



ACS SYMPOSIUM SERIES **555**

Inorganic Fluorine Chemistry

Toward the 21st Century

Joseph S. Thrasher, EDITOR
University of Alabama

Steven H. Strauss, EDITOR
Colorado State University

Developed from a symposium sponsored
by the Division of Fluorine Chemistry
at the 203rd National Meeting
of the American Chemical Society,
San Francisco, California,
April 5–10, 1992



American Chemical Society, Washington, DC 1994

Inorganic fluorine chemistry



Library of Congress Cataloging-in-Publication Data

Inorganic fluorine chemistry: toward the 21st century: developed from a symposium sponsored by the Division of Fluorine Chemistry at the 203rd National Meeting of the American Chemical Society, San Francisco, California, April 5-10, 1992 / Joseph S. Thrasher, editor, Steven H. Strauss, editor.

p. cm.—(ACS symposium series, ISSN 0097-6156; 555)

Includes bibliographical references and index.


ISBN 0-8412-2869-8

1. Fluorine compounds—Congresses. 2. Organofluorine compounds—Congresses.

I. Thrasher, Joseph S., 1956— II. Strauss, Steven H.
III. American Chemical Society. Division of Fluorine Chemistry.
IV. American Chemical Society. Meeting (203rd: 1992: San Francisco, Calif.) V. Series.

QD181.F1156 1994
546'.731—dc20

94-2547
CIP

The paper used in this publication meets the minimum requirements of American National Standard for Information Sciences—Permanence of Paper for Printed Library Materials, ANSI Z39.48-1984. 

Copyright © 1994

American Chemical Society

All Rights Reserved. The appearance of the code at the bottom of the first page of each chapter in this volume indicates the copyright owner's consent that reprographic copies of the chapter may be made for personal or internal use or for the personal or internal use of specific clients. This consent is given on the condition, however, that the copier pay the stated per-copy fee through the Copyright Clearance Center, Inc., 27 Congress Street, Salem, MA 01970, for copying beyond that permitted by Sections 107 or 108 of the U.S. Copyright Law. This consent does not extend to copying or transmission by any means—graphic or electronic—for any other purpose, such as for general distribution, for advertising or promotional purposes, for creating a new collective work, for resale, or for information storage and retrieval systems. The copying fee for each chapter is indicated in the code at the bottom of the first page of the chapter.

The citation of trade names and/or names of manufacturers in this publication is not to be construed as an endorsement or as approval by ACS of the commercial products or services referenced herein; nor should the mere reference herein to any drawing, specification, chemical process, or other data be regarded as a license or as a conveyance of any right or permission to the holder, reader, or any other person or corporation, to manufacture, reproduce, use, or sell any patented invention or copyrighted work that may in any way be related thereto. Registered names, trademarks, etc., used in this publication, even without specific indication thereof, are not to be considered unprotected by law.

PRINTED IN THE UNITED STATES OF AMERICA

American Chemical Society

Library

1155 16th St., N.W.

Inorganic Fluorine Chemistry: Thrasher, J., et al.;
ACS Symposium Series; American Chemical Society: Washington, DC, 1994.

1994 Advisory Board

ACS Symposium Series

M. Joan Comstock, *Series Editor*

- | | |
|---|---|
| Robert J. Alaimo
Procter & Gamble Pharmaceuticals | Douglas R. Lloyd
The University of Texas at Austin |
| Mark Arnold
University of Iowa | Cynthia A. Maryanoff
R. W. Johnson Pharmaceutical
Research Institute |
| David Baker
University of Tennessee | Julius J. Menn
Plant Sciences Institute,
U.S. Department of Agriculture |
| Arindam Bose
Pfizer Central Research | Roger A. Minear
University of Illinois
at Urbana–Champaign |
| Robert F. Brady, Jr.
Naval Research Laboratory | Vincent Pecoraro
University of Michigan |
| Margaret A. Cavanaugh
National Science Foundation | Marshall Phillips
Delmont Laboratories |
| Arthur B. Ellis
University of Wisconsin at Madison | George W. Roberts
North Carolina State University |
| Dennis W. Hess
Lehigh University | A. Truman Schwartz
Macalaster College |
| Hiroshi Ito
IBM Almaden Research Center | John R. Shapley
University of Illinois
at Urbana–Champaign |
| Madeleine M. Joullie
University of Pennsylvania | L. Somasundaram
DuPont |
| Lawrence P. Klemann
Nabisco Foods Group | Michael D. Taylor
Parke-Davis Pharmaceutical Research |
| Gretchen S. Kohl
Dow-Corning Corporation | Peter Willett
University of Sheffield (England) |
| Bonnie Lawlor
Institute for Scientific Information | |

Foreword

THE ACS SYMPOSIUM SERIES was first published in 1974 to provide a mechanism for publishing symposia quickly in book form. The purpose of this series is to publish comprehensive books developed from symposia, which are usually "snapshots in time" of the current research being done on a topic, plus some review material on the topic. For this reason, it is necessary that the papers be published as quickly as possible.

Before a symposium-based book is put under contract, the proposed table of contents is reviewed for appropriateness to the topic and for comprehensiveness of the collection. Some papers are excluded at this point, and others are added to round out the scope of the volume. In addition, a draft of each paper is peer-reviewed prior to final acceptance or rejection. This anonymous review process is supervised by the organizer(s) of the symposium, who become the editor(s) of the book. The authors then revise their papers according to the recommendations of both the reviewers and the editors, prepare camera-ready copy, and submit the final papers to the editors, who check that all necessary revisions have been made.

As a rule, only original research papers and original review papers are included in the volumes. Verbatim reproductions of previously published papers are not accepted.

M. Joan Comstock
Series Editor

Preface

INORGANIC FLUORINE CHEMISTRY'S RELEVANCE to the broader field of inorganic chemistry and to the chemical industry as a whole cannot and should not be overlooked. This book provides an up-to-date account of both fundamental and applied research in inorganic fluorine chemistry and emphasizes the important interdisciplinary nature of most research in the fluorine chemistry field as it applies to the future well-being of our country and the world. The development of chlorofluorocarbon alternatives to help halt the depletion of stratospheric ozone serves as a vivid example of this point. Although the alternatives will almost certainly be organofluorine compounds, the processes being developed to produce these materials cannot escape the use of inorganic fluorine chemistry in terms of such applications as catalysts and halogen-exchange reagents. Materials science is another area of increasing interest to the chemical industry as a result of the recent development of new precursors for the chemical vapor deposition of inorganic materials. Chapters on both topics are included in this volume.

Although a few recent books contain chapters on inorganic fluorine chemistry, no volume exists that is totally dedicated to the subject. This volume contains 26 authoritative accounts from recognized leaders in the field. Several chapters, particularly those by Burton, Farnham, and Lagow, may appear to look like organofluorine chemistry, but the results given in these chapters would not have been possible without the use of inorganic reagents and methodologies. This situation attests to the interdisciplinary nature of most research in fluorine chemistry.

The goals of this book and the symposium from which it evolved are to broaden and renew interest and expertise in inorganic fluorine chemistry and to help inorganic fluorine chemists gain wider acceptance in the field of inorganic chemistry. The incredible response shown by the speakers and authors, the large attendance and participation shown by the audience, and the financial support from the fluorochemical industry for the symposium reveal a strong interest in inorganic fluorine chemistry. We have attempted to foster this interest by co-listing the symposium program with programs of the Division of Inorganic Chemistry; inviting speakers and authors from a broad range of inorganic chemists who rarely attend divisional, European, or international fluorine chemistry symposia; and seeking out and inviting junior investigative scientists and young authors to attend the meeting. We hope that this book and future

symposia will provide a continuing platform to expand and promote interest in inorganic fluorine chemistry in the United States and around the world.

Acknowledgments

This volume would not have been possible without the hard work and cooperation of the authors, reviewers, and staff at the American Chemical Society Books Department. We thank Richard E. Fernandez of DuPont for all of his assistance during Joe Thrasher's sabbatical, where much of the planning for both the symposium and this book took place. We also gratefully acknowledge the following for financial support of the symposium: American Chemical Society's Division of Fluorine Chemistry; American Chemical Society Petroleum Research Fund; Advance Research Chemicals, Inc.; Air Products and Chemicals, Inc.; Allied-Signal Corporation; Anaquest/BOC Group, Inc.; Ausimont; DuPont; Hemagen/PFC; Occidental Chemical Corporation; and 3M Company, Inc.

JOSEPH S. THRASHER
Department of Chemistry
University of Alabama
P.O. Box 870336
Tuscaloosa, AL 35487-0336

STEVEN H. STRAUSS
Department of Chemistry
Colorado State University
Fort Collins, CO 80523

October 15, 1993

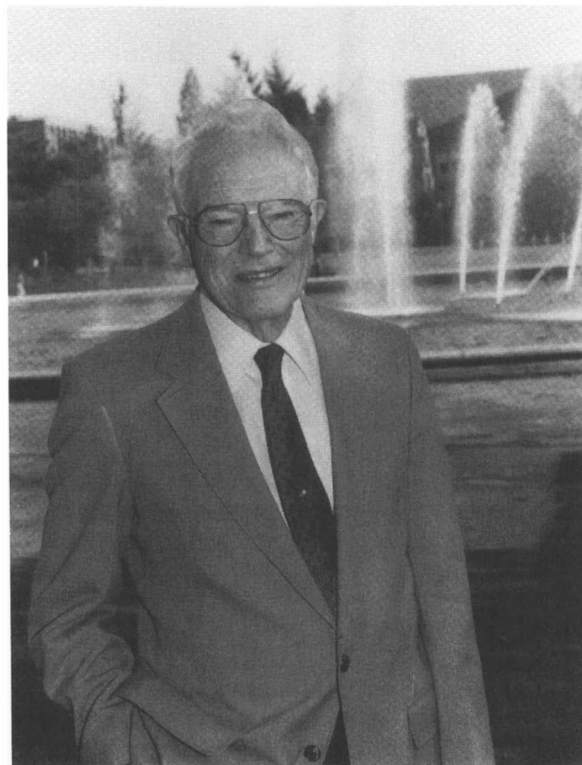


Photo courtesy of Davis Freeman, University Photography

To

**George H. Cady
1906–1993**

An inspirational teacher and scientist.

Chapter 1

Inorganic Fluorine Chemistry Toward the 21st Century

Joseph S. Thrasher¹ and Steven H. Strauss²

¹Department of Chemistry, The University of Alabama, P.O. Box 870336,
Tuscaloosa, AL 35487-0336

²Department of Chemistry, Colorado State University,
Fort Collins, CO 80523

Fluorine and fluorinated substituent groups play an increasingly important role in modern inorganic chemistry. Many advances in solid-state chemistry, coordination chemistry, main group element chemistry, and organometallic chemistry rely on the unique physical and chemical properties of the most electronegative of the chemical elements. This chapter lists the important monographs and reviews that have been published during the last twenty-five years in this area as well as some thoughts about where the field of inorganic fluorine chemistry is heading.

The unusual properties exhibited by numerous materials upon the incorporation of either fluorine or fluorine-containing substituents are no longer just topics of idle curiosity for the academician, but are the driving force behind developments in the field of fluorine chemistry. Many advances have either recently found or await commercialization as witnessed by the increasing diversity of industrial applications of fluorine compounds (1-7). Two illustrative examples of the current importance of inorganic fluorine chemistry to industry are the development of both chlorofluorocarbon (CFC) alternatives and new precursors for chemical vapor deposition (CVD) of inorganic materials. Although the CFC alternatives will almost certainly be organofluorine compounds, the processes being developed to produce these materials cannot escape the use of inorganic fluorine chemistry in terms of catalysts (8-15), halogen exchange reagents (16-20), and the like. The references given here serve only as representative examples; the current patent literature is full of references in light of the global concern to help halt the depletion of stratospheric ozone. The second aforementioned case falls into the increasingly important area of materials science. For example, a number of groups have recently taken advantage of the well-known increase in volatility associated with fluorine incorporation to make a series of volatile metal alkoxides which serve as new precursors for CVD of metal fluorides (21-28). Separate chapters on both of these topics of industrial importance appear later in this book.

0097-6156/94/0555-0001\$08.54/0
© 1994 American Chemical Society

A number of other topical areas that are of current interest in inorganic fluorine chemistry and promise to be of continued interest towards the 21st century will be surveyed in the following pages. Many of these topics, but not all, are then described in more detail in later chapters.

Coordination Numbers Greater than Six Among Fluorides and Oxofluorides

The recent and continuing explosion in terms of the number of examples, as well as our understanding of their structures and bonding, of fluorides and oxofluorides with coordination numbers greater than six can be attributed almost solely to the development of a synthetic procedure for truly anhydrous tetramethylammonium fluoride by Christe and co-workers (29). With this source of more active fluoride, the groups of Christe, Schrobilgen, and Seppelt have been able to prepare and characterize the following remarkable species: XeF_5^- (30), ClF_6^- (31), BrF_6^- (32-34), IF_6^- (32,35), TeF_7^- (36-38), $\text{TeF}_6(\text{OCH}_3)^-$ (38), $\text{TeF}_5(\text{OCH}_3)_2^-$ (38), TeOF_6^{2-} (39), IOF_6^- (40), TeF_8^{2-} (36), and IF_8^- (36,41). The concept of coordination numbers greater than six has also been extended to *d*- and *f*-block metal fluorides, namely MoF_7^- , WF_7^- , and UF_7^- (42). In addition, other novel species such as the PF_4^- anion (43), which was previously only known in a low-temperature matrix (44), have now been prepared from tetramethylammonium fluoride. All of the aforementioned anions, as well as the ones remaining to be discovered, will almost certainly become the textbook examples of the future (45). The current viewpoint on the structure and bonding in these novel species is the topic of two chapters in this monograph.

From Naked Fluoride to Least Coordinating Anion

Obviously, the fluoride ion cannot be totally naked in a real chemical environment; however, successes such as those mentioned above can be attributed totally to more basic or nucleophilic sources of fluoride such as cesium fluoride, tetramethylammonium fluoride, and the phosphazanium fluoride [$\{(\text{CH}_3)_2\text{N}\}_3\text{P}=\text{N}=\text{P}\{\text{N}(\text{CH}_3)_2\}_3\}^+\text{F}^-$ (46). In each case, a bulky cation is used in order to maximize the cation-anion distance and thus minimize their interaction. In addition, it is important to have a cation that is as stable as possible towards oxidation. Furthermore, it is necessary for the fluoride source to be anhydrous. It is with these reasons in mind, and the well-known stabilization of a complex anion by the use of a bulky cation (47,48), that Thrasher and co-workers prepared a potentially "naked" SF_5^- salt using $\text{Cs}\cdot([\text{18}]\text{crown-6})_2^+$ as the cation. Although the closest cation-anion contacts in this salt were over 7 Å, the SF_5^- anion in this salt failed to act as a nucleophile when reacted with methyl iodide (49). Seppelt and co-workers have recently published the structures of an SeF_5^- salt and several TeF_5^- salts in which they describe weak interactions between the chalcogen atom of one anion with the fluorine atom of a neighboring anion (50).

Just as bulky cations have been used to disperse the positive charge over the cation and minimize cation-anion interactions, so has the search continued for more and more weakly coordinating anions. Again fluorine chemistry has played an

important role in this search, not only in terms of aromatic C-F bonds in tetraarylborates, but also in terms of the pentafluorooxotellurate, OTeF_5^- , and related anions (51,52). For example, Strauss and co-workers have recently extended their search to anions such as $\text{Ti}(\text{OTeF}_5)_6^{2-}$, $\text{Nb}(\text{OTeF}_5)_6^-$, $\text{Ta}(\text{OTeF}_5)_6^-$, and $\text{Sb}(\text{OTeF}_5)_6^-$ in which the negative charge(s) is(are) spread primarily over thirty fluorine atoms. The high solubility of the silver salts of these anions in solvents like CFC-113 shows that appreciable concentrations of metal ions can be produced in solvents that are even more weakly coordinating than dichloromethane if the counterion is large enough and weakly coordinating enough (51). Winter and co-workers, as described in a later chapter, have successfully utilized more or less the same concept to produce a series of highly soluble organotitanium Lewis acids (53,54). Strauss' search has allowed the preparation and characterization of the first isolable silver carbonyls $\text{Ag}(\text{CO})^+$ and $\text{Ag}(\text{CO})_2^+$ (55,56) where the would-be coordinatively unsaturated metal cation binds to weak ligands such as carbon monoxide. Aubke and co-workers have also recently been able to stabilize the $\text{Au}(\text{CO})_2^+$ cation either in highly acidic media (57) or in the solid state with the weakly basic fluoro anion $\text{Sb}_2\text{F}_{11}^-$ (58). These silver and gold carbonyl cations are particularly interesting in that they possess C-O stretching frequencies higher than that in free CO which is an indication of an increase in bond order between the carbon and oxygen upon coordination to silver or gold. A more detailed overview of these complexes and their structures and bonding is included in two separate chapters in this monograph. In terms of what the future holds, the intriguing question has been posed "Carbon monoxide. A ligand for main group elements?" (59).

Fluorinated Allotropes of Carbon

From the initial report of synthetic quantities of buckminsterfullerene, one could realistically think of the possibility of preparing better lubricants than the graphite fluorides (60). Several research groups have undertaken the fluorination of C_{60} and other fullerenes (61-65), and although there may be some debate as to the degree of fluorination, highly fluorinated C_{60} is rather susceptible to nucleophilic substitution which precludes its use as a lubricant (66-68). On the other hand, the reactivity of fluorinated C_{60} provides a potential route to many new fullerene derivatives (66-69), and high quality thin films of fluorinated C_{60} have already been prepared and studied (70). In addition, buckyballs have recently been coated with perfluoroalkyl groups by a team of scientists at Du Pont (71). As far as the other allotrope of carbon is concerned, Margrave's group has been studying the fluorination of diamond for a number of years (72-75). More recently, Margrave and co-workers have been looking at the halogen-assisted CVD of diamond (76-79), including the potential disposal of CFCs and Halons via this technique (80). It will be interesting to examine the economics of this latter proposal when done on a large scale.

Novel Bond Types to Noble Gases

It has been almost twenty years since DesMarteau reported the first example of a compound with a xenon-nitrogen bond (81) and approximately ten years since

Schrobilgen published the first structural evidence for this bond type (82). In the intervening time, the majority of new compounds with a xenon-nitrogen bond have resulted from the exploitation of the Lewis acid properties of noble gas cations by Schrobilgen and co-workers (83-88). These workers have further exploited these properties to prepare the first compounds with a krypton-nitrogen bond (87,89). The majority of these new Xe-N and Kr-N compounds are solution species; they have been characterized predominately by multinuclear NMR and vibrational spectroscopy and are generally too unstable to be isolated in a pure form.

In 1979, Lagow and co-workers reported the first evidence for a compound with a bond between xenon and carbon, namely Xe(CF₃)₂ (90). While the evidence for this compound still receives much scrutiny, the groups of Frohn and Naumann independently synthesized the first definitive examples of compounds with a xenon-carbon bond (91-96). Until recently all of the examples of xenon-carbon bonds were cationic species. However, earlier this year Frohn reported the preparation, characterization, and structure of C₆F₅XeO₂CC₆F₅, the first truly covalent compound with not only a xenon-carbon bond, but a xenon-oxygen bond as well (97).

The recently prepared Kr(OTeF₅)₂ represents the first compound with krypton-oxygen bonds (98). Again, this compound is only a solution species which has been characterized by its ¹⁹F and ¹⁷O NMR spectra. Much technical expertise on updated procedures for noble gas fluorides has come from the groups of Zemva and Kinkead (99-103). A detail discussion of the preparation of one of these noble gas fluorides, namely KrF₂, is given in a following chapter. In addition, these research groups have led the way recently in the synthesis of new *d*-block metal fluorides (104-106) and *f*-block metal compounds (107), respectively. The future of noble gas chemistry will likely see the synthesis of compounds containing new types of xenon-carbon bonds as well as a xenon-nitrogen double bond, a xenon-boron bond, and an argon-fluorine bond. The Ar-F⁺ species is fundamentally the most likely target for the latter (108,109), and the practicalities of this synthetic challenge are discussed in detail by Bartlett in a later chapter.

Marriage Between Computational and Experimental Chemistry

Both authors firmly believe in the ability of computational chemistry to aid the direction of and thus complement their synthetic chemistry (49,110-115). Today there is an ever increasing number of examples where computational chemistry has helped to point out either an incorrect structural solution, vibration assignment, etc. Dixon and Christie have recently published a number of salient examples in inorganic fluorine chemistry which display the benefits of this marriage (30,39,40,116-119). For example, their recent publication on TeOF₆²⁻ may not have been possible if it were not for computational chemistry, as the insolubility and instability of the tetramethylammonium salt of this anion precluded its characterization by methods outside of vibrational spectroscopy. In addition, the vibrational spectra were fraught with difficulty from the unavoidable presence of the corresponding TeOF₅⁻ salt (39). Christie and Dixon have also developed for the first time a quantitative scale for the oxidizer strengths of oxidative fluorinators. The availability of such a scale should have a major impact on the future syntheses of new as well as known oxidative

fluorination reagents (118). A much more detailed and certainly correct understanding of the structure, bonding, and rigidity of the prototypical seven-coordinate molecule IF₇ is now available through the union of experimental and computational chemistry (116). (This particular topic is expounded upon in considerable detail in a later chapter.) In fact, we have borrowed the section title from the title of a recent presentation by Christie and Dixon: "Experimental and Computational Chemistry. A Marriage Made in Heaven" (120). We are convinced that computational chemistry will become every bit as common place a tool for the synthetic chemist in the 21st century as the NMR spectrometer and X-ray diffractometer are today.

Obviously, Dixon and Christie are not alone in applying computational chemistry to inorganic fluorine chemistry. One needs only to look at the continuing saga on the existence and structure of CrF₆ to see a number of other players in the field (121-127). Space limitations prohibit us from being comprehensive in coverage.

New Fluorine-Containing Ligands

Pentafluorocyclopentadienyl. In the 1980s, Seppelt and co-workers succeeded in preparing the C₅F₅⁻ anion, but their inability to prepare transition metal complexes from metathesis reactions of this anion, or from 5H-pentafluorocyclopentadiene and its 5-bromo analogue, left them wondering if the desired transition metal complexes might be unstable (128-130). More recently, Curnow and Hughes have prepared the first transition metal complex containing the pentafluorocyclopentadienyl ligand by extrusion of CO from a η⁵-bound pentafluorophenoxide ligand (131). Winter and co-workers have also succeeded in preparing an η⁵-C₅F₅ complex (132,133). A detailed account of the synthesis and characterization of the first η⁵-C₅F₅ transition metal complex Ru(η⁵-C₅Me₅)(η⁵-C₅F₅), as well as other new transition metal chemistry involving fluoro-olefins and -dienes, is given by Hughes in a later chapter.

Difluoroethyne. Just as Curnow and Hughes were able to build the η⁵-C₅F₅ ligand directly on the metal center, Lentz and co-workers have succeeded in preparing the first difluoroethyne (FCCF) complexes either by coupling two fluoromethylidyne ligands in a cluster expansion reaction (134) or by bridging two tetracarbonylcobalt fragments with difluorofumaric dichloride followed by subsequent loss of two equivalents of carbon monoxide (135). Previously, the extreme instability of difluoroethyne was thought to have prevented its use in the synthesis of complexes. This belief has found support in the recent isolation and characterization of free difluoroethyne, as the molecule was found to decompose slowly even at liquid nitrogen temperature (136).

Fluoromethylidyne and Difluoromethylidene. Bismethylidyne complexes of iron are themselves somewhat rare. For example, when Lentz and co-workers first prepared nonacarbonylbis(μ₃-fluoromethylidyne)triiron, [Fe₃(CO)₉(μ₃-CF)₂] (137), it was only the second known compound to contain the Fe₃(CR)₂ moiety. Since then, Lentz has extended the chemistry of this compound by studying (1) its reactions with alkynes (138-140), a phosphalkyne (140,141), and Lewis acids (140,142), (2) its carbonyl substitution chemistry with nitriles and phosphines (143),

(3) its reduction to the corresponding μ_3 -methylidyne complex (144), and (4) its electronic structure via photoelectron spectroscopy (145,146). Just as the μ_3 -fluoromethylidyne ligand bridges three metal centers, a few complexes with μ_2 -difluoromethylidene (difluoromethylene) ligands bridging two metal centers have recently been prepared and structurally characterized (147,148). While, the difluoromethylidene ligand can also be found as a terminal (difluorocarbene) ligand (149-154), an example of a complex with a terminal (mononuclear) fluoromethylidyne ligand does not yet exist.

Fluorinated Isocyanides. In addition to his contributions in the area of cluster chemistry, Lentz has also contributed heavily in the area of organometallic chemistry of fluorinated isocyanides. He and his co-workers have prepared numerous complexes of CF_3NC (155) and the first complexes of $\text{C}_6\text{F}_5\text{NC}$ (156,157), HCF_2NC , H_2CFNC (158), and $\text{CF}_2=\text{CFNC}$ (159). Again, Lentz has had to use indirect routes to build some of the new fluorinated isocyanide ligands directly on metal centers in situations where it was not possible to prepare and/or isolate the free isocyanides. Having also recently prepared and characterized ethynyl isocyanide, $\text{HC}\equiv\text{C}-\text{N}\equiv\text{C}$ (160), Lentz's attention now turns towards the fluorine analogue $\text{FC}\equiv\text{C}-\text{N}\equiv\text{C}$. A detailed overview of this chemistry is given in a later chapter by Lentz.

Fluorophosphines. King (161) and Nixon (162,163) are two names that are synonymous with the early development of the chemistry of fluorophosphine transition metal complexes. While PF_3 complexes are certainly the most well-studied, there appears to be a renewed interest in the study of the ligating properties of (fluoroalkyl)phosphines in terms of being able to fine tune the reactivity of metal centers, especially for low valent transition metals. For example, tungsten and molybdenum complexes of $(\text{CF}_3)_2\text{PH}$ and CF_3PH_2 have been prepared by the research groups of Grobe (164) and O'Brien (165). These researchers have also initiated a study of the ligating properties of $\text{CF}_3\text{P}=\text{CF}_2$ (165-167) and $\text{CF}_3\text{P}=\text{C}(\text{F})\text{NR}_2$ (168), ligands which may be viewed as having multiple sites for coordination. More recently, O'Brien has reported the preparation of the first complexes of $(\text{HCF}_2\text{CF}_2)_2\text{PH}$ and $\text{HCF}_2\text{CF}_2\text{PH}_2$ (169). Schmutzler and co-workers have also recently reported a variety of new monofluorophosphines as well as their transition metal complexes (170). In terms of chelating (fluoroalkyl)phosphine ligands, Roddick and co-workers have concentrated their studies on the ligand $(\text{C}_2\text{F}_5)_2\text{PCH}_2\text{CH}_2\text{P}(\text{C}_2\text{F}_5)_2$ (171-173). In fact, a more detail account of these and related results is given in a later chapter by Roddick and Schnabel.

Other Fluorine-Containing Main Group Element Ligands. Of the novel fluorine-containing ligands that have been prepared over the last few years, the examples from Ebworth's group are especially noteworthy. For example, these researchers have prepared the first fluoroacyl complexes by reacting iridium carbonyl complexes with XeF_2 (175,176). They have also prepared the first transition metal complexes with SF_3 , SeF_3 , and TeF_3 ligands by reacting the iridium or rhodium complexes $[\text{M}(\text{CO})\text{X}(\text{PEt}_3)_2]$ (where X = halogen or pseudohalogen) with the respective nonmetal tetrafluoride (177,178). A later chapter by Ebsworth and co-

workers describes in detail these and other interesting results, including complexes with PF₂, PF₄, and PF₂H₂ ligands.

A variety of organocobaloximes containing fluoroalkyl and fluoroalkenyl ligands have been reported by Toscano and co-workers (179-182). These complexes are of special interest in helping to determine the factors which affect cobalt-carbon energies. For example, a very short Co-C(sp³) bond was found in the cobaloximes with a CF₃ ligand (181), and the first case of a steric trans effect for ligand substitution in a cobaloxime was observed with the bulky CF(CF₃)₂ ligand (179). The syntheses, structures, and reactivities of these and related complexes are given in a later chapter by Toscano and co-workers.

C-F Bond Activation

The activation of hydrocarbons by metal centers has been an area of intense study during the last ten to fifteen years especially in view of the potential for selectively modifying petroleum feed stocks under mild conditions (45). The idea that perfluorocarbons could not easily be modified in a similar manner, primarily because of the increased C-F bond energy, makes the increasing number of current examples of C-F bond activation all the more interesting. The report by MacNicol in 1988 (183) of the unexpected reactivity of arenethiolate nucleophiles with perfluorocarbons such as perfluorodecalin under ambient conditions seems to have sparked a renewed interest in this area. Reports of intermolecular C-F bond activation have appeared from no fewer than eight laboratories since that time (184,185). It is interesting to note that there are also several structural reports of transition metal complexes with agostic C-F interactions (186-188). While most of the reports of C-F bond activation involve unsaturated or aromatic fluorocarbons, the most recent reports from the laboratories of Andersen (184) and Richmond (185) also involve saturated fluorocarbons. A more detailed discussion of this most intriguing area is given later in two separate chapters, one by Andersen on *f*-block metal complexes and another by Richmond on *d*-block metal complexes.

Fluorine-Containing Substituent Groups

There have clearly been more advances in the area of fluorine-containing substituent groups, especially in the area of main group chemistry, than under any of the aforementioned headings, and thus the title of the book. Unfortunately, space limitations again prohibit us from being comprehensive in coverage; however, the reader's attention will be drawn to a large number of the remaining chapters which are on this topic. In addition, a number of researchers who have made significant contributions in this area, but whose contributions are not covered by separate chapters, will be pointed out.

The syntheses of a large number of Group 15-17 onium cations such as S₂F⁺, H₂SF⁺, H₂OF⁺, and Br₅⁺ from the reactions of the monfluoroxenonium hexafluorometalates XeF⁺MF₆⁻ where M = As or Sb are described in a later chapter by Minkwitz and Bäck. As a further example of the utility of the element displacement principle (189-192), Haas and Brosius demonstrate the influence of fluorine, trifluoromethyl, trifluoromethylsulfenyl, and trifluoromethylselenyl on the

chemistry of selected functional groups including carbenes, nitrenes, carbonyls, thiocarbonyls, selenocarbonyls, tellurocarbonyls, ketenes, thioketenes, sulfines, isocyanates, and sulfinylamines. In another chapter, Winter and Gard review the functionalization of SF₅-containing olefins and acetylenes. A number of other laboratories have carried out work with the SF₅ and related functional groups, including the laboratories of Lagow (193) and Seppelt (114,194), primarily on SF₅-carbon compounds, and the laboratories of DesMarteau (195), Mews (196-198), Shreeve (199-203), and Thrasher (49,204-206) on SF₅-nitrogen compounds. A chapter on the recent advances in the area of fluoro-sulfur anions by Mews is included in this volume. Another sterically and electronically demanding group is the 2,4,6-tris(trifluoromethyl)phenyl group which has been used extensively by Edlmann to stabilize a number of organic and main group systems. Although Edlmann has recently reviewed the chemistry of this group (207), he provides an overview herein of the more important aspects and latest developments of its chemistry.

Other noteworthy topics not covered by the present volume include advances in the chemistry of hypofluorites, new superacids of carbon and nitrogen, selenium-nitrogen-fluorine chemistry and related cations, and the fluorine chemistry of homopolyatomic cations. A number of new hypofluorites including CF₃SO₂OF (208), (CH₃)₃COF (209), CH₃C(O)OF (210), and CH₃OF (211,212) have recently been prepared and characterized by Appelman and co-workers. DesMarteau and co-workers have developed a new family of polyprotic superacids of carbon and nitrogen based on the CF₃SO₂ group. These materials are unique in that the protons all ionize at virtually the same pH and not stepwise like in a normal polyprotic acid. Although no review exists on this subject, some representative references are given (213-215). Both of the fluorine chemistry of selenium-nitrogen compounds and homopolyatomic cations have been reviewed recently by Klapötke (217) and Passmore (218,219), respectively.

Finally, a list of the important monographs and reviews that have been published in the area of inorganic fluorine chemistry during the last twenty-five years is included at the end of the Literature Cited section (220-346).

Conclusion

Traditionally, fluorine chemistry has been viewed as a highly specialized area in which only experts contributed to the literature. However, as we approach the 21st century, all chemists are becoming more interdisciplinary in their search for solutions to complex scientific and technological problems. We predict that more and more chemists will include various aspects of inorganic fluorine chemistry in their work, and in doing so, will become *de facto* fluorine chemists.

Literature Cited

1. *Preparation, Properties, and Industrial Applications of Organofluorine Compounds*; Banks, R. E., Ed.; Ellis Horwood: Chichester, 1982.
2. *Organofluorine Compounds and their Industrial Applications*; Banks, R.E., Ed.; Ellis Horwood: Chichester, 1979.
3. Gerstenberger, M. R. C.; Haas, A. *Angew. Chem., Int. Ed. Engl.* **1981**, *20*, 647.

4. Meshri, D. T. In *Fluorine: The First Hundred Years (1886-1986)*; Banks, R. E.; Sharp, D. W. A.; Tatlow, J. C., Eds.; Elsevier: New York, 1986; Chapter 10.
5. Büchner, W.; Schliebs, R.; Winter, G.; Büchel, K. H. *Industrial Inorganic Chemistry*; VCH: New York, 1989.
6. Swaddle, T. W. *Applied Inorganic Chemistry*; University of Calgary Press: Calgary, 1990.
7. Austin, G. T. *Shreve's Chemical Process Industries*, 5th ed.; McGraw-Hill: New York, 1984.
8. Butcher, J. L.; Ryan, T. A.; Burgess, L. Eur. Patent 518 506, 1992.
9. Tung, H. S.; Smith, A. M. U.S. Patent 5 155 082, 1992.
10. Ikawa, T.; Morikawa, Y.; Ueda, W. Eur. Patent 499 984, 1992.
11. Eicher, J.; Razniewscy, K. H.; Rudolph, W.; Swidersky, H. W. Eur. Patent 451 746, 1991.
12. Thomson, J.; Winfield, J. M.; Webb, G. Eur. Patent 439 338, 1991.
13. Blanchard, M.; Wendlinger, L.; Canesson, P. *Appl. Catal.* **1990**, *59*, 123.
14. Vachta, J.; Grunt, M.; Roh, Z.; Mekota, F.; Pacha, J.; Siler, J.; Krasl, K.; Posta, A.; Barta, M. Czech. Patent 237 613, 1987.
15. Ruderhausen, C. G. U.S. Patent 4 678 859, 1987.
16. Dukat, W. W.; Holloway, J. H.; Hope, E. G.; Rieland, M.; Townson, P. J.; Powell, R. L. Eur. Patent 503 792, 1992.
17. Holloway, J. H.; Hope, E. G.; Townson, P. J.; Powell, R. L. Eur. Patent 503 793, 1992.
18. Cassel, W. R.; Fernandez, R. E.; Mader, F. W. U.S. Patent 4 990 701, 1991.
19. Cassel, W. R.; Fernandez, R. E.; Mader, F. W. U.S. Patent 4 990 702, 1991.
20. Fernandez, R. E.; Gumprecht, W. H.; Kaplan, R. B. U.S. Patent 5 045 634, 1991.
21. Samuels, J. A.; Lobkovsky, E. B.; Streib, W. E.; Foltling, K.; Huffman, J. C.; Zwanziger, J. W.; Caulton, K. G. *J. Am. Chem. Soc.* **1993**, *115*, 5093.
22. Purdy, A. U.S. Patent Appl. 92-828 634, 1992; *Chem. Abstr.* **1992**, *118*, 180615.
23. Thompson, S. C.; Cole-Hamilton, D. J.; Gilliland, D. D.; Hitchman, M. L.; Barnes, J. C. *Adv. Mater. Opt. Electron.* **1992**, *1*, 81.
24. Gilliland, D. G.; Hitchman, M. L.; Thompson, S. C.; Cole-Hamilton, D. J. *J. Phys. III* **1992**, *2*, 1381.
25. Brooks, K. C.; Turnipseed, S. B.; Barkley, R. M.; Sievers, R. E.; Tulchinsky, V.; Kaloyeros, A. E. *Chem. Mater.* **1992**, *4*, 912.
26. Lingg, L. J.; Berry, A. D.; Purdy, A. P.; Ewing, K. J. *Thin Solid Films* **1992**, *209*, 9.
27. Purdy, A. P.; Berry, A. D.; Holm, R. T.; Fatemi, M.; Gaskill, D. K. *Inorg. Chem.* **1989**, *28*, 2799.
28. Zhao, J.; Dahmen, K.; Marcy, H. O.; Tonge, L. M.; Marks, T. J.; Wessels, B. W.; Kannewurf, C. R. *Appl. Phys. Lett.* **1988**, *53*, 1750.
29. Christe, K. O.; Wilson, W. W.; Wilson, R. D.; Bau, R.; Feng, J. *J. Am. Chem. Soc.* **1990**, *112*, 7619.
30. Christe, K. O.; Curtis, E. C.; Dixon, D. A.; Mercier, H. P.; Sanders, J. C. P.; Schrobilgen, G. J. *J. Am. Chem. Soc.* **1991**, *113*, 3351.

31. Christe, K. O.; Wilson, W. W.; Chirakal, R. V.; Sanders, J. C. P.; Schrobilgen, G. J. *Inorg. Chem.* **1990**, *29*, 3506.
32. Christe, K. O.; Wilson, W. W. *Inorg. Chem.* **1989**, *28*, 3275.
33. Wilson, W. W.; Christe, K. O. *Inorg. Chem.* **1989**, *28*, 4172.
34. Mahjoub, A. R.; Hoser, A.; Fuchs, J.; Seppelt, K. *Angew. Chem., Int. Ed. Engl.* **1989**, *28*, 1526.
35. Mahjoub, A. R.; Seppelt, K. *Angew. Chem., Int. Ed. Engl.* **1991**, *30*, 323.
36. Christe, K. O.; Sanders, J. C. P.; Schrobilgen, G. J.; Wilson, W. W. *J. Chem. Soc., Chem. Commun.* **1991**, 837.
37. Mahjoub, A. R.; Seppelt, K. *J. Chem. Soc., Chem. Commun.* **1991**, 840.
38. Mahjoub, A. R.; Drews, T.; Seppelt, K. *Angew. Chem., Int. Ed. Engl.* **1992**, *31*, 1036.
39. Christe, K. O.; Dixon, D. A.; Sanders, J. C. P.; Schrobilgen, G. J.; Wilson, W. W. *Inorg. Chem.* **1993**, *32*, 4089.
40. Christe, K. O.; Dixon, D. A.; Mahjoub, A. R.; Mercier, H. P. A.; Sanders, J. C. P.; Seppelt, K. Schrobilgen, G. J.; Wilson, W. W. *J. Am. Chem. Soc.* **1993**, *115*, 2696.
41. Mahjoub, A. R.; Seppelt, K. *Angew. Chem., Int. Ed. Engl.* **1991**, *30*, 876.
42. Giese, S.; Seppelt, K. *J. Fluorine Chem.* **1992**, *58*, 368.
43. Wilson, W. W.; Christe, K. O.; Sanders, J. C. P.; Schrobilgen, G. J.; Dixon, D. A.; Bau, R. *Abstracts of Papers*, 203rd National Meeting of the American Chemical Society, San Francisco, CA; American Chemical Society: Washington, DC, 1992; FLUO 27.
44. Werner, P.; Ault, B. S. *Inorg. Chem.* **1981**, *20*, 970.
45. Huheey, J. E.; Keiter, E. A.; Keiter, R. L. *Inorganic Chemistry: Principles of Structure and Reactivity*, 4th ed.; HarperCollins College Publishers: New York, 1993.
46. Seppelt, K. *Angew. Chem., Int. Ed. Engl.* **1992**, *31*, 292 and references therein.
47. Steudel, R. *Chemistry of the Non-Metals*; Walter de Gruyter: Berlin, 1977; Chapter 5.
48. Douglas, B. E.; McDaniel, D. H.; Alexander, J. J. *Concepts and Models of Inorganic Chemistry*, 2nd ed.; John Wiley & Sons: New York, 1983; p 229.
49. Clark, M.; Kellen-Yuen, C. J.; Robinson, K. D.; Zhang, H.; Yang, Z.-Y.; Madappat, K. V.; Fuller, J. W.; Atwood, J. L.; Thrasher, J. S. *Eur. J. Solid State Inorg. Chem.* **1992**, *29*, 809.
50. Mahjoub, A. R.; Leopold, D.; Seppelt, K. *Z. Anorg. Allg. Chem.* **1992**, *618*, 83.
51. Strauss, S. H. *Chem. Rev.* **1993**, *93*, 927 and references therein.
52. Seppelt, K. *Angew. Chem., Int. Ed. Engl.* **1993**, *32*, 1025.
53. Winter, C. H.; Zhou, X. X.; Heeg, M. J. *Inorg. Chem.* **1992**, *31*, 1808.
54. Winter, C. H.; Zhou, X. X.; Heeg, M. J. *Organometallics* **1991**, *10*, 3799.
55. Hurlburt, P. K.; Anderson, O. P.; Strauss, S. H. *J. Am. Chem. Soc.* **1991**, *113*, 6277.
56. Hurlburt, P. K.; Rack, J. J.; Dec, S. F.; Anderson, O. P.; Strauss, S. H. *Inorg. Chem.* **1993**, *32*, 373.
57. Willner, H.; Aubke, F. *Inorg. Chem.* **1990**, *29*, 2195.

58. Willner, H.; Schaebbs, J.; Hwang, G.; Mistry, F.; Jones, R.; Trotter, J.; Aubke, F. *J. Am. Chem. Soc.* **1992**, *114*, 8972.
59. Strauss, S. H. *Abstracts of Papers*, 206th National Meeting of the American Chemical Society, Chicago, IL; American Chemical Society: Washington, DC, 1992; INOR 233.
60. Watanabe, N.; Nakajima, T.; Touhara, H. *Graphite Fluorides*; Elsevier: New York, 1988.
61. Holloway, J. H.; Hope, E. G.; Taylor, R.; Langley, G. J.; Avent, A. G.; Dennis, T. J.; Hare, J. P.; Kroto, H. W.; Walton, D. R. M. *J. Chem. Soc., Chem. Commun.* **1991**, 966.
62. Selig, H.; Lifshitz, C.; Peres, T.; Fischer, J. E.; McGhie, A. R.; Romanow, W. J.; McCauley, J. P., Jr.; Smith, A. B., III *J. Am. Chem. Soc.* **1991**, *113*, 5475.
63. Tuinman, A. A.; Mukherjee, P.; Adcock, J. L.; Hettich, R. L.; Compton, R. N. *J. Phys. Chem.* **1992**, *96*, 7584.
64. Nakajima, T.; Matsuo, Y. *Carbon*, **1992**, *30*, 1119.
65. Tuinman, A. A.; Gakh, A. A.; Adcock, J. L.; Compton, R. N. *J. Am. Chem. Soc.* **1993**, *115*, 5885.
66. Taylor, R.; Avent, A. G.; Dennis, T. J.; Hare, J. P.; Kroto, H. W.; Walton, D. R. M.; Holloway, J. H.; Hope, E. G.; Langley, G. J. *Nature*, **1992**, *355*, 27.
67. Taylor, R.; Holloway, J. H.; Hope, E. G.; Avent, A. G.; Langley, G. J.; Dennis, T. J.; Hare, J. P.; Kroto, H. W.; Walton, D. R. M.; *J. Chem. Soc., Chem. Commun.* **1992**, 665.
68. Taylor, R.; Avent, A. G.; Birkett, P. R.; Dennis, T. J.; Hare, J. P.; Hitchcock, P. B.; Holloway, J. H.; Hope, E. G.; Kroto, H. W.; Langley, G. J.; Meidine, M. F.; Parsons, J. P.; Walton, D. R. M. *Pure Appl. Chem.* **1993**, *65*, 135.
69. Gakh, A. A.; Tuinman, A. A.; Adcock, J. L.; Compton, R. N. *Tetrahedron Lett.* **1993**, *34*, 7167.
70. Belaish, I.; Entin, I.; Goffer, R.; Davidov, D.; Selig, H.; McCauley, J. P., Jr.; Coustel, N.; Fischer, J. E.; Smith, A. B., III *J. Appl. Phys.* **1992**, 5248.
71. Fagan, P. J.; Krusic, P. J.; McEwen, C. N.; Lazar, J.; Parker, D. H.; Herron, N.; Wasserman, E. *Science* **1993**, *262*, 404.
72. Margrave, J. L.; Bautista, R. G.; Ficalora, P. J.; Badachhape, R. B. U.S. Patent 3 711 595, 1973.
73. Margrave, J. L.; Badachhape, R. B. *Proc. - Electrochem. Soc.* **1984**, *84-5*, 525.
74. Patterson, D. E.; Hauge, R. H.; Margrave, J. L. *Mater. Res. Soc. Symp. Proc.* **1989**, *140*, 351.
75. Gardos, M. N.; Soriano, B. L.; Patterson, D. E.; Hauge, R. H.; Margrave, J. L. *Proc. - Electrochem. Soc.* **1991**, *91-8*, 365.
76. Patterson, D. E.; Hauge, R. H.; Chu, C. J.; Margrave, J. L. World Patent 9 118 128, 1991.
77. Patterson, D. E.; Chu, C. J.; Bai, B. J.; Komplin, N. J.; Hauge, R. H.; Margrave, J. L. *Mater. Sci. Monogr.* **1991**, *73*, 569.
78. Patterson, D. E.; Chu, C. J.; Bai, B. J.; Xiao, Z. L.; Komplin, N. J.; Hauge, R. H.; Margrave, J. L. *Diamond Relat. Mater.* **1992**, *1*, 768.
79. Patterson, D. E.; Hauge, R. H.; Chu, C. J.; Margrave, J. L. World Patent 9 219 791, 1992.

80. Patterson, D. E.; Bai, B. J.; Schmidt, H. K.; Hauge, R. H.; Margrave, J. L. *Abstracts of Papers*, 203rd National Meeting of the American Chemical Society, San Francisco, CA; American Chemical Society: Washington, DC, 1992; FLUO 81.
81. LeBlond, R. D.; DesMarteau, D. D. *J. Chem. Soc., Chem. Commun.* **1974**, 555.
82. Sawyer, J. F.; Schrobilgen, G. J.; Sutherland, S. J. *Inorg. Chem.* **1982**, *21*, 4064.
83. Emara, A. A. A.; Schrobilgen, G. J. *Inorg. Chem.* **1992**, *31*, 1323.
84. Schrobilgen, G. J. In *Synthetic Fluorine Chemistry*; Olah, G. A.; Chambers, R. D.; Prakash, G. K. S., Eds.; John Wiley & Sons: New York, 1992; Chapter 1.
85. MacDougall, P. J.; Schrobilgen, G. J.; Bader, R. F. W. *Inorg. Chem.* **1989**, *28*, 763.
86. Emara, A. A. A.; Schrobilgen, G. J. *J. Chem. Soc., Chem. Commun.* **1988**, 257.
87. Schrobilgen, G. J. *J. Chem. Soc., Chem. Commun.* **1988**, 1506.
88. Emara, A. A. A.; Schrobilgen, G. J. *J. Chem. Soc., Chem. Commun.* **1987**, 1646.
89. Schrobilgen, G. J. *J. Chem. Soc., Chem. Commun.* **1988**, 863.
90. Turbini, L. J.; Aikman, R. E.; Lagow, R. J. *J. Am. Chem. Soc.* **1979**, *101*, 5833.
91. Frohn, H. J.; Jakobs, S. *J. Chem. Soc., Chem. Commun.* **1989**, 625.
92. Naumann, D.; Tyrra, W. *J. Chem. Soc., Chem. Commun.* **1989**, 47.
93. Frohn, H. J.; Jakobs, S.; Henkel, G. *Angew. Chem., Int. Ed. Engl.* **1989**, *28*, 1506.
94. Frohn, H. J.; Jakobs, S.; Rossbach, C. *Eur. J. Solid State Inorg. Chem.* **1992**, *29*, 729.
95. Butler, H.; Naumann, D.; Tyrra, W. *Eur. J. Solid State Inorg. Chem.* **1992**, *29*, 739.
96. Naumann, D.; Butler, H.; Gnann, R.; Tyrra, W. *Inorg. Chem.* **1993**, *32*, 861.
97. Frohn, H. J.; Klose, A.; Henkel, G. *Angew. Chem., Int. Ed. Engl.* **1993**, *32*, 99.
98. Sanders, J. C. P.; Schrobilgen, G. J. *J. Chem. Soc., Chem. Commun.* **1989**, 1576.
99. Smalc, A.; Lutar, K.; Zemva, B.; Kinkead, S. A. *Inorg. Synth.* **1992**, *29*, 11.
100. Lutar, K.; Smalc, A.; Zemva, B.; Kinkead, S. A. *Inorg. Synth.* **1992**, *29*, 4.
101. Smalc, A.; Lutar, K.; Kinkead, S. A. *Inorg. Synth.* **1992**, *29*, 1.
102. Nielsen, J. B.; Kinkead, S. A.; Eller, P. G. *Inorg. Chem.* **1990**, *29*, 3621.
103. Nielsen, J. B.; Kinkead, S. A.; Purson, J. D.; Eller, P. G. *Inorg. Chem.* **1990**, *29*, 1779.
104. Zemva, B.; Lutar, K.; Jesih, A.; Casteel, W. J., Jr.; Wilkinson, A. P.; Cox, D. E.; Von Dreele, R. B.; Borrmann, H.; Bartlett, N. *J. Am. Chem. Soc.* **1991**, *113*, 4192.
105. Zemva, B.; Hagiwara, R.; Casteel, W. J., Jr.; Lutar, K.; Jesih, A.; Bartlett, N. *J. Am. Chem. Soc.* **1990**, *112*, 4846.
106. Zemva, B.; Lutar, K.; Jesih, A.; Casteel, W. J., Jr.; Bartlett, N. *J. Chem. Soc., Chem. Commun.* **1989**, 346.
107. Eller, P. G.; Kinkead, S. A.; Nielsen, J. B. In *Transuranium Element Symposium*; Morss, L. R.; Fuger, J., Eds.; American Chemical Society: Washington, DC, 1992; pp 202-212.

108. Berkowitz, J.; Chupka, W. A. *Chem. Phys. Lett.* **1970**, *7*, 447.
109. Frenking, G.; Koch, W.; Deakyne, C. A.; Liebman, J. F.; Bartlett, N. *J. Am. Chem. Soc.* **1989**, *111*, 31.
110. Miller, P. K.; Abney, K. D.; Rappe, A. K.; Anderson, O. P.; Strauss, S. H. *Inorg. Chem.* **1988**, *27*, 2255.
111. Madappat, K. V.; Sun, J.; Thrasher, J. S.; Xie, Y.; Jin, S.; Colegrove, B. T.; Schaefer, H. F., III *Abstracts of Papers*, 203rd National Meeting of the American Chemical Society, San Francisco, CA; American Chemical Society: Washington, DC, 1992; FLUO 74.
112. Xie, Y.; Schaefer, H. F., III; Thrasher, J. S. *J. Mol. Struct. (Theochem)* **1991**, *234*, 247.
113. Thrasher, J. S.; Madappat, K. V. *Angew. Chem., Int. Ed. Engl.* **1989**, *28*, 1256.
114. Damerius, R.; Seppelt, K.; Thrasher, J. S. *Angew. Chem., Int. Ed. Engl.* **1989**, *28*, 769.
115. Bott, S. G.; Clark, M.; Thrasher, J. S.; Atwood, J. L. *J. Crystallogr. Spectrosc. Res.* **1987**, *17*, 187.
116. Christe, K. O.; Curtis, E. C.; Dixon, D. A. *J. Am. Chem. Soc.* **1993**, *115*, 1520.
117. Christe, K. O.; Dixon, D. A.; Goldberg, I. B.; Schack, C. J.; Walther, B. W.; Wang, J. T.; Williams, F. *J. Am. Chem. Soc.* **1993**, *115*, 1129.
118. Christe, K. O.; Dixon, D. A. *J. Am. Chem. Soc.* **1992**, *114*, 2978.
119. Christe, K. O.; Wilson, R. D.; Wilson, W. W.; Bau, R.; Sukumar, S.; Dixon, D. A. *J. Am. Chem. Soc.* **1991**, *113*, 3795.
120. Christe, K. O.; Wilson, W. W.; Dixon, D. A. *Abstracts of Papers*, American Chemical Society 11th Winter Fluorine Conference, St. Petersburg, FL; American Chemical Society: Washington, DC, 1993; 64.
121. Jacobs, J.; Müller, H. S. P.; Willner, H.; Jacob, E.; Bürger, H. *Inorg. Chem.* **1992**, *31*, 5357.
122. Pierloot, K.; Roos, B. O. *Inorg. Chem.* **1992**, *31*, 5353.
123. Neuhaus, A.; Frenking, G.; Huber, C.; Gauss, J. *Inorg. Chem.* **1992**, *31*, 5355.
124. Hope, E. G.; Levason, W.; Ogden, J. S. *Inorg. Chem.* **1991**, *30*, 4873.
125. Joergenson, C. K. *Eur. J. Solid State Inorg. Chem.* **1991**, *28*, 799.
126. Marsden, C. J.; Wolyneec, P. P. *Inorg. Chem.* **1991**, *30*, 1681.
127. Jacob, E.; Willner, H. *Chem. Ber.* **1990**, *123*, 1319.
128. Paprott, G.; Seppelt, K. *J. Am. Chem. Soc.* **1984**, *106*, 4060.
129. Paprott, G.; Lentz, D.; Seppelt, K. *Chem. Ber.* **1984**, *117*, 1153.
130. Paprott, G.; Lehmann, S.; Seppelt, K. *Chem. Ber.* **1988**, *121*, 727.
131. Curnow, O. J.; Hughes, R. P. *J. Am. Chem. Soc.* **1992**, *114*, 5895.
132. Winter, C. H., personal communication.
133. Winter, C. H.; Han, Y.-H.; Ostrander, R. L.; Rheingold, A. L. *Angew. Chem., Int. Ed. Engl.* **1993**, *32*, 1161.
134. Lentz, D.; Michael, H. *Angew. Chem., Int. Ed. Engl.* **1988**, *27*, 845.
135. Lentz, D.; Preugschat, D. *Angew. Chem., Int. Ed. Engl.* **1990**, *29*, 315.
136. Bürger, H.; Sommer, S. *J. Chem. Soc., Chem. Commun.* **1991**, 456.
137. Lentz, D.; Brüdgam, I.; Hartl, H. *Angew. Chem., Int. Ed. Engl.* **1985**, *24*, 119.
138. Lentz, D.; Michael-Schulz, H. *Inorg. Chem.* **1990**, *29*, 4396.
139. Lentz, D.; Reuter, M. *Z. Anorg. Allg. Chem.* **1992**, *618*, 111.
140. Lentz, D. Michael, H. *J. Organomet. Chem.* **1989**, *372*, 109.

141. Lentz, D. Michael, H. *Angew. Chem., Int. Ed. Engl.* **1989**, *28*, 321.
142. Lentz, D. Michael, H. *Inorg. Chem.* **1989**, *28*, 3396.
143. Lentz, D.; Michael-Schulz, H. *Z. Anorg. Allg. Chem.* **1992**, *614*, 121.
144. Lentz, D.; Michael, H. *Chem. Ber.* **1990**, *123*, 1481.
145. Casarin, M.; Gulino, A.; Lentz, D.; Michael-Schulz, H.; Vittadini, A. *Inorg. Chem.* **1993**, *32*, 1383.
146. Casarin, M.; Ajò, D.; Lentz, D.; Bertoncello, R.; Granozzi, G. *Inorg. Chem.* **1987**, *26*, 465.
147. Crespi, A. M.; Sabat, M.; Shriver, D. F. *Inorg. Chem.* **1988**, *27*, 812.
148. Schulze, W.; Hartl, H.; Seppelt, K. *Angew. Chem., Int. Ed. Engl.* **1986**, *25*, 185.
149. Koola, J. D.; Roddick, D. M. *Organometallics* **1991**, *10*, 591.
150. Brothers, P. J.; Burrell, A. K.; Clark, G. R.; Rickard, C. E. F.; Roper, W. R. *J. Organomet. Chem.* **1990**, *394*, 615.
151. Campen, A. K.; Mahmoud, K. A.; Rest, A. J.; Willis, P. A. *J. Chem. Soc., Dalton Trans.* **1990**, 2817.
152. Burrell, A. K.; Clark, G. R.; Jeffrey, J. G.; Rickard, C. E. F.; Roper, W. R. *J. Organomet. Chem.* **1990**, *388*, 391.
153. Clark, G. R.; Hoskins, S. V.; Jones, T. C.; Roper, W. R. *J. Chem. Soc., Chem. Commun.* **1983**, 719.
154. Clark, G. R.; Hoskins, S. V.; Roper, W. R. *J. Organomet. Chem.* **1982**, *234*, C9.
155. Lentz, D. *Ann. Chim. Fr.* **1984**, *9*, 665 and references therein.
156. Lentz, D.; Graske, K.; Preugschat, D. *Chem. Ber.* **1988**, *121*, 1445.
157. Lentz, D.; Preugschat, D., unpublished results.
158. Lentz, D.; Preugschat, D. *J. Organomet. Chem.* **1992**, *436*, 185.
159. Lentz, D.; Preugschat, D. *J. Chem. Soc., Chem. Commun.* **1992**, 1523.
160. Krüger, M.; Dreizler, H.; Preugschat, D.; Lentz, D. *Angew. Chem., Int. Ed. Engl.* **1991**, *30*, 1644.
161. King, R. B. *Acc. Chem. Res.* **1980**, *13*, 243.
162. Nixon, J. F. *Endeavour* **1973**, *32*, 19.
163. Nixon, J. F. *Adv. Inorg. Chem. Radiochem.* **1970**, *13*, 363.
164. Grobe, J.; Le Van, D.; Meyring, W. *Z. Anorg. Allg. Chem.* **1990**, *586*, 149.
165. O'Brien, B. A., personal communication.
166. Grobe, J.; Lange, G.; Le Van, D. *J. Organomet. Chem.* **1990**, *399*, 189.
167. Grobe, J.; Le Van, D.; Schulze, J.; Szameitat, J. *Phosphorus Sulfur* **1986**, *28*, 239.
168. Grobe, J.; Le Van, D.; Nientiedt, J.; Krebs, B.; Dartmann, M. *Chem. Ber.* **1988**, *121*, 655.
169. Chamberlain, B. M.; O'Brien, B. A. *Abstracts of Papers*, 206th National Meeting of the American Chemical Society, Chicago, IL; American Chemical Society: Washington, DC, 1993; FLUO 15.
170. Meyer, T. J.; Jones, P. G.; Schmutzler, R. *Z. Naturforsch.* **1993**, *48b*, 875.
171. Schnabel, R. C.; Roddick, D. M. *Inorg. Chem.* **1993**, *32*, 1513.
172. Schnabel, R. C.; Roddick, D. M. *Organometallics* **1993**, *12*, 704.
173. Koola, J. D.; Roddick, D. M. *J. Am. Chem. Soc.* **1991**, *113*, 1450.
174. Ernst, M. F.; Roddick, D. M. *Organometallics* **1990**, *9*, 1586.

175. Ebsworth, E. A. V.; Robertson, N.; Yellowlees, L. J. *J. Chem. Soc., Dalton Trans.* **1993**, 1031.
176. Blake, A. J.; Cockman, R. W.; Ebsworth, E. A. V.; Holloway, J. H. *J. Chem. Soc., Chem. Commun.* **1988**, 529.
177. Ebsworth, E. A. V.; Holloway, J. H.; Watson, P. G. *J. Chem. Soc., Chem. Commun.* **1991**, 1443.
178. Cockman, R. W.; Ebsworth, E. A. V.; Holloway, J. H. *J. Am. Chem. Soc.* **1987**, *109*, 2194.
179. Toscano, P. J.; Brand, H.; Geremia, S.; Randaccio, L.; Zangrando, E. *Organometallics* **1991**, *10*, 713.
180. Toscano, P. J.; Brand, H.; Liu, S.; Zubieta, J. *Inorg. Chem.* **1990**, *29*, 2101.
181. Toscano, P. J.; Konieczny, L.; Liu, S.; Zubieta, J. *Inorg. Chem. Acta* **1989**, *166*, 163.
182. Toscano, P. J.; Barren, E. *J. Chem. Soc., Chem. Commun.* **1989**, 1159.
183. MacNicol, D. D.; Robertson, C. D. *Nature* **1988**, *332*, 59.
184. Weydert, M.; Andersen, R. A.; Bergman, R. G. *J. Am. Chem. Soc.* **1993**, *115*, 8837 and references therein.
185. Harrison, R. G.; Richmond, T. G. *J. Am. Chem. Soc.* **1993**, *115*, 5303 and references therein.
186. Catalá, R.-M.; Cruz-Garriz, D.; Sosa, P.; Terreros, P.; Torrens, H.; Hills, A.; Hughes, D. L.; Richards, R. L. *J. Organomet. Chem.* **1989**, *359*, 219.
187. Kulawiec, R. J.; Holt, E. M.; Lavin, M.; Crabtree, R. H. *Inorg. Chem.* **1987**, *26*, 2559.
188. Uson, R.; Forniés, J.; Tomás, M.; Cotton, F. A.; Falvello, L. R. *J. Am. Chem. Soc.* **1984**, *106*, 2482.
189. Haas, A. *Pure Appl. Chem.* **1991**, *63*, 1577.
190. Haas, A. *Kontakte* **1988**, 3.
191. Haas, A. *Adv. Inorg. Chem. Radiochem.* **1984**, *28*, 167.
192. Haas, A. *Chem.-Ztg.* **1982**, *106*, 239.
193. Representative example: Huang, H. N.; Lagow, R. J.; Roesky, H. W. *Inorg. Chem.* **1991**, *30*, 789.
194. Representative example: Seppelt, K. *Angew. Chem., Int. Ed. Engl.* **1991**, *30*, 361 and references therein.
195. Representative example: O'Brien, B. O.; DesMarteau, D. D. *Inorg. Chem.* **1984**, *23*, 2188.
196. Representative example: Meier, T.; Hoppenheit, R.; Mews, R. *Z. Anorg. Allg. Chem.* **1993**, *619*, 1241.
197. Representative example: Heilemann, W.; Mews, R. *Eur. J. Solid State Inorg. Chem.* **1992**, *29*, 799.
198. Glemser, O.; Mews, R. *Angew. Chem., Int. Ed. Engl.* **1980**, *19*, 883.
199. Representative example: Sandhu, A.; Gard, G. L.; Patel, N. R.; Kirchmeier, R. L.; Shreeve, J. M. *Inorg. Chem.* **1993**, *32*, 3205.
200. Representative example: John, E. O.; Mack, H. G.; Oberhammer, H.; Kirchmeier, R. L.; Shreeve, J. M. *Inorg. Chem.* **1993**, *32*, 287.
201. Kirchmeier, R. L.; Shreeve, J. M.; Verma, R. D. *Coord. Chem. Rev.* **1992**, *112*, 169.

202. Shreeve, J. M. In *Sulfur Org. Inorg. Chem.*; Senning, A., Ed.; Dekker: New York, 1982; Vol. 4., pp 131-191.
203. Shreeve, J. M. *Isr. J. Chem.* **1978**, *17*, 1.
204. Representative example: Nielsen, J. B.; Thrasher, J. S. *J. Fluorine Chem.* **1990**, *48*, 407.
205. Representative example: Thrasher, J. S.; Madappat, K. V. *Angew. Chem., Int. Ed. Engl.* **1989**, *28*, 1256.
206. Representative example: Thrasher, J. S.; Nielsen, J. B.; Bott, S. G.; McClure, D. J.; Morris, S. A.; Atwood, J. L. *Inorg. Chem.* **1988**, *27*, 570.
207. Edelmann, F. T. *Comments Inorg. Chem.* **1992**, *12*, 259.
208. Appelman, E. H.; Jache, A. W. *J. Am. Chem. Soc.* **1993**, *115*, 1376.
209. Appelman, E. H.; French, D.; Mishani, E.; Rozen, S. *J. Am. Chem. Soc.* **1993**, *115*, 1379
210. Appelman, E. H.; Mendelsohn, M. H.; Kim, H. *J. Am. Chem. Soc.* **1985**, *107*, 6515.
211. Ruscic, B.; Appelman, E. H.; Berkowitz, J. *J. Chem. Phys.* **1991**, *95*, 7957.
212. Kol, M.; Rozen, S.; Appelman, E. *J. Am. Chem. Soc.* **1991**, *113*, 2648.
213. Appleby, A. J.; Velez, O. A.; LeHelloco, J. G.; Parthasarthy, A.; Srinivasan, S. DesMarteau, D. D.; Gillette, M. S.; Ghosh, J. K. *J. Electrochem. Soc.* **1993**, *140*, 109.
214. Singh, S.; DesMarteau, D. D. *Inorg. Chem.* **1990**, *29*, 2982.
215. Razaq, M.; Razaq, A.; Yeager, E.; DesMarteau, D. D.; Singh, S. *J. Electrochem. Soc.* **1989**, *136*, 385.
216. Razaq, M.; Razaq, A.; Yeager, E.; DesMarteau, D. D.; Singh, S. *J. Appl. Electrochem.* **1987**, *17*, 1057.
217. Klapötke, T. M. In *The Chemistry of Inorganic Ring Systems*; Steudel, R., Ed.; Elsevier: New York, 1992; Chapter 20.
218. Passmore, J. In *The Chemistry of Inorganic Ring Systems*; Steudel, R., Ed.; Elsevier: New York, 1992; Chapter 19.
219. Burford, N.; Passmore, J.; Sanders, J. C. P. In *From Atoms to Polymers: Isoelectronic Analogies*; Liebman, J. F.; Greenberg, A., Eds.; VCH: New York, 1989; Chapter 2.

Inorganic Fluorine Chemistry Monographs and Reviews

220. Strauss, S. H., "The Search for Larger and More Weakly Coordinating Anions," *Chem. Rev.* **1993**, *93*, 927.
221. Seppelt, K., "Noncoordinating' Anions, II," *Angew. Chem., Int. Ed. Engl.* **1993**, *32*, 1025.
222. Various authors, "Fluorine Compounds, Inorganic," *Kirk-Othmer Encycl. Chem. Technol.*, 4th Ed., Volume X, **1993**.
223. Milicev, S., "Vibrational Spectroscopy of Inorganic Coordination Compounds of Fluorine," *Croat. Chem. Acta* **1992**, *65*, 125.
224. Witt, M.; Roesky, H. W., "Sterically Demanding Fluorinated Substituents and Metal Fluorides with Bulky Ligands," *Prog. Inorg. Chem.* **1992**, *40*, 353.

225. Schrobilgen, G. J., "Lewis Acid Properties of Fluorinated Noble Gas Cations," In *Synthetic Fluorine Chemistry*; Olah, G. A.; Chambers, R. D.; Prakash, G. K. S., Eds.; Wiley: New York, **1992**; p 1.
226. Christe, K. O.; Wilson, W. W.; Schack, C. J., "Controlled Replacement of Fluorine by Oxygen in Fluorides and Oxyfluorides," In *Synthetic Fluorine Chemistry*; Olah, G. A.; Chambers, R. D.; Prakash, G. K. S., Eds.; Wiley: New York, **1992**; p 31.
227. Aubke, F.; Cader, M. S. R.; Mistry, F., "Transition Metal Derivatives of Strong Protonic Acids and Superacids," In *Synthetic Fluorine Chemistry*; Olah, G. A.; Chambers, R. D.; Prakash, G. K. S., Eds.; Wiley: New York, **1992**; p 43.
228. Seppelt, K., "Fluorine Stabilized Carbon-Sulfur Multiple Bonding," In *Synthetic Fluorine Chemistry*; Olah, G. A.; Chambers, R. D.; Prakash, G. K. S., Eds.; Wiley: New York, **1992**; p 87.
229. Rozen, S., "Electrophilic Fluorination Reactions with Fluorine and Some Reagents Directly Derived From It," In *Synthetic Fluorine Chemistry*; Olah, G. A.; Chambers, R. D.; Prakash, G. K. S., Eds.; Wiley: New York, **1992**; p 143.
230. Burton, D. J., "Organometallics in Synthetic Organofluorine Chemistry," In *Synthetic Fluorine Chemistry*; Olah, G. A.; Chambers, R. D.; Prakash, G. K. S., Eds.; Wiley: New York, **1992**; p 205.
231. Piraux, L.; Amine, K.; Bayot, V.; Issi, J. P.; Di Vittorio, S. L.; Dresselhaus, M. S.; Tressaud, A.; Mayorga, S. F.; Endo, M.; Nakajima, T., "2D Electronic Transport in Fluorine and Transition Metal Fluoride GICs," *Mater. Sci. Forum* **1992**, 91-93, 481.
232. Ma, T. P., "Metal-Oxide-Semiconductor Gate Oxide Reliability and the Role of Fluorine," *J. Vac. Sci. Technol.* **1992**, 10, 705.
233. Lerner, M.; Hagiwara, R.; Bartlett, N., "Synthesis of Main-Group Graphite Fluoroanion Salts with Chlorine-Assisted Oxidation by Lewis-Acid Fluorides," *J. Fluorine Chem.* **1992**, 57, 1.
234. Kirchmeier, R. L.; Shreeve, J. M.; Verma, R. D., "Fluorinated Compounds That Contain Catenated Oxygen, Sulfur or Nitrogen Atoms," *Coord. Chem. Rev.* **1992**, 112, 169.
235. Poulain, M., "Compositional Dependence of Physical Properties in Fluoride Glasses," In *Phys. Non-Cryst. Solids*; Pye, L., D.; La Course, W. C.; Stevens, H. J., Eds.; Taylor & Francis: London, UK, **1992**; 167.
236. Seppelt, K., "Structure, Color, and Chemistry of Pentaaryl Bismuth Compounds," *Adv. Organomet. Chem.* **1992**, 34, 207.
237. Edelmann, F. T., "The 2,4,6-Tris(Trifluoromethyl)Phenyl Substituent: An Ideal," *Comments Inorg. Chem.* **1992**, 12, 259.
238. Seppelt, K., "Is There a Naked Fluoride Ion?," *Angew. Chem., Int. Ed. Engl.* **1992**, 31, 292.
239. Passmore, J., "Homopolyatomic Selenium Cations and Related Halopolyselenium Cations," In *The Chemistry of Inorganic Ring Systems*; Steudel, R., Ed.; Elsevier: New York, **1992**; p 373.
240. Klapötke, T. M., "Binary Selenium-Nitrogen Species and Related Compounds," In *The Chemistry of Inorganic Ring Systems*; Steudel, R., Ed.; Elsevier: New York, **1992**; p 409.

241. Seppelt, K., "Coordination Numbers Larger Than Six Among Electronegative Elements," *Comments Inorg. Chem.* **1991**, *12*, 199.
242. Seppelt, K., "Fluorine-Stabilized Sulfur-Carbon Multiple Bonds," *Angew. Chem., Int. Ed. Engl.* **1991**, *30*, 361.
243. Touhara, H.; Okino, F.; Suganuma, S., "Synthesis, Properties, and Functions of Graphite-Fluorine Intercalation Compounds," *Kino Zairyo* **1991**, *11*, 18.
244. Touhara, H.; Suganuma, S.; Okino, F., "Lithium Batteries with Fluorine-Graphite Intercalation Compound Cathodes. Post-Graphite Fluoride Cathode," *Tanso* **1991**, *150*, 328.
245. Thomas, M. J. K., "Fluorine, Chlorine, Bromine, Iodine and Noble Gases," *Annu. Rep. Prog. Chem.* **1991**, *86*, 49.
246. Nakajima, T., "Graphite Intercalation Compounds as Highly Conductive Materials and Battery Materials," *Nyu Seramikkusu* **1991**, *4*, 71.
247. Takeuchi, Y., "Development of Fluorine-Containing Synthetic Blocks," *Farumashia* **1991**, *27*, 1036.
248. Harris, R. K.; Jackson, P., "High-Resolution Fluorine-19 Magnetic Resonance of Solids," *Chem. Rev.* **1991**, *91*, 1427.
249. Nakajima, T., "Fluorine-Graphite Intercalation Compounds. Their Synthesis, Structures, and Physical and Chemical Properties," *Tanso*, **1990**, *145*, 295.
250. Devilliers, D.; Groult, H.; Vogler, M., "Elementary Fluorine in Inorganic Synthesis," *Actual. Chim.* **1990**, *2*, 81.
251. Bartlett, N.; Okino, F.; Mallouk, T. E.; Hagiwara, R.; Lerner, M.; Rosenthal, G. L.; Kourtakis, K., "Oxidative Intercalation of Graphite by Fluoroanionic Species. Evidence for Thermodynamic Barrier," *Adv. Chem. Ser.* **1990**, *226*, 391.
252. Hughes, R. P., "Organo-Transition Metal Compounds Containing Perfluorinated Ligands," *Adv. Organomet. Chem.* **1990**, *31*, 183.
253. Klimov, V. D., "Structural Features of Inorganic Fluorides," *Zh. Neorg. Khim.* **1990**, *35*, 2758.
254. Emeleus, H. J.; Shreeve, J. M.; Verma, R. D., "The Nitrogen Fluorides and Some Related Compounds," *Adv. Inorg. Chem.* **1989**, *33*, 139.
255. Burford, N.; Passmore, J.; Sanders, J. C. P., "The Preparation, Structure, and Energetics of the Homopolyatomic Cations of Group 16 (the Chalcogens) and 17 (the Halogens)," In *From Atoms to Polymers: Isoelectronic Analogies*; Liebman, J. F.; Greenberg, A., Eds.; VCH: New York, **1989**; p 53.
256. Watanabe, N.; Nakajima, T.; Touhara, H. *Graphite Fluorides*; Elsevier: New York, **1988**.
257. Bartlett, N., "Valency in the Periodic Table - Concerning the Limits of Oxidation of the Elements," *Proc. Robert A. Welch Found. Conf. Chem. Res.* **1988**, *32*, 258.
258. Zemva, B., "Binary Fluorides of Noble-Gases and Their Compounds," *Croat. Chem. Acta* **1988**, *61*, 163.
259. Oberhammer, H., "Fluorine Derivatives," *Methods Stereochem. Anal.* **1988**, *10*, 147.
260. Burton, D. J., "Stereospecific Preparation, Reactivity, and Utility of Polyfluorinated Alkenyl," In *Fluorine-Containing Molecules: Structure,*

- Reactivity, Synthesis, and Applications*; Liebman, J. F.; Greenberg, A.; Dolbier, W. R., Jr., Eds.; VCH: New York, **1988**; p 149.
261. Jache, A. W., "The Inorganic Chemistry of Hydrogen Fluoride," In *Fluorine-Containing Molecules: Structure, Reactivity, Synthesis, and Applications*; Liebman, J. F.; Greenberg, A.; Dolbier, W. R., Jr., Eds.; VCH: New York, **1988**; p 165.
262. Peters, N. J. S.; Allen, L. C., "Structure and Bonding in N, O, F Compounds," In *Fluorine-Containing Molecules: Structure, Reactivity, Synthesis, and Applications*; Liebman, J. F.; Greenberg, A.; Dolbier, W. R., Jr., Eds.; VCH: New York, **1988**; 199.
263. Seppelt, K., "Sulfur/Carbon Double and Triple Bonds," *Pure Appl. Chem.* **1987**, *59*, 1057.
264. Glemser, O., "Inorganic Fluorine Chemistry, 1900 - 1945," In *Fluorine: The First Hundreded Years (1886-1986)*; Banks, R. E.; Sharp, D. W. A.; Tatlow, J. C., Eds.; Elsevier: New York, **1986**; p 45. See also Glemser, O. *J. Fluorine Chem.* **1986**, *33*, 45.
265. Holloway, J. H., "Noble Gas Fluorides," In *Fluorine: The First Hundreded Years (1886-1986)*; Banks, R. E.; Sharp, D. W. A.; Tatlow, J. C., Eds.; Elsevier: New York, **1986**; p 149. See also Holloway, J. H. *J. Fluorine Chem.* **1986**, *33*, 149.
266. Winfield, J. M., "Transition Metal Fluorides," In *Fluorine: The First Hundreded Years (1886-1986)*; Banks, R. E.; Sharp, D. W. A.; Tatlow, J. C., Eds.; Elsevier: New York, **1986**; p 159. See also Winfield, J. M. *J. Fluorine Chem.* **1986**, *33*, 149.
267. Shreeve, J. M., "Recent Advances in Main-Group Fluoride Chemistry," In *Fluorine: The First Hundreded Years (1886-1986)*; Banks, R. E.; Sharp, D. W. A.; Tatlow, J. C., Eds.; Elsevier: New York, **1986**; p 179. See also Shreeve, J. M. *J. Fluorine Chem.* **1986**, *33*, 179.
268. Meshri, D. T., "The Modern Inorganic Fluorochemical Industry," In *Fluorine: The First Hundreded Years (1886-1986)*; Banks, R. E.; Sharp, D. W. A.; Tatlow, J. C., Eds.; Elsevier: New York, **1986**; p 195. See also Meshri, D. T. *J. Fluorine Chem.* **1986**, *33*, 195.
269. Lagow, R. J., "High-Yield Reactions of Elemental Fluorine," In *Fluorine: The First Hundreded Years (1886-1986)*; Banks, R. E.; Sharp, D. W. A.; Tatlow, J. C., Eds.; Elsevier: New York, **1986**; p 321. See also Lagow, R. J. *J. Fluorine Chem.* **1986**, *33*, 321.
270. Seppelt, K., "The Nature of Sulfur-Carbon Double and Triple Bonds," *Nova Acta Leopold.* **1985**, *59*, 247.
271. Hagenmuller, P., "General Trends," In *Inorganic Solid Fluorides: Chemistry and Physics*; Hagenmuller, P., Ed.; Academic: Orlando, FL, **1985**; p 1.
272. Grannec, J.; Lozano, L., "Preparative Methods," In *Inorganic Solid Fluorides: Chemistry and Physics*; Hagenmuller, P., Ed.; Academic: Orlando, FL, **1985**; p 17.
273. Hoppe, R., "High Oxidation States in Fluorine Chemistry," In *Inorganic Solid Fluorides: Chemistry and Physics*; Hagenmuller, P., Ed.; Academic: Orlando, FL, **1985**; p 275.

274. Watanabe, N.; Touhara, H.; Nakajima, T.; Bartlett, N.; Mallouk, T.; Selig, H., "Fluorine Intercalation Compounds of Graphite," In *Inorganic Solid Fluorides: Chemistry and Physics*; Hagenmuller, P., Ed.; Academic: Orlando, FL, **1985**; p 331.
275. Cochet-Muchy, B.; Portier, J. "Industrial Uses of Inorganic Fluorides," In *Inorganic Solid Fluorides: Chemistry and Physics*; Hagenmuller, P., Ed.; Academic: Orlando, FL, **1985**; p 565.
276. Shurin, I. V., "Superionic Conductors. Anomalous High Ionic Conductivity in Inorganic Fluorides. Problem of Superionic Conductivity," *Izv. Sib. Otd. Akad. Nauk SSSR, Ser. Khim. Nauk* **1984**, *1*, 53.
277. Rakov, E. G. and Yagodin, G. A., "Problems of the Chemistry of Inorganic Fluorides," *Zh. Neorg. Khim.* **1984**, *29*, 489.
278. Haas, A., "The Element Displacement Principle: A New Guide in P-Block Element Chemistry," *Adv. Inorg. Chem. Radiochem.* **1984**, *28*, 167.
279. Winfield, J. M., "Acetonitrile, A Convenient Solvent for Inorganic Fluorides," *J. Fluorine Chem.* **1984**, *25*, 91.
280. Holloway, J. H. and Laycock, D., "Preparations and Reactions of Inorganic Main-Group Oxide Fluorides," *Adv. Inorg. Chem. Radiochem.* **1983**, *27*, 157.
281. Shreeve, J. M., "Fluorinated Hypofluorites and Hypochlorites," *Adv. Inorg. Chem. Radiochem.* **1983**, *26*, 119.
282. Flamm, D. L.; Ibbotson, D. E.; Mucha, J. A.; Donnelly, V. M., "Xenon Difluoride and Fluorine Atom Reactions with Silicon: Their Significance for Plasma Etching," *Solid State Technol.* **1983**, *26*, 117.
283. Margrave, J. L.; Hauge, R. H.; Ismail, Z. K.; Fredin, L.; Billups, W. E., "Synthetic Inorganic Chemistry in Low-Temperature Matrixes," *ACS Symp. Ser.*, **1983**, *211*, 329.
284. Seppelt, K., "Stabilization of Unusual Oxidation and Coordination States by the Ligands OSF₅, OSeF₅, and OTeF₅," *Angew. Chem., Int. Ed. Engl.* **1982**, *21*, 877.
285. Shreeve, J. M., "The Sulfur-Fluorine Bond," *Sulfur Org. Inorg. Chem.* **1982**, *4*, 131.
286. Seppelt, K.; Lentz, D., "Novel Developments in Noble Gas Chemistry," *Prog. Inorg. Chem.* **1982**, *29*, 167.
287. Hoppe, R., "Recent Progress in Oxo- and Fluorometalate Chemistry," *Angew. Chem., Int. Ed. Engl.* **1981**, *93*, 64.
288. Tressaud, A., "Chemistry and Physics of Solid Inorganic Fluorides," *Yoyuen* **1981**, *24*, 141.
289. Woolf, A. A., "Thermochemistry of Inorganic Fluorine Compounds," *Adv. Inorg. Chem. Radiochem.* **1981**, *24*, 1.
290. Engelbrecht, A.; Sladky, F., "Selenium and Tellurium Fluorides," *Adv. Inorg. Chem. Radiochem.* **1981**, *24*, 189.
291. Clark, H. C., "An Organometallic Journey From Fluorine to Platinum," *J. Organomet. Chem.* **1980**, *200*, 63.
292. Winfield, J. M., "Preparation and Use of 18-Fluorine Labeled Inorganic Compounds," *J. Fluorine Chem.* **1980**, *16*, 1.

293. Glemser, O. and Mews, R., "Chemistry of Thiazyl Fluoride (NSF) and Thiazyl Trifluoride (NSF₃): A Quarter of a Century of Sulfur-Nitrogen-Fluorine Chemistry," *Angew. Chem., Int. Ed. Engl.* **1980**, *19*, 883.
294. Lagow, R. J.; Margrave, J. L., "Direct Fluorination: A New Approach to Fluorine Chemistry," *Prog. Inorg. Chem.* **1979**, *26*, 161.
295. Seppelt, K., "Recent Developments in the Chemistry of Some Electronegative Elements," *Acc. Chem. Res.* **1979**, *12*, 211.
296. Seppelt, K., "Structural Chemistry of Fluorides and Oxide Fluorides of Nonmetals" *Angew. Chem., Int. Ed. Engl.* **1979**, *18*, 186.
297. Appelman, E. H. and Clyne, M. A. A., "Elementary Reaction Kinetics of Fluorine Atoms, FO, and NF Free Radicals," In ACS Symposium Series 66; American Chemical Society: Washington, DC, **1978**; p 3.
298. Morton, J. R.; Preston, K. F., "ESR Spectra and Structure of Inorganic Fluorine-Containing Free Radicals," In ACS Symposium Series 66; American Chemical Society: Washington, DC, **1978**; p 386.
299. Shreeve, J. M., "Tri- and Tetracoordinate Fluorosulfur(IV) and Pentacoordinate Fluorosulfur(VI) Compounds," *Isr. J. Chem.* **1978**, *17*, 1.
300. Aubke, F.; DesMarteau, D. D., "Halogen Derivatives of Group VIA Oxyacids," *Fluorine Chem. Rev.* **1977**, *8*, 73.
301. Fielding, H. C.; Lee, B. E., "Hydrofluoric Acid, Inorganic Fluorides and Fluorine," *Spec. Publ. - Chem. Soc.* **1977**, *31*, 149.
302. Wechsberg, M.; Schabacher, W.; Nieder, H.; Schneider, S.; Beyl, V., "Fluorine and Inorganic Fluorine Compounds," *Ullmanns Encykl. Tech. Chem.* **1976**, *11*, 587.
303. Shreeve, J. M., "Fluorinated Peroxides," *Endeavour* **1976**, *35*, 79.
304. Christe, K. O. and Schack, C. J., "Chlorine Oxyfluorides," *Adv. Inorg. Chem. Radiochem.* **1976**, *18*, 319.
305. Mews, R., "Nitrogen-Sulfur-Fluorine Ions," *Adv. Inorg. Chem. Radiochem.* **1976**, *19*, 185.
306. Zingaro, R. A., "Reactions in Inorganic Solvents," *Tech. Chem.* **1976**, *8*, 235.
307. Haas, A.; Niemann, U., "Preparation and Reactions of Perfluorohaloorganosulphenyl Halides," *Adv. Inorg. Chem. Radiochem.* **1976**, *18*, 143.
308. Haas, A., "New Developments in Perfluoroorganoselenium Chemistry," *Chem. Scr.* **1975**, *8A*, 75.
309. Makeev, G. N.; Sokolov, V. B.; Chaivanov, B. B., "*Khim. Plazmy* **1975**, *2*, 62.
310. Ikrami, D. D.; Dadabaeva, G.; Okhunov, R., "Solubility and Interaction of Inorganic Fluorides in Hydrogen Fluoride," *Izv. Akad. Nauk Tadzh. SSR, Otd. Fiz.-Mat. Geol.-Khim. Nauk* **1975**, *3*, 130.
311. Augustyn, W.; Grobelny, M.; Chmiel-Pela, J.; Rozycka, D., "New Technological Procedures in the Production of Inorganic Fluorine Compounds," *Chem. Prum.* **1974**, *24*, 57.
312. Yagupol'skii, L. M.; Il'chenko, A. Y.; Kondratenki, N. V., "Electronic Nature of Fluorine-Containing Substituents," *Usp. Khim.* **1974**, *43*, 64.
313. De Marco, R. A.; Shreeve, J. M., "Fluorinated Peroxides," *Adv. Inorg. Chem. Radiochem.* **1974**, *16*, 109.

314. Lustig, M.; Shreeve, J. M., "Fluoroxyfluoroalkanes and Perfluoroacyl and Inorganic Hypofluorites," *Advan. Fluorine Chem.* **1973**, *7*, 175.
315. Shreeve, J. M., "Precursors and Derivatives of Bis(Perfluoroalkyl) Sulfoxides," *Acc. Chem. Res.* **1973**, *6*, 387.
316. Reynolds, D. J., "Vibrational Spectra of Inorganic Fluorides," *Advan. Fluorine Chem.* **1973**, *7*, 1.
317. Ohno, H.; Furukawa, K., "Phase Diagrams and Data for Liquid Metals and Inorganic Molten Salts. Alkali Metal Tetrafluoroborates," *Nucl. Sci. Abstr.* **1973**, *28*, 17945.
318. Emeleus, H. J., "Sulfur-Nitrogen Compounds," *Endeavour* **1973**, *32*, 76.
319. Rowland, F. S.; Cramer, J. A.; Iyer, R. S.; Milstein, R.; Williams, R. L., "Chemical Reactions of Atomic Fluorine Atoms, as Studied with Tracer Fluorine-18," *Nippon Aisotopu Kaigi Hobunshu* **1973**, *11*, 360.
320. Emeleus, H. J., "Recent Advances in Fluorine Chemistry," *Ind. Chim. Belge* **1972**, *37*, 317.
321. Bartlett, N., "Noble-Gas Compounds," *Endeavour* **1972**, *31*, 107.
322. Glemser, O.; Mews, R., "Sulfur-Nitrogen-Fluorine Compounds," *Adv. Inorg. Chem. Radiochem.* **1972**, *14*, 333.
323. Haas, A.; Hinsch, W., "Fluorochloroalkanesulfenyl Chlorides and Pseudohalides. Starting Materials for the Synthesis of New Fluorinated Substances," *Chem.-Ztg.* **1972**, *96*, 75.
324. Nikolaev, N. S.; Buslaev, Y. A.; Ippolitov, E. G.; Alenchikova, I., "Physicochemical Analysis in the Study of Inorganic Fluorides," In Zhavoronkov, N. M. "Nauka": *Issled. Teor. Prikl. Neorg. Khim.* **1971**, *322*, Moscow, USSR.
325. Rigny, P., "NMR of Inorganic Solids: Applications to Some Solid Fluorides," *Semin. Chim. Etat Solide* **1971**, *4*, 33.
326. Cady, G. H., "Fluorides and Oxofluorides of Sulfur," *Intra-Sci. Chem. Rep.* **1971**, *5*, 1.
327. Von Halasz, S. P.; Glemser, O., "Sulfur-Fluorine Bond," In *Sulfur Org. Inorg. Chem.*; Senning, A., Ed.; Dekker: New York, **1971**; p 209.
328. Glemser, O. M., "Sulfur-Nitrogen-Halogen Compounds," *Int. J. Sulfur Chem.* **1971**, *6*, 35.
329. Kidd, R. G., "Nuclear-Magnetic-Resonance Spectroscopy of Organometallic Compounds," *Character. Organometal. Compounds* **1971**, *26*, 373.
330. Hoppe, R., "Metal Binary and Ternary Fluorides and Oxides," *20 [Zwanzig] Jahre Fonds Chem. Ind., Beitr. Wiss. Verantst.* **1970**, *15*.
331. Batty, W. E., "Inorganic High Energy Oxidizers," *Chem. Ind.* **1969**, *35*, 1231.
332. Fild, M.; Glemser, O., "Phosphorus, Arsenic, and Antimony Pentafluorophenyl Compounds," *Fluorine Chem. Rev.* **1969**, *3*, 129.
333. Glemser, O., "Developments in the Chemistry of Sulfur-Nitrogen-Fluorine Compounds," *Endeavour* **1969**, *28*, 86.
334. Malm, J. G.; Appelman, E. H., "Chemical Compounds of Xenon and Other Noble Gases," *At. Energy Rev.* **1969**, *7*, 3.
335. Haas, A., "Fluorine, An Element With Many Possibilities," *Chem. Unserer. Zeit.* **1969**, *3*, 17.

336. Haas, A., "Perfluoropseudohalides and the Chemistry of Chlorofluoromethyl-sulphenyl Compounds," In *New Pathways Inorg. Chem.*; Ebsworth, E. A. V., Ed.; University Press: Cambridge, England, **1968**; p 87.
337. Pankratov, A. V., "Chemistry of Inorganic Nitrogen Fluorides," *Izv. Sib. Otd. Akad. Nauk SSSR, Ser. Khim. Nauk* **1968**, *1*, 61.
338. Bartlett, N., "The Oxidizing Properties of the Third Transition Series Hexafluorides and Related Compounds," *Angew. Chem. Int. Ed. Engl.* **1968**, *7*, 433.
339. Emeleus, H. J., "Advances in the Field of Fluorinated Inorganic Radicals," *Allg. Prakt. Chem.* **1968**, *19*, 1.
340. Lawless, E. W.; Rowatt, R. J., "Review of Advanced Inorganic Oxidizers," *Amer. Chem. Soc.* **1968**, *12*, 108.
341. Lawless, E. W.; Smith, I. C. *Inorganic High-Energy Oxidizers: Synthesis, Structure, and Properties*; Marcel Dekker: New York, **1968**.
342. Mooney, E. F.; Winson, P. H., "Fluorine-19 Nuclear Magnetic Resonance Spectroscopy," *Annu. Rev. NMR (Nucl. Magn. Resonance) Spectrosc.* **1968**, *1*, 243.
343. Kwasnik, W., "Advances in Fluorine Preparation and Electrochemical Fluorination of Inorganic Compounds," *Fortschr. Chem. Forsch.* **1967**, *8*, 309.
344. Glemser, O.; Fild, M., "Sulfur-Nitrogen-Halogen Compounds," *Halogen Chem.* **1967**, *2*, 1.
345. Mueller, R., "Organofluorosilicates and Their Application to the Synthesis of Organometallic Compounds," *Organomet. Chem. Rev.* **1966**, *1*, 359.
346. Holloway, J. H., "Reactions of the Noble Gases," *Prog. Inorg. Chem.* **1964**, *6*, 241.

RECEIVED January 6, 1994

Chapter 2

Thermodynamic Aspects of the Remarkable Oxidizing Capabilities of Fluorine–Lewis-Fluoroacid Mixtures

Ciping Shen, Rika Hagiwara, Thomas E. Mallouk, and Neil Bartlett¹

Chemical Sciences Division, Lawrence Berkeley Laboratory,
and Department of Chemistry, University of California,
Berkeley, CA 94720

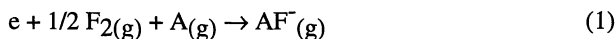
Xenon and F₂, in liquid AsF₅, at -60°C interact rapidly even in the dark to yield XeF⁺AsF₆⁻. The same reaction, substituting O₂ for Xe, does not proceed to O₂⁺AsF₆⁻. This difference is attributed to the formation of a (Xe-F)⁺ bond in a concerted Xe → F - F - AsF₅ interaction which simultaneously undoes the F-F bonding, and makes a F-As bond, in a heterolytic cleavage, there being no comparable energetic counterpart of the Xe-F bonding in the O₂/F₂/AsF₅ interaction. Even the modest fluoroacid, HF, brings about combination of Xe with F₂ in the dark (at 20°C) to form XeF₂. Evaluation of fluoride-ion affinities and lattice energies gives quantitative measure of F₂-fluoroacid oxidizing effects. Enthalpy and entropy evaluations account for instability of O₂⁺BF₄⁻ and O₂⁺PF₆⁻ and the thermodynamic stability of O₂⁺AsF₆⁻ and XeF⁺AsF₆⁻ at 20°C.

The (Ar-F)⁺ species is known to be well bound (1, 2). Salts of such a cation would be oxidizing reagents of unprecedented power. But can such salts be made? To explore the practicalities of this problem, it is instructive to examine the features that provide for the stabilization of salts containing the O₂⁺ and XeF⁺ cations.

Seel and Detmer were the first to show (3) that 1:1 adducts of SF₄, SeF₄ and TeF₄ with the Lewis acids BF₃, AsF₅ and SbF₅, described by Bartlett and Robinson (4), were fluoroonium salts (SF₃⁺ etc). Indeed Seel and Detmer (3) also gave convincing vibrational spectroscopic evidence to show that AsF₅ had the capability of removing F⁻ from the highest valence iodine fluoride, IF₇, to yield the remarkable cation IF₆⁺. In so doing, they gave the first clear evidence of the highly energetic F⁻ acceptor capability of these Lewis acids. Cotton (5) and his coworkers determined the enthalpy change $\Delta H^\circ(\text{F}^-(\text{g}) + \text{BF}_3(\text{g}) \rightarrow \text{BF}_4^-(\text{g}))$ to be -91 kcal mol⁻¹ and more recently Bartlett and his coworkers (6) were able to confirm that value and also assess the F⁻ affinities of PF₅, GeF₄ and (roughly) AsF₅. Because of the low enthalpy of

¹Corresponding author

dissociation (7) of F_2 ($37.72 \text{ kcal mol}^{-1}$) and the high electron affinity of the F atom (8) ($78.38 \text{ kcal mol}^{-1}$), the electron affinities, E, for the overall process:



exceed that for the fluoride affinity, FA, defined as $-\Delta H^\circ (F^-(g) + A(g) \rightarrow AF^-(g))$ by 60 kcal mol^{-1} , giving (9) E values for (1), where $A = BF_3, GeF_4$ and AsF_5 of 152, 161 and $>171 \text{ kcal mol}^{-1}$ respectively. These electron affinities are to be compared with that of the powerfully oxidizing hexafluoride (10) PtF_6 , where E is $\approx 184 \text{ kcal mol}^{-1}$. This, alone, indicates extraordinary oxidizing power for the F_2/A combinations but, for a more quantitative assessment of that power, lattice energy and entropy change evaluations need to be made for each salt contemplated.

There are many observations that indicate the extraordinary oxidizing power of Lewis acid-elemental fluorine combinations, perhaps the most dramatic early examples being the synthesis of $O_2^+AsF_6^-$ from $O_2/F_2/AsF_5$ mixtures both thermally (11), by Beal, Pupp and White and photochemically (12) by Shamir and Binnenboym. Another was the observation by Stein (13), that fluorine in combination with liquid SbF_5 was able to oxidize xenon at room temperature.

In this study, it is shown that F_2 , in combination even with the relatively weak fluoroacid (6, 14) HF, is capable of oxidizing xenon at room temperature in the absence of light or other excitation, to XeF_2 . The powerful fluoroacid AsF_5 , as the liquid, in combination with F_2 at -60°C , oxidizes xenon rapidly to yield the previously known salt (15) $XeF^+AsF_6^-$. On the other hand, the salt $O_2^+AsF_6^-$, which is also thermodynamically stable (11), is not formed from mixtures of O_2, F_2 and liquid AsF_5 in the absence of light or thermal activation. Thermodynamic and mechanistic aspects of such reactions as these are discussed, and a more quantitative assessment of the oxidizing power of fluorine with fluoroacid mixtures is made to compare these systems to the more powerfully oxidizing hexafluorides such as PtF_6 .

Experimental

Reagents. Anhydrous HF (AHF) (98%, Matheson, Newark, CA) was treated with K_2NiF_6 (Ozark-Mahoning-Pennwalt, Tulsa, OK). F_2 (Matheson, Newark, CA) was used as received. BF_3 (Matheson, Newark, CA) and AsF_5 (Ozark-Mahoning-Pennwalt, Tulsa, OK) were checked by IR spectroscopy, and were used as received. When AsF_5 was used in glass reactors, it was passed through a column of NaF to ensure its freedom from HF. Xenon and krypton (Aircro, Riverton, NJ) were used as received. O_2 was passed slowly through a copper coil cooled down to -78°C to remove any moisture. IF_5 (Matheson, Newark, CA) was treated with F_2 at low temperature and then evacuated briefly under vacuum.

Reactors. Pyrex reactors were made by joining a heavy-walled Pyrex vessel to a greaseless J. Young glass valve provided with Teflon O-rings. The Pyrex reactors were flame-dried under a vacuum of 10^{-7} torr. The reactors were made of $1/2$ " diameter

fluorinated ethylene propylene (FEP) tubing (AIN plastics, Berkeley, CA) joined to a Teflon valve.

Reactions. Except for the first, all of the following reactions were carried out in the dark. Reactions at low temperatures were cooled by an acetone bath with its temperature regulated by dry ice.

X-ray Powder Diffraction. Photographs were taken on products in quartz capillaries using Debye-Scherrer cameras.

A mixture of **Xe**, **AsF₅**, and **F₂** (50.4 torr, 51.7 torr, and 101.8 torr, respectively) in a Pyrex reactor (1 liter) was exposed to sunlight for ~12 hrs. The glass wall of the reactor was quickly coated with a finely divided white powder which was collected with a Teflon-coated magnet. It was shown (15) by X-ray powder diffraction and Raman spectroscopy to be $\text{XeF}^+\text{AsF}_6^-$. Yield: 0.4053 g, 1.19 mmole, ~43%.

Xe, **AsF₅**, and **F₂** (each 3.5 mmole) were condensed into the Pyrex reactor (25 ml). The mixture was warmed to 20 °C to a total pressure of ~10 atm. After ~24 hrs no solid product was observable. When this same reactor and its contents were cooled to -60 °C (**AsF₅** now liquid) rapid reaction to produce **XeFAsF₆**, as described next, occurred.

AsF₅ (14 mmole), **Xe** (1.42 mmole), and **F₂** (2.13 mmole) in a heavy-walled Pyrex reactor (25 ml) at -60°C (liquid **AsF₅** was ~1 ml) was stirred vigorously. The liquid **AsF₅** rapidly became opalescent and a white granular precipitate formed within 2 to 3 min. After 12 hrs a bulky greenish-white solid lay in the liquid **AsF₅**. Volatiles were removed, and the solid was shown (15) by Raman spectroscopy and X-ray powder diffraction to be **XeFAsF₆**. Yield: 0.377 g, 1.11 mmole, ~78%.

WF₆ (2 ml), **AsF₅** (0.64 mmole), **Xe** (0.71 mmole) and **F₂** (0.75 mmole) were condensed into the Pyrex reactor (25 ml). The reactor was shaken mechanically at 20 °C for 2 days. Large white crystals were formed on the glass wall. The unreacted volatiles were removed under vacuum, and the crystals vacuum-dried at -15 °C (10^{-3} torr). The crystals had a pale green tinge, and were shown (15) by Raman spectroscopy to be **XeFAsF₆**. Yield: 0.1177 g, 0.347 mmole, ~54%.

WF₆ (2 ml) and **Xe** (0.69 mmole) and **F₂** (0.71 mmole) in a Pyrex reactor (25 ml) were shaken mechanically at 20 °C for 2 days. No solid product was formed.

AHF (2 ml), **Xe** (0.58 mmole), **AsF₅** (0.71 mmole), and **F₂** (0.90 mmole) in a FEP reactor (35 ml) at 20 °C were shaken for 24 hrs. The removal of volatiles at -20 °C left a greenish tinged white solid, which Raman spectroscopy and X-ray powder diffraction showed (15) to be only **XeFAsF₆**. Yield: 0.1144 g, 0.337 mmole, ~58%.

F₂ (0.51 mmole), **Xe** (0.51 mmole), **BF₃** (1.02 mmole) and **AHF** (2 ml) in a FEP reactor (38 ml) were shaken mechanically for 24 hrs. As the last of the solvent was removed at -30°C, an orange-red solid separated. When all the liquid had been removed, the reactor was cooled to ~-35°C and evacuated for another 1½ hrs. A white solid remained which Raman spectroscopy proved (16) to be **XeF₂** (identified by its

strong Raman band at 495 cm^{-1}). Yield: 0.029 g, 0.17 mmole, ~33%. The evanescent orange-red species was not identified.

A mixture of F_2 (1.65 mmole) and Xe (1.26 mmole) and AHF (2 ml) in a FEP reactor (42 ml) was vigorously stirred with a Teflon-coated magnet at $20\text{ }^\circ\text{C}$ for 12 hrs. Removal of volatiles at $-30\text{ }^\circ\text{C}$ left a white solid which Raman spectroscopy proved (16) to be XeF_2 (identified by its strong Raman band at 495 cm^{-1}). Yield: 0.134 g, 0.792 mmole, ~63%.

WF_6 (2 ml) and AsF_5 (0.64 mmole), O_2 (0.82 mmole) and F_2 (0.43 mmole) in a Pyrex reactor (25 ml) was shaken mechanically at $20\text{ }^\circ\text{C}$ for 2 days. No solid was produced.

AsF_5 in AHF with O_2 and F_2 . A $\frac{1}{2}$ " diam. T-shaped FEP reactor (30 ml) with a Teflon-coated magnetic stirring bar in the main tube was used. AsF_5 (1 ml) and HF (2 ml) in the main tube were exposed to a mixture of O_2 and F_2 in 10:7 ratio to a total pressure of ~2.5 atm (O_2 ~1.8 mmole and F_2 ~1.3 mmole). The mixture was kept at $-78\text{ }^\circ\text{C}$ and stirred vigorously for $2\frac{1}{2}$ days. The pressure did not change and no solid formed.

AsF_5 (0.35 ml), O_2 (2.69 mmole), and F_2 (1.46 mmole) in a heavy-walled Pyrex reactor (13 ml) were maintained at $-60\text{ }^\circ\text{C}$ to $-80\text{ }^\circ\text{C}$ with vigorous shaking for one week. No solid product was formed.

IF_5 , AsF_5 , with F_2 in absence of light. A mixture of IF_5 (14.4 mmole, 1 ml), AsF_5 (1.52 mmole), and F_2 (1.87 mmole) in a FEP reactor (45 ml) was vigorously stirred at $20\text{ }^\circ\text{C}$ for 12 hrs. No solid formed in the liquid IF_5 . Removal of volatiles at $20\text{ }^\circ\text{C}$ gave a white solid shown by X-ray powder diffraction (17, 18) to be $\text{IF}_6^+\text{AsF}_6^-$. Yield: 0.074 g, 0.172 mmole, ~11%. That this was a product of the separate reaction of IF_5 and F_2 to form IF_7 was indicated by the following experiments: IF_5 (14.4 mmole, 1 ml) and F_2 (1.87 mmole) were agitated in a FEP reactor as in the earlier experiment. After 12 hrs, F_2 was removed at $-196\text{ }^\circ\text{C}$. The characteristic bands of IF_7 at 748, 676, 426 and 365 cm^{-1} were very prominent in the IR spectrum (19, 20) of the resulting product. In a separate reaction, IF_5 (1.44 mmole, 1 ml) and F_2 (1.87 mmole) were first allowed to react for 12 hrs, F_2 was removed at $-196\text{ }^\circ\text{C}$, and AsF_5 (1.52 mmole) was added and the mixture was stirred for several hours. Removal of volatiles gave a yield similar to that of the first experiment. Yield: 0.0812 g, 0.189 mmole, ~12%.

Kr , F_2 and A (A = liquid AsF_5 , AsF_5 in AHF , or SbF_5 in AHF). Attempts to prepare KrF^+ and Kr_2F_3^+ salts at low temperatures, using the conditions effective in fixing Xe , failed.

NF_3 , F_2 and liquid AsF_5 . Attempts to prepare $\text{NF}_4^+\text{AsF}_6^-$ salt, from NF_3 , F_2 and liquid AsF_5 , at $-65\text{ }^\circ\text{C}$, using the conditions effective in fixing Xe , failed.

Results and Discussion

The spontaneous oxidation of xenon by fluorine in the presence of a Lewis acid fluoride, A , was observed to occur only in the liquid phase. There was no interaction between Xe , F_2 and AsF_5 (strongest A) in the gas phase, in the dark, at $20\text{ }^\circ\text{C}$ at a total pressure of 10 atmospheres, over one day. When this mixture was cooled to $-60\text{ }^\circ\text{C}$

interaction to produce $\text{XeF}^+\text{AsF}_6^-$ occurred rapidly. But Xe did not interact with F_2 in solution in WF_6 (weak A). Spontaneous oxidation of O_2 , which has the same ionization potential as Xe (12.13 eV for each) (21), to yield O_2^+ salts was never observed even with $\text{A} = \text{AsF}_5$. Yet, the effective synthesis of $\text{O}_2^+\text{AsF}_6^-$ by Beal *et al* (11) gives clear indication that this O_2^+ salt is thermodynamically stable.

There were other instances of the powerfully oxidizing F_2/A mixtures failing to bring about thermodynamically allowed oxidations. Thus IF_5 with AsF_5/F_2 did not yield $\text{IF}_6^+\text{AsF}_6^-$ in the dark at room, or lower temperatures. Yet IF_7 was produced slowly from the interaction of IF_5 with F_2 alone, under similar conditions. This failure to efficiently make $\text{IF}_6^+\text{AsF}_6^-$ can be attributed to a strong donor-acceptor interaction between the Lewis base, IF_5 , and the AsF_5 . Under such circumstances the F_2 cannot itself act as a donor to the acid and so serves as the acceptor to the base. This suggests that the donor, D, must not be greatly superior to F_2 , as a Lewis base, if spontaneous oxidation of D is to occur.

Why a modest fluoroacid (6, 14) such as HF is able to promote oxidation of Xe, whereas even the potent acid AsF_5 fails to bring about spontaneous oxidation of O_2 , requires a more detailed analysis of the thermodynamic features of the system.

Impact of Size on Lattice Enthalpy. The conventional formulae for lattice energy evaluation (22, 23) express that energy as inversely proportional to the sum of the ionic radii of the system. There are, however, difficulties in arriving at acceptable radii, and this is especially so when the cation is a complex cation, of low symmetry. We have avoided this difficulty by replacing the sum of the cationic and anionic radii with the cube root of the formula unit volume (FUV), as in earlier studies (6). Figure 1 shows lattice enthalpies calculated by the simple Kapustinskii formula (22) (filled circles) as a function of the reciprocal of the cube root of the observed FUV. Open circle lattice enthalpies are those derived by detailed evaluation using the method described by Bertot (24), as modified by Templeton (25). Differences between the Kapustinskii or Bertot/Templeton values, and those given by the best straight line relationship for all of the data, are usually within the uncertainties occurring even in the best lattice energy evaluations (6). These are all close packed solids, and at least for these unit-charged salts, D^+X^- , it appears that the lattice enthalpy is given, to within $\pm 5 \text{ kcal mol}^{-1}$, by the relationship previously given (6):

$$U(\text{kcal mol}^{-1}) = 556.3(\text{FUV})^{-1/3} (\text{\AA}^{-1}) + 26.3$$

The smaller fluoroborate ion confers more favorable lattice energy than a hexafluorometallate ion, MF_6^- . The difference in FUV, is typically about 30\AA^3 (e.g. the unit cell volumes (26) of KBF_4 and KPF_6 (cubic) are 83.4 and 114.6\AA^3 , respectively). This gives lattice enthalpies $\text{KBF}_4 = 153.6 \text{ kcal mol}^{-1}$ and $\text{KPF}_6 = 140.8 \text{ kcal mol}^{-1}$. This means that, for cations of about the size of K^+ , each additional F ligand in the anion is disadvantageous by about 6 kcal mol^{-1} . In the case of BF_4^- compared with PF_6^- , this lattice energy advantage, of the former anion, almost matches and cancels the effect of the difference in the fluoride affinities of BF_3 and PF_5 (92 and $101 \text{ kcal mol}^{-1}$ respectively (6)). Because the isomorphous rhombohedral salts $\text{O}_2^+\text{PtF}_6^-$ and KPtF_6 have nearly the same volume (27), the lattice energies (and

the cation volumes), must be nearly the same. Since the unit cell of $\text{O}_2^+\text{PF}_6^-$ is not known, FUV of this salt is taken to be the same as that of KPF_6 , i.e. the lattice energy of $\text{O}_2^+\text{PF}_6^-$ is taken to be $-141 \text{ kcal mol}^{-1}$. For $\text{O}_2^+\text{BF}_4^-$ (FUV = 86.2 \AA^3) the lattice energy is $-152 \text{ kcal mol}^{-1}$.

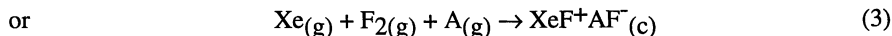
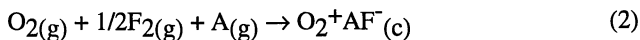
Since HF_2^- and other hydrofluoride anions must be small they can provide higher Coulomb energy than fluoroborate. In such cases, however, the fluoride affinity of A is far less (14) than in the BF_3 case (5, 6). One must conclude that the favorable impact of the small anion size, as well as the Xe-F⁺ bond formation (see below), provides the driving force for XeF_2 formation from Xe, F_2 and HF via some $\text{XeF}^+\text{F}(\text{HF})_x^-$ intermediate.

Since hexafluorometallates of a given cation are all much closer in FUV than are BF_4^- and PF_6^- salts (e.g. the FUV of cubic KPF_6 = 114.6 \AA^3 and that of rhombohedral KAsF_6 = 114.9 \AA^3), lattice energies do not change greatly with change in MF_6^- . For such MF_6^- salts, differences in the enthalpies of dissociation, with change in A, $\Delta H^\circ(\text{D}^+\text{AF}^-(\text{c}) \rightarrow \text{DF}(\text{g}) + \text{A}(\text{g}))$ must therefore depend primarily on the fluoride-ion affinity of A. Since the F^- affinity of AsF_5 exceeds that (6) of PF_5 by at least 10 kcal mol^{-1} the enthalpy of formation of an AsF_6^- salt, of a given cation, must exceed that of the PF_6^- salt by approximately that amount. In general, the better the F^- affinity of A, the more likely is AF^- to stabilize high oxidation states.

The High F^- Affinity of AsF_5 and SbF_5 . The group number oxidation states of the elements succeeding the first transition series (particularly As(V), Se(VI) and Br(VII)) are difficult to generate, even with potent oxidizers (28). This is a consequence of the high effective nuclear charge build-up accompanying the filling of the $3d$ sub-shell. The F^- affinity of AsF_5 exceeds that of PF_5 by at least 10 kcal mol^{-1} because of this greater effective nuclear charge at the As atom. Since SbF_6^- salts of cations, such as KrF^+ , are more thermally stable (29) than their AsF_6^- relatives, it appears that the F^- affinity of SbF_5 , perhaps for reasons related to those given for AsF_5 , is even higher. Possibly, in BiF_5 , we will have the highest F^- affinity of all, since here the effective nuclear charge, at the Bi atom, should also be enhanced because of the $4f$ filled sub-shell effect. The MF_6^- increases modestly in size (30), with increase in the mass of M. Lattice energies of the MF_6^- salts of a common cation, since they depend upon the cube root of the inverse of the volume, decrease only slightly with increase in the mass of M.

Because of their large F^- affinities, the heavier group V pentafluorides do appear, therefore, to be particularly effective in providing favorable enthalpies of formation for salts D^+AF^- . But, to assess the thermodynamic stabilities of such salts, it is also necessary to estimate entropy changes.

Estimating Entropy. The standard entropies of many known simple gaseous species have been evaluated (7), so in the processes



the evaluation of ΔS° depends on the determination of the standard entropy for the salts $O_2^+AF^-(c)$ or $XeF^+AF^-(c)$.

From experimental data in which ΔS° for processes $DF(g) + A(g) \rightarrow D^+AF^-(c)$ have been derived from dissociation pressure dependence upon temperature (van't Hoff relation) the standard entropy for salts $D^+AF^-(c)$ have been evaluated. Table I contains data from these investigations, which are also pertinent to Figure 2. Standard entropies (7), for a wide variety of these and other salts (all of which are close-packed solids), show a linear dependence on volume, as illustrated in Figure 2. As may be seen, the linear relationship does satisfy the expectation that S° should become zero at zero volume. The standard entropy for a close-packed salt D^+AF^- is therefore assumed, from this experience, to be determined by its FUV, the numerical relationship being:

$$S^\circ (\text{cal deg}^{-1} \text{mol}^{-1}) = 0.42 \times \text{FUV} (\text{\AA}^3)$$

For the process represented in equation (2), since the FUV for $O_2^+BF_4^-$ and $O_2^+AsF_6^-$ are, respectively, 86.2 and 131.9\AA^3 , the S° values are 36 and 55 $\text{cal deg}^{-1} \text{mol}^{-1}$, respectively. This yields, for equation (2), ΔS° for $A = AsF_5$ and BF_3 respectively -96 and -98 $\text{cal deg}^{-1} \text{mol}^{-1}$. For $A = PF_5$, $\Delta S^\circ \approx -97 \text{ cal deg}^{-1} \text{mol}^{-1}$. It is probably much the same for any other gaseous acid fluoride, A. A general value for ΔS° of $\sim -97 \text{ cal deg}^{-1} \text{mol}^{-1}$ may be used; this, for the most part, expressing the loss of translational freedom for the two and a half molecules on the left hand side of equation (2).

From this it appears likely that changing A in either (2) or (3) is not likely to have a large impact on the $T\Delta S$ term for either reaction. If so, the change in ΔG° for either reaction (2) or (3), associated with change in fluoroacid A will be determined primarily by change in the enthalpy. However, reaction (3) is slightly more unfavorable entropically than reaction (2).

Physical Properties of $O_2^+AF^-$ Salts. The physical properties of the $O_2^+AF^-(c)$ salts $A = BF_3$, PF_5 and AsF_5 fit the expectations based on these simple thermodynamic evaluations. At least the relative stabilities of the salts are accounted for. Because of inherent imprecision (particularly in lattice energy evaluation (6)), the ΔG° values for process (2) and (3) are not accurate to more than $\pm 5 \text{ kcal mol}^{-1}$. As we have already seen the lattice enthalpy advantage of about 11 kcal mol^{-1} for $O_2^+BF_4^-$ over $O_2^+PF_6^-$ approximately balances the difference in the F^- affinities of PF_5 and BF_3 . The thermodynamic stability of $O_2^+BF_4^-$ should only be slightly better than $O_2^+PF_6^-$.

$O_2^+PF_6^-$ is reported (38) to decompose slowly at -80°C and rapidly at room temperature. $O_2^+BF_4^-$ is described (39) as decomposing at a moderate rate at 0°C . Clearly both are thermodynamically unstable. The evaluation for $O_2^+BF_4^-(c)$ shows why. For reaction (2), ΔH° is $-23 \text{ kcal mol}^{-1}$ (see Figure 3) and $\Delta S^\circ = -98 \text{ cal deg}^{-1} \text{mol}^{-1}$, from which at 0°C , $-T\Delta S \approx +27 \text{ kcal mol}^{-1}$, from which $\Delta G \approx +4 \text{ kcal mol}^{-1}$. For comparison of BF_4^- with PF_6^- salts of cations similar in size to K^+ (as O_2^+ salts

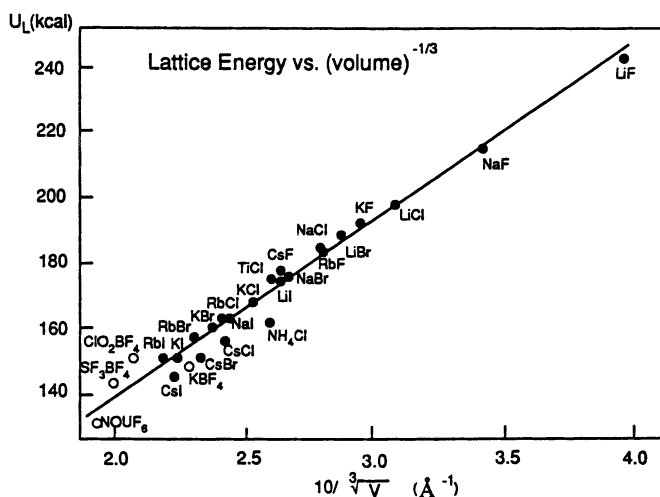


Figure 1. Correlation of lattice energy for A^+B^- salts with formula unit volume.

Table I. Entropy evaluations^a for dissociable fluoro-complexes

	S°_{298K}	S°_{298K}	S°_{298K}	ΔS	Ref.	FUV (\AA^3)	Ref.
	DF	+ A	\rightarrow D ⁺ AF _(c)				
(SF ₃) ₂ GeF ₆	2SF ₄ 144	GeF ₄ 72	(SF ₃) ₂ GeF ₆ (91)	-125	6	219.7	6
SF ₃ PF ₆	SF ₄ 72	PF ₅ 72	SF ₃ PF ₆ (69)	-75	31	161.8	31
SF ₃ BF ₄	SF ₄ 72	BF ₃ 61	SF ₃ BF ₄ (60.5)	-72.5	4	123.9	32
ClO ₂ GeF ₅	ClO ₂ F 67	GeF ₄ 72	ClO ₂ GeF ₅ (49)	-90	33, 6	123.4	34
ClO ₂ PF ₆	ClO ₂ F 67	PF ₅ 72	ClO ₂ PF ₆ (64)	-75	31	142.8	31
ClO ₂ BF ₄	ClO ₂ F 67	BF ₃ 61	ClO ₂ BF ₄ (55)	-73	33, 35	112.9	6

^aThe entropies of the salts (in parentheses) were calculated from the entropies of the reactants and the entropy change of the reaction.

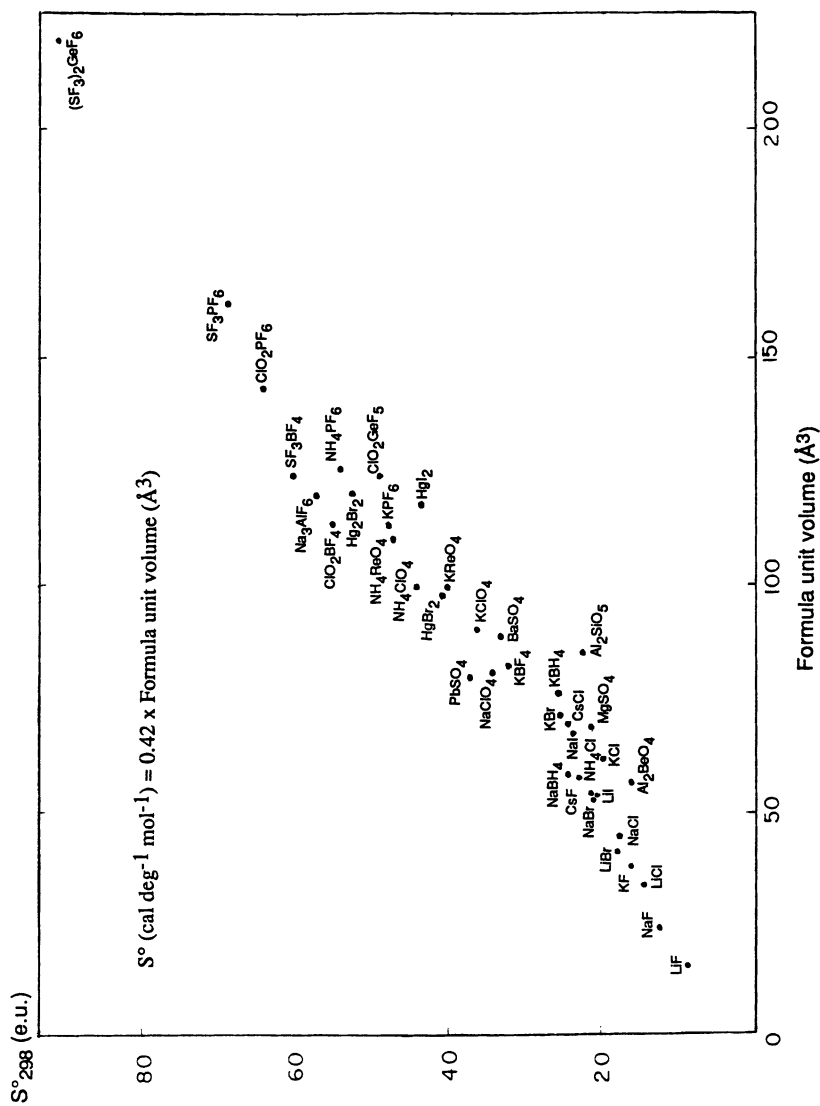
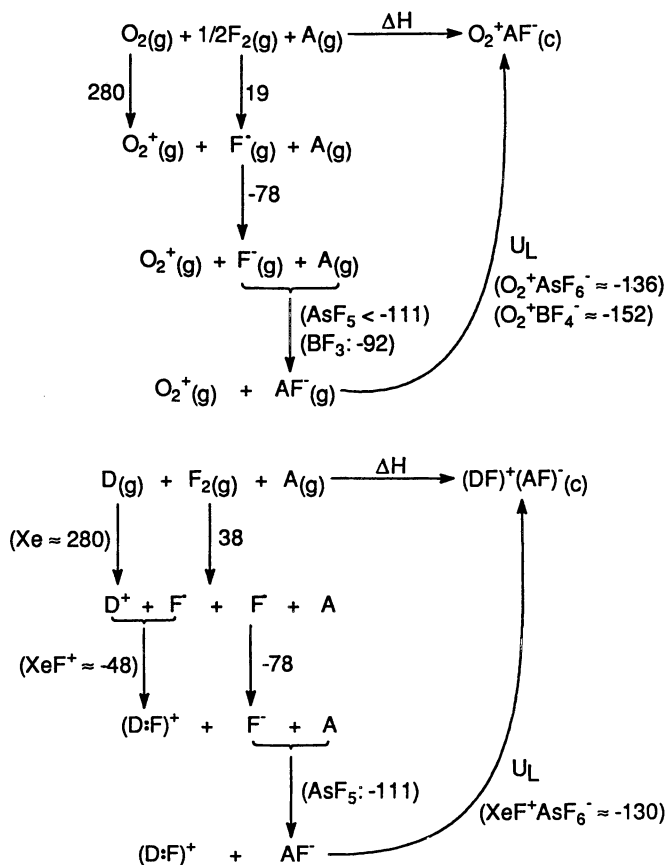


Figure 2. Correlation of S°_{298} with the formula unit volumes of the solids.

Figure 3. Thermochemical cycles for O_2^+AF^- and DF^+AF^- salts.

are), the enthalpy change disadvantage of 2 kcal mol^{-1} of the PF_6^- salts for reaction (2) leads to an estimated ΔG (at 0°C) for $\text{O}_2^+\text{PF}_6^-$ of $\sim +6 \text{ kcal mol}^{-1}$ (assuming $-\text{T}\Delta\text{S} \approx 27 \text{ kcal mol}^{-1}$ for each case).

Because the F^- affinity of AsF_5 is at least 10 kcal mol^{-1} higher than that of PF_5 , and could be 15 kcal mol^{-1} higher (40), we expect ΔG° for the process (2) to be that much more advantageous for the AsF_6^- salt than for the PF_6^- case (see Figure 3). From FUV of $\text{O}_2^+\text{AsF}_6^-$ the lattice energy $\approx -26 \text{ kcal mol}^{-1}$. For reaction (2) $-\text{T}\Delta\text{S}$ term at 0°C is $\approx +26 \text{ kcal mol}^{-1}$, whence $\Delta G \approx 0$. Because the fluoride affinity of AsF_5 is probably undervalued, ΔG would be negative by the amount of that undervaluation. $\text{O}_2^+\text{AsF}_6^-$ is therefore anticipated to be thermodynamically stable at ordinary temperatures. That is consistent with its synthesis (11) from F_2 , O_2 , AsF_5 mixtures under pressure at 200°C . That it does not form spontaneously from a $\text{O}_2/\text{F}_2/\text{AsF}_5$ mixture, whereas $\text{XeF}^+\text{AsF}_6^-$ does do so from a $\text{Xe}/\text{F}_2/\text{AsF}_5$ mixture, may be associated with differing mechanistic features of the reactions.

Comparison of $\text{O}_2^+\text{AsF}_6^-$ and $\text{XeF}^+\text{AsF}_6^-$. Figure 3 represents the thermodynamic steps for this comparison. As a consequence of its larger cation size (15), $\text{XeF}^+\text{AsF}_6^-$ (FUV = 156.2 \AA^3) has a smaller lattice energy than $\text{O}_2^+\text{AsF}_6^-$ (FUV = 131.9 \AA^3). The lattice energies calculated simply from the volume formula are 130 and $136 \text{ kcal mol}^{-1}$, respectively. The bonding (41) of Xe^+ with F ($\geq 48 \text{ kcal mol}^{-1}$) more than compensates for the additional F-F bond dissociation energy (7) (which is only 19 kcal mol^{-1} for the $\text{O}_2^+\text{AsF}_6^-$ salt, but 38 kcal mol^{-1} for $\text{XeF}^+\text{AsF}_6^-$) and also more than compensates for the inferior lattice energy of the latter. The entropy changes for the XeF^+AF^- salt syntheses are, however, slightly less favorable than for their O_2^+AF^- relatives {reaction (3) versus reaction (2)}. For the O_2^+AF^- salt formation, expressed in equation (2), the representative ΔS° value as we have seen is $\approx -97 \text{ cal deg}^{-1} \text{ mol}^{-1}$. For the comparable XeF^+AF^- salt {equation (3)} ΔS° is $\approx -101 \text{ cal deg}^{-1} \text{ mol}^{-1}$, hence the $\text{T}\Delta\text{S}^\circ$ term at 298K is $-30 \text{ kcal mol}^{-1}$ for $\text{XeF}^+\text{AsF}_6^-$ and $-29 \text{ kcal mol}^{-1}$ for O_2AsF_6^- . The observed thermodynamic stability of each AsF_6^- salt, at ordinary temperatures, requires that the sum of (a) the high ionization energy needed to produce each cation, (b) the energy required to split the F_2 molecule, and (c) the achievement of the entropy diminution, is more than provided for by the lattice energy, the electron affinity of $\text{F}(\text{g})$ and the F^- affinity of A.

From Figure 3, we see that the $(\text{XeF})^+$ bonding energy gives a decisive thermodynamic advantage to the oxidation of xenon, relative to O_2 , in spite of the lattice energy disadvantage of the $(\text{XeF})^+$ salts. This signifies a standard free energy of formation advantage of $\approx -23 \text{ kcal mol}^{-1}$ for any XeF^+ salt in comparison with its O_2^+ relative.

There is a further practical advantage to the XeF^+ salt syntheses, which derives from the greater solubility of Xe (a soft atom) over O_2 (a hard molecule) in the HF solvent. This immediately enhances the thermodynamic activity of the Xe over O_2 in any equilibria.

The $-60\text{ }^{\circ}\text{C}$ reaction temperature (since kT is only $0.42\text{ kcal mol}^{-1}$) indicates that the reaction $\text{Xe} + \text{F}_2 + \text{AsF}_5 \rightarrow \text{XeF}^+\text{AsF}_6^-$ occurs without a sizable barrier. This may not be so in the O_2^+ case.

Concerning the Pathway for the $\text{Xe}/\text{F}_2/\text{A}$ and the $\text{O}_2/\text{F}_2/\text{A}$ Reactions. The failure of $\text{O}_2\text{F}^+\text{AF}^-$ salts to be formed in the interaction (38) of O_2F_2 and A, already suggests that the cation O_2F^+ is not an energetically favorable entity. Indeed the formation of a sigma bond between the electron rich F atom and O_2^+ would bring the π electrons of the former into antibonding influence in the O_2^+ . Any strong sigma bonding of F to O_2^+ would therefore be offset, at least partially, by antibonding effects in the O_2^+ . This accounts for the long, weak bond (probably a single-electron bond) between O_2 and each F ligand, apparent in O_2F_2 , where the interatomic distance (42) O-F is $1.575 \pm 0.003\text{ \AA}$. That long O-F bond contrasts with that (43) of OF_2 (electron pair bonded), where O-F = $1.4053 \pm 0.0004\text{ \AA}$. The similarity of the O-O bond in O_2F_2 with that in O_2 itself (44) (O-O distance in $\text{O}_2\text{F}_2 = 1.217 \pm 0.003\text{ \AA}$; O-O in $\text{O}_2 = 1.20741 \pm 0.00002\text{ \AA}$) indicates minimal π^* effect of the long-bonded F ligands on the O-O bonding in the O_2F_2 molecule. The 48 kcal bonding energy (41) advantage of F atom with Xe^+ is therefore unlikely to have a counterpart in the F + O_2^+ interaction. The ready formation of XeF^+ and the failure to form an analogous strong O-F bond in O_2F^+ must have an important impact on the way the $\text{D} + \text{F}_2 + \text{A}$ reactions proceed.

The $\text{Xe} + \text{F}_2 + \text{A}$ reactions may be perceived as proceeding by a three body interaction. This is consistent with the rapid interactions observed in the condensed phase and the failure of such reactions in the gas phase (at modest pressures).

An F_2 molecule sigma bonded (albeit weakly) to A will be more likely to receive an electron pair from the donor (D) into the σ^* LUMO of F_2 . Such an event leads to the loss of F-F bonding and, in effect, an F^+ is transferred to D (this differs from the thermodynamic convention of considering F atom with D^+ as in our thermodynamic cycles, but does not change the outcome). Clearly, for the xenon case, this process can smoothly occur, to generate XeF^+AF^- , but if the O_2 is unable to make an effective bond to F^+ (which is essentially the same as the $\text{O}_2^+ + \text{F}$ atom situation), as seems likely, then the breaking of the F-F linkage poses a sizable activation energy barrier. This may be the reason why thermodynamically stable $\text{O}_2^+\text{AsF}_6^-$ does not form from $\text{O}_2 + \text{F}_2 + \text{AsF}_5$ without activation.

Prospects for ArF^+ Salts. Here we shall ignore questions of synthetic strategies attendant upon the nonexistence of a bound ArF_2 molecule (10) and concentrate solely on the thermodynamic features. As we have seen, the bonding of the noble-gas species, G^+ , to F^{\bullet} provides important energy to the benefit of $(\text{GF})^+\text{AF}^-$ salt formation. The greatest difficulty springs from the electron affinity of the $(\text{Ar-F})^+$. Since Ar-F radical is not bound, but $(\text{Ar-F})^+$ is bound (with respect to ground-state Ar^+ and F^{\bullet} species) by $\sim 50\text{ kcal mol}^{-1}$, the electron affinity of the cation is the ionization enthalpy (7) of Ar (365 kcal mol^{-1}) less this bond energy, i.e. 315 kcal mol^{-1} . The best anion to stabilize this cation is likely to be a hexafluorometallate

MF_6^- , for which the lattice energy for $\text{ArF}^+\text{MF}_6^-$ will be between the values for $\text{O}_2^+\text{AsF}_6^-$ and $\text{XeF}^+\text{AsF}_6^-$. Optimistically, it could be $-136 \text{ kcal mol}^{-1}$.

Since the entropy change, for equation (3), is again likely to be $\approx -101 \text{ cal deg}^{-1} \text{ mol}^{-1}$ (as in the $\text{XeF}^+\text{AsF}_6^-$ case), the $-\Delta S$ term is $\approx +20 \text{ kcal mol}^{-1}$, even at -75°C . This means that for an $\text{ArF}^+\text{MF}_6^-$ salt to be thermodynamically stable, even at -75°C , the electron affinity for MF_6^- must exceed $199 \text{ kcal mol}^{-1}$. This could be satisfied (10) by AuF_6^- . When allowance is made for a salt, which, although unstable with respect to F_2 loss, is yet stable with respect to F atom loss, the electron affinity requirement is decreased by 19 kcal mol^{-1} (see Figure 3). This then, perhaps, extends the possibilities to include $\text{ArF}^+\text{SbF}_6^-$, and possibly $\text{ArF}^+\text{BiF}_6^-$.

Acknowledgments

This work was supported by the Director, Office of Energy Research, Office of Basic Energy Sciences, Chemical Science Division of the U.S. Department of Energy, under Contract No. DE-AC03-76SF00098.

References

- Berkowitz, J.; Chupka, W. A. *Chem. Phys. Lett.* **1970**, *7*, 447.
- Frenking, G.; Koch, W.; Deakyne, C. A.; Liebman, J. F.; and Bartlett, N. *J. Am. Chem. Soc.* **1989**, *111*, 31.
- Seel, F.; Detmer, O. Z. *Anorg. Allg. Chem.* **1959**, *301*, 113.
- Bartlett, N.; Robinson, P. L. *Chem. Ind. (London)* **1956**, 1351; *J. Chem. Soc.* **1961**, 3417.
- Cotton, F. A.; George, G. W. *J. Inorg. Nucl. Chem.* **1960**, *12*, 386.
- Mallouk, T. E.; Rosenthal, G. L.; Müllen, G.; Brusasco, R.; and Bartlett, N. *Inorg. Chem.* **1984**, *23*, 3167.
- "JANAF Tables", Dow Chemical Co., Midland, MI, 1977.
- Hotop, H.; Lineberger, W. C. *J. Phys. Chem. Ref. Data*, **1975**, *4*, 539.
- Bartlett, N.; Okino, F.; Mallouk, T. E.; Hagiwara, R.; Lerner, M.; Rosenthal, G. L.; and Kourtakis, K. in *Advances in Chemistry Series No. 226*, **1990**, 391.
- Bartlett, N. *Proc. R. A. Welch Foundation Conf. on Chem. Research XXXII Valency* **1988**, 259.
- Beal, J. B.; Pupp, C.; White, W. E. *Inorg. Chem.* **1969**, *8*, 828.
- Shamir, J.; Binenboym, J. *Inorg. Chim. Acta.* **1968**, *2*, 37.
- Stein, L. *J. Fluorine Chem.* **1982**, *20*, 65.
- Harrell, S. A.; McDaniel, D. H. *J. Am. Chem. Soc.* **1964**, *86*, 4497.
- Zalkin, A.; Ward, D. L.; Biagioni, R. N.; Templeton, D. H.; and Bartlett, N. *Inorg. Chem.* **1978**, *17*, 1318.
- Agron, P. A.; Begum, G. M.; Levy, H. A.; Mason, A. A.; Jones, C. F.; and Smith, D. F. *Science*, **1963**, *139*, 842. Smith, D. F. *J. Chem. Phys.* **1963**, *38*, 270.
- Beaton, S. P. Ph. D. Thesis, University of British Columbia, Vancouver, B. C., Canada, **1966**, 67.
- Christie, K.O.; Sawodny, W. *Inorg. Chem.* **1967**, *6*, 1783.

19. Bartlett, N.; Levchuk, L. E. *Proc. Chem. Soc.* **1963**, 342.
20. Eyesel, H. H.; Seppelt, K. *J. Chem. Phys.* **1972**, *56*, 5081.
21. "Ionization Potential and Appearance Potential Measurements, 1971-81," R.D. Levin, and S.G. Lias, eds., NSRDS-NBS 71, U.S. Dept. of Commerce, Washington D.C., 20403, October 1982.
22. Kapustinskii, A. F. *Quart. Rev. (Chem. Soc., London)* **1956**, *10*, 283.
23. Waddington, T. C. *Advances Inorg. Chem. Radiochem.* **1959**, *1*, 157.
24. Bertaut, E. F. *J. Phys. Radium* **1952**, *13*, 499.
25. Templeton, D. H. *J. Chem. Phys.* **1955**, *21*, 1629.
26. JCPDS - International Center for Diffraction Data, Swarthmore, PA, 1989.
27. Bartlett, N.; Lohmann, D. H. *J. Chem. Soc.* **1962**, 5253.
28. Dasent, W. E. "Inorganic Energetics, An Introduction", Cambridge University Press, Cambridge, London, 1982.
29. Gillespie, R. J.; Schrobilgen, G. J. *Inorg. Chem.* **1976**, *15*, 22.
30. Babel, D. *Structure and Bonding* **1967**, *3*, 1.
31. Rothensal, G. Ph. D. Thesis, University of California, Berkeley, CA. 1984.
32. Gibler, D. D.; Adams, C. J.; Fischer, M.; Zalkin, A.; and Bartlett, N. *Inorg. Chem.* **1972**, *11*, 2325.
33. Since ClO_2F is similar in size and symmetry to SOF_2 , the S° value for the latter ($66.6 \text{ cal deg}^{-1} \text{ mol}^{-1}$) has been taken to be a reliable estimate of S° for ClO_2F .
34. Mallouk, T. E.; Desbat, B.; and Bartlett, N. *Inorg. Chem.* **1984**, *23*, 3160.
35. Christe, K. O.; Schack, C. J.; Pilopovich, D.; and Sawodny, W. *Inorg. Chem.* **1969**, *8*, 2489.
36. Wilson, J. W.; Curtis, R. M.; and Goetschel, C. T. *J. Appl. Crystallogr.* **1971**, *4*, 260.
37. Edwards, A. J.; Falconer, W. E.; Griffiths, J. E.; Sunder, W. A.; Vasile, M. J. *J. Chem. Soc. Dalton* **1974**, 1129.
38. Young, A. R. II; Hirata, T.; and Morrow, S. I. *J. Amer. Chem. Soc.* **1964**, *86*, 20.
39. Keith, J. N.; Solomon, I. J.; Sheft, I.; and Hyman, H. H. *Inorg. Chem.* **1968**, *7*, 230.
40. The fluoride ion affinity of $111 \text{ kcal mol}^{-1}$ given previously was conservatively evaluated. The value is probably higher and could be as great as $115 \text{ kcal mol}^{-1}$.
41. Berkowitz, W.A. Chupka, P.M. Guyon, J.H. Holloway, and R. Spohr, *J. Phys. Chem.*, **1971**, *75*, 1461.
42. Jackson, R. H. *J. Chem. Soc.* **1962**, 4585.
43. Morino, Y. and Saito, S. *J. Mol. Spectrosc.* **1966**, *19*, 435.
44. Tinkham, M. and Stranberg, M. W. P. *Phys. Rev.* **1955**, *97*, 951.

RECEIVED November 4, 1993

Chapter 3

Photochemical and Thermal Dissociation Synthesis of Krypton Difluoride

S. A. Kinkead¹, J. R. FitzPatrick¹, J. Foropoulos, Jr.², R. J. Kissane³,
and J. D. Purson⁴

¹Isotope and Nuclear Chemistry Division, ²Nuclear Material Division,
³Health and Safety Division, and ⁴Material Science Division, Los Alamos
National Laboratory, Los Alamos, NM 87545

Like dioxygen difluoride (O_2F_2), KrF_2 can be produced by thermal dissociation or photochemical synthesis from the elements; however, the yields are invariably much less than those obtained for O_2F_2 . For example, while irradiation of liquid O_2/F_2 mixtures at $-196^\circ C$ through a sapphire window with an unfiltered 1000W UV lamp provides in excess of 3g of O_2F_2 per hour, the yield of KrF_2 under identical circumstances is approximately 125 mg/hr. In this report, the yield of KrF_2 in quartz and Pyrex photochemical reactors has been examined as a function of irradiation wavelength, irradiation power, and Kr: F_2 mole ratio. The UV-Visible spectrum of KrF_2 has also been recorded for comparison with earlier work, and the quantum yield for photodissociation at two wavelengths determined. The synthesis of KrF_2 using large thermal gradients has also been examined using resistively heated nickel filaments to thermally dissociate the F_2 in close proximity to liquid nitrogen-cooled metal surfaces. As a net result, KrF_2 has been produced in yields in excess of 1.75 g/hr for extended periods in photochemical systems, and 2.3 g/hr for shorter periods in thermally dissociative reactors. This paper summarizes the results of examining parametrically several different types of reactors for efficiency of producing krypton difluoride.

Krypton difluoride, the last of the binary noble gas fluorides to be discovered, has been shown to be one of the strongest oxidizers known, rivaling PtF_6 and O_2F_2 in its ability to oxidize Pu(IV) to $PuF_6(1,2)$. In addition, this reagent has found a unique place in the repertoire of preparative fluorine chemistry and has been used to prepare a wide variety of novel materials, including AgF_3 (3), *cis*- OsO_2F_4 (4), numerous ClF_6^+ and BrF_6^+ compounds (5,6), and other novel materials. In addition to its value in the synthesis of novel and known high-valent inorganic compounds, krypton difluoride has been evaluated for use as an agent for decontaminating plutonium processing equipment, as well as a storable solid precursor for a chemically-pumped KrF laser.

Both of these applications, as well as other potential commercial applications require a greater availability of the reagent. The two syntheses discussed here are extensions of well-known methods for preparing a variety of high-valent inorganic materials, and offer relatively convenient routes to useful quantities of KrF_2 . While dioxygen difluoride (FOOF) is more reactive than KrF_2 at subambient temperatures, the poorer thermal stability of FOOF at room temperature renders this material less attractive for many applications. For example, where apparatus cannot be conveniently cooled to subambient temperatures, or where the necessary equipment is unavailable to produce O_2F_2 or O_2F *in-situ* in sufficient quantities, KrF_2 is far easier to store, handle, and much more efficient in fluorinating ability. The striking contrast in ambient temperature-low temperature behavior is a reflection of the widely differing volatilities as well as thermal stabilities, as shown in Table I below. In practice, KrF_2 and O_2F_2 are complementary in their fluorination capabilities.

Table I. Physical Properties of KrF_2 and O_2F_2

Property	$\text{KrF}_2(7)$	$\text{O}_2\text{F}_2(8)$
Melting Point ($^{\circ}\text{C}$)	+77 (subl.,dec.)(9)	-163.5
Boiling Point ($^{\circ}\text{C}$)	--	-57 (dec.)
Solubility in HF (wt %)	200	>11*
Decomposition at -78°C (%/day)	none	4.3(10)
Vapor Pressure at -78°C (torr)	0	~240
Lifetime at 25°C	days	3 sec. (11)
Vapor Pressure at 25°C (torr)	134	>1000

*at -78°C

Unlike the binary xenon fluorides, KrF_2 cannot be prepared by photolysis of the elements at room temperature nor by high temperature-high pressure methods. Also unlike the binary xenon fluorides, there has been little success in achieving a higher yield (i.e. multiple grams per hour) synthesis of KrF_2 . Aside from oxidative

fluorinations, the predominate reactions of KrF_2 are the formation of KrF^+ and Kr_2F_3^+ salts, although the chemistry of this compound may yet be emerging, as evidenced by the claimed and confirmed preparation of $\text{Kr}(\text{OTeF}_5)_2$ (12,13) containing the first Kr-O bond, and recent reports of the unusual salts $[\text{R}_f\text{-Kr-N}\equiv\text{C-H}]^+ \text{AsF}_6^-$ [$\text{R}_f = \text{F}, \text{CF}_3, \text{C}_2\text{F}_5, \text{n-C}_3\text{F}_7$] containing the novel Kr-N bond (14, 15).

Numerous methods have been employed to prepare KrF_2 , including electric discharge (16, 17), photochemical (18) or electron beam (19) irradiation, and proton (10 MeV) (20) or α (40 MeV) bombardment (20). Irrespective of the method of synthesis, a common feature of all of these preparations is that low temperatures (< -150°C) are required to achieve high yields of the product. Thus, while KrF_2 has been prepared at temperatures as high as -60°C (via proton bombardment) and at -150°C

(electron beam irradiation), better yields are generally obtained at much lower temperatures; e.g. -196°C for UV photolysis or -183°C for electric discharge. The literature yield for early photochemical synthesis was reported to be 200 mg/hr (21) for a 2.5 kW UV lamp, while electric discharge has been reported to provide as much as 250 mg/hr (1). For comparison, the yield of O_2F_2 under conditions of photochemical synthesis is approximately 3g/hr (11). In spite of the lower yields of KrF_2 reported from photochemical preparation, later reports (22) suggest that a substantial improvement in the yield is possible.

In a unique preparation, Bezmel'nitsyn and coworkers have reported the synthesis of KrF_2 using thermally generated atomic fluorine (23). In this synthesis, large thermal gradients ($>900^{\circ}\text{C}/\text{cm}$) are created using a resistively heated nickel filament—which catalytically and thermally dissociates elemental fluorine—in close proximity to a cold surface covered with solid krypton. According to the authors, the filament temperature, distance from the wall, and pretreatment are critical parameters (the latter being poorly defined) in the operation of this reactor. Under proper conditions, optimum yields of this reactor (at a filament temperature of 680°C and 1 cm filament-wall distance) are in the range of 5-6 g/hr, far in excess of any other known preparation of KrF_2 . According to the authors, this design is also amenable to the large-scale production of other strong oxidizers such as O_2F_2 and chlorine- and nitrogen fluorides and oxyfluorides. In this report, we investigate two useful preparations, and relevant physical and chemical characteristics of KrF_2 .

Experimental

[CAUTION: Elemental fluorine and krypton difluoride are extremely potent oxidizers, and react violently with skin, water, or organic matter. Contact with these materials should be scrupulously avoided. In addition, condensed liquid fluorine and solid krypton, used in both of these syntheses, can rupture apparatus if allowed to warm beyond their boiling points (-187.9° and -152°C , respectively).]

Materials. Krypton (Linde, Research grade or Spectra Gases Inc. 99.995% purity) was used as received without further purification. Fluorine (Air Products and Chemicals Inc., nominal 98%) was purified by passing the gas through two NaF traps to remove HF and SiF_4 . Ultrapure fluorine was prepared by the method of Asprey (24). Boron trifluoride (Ozark-Mahoning) was used as received after verification of its infrared spectrum.

General. Infrared spectra were recorded on either a Nicolet model 20SX FTIR infrared spectrometer or a Perkin-Elmer model 283 spectrometer using a stainless steel 10 cm-pathlength gas cell fitted with AgCl windows. UV-visible spectra were recorded on a Perkin-Elmer model 330 UV-VIS-NIR spectrometer, using a 9.4 cm nickel cell fitted with UV grade sapphire windows (Saphikon) and a portable metal vacuum line and pumping station. To measure quantum yields, this same cell and vacuum system was used in conjunction with a Lambda-Physik model EMG-102ES excimer laser operating at 308 nm, or a Questek model 2140 excimer laser operating at 248 nm. Laser power (and hence photon input) was measured with a Scientech 362 power meter, while the KrF_2 decomposed was measured from pressure increase in the cell after correction for thermal decomposition and verification of the amount lost by FTIR.

Photochemical Synthesis Apparatus. A metal manifold (stainless steel and Monel) was used to handle all gases and products. All reactants were measured by

manometric techniques in either of the two calibrated ballast volumes on the gas handling line. The amount of KrF_2 product was determined by weighing in an all-metal stainless 75 ml stainless steel cylinder (Whitey) fitted with 1/4" Nupro Bellows valves. An all-quartz photolysis lamp well (Ace model 7858-45 vacuum insulated immersion well; see Figure 1a) was used to with a Canrad-Hanovia medium pressure 450 watt Hg lamp. The central tube, closed at one end, of either quartz, Vycor, or Pyrex glass, filtered the light as necessary. The reactor outer section is patterned after the design of Šmalc et al.(22). To measure the yield with 550 and 1200 Watt immersion lamps, a larger version of the immersion well reactor was constructed (Figure 1b). Apart from its size, the major difference from the smaller reactor is that only Pyrex was used for the lamp well and reactor. To allow extended operation, an automatic dual-setpoint liquid nitrogen controller (Thermionics Laboratory, Inc. model LNC-400) was employed with Neslab RTE-110 and CFT-25 recirculating chillers—operating in series and fitted with an Ace model 12160 water flow power cut-off sensor and power supply to shut down the lamp power supply in the event water flow is interrupted—cooled the reactor and lamp well, respectively. Should the liquid nitrogen coolant supply be lost an air actuated valve (Varian model NW-16)—controlled by the relay from an MKS model PDR-C-1B power supply readout and a 1000 torr MKS model 222CA pressure transducer—will open at 600 torr, venting the gases into a fume hood.

Thermal Synthesis Apparatus. Several hot-wire reactors similar in design to that used by Bezmelnitsyn et. al. (23) have been constructed; the latest design, of stainless steel and Monel is as follows. The smaller reactor consisted of a 1.5 in. dia. x 20 in. long stainless steel tube with MDC 2.75 in. dia. knife-edge (Del-Seal) flanges welded to the top and bottom. The filament was a coiled nickel 200 rod (Castle metals) or nickel 200 chromatography tubing (0.125 in. dia., Alltech). The electrical feedthrough was an MDC model MMC-150 medium current flanged feedthrough. A larger reactor was also designed and constructed. The body of this reactor was constructed of a 4 in. dia. by 22 in. long section of schedule 40 Monel pipe with an 8 in. dia. Monel knife-edge flange machined and welded to the end of the pipe. The bottom of the reactor was capped with a 0.5 in. thick section of Monel plate; the top of the reactor was an eight inch stainless MDC knife-edge flange fitted with a gas inlet and dual medium current electrical feedthroughs as well as connectors for a pressure transducer and observation/temperature measurement window. Electrical feedthroughs were MDC Vacuum Products Corporation models MCT-150 or MMC-150. To heat the nickel filament, a Lambda model LK-361-FMOV DC or Electronic Measurements model 40-275-1-O-0650-OV DC power supply was connected to the electrical feedthroughs. The filaments consisted of a 0.0625 in. dia. nickel rod (nickel 200, Castle Metals) or 0.0625 in. dia. nickel 200 chromatography tubing (Alltech) wound around a 0.375 in. dia. alumina tube to provide mechanical support at high temperatures. Copper-Constantan (E type) thermocouples were attached to the outside of the reactor to monitor the surface temperature during the reaction. A window at the top of the reactor provides a means to monitor the filament temperature and condition. The temperature of the filament was determined by visual comparison with a blackbody source at 700° C. An infrared pyrometer (Omega model OS-2000AS-CSS) focused through an AgCl window was thought to provide more accurate temperature measurements; however, this proved not to be the case and this method was abandoned. Reactants were introduced through a gas inlet at the top of the reactor; the lower inlet permitted recirculation of the reactants as well as removal of the products at the conclusion of the experiments. A three-liter ballast can allowed the fluorine to be admitted at more or less constant pressure. When larger scale KrF_2 experiments were conducted, a recirculating system employing a Metal Bellows model 602 recirculating pump and larger steel ballast volumes was constructed. The KrF_2 product was purified

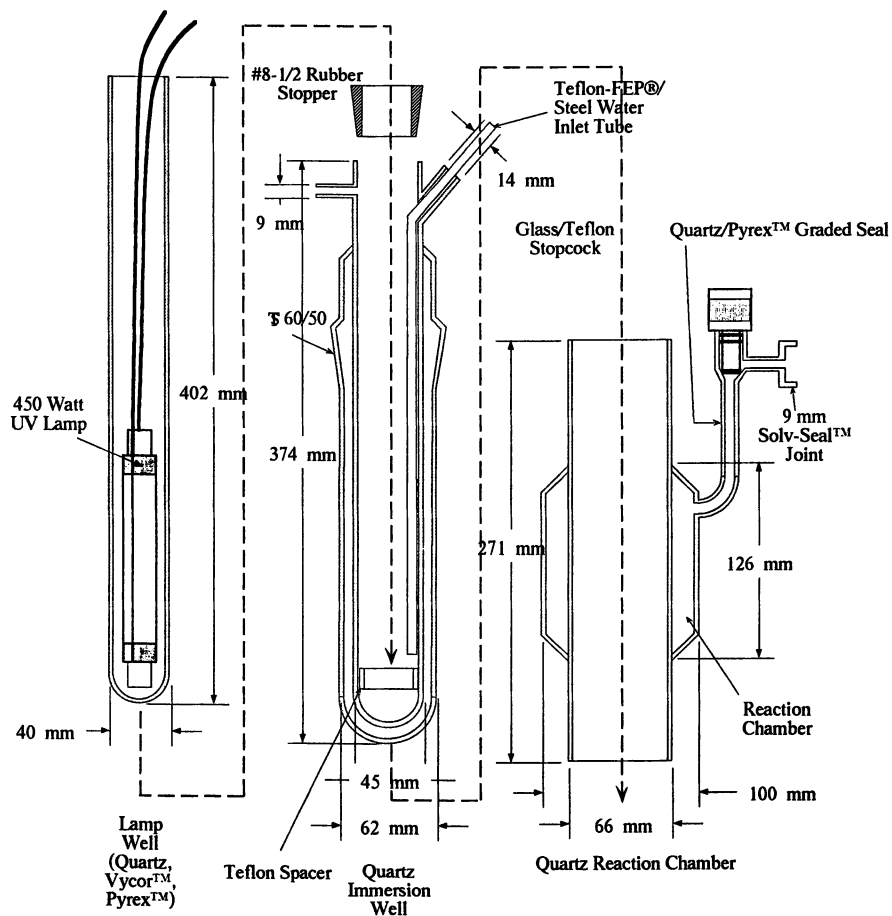


Figure 1a. Small Photochemical Immersion Well for Low-Temperature KrF_2 Synthesis. The immersion well and reaction chamber are of quartz; the lamp well is of Quartz, Vycor, or Pyrex, as desired. The lamp well is sized for a 450 watt or smaller medium pressure UV lamp (37 mm O.D.)

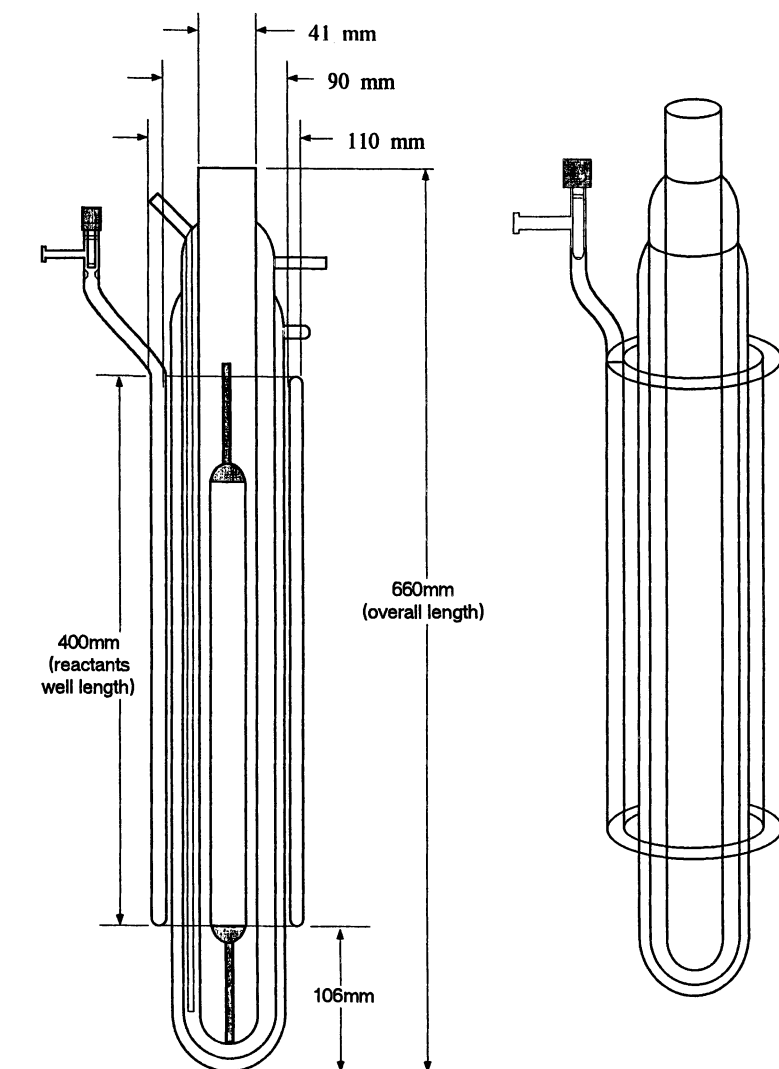


Figure 1b. Photochemical Reactor for 550- and 1200 Watt Medium Pressure UV Lamps. Material is all Pyrex.

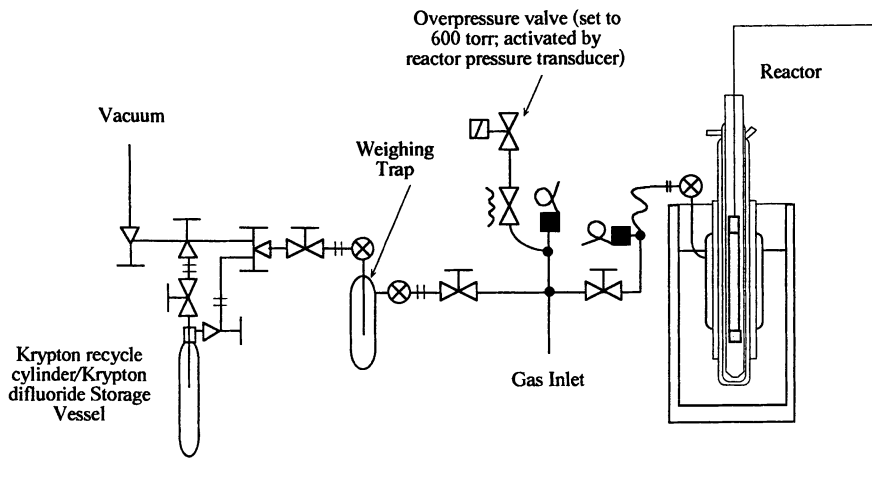


Figure 1c. Section of Vacuum Line for Purification of KrF_2 Product from Photochemical Synthesis.

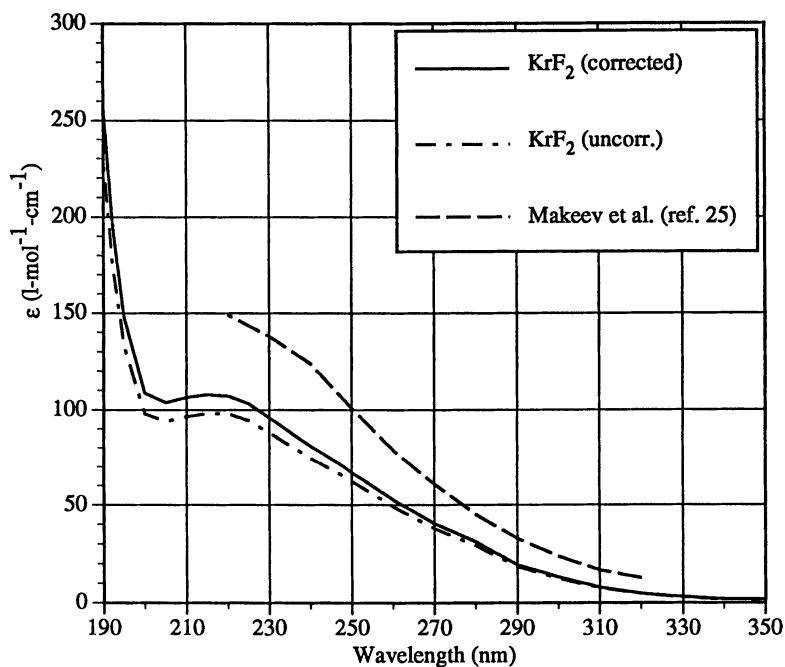


Figure 2. UV-visible spectrum of KrF_2 . In addition to the corrected (solid line) and uncorrected for thermal decomposition (alternating dash) data, the earlier reported data (dash) is shown.

from Kr and F₂ through a stainless steel trap cooled to -78° C and transferred to the storage vessel (a 300 ml Whitey SS-304 cylinder fitted with a dip tube and medium pressure autoclave engineers valves).

Photochemical Synthesis Procedure. To prevent freezing of water in the lamp well, cooling water was circulated through the water jacket prior to cooling the reactor with liquid nitrogen. After the lower part of the reactor was at -196° C, krypton was condensed into the reactor to a residual pressure of 2–10 torr. Then, after any other reagent (e.g. BF₃) was added, elemental fluorine was added to the reactor after which the lamp was ignited. During the course of the reaction, the liquid nitrogen level was maintained with the liquid nitrogen level controller, connected to a pressurized 160 liter dewar. At the completion of the reaction, residual F₂ was removed through a trap containing coarse charcoal while the reactor was held at -196° C. [For larger quantities of F₂, a small (150 ml) stainless steel cylinder (Whitey) attached to the line was cooled to -196° C, and the dewar around the reactor was replaced with one containing liquid oxygen (b.p. -183°C) to distill the fluorine back into a 10 liter ballast volume on the vacuum line for reuse.] Subsequently, the removable product trap was cooled to -78° C, and a 300 ml Kr storage cylinder (Whitey) containing molecular sieves (type 4A, 30g) cooled to -196° C connected in line after the trap, and the dewar surrounding the reactor was gradually lowered while maintaining the pressure below 200 torr to remove the krypton to the storage cylinder for subsequent reuse (Figure 1c). When all the krypton had been evacuated, the reactor was gently warmed with a heat gun or warm water to sublime the KrF₂ to the trap, and the product weighed. Finally, the KrF₂ was transferred to a nickel or stainless cylinder for storage at -78° C.

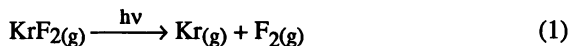
Thermal Synthesis Procedure. The filament was preconditioned by heating to 700°C first in an atmosphere of hydrogen to reduce any nickel fluoride passivation to metal, after which the filament was heated in oxygen according to the procedure of Bezmel'nitsyn (23). After preconditioning the filament, a 25 liter dewar of liquid nitrogen was raised around the reactor to cool it to -196° C. To cover the reactor walls with a uniform layer of krypton, the three liter ballast can was first filled to a pressure of 700 torr (~110 mmole), and the gas rapidly admitted to the cold reactor. By visual examination, this method resulted in a more or less uniform layer of Kr. With the valve between the reactor and ballast can open, the system was filled to a pressure of approximately 40 torr of F₂. The power supply was turned on, and the current slowly increased to achieve the proper filament temperature. Once the F₂ pressure began to decrease (after an initial rise due to dissociation and heating), fluorine was added continuously to maintain the pressure nominally at 40 torr. To maintain the cooling capability, liquid nitrogen was continuously added *via* a similar arrangement as in the photolytic synthesis. At the completion of the reaction (when the fluorine consumption approached zero), the power supply was turned off and the residual fluorine pumped out through a trap of coarse charcoal. The dewar was lowered slowly to maintain a pressure in the reactor of less than 20 torr, and the Kr and KrF₂ were pumped through the purification traps held at -78° and -196° C. The remainder of the purification was the same as in the photosynthetic preparation.

Results and Discussion

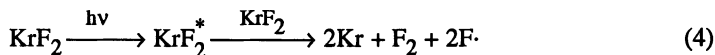
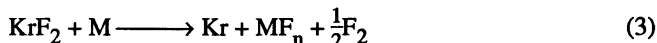
While the synthesis and properties of small laboratory quantities of KrF₂ have long been worked out, a careful reexamination of the relevant spectroscopic data was in order before the syntheses were scaled to multigram size. In the case of the photosynthetic preparation, this was essential both to confirm the reported UV-visible spectra of KrF₂ (25), and to correlate the absorption features with yield. If, for example, the absorption band at 220 nm reported by the Russian workers was photodissociative, then wavelengths in this region must be carefully filtered out if the yields are to be maximized. The resulting spectrum in Figure 2 is shown corrected and

uncorrected for the decomposition of KrF_2 during the course of the experiment (nominally 10-15 % per experiment). The abnormally high decomposition resulted from the proximity of the spectrometer source to the sample compartment in our instrument, which in turn caused the sample cell temperature to be in excess of 35°C . While the Russian report shows only a broad rise from 320 to 230 nm ($\epsilon = 147 \text{ l/mole-cm}$), the spectrum we obtained shows a less intense absorption at 218 nm ($\epsilon = 105 \text{ l/mole-cm}$) with another, more intense feature near 188–190 nm ($\epsilon = 250 \text{ l/mole-cm}$). The position and shape of this latter band varied slightly from experiment to experiment, probably due to the intensity of the band as well as instrument resolution near the spectrometer wavelength limit (185nm).

The dissociative quantum yields were measured at 248 nm and 308 nm to determine if the absorption feature which has its maximum at 218 nm arises from a dissociative electronic transition; e. g. $\sigma \rightarrow \sigma^*$. By measuring the photodecomposition reaction, e.g.



a single reaction (1) may be examined for its effect on the formation of KrF_2 . Obviously other reactions such as those shown below, can play a significant role in the photodecomposition of KrF_2 by initiating or propagating a chain reaction.



If instead the quantum yield for photosynthesis is measured, only the overall reaction can be studied; i. e., the photodecomposition of either KrF_2 or $\text{KrF}\cdot$, which may occur coincidentally, are indistinguishable. Also, the quantum yields are so low—approximately 0.02 for solid Kr and liquid F_2 (28)—as to require an extended measurement period and correspondingly difficult-to-maintain control over reaction conditions. Since the average Kr-F bond energy in KrF_2 is only 10–12 Kcal/mole ($\sim 0.5 \text{ eV}$), an electronic transition at 218 nm (5.7 eV) is more than energetic enough to result in dissociation. As seen below in Table II the quantum yield at 248 nm is near unity, indicating a strongly dissociative process, and substantially higher than that at 308 nm.

From these experiments, hard UV radiation is shown to have a deleterious effect on KrF_2 formation. To determine the magnitude of the effect of filtering short wavelength UV light on the yield of material, as as determined by the effect on the overall synthesis, experiments using an immersion well reactor, with a variable wavelength cutoff, were conducted. Using a constant krypton to fluorine ratio of 4:1 (200:50 mmol), KrF_2 was prepared employing alternately a quartz, Vycor 7913, and a Pyrex 7740 glass insert. While there was only a slight difference in yield between experiments where a quartz or Vycor insert was used, a dramatic effect was observed when Pyrex was substituted. The results, shown in Table III, are striking evidence of the deleterious effect of short wavelengths on the production of KrF_2 .

From this data, as well as the previous data on the photodissociative quantum yield, it is evident that short wavelength UV light is extremely detrimental to the

Table II. Quantum Yield for the Photodecomposition of KrF₂

Wavelength (nm)	Laser Power (mJ/pulse)	KrF ₂ Init. Pressure (torr)	mmol KrF ₂ Photolyzed*	Φ (mmol/quanta)
248	140	11.23	0.019	1.17
	139	20.00	0.035	1.19
308	51.5	12.12	0.0011	0.45
	49.0	20.10	0.0045	0.53

*5 min. photolysis, corrected for thermal decomposition

Table III. Synthesis of KrF₂ in Well Reactor

INSERT MATERIAL	UV CUTOFF (nm)‡	YIELD (mg/hr)	COMMENTS
Quartz	170	130†	(avg. = 158 ± 20)
		161†	
		138†	
		193†	
		155†	
		171◊	
Vycor 7913	210	222*	(avg. = 204 ± 30)
		139*	
		250†	
Pyrex 7740	280	484◊	(avg. = 507 ± 50) 10 mmol BF ₃ added
		557◊	
		456◊	

Note: All experiments are at least 3 hours in length

‡ Wavelength at 0% Transmission

* Amount by thermal decomposition of product

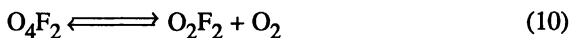
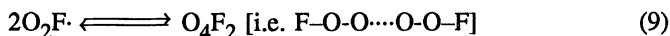
† By weight in a Teflon FEP/PFA trap

◊ By weight in a Glass trap

synthesis of KrF_2 and must be carefully filtered out. We also find that earlier reports that addition of BF_3 enhances the formation of KrF_2 either with filtered or unfiltered (data not shown) UV light are unsupported (28).

In the above experiments, the krypton fraction was fixed at 80 mole-% (4:1 Kr:F₂) based on information provided by Slovenian workers (26) that the best yields of KrF_2 were obtained at this ratio. To confirm this data, yields were obtained for krypton mole fractions from 0.25 to 0.90 (with the total amount of reactants held constant at 250 mmol). The resulting data are plotted in Figure 3, showing that a maximum in the yield curve exists near 80 mole % krypton, confirming the work of Šmalc and coworkers (22).

Since, for the synthesis of O_2F_2 a ratio of oxygen to fluorine of 1 provides the best yields, the markedly higher yields at 4:1 vs. 1:1 Kr:F₂ suggest that the formation of KrF_2 may involve a different mechanism than for O_2F_2 formation. The synthesis of O_2F_2 has been well studied and likely proceeds *via* the following series of reactions:



All of these reactions except (8) involve the stable intermediate $\text{O}_2\text{F}\cdot$ species, and are coincidentally two-body collision processes. Being a three-body process, reaction (8) would be expected to contribute less to the overall yield than equations (6) and (7). In the case of KrF_2 , the intermediate $\text{KrF}\cdot$ radical is unstable at room temperature and is stable only at cryogenic temperatures (27). According to Artyukhov and coworkers (28), $\text{KrF}\cdot$ may be stabilized by association or electron sharing with other krypton atoms (i. e. a Van der Waals molecule such as $\text{Kr-F}\cdots\text{Kr}$). This may explain why the synthesis of KrF_2 from gaseous Kr and F_2 proceeds with poorer yields (quantum yields less than 0.001 vs. 0.021 in liquid fluorine-solid krypton (28)) as well as why larger proportions of krypton are required for optimum yields.

In the studies of the optimum Kr:F mole ratio and irradiation wavelength, we were unable to confirm the claim of Slovenian workers to produce in excess of 1.0 grams of KrF_2 . However, we believe this in fact is a reflection of the scale of reaction. For example, while the total amount of starting material in many of these experiments never exceeded 250 mmol (e.g. 200 mmol Kr and 50 mmol F_2 at 4:1 Kr:F₂) or 0.25 mole, Šmalc and coworkers (22) routinely use 4 moles Kr and 1 mole F_2 in a similar size reactor (i.e. 100–200 ml internal volume). When the reaction was scaled to 1.25 mole reactants (0.25 mole F_2 and 1 mole Kr), yields of 1.0–1.1 g/hr over 20–24 hours were obtained. Obviously, the increase in yield supports the Russian workers' data of the higher quantum yield in the solid phase versus the gas phase (28). Because of the high initial Kr:F₂ ratio, the extended reaction time (20–24 h), and the high rate of formation of KrF_2 , we expect that a substantial increase of the Kr:F₂ ratio will occur

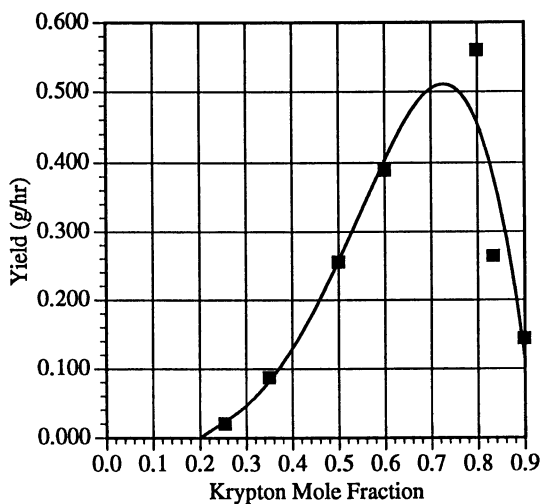


Figure 3. Variation of KrF_2 yield (in grams/hour) with mole fraction krypton. Total quantity of reactants are constant at 0.25 moles. The data are fitted to the following polynomial:

$$\text{KrF}_2 \text{ yield (g/hr)} = -15.81664 \cdot \chi_{\text{Kr}}^4 + 23.90729 \cdot \chi_{\text{Kr}}^3 - 11.03569 \cdot \chi_{\text{Kr}}^2 + 2.466380 \cdot \chi_{\text{Kr}} - 0.2180971.$$

with time, shifting to a lower than optimum rate. To avoid this degradation in the expected yield, fluorine is periodically added to sustain the ideal Kr:F₂ ratio.

Substantial dependence of the hourly yield on lamp power were also observed. As can be readily seen in Table IV, use of a 550 Watt lamp provided a measurable increase in yield over the use of a 450 watt lamp.

Table IV. Photosynthetic Yields of KrF₂ with Varying Lamp Power

Lamp Power (Watts)	Total Yield (g)	Hourly Yield (g/hr)	Comments
450	22.	1.1	1 mole Kr; 0.25 mole F ₂
550	24.4	1.22	2 mole Kr; 0.5 mole F ₂ ; larger reactor

While some experiments using a 1200 Watt medium-pressure Canrad-Hanovia UV lamp in the larger reactor have been done, the large amount of heat produced by this lamp repeatedly tripped the high-temperature breaker. In one experiment, 40.9 grams of KrF₂ were produced in 23 hours; however this must be regarded as a minimum since the lamp chiller required replacement in the middle of the experiment, resulting in approximately a two-hour interruption in the experiment. From this data, we believe it should be possible to further increase the synthesis rate by additional increases in lamp power.

Thermal Dissociation of Fluorine. The first step in the synthesis of KrF₂ or many other highly oxidized fluorine compounds is the dissociation of F₂ into atomic fluorine. While thermal dissociation of fluorine is often used in the synthesis of thermodynamically stable fluorine compounds, the rapid decomposition of thermally unstable compounds in the presence of hot fluorine atoms limits the utility of this method for such materials (e.g. O₂F₂, KrF₂). However, the use of large thermal gradients provides an analogous situation to the use of UV photolysis in low temperature environments: Energetic species (fluorine atoms) created in close proximity to unstable products or intermediates. From thermochemical tables (29), elemental fluorine is about 18-22% dissociated at 700° C, depending on pressure. In order to take advantage of the extensive dissociation of fluorine at relatively low energies, it is essential to rapidly quench the KrF₂ reaction product. The principle here is to generate large quantities of atomic fluorine (i.e. at low pressures) in close proximity to the cold Kr to achieve rapid conversion of the short-lived KrF· to KrF₂, or alternately to sustain a high rate of three-body kinetics (2F· + Kr). To achieve this result, Bezmelnitsyn and coworkers (23) employed thermal gradients of up to 900°/cm to keep Kr, KrF₂, and KrF· radicals frozen in the immediate vicinity of hot fluorine. A coiled nickel filament, located in the center of the reactor, is resistively heated to 680–700° C using a DC power supply to catalytically dissociate the fluorine. According to this report, at a distance between the filament and wall of 1 cm, the yield of KrF₂ is 6.0 grams in one hour. Not surprisingly, the yield of KrF₂ drops off rapidly with distance to the wall: At 2 cm the yield is 5 g/hr; at 4 cm, 2.8 g/hr. A notable feature of this report is the emphasis on pretreating the filament by heating to >800°C in an oxygen atmosphere for a brief period of time, which forms a high surface area oxide coating. Presumably, subsequent reaction of this coating in a fluorine atmosphere would provide a higher surface-area fluoride coating capable of producing larger quantities of

atomic fluorine. Experimental evaluation of filament pretreatment by resistively heating in an oxygen atmosphere at 800–900° C produced no measurable effect on the yield, although reaction of the nickel filament with oxygen was evident: O₂ pressure drops of 50–100 torr were reproducibly observed.

Since these yields are the highest ever reported for the production of KrF₂, we sought to confirm these values in our own laboratories. Using the Soviet design as a point of departure, a reactor was designed and constructed to test this preparation. Although a complete discussion of the thermal dissociation reactor is inappropriate for this report, the results of scoping experiments are promising although highly variable. In a series of fourteen experiments to evaluate baseline conditions for this reactor, yields in excess of 2 g/h have been obtained. While yields were not measured for some individual experiments, average yields (cumulative KrF₂ produced per operating time) were obtained for a series of experiments, as shown in Table V, below.

Table V. Yields of KrF₂ from a Hot-Wire Reactor

EXPERIMENT	YIELD (mg/hr)	COMMENTS
1	200.*	0.062 in. dia. Ni-61 welding rod [§] ; rapid burnout, extensive corrosion of filament.
2	250.*	
3	125.*	Pure Ni (Ni-200) filament
4-8	950.†	Five one-hour experiments without removing product between reactions.
9-14	880.†	Six one-hour experiments without removing product between reactions.
15	830.†	Five-hour experiment (4. g product)
16	2300.†	2 hour experiment

Conditions: Filament electrically heated to ~700 ± 100° C; approximately 1.0 cm from reactor wall.

*Estimated from fluorine pressure drop.

[§]Ni-61 composition: 96.3% Ni, 2.95% Ti, 0.43% Si, 0.20% Mn; C, Fe, S, Cu, Al, P all <0.1%.

†By weighing in a S. S. storage vessel.

Difficulties in measuring the filament temperature prevented more precise control of this parameter, and obviously affected the reproducibility as well as the optimum yield. In experiments 4 -14, over 20 grams of KrF₂ were produced in multiple 2 to 4 hour runs. Even though there were significant reliability problems with the filaments, this indicates a substantial capability to produce multigram amounts of material. Because the yield falls off rapidly after approximately an hour, most of the experiments reported here are of short duration, with repeated additions of krypton to the reactor. Due to the promise shown in these early experiments as well as the versatility of this reactor, we plan to continue research with this reactor. To improve

reliability and reproducibility, a repeatable method for winding filaments has been developed.

Since it is possible that the surface area of both the heated filaments and cold area of the reactor are crucial variables in this system, a larger reactor was constructed and evaluated. A unique feature of this reactor is that multiple filaments (from four to twelve) could be connected to the current source, increasing the area of the catalytic surface responsible for dissociating fluorine. In spite of the larger cold surface of this reactor relative to the 1.5 in. dia. reactor, there was no measurable improvement in the KrF_2 production rate, although this reactor has been shown to be capable of producing multigram quantities of XeF_6 (30).

Conclusions

In the synthesis of high-valent inorganic compounds, krypton difluoride enjoys an position shared by few other materials. Not only is it an extremely powerful oxidizer in its own right, but its cationic salts, KrF^+ , are quite possibly the strongest oxidizers available aside from the fluorine atom. A large number of novel high valent fluorides, such as AgF_3 , ClF_6^+ salts, and others, either require KrF_2 (or KrF^+ salts) for their synthesis or are prepared more easily or more purely with KrF_2 . Much of the chemistry of this oxidizer has developed only slowly, due to the specialized equipment and techniques required for its preparation as well as the lower rates which generally occur. The two methods described and evaluated in this paper are the highest yield, most readily adaptable (to the laboratory) routes to this synthetically valuable reagent. Photochemical synthesis provides a high sustained production rate of material, which with proper precautions, can be conducted safely. Thermal gradient synthesis is useful for preparing smaller amounts of KrF_2 , and due to the lower pressures and smaller quantities of fluorine involved is inherently safer. In addition, the thermal gradient synthesis technique is easily adapted to the synthesis of other oxidizers such as ClF_5 , XeF_6 , and O_2F_2 by substitution of ClF_3 , Xe, or O_2 for krypton in the preparation.

Acknowledgements

The authors gratefully acknowledge the support of the U.S. Department of Energy, Office of Nuclear Material Production. S.K. also acknowledges the support of the USAF Phillips Laboratory, the National Research Council (Office of Eastern European Affairs), the Academy of Arts and Sciences, Slovenia, and the Jožef Stefan Institute, Ljubljana, Slovenia. The support of colleagues at the Los Alamos National Laboratory—Drs. Larned Asprey, P. Gary Eller, Jon Nielsen, and Kent Abney—and at the Jožef Stefan Institute—Prof. Boris Žemva, and Drs. Karel Lutar and Adolf Jesih—also gratefully appreciated.

Literature Cited

1. Weinstock, B.; Malm, J. G.; Weaver, E. E. *J. Am. Chem. Soc.* **1961**, *83*, 4310.
2. Asprey, L. B.; Eller, P. G.; Kinkead, S. A. *Inorg. Chem.* **1986**, *25*, 670.
3. Žemva, B.; Lutar, K.; Jesih, A.; Casteel, W.J.Jr.; Wilkinson, A.P.; Cox, D.E.; Von Dreele, R.B.; Borrmann, H.; Bartlett, N. *J. Am. Chem. Soc.* **1991**, *113*, 4192.
4. Christe, K.O.; Bougon, R. *J. Chem. Soc., Chem. Comm.* **1992**, *15*, 1056.
5. Christe, K.O.; Wilson, W.W.; Curtis, E.C. *Inorg. Chem.* **1983**, *22*, 3056.
6. Gillespie, R.J.; Schrobilgen, G.J. *Inorg. Chem.* **1974**, *13*, 1230.

7. Prusakov, V. N.; Sokolov, V. B. *Atom. Energ. (Engl. Trans.)* **1971**, *31*, 990; *Atom. Energ.* **1971**, *31*, 259.
8. Streng, A. G. *Chem. Rev.* **1963**, *63*, 607.
9. Al-Mukthar, M.; Holloway, J.H.; Hope, E.G.; Schrobilgen, G.J. *J. Chem. Soc., Dalton Trans.* **1991**, 2831.
10. Kirshenbaum, A.D.; Grosse, A.V. *J. Am. Chem. Soc.* **1959**, *81*, 1277.
11. Abney, K.D.; Eller, P.G.; Kinkead, S.A.; Kissane, R.J.; Asprey, L.B. *J. Fluorine Chem.* submitted.
12. Jacob, E.; Lentz, D.; Seppelt, K; Simon, A. *Z. anorg. allgem. Chem.* **1981**, *472*, 7.
13. Sanders, J.C.P.; Schrobilgen, G.J. *J. Chem. Soc., Chem. Comm.* **1989**, 1576.
14. Schrobilgen, G.J. *J. Chem. Soc., Chem. Comm* **1988**, 863.
15. Schrobilgen, G.J. *J. Chem. Soc., Chem. Comm* **1988**, 1506.
16. Grosse, A. V.; Kirshenbaum, A. D.; Streng, A. G.; Streng, L. V. *Science* **1963**, *139*, 1047.
17. Schreiner, F; Malm, J. G.; Hindman, J. C. *J. Am. Chem. Soc.* **1965**, *87*, 25.
18. Turner, J. J.; Pimentel, G. C. *Science* **1963**, *140*, 974.
19. MacKenzie, D. R. *Science* **1963**, *141*, 1171.
20. MacKenzie, D. R.; Fajer, J. *Inorg. Chem.* **1966**, *5*, 699.
21. Bougon, R.; Lance, M C. *R. Acad. Sci. Paris* **1983**; *297*; 117.
22. Šmalc, A.; Lutar, K.; Žemva, B. *Inorg. Synth.* **1992**; *29*, 11.
23. Bezmel'nitsyn, V. N.; Legasov, V. A.; Chaivanov, B. B. *Proc. Acad. Sci. USSR (Engl. Trans.)* **1977**; *235*, 365; *Dokl. Akad. Nauk SSSR.* **1977**; *235*; 96.
24. Asprey, L.B. *J. Fluorine Chem.* **1976**, *7*, 359.
25. Makeev, G. H.; Cynanskii, B. F.; Smirnov, V. M. *Proc. Acad. Sci. USSR (Engl. Trans.)* **1975**; *222*; 452; *Dokl. Akad. Nauk SSSR* **1975**; *222*; 151.
26. Žemva, B. *Personal Communication*, see also reference 22.
27. Falconer, W.E.; Morton, J.R.; Streng, A.G. *J. Chem. Phys.* **1964**, *41*, 902.
28. Artyukhov, A. A.; Legasov, V. A.; Makeev, G. N.; Smirnov, B. B.; Chaivanov, B. B. *High Energ. Chem. (Engl. Trans.)* **1976**, *10*; 450; *Khim. Vysok. Énerg.* **1976**; *10*; 512.
29. *JANAF Thermochemical Tables*; Stull, D.R.; Prophet, H., Eds.; National Bureau of Standards: Washington, D.C. 1970, No. 37, 2nd ed.
30. Nielsen, J.B.; Kinkead, S.A. *Inorg. Chem.* **1990**, *29*, 1779.

RECEIVED October 25, 1993

Chapter 4

Main-Group Fluorides with Coordination Numbers Greater Than Six

Konrad Seppelt

Institut für Anorganische und Analytische Chemie, Freie Universität
Berlin, Fabeckstrasse 34–36, D–14195 Berlin, Germany

The principal geometries for neutral or anionic AF_7 and AF_8 species are the pentagonal bipyramid and the square antiprism, respectively (A = heavy main group element). Examples of the first geometry include IF_7 , IOF_6^- , TeF_7^- , $CH_3OTeF_6^-$, and $(CH_3O)_2TeF_5^-$. The ion IF_8^- provides an example of the second geometry. The pentagonal bipyramid is not ideally realized: there are systematic deviations from planarity for the equatorial positions. The nonbonding electron pair, E, in species such as AF_6E and AF_8E plays a dual role depending on the size of the central atom. For example, its stereochemical activity disappears if crowding of the structure becomes severe, as in BrF_6^- and XeF_8^{2-} . On the other hand, the stereochemical activity of the nonbonding pair is clearly apparent, in less crowded fluoride species such as IF_6^- as well as in the classic case of XeF_6 .

The principal geometries for molecules or ions of the type AB_2 , AB_3 , AB_4 , AB_5 , and AB_6 are well established. The most complicated case is clearly AB_5 : the trigonal-bipyramidal and square-pyramidal geometries are close in energy. In most cases involving main group compounds, the trigonal bipyramid is the dominating structure, with the square pyramid proposed as a transition state for intramolecular ligand exchange *via* the Berry mechanism. Besides a few cases for which chelating ligands enforce a square-pyramidal geometry, there are only a handful of square-pyramidal main group compounds, namely $Bi(C_6H_5)_5$ (1) and its many derivatives (1) and $Sb(C_6H_5)_5$ (2). It has become clear very recently that the highly symmetric octahedron is *not* always the principal geometry for AB_6 compounds: an exception to the rule is $W(CH_3)_6$, which possesses a trigonal prismatic structure (3).

Coordination Number 7

Keeping these facts in mind, it is immediately clear that structural preferences for compounds of the type AB_7 (and AB_8 , see below) should not be easy to predict.

0097-6156/94/0555-0056\$08.00/0
© 1994 American Chemical Society

Keperth has thoroughly analyzed the AB₇ case under the assumption that only electrostatic forces determine the structure (4). In that case, there are three limiting geometries, the pentagonal bipyramid, the monocapped octahedron, and the monocapped trigonal prism, all three of which are shown in Figure 1. The monocapped octahedron is lowest in repulsive energy, followed very closely by the other two. Furthermore, relatively small angle deformations can interconvert all three geometries. Therefore, as a function of certain deformation angles, the repulsive energy hypersurface contains the monocapped octahedron as the global minimum, with the pentagonal bipyramid and the monocapped trigonal prism as saddle points only a little above the minimum. In other words, this model predicts that AB₇ compounds should have low barriers for intramolecular ligand exchange. The compound IF₇ is the only example of a binary main group *molecule* of the type AB₇. It adopts a pentagonal-bipyramidal structure, but electron diffraction data indicate certain systematic deviations, in terms of pentagonal ring puckering, from the ideal structure in the gas phase (5). The solid state structure of IF₇ remains uncertain (6).

We have studied the question of the principal structure of AB₇ species by looking at ionic relatives of IF₇, namely the anions TeF₇⁻, (CH₃O)TeF₆⁻, (CH₃O)₂TeF₅⁻, and IOF₆⁻. The influence of lattice energy on the structures was kept at a minimum because the anions are monovalent. Furthermore, the relatively large (CH₃)₄N⁺ counterion was chosen to further minimize cation-anion interactions that might influence the structure. X-ray crystallography showed that TeF₇⁻, CH₃OTeF₆⁻, (CH₃O)₂TeF₅⁻, and IOF₆⁻ all exhibit slightly distorted pentagonal-bipyramidal geometries, as shown in Figure 2 (7,8).

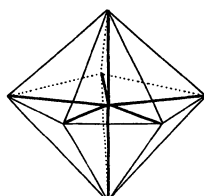
These results can be translated into rules for the geometry of seven-coordinate main group compounds:

(1) *The principal geometry is the pentagonal bipyramid.* This is against the electrostatic model. This finding indicates that among main group elements the principal geometry is always the one with highest symmetry. The pentagonal bipyramid needs only two parameters (two bond lengths) to be completely described, in comparison to five parameters for the other two geometric alternatives. This seems to be a general principle, in that it also holds for the trigonal bipyramid vs. the square pyramid as well as for the square antiprism vs. the trigonal dodecahedron (see below).

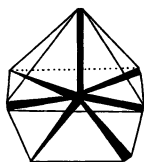
(2) *The pentagonal-bipyramidal structure is never completely ideal.* All structures show deviations in the location of the equatorial groups (i.e., pentagonal ring puckering). Most often the sequence *up, down, up, down, in plane* is observed. These distortions apparently diminish the considerable steric repulsions among the equatorial groups, which are a consequence of the very small B–A–B angles of ~72°.

(3) *Oxygen ligands, considered to be larger ligands than fluorine atoms, always occupy the sterically less crowded axial positions.*

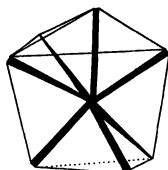
(4) *The pentagonal bipyramid undergoes intramolecular ligand exchange in solution.* This is clearly proven by the ¹⁹F and ¹²⁵Te NMR spectra of TeF₇⁻ and CH₃OTeF₆⁻, which show seven and six equivalent fluorine atoms on the NMR time scale, respectively (6). In case of (CH₃O)₂TeF₅⁻, the question of non-rigidity cannot be simply answered, since all five fluorine atoms are chemically equivalent in the observed solid-state structure. The anion IOF₆⁻ is clearly an exception, however. The doublet-sextet pattern in its ¹⁹F NMR spectrum indicates a rigid species. Most



1 : 5 : 1



1 : 4 : 2



1 : 3 : 3

Figure 1. The principal geometries of AB_7 compounds: the pentagonal bipyramid, the monocapped octahedron, and the monocapped trigonal prism.

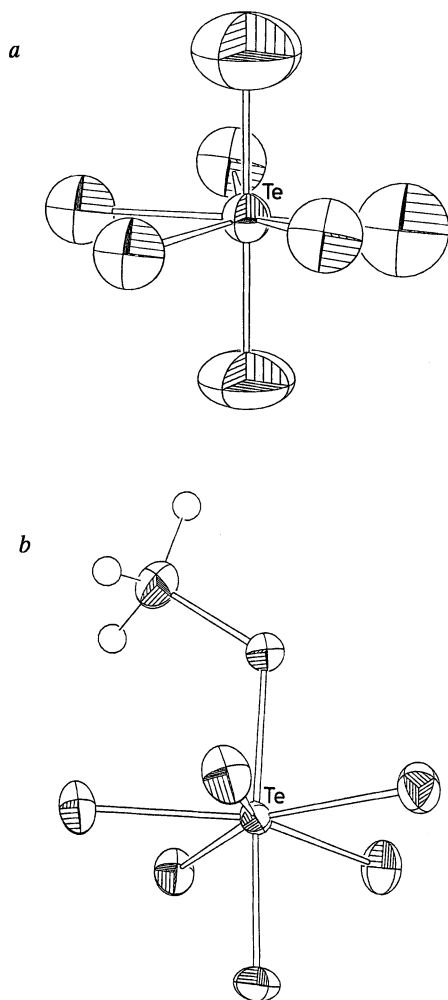
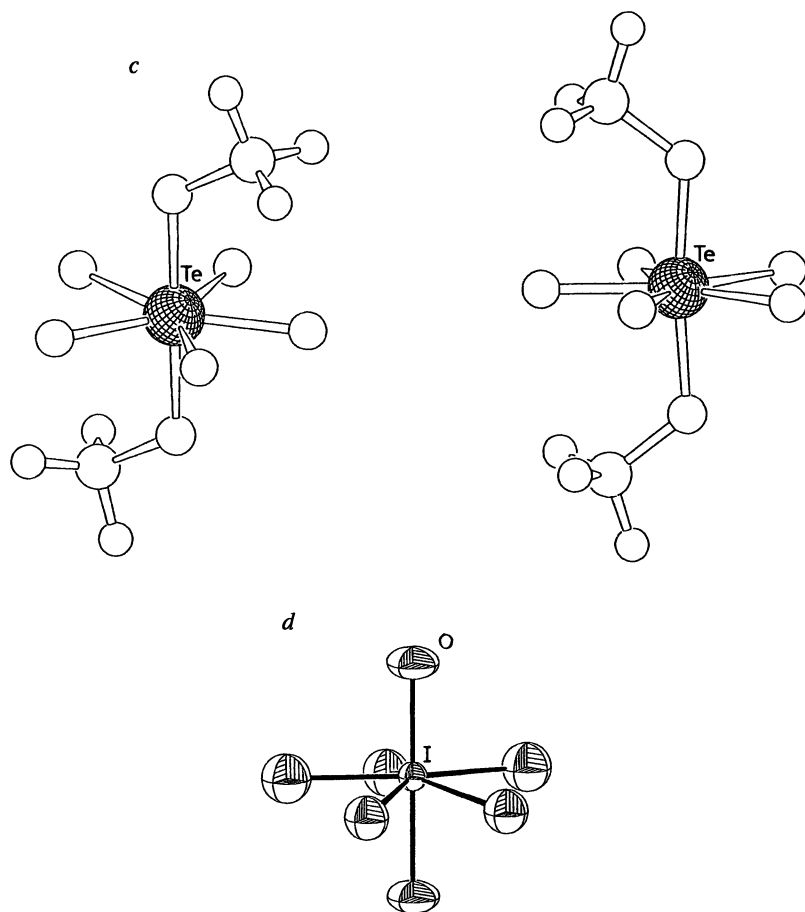


Figure 2. Crystal structures of TeF_7^- , $\text{CH}_3\text{OTeF}_6^-$, $(\text{CH}_3\text{O})_2\text{TeF}_5^-$, and IOF_6^- as examples of pentagonal bipyramids. *Continued on next page.*

Figure 2. *Continued.*

probably, the considerable double bond character of the I–O bond locks the oxygen atom into an axial position and thus prevents further intramolecular exchange (6).

The Outlook for Transition Metal Compounds. Relatively little is known about this problem among seven-coordinate transition metal complexes like ReF_7 , WF_7^- , NoF_7^- , and UF_7^- . We have crystallized the salts Cs^+WF_7^- and $\text{Cs}^+\text{MoF}_7^-$ from acetonitrile and have found that both anions exhibit a monocapped octahedral structure (9). Whether this is the result of cation-anion interactions in the cubic lattice, or whether there is a different rule governing the structures of seven-coordinate transition metal compounds, remains to be seen. Further work is in progress.

Coordination Number 8

The two principal geometries for AB_8 compounds that result from D. L. Kepert's purely electrostatic model are the square (archimedean) antiprism and the trigonal dodecahedron, as shown in Figure 3. The cube, however, is quite unfavorable (4). Chemical realizations, however, are rare. No binary material AB_8 exists for main group elements or for any transition metal; compounds such as XeF_8 and OsF_8 are unknown. We addressed the question of the principal structure for coordination number 8 by looking at anions. According to X-ray crystallographic results for $\text{NO}^+\text{IF}_8^- \cdot 2\text{NOF}$ and $(\text{CH}_3)_4\text{N}^+\text{IF}_8^-$, the IF_8^- anion exhibits a very regular square-antiprismatic structure, as shown in Figure 4 (10).

While it is not yet proper to generalize this finding, it is interesting that nature has once again chosen the more symmetric geometry. The square antiprism is defined by only two parameters, while the trigonal dodecahedron requires four. The two parameters for the square antiprism may be defined as one bond length and one angle that expresses the elongation or flatness of this geometry. In the case of IF_8^- all of the I–F bond lengths are equal. All fluorine-fluorine distances are also quite similar, independent of whether the two fluorine atoms are within one hemisphere of the anion or belong to two hemispheres. Our finding indicates that, in this case, the electrostatic model governs the geometry. Whether or not this finding will be valid for transition metal compounds remains to be seen.

High Coordination Number Species with One Nonbonding Electron Pair.

The Valence Shell Electron Pair Repulsion model correctly predicts the structures of main group compounds and d^0 transition metal compounds in most cases. The structures of less symmetric molecules can be predicted semi-quantitatively. The model is particularly successful if the coordination number (including the count of nonbonding electron pairs) does not exceed six. A peculiarity of the model is the stereochemical activity of the free electron pair. Whether the VSEPR model can be successfully extended to coordination numbers larger than 6 is the topic of the following discussion.

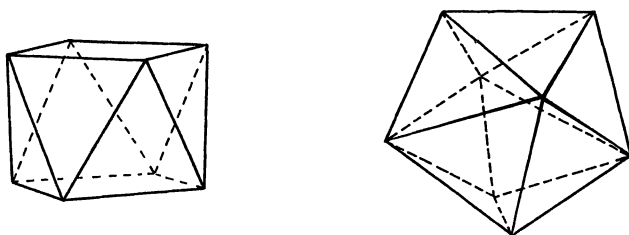


Figure 3. The principal geometries of AB_8 compounds: the square antiprism and the trigonal dodecahedron.

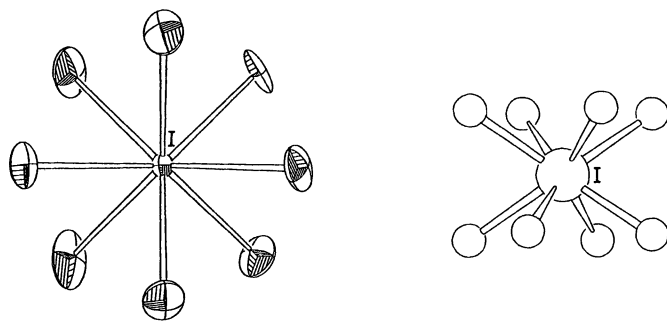


Figure 4. Crystal structure of IF_8^- as an example of a square antiprism.

A case of long dispute is the structure of XeF_6 . It is now clear that XeF_6 is not octahedral in the gas phase, having a monocapped octahedral structure in which the cap is the free electron pair. This structure undergoes, of course, rapid intramolecular ligand exchange (11). To complicate matters further, XeF_6 is tetrameric and hexameric in solid phases (12). These oligomers are composed of square pyramidal XeF_5^+ units, that are bridged by F^- ions. In solution, however, the tetramers exist as isolated non-rigid species with four magnetically equivalent xenon atoms and 24 magnetically equivalent fluorine atoms, indicating that the bridging fluorine atoms in the solid state structure cannot be left out when computing the coordination number count (13).

The question is, will this complicated structural problem be found in the structures of IF_6^- and BrF_6^- ? In the crystal structure of $(\text{CH}_3)_4\text{N}^+\text{IF}_6^-$, the IF_6^- units appear as dimer dianions (14). Each IF_6^- anion has a distorted octahedral structure; the seventh coordination site, the cap, can be thought to be occupied by the nonbonding electron pair, as shown in Figure 5. If dimer formation by two bridging fluorine atoms is overlooked, this structure is identical to the gas phase structure of XeF_6 . The bridging fluorine atoms exchange with the residual IF_5 units upon warming to room temperature. This underscores the need for low temperature crystallography as a routine method. Interestingly, by changing the cation to NO^+ , the IF_6^- anion appears as a tetramer (14). This arrangement is nearly identical to the XeF_6 tetramer, except that the bridging fluorine atoms are more regularly spaced in $(\text{IF}_6)_4^{4-}$ than in $(\text{XeF}_6)_4$. All in all, it can be said that IF_6^- is a true structural relative to XeF_6 . It is possible that with a cation larger than $(\text{CH}_3)_4\text{N}^+$, a non-bridged IF_6^- monomer will be found. Note that the iodine analogue to the non-rigid $(\text{XeF}_6)_4$ tetramer in solution has not been established.

The BrF_6^- anion, on the other hand, has a regular octahedral structure. This conclusion was reached based on X-ray crystallographic results for $\text{Cs}^+\text{BrF}_6^-$ as well as on vibrational spectroscopic results for $(\text{CH}_3)_4\text{N}^+\text{BrF}_6^-$ in the solid state and in solution (15,16). The surprising disappearance of the stereochemical activity of the nonbonding electron pair may be explained in two ways. First of all, crowding of the smaller bromine atoms (i.e., smaller relative to iodine or xenon atoms) by six fluorine atoms leaves no room for the free electron pair. Alternatively, the electron pair in BrF_6^- may occupy a centrosymmetric (but not necessarily spherically symmetric) orbital. The nonbonding electron pair has no other effect on the structure other than causing a considerable lengthening of the Br-F bonds in BrF_6^- relative to the bond lengths in BrF_6^+ . The preference for an a_{1g} orbital in BrF_6^- may be the result of the transition metal contraction: the imperfect shielding of the positive charge on the bromine nucleus by electrons in the first d -subshell increases the effective nuclear charge for centrosymmetric and inner orbitals (see Figure 6).

There is a second case in which the stereochemical activity of a nonbonding electron pair disappears, and not surprisingly, it also involves a species with a high coordination number, XeF_8^{2-} (17). The structure, determined long ago, was found to be a regular square antiprism. Interestingly, the Xe-F bond distances are longer than the I-F distances in IF_8^- , although a xenon atom is smaller than an iodine atom.

Therefore, in two separate cases the formal redox reactions $\text{BrF}_6^- \xrightleftharpoons[-2e^-]{+2e^-} \text{BrF}_6^+$ and $\text{XeF}_8^{2-} \xrightleftharpoons[-2e^-]{+2e^-} \text{IF}_8^-$ leaves the structure unchanged. Addition or subtraction

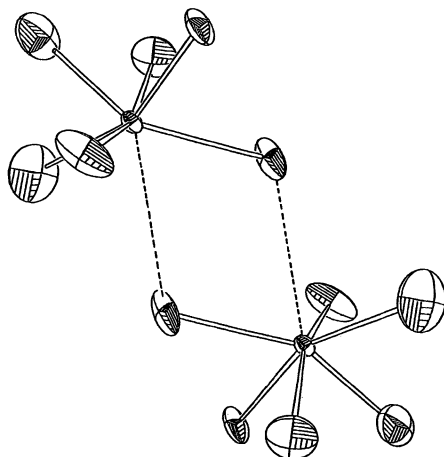


Figure 5. Crystal structures of the IF_6^- dimer.

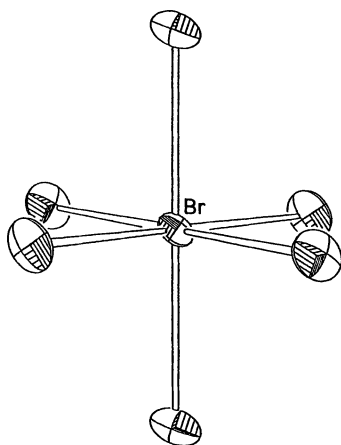


Figure 6. Crystal structure of octahedral BrF_6^- in $\text{Cs}^+\text{BrF}_6^-$.

of the two nonbonding electrons only results in a symmetric "breathing" of the entire anion.

The series XeF_5^+ , XeF_6 , XeF_8^{2-} serves as a perfect example of the gradual disappearance of the stereochemical activity of a nonbonding electron pair with increasing crowding: in XeF_5^+ , the electron pair serves as a ligand larger than fluorine, since the cation has a square-pyramidal umbrella structure; in XeF_6 (or in IF_6^-), the electron pair is stereochemically active enough to strongly disturb the octahedral geometry; in XeF_8^{2-} , however, the stereochemical activity of the electron pair is negligible. An interesting, but as yet unknown, case would be the structure of XeF_7^- .

Literature Cited

1. (a) Schmuck, A.; Buschmann, J.; Fuchs, J.; Seppelt, K. *Angew. Chem., Int. Ed. Engl.* **1987**, *26*, 1180. (b) Schmuck, A.; Leopold, D.; Wallenhauer, S.; Seppelt, K. *Chem. Ber.* **1990**, *123*, 761.
2. (a) Wheatley, P. J. *J. Chem. Soc. A* **1964**, 3718. (b) Beauchamp, A. L.; Bennett, M. J.; Cotton, F. A. *J. Am. Chem. Soc.* **1968**, *90*, 6675.
3. Haaland, A.; Hammel, A.; Rypdal, K.; Volden, H. V. *J. Am. Chem. Soc.* **1990**, *112*, 4547.
4. Kepert, D. L. *Inorganic Stereochemistry*; Springer: Berlin, 1982.
5. Adams, W. J.; Thompson, H. B.; Bartell, L. S. *J. Chem. Phys.* **1970**, *53*, 4040.
6. (a) Burbank, R. D.; Bensey, F. N. *J. Chem. Phys.* **1957**, 981. (b) Burbank, R. D. *Acta Crystallogr.* **1962**, *15*, 1207. (c) Burbank, R. D. *J. Chem. Phys.* **1963**, *16*, 700. (d) Donehue, J. *J. Chem. Phys.* **1959**, *30*, 1618.
7. Mahjoub, A.-R.; Seppelt, K. *J. Chem. Soc. Chem. Commun.* **1991**, 840.
8. Mahjoub, A.-R.; Drews, T.; Seppelt, K. *Angew. Chem., Int. Ed. Engl.* **1992**, *31*, 1036.
9. Geise, S.; Seppelt, K. Manuscript in preparation.
10. Mahjoub, A.-R.; Seppelt, K. *Angew. Chem., Int. Ed. Engl.* **1991**, *30*, 876.
11. (a) Gavin, R. M.; Bartell, L. S. *J. Chem. Phys.* **1968**, *48*, 2460. (b) Bartell, L. S.; Gavin, R. M. *ibid.* **1968**, *48*, 2466.
12. Burbank, R. D.; Jones, G. R. *J. Am. Chem. Soc.* **1974**, *96*, 43.
13. Rupp, H. H.; Seppelt, K. *Angew. Chem., Int. Ed. Engl.* **1974**, *13*, 612. (b) Seppelt, K.; Rupp, H. H. *Z. Anorg. Allg. Chem.* **1974**, *409*, 331. (b) Schrobilgen, G. J.; Holloway, J. H.; Granger, P.; Brevard, C. *Inorg. Chem.* **1977**, *17*, 980.
14. Mahjoub, A.-R.; Seppelt, K. *Angew. Chem., Int. Ed. Engl.* **1991**, *30*, 323.
15. Mahjoub, A.-R.; Hoser, A.; Fuchs, J.; Seppelt, K. *Angew. Chem., Int. Ed. Engl.* **1989**, *28*, 1526.
16. Christe, K. O.; Wilson, W. W. *Inorg. Chem.* **1989**, *28*, 3275. (b) Wilson, W. W.; Christe, K. O. *ibid.* **1989**, *28*, 4172.
17. Peterson, S. W.; Holloway, J. H.; Coyle, B. A.; Williams, J. M. *Science* **1971**, *173*, 1238.

RECEIVED May 4, 1993

Chapter 5

Heptacoordinated Main-Group Fluorides and Oxofluorides

K. O. Christe¹, E. C. Curtis¹, D. A. Dixon², H. P. A. Mercier³,
J. C. P. Sanders³, G. J. Schrobilgen³, and W. W. Wilson¹

¹Rocketdyne, Division of Rockwell International Corporation,
Canoga Park, CA 91309

²Central Research and Development, DuPont, Experimental Station,
Wilmington, DE 19880-0328

³Department of Chemistry, McMaster University, Hamilton,
Ontario L8S 4M1, Canada

The major problems associated with heptacoordination in main-group fluorides and oxofluorides have been resolved. A detailed discussion of the structures of ClF_6^- , BrF_6^- , IF_6^- , XeF_5^- , IF_7 , TeF_7^- , IOF_6^- and TeOF_6^{2-} is given. It is shown (i) that the steric activity of a free valence electron pair (E) in XF_6E species depends on the size of X; (ii) that in the XeF_5^- anion, which is the first known example of a pentagonal planar XF_5E_2 species, the two free valence electron pairs are sterically active and occupy the two axial positions; (iii) that the XF_7 and XOF_6 species possess pentagonal bipyramidal structures with five equatorial fluorine ligands which, in free molecules, are highly fluxional and dynamically distorted; (iv) that the dynamic distortion in XF_7 is the result of a rapid puckering motion of the five equatorial fluorines and of a much slower intramolecular, axial-equatorial ligand exchange; (v) that, in the XOF_6 species, this axial-equatorial ligand exchange is precluded by the more repulsive oxygen ligand which resides exclusively in one of the less congested axial positions; (vi) that, in solid $\text{N}(\text{CH}_3)_4^+\text{IOF}_6^-$, the dynamic puckering of the equatorial ligands is frozen out by hydrogen-fluorine bridges; (vii) that the pentagonal bipyramidal structures of these fluorides and oxofluorides cannot be explained by the VSEPR rules of repelling points on a sphere but are governed by the spatial distribution of the valence orbitals of the central atom; and (viii) that the bonding in these heptacoordinated species is best explained by a model involving delocalized $p_{x,y}$ hybrid orbitals of the central atom for the formation of a coplanar, semi-ionic, 6-center 10-electron bond system for the five equatorial bonds and of an sp_z hybrid orbital for the formation of two, more covalent, colinear, axial bonds; this bonding scheme can account for all the observed structural features and also the observed differences in bond lengths.

Inorganic main-group fluorides or oxofluorides offer a unique opportunity to study unusually high coordination numbers and problems associated with them, such as the steric activity of free valence electron pairs, steric crowding of the ligands, and fluxionality. Of particular interest are heptacoordinated species which could exist either

0097-6156/94/0555-0066\$08.72/0
© 1994 American Chemical Society

as a monocapped octahedron, a monocapped trigonal prism, or a pentagonal bipyramid. According to the VSEPR model of "repelling points on a sphere", the preferred structures should be the monocapped octahedron or trigonal prism (1,2). However, for main-group elements, the pentagonal bipyramid is favored (3), as found for IF_7 (4) and TeF_7^- (5-7). These pentagonal bipyramidal structures possess five-fold symmetry. Their highly congested equatorial planes result in increased equatorial bond lengths and usually some kind of puckering. The puckering of the five equatorial ligands represents a special problem. The odd number of ligands does not allow for a highly symmetric arrangement in which all five equatorial ligands can be placed into equivalent positions, i.e., with identical displacements alternately above and below the equatorial plane. This poses several interesting questions, such as: (i) are the five equatorial ligands equivalent and, if so, how is this equivalency achieved; (ii) are these molecules rigid or fluxional and, if they are fluxional, on what time scale; and (iii) what causes these heptacoordinated molecules to adopt, contrary to the VSEPR rules (1,2), pentagonal bipyramidal structures with either planar or only slightly puckered equatorial fluorines? In this paper we will give a brief review of the work recently done in our laboratories in this field which, to a large extent, was made possible by the development of a convenient preparative scale synthesis of truly anhydrous $\text{N}(\text{CH}_3)_4^+\text{F}^-$ (8) and the realization that this salt is an excellent reagent for the preparation of novel, high-oxidation state complex fluoro- or oxofluoro-anions (9,10). Furthermore, the high solubilities of these $\text{N}(\text{CH}_3)_4^+$ salts in solvents such as CH_3CN or CHF_3 permit the gathering of valuable structural information through NMR and vibrational studies and the growth of single crystals suitable for X-ray structure determinations.

XF_6E Species

Typical representatives of this structural type are the hexafluorohalate (V) anions, ClF_6^- , BrF_6^- and IF_6^- . Vibrational spectroscopy on the BrF_6^- (11,12) and IF_6^- (12,13) anions strongly indicated that BrF_6^- is octahedral while IF_6^- is strongly distorted. This was subsequently confirmed by X-ray crystal structure determinations (14,15). For ClF_6^- , only vibrational data are known (10) which show that this anion is also octahedral. These results demonstrate that in the HalF_6^- anions the steric activity of the free valence electron pair on the central atoms is governed by the size of the central atom. For the relatively large iodine atom, the maximum coordination number (CN) towards fluorine exceeds six, thus providing sufficient space for a sterically active free electron pair, whereas for the smaller bromine and chlorine atoms, the maximum CN is only six and, hence, the free valence electron pair occupies a centrosymmetric s orbital and is sterically inactive (12).

XF_5E_2 Species

Only one representative of this type is known, namely the XeF_5^- anion. The structure of this anion was established by ^{19}F and ^{129}Xe NMR and infrared and Raman spectroscopy and an X-ray crystal structure determination (16). The structure of this unique anion is shown in Figures 1 and 2 and demonstrates that the two free valence electron pairs are sterically active and, as expected from their increased repulsive character, occupy the two less congested axial positions of a pentagonal bipyramid. The chemical equivalence of the five equatorial fluorine ligands in XeF_5^- was confirmed by its ^{129}Xe NMR spectrum which displays a well-resolved binominal sextet (see Figure 3). Due to its relatively long Xe-F bonds, the XeF_5^- anion experiences only mild congestion in the equatorial plane (as shown below, the in-plane deformation force

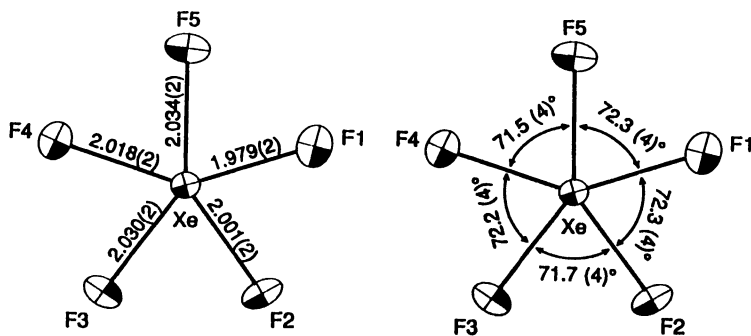


Figure 1. Atom numbering scheme, bond lengths (Å) and angles (deg) for XeF_5^- at -86°C in $[\text{N}(\text{CH}_3)_4]^+[\text{XeF}_5]^-$. Projection of the XeF_5^- anion on (111). Esd's are given in parentheses; thermal ellipsoids are shown at the 50% probability level.

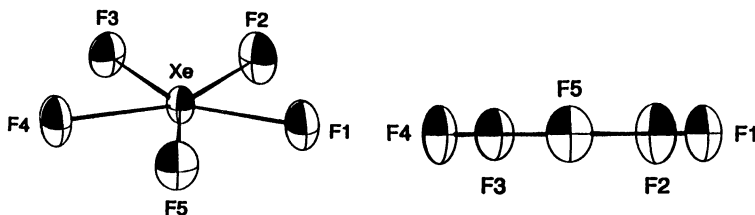


Figure 2. Projections of the XeF_5^- anion on (130) (left) and (010) (right). Thermal ellipsoids are shown at the 50% probability level.

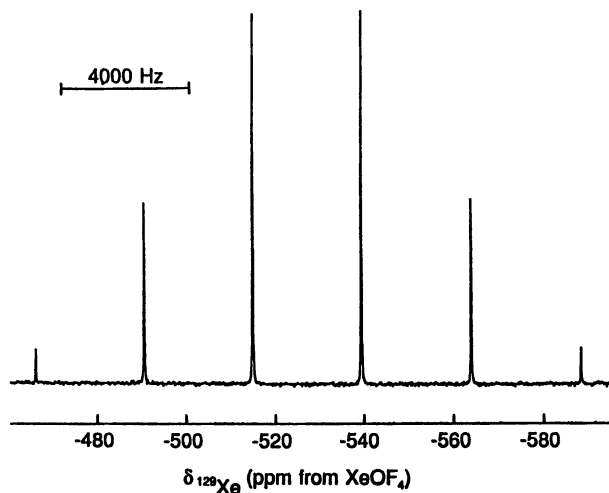


Figure 3. ^{129}Xe NMR spectrum (139.05 MHz) at 24°C of a saturated solution of $\text{N}(\text{CH}_3)_4^+\text{XeF}_5^-$ in CH_3CN containing a 1 M excess of $\text{N}-(\text{CH}_3)_4^+\text{F}^-$.

constant, f_{α} , is only 0.364 mdyn/Å) and therefore is, within experimental error, unpuckered.

XF₇ Species, IF₇

The two representatives, known for this type, are the IF₇ molecule and the TeF₇⁻ anion. Although IF₇ had been known for 61 years (17) and numerous papers dealing with its properties had been published, this molecule was only poorly understood and presented many mysteries. Since IF₇ is the prototype of a pentagonal bipyramidal, heptacoordinated species, it was imperative to better understand this molecule. The following paragraph summarizes the salient features and conclusions from the previous studies: (i) Crystal structure determinations of solid IF₇ were inconclusive due to disorder problems (18-23). (ii) In the liquid and gas phases, all seven fluorine ligands were shown to be magnetically equivalent on the time scale of NMR spectroscopy due to an intramolecular exchange of equatorial and axial fluorines (24-28). (iii) Gaseous IF₇ at room temperature does not possess a permanent dipole moment, as shown by the absence of microwave transitions (29) and of deflections in inhomogeneous electric fields (30). (iv) Gas phase electron diffraction data (4,31,32) show that IF₇ closely approaches D_{5h} symmetry with a misfit in the 2.1-2.7 Å region which is not much larger than common amplitudes of vibration. The breadth and skewing of the 2.5 Å nonbonded F_{ax...Feq} radial distribution peak were explained by an asymmetric molecule involving fluxionality and a dynamic pseudorotational ring-puckering which resulted in average displacements of 7.5° for the equatorial fluorines and of 4.5° for the axial fluorines (4). (v) At least nine studies of the vibrational spectra of IF₇ have previously been reported (33-42), and although all nine studies analyzed the observed spectra in point group D_{5h}, all sets of assignments were different and none was able either to duplicate the experimental mean square amplitudes of vibration (4) or to assign the observed infrared combination bands without violations of the D_{5h} selection rules. (vi) Results from a pseudopotential SCF-MO study (43) yielded a minimum energy structure with D_{5h} symmetry and an alternative assignment for the vibrational spectra, however, the agreement between calculated and observed frequencies was poor, and a complete vibrational spectrum was not calculated at that time due to the lack of analytic second derivative methods for pseudopotentials.

Ab Initio Calculations for IF₇. Because our results on the vibrational spectra and structures of the pentagonal planar XeF₅⁻ (16) and pentagonal bipyramidal IOF₆⁻ anions substantially differed from those (4,33-43) previously reported for pentagonal bipyramidal IF₇, ab initio calculations were carried out for IF₇ at the following levels of theory: (i) local density functional (LDF) theory with numerical functions; (ii) all electron MO calculations; and (iii) MO calculations with an effective core potential (ECP) on iodine. All three calculations resulted in a pentagonal bipyramid of D_{5h} symmetry as the lowest energy structure. The calculated geometries and vibrational frequencies are summarized in Table I and compared with the revised (see below) experimental values. Reducing the symmetry to C₂ or C₁ resulted at the LDF level in structures with only one component of the E₂^{''} mode being imaginary and having smaller values, but led to structures that were higher in energy by <0.05 kcal/mol. The remaining frequencies, excluding the E₂^{''} mode, were within 10 cm⁻¹ of those for the LDF D_{5h} structure. As can be seen from Table I, the resulting changes in the frequencies and geometries for the C₂ and C₁ structures from the D_{5h} structure are rather small and demonstrate the great similarities between the ideal D_{5h} structure and the other structures which are somewhat deformed by equatorial puckering and slight axial bending. This is in accord with the previous conclusion that the potential energy well for IF₇ at D_{5h} is very flat and shallow and has a nearly quartic contour for buckling along either a C₂ or a C_s symmetry coordinate (3). Table I shows that the effective core

Table I. Observed and Calculated Vibrational Frequencies and Geometries for IF₇

assignments and approximate mode descriptions in point group D _{5h}	obsd frequencies, cm ⁻¹			calculated frequencies, cm ⁻¹		
	IR		ECPa	SCF		LDF
	—	Ra	D _{5h}	D _{5h}	D _{5h}	C ₁
A ₁ '	v ₁ v sym XF ₂ ax	676(2)p	673	743	630	629
	v ₂ v sym XF ₅ eq	635(10)p	644	704	598	596
A ₂ ''	v ₃ v as XF ₂ ax	—	753	834	710	708
	v ₄ δ umbrella XF ₅ eq	—	368	366	304	310
E ₁ '	v ₅ v as XF ₅ eq	—	681	761	647	644
	v ₆ δ as XF ₅ in plane	—	441	454	377	375
	v ₇ δ sciss XF ₂ ax	—	265	261	213	211
E ₁ ''	v ₈ δ rock XF ₂ ax	319(0.6) ^b	320	321	259	268
	v ₉ } mixture of δ sciss XF ₅ in plane	596(0.2)	605	651	561	559
	v ₁₀ } and v as XF ₅ eq	510(1.7)	515	555	467	464
E ₂ ''	v ₁₁ δ pucker XF ₅ eq	[68] ^c	59	39	50i	41,33i
Total Energy						
Geometry		observed[4]			calculated	
	C ₂ - C _s	D _{5h}				
	r (I - F _{ax}) (Å)	1.786(7)	1.781	1.807	1.870	1.874
	r (I - F _{eq}) (Å)	1.858(4)	1.857	1.862	1.918	1.917
	average equat. puckering angle (deg)	7.5	0	0 ^d	0 ^d	4.0 ^e
	deviation of ax. bonds from 180°	4.5	0	0	0	1.7 ^e

^aThe ECP frequencies were scaled by a factor of 0.932. ^bThis frequency value was derived from the two Raman bands at 310(0.6) and 352(0.6) by correction for Fermi resonance (see text). ^cEstimated from the (v₇ + v₁₁) combination band (see text). ^dAlthough D_{5h} symmetry requires the equatorial plane in the average to be planar, the low frequency of v₁₁ combined with the large F_{ax}...F_{eq} amplitude of vibration makes the effective equatorial puckering comparable to that found for the lower symmetries (see text). ^eThe actual displacements of the five equatorial fluorines from the ideal plane in a clockwise sense were (deg): +0.35, -3.15, +6.65, -6.65, +3.25 with the axial fluorines being bent toward the equatorial fluorine with the smallest (0.35) equatorial displacement.

potential data set, after scaling by a factor of 0.932 to account for electron correlation and anharmonicity effects, duplicates best the experimental frequencies (37,40) with an average frequency deviation of only 7 cm^{-1} . This small deviation is excellent considering that the original calculated values are harmonic, gas-phase frequencies, while the observed values are anharmonic frequencies measured in some cases even in liquid or solid phases.

Raman Spectrum of Solid IF₇. A comparison between the calculated (see Table I) and previously reported (33-42) vibrational frequencies, irrespective of their detailed assignments, revealed the following general problems: (i) a Raman active mode having a predicted frequency of about 605 cm^{-1} was missing; (ii) there was one excess fundamental vibration in the $300\text{-}400\text{ cm}^{-1}$ region; and (iii) the puckering mode of the equatorial plane which should be inactive in both the Raman and infrared spectra, should have a very low frequency of about 60 cm^{-1} and be observable only indirectly in the form of combination bands.

For these reasons, the Raman spectrum of solid IF₇ was reinvestigated at different temperatures. As can be seen from Figure 4, at -142°C a distinct Raman band is observed at 596 cm^{-1} exhibiting about the right intensity for the missing equatorial IF₅ antisymmetric stretching or in-plane scissoring modes. At higher temperature, this band becomes hidden in the foot of the intense 635 cm^{-1} band due to the increased line widths. In the $300\text{-}360\text{ cm}^{-1}$ region, two fundamental vibrations had previously been identified (37) at 310 and 352 cm^{-1} . Figure 4 shows that on cooling from -13° to -142°C , the frequency separation of these two bands decreases from 42 to 29 cm^{-1} while at the same time the relative intensity of the higher frequency band decreases markedly. This behaviour is characteristic for a Fermi resonance between a fundamental vibration and a combination band where the population of the combination band decreases with decreasing temperature. Therefore, the 352 cm^{-1} Raman band does not represent a fundamental vibration. It is due (see below) to a combination band which involves the inactive equatorial ring puckering mode and confirms the predicted low frequency value of the latter.

Vibrational Assignments. In view of the above findings, the vibrational assignments for IF₇ (see Table I) can now be easily made by comparison with the calculated ECP frequencies. All bands strictly follow the selection rules for D_{5h} symmetry, $2A_1'(R) + 2A_2''(IR) + 3E_1'(IR) + 1E_1''(R) + 2E_2'(R) + 1E_2''(ia)$, and exhibit the expected relative intensities, infrared gas-phase band contours and Raman polarization. The agreement between calculated and observed frequencies (average $\Delta\nu = 7\text{ cm}^{-1}$) is excellent and supports the present assignments.

The difficulty of assigning the vibrational spectra of IF₇ without the help of reliable ab initio calculations is best reflected by the failures of the previous vibrational analyses (33-42) in which no more than four out of the eleven fundamental vibrations had been correctly assigned, a disappointing result if one considers the large number of studies and the expertise of the previous investigators. The only significant improvement over these poor results had previously been achieved by Bartell and coworkers who, with the aid of pseudopotential SCF-MO calculations, correctly located seven of the eleven fundamental vibrations and predicted the right frequency range for two additional ones (43). Most of these difficulties can be attributed to the fact that the previous investigators did not realize that the equatorial in-plane bending modes of IF₇ have such unusually high frequencies.

In several of the previous studies, the inability to assign the observed infrared combination bands of IF₇ without violations of the D_{5h} selection rules had been explained by a strong coupling between the E₂'' and E₁' modes which should make the E₂'' overtones and the pseudoradial, pseudoangular combination bands slightly infrared

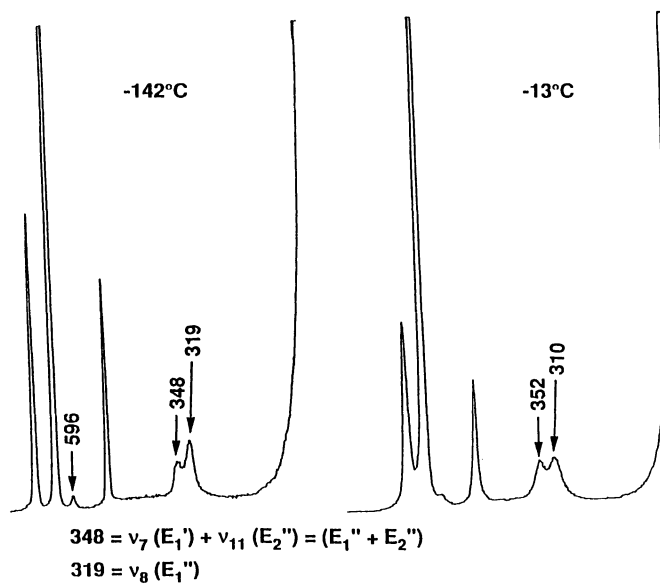


Figure 4. Raman spectra of solid IF₇ recorded at -142 and -13 °C.

active, with intensity borrowed from the induced E_1' displacements (4,40,44). The revised assignments for IF_7 given in Table I permit the assignment of all the observed infrared overtones and combination bands without any violations of the D_{5h} selection rules, thus eliminating one of the arguments previously advanced (40,43) against IF_7 having an average symmetry of D_{5h} .

The aforementioned, Raman active combination band at 352 cm^{-1} which is in Fermi resonance with $\nu_8 (E_1'')$ requires some special comment. First of all, Fermi resonance requires this band to have the same E_1'' symmetry as ν_8 ; secondly, the band cannot be assigned using any of the remaining fundamental vibrations of IF_7 ; and thirdly, there are only two fundamental vibrations, $\nu_7 (E_1')$ and $\nu_{11} (E_2'')$, that have frequencies lower than that of ν_8 . Therefore, the 352 cm^{-1} band can only be due to a combination of $\nu_7 (E_1')$ with the inactive equatorial ring puckering mode, $\nu_{11} (E_2'')$, which results in the required E_1'' symmetry for the ensuing combination band. After a correction for the Fermi resonance induced frequency shift (45), a frequency of about 68 cm^{-1} is obtained for the ring puckering mode, ν_{11} , which is in good agreement with the value of 59 cm^{-1} predicted by our ECP calculations. Furthermore, this [$\nu_7 (E_1') + \nu_{11} (E_2'')$] combination band represents the mode proposed (4,43) by Bartell for the pseudorotation in IF_7 .

Force Constants and Mean Square Amplitudes of Vibration. Another problem in the previous IF_7 studies (33-43) was the discrepancy between the mean square amplitudes of vibration from the electron diffraction study (4) and those derived from normal coordinate analyses of the vibrational spectra. Since all the previous normal coordinate analyses for IF_7 had been carried out with partially incorrect assignments, such an analysis was repeated using our ab initio (ECP) force field. Inspection of the internal force constants of IF_7 (see Table II) reveals several interesting features: (i) the stretching force constant of the axial bonds, f_D , is considerably larger than that of the equatorial bonds, as expected from the observed bond lengths (4) and general valence shell electron pair repulsion (VSEPR) arguments (1,2) which attribute the longer equatorial bonds to the congestion and increased mutual repulsion of the ligands in the equatorial plane. The absolute value of f_D , 5.01 mdyn/\AA , is lower than that of 5.42 mdyn/\AA previously found for the IF_6^+ cation (46), as expected for going from a fluorocation to its parent molecule, and (ii) the values of the equatorial angle deformation constants, f_α and f_β , exhibit a huge difference. As expected, the in-plane deformation, f_α , is very large (0.84 mdyn/\AA) due to the severe crowding in the equatorial plane, while the out-of-plane deformation, f_β , is very small (0.16 mdyn/\AA) because of the ease of equatorial ring puckering. These force constants lend strong support to our model of the bonding and fluxionality in IF_7 (see below).

The previous electron diffraction study (4) had resulted in two different sets of mean square amplitudes of vibration which, depending on the choice of the structural model, strongly differed in their value for the nonbonded $\ell(F_{ax}\cdots F_{eq})$ amplitude. For a static D_{5h} model, this amplitude had a value of 0.169 \AA , whereas for the statically or dynamically distorted C_2 , (50% $C_2 + 50\%$ C_s), or C_s models values ranging from 0.104 to 0.107 \AA were obtained. Since the analysis of the vibrational spectra provides an independent experimental set of mean square amplitudes for IF_7 , this set can be used to distinguish between the two structural models which were proposed (4) on the basis of the electron diffraction data. As can be seen from Table III, the mean square amplitudes from the vibrational spectra are in good agreement with the D_{5h} but not the other models. It must be kept in mind, however, that the unusually large vibrational amplitude of 0.16 \AA for $\ell(F_{ax}\cdots F_{eq})$ in the D_{5h} model corresponds to a 6.9° displacement of a fluorine ligand from the equatorial plane and is very close to the

average equatorial puckering angle of 7.5° deduced from the electron diffraction data for the distorted models (4). The good agreement between the mean square amplitudes of vibration, derived from our force field, and those deduced for the D_{5h} model from the electron diffraction data (4), is very gratifying and attests to the correctness of our revised assignments.

Table II. Internal Force Constants^a (mdyn/Å)^b of IF₇

$f_D = 5.005$	$f_\beta = 0.163$
$f_{DD} = 0.058$	$f_{\beta\beta} = 0.078$
$f_{Dd} = -0.0018$	$f_{\beta\beta'} = -0.042$
$f_d = 3.947$	$f_{\beta\beta''} = -0.038$
$f_{dd} = 0.326$	$f_{\beta\beta'''} = -0.044$
$f_{dd'} = 0.0265$	$f_{\beta\beta''''} = -0.058$
$f_\alpha = 0.841$	$f_{d\beta} = 0.090$
$f_{\alpha\alpha} = -0.187$	$f_{d\beta'} \equiv f_{d\beta''} \equiv 0$
$f_{\alpha\alpha'} = -0.243$	$f_{\alpha\beta} \equiv f_{\alpha\beta'} \equiv -f_{\alpha\beta''} = -0.021$
$f_{d\alpha} \equiv f_{d\alpha'} \equiv -f_{d\alpha''} = -0.238$	$f_{D\beta} \equiv -f_{D\beta'} = 0.042$

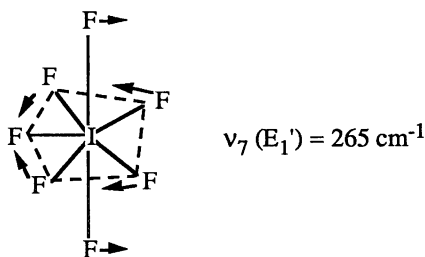
^a $D = IF_{ax}$, $d = IF_{eq}$, $\alpha = \nabla F_{eq}IF_{eq}$, $\beta = \nabla F_{ax}IF_{eq}$, $dd =$ coupling to adjacent d , $dd' =$ coupling to opposite d , $\alpha\alpha =$ adjacent α , $\alpha\alpha' =$ opposite α , $d\alpha = \alpha$ opposite to d , $d\alpha' =$ remote α , $d\alpha'' =$ adjoining α , $\beta\beta =$ common D and adjoining d , $\beta\beta' =$ noncommon D and common d , $\beta\beta'' =$ common D and remote d , $\beta\beta''' =$ noncommon D and adjoining d , $\beta\beta'''' =$ noncommon D and remote d , $d\beta =$ common d , $d\beta' =$ adjoining d , $d\beta'' =$ remote d , $\alpha\beta =$ opposite d , $\alpha\beta' =$ adjoining d , $\alpha\beta'' =$ common d , $D\beta =$ common D , $D\beta' =$ opposite D . ^bThe internal force constants have been normalized for distance assuming $D = 1.781\text{Å}$ and $d = 1.857\text{Å}$.

Table III. Comparison of the Mean Square Amplitudes (Å) of Vibration of IF₇ Obtained from the Vibrational Spectra with Those Derived from the Electron Diffraction Study under the Assumption of Different Structural Models

	Vibrational Spectra (D_{5h})	Electron Diffraction ⁵	
		D_{5h}	50% C_2 - 50% C_s
$\ell(I \dots F_{ax})$	0.039	0.042 ^a	0.043±0.003
$\ell(I \dots F_{eq})$	0.043	0.044	0.045±0.003
$\ell(F_{eq} \dots F_{eq})$ short	0.061	0.061	0.061±0.005
$\ell(F_{eq} \dots F_{eq})$ long	0.060	0.093 ^b	0.091 ^b ±0.006
$\ell(F_{ax} \dots F_{ax})$	0.053		
$\ell(F_{eq} \dots F_{ax})$	0.163	0.169	0.106±0.008

^aObtained from constraint $\ell(I \dots F_{ax}) = \ell(I \dots F_{eq}) - 0.002\text{Å}$. ^bOverlapping peak which could not be resolved into its two components.

Axial-Equatorial Ligand Exchange. In addition to the above described very fast, dynamic puckering of the pentagonal equatorial fluorine plane which requires very little energy ($\nu_{11} = 59 \text{ cm}^{-1} = 0.17 \text{ kcal mol}^{-1}$) and hence is thermally populated at higher vibrational levels even at low temperatures, a second type of fluxionality is possible for IF_7 . This second type of fluxionality involves an intramolecular exchange of axial and equatorial fluorines. This was shown by the magnetic equivalence of all seven fluorine ligands of IF_7 (24-28) or the isoelectronic TeF_7^- anion (6,7) on the NMR time scale. This exchange process, with an estimated (27) lifetime of a given configuration of $\sim 2.5 \times 10^{-3} \text{ sec}$, is considerably slower than that for ring puckering and involves higher vibrational levels of ν_7 (E_1'). This motion can best be described as an antisymmetric combination of the axial and equatorial bending symmetry coordinates, S_6 and S_7 , which is accompanied by an out-of-plane twisting motion of the three remote equatorial fluorine ligands.



This axial-equatorial exchange mechanism is analogous to that previously proposed by Berry (47) for trigonal bipyramidal molecules, such as PF_5 or SF_4 , and involves a substantial energy barrier of several vibrational levels of ν_7 .

Structure and Bonding of IF_7 . Whereas the results of the ab initio calculations, the microwave study and the normal coordinate analysis are best interpreted in terms of a structural model of average D_{5h} symmetry that undergoes a rapid dynamic puckering of the equatorial plane with very large vibrational amplitudes, the previous electron diffraction data (4) favored a pseudorotational C_2-C_3 model with an equilibrium structure that is distorted from D_{5h} symmetry. The question then arises whether one of these seemingly different models is incorrect or if the differences are only due to the semantics of how to best describe a highly fluxional and dynamically distorted molecule.

First of all, one must understand what type of information can be gained from the different methods of investigation. Electron diffraction results generally describe the average structure of vibrating molecules and not the minimum energy geometries (48). If a highly fluxional molecule, such as IF_7 , undergoes a large dynamic distortion at low energy, then electron diffraction will only see a distorted molecule. A classic example for such a case is the linear CO_2 molecule which, according to its electron diffraction data, would be bent because in the vibrating molecule the average nonbonded $\text{O}\cdots\text{O}$ distance becomes shorter than twice the bonded $\text{C}-\text{O}$ distance (48). Returning to the electron diffraction data for IF_7 , the conclusions (4,43) reached by Bartell and coworkers are compelling by their logic and thoroughness. The plane of the five equatorial fluorines of IF_7 is highly congested. This congestion can be relieved by a large-amplitude, dynamic puckering. For a five-fold symmetry, the five ligands cannot be displaced from the equatorial plane in a manner which renders them at any given time equivalent and equidistant from the ideal equatorial plane as shown by the previously published (4) geometries of the C_2 or C_3 models of IF_7 . As a consequence of these

uneven equatorial ligand displacements, the axial ligands experience an uneven repulsion from the equatorial plane and will bend away from those ligands which exhibit the largest displacements from the equatorial plane (1). Since the experimental evidence overwhelmingly suggests that all the equatorial ligands are equivalent, a rapid dynamic pseudorotation of the puckering motion must be invoked which is phase-coupled to a precession of the slightly bent axial FIF group (i.e., Bartell's pseudorotational model) (4). Due to the short time scale of the electron diffraction technique, it detects at all times a distorted IF₇ molecule that exhibits a strong and uneven equatorial puckering and as a consequence also an axial bend which results in an equilibrium symmetry lower than D_{5h}.

On the other hand, ab initio calculations and vibrational spectroscopy generally describe the symmetry of the minimum energy geometry which for IF₇ would be D_{5h} if the distortions are only dynamic in nature and not static. Although the knowledge of the exact potential energy curve of IF₇ would be desirable to distinguish between a distorted and an undistorted ground state configuration, the absence of a permanent dipole moment (30) and microwave transitions (29) and the results from this study strongly favor an undistorted D_{5h} ground state which undergoes facile dynamic distortion, most likely by Bartell's pseudorotation mechanism (4). This signifies that both the D_{5h} and the dynamically distorted model descriptions for IF₇ are, in principal, correct because they describe different time domains. The undistorted D_{5h} model describes the nonvibrating ground state whereas the distorted, dynamically puckered, pseudorotational model depicts the vibrating molecule.

Corroborating evidence that heptacoordinated molecules, with either fluorine, oxygen or free valence electron pairs as ligands, possess in their ground states pentagonal bipyramidal structures with an unpuckered equatorial plane, comes from ongoing ab initio calculations and two X-ray crystal structure determinations. It has experimentally been shown that in XeF₅⁻, in which the longer Xe-F bond distances of 1.979(2)-2.034(2)Å lessen the equatorial ligand-ligand repulsions ($f_{\alpha} = 0.364$ mdyn/Å), the equatorial fluorines are essentially coplanar (16). It has also been shown (see below) that in IOF₆⁻ ($f_{\alpha} = 0.690$ mdyn/Å), which has considerably shorter (1.88Å) equatorial bonds than XeF₅⁻, the equatorial fluorines are puckered, but that with decreasing temperature the degree of puckering strongly decreases (49).

The fact that heptacoordinated species in their ground states exhibit pentagonal bipyramidal structures with an unpuckered equatorial plane, cannot be rationalized by VSEPR theory (1,2) in terms of a "repelling points on a sphere" (POS) model which should result in either a monocapped octahedron or a monocapped trigonal prism. Furthermore, it cannot be explained by conventional bonding schemes involving localized electron orbitals of the central atom to enforce the coplanarity of a central atom and five equatorial ligands. The best explanation to account for this planarity is the bonding scheme first proposed (16) for XeF₅⁻ based on an ab initio calculation of the molecular orbital population. In this scheme, the structure and bonding of XeF₅⁻ are explained by a simple model derived from XeF₄. The bonding in the square planar XeF₄ can be described by two semi-ionic, 3-center 4-electron (3c-4e) bonds (50-52) for the four Xe-F bonds and two lone valence electron pairs on Xe ($s^2p_z^2$ hybrids). The 3c-4e bonds involve the p_x^2 and p_y^2 orbitals of xenon. Addition of an F⁻ ion to the equatorial plane in XeF₄ results in pentagonal planar XeF₅⁻ and the formation of a semi-ionic, 6-center 10-electron (6c-10e) bond involving the delocalized $p_x^2p_y^2$ hybrid orbitals of Xe and 6 electrons on the 5 F ligands (16). The two lone valence electron pairs on Xe in XeF₅⁻ are analogous to those in XeF₄.

The planar IF₅ fragment of IF₇ has essentially the same bonding as XeF₅⁻, as shown by the atomic population calculations given in Table IV. As expected for the

Table IV. Atomic Populations (e) in the Valence Electron Orbitals and Total Charge Distributions for XeF₅⁻, IF₇ and IOF₆^{-a}

<i>Central Atom</i>				
	<i>XeF₅⁻</i>	<i>IF₇</i>	<i>IOF₆⁻</i>	
s	2.22	1.35	1.43	
p _x = p _y	0.61	0.64	0.64	
p _z	2.02	0.60	0.71	
d _z ²	0.03	0.11	0.14	
d _x ² = d _y ²	0.06	0.12	0.09	
d _{xy}	0.14	0.20	0.16	
d _{xz} = d _{yz}	0.04	0.14	0.15	
d total	0.37	0.83	0.78	
<i>Equatorial Fluorines</i>				
s	1.98	1.93	1.94	
p bond	1.70	1.57	1.64	
p in plane	1.98	1.96	1.97	
p _z	1.97	1.94	1.95	
d	0	0.03	0.02	
<i>Axial Fluorines and Oxygens</i>				
			<i>F</i>	<i>O</i>
s	—	1.92	1.92	1.86
p _z	—	1.54	1.57	1.16
p _x = p _y	—	1.94	1.95	1.83
d	—	0.04	0.03	0.04
<i>Total Charges</i>				
Central Atom	2.15	2.94	2.81	
F _{eq}	-0.63	-0.43	-0.53	
F _{ax}	—	-0.39	-0.44	
O _{ax}	—	—	-0.74	

^aThe Z axis is the five-fold axis.

replacement of two free valence electron pairs on the central atom by two bonded ligands, each of which contributes one electron to its bond, the population of the s² and p_z² orbitals of I in IF₇ has decreased by about two electrons, compared to XeF₄ and XeF₅⁻. The higher oxidation state of the central atom in IF₇ (+VII) results in I having a higher positive charge than Xe (+IV) in XeF₅⁻. This causes the effective electronegativity difference between the central atom and the ligands in IF₇ to be smaller than those in XeF₄ and XeF₅⁻ and results in an increased covalency and a shortening of

the central atom-fluorine bonds. Furthermore, the axial fluorine ligands in IF_7 carry less of a negative charge than the equatorial ones and their bonds have higher s-character which accounts for the axial I-F bonds to be shorter than the equatorial ones.

Of course, the above model does not account for the fact that the electrons will try to minimize their mutual repulsions and occupy all of the available orbitals to do so. This results in the participation of some d functions. Although we are not proposing a d hybridization model, the population in the d orbitals does suggest a redistribution into these orbitals beyond that expected if the d orbitals were acting solely as polarization functions.

The above atomic population and total charge distribution analysis qualitatively confirms our simple bonding model for pentagonal bipyramidal molecules. This model involves the use of delocalized p_x^2 and p_y^2 hybrid orbitals of the central atom for the formation of a semi-ionic, 6c-10e bond with the five equatorial ligands and of an sp_z hybrid orbital for the formation of two, more covalent, axial bonds. This bonding scheme can account for all the observed structural features and also the observed bond length differences. The planarity of the p_x^2 and p_y^2 hybrid orbitals of the central atom also provides the explanation why the heptacoordinated main-group fluorides prefer pentagonal-bipyramidal structures and not the monocapped octahedral or trigonal prismatic ones expected from VSEPR arguments (1,2).

The possible puckering of the equatorial plane in pentagonal bipyramidal molecules is due to the high degree of congestion in this plane. In XeF_5^- ($r_{\text{XeF}} \approx 2.00 \text{ \AA}$) (16), the congestion is relatively low and, therefore, the anion is still planar, whereas the considerably shorter equatorial I-F bonds ($r = 1.857 \text{ \AA}$) (4) in IF_7 result in increased repulsion and significant dynamic puckering.

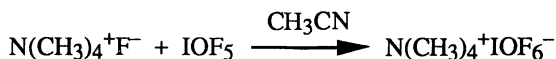
XF_7 Species, TeF_7^-

The structure of the TeF_7^- anion which is isoelectronic with IF_7 was shown by ^{19}F NMR and vibrational spectroscopy to be analogous to that of IF_7 (6,7). The ^{125}Te NMR spectrum (see Figure 5) of TeF_7^- in CH_3CN solution demonstrated that on the NMR time scale all seven fluorine ligands are chemically equivalent and, therefore, the free TeF_7^- anion is fluxional. The pentagonal bipyramidal structure of TeF_7^- has also been recently confirmed by the results from an X-ray crystal structure determination (53) and, hence, does not require any further discussion.

XOF_6 Species

Two isoelectronic anions, IOF_6^- and TeOF_6^{2-} , have been prepared (6,7) and are the only known main-group representatives of this structural type. Of the two, the IOF_6^- has been fully characterized by ab initio calculations, NMR and vibrational spectroscopy and an X-ray crystal structure determination, while for TeOF_6^{2-} only the vibrational spectra are known.

Synthesis and Properties of $\text{N}(\text{CH}_3)_4^+\text{IOF}_6^-$. This salt was prepared according to



and is a very pale yellow solid which is thermally stable up to about 137°C where it starts to decompose to IOF_4^- , CF_4 and COF_2 as the major products. Its crystal

structure consists of well separated $\text{N}(\text{CH}_3)_4^+$ and IOF_6^- ions. The packing of the ions (see Figure 6) can be described as a cubic close packing of alternating layers of IOF_6^- anions and $\text{N}(\text{CH}_3)_4^+$ cations in which the alternating orientation of the tetrahedral cations results in a cuboctahedral (54) unit cell with $Z = 2$. While the cation is perfectly ordered with the expected bond lengths, the IOF_6^- anion is subject to a positional four-fold disorder in the equatorial plane. The model results from the superposition of four anions in which the central I atom and the axial O and F(1) atoms occupy identical positions. One of these anions is shown in Figure 7. There are no significant contacts to iodine other than the directly bonded oxygen and six fluorine ligands, and the anion exhibits a gross pentagonal bipyramidal geometry. The O-I-F_{ax} angle is constrained by symmetry to be 180° , while there are no constraints on the positions of the equatorial fluorines. The equatorial fluorines are bent away from the axial oxygen ligand, as expected for a doubly bonded oxygen being more repulsive than a singly bonded fluorine ligand (2).

The I-O bond length (1.75-1.77 Å) indicates significant double bond character for the I-O bond (55-60). Its temperature dependence will be discussed below. The greater I-O bond length in IOF_6^- , when compared with that in IOF_5 [1.715(4) Å] (55), is consistent with the placement of some of the negative charge on oxygen, thereby increasing the polarity and decreasing the bond order of the I-O bond. The axial I-F bond [1.823(3) Å] is, within experimental error ($\pm 3\sigma$), significantly shorter than all of the equatorial I-F bonds (average 1.88 Å), and both types of I-F bonds in IOF_6^- are significantly longer than the corresponding bonds in IF_7 [1.786(7) Å and 1.858(4) Å, respectively] (4). These differences can be attributed again to the formal negative

charge on IOF_6^- , which leads to greater $\delta^+ \delta^-$ I-F bond polarities and consequently longer bonds. The greater length of the equatorial bonds in IOF_6^- and IF_7 relative to their axial ones is due to the increased mutual repulsion of the fluorine ligands in the highly congested equatorial plane and their higher ionicity.

Nature of the Equatorial Puckering in IOF_6^- . As mentioned above, the equatorial fluorine atoms in IOF_6^- are bent away from the doubly bonded oxygen atom by about 5° . Furthermore, the plane of the equatorial fluorine atoms is puckered and its I-F bonds are elongated in order to lessen the high degree of ligand-ligand repulsion encountered for these fluorines. Contrary to the rapid dynamic puckering in free, pentagonal bipyramidal molecules, such as IF_7 (see above), the puckering in solid $\text{N}(\text{CH}_3)_4^+\text{IOF}_6^-$ is frozen out by hydrogen...fluorine bridging between the two F(2) atoms of IOF_6^- and hydrogen atoms from two different cations. This bridging results in two close F...C contacts of 3.175(9) Å and 3.271(9) Å, while the remaining closest F...C contacts occur at 3.317(9), 3.473(9) and 3.416(9) Å and are very close to the accepted sum of the van der Waals radii of CH_3 (2.00 Å) (61) and F (1.35-1.40 Å) (61,62) which is 3.35-3.40 Å.

A pentagonal plane can be puckered in two ways resulting in structures of either C_s or C_2 symmetry, respectively.



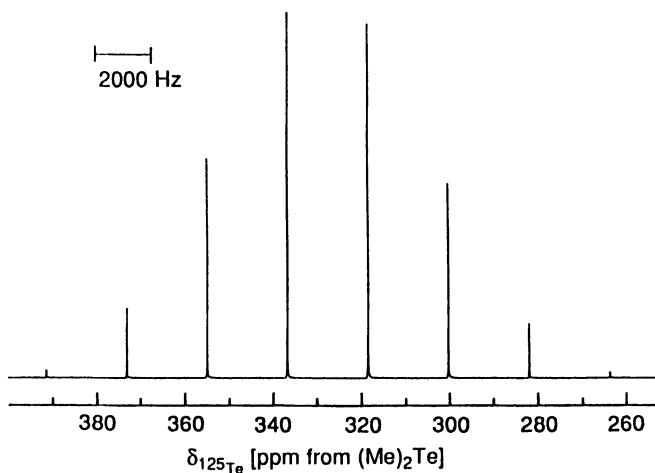


Figure 5. The ^{125}Te NMR spectrum of $\text{N}(\text{Me})_4^+\text{TeF}_6^-$ recorded at 157.792 MHz in MeCN solvent at 30 °C.

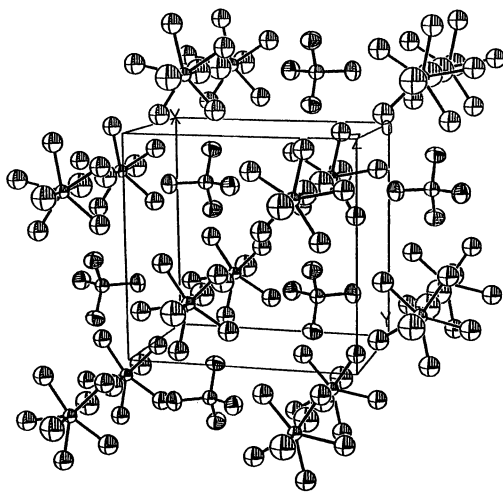
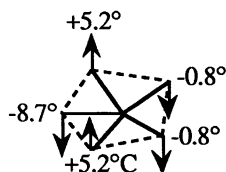


Figure 6. Packing diagram of $\text{N}(\text{CH}_3)_4^+\text{IOF}_6^-$ viewed along the c -axis.

As mentioned above, the doubly bonded, axial oxygen ligand in IOF_6^- is more repulsive than the singly bonded, axial fluorine ligand. Therefore, the average equatorial plane, which can be defined as a plane perpendicular to the O-I-F_{ax} axis containing all five equatorial fluorine ligands at the averaged F_{eq}-I-O bond angle, drops below the center of the iodine atom. As can be seen from Figure 7, the puckered plane of IOF_6^- definitely exhibits C₃ symmetry with the following out of plane displacements.



^{19}F NMR Spectrum of the IOF_6^- Anion. The ^{19}F NMR spectrum of $\text{N}(\text{CH}_3)_4^+\text{IOF}_6^-$ was recorded at -40°C in CH_3CN solution and is in agreement with a pentagonal bipyramidal structure for the IOF_6^- anion. This structure is expected to have an average C_{5v} point group symmetry with the oxygen in the axial position. Accordingly, the ^{19}F NMR spectrum (Figure 8) displays a broad doublet ($\Delta\nu_{1/2} \approx 170$ Hz) at 166.0 ppm, assigned to the equatorial fluorines, and a broad binomial sextet ($\Delta\nu_{1/2} \approx 360$ Hz) at 111.1 ppm, assigned to the axial fluorine trans to oxygen. The observation of separate ^{19}F resonances for the axial and equatorial ligand environments of IOF_6^- is unusual for a pentagonal bipyramidal species and demonstrates that the IOF_6^- anion does not undergo intramolecular ligand exchange (i.e., pseudorotation) in solution, in contrast with the related TeF_7^- anion (6,7) and IF_7 molecule (see above). This is not surprising because any plausible intermediate in the pseudorotation process for IOF_6^- would require the doubly bonded oxygen ligand to move into an equatorial position. The greater space requirement of the oxygen double bond domain, compared with that of a fluorine single bond domain, would render the placement of the oxygen ligand in the more sterically crowded equatorial position energetically unfavorable, thereby creating a high activation barrier for the process. Although the X-ray crystal structure reveals that, in the solid state, the equatorial fluorine ligands of the IOF_6^- anion are unevenly puckered, only a single resonance is observed for these ligands in the ^{19}F NMR spectrum of the solution. Clearly, the puckering, which is frozen out in the solid state, becomes a dynamic process in solution which is fast on the NMR time scale.

Vibrational Spectra. The infrared and Raman spectra of solid $\text{N}(\text{CH}_3)_4^+\text{IOF}_6^-$ and the Raman spectra of its CH_3CN solution were recorded and are shown in Figure 9. A comparison of the observed and calculated (see below) frequencies of IOF_6^- with those of the closely related pentagonal IF_7 molecule (see above) and XeF_5^- anion (16), together with their approximate mode descriptions, are given in Table V. After subtraction of the well known (8,61) bands of the $\text{N}(\text{CH}_3)_4^+$ cation, the remaining bands, which are due to IOF_6^- , can be readily assigned based on the data given in Table V. Since the vibrational spectra of IOF_6^- in solid $\text{N}(\text{CH}_3)_4^+\text{IOF}_6^-$ do not appear to be noticeably affected by the slight equatorial puckering, they were assigned (see Table V) in point group C_{5v} which is the lowest energy structure of the free anion (see below).

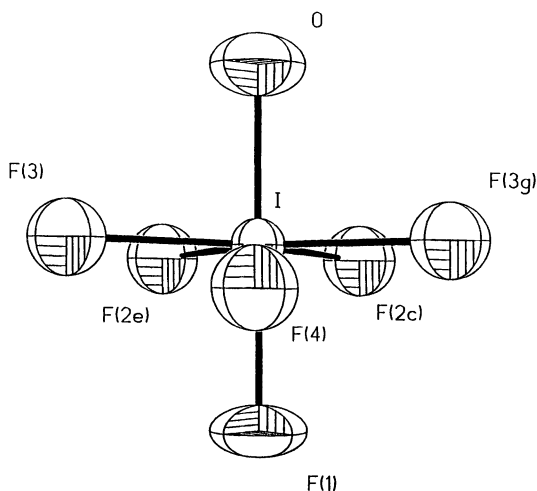


Figure 7. The structure of the IOF_6^- anion showing the puckering pattern of the equatorial fluorine ligands.

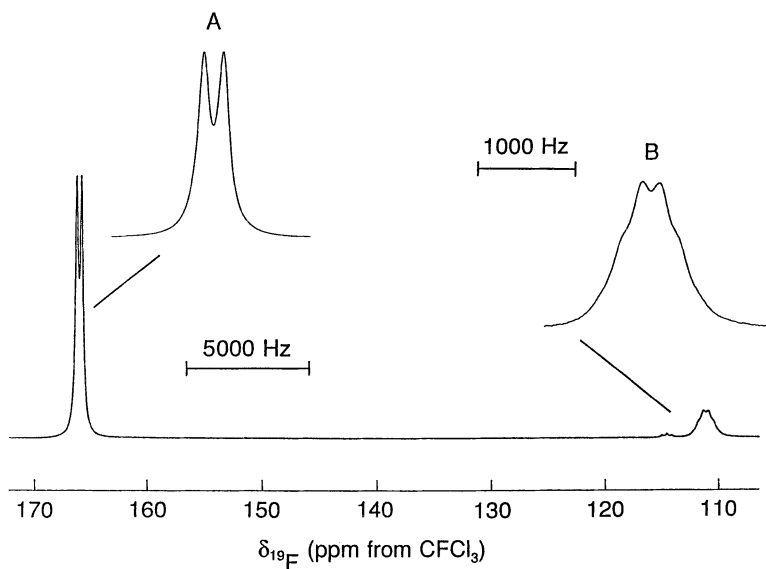


Figure 8. The ^{19}F NMR spectrum (470.599 MHz) of a saturated solution of $\text{N}(\text{CH}_3)_4^+ \text{IOF}_6^-$ in CH_3CN at -40°C . (A) F_{eq} environment of ; (B) F_{ax} environment of IOF_6^- .

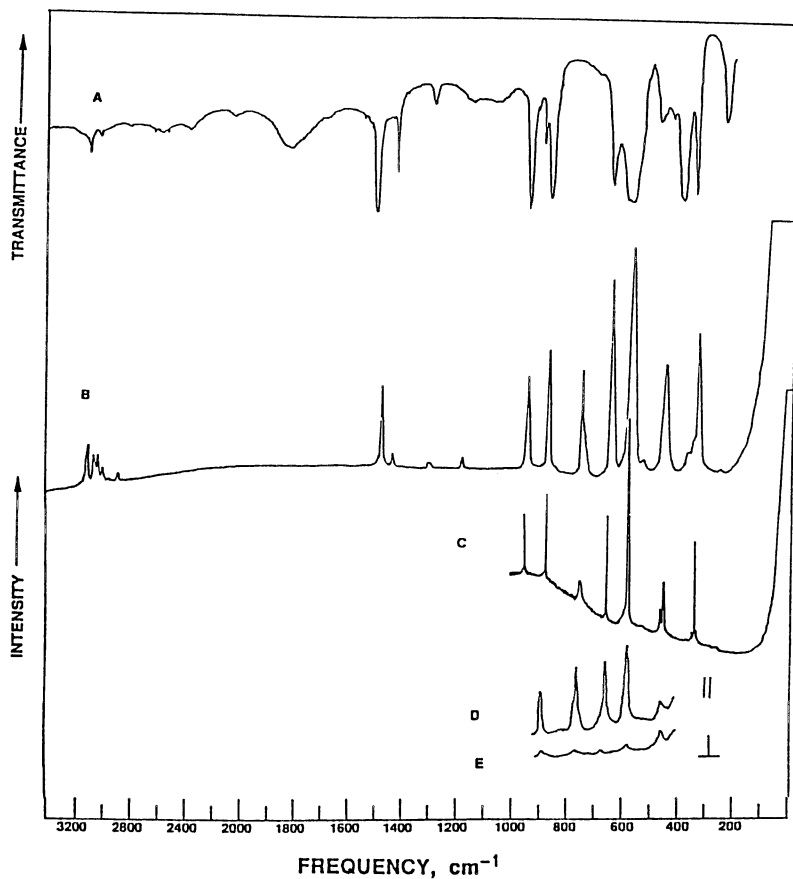


Figure 9. Vibrational spectra of $N(CH_3)_4^+IOF_6^-$. Trace A, infrared spectrum of the solid as an AgBr disk; traces B and C, Raman spectra of the solid at 25 and -146 °C; traces D and E, Raman spectra of the CH_3CN solution with parallel and perpendicular polarization, respectively.

Table V. Comparison of Observed and Calculated Frequencies of IOF₅, IF₅, and XeF₅, Together with Their Approximate Mode Descriptions

IOF ₅ (C _{2v})			IF ₅ (D _{3h}) ^a			XeF ₅ (D _{3h})					
assign- ment	approximate mode description	obsd freq, cm ⁻¹ , int (IR, Ra)	calcd freq, cm ⁻¹	assign- ment	approximate mode description	obsd freq, cm ⁻¹ , int (IR, Ra)	calcd freq, cm ⁻¹	assign- ment	approximate mode description	obsd freq, cm ⁻¹ , int (IR, Ra) ^f	calcd freq, cm ⁻¹
			ECP ^a				ECP ^c				ECP ^d
		LDF			LDF				LDF		
A ₁ v ₁	ν ₁ =O	873 (vs, 53p)	860 ^b	ν ₃ (A ₂ '')	v as IF ₂ ax	746 (s, -)	733	—	—	—	—
v ₂	ν ₁ F _{ax}	649 (s, 88p)	625	ν ₁ (A ₁ ')	v sym IF ₂ ax	676 (-20p)	673	—	—	—	—
v ₃	v sym IF ₅	584 (vs, 100p)	566	ν ₂ (A ₁ ')	v sym IF ₅	635 (-100p)	644	ν ₁ (A ₁ ')	v sym XeF ₅	502 (-100)	498
v ₄	δ umbrella IF ₅	359 (s, 4)	371	ν ₄ (A ₂ '')	δ umbrella IF ₅	365 (s, -)	368	ν ₂ (A ₂ '')	δ umbrella XeF ₅	290 (m, sh, -)	301
E ₁ v ₅	v as IF ₅	585 (vs, ν ₃)	583	ν ₅ (E ₁)	v as IF ₅	670 (vs, -)	681	ν ₃ (E ₁)	v as XeF ₅	450 (vs, -)	449
v ₆	δ as IF ₅ in plane	405 (vs, -)	415	ν ₆ (E ₁)	δ as IF ₅ in plane	425 (vs, -)	441	ν ₄ (E ₁)	δ as XeF ₅ in plane	274 (s, -)	273
v ₇	δ rock O=L-F _{ax}	341 (-62)	340	ν ₈ (E ₁ '')	δ rock IF ₂ ax	319 (-6)	320	ν ₅ (E ₂)	v as XeF ₅	423 (-16)	420
v ₈	δ sciss O=L-F _{ax}	260 (s, 2)	273	ν ₇ (E ₁)	δ sciss IF ₂ ax	257 (w, -)	265	ν ₆ (E ₂)	δ sciss XeF ₅ in-plane	377 (-23)	373
E ₂ v ₉	δ sciss IF ₅ in plane	530 (-4)	530	ν ₉ (E ₂)	mixture of δ sciss	596 (-2)	605	ν ₇ (E ₂ '')	δ pucker XeF ₅	n. obsd	105
v ₁₀	v as IF ₅	457 (-49)	446	ν ₁₀ (E ₂ '')	in-plane and v as IF ₅	510 (-17)	515	ν ₈ (E ₂ '')	δ pucker XeF ₅	n. obsd	79
v ₁₁	δ pucker IF ₅	n. obsd	141	ν ₁₁ (E ₂ '')	δ pucker IF ₅	[68]	59	ν ₉ (E ₂ '')	δ pucker XeF ₅	n. obsd	50t

^aFrequency values were scaled by an empirical factor of 0.9038. ^bUnscaled frequency value; scaled frequency value is 789 cm⁻¹. ^cFrequency values were scaled by an empirical factor of 0.932.

^dFrequency values were scaled by an empirical factor of 0.8618. ^eData from ref. 8. ^fData from ref. 49.

Ab Initio Calculations and Normal Coordinate Analyses. The

electronic structure of IOF_6^- was calculated at the ab initio level by using both local density functional (LDF) theory and molecular orbital theory with an effective core potential (ECP) for the core electrons of iodine. Both types of calculations resulted in minimum energy structures of C_{5v} symmetry with the ECP calculations duplicating the experimentally observed geometry (see Table VI) and vibrational frequencies (see Table V) much better than the LDF calculations. In view of the superiority of the ECP calculations, we have also recalculated the structure of the closely related XeF_5^- anion, for which previously (16) only LDF values had been available. As can be seen from Tables V and VI, the ECP calculations are in excellent agreement with the observed values, after scaling of the calculated frequencies by empirical factors to maximize their fit with the experimental data, and therefore, are invaluable for the correct assignments of the vibrational spectra. For XeF_5^- , for example, they clearly indicate that the previous assignments (16) for $\nu_2(A_2'') = 274 \text{ cm}^{-1}$ and $\nu_4(E_1') = 290 \text{ cm}^{-1}$ should be reversed. In view of the closeness of these two frequencies, the reversal of their assignments has very little or no impact on the conclusions previously reached (16) for XeF_5^- .

A normal coordinate analysis was carried out for IOF_6^- , and the most important internal force constants are compiled in Table VII and compared to those of IF_7 and XeF_5^- . As can be seen, the $X\text{-F}_{\text{ax}}$ bonds are considerably stronger than the $X\text{-F}_{\text{eq}}$ ones for a given compound, as expected from the bonding scheme proposed below. Furthermore, the stretching force constants decrease significantly on going from IF_7 to IOF_6^- and XeF_5^- , as expected from an increasing ionicity of the X-F bonds caused by the formal negative charge in the anions and the reduction in the formal oxidation state of the central atom from +VII in IF_7 and IOF_6^- to +IV in XeF_5^- . The large increase in the value of $f_{\text{rr}'}$, the coupling to opposite bonds, from IOF_6^- to XeF_5^- is analogous to those previously observed (62) for going from either *trans*- IO_2F_4^- ($f_{\text{rr}'} = 0.27 \text{ mdyn/\AA}$) to IOF_4^- ($f_{\text{rr}'} = 0.45 \text{ mdyn/\AA}$) and IF_4^- ($f_{\text{rr}'} = 0.47 \text{ mdyn/\AA}$) or IOF_5 ($f_{\text{rr}'} = 0.18 \text{ mdyn/\AA}$) to IF_5 ($f_{\text{rr}'} = 0.38 \text{ mdyn/\AA}$) and, hence, appears to be associated with the introduction of a sterically active, free valence electron pair into the ligand sphere around the central atom.

The in-plane deformation constants, f_{α} , are a measure for the strength of the mutual repulsion of the equatorial ligands and hence, for the degree of congestion in this plane which, in turn, is responsible for the puckering. As can be seen from Table VII, the value of f_{α} decreases markedly on going from IF_7 to IOF_6^- and XeF_5^- . In IF_7 , the in-plane deformation constant, f_{α} , is about five times larger than the out-of-plane deformation constant, f_{β} , and accounts for the puckering of the equatorial plane in IF_7 . On the other hand, in XeF_5^- the f_{α} value has become much smaller and approaches the range of values expected for the out-of-plane deformation constants, f_{β} . This is in good agreement with the x-ray crystal structure of $\text{N}(\text{CH}_3)_4^+\text{XeF}_5^-$ which showed (16) that XeF_5^- is planar and not puckered. Hence, it appears that the value of the in-plane deformation force constant, f_{α} , is a useful parameter for measuring the degree of congestion and the likely occurrence of puckering in the equatorial ligand plane.

Structure and Bonding in IOF_6^- . The structure and bonding of IOF_6^- can be rationalized by the same 6-center 10-electron bonding scheme outlined above for IF_7 (see Table IV). The only significant differences between IOF_6^- and IF_7 are that in IOF_6^- the congestion in the equatorial plane is lessened due to more ionic and, hence,

Table VI. Observed and Calculated Geometries of IOF_6^- and the Closely Related IF_7 and XeF_5^-

	IOF_6^-		IF_7		XeF_5^-	
	exp ^a	calcd ^a ECP LDF	exp ^b	calcd ^a ECP LDF	exp ^c	calcd ECP LDF
r I-O(Å)	1.75-1.77	1.7255 1.791	r I-F _{ax}	1.781 1.7705 1.870	r Xe-F _{eq}	2.012 1.9924 2.077
r I-F _{ax} (Å)	1.82	1.8087 1.913	r I-F _{eq}	1.857 1.8333 1.918		
r I-F _{eq} (Å)	1.88	1.8819 1.969	∠F _{ax} -I-F _{eq}	90 90 90		
∠O-I-F _{ax} (deg)	94-96	95.76 96.0				

^aData from this study. ^bData from ref. 4. ^cData from ref. 49.

Table VII. Internal Force Constants^{a,b} (mdyn/Å) of IF₇, IOF₆⁻ and XeF₅⁻

	IF ₇	IOF ₆ ⁻	XeF ₅ ⁻
f_R	5.005	3.897	—
f_r	3.947	2.938	2.062
f_{π}	0.326	0.306	0.198
$f_{\pi'}$	0.0265	0.0536	0.317
$f\alpha$	0.847	0.690	0.364
$f\alpha\alpha$	-0.183	-0.147	-0.081
$f\alpha\alpha'$	-0.240	-0.198	-0.102
$f\beta$	0.163		

(a) The deformation constants have been normalized for the following bond distances: IF₇, r I–F_{eq} = 1.857 Å; IOF₆⁻, r I–F_{eq} = 1.877 Å; XeF₅⁻, r Xe–F = 2.0124 Å. (b) f_{π} and $f_{\pi'}$ denote coupling to adjacent and opposite bonds, respectively, and $f\alpha\alpha$ and $f\alpha\alpha'$ coupling to adjacent and opposite bond angles, respectively.

longer bonds and that in IOF₆⁻ the intramolecular, equatorial-axial ligand exchange is precluded.

The TeOF₆²⁻ Anion. The [N(CH₃)₄⁺]₂TeOF₆²⁻ salt was prepared from N(CH₃)₄⁺TeOF₅⁻ and excess N(CH₃)₄⁺F⁻ in CH₃CN solution. It could not be isolated in pure form and always contained some unreacted N(CH₃)₄⁺TeOF₅⁻ starting material as a byproduct. Due to its insolubility in CH₃CN, its characterization was limited to vibrational spectroscopy of the solid. These vibrational spectra were completely analogous to those of IOF₆⁻, thereby confirming the close structural relationship of the two anions.

Conclusions

The present study shows that the preferred structures of heptacoordinated main-group fluorides and oxofluorides are pentagonal bipyramids. The structure, bonding, and fluxionality of these molecules is now well understood. The pentagonal bipyramidal arrangement cannot be explained by VSEPR-type arguments of repelling points on a sphere but is due to the spatial distribution of the valence orbitals on the central atom. The extensive ligand congestion in the equatorial plane, combined with the special requirements for five-fold symmetry, result in facile, dynamic puckering of the equatorial plane and high degrees of fluxionality. The novel XeF₅⁻, IOF₆⁻, and TeOF₆²⁻ anions have been prepared and characterized and are the first known examples of pentagonal bipyramidal XF₅E₂ and XOF₆ species.

Acknowledgments

The work at Rocketdyne was financially supported by the U.S. Air Force Phillips Laboratory and the U.S. Army Research Office, and that at McMaster University by the U.S. Air Force Phillips Laboratory and the Natural Sciences and Engineering Research Council of Canada.

Literature Cited

- (1) Gillespie, R.J. *Molecular Geometry*; Van Nostrand Reinhold Co.: London, 1972.
- (2) Gillespie, R.J.; Hargittai, I. *The VSEPR Model of Molecular Geometry*; Allyn and Bacon, A Division of Simon & Schuster, Inc: Needham Heights, MA, 1991; p 58.
- (3) Bradford-Thompson, H.; Bartell, L.S. *Inorg. Chem.* **1968**, *7*, 488.
- (4) Adams, W.J.; Bradford-Thompson, H.; Bartell, L.S. *J. Chem. Phys.* **1970**, *53*, 4040.
- (5) Selig, H.; Sarig, S.; Abramowitz, S. *Inorg. Chem.* **1974**, *13*, 1508.
- (6) Christe, K.O.; Sanders, J.C.P.; Schrobilgen, G.J.; Wilson, W.W. *J. Chem. Soc., Chem. Commun.* **1991**, 837.
- (7) Majhoub, A.R.; Seppelt, K. *J. Chem. Soc., Chem. Commun.* **1991**, 840.
- (8) Christe, K.O.; Wilson, W.W.; Wilson R.D.; Bau, R.; Feng, J. *J. Am. Chem. Soc.* **1990**, *112*, 7619.
- (9) Wilson, W.W.; Christe, K.O. *Inorg. Chem.* **1989**, *28*, 4172.
- (10) Christe, K.O.; Wilson, W.W.; Chirakal, R.V.; Sanders, J.C.P.; Schrobilgen, G.J. *Inorg. Chem.* **1990**, *29*, 3506.
- (11) Bougon, R.; Charpin, P.; Soriano, J. *C.R. Hebd. Seances Acad. Sci., Ser. C* **1971**, *272*, 565.
- (12) Christe, K.O.; Wilson, W.W. *Inorg. Chem.* **1989**, *28*, 3275.
- (13) Christe, K.O. *Inorg. Chem.* **1972**, *11*, 1215.
- (14) Mahjoub, A.R.; Hoser, A.; Fuchs, J.; Seppelt, K. *Angew. Chem., Int. Ed. Engl.* **1989**, *28*, 1526.
- (15) Mahjoub, A.R.; Seppelt, K. *Angew. Chem. Int. Ed. Engl.* **1991**, *30*, 323.
- (16) Christe, K.O.; Curtis, E.C.; Dixon, D.A.; Mercier, H.P.; Sanders, J.C.P.; Schrobilgen, G.J. *J. Am. Chem. Soc.* **1991**, *113*, 3351.
- (17) Ruff, O.; Keim, R. *Z. Anorg. Chem.* **1931**, *201*, 245.
- (18) Burbank, R.D.; Bensey, Jr., F.N. *J. Chem. Phys.* **1957**, *27*, 981.
- (19) Donohue, J. *J. Chem Phys.* **1959**, *30*, 1618.
- (20) Burbank, R.D. *J. Chem Phys.* **1959**, *30*, 1619.
- (21) Lohr, Jr., L.L.; Lipscomb, W.N. *J. Chem. Phys.* **1962**, *36*, 2225.
- (22) Burbank, R.D. *Acta Crystallogr.* **1962**, *15*, 1207.
- (23) Donohue, J. *Acta Crystallogr.* **1965**, *18*, 1018.
- (24) Gutowski, H.S.; Hoffmann, C.J. *J. Chem. Phys.* **1951**, *19*, 1259.
- (25) Muetterties, E.L.; Packer, K.J. *J. Am. Chem. Soc.* **1964**, *86*, 293.
- (26) Alexakos, L.G.; Cornwell, C.D.; Pierce, St. B. *Proc. Chem. Soc. (London)* **1963**, 341.
- (27) Bartlett, N.; Beaton, S.; Reeves, L.W.; Wells, E.J. *Can. J. Chem.* **1964**, *42*, 2531.
- (28) Gillespie, R.J.; Quail, J.W. *Can. J. Chem.* **1964**, *42*, 2671.
- (29) Kukolich, S.G. private communication, 1991.
- (30) Kaiser, E.W.; Muentner, J.S.; Klemperer, W.; Falconer, W.E. *J. Chem. Phys.* **1970**, *53*, 53.
- (31) Bradford-Thompson, H.; Bartell, L.S. *Trans. Am. Cryst. Soc.* **1966**, *2*, 190.
- (32) La Villa, R.E.; Bauer, S.H. *J. Chem. Phys.* **1960**, *33*, 182.
- (33) Lord, R.C.; Lynch, M.A.; Schumb, W.C.; Slowinski, E.J. *J. Am. Chem.* **1950**, *72*, 522.
- (34) Nagarajan, G. *Curr. Sci. (India)* **1961**, *30*, 413; *Bull. Soc. Chim. Belges* **1962**, *71*, 82.
- (35) Khanna, R.K. *J. Mol. Spectrosc.* **1962**, *8*, 134.
- (36) Arighi, L.S. Ph.D. Thesis, University of Wisconsin, **1965**.
- (37) Claassen, H.H.; Gasner, E.L.; Selig, H. *J. Chem. Phys.* **1968**, *49*, 1803.
- (38) Ramaswamy, K.; Muthusubramanian, J. *Mol. Struct.* **1970**, *6*, 205.

- (39) Wendling, E.; Mahmoudi, S. *Bull. Soc. Chim.* **1972**, *33*.
(40) Eysel, H.H.; Seppelt, K. *J. Chem. Phys.* **1972**, *56*, 5081.
(41) Mohan, S. *Acta Cient Indica* **1978**, *1*, 31.
(42) Bernstein, L.S. Ph.D. Thesis, University of California, Berkeley, **1974**.
(43) Bartell, L.S.; Rothman, M.J.; Gavezzotti, A. *J. Chem. Phys.* **1982**, *76*, 4136.
(44) Jacob, E.J.; Bartell, L.S. *J. Chem. Phys.* **1970**, *53*, 2235.
(45) Weidlein, J.; Müller, U.; Dehnicke, K. In *Schwingungsspektroskopie*; Georg Thieme Verlag: Stuttgart, 1982; p 37.
(46) Christe, K.O.; Wilson, R.D. *Inorg. Chem.* **1975**, *14*, 694.
(47) Berry, R.S. *J. Chem. Phys.* **1960**, *32*, 933.
(48) Bartell, L.S. In *Physical Methods of Chemistry*; Weissberger, A.; Rossiter, B.A., Ed. Wiley Interscience: New York, 1972, Vol. I, Part III; p 125.
(49) Christe, K.O.; Dixon, D.A.; Mahjoub, A.R.; Mercier, H.P.A.; Sanders, J.C.P.; Seppelt, K.; Schrobilgen, G.J.; Wilson, W.W. to be published.
(50) Pimentel, G.C. *J. Chem. Phys.* **1951**, *10*, 446.
(51) Hach, R.J.; Rundle, R.E. *J. Am. Chem. Soc.* **1951**, *73*, 4321.
(52) Rundle, R.E. *J. Am. Chem. Soc.* **1963**, *85*, 112.
(53) Mahjoub, A.R.; Drews, T.; Seppelt, K. *Angew. Chem., Int. Ed. Engl.* **1992**, *31*, 1036.
(54) Hyde, B.G.; Anderson, S. *Inorganic Crystal Structures*; John Wiley & Sons: New York, 1989; p 7.
(55) Bartell, L.S.; Clippard, F.B. Jacob, J.E. *Inorg. Chem.* **1976**, *15*, 3009.
(56) Smart, L.E. *J. Chem. Soc., Chem. Commun.* **1977**, 519.
(57) Selte, K.; Kjekshus, A. *Acta Chem. Scand.* **1970**, *24*, 1912.
(58) Kálmán, K.; Cruickshank, D.W.J. *Acta Crystallogr.* **1970** B26, 1782.
(59) Feikeman, Y.D. *Acta Crystallogr.* **1961**, *14*, 315.
(60) Feikeman, Y.D. *Acta Crystallogr.* **1966**, *20*, 765.
(61) Christe, K.O.; Wilson, W.W.; Bau, R.; Bunte, S.W. *J. Am. Chem. Soc.* **1992**, *114*, 3411, and references cited therein.
(62) Christe, K.O.; Wilson, R.D.; Schack, C.J. *Inorg. Chem.* **1981**, *20*, 2104.

RECEIVED June 16, 1993

Chapter 6

Monofluoroxenonium Hexafluorometalates

$\text{XeF}^+\text{MF}_6^-$ (M = As or Sb)

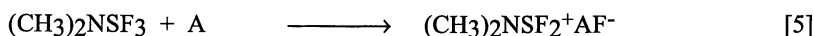
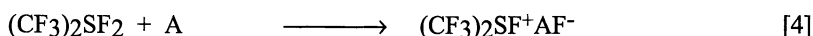
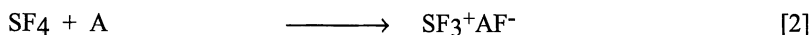
A Course to Different Onium Cations

Rolf Minkwitz and Birgit Bäck

Fachbereich Chemie, Anorganische Chemie, Universität Dortmund,
D-44227 Dortmund, Germany

A summary of the reactions which have been carried with $\text{XeF}^+\text{MF}_6^-$ (M = As, Sb) is given. This summary describes the development of the use of these salts to prepared a variety of different onium cations. Starting with the oxidative fluorination of sulfanes, the investigations in this field are extended towards the reactivity and regioselectivity of $\text{XeF}^+\text{MF}_6^-$ via the directed use of specially substituted sulfanes. The results of the reactions of XeF^+ salts with sulfuranes are also reported and discussed. When reactants with central atoms of the fifth main group are involved various differences are given regarding the reaction pathways and products. In addition, the results of reactions with H_2O leading to monofluorooxonium(0) hexafluorometalates are described, as well as the synthesis of polyhalonium cations by the oxidative fluorination of halogens.

Until a short time ago only a few fluorinated sulfonium cations were known. These cations have generally been obtained by Lewis acid-base reactions of sulfuranes or persulfuranes with strong Lewis acids (equation 1-6) (1-6).



(A = BF_3 , AsF_5 , SbF_5 , PF_5)

0097-6156/94/0555-0090\$08.00/0
© 1994 American Chemical Society

Another method of preparation is represented by the formation of $(\text{CH}_3)_2\text{SF}^+\text{BF}_4^-$ and $(\text{CH}_3)_2\text{SF}^+\text{AsF}_6^-$. For example, Forster and Downs obtained the hexafluoroarsenate salt by the reaction of the dimethylsulfane arsenic pentafluoride adduct with xenon difluoride in HF (equation 7) (7).



Reactions with Sulfanes

It is very likely that $\text{XeF}^+\text{AsF}_6^-$ occurs as a reactive intermediate in equation 7. We decided to test this idea by carrying out a number of direct reactions of the monofluoroxenonium hexafluorometalates $\text{XeF}^+\text{AsF}_6^-$ and $\text{XeF}^+\text{SbF}_6^-$, both of which can be readily obtained by reaction of XeF_2 with MF_5 ($\text{M} = \text{As}, \text{Sb}$) in HF (equation 8) (8). We first studied the fluorination of the alkyl and perfluoroalkyl



sulfanes RSR' ($\text{R}, \text{R}' = \text{CF}_3, \text{CH}_3, \text{C}_6\text{F}_5$) (4, 9, 10). The reactions proceed quantitatively in anhydrous HF to the monofluorosulfonium hexafluorometalates $\text{RS}(\text{R}')\text{F}^+\text{MF}_6^-$ ($\text{R}, \text{R}' = \text{CH}_3, \text{CF}_3, \text{C}_6\text{F}_5$; $\text{M} = \text{As}, \text{Sb}$) (see Figure 1) with elimination of xenon within a few hours at temperatures between 213 and 233 K. The formation of these salts provides a confirmation of our assumption that the reaction of Forster and Downs proceeds via the intermediate $\text{XeF}^+\text{AsF}_6^-$.

In the case of $(\text{C}_6\text{F}_5)_2\text{SF}^+\text{SbF}_6^-$, single crystals could be obtained from an $\text{SO}_2/\text{SO}_2\text{ClF}$ solution (10), and thus this compound represents the first monofluorinated sulfonium salt which could be investigated by X-ray diffraction. In the cation, the two pentafluorophenyl groups and the fluorine atom are arranged around the sulfur atom in the form of a trigonal pyramid (Figure 2). The S-F bond distances in several SF_3^+ cations have been found to be 149.6 pm (11) or 151.2 and 151.5 pm (12), while for the difluorinated cations CF_3SF_2^+ (13) and $(\text{CH}_3)_2\text{NSF}_2^+$ (14) this distance was found to be 152.5 pm and 155 pm, respectively. In continuation of an apparent trend of increasing S-F bond distance with decreasing fluorine content, the S-F distance in the $(\text{C}_6\text{F}_5)_2\text{SF}^+$ cation turns out to be 158.4 pm. Zigzag chains are formed in the crystal structure from the association of sulfur atoms in the cations with two fluorine atoms belonging to different octahedral anions (Figure 3). The cations and anions are arranged along chains in form of ABAB sequences. This confirms the observation of Mews that stronger Lewis basic fluorosulfonium cations are associated with complex fluoroanions in the shape of chains (15).

Further reactions between $\text{XeF}^+\text{MF}_6^-$ ($\text{M} = \text{As}, \text{Sb}$) and the sulfanes SCl_2 (16) and CF_3SCl (17) led to the mixed halogenated chlorofluorosulfonium salts (Figure 1). Attempts to obtain single crystals of these compounds failed due to a strong tendency towards disproportionation, even in the solid state. For this reason, in the

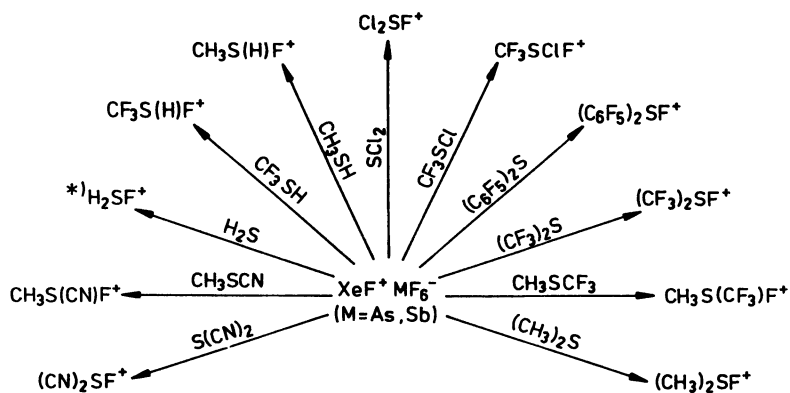


Figure 1. Reactions of $\text{XeF}^+ \text{MF}_6^-$ (M = As, Sb) with sulfanes.
 *) only $\text{H}_2\text{SF}^+ \text{SbF}_6^-$.

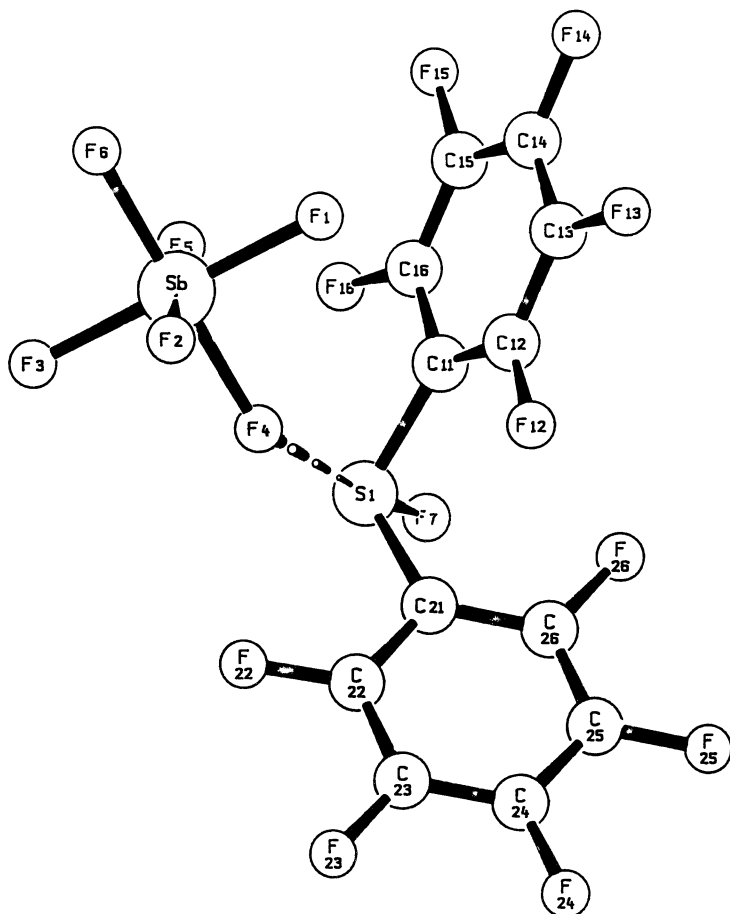


Figure 2. Asymmetric unit of $(\text{C}_6\text{F}_5)_2\text{SF}^+ \text{SbF}_6^-$ (adapted from ref. 10).

case of $\text{CF}_3\text{SClF}^+\text{SbF}_6^-$ only crystals of $\text{CF}_3\text{SCl}_2^+\text{SbF}_6^-$, obtained from SO_2 solutions, could be investigated by X-ray diffraction (17).

The synthetic principle of oxidative fluorination is also applicable to pseudohalido derivatives. Difunctional nucleophiles represent an especially important group because of the possible regioselectivity of the monofluoroxenonium salts. In both cyano(methyl)sulfane and dicyanosulfane two different basic centers are possible for the electrophilic attack of the XeF^+ cation. In each case, the corresponding fluorosulfonium salt is formed in HF at 213 K (Figure 1) (18). While $\text{S}(\text{CN})_2\text{F}^+\text{MF}_6^-$ is observed to disproportionate rapidly in SO_2 solution to $\text{SF}_3^+\text{MF}_6^-$ (2) and $\text{S}(\text{CN})_3^+\text{MF}_6^-$ (19), there is no evidence for such a behavior in the case of $\text{CH}_3\text{S}(\text{CN})\text{F}^+\text{MF}_6^-$ ($\text{M} = \text{As}, \text{Sb}$).

Reactions with Disulfanes

The high selectivity of the extremely mild fluorinating agent $\text{XeF}^+\text{MF}_6^-$ ($\text{M} = \text{As}, \text{Sb}$) is also confirmed by its reaction with the disulfanes RSSR' ($\text{R}, \text{R}' = \text{CF}_3, \text{CH}_3, \text{C}_6\text{F}_5, \text{Cl}$), which can be fluorinated without cleavage of the S-S bond (Figure 4) (20-22). The regioselectivity of this reaction is demonstrated with the mixed disulfane CF_3SSCH_3 . In this case, only the methylated sulfur atom is attacked by the monofluoroxenonium cation, as clearly demonstrated by NMR investigations. All of these salts are sensitive to hydrolysis and can be kept without decomposition up to 243 K. At higher temperatures, formation of the intensively blue solid $\text{Sg}^{2+}(\text{SbF}_6^-)_2$ (23) occurs both in solution and in the solid state. No difference in stability was observed between the hexafluoroarsenate and -antimonate salts. In addition, the $\text{S}_2\text{Cl}_2\text{F}^+$ cation was characterized by sulfur-32/34 isotopic exchange. This made it possible to assign exactly both the S-Cl and the S-S valence frequencies, which would have otherwise been difficult as these bands are expected in the same range.

Reactions with SH Derivatives

The next logical step was the extension of this chemistry to SH derivatives. Attempts to oxidatively fluorinate CF_3SSH with monofluoroxenonium hexafluorometalates failed, even at 195 K. Only decomposition into the already mentioned Sg^{2+} salts could be observed (24). On the other hand, the synthesis of the fluoro(trifluoromethyl)sulfonium- and fluoro(methyl)sulfonium cations from the SH acidic sulfanes CF_3SH and CH_3SH proceeded without difficulty at 213 K (Figure 1) (25). The elimination of HF at 213 K is expected to be preferred from a thermodynamic point of view, although HF elimination is probably kinetically inhibited in this case. However, at 233 K decomposition of all of these compounds into the characteristic blue Sg^{2+} salts is observed. By reaction with chlorine $\text{CF}_3\text{S}(\text{H})\text{F}^+\text{MF}_6^-$ and $\text{CH}_3\text{S}(\text{H})\text{F}^+\text{MF}_6^-$ ($\text{M} = \text{As}, \text{Sb}$) can be transferred into the corresponding chlorosulfonium salts with formation of HCl (equations 9 and 10) (25).



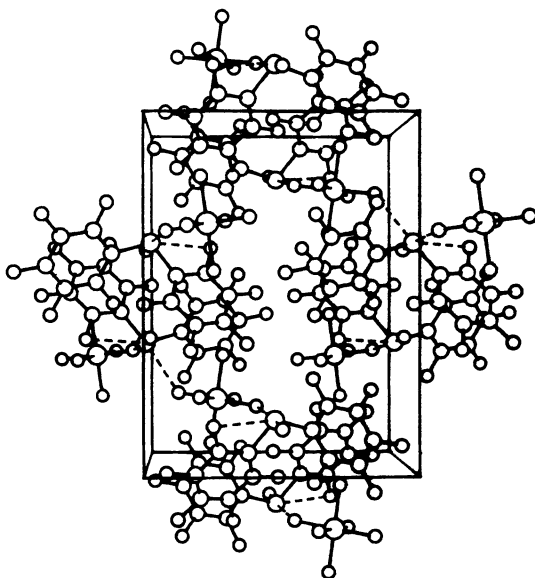


Figure 3. Unit cell packing of $(C_6F_5)_2SF^+SbF_6^-$ (adapted from ref. 10).

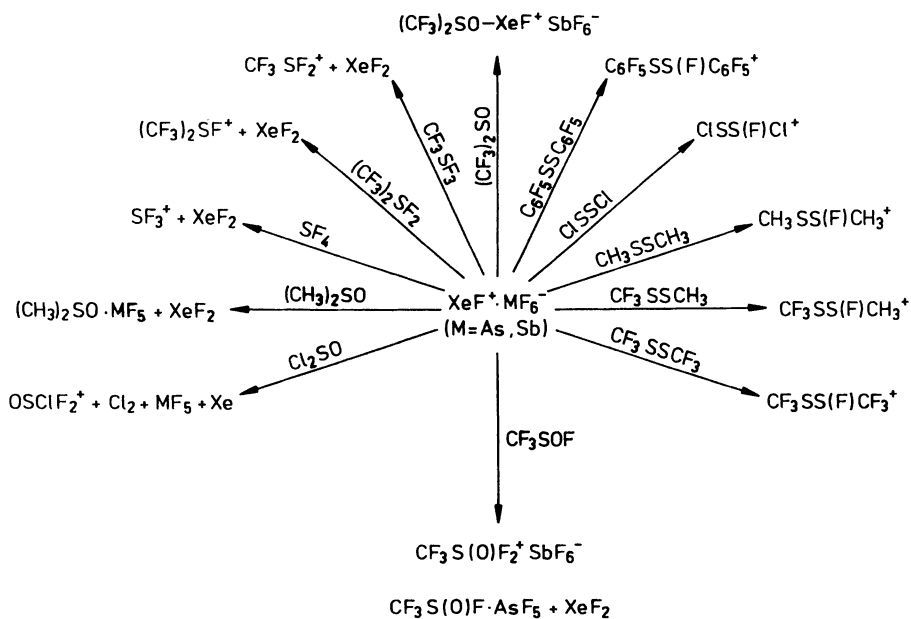
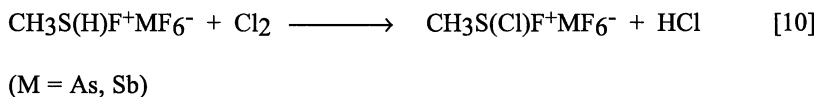
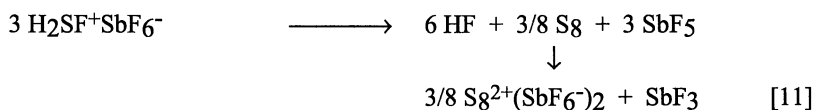


Figure 4. Reactions of $XeF^+MF_6^-$ ($M = As, Sb$) with disulfanes and sulfuranes.



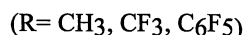
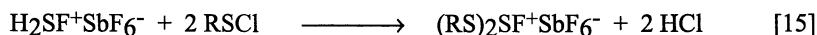
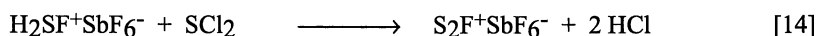
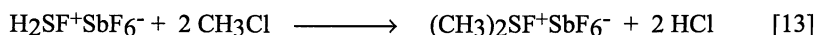
Preparation and Reactions of $\text{H}_2\text{SF}^+\text{SbF}_6^-$

During the search for the missing link within the series of monofluorosulfonium cations, namely H_2SF^+ , many unsuccessful attempts were carried out. Finally, a reaction between H_2S and $\text{XeF}^+\text{SbF}_6^-$ at 195 K led to the formation of the extremely thermolabile monofluorosulfonium hexafluoroantimonate $\text{H}_2\text{SF}^+\text{SbF}_6^-$ (Figure 1) (26). This salt readily decomposes at only a few degrees above the reaction temperature as well as sometimes when the solvent is being pumped off of the reaction mixture (equation 11). In a well-closed vessel, the slightly yellow sulfonium salt remains



stable for several days at 195 K and for approximately 5 hours at 213 K, after which time, $\text{S}_8^{2+}(\text{SbF}_6^-)$, S_8 , and HF are identified as decomposition products spectroscopically. Decomposition products analogous to those in equation 11 are observed when the synthesis of $\text{H}_2\text{SF}^+\text{AsF}_6^-$ is attempted, a result which indicates that the hexafluoroarsenate salt exists only below the melting point of HF, i.e. 189 K. Investigations concerning the quantitative nature of the reaction indicate that more than 90% of the expected xenon can be collected during the formation of $\text{H}_2\text{SF}^+\text{SbF}_6^-$. On average, the sulfur/antimony ratio in the salt as determined by chemical analysis amounts to 1:1 with a deviation of 10%. The cation is characterized by its vibrational spectra, including $^{32/34}\text{S}$ and H/D markings, as well as by NMR spectroscopy.

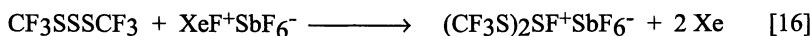
The H_2SF^+ cation has also been shown to possess high synthetic potential itself. Various reactions of the cation have led to different monofluorinated sulfonium salts with the formation of HCl as shown in equations 12-15. The salts emerging



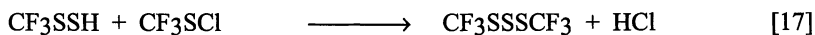
from equation 13 and 14 have previously been prepared by the oxidative fluorination of the corresponding sulfanes with $\text{XeF}^+\text{SbF}_6^-$ (15,9) and successful derivatization.

The reaction of $\text{H}_2\text{SF}^+\text{SbF}_6^-$ with SCl_2 leading to monofluorothiosulfonium hexafluoroantimonate (equation 15) (27) is of special interest. The existence of this compound was first postulated by Seel (28) in 1971. $\text{S}_2\text{F}^+\text{SbF}_6^-$ is a bright yellow, moisture sensitive salt which remains stable at 195 K for approximately two weeks. At 233 K it decomposes within several hours. The measured vibrational frequencies of this salt were assigned by sulfur- 32/34 isotopic exchange.

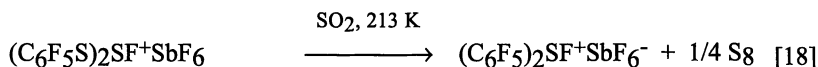
Simple condensation reactions of $\text{H}_2\text{SF}^+\text{SbF}_6^-$ with chlorosulfanes (equation 15) result in the formation of formally fluorinated trisulfanes (29) with the release of HCl . The perfluoromethylated dithiosulfonium hexafluoroantimonate salt was also synthesized by the oxidative fluorination of the corresponding trisulfane with $\text{XeF}^+\text{SbF}_6^-$ (equation 16), and its identity was confirmed by NMR spectroscopy.



However, the latter synthetic route is very problematic due to difficulties in preparing pure trisulfane (equation 17) (30). For example, small amounts of the impurity



CF_3SSH lead to the formation of the blue solid $\text{S}_8^{2+}(\text{SbF}_6^-)_2$. The new salts $(\text{RS})_2\text{SF}^+\text{SbF}_6^-$ ($\text{R} = \text{CH}_3, \text{CF}_3, \text{C}_6\text{F}_5$) are characterized by vibrational and NMR spectroscopy and are stable up to 14 days at 195 K. The compounds are extremely sensitive towards hydrolysis and elimination of sulfur. The latter fact has been confirmed by the reaction of $\text{H}_2\text{SF}^+\text{SbF}_6^-$ with $\text{C}_6\text{F}_5\text{SCl}$ in liquid SO_2 at 213 K (equation 15). In this case, the already known $(\text{C}_6\text{F}_5)_2\text{SF}^+\text{SbF}_6^-$ salt (10) was detected by NMR spectroscopy, and the by-product sulfur was identified by Raman spectroscopy (equation 18) (29).



Reactions with Sulfuranes

In order to extend the investigations concerning the oxidation potential of monofluoroxenonium hexafluorometalates, sulfuranes were used as reactants, leading to some unexpected results. Reactions of the fluorosubstituted sulfuranes $(\text{CF}_3)_n\text{SF}_{4-n}$ ($n = 0 - 2$) with $\text{XeF}^+\text{MF}_6^-$ ($\text{M} = \text{As}, \text{Sb}$) produce the corresponding fluorosulfonium salts and XeF_2 (Figure 4) (31). Here, the oxidizing properties of the monofluoroxenonium cations do not occur, but their Lewis-acidic character is

observed. These reactions are facilitated through the weak axial S-F bonds with long distances between 164.3 and 168.1 pm (32-35). This confirms the existence of a structure-activity relationship for sulfur-fluorine compounds and fits well with the empirical rule that sulfur fluorides with S-F bonds longer than 159.5 pm react with strong Lewis acids such as AsF_5 and SbF_5 , leading to hexafluorometalates under F⁻ abstraction (36). Oxosulfuranes like CF_3SOF and R_2SO ($\text{R} = \text{CF}_3, \text{CH}_3, \text{Cl}$) react in a different manner (Figure 4) (33). In the reaction of CF_3SOF with $\text{XeF}^+\text{SbF}_6^-$ oxidative fluorination of the sulfurane occurs, forming difluoro(oxo)trifluoromethylpersulfonium(VI) hexafluoroantimonate. In contrast to this, the analogous reaction with $\text{XeF}^+\text{AsF}_6^-$ yields the thermosensitive adduct $\text{CF}_3\text{S(O)F}\cdot\text{AsF}_5$ (37). The corresponding result is observed with $(\text{CH}_3)_2\text{SO}$. With $\text{XeF}^+\text{MF}_6^-$ ($\text{M} = \text{As}, \text{Sb}$) the two known adducts $(\text{CH}_3)_2\text{SO}\cdot\text{MF}_5$ (38) are produced. The reaction of the XeF^+ salts and OSCl_2 forms neither monofluoropersulfonium compounds nor XeF_2 and adducts with the Lewis acids AsF_5 or SbF_5 . Instead, $\text{OSClF}_2^+\text{MF}_6^-$ salts, which were first prepared by Passmore et al. (39), are formed along with Cl_2 (Figure 4). The reaction of $(\text{CF}_3)_2\text{SO}$ with $\text{XeF}^+\text{SbF}_6^-$ gives yet another result. In this case, the corresponding fluoropersulfonium salt is not obtained. Instead, the reaction remains at the intermediate stage of $(\text{CF}_3)_2\text{SOXeF}^+\text{SbF}_6^-$ (Figure 4) (31). This isolation of this compound confirms earlier ideas concerning the reaction mechanism with monofluoroxenonium hexafluorometalates (16).

In the first step, the formation of a transition state with an intermediate E- XeF^+ bonding occurs, followed by the concomitant transfer of a fluorine atom onto the central atom E and elimination of the xenon atom. There is no evidence yet which indicates whether the fluorine atom transfer is an inter- or intramolecular process.

Reactions with Fifth Main Group Elements

Further examples of the transition state of this oxidative fluorination are given in the preparation of fluoronitrilium salts by Schrobilgen et al. (40-43). During the reaction of $\text{XeF}^+\text{AsF}_6^-$ with alkyl- and aryl nitriles various nitrilium cations containing the N- XeF^+ structural unit are formed (Figure 5). Another interesting intermediate with this structural unit has been prepared by Schrobilgen by reaction of trifluoro-s-triazine with $\text{XeF}^+\text{AsF}_6^-$ (Figure 5) (42). In this case, XeF^+ is coordinated to a nitrogen atom of the heterocycle.

In contrast to the reactions of nitriles with XeF^+ salts, the use of the stronger oxidant $\text{N}_2\text{F}^+\text{AsF}_6^-$ does not lead to an analogous stable intermediate $\text{R-CN-N}_2\text{F}^+$, as shown by the reaction of CH_3CN with $\text{N}_2\text{F}^+\text{AsF}_6^-$ (27). In this case, only the secondary products of a possible fluorination product of CH_3CN could be obtained, but these products have not yet been completely identified.

This behavior corresponds well to the theoretical determinations by Christe and Dixon (44) of the oxidizer strengths of both XeF^+ (164.8 kcal/mol) and N_2F^+ (139.3 kcal/mol) where the F⁺ detachment energies, when used as a measure of oxidizer strength, differ by about 25.5 kcal/mol. One example that the reaction

products of the fluorination in the special case of nitriles are not only dependent upon the oxidizer strength of the fluorinator is given by the already stronger oxidant KrF^+ (115.9 kcal/mol) (44). Various nitrilium salts of the form RCN-KrF^+ ($\text{R} = \text{H}, \text{CF}_3, \text{C}_2\text{F}_5, n\text{-C}_3\text{F}_7$) have recently been prepared (42,45), and no oxidative fluorination of the nitrogen was observed in these cases. We are currently trying to find an explanation for these different reaction behaviors by means of further experiments.

The aforementioned $\text{N}_2\text{F}^+\text{AsF}_6^-$ salt can only be prepared from *trans*- N_2F_2 and has recently been studied crystallographically by Christe et al. (46). As such it represents the compound with the shortest N-F bond. The compound has also been shown to be a good alternative for oxidative fluorination in cases where working in HF solution is not possible. While nitrosyl fluoride reacts in HF with $\text{XeF}^+\text{MF}_6^-$ ($\text{M} = \text{As}, \text{Sb}$) to form difluoronitryl hexafluorometalates (Figure 5) (47), the analogous synthesis with nitrosyl chloride does not work since ONCl reacts with HF, giving $\text{ONF} \cdot 3 \text{HF}$ and HCl (48). For this reason $\text{N}_2\text{F}^+\text{AsF}_6^-$ is used for oxidative fluorination of ONCl (equation 19) (47). The reaction is carried out in a



heterogeneous system at 195 K in CCl_3F . At this temperature, $\text{N}_2\text{F}^+\text{AsF}_6^-$ does not attack the solvent. The solvent is attacked only at room temperature after several days where higher fluorinated chlorofluorocarbons CF_2Cl_2 and CClF_3 are formed in NMR traceable amounts. The compound CF_3NO reacts in a similar fashion giving $\text{ON}(\text{CF}_3)\text{F}^+\text{AsF}_6^-$ (equation 20) (47).



The reactants PCl_3 and AsCl_3 can be handled in HF solution without any problems. Thus, the oxidative fluorination of these molecules with monofluoroxenonium hexafluoroarsenate proceeds at 213 K in HF (Figure 5) (49,50). Due to the fast symmetrization of AsCl_3F^+ (equation 21), small amounts of $\text{AsCl}_4^+\text{AsF}_6^-$ could already be determined by vibrational spectroscopy after a reaction time of ten minutes. Within 15 hours a complete symmetrization is

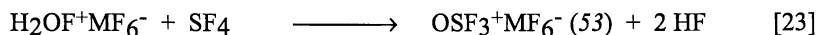


observed, and therefore the isolation of pure $\text{AsCl}_3\text{F}^+\text{AsF}_6^-$ was not possible.

Reactions with Sixth Main Group Elements

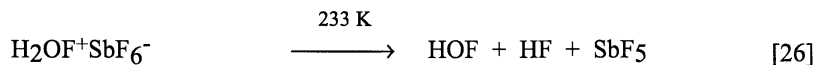
An example of the strength of the oxidative fluorinator $\text{XeF}^+\text{MF}_6^-$ ($\text{M} = \text{As}, \text{Sb}$) is given by the reaction with H_2O . In spite of the high ionization potential of 12.6 eV (51), the fluorination of H_2O leads to reddish colored monofluorooxonium(0) hexafluorometalates (Figure 5) (52). Both salts are stable in a well-closed vessel for

up to several weeks at 233 K and can be handled at room temperature in the pure, isolated state for about two hours. Various reactions have been carried out to show the synthetic potential of these compounds (equation 22 - 25). These equations show



(M = As, Sb)

some interesting results. The H_2OF^+ cation is able to either transfer formally an OF^+ or an OH_2^+ group, and therefore it possesses a bifunctional character. In a dynamic, high vacuum at 233 K, $\text{H}_2\text{OF}^+\text{SbF}_6^-$ decomposes to hypofluorous acid (56), HF and SbF_5 which can be isolated in an inert gas matrix (equation 27).



Reactions with Seventh Main Group Elements

All reactions with $\text{XeF}^+\text{MF}_6^-$ (M = As, Sb) mentioned so far for elements of the fifth and sixth main group have been examples of either oxidative fluorination forming E-F^+ cations or the synthesis of a transition state with an E-XeF^+ structural unit. It seemed logical to extend our investigations to the elements of the seventh main group in order to prepare Hal_2F^+ or possibly Hal_2XeF^+ salts. However, the analytical and spectroscopic data obtained from the reactions of $\text{XeF}^+\text{MF}_6^-$ (M = As, Sb) with chlorine and bromine as well as the X-ray crystal structure determination of the bromine species reveal some surprising results (Figure 5) (57-59). As was expected, $\text{Hal}_2\text{F}^+\text{MF}_6^-$ (Hal = Cl, Br; M = As, Sb) salts are formed in the first step of all reactions, but the presence of excess halogen leads to the homology of the polyhalonium ions (equations 27 and 28).



(Hal = Cl, Br; M = As, Sb)

Using this method, $\text{Cl}_3^+\text{SbF}_6^-$ was first reported by Clegg and Downs (59). In the case of the bromine compound, the BrF formed disproportionates into BrF_3 and Br_2 (60). While $\text{Cl}_3^+\text{SbF}_6^-$ can be isolated in pure form (57), only mixtures of $\text{Br}_3^+\text{MF}_6^-$ and crystalline $\text{Br}_5^+\text{MF}_6^-$ ($\text{M} = \text{As}, \text{Sb}$) are obtained (58). The addition of another mole of bromine to the Br_3^+ cation was incomplete under all conditions tried. In some cases a dark green liquid was observed besides the Cl_3^+ salt, as already mentioned by Downs (59). Attempts to isolate these compounds were unsuccessful; however, colorless single crystals were obtained within three months from a sample of the green liquid in a glass ampule. These crystals were determined by X-ray diffraction to be $\text{ClO}_2^+\text{MF}_6^-$ ($\text{M} = \text{As}, \text{Sb}$) (61). An improved force field was also calculated for $\text{Cl}_3^+\text{SbF}_6^-$ from the isotopic shifts in its Raman spectra (57). The X-ray structure analysis of $\text{Br}_5^+\text{MF}_6^-$ ($\text{M} = \text{As}, \text{Sb}$) shows a centrosymmetric Z -configuration of the pentabromine(1⁺) cation (Figure 6) in analogy to the cations I_5^+ , I_3Cl_2^+ and I_3Br_2^+ (62,63) with two short terminal (227.5 and 226.8 pm) and two longer central Br-Br distances (251.4 and 251.2 pm). The structure can formally be described as an adduct of two halogen molecules to the central halonium ion with a linear 3-center, 4-electron bond and an AX_2E_3 coordination. In both $\text{Br}_5^+\text{MF}_6^-$ ($\text{M} = \text{As}, \text{Sb}$) salts, the cations are linked into layers by four fluorine atoms of each MF_6^- octahedron. The $\text{Br}\cdots\text{Br}\cdots\text{F}$ groups are nearly linear, and the fluorine atoms joined in the anion-cation contacts have about 3 pm longer M-F distances than the others. Comparable interionic contacts are observed for other polyhalonium salts. The geometry of Br_5^+ was also calculated by the use of the local density functional method (64). In contrast to the planar trans configuration of C_{2h} symmetry found for the cation in solid $\text{Br}_5^+\text{MF}_6^-$ ($\text{M} = \text{As}, \text{Sb}$) (58), the lowest energy configuration for free Br_5^+ is a skewed structure with the three central Br atoms forming an angle of 168° and the two terminal Br atoms exhibiting a dihedral angle of 82° .

Conclusions

The reactions described in this paper have shown that a number of different molecules can be prepared by the use of the monofluoroxenonium hexafluorometalates. These salts are extremely mild and regioselective agents for oxidative fluorination. Thus, the synthetic potential of $\text{XeF}^+\text{MF}_6^-$ ($\text{M} = \text{As}, \text{Sb}$) offers the possibility to obtain monofluorinated onium salts as well as compounds containing an E-XeF⁺ element bond or even polyhalonium cations. It is clear that many unexpected results remain to be discovered in this area.

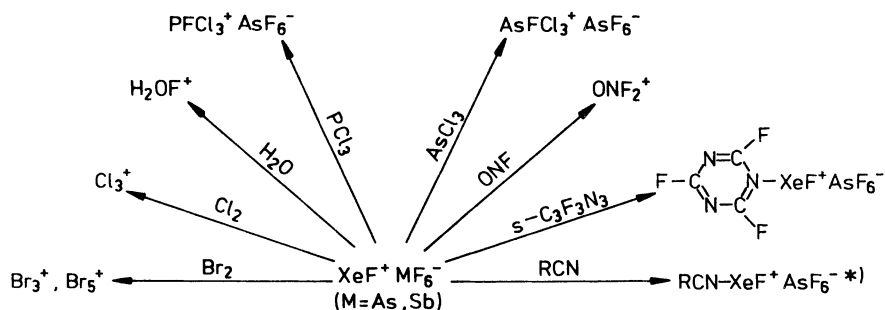


Figure 5. Reactions of $\text{XeF}^+\text{MF}_6^-$ (M = As, Sb) with different molecules. *) R = H, CH₃, CH₂F, C₂H₅, C₂F₅, C₃F₇, C₆F₅.

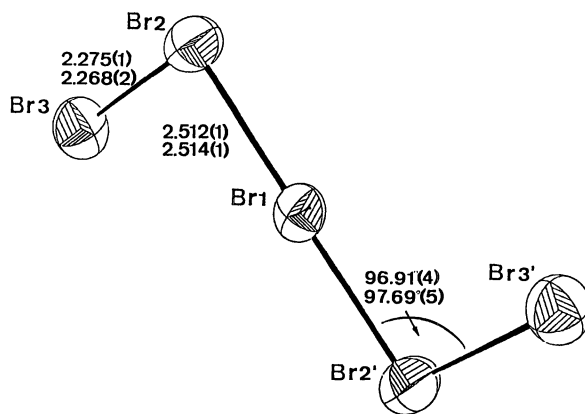


Figure 6. ORTEP plot of Br_5^+ (adapted from ref. 58). Upper values belong to $\text{Br}_5^+\text{AsF}_6^-$, lower values to $\text{Br}_5^+\text{SbF}_6^-$.

Acknowledgments

We thank the Minister für Wissenschaft und Forschung Nordrhein-Westfalen, the Bundesminister für Forschung und Technologie, the Deutsche Forschungsgemeinschaft, and the Fonds der Chemischen Industrie for financial support.

Literature Cited

- (1) Alam, K.; Shreeve, J. M. *Inorg. Chem.* **1988**, *27*, 1374.
- (2) Azeem, M.; Brownstein, M.; Gillespie, R. J. *Can. J. Chem.* **1969**, *47*, 4159.
- (3) Kramar, M.; Duncan, L. C. *Inorg. Chem.* **1971**, *10*, 647.
- (4) Minkwitz, R.; Werner, A. *J. Fluorine Chem.* **1988**, *39*, 141.
- (5) Mews, R.; Henle, H. *J. Fluorine Chem.* **1979**, *14*, 495.
- (6) Downs, A. J.; Forster, A. M.; McGrady, G. S.; Taylor, B. J. *J. Chem. Soc., Dalton Trans.* **1991**, 81.
- (7) Downs, A. J.; Forster, A. M. *J. Chem. Soc., Dalton Trans.* **1984**, 2827.
- (8) Gillespie, R. J.; Landa, B. *Inorg. Chem.* **1973**, *12*, 1383.
- (9) Minkwitz, R.; Werner, A. *Z. Naturforsch.* **1988**, *43b*, 403.
- (10) Minkwitz, R.; Nowicki, G.; Preut, H. *Z. Anorg. Allg. Chem.* **1992**, *611*, 23.
- (11) Gibbler, D. D.; Adams, C. J.; Zalkin, A.; Bartlett, N. *Inorg. Chem.* **1973**, *11*, 3417.
- (12) Mallouk, T. E.; Rosenthal, G. L.; Müller, G.; Brusasco, R.; Bartlett, N. *Inorg. Chem.* **1984**, *23*, 3167.
- (13) Minkwitz, R.; Molsbeck, W.; Bäck, B.; Preut, H. *Z. Anorg. Allg. Chem.* **1993**, *619*, 174.
- (14) Pauer, F.; Erhardt, M.; Mews, R.; Stalke, D. *Z. Naturforsch.* **1990**, *45b*, 271.
- (15) Erhart, M.; Mews, R.; Pauer, F.; Stalke, D.; Sheldrick, G. M. *Chem. Ber.* **1991**, *124*, 31.
- (16) Minkwitz, R.; Nowicki, G. *Z. Naturforsch.* **1989**, *44b*, 1343.
- (17) Minkwitz, R.; Nowicki, G.; Preut, H. *Z. Anorg. Allg. Chem.* **1989**, *573*, 185.
- (18) Minkwitz, R.; Nowicki, J.; Jahnkow, B.; Koch, M. *Z. Anorg. Allg. Chem.* **1991**, *596*, 77.
- (19) Minkwitz, R.; Gerhard, V. *Z. Naturforsch.* **1991**, *46b*, 265.
- (20) Minkwitz, R.; Nowicki, G. *Inorg. Chem.* **1991**, *30*, 4426.
- (21) Minkwitz, R.; Bäck, B., unpublished results.
- (22) Minkwitz, R.; Nowicki, G., unpublished results.
- (23) Gillespie, R. J.; Passmore, J. *J. Chem. Soc., Chem. Commun.* **1969**, 1333.
- (24) Nowicki, G., University of Dortmund, personal communication.
- (25) Minkwitz, R.; Nowicki, G. *Inorg. Chem.* **1992**, *31*, 225.
- (26) Minkwitz, R.; Nowicki, G.; Bäck, B.; Sawodny, W. *Inorg. Chem.* **1993**, *32*, 787.
- (27) Minkwitz, R.; Bäck, B., unpublished results.
- (28) Seel, F.; Hartmann, V.; Molnar, I.; Budenz, R.; Gombler, W. *Angew. Chem.* **1971**, *83*, 173; *Angew. Chem., Int. Ed. Engl.* **1971**, *10*, 186.
- (29) Minkwitz, R.; Bäck, B., unpublished results.
- (30) Gaensslen, M.; Minkwitz, R.; Molsbeck, W.; Oberhammer, H. *Inorg. Chem.* **1992**, *31*, 4147.

- (31) Minkwitz, R.; Molsbeck, W. *Z. Anorg. Allg. Chem.* **1992**, *612*, 35.
- (32) Tolles, M. W.; Gwinn, W. G. *J. Chem. Phys.* **1962**, *36*, 1119.
- (33) Kimura, K.; Bauer, S. H. *J. Chem. Phys.* **1963**, *39*, 3172.
- (34) Downs, A. J.; McGrady, G. S.; Bamfield, E. A.; Rankin, D. W. H.; Robertson, H. E.; Boggs, J. E.; Dobbs, K. D. *Inorg. Chem.* **1989**, *28*, 3286.
- (35) Oberhammer, H.; Kumar, R. C.; Knerr, G. D.; Shreeve, J. M. *Inorg. Chem.* **1981**, *20*, 3871.
- (36) Minkwitz, R.; Molsbeck, W.; Oberhammer, H.; Weiss, I. *Inorg. Chem.* **1992**, *31*, 2104.
- (37) Minkwitz, R.; Molsbeck, W. *Z. Naturforsch.* **1991**, *46b*, 1733.
- (38) Webster, M. *Chem. Rev.* **1966**, *66*, 87.
- (39) Lau, C.; Passmore, J. *J. Chem. Soc., Dalton Trans.* **1973**, 2528.
- (40) Emar, A. A. A.; Schrobilgen, G. J. *Inorg. Chem.* **1992**, *31*, 1323.
- (41) Emar, A. A. A.; Schrobilgen, G. J. *J. Chem. Soc., Chem. Commun.* **1987**, 1646.
- (42) Schrobilgen, G. J. *J. Chem. Soc., Chem. Commun.* **1988**, 1506.
- (43) Emar, A. A. A.; Schrobilgen, G. J. *J. Chem. Soc., Chem. Commun.* **1988**, 257.
- (44) Christe, K. O.; Dixon, D. A. *J. Am. Chem. Soc.* **1992**, *114*, 2978.
- (45) Schrobilgen, G. J. *J. Chem. Soc., Chem. Commun.* **1988**, 863.
- (46) Christe, K. O.; Wilson, R. D.; Wilson, W. W.; Bau, R.; Sukumar, S.; Dixon, D. A. *J. Am. Chem. Soc.* **1991**, *113*, 3795.
- (47) Minkwitz, R.; Bernstein, D.; Preut, H.; Sartori, P. *Inorg. Chem.* **1991**, *30*, 2159.
- (48) Seel, F.; Birnkraut, W. *Angew. Chem.* **1961**, *73*, 531.
- (49) Minkwitz, R.; Molsbeck, W. *Z. Anorg. Allg. Chem.* **1992**, *607*, 175.
- (50) Lennhoff, D., University of Dortmund, personal communication.
- (51) Rosenstock, H. M.; Draxl, K.; Steiner, B. W.; Herron, J. T. *J. Phys. Chem. Ref. Data* 1977, Supplement No. 1, 6.
- (52) Minkwitz, R.; Nowicki, G. *Angew. Chem.* **1990**, *102*, 692; *Angew. Chem., Int. Ed. Engl.* **1990**, *29*, 688.
- (53) Brownstein, M.; Dean P. A. W.; Gillespie, R. J. *J. Chem. Soc., Chem. Commun.* **1970**, 9.
- (54) Christe, K. O.; Schack, C. J. *Inorg. Chem.* **1972**, *11*, 2212.
- (55) Christe, K. O.; Wilson, W. W.; Curtis, E. C. *Inorg. Chem.* **1979**, *18*, 2578.
- (56) Goleb, J. A.; Claassen, H. H.; Studier, M. H.; Appelman, E. H. *Spectrochim. Acta* **1972**, *28A*, 65.
- (57) Minkwitz, R.; Nowicki, J.; Härtner, H.; Sawodny, W. *Spectrochim. Acta* **1991**, *47A*, 1673.
- (58) Hartl, H.; Nowicki, J.; Minkwitz, R. *Angew. Chem.* **1991**, *103*, 311; *Angew. Chem., Int. Ed. Engl.* **1991**, *30*, 328.
- (59) Clegg, M. J.; Downs, A. J. *J. Fluorine Chem.* **1989**, *45*, 13.
- (60) Naumann, D.; Lehmann, E. *J. Fluorine Chem.* **1975**, *5*, 307.
- (61) Minkwitz, R.; Nowicki, J.; Hartl, H., unpublished results.
- (62) Apblett, A.; Grein, F.; Johnson, J. P.; Passmore, J.; White, P. S. *Inorg. Chem.* **1986**, *25*, 422.
- (63) Pohl, S.; Saak, W. *Z. Naturforsch.* **1985**, *40b*, 45.
- (64) Christe, K. O.; Dixon, D. A.; Minkwitz, R. *Z. Anorg. Allg. Chem.* **1992**, *612*, 51.

RECEIVED December 16, 1993

Chapter 7

Influence of Fluorine and Parahalogen Substituents on the Chemistry of Some Functional Groups

A. Haas and A. Brosius

Lehrstuhl für Anorganische Chemie II, Ruhr-Universität Bochum,
D-44780 Bochum, Germany

The influence of fluorine, trifluoromethyl, trifluoromethylsulphenyl or trifluoromethylselenenyl on the chemistry of selected functional groups such as carbene, nitrene, $C=X$ ($X = O, S, Se, Te$), $=CCO$ and $-NSO$ will be presented. After describing evidence for the existence of $(CF_3S)_2C:$ and $CF_3SN:$, their stability and reactivity will be compared with those of F- and CF_3 -substituted carbenes and nitrenes. Tellurocarbonyl difluoride, $(CF_3S)_2CCO$, and CF_3SNSO are other key compounds that will be treated in a similar manner. Their preparation, chemical and physical properties will be discussed in comparison with either their fluorine, CF_3 , CF_3S or CF_3Se analogues. An attempt will be made to offer rules for planning successful syntheses.

The aim of this chapter is to demonstrate the influence of the three important ligands F, CF_3 , and CF_3S on the stability and chemistry of some selected functional groups. First, it is informative to compare the constants for the three ligands as aromatic substituents (see Table I). Group electronegativity decreases regularly from a value of 4.00 for F to a value of 2.7 for CF_3S , while π effects increase from 0.14 to 1.44, respectively. The other constants show substantial differences between fluorine and the other two ligands. For example, CF_3 and CF_3S have rather similar Hammett and Taft constants; however, overall there is no unique trend in the data shown in Table I.

On the other hand, little is known in terms of constants for these ligands as aliphatic substituents. No data could be found for the CF_3S group, but its hydrophobicity should increase and its electron withdrawing effect decrease slightly with respect to F and CF_3 . Tentative extrapolations are given in Table I.

0097-6156/94/0555-0104\$08.72/0
© 1994 American Chemical Society

The functional groups selected are carbenes and nitrenes and their derivatives with a chalcogen or parachalcogen (=CO, =SO) ligand. They are summarized in Scheme 1. These functional groups are incorporated into the periodic system as shown in Scheme 2. In particular the stability and chemistry of $(\text{CF}_3\text{S})_2\text{C}\cdot$, $\text{CF}_3\text{SN}\cdot$, $\text{F}_2\text{C}=\text{Te}$, $(\text{CF}_3\text{S})_2\text{C}=\text{C}=\text{O}$, and $\text{CF}_3\text{SN}=\text{S}=\text{O}$ shall be discussed.

Fluorine-Containing Carbenes

Fluorinated carbenes are a well known and thoroughly investigated class of reactive intermediates. Their stability decreases in the order $:\text{CF}_2 > :\text{CFR}_f > :\text{C}(\text{R}_f)_2$ and $:\text{CF}_2 > :\text{CCl}_2 > :\text{CBr}_2 > :\text{Cl}_2$. Since $:\text{CCl}_2$ is an important reagent in synthetic chemistry and the comparability of $\text{Cl}/\text{CF}_3\text{S}$ (*I*) has been demonstrated in many cases, the preparation and characterization of $(\text{CF}_3\text{S})_2\text{C}\cdot$ became important to us.

Almost all reactions providing carbenes were carried out when the corresponding CF_3S -substituted derivative was available. But only the photolysis of $(\text{CF}_3\text{S})_2\text{C}=\text{C}=\text{O}$, either neat or in C_6F_6 solution, provided low yields of $(\text{CF}_3\text{S})_2\text{C}=\text{C}(\text{SCF}_3)_2$, thus indicating the formation of $(\text{CF}_3\text{S})_2\text{C}\cdot$ as an intermediate. In protic solvents or in the presence of olefins such as cyclohexene, formation of either $(\text{CF}_3\text{S})_2\text{C}=\text{C}(\text{SCF}_3)_2$ or 2+1 cycloadducts could not be detected. The reactions that were carried out are summarized in Scheme 3.

An explanation of these contradictory observations was found by investigating the photolysis of $(\text{CF}_3\text{S})_2\text{C}=\text{C}=\text{O}$ by esr and matrix isolation IR spectroscopic methods. Irradiating a solution of $(\text{CF}_3\text{S})_2\text{C}=\text{C}=\text{O}$ in *n*-hexane treated with argon in a flow cell provided an esr spectrum consisting of a doublet of septets as shown in Figure 1. This spectrum is assigned to the $(\text{CF}_3\text{S})_2\text{CH}$ radical formed by intermediate formation of $(\text{CF}_3\text{S})_2\text{C}\cdot$ in the triplet state, which then abstracts a hydrogen atom from the solvent. This secondary reaction is probably one reason why the carbene was not detected in earlier experiments. The following data for $(\text{CF}_3\text{S})_2\text{CH}$ were measured and compared with literature values.

$T[\text{K}]$	$a(^1\text{H}\alpha)[\text{G}]$	$a(^{19}\text{F}\gamma)[\text{G}]$	<i>g</i> -Factor
283	13.9	2.2	2.00516
253*	17.5*	2.75*	-

*(2)

When the ketene is irradiated in an argon matrix at 10 K ($\lambda = 230$ nm) the formation of CO, CS_2 and C_2F_6 can be detected in addition to the bands of the ketene. These results prove the great instability of the carbene $(\text{CF}_3\text{S})_2\text{C}\cdot$: which decomposes to the final products CS_2 and C_2F_6 according to Scheme 4. As far as carbenes are concerned, a decrease in stability is observed going from F to CF_3 to CF_3S (3).

Fluorine-Containing Nitrenes

A similar situation is observed with nitrenes. Representatives such as $\text{FN}\cdot$ and $\text{CF}_3\text{N}\cdot$ are reactive intermediates, but they do not reach the importance of carbenes. In the

Table I. Aromatic Substituent Constants

	<i>EN</i>	σ_p	σ_m	σ_E	σ_R	π	<i>Steric Effects</i>
F	4.00	0.06	0.34	0.43	-0.34	0.14	-0.46
CF ₃	3.3	0.54	0.43	0.38	0.19	0.88	-2.40
CF ₃ S	2.7	0.50	0.40	0.35	0.18	1.44	-1.07

Aliphatic Substituent Constants

	<i>Hydrophobicity</i> π	<i>Electronic Effect</i> σ
F	-0.61	3.08
CF	0.06	2.85
CF ₃ S	-0.74?	-2.5?

Carbenes	Nitrenes
	F-N̄ F ₃ C-N̄ F ₃ C-S-N̄ ⇌ CF ₃ S=N̄
	C FS-N̄ ⇌ FS=N̄ CIS-N̄ ⇌ CIS=N̄

Chalcogenated Carbenes and Nitrenes

F ₂ C=Q̄	(F ₃ C) ₂ C=Q̄	(F ₃ CS) ₂ C=Q̄	FNO
F ₂ C=S̄	(F ₃ C) ₂ C=S̄	(F ₃ CS) ₂ C=S̄	F ₃ CNO
F ₂ C=Sē	(F ₃ C) ₂ C=Sē	(F ₃ CS) ₂ C=Sē	F ₃ CSNO
F ₂ C=Tē	(F ₃ C) ₂ C=Tē	(F ₃ CSe) ₂ C=Sē	
		(F ₃ CS) ₂ C=Tē	
		(F ₃ CTe) ₂ C=Tē	

CO- and SO-substituted Carbenes and Nitrenes

F ₂ C=C=Q̄	F ₂ C=S=Q̄	FN̄=C=Q̄	FN̄=S=Q̄
(F ₃ C) ₂ C=C=Q̄	(F ₃ C) ₂ C=S=Q̄	F ₃ C-N̄=C=Q̄	F ₃ C-N̄=S=Q̄
(F ₃ CS) ₂ C=C=Q̄	(F ₃ CS) ₂ C=S=Q̄	F ₃ CS-N̄=C=Q̄	F ₃ CS-N̄=S=Q̄

Scheme 1

**Incorporation of the Substituted Functional Groups
or Molecules in the Periodic System**

A: With X=F,CF₃,CF₃S) as a Ligand to Carbon and Nitrogen

C	N X-C	O XN X ₂ C
---	----------	-----------------------------

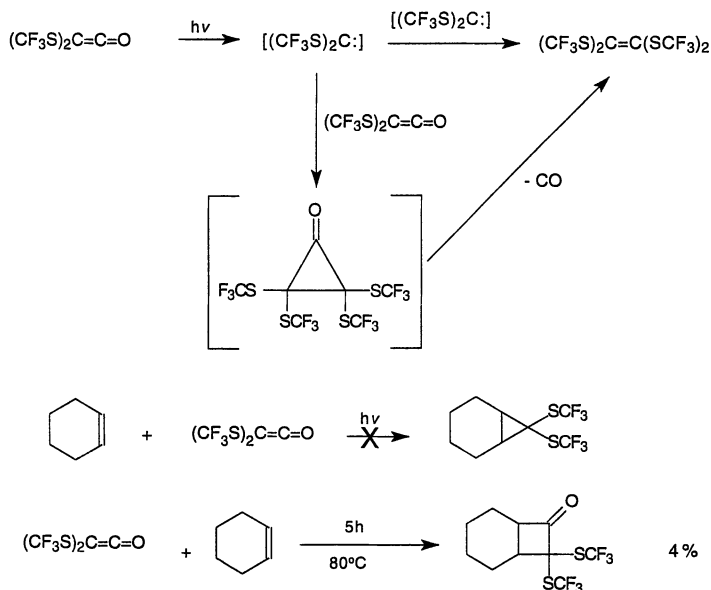
B: With Chalcogens as Ligands to X-N̄ and X₂C̄

Group 16 (Chalcogens)	Group 17 (Halogens)	Group 18 (Noble Gas)
XN		XNO
X ₂ C		X ₂ CO X ₂ CS X ₂ CSe X ₂ CTe

C: With =C=O and =S=O as Ligands to X-N̄ and X₂C̄

X-N̄	XN=C=O XN=S=O
X ₂ C̄	X ₂ C=C=O X ₂ C=S=O

Scheme 2



Scheme 3

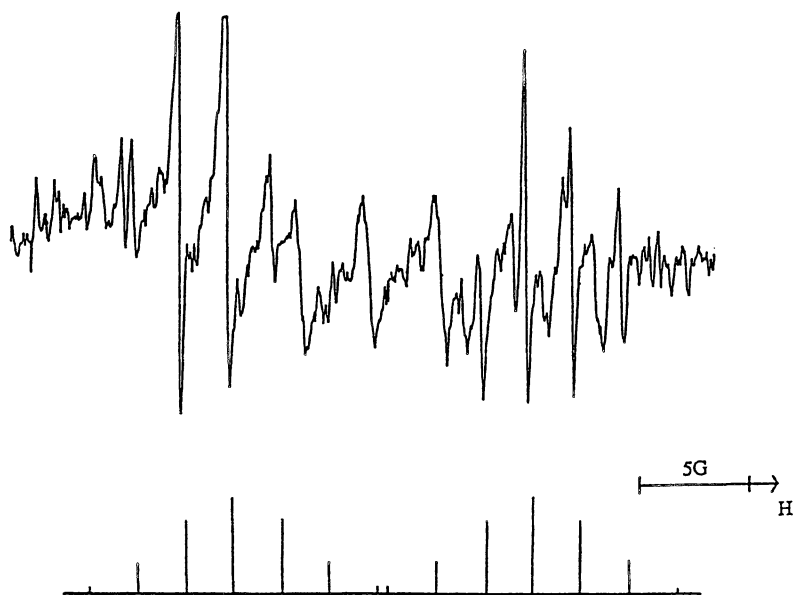
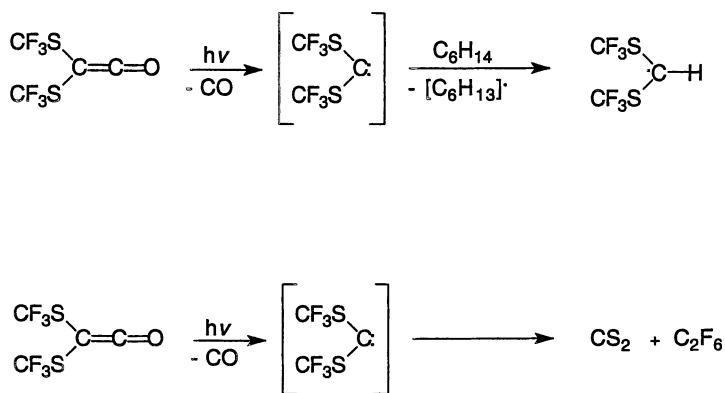


Figure 1. Esr spectrum of the $(\text{CF}_3\text{S})_2\text{CH}$ radical.



Scheme 4

case of CF_3SN one must consider a thiazyl molecular structure in addition to that of a nitrene



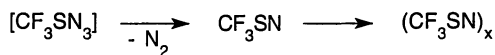
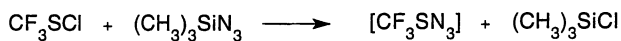
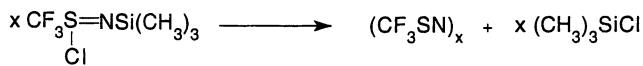
One would expect $\text{CF}_3\text{S}=\text{N}|$ to be the thermodynamically more stable structure. In the literature CF_3SN (4) was mentioned as an unstable intermediate which oligomerizes to $(\text{CF}_3\text{SN})_x$. It is formed according to Scheme 5.

Decomposition of $\text{CF}_3\text{S}(\text{Cl})=\text{NSi}(\text{CH}_3)_3$ in the presence of dienes such as butadiene, cyclopentadiene, hexachlorocyclopentadiene and tetraphenyl cyclopentadienone affords no addition products, thereby proving that decomposition of the starting material proceeds via inter- instead of intramolecular condensation. The other synthetic method, which is based on CF_3SN_3 as an intermediate (see Scheme 5), should be more promising since CF_3SN (and N_2) will be formed through an intramolecular process. In the presence of hexachlorocyclopentadiene a 1:1 addition product is formed in rather low yield. Single crystal X-ray structure analysis of this material shows that CF_3SN reacts as a nitrene and not as a thiazyl, giving hexachloro-3-cyclopentenylidene amino-trifluoromethylsulfide according to Figure 2. A possible reaction pathway is provided in Scheme 6. This result raises the question of how ClSN or FSN would interact with C_5Cl_6 . The reaction with ClSN produces the corresponding sulphenyl chloride as proven by the X-ray crystallography. An almost identical structure is observed as is shown in the ORTEP plot in Figure 3. Again ClSN reacts as a nitrene. Additional proof for the presence of an $-\text{SCl}$ group is provided by treating the product with $\text{Hg}(\text{SCF}_3)_2$ and SbCl_5 in SO_2 (see Scheme 7).

The reaction of C_5Cl_6 with FSN is more complicated since the first reaction product, a sulphenyl fluoride, is unstable and undergoes metathetical reactions with C_5Cl_6 as shown in Scheme 8 (5). With perfluoro olefins, however, FSN reacts differently. The reaction products formed depend on both the reaction conditions and the nature of the olefin. A [4+2] cycloaddition reaction is observed between FSN and perfluorobutadiene (6); however, a [2+1] cycloaddition cannot be excluded, since the six-membered ring is postulated only on the basis of NMR data. A Cl/F exchange was achieved with $(\text{CH}_3)_3\text{SiCl}$ (6) or by treating $\text{CF}_2=\text{CFCF}=\text{CF}_2$ with $(\text{ClSN})_3$ at 22°C (7) according to Scheme 9.

A low temperature X-ray crystal structure analysis proved unambiguously the six-membered ring structure shown in Figure 4. The S-Cl bond of the 1,2-thiazine is converted by NaF or KF in good yields to the fluorinated derivative leaving no doubt that in both cases a [4+2] cycloaddition takes place. The reactions studied so far, at least with C_5Cl_6 as a reaction partner, strongly suggest that the XSN ($\text{X} = \text{CF}_3, \text{Cl}, \text{F}$) compounds react not only as thiazyls but also as nitrenes. Obviously the mesomeric structures shown in Scheme 10 explain their reactivity (7).

One can conclude that perfluorinated nitrenes are unstable, reactive intermediates. However, a stability trend caused by the ligands $\text{F}, \text{CF}_3, \text{CF}_3\text{S}$ cannot be demonstrated.



Scheme 5

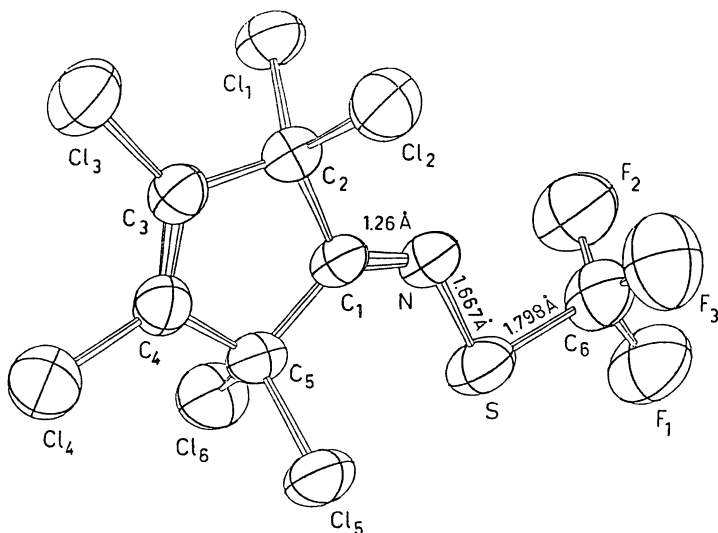
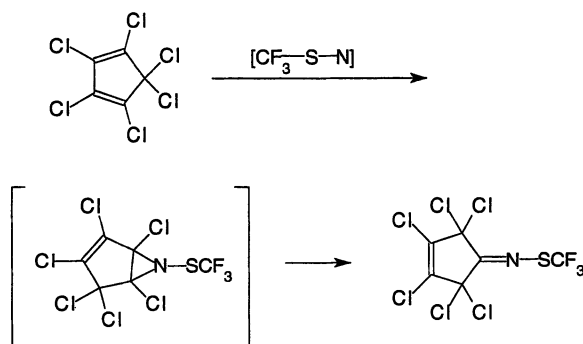


Figure 2. Molecular structure of hexachloro-3-cyclopentenyldene amino-trifluoromethylsulfide.



Scheme 6

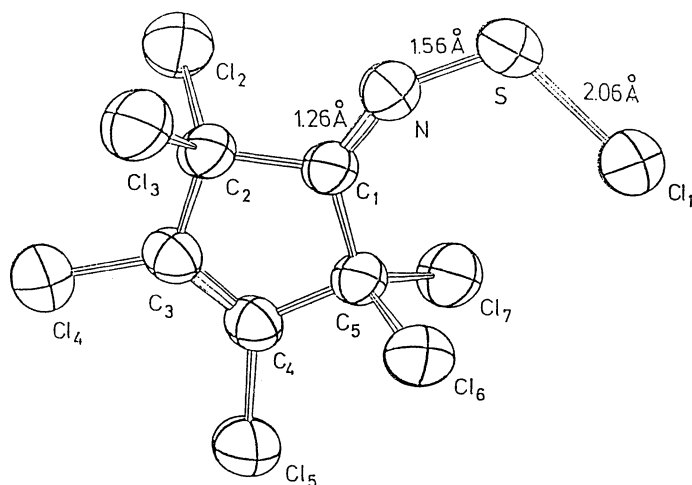
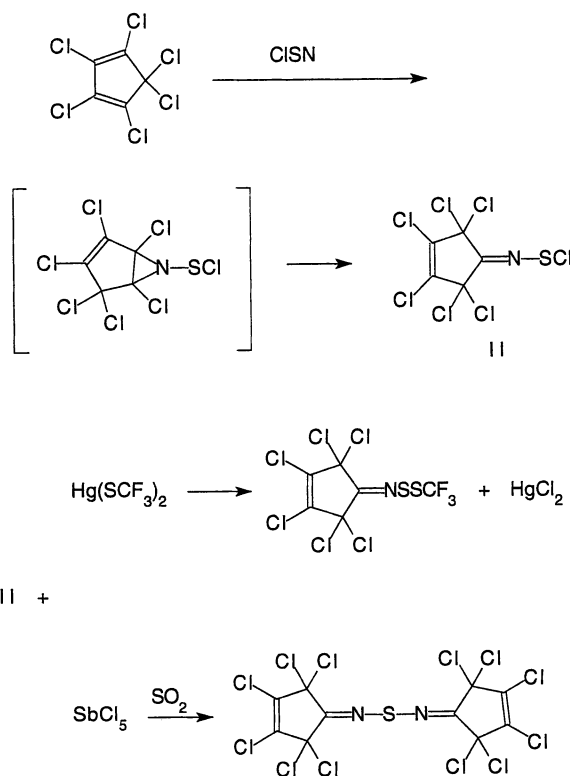
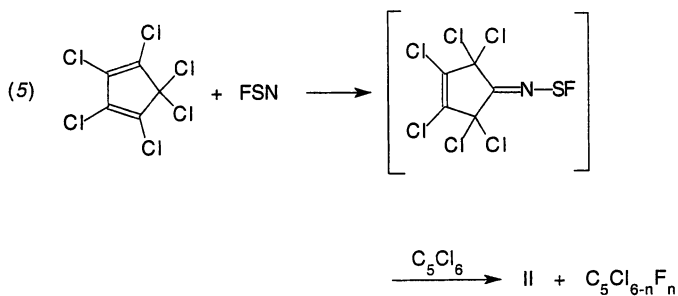


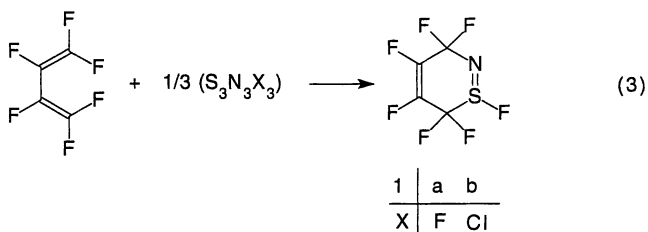
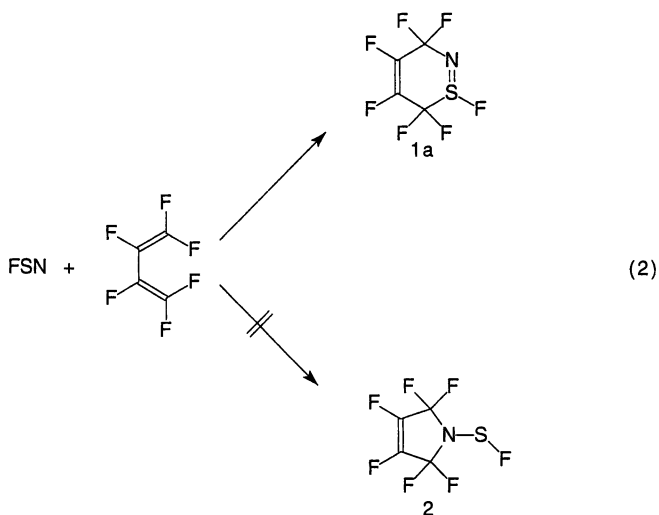
Figure 3. Molecular structure of hexachloro-3-cyclopentenyldene amino-sulfonyl chloride.



Scheme 7



Scheme 8



Scheme 9

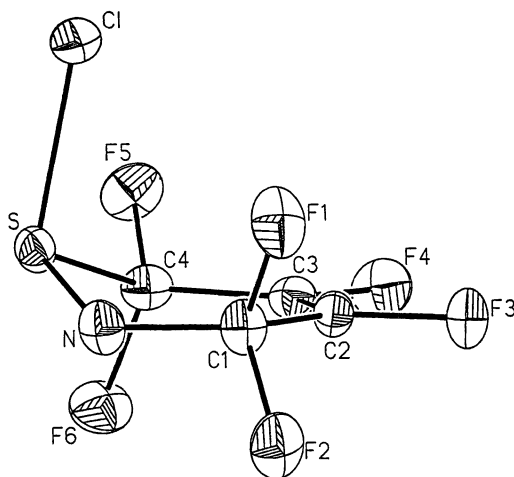
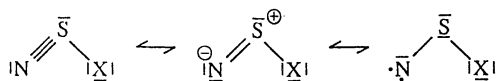


Figure 4. Molecular structure of 1-Chloro-3,3,4,5,6,6-hexafluoro-3,6-dihydro-1 λ ⁴,2-thiazine.



Scheme 10

Fluorine-Containing Carbonyls, Thiocarbonyls, Selenocarbonyls and Tellurocarbonyls

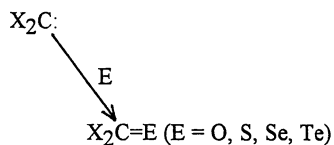
Carbenes coordinated with a chalcogen ligand are transformed to electronically saturated compounds with a C=E group such as $X_2C=E$ (E = O, S, Se, Te). In this series the hitherto unknown substance is $X_2C=Te$.

The preparations of $F_2C=Se$ can be expressed with one reaction as shown in Scheme 11. It is necessary to synthesize first of all a material containing an element- $SeCF_3$ group which decomposes on heating in vacuo to an element-fluorine moiety and $F_2C=Se$ (8-10). This strategy was also applied to the first synthesis of $F_2C=Te$. The reaction between $Hg(TeCF_3)_2$ and $(C_2H_5)_2AlI$ proceeds at $20\text{ }^\circ\text{C}/10^{-4}$ torr as shown in Scheme 12 and provides a deep violet-colored, thermally very unstable substance in about 10% yield. The product already dimerizes during removal of the liquid nitrogen Dewar to its dark red-colored cyclic dimer. Cocondensation with excess F_2CSe gives for the first time an orange-colored four-membered ring with two different chalcogen heteroatoms. X-ray crystal structure analysis of the dimer proved the postulated ring. An ORTEP projection and selected parameters are provided in Figure 5 (11).

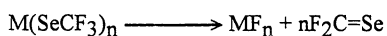
An additional two step route to $F_2C=Te$ — preparation of the tin derivative and its thermal decomposition — is shown in Scheme 13 (12). This method gives better yields, and it was possible to demonstrate that $F_2C=Te$ undergoes a [4+2] cycloaddition with e.g. dimethylhexadiene. For the first time it was also possible to obtain an IR-spectrum in the gas phase. In the region 4000 to 400 cm^{-1} the bands observed are shown in Figure 6a. Upon expansion of the range 1300 to 1100 cm^{-1} one clearly recognizes band contours. At about 1240 cm^{-1} , ν_1 shows a PQR splitting with $\Delta PR = 12.2\text{ cm}^{-1}$, and ν_4 a PR branch at 1206.7 and 1195.4 cm^{-1} , respectively. These bands are in complete agreement with the ones observed for $F_2C=Se$ as shown in Figure 6b. The other four bands are either too weak to be observed or appear below 400 cm^{-1} . The mass spectrum of $F_2C=Te$, shown in Figure 7, exhibits M^+ with the correct isotopic pattern and the fragments $FCTe^+$, Te^+ , and CF_2^+ . In addition, the fragments $C_2F_4^+$ and $C_2F_3^+$ are observed.

The cyclic dimer is a good starting material for further reactions. Halogen exchange with BCl_3 or BBr_3 gives tetrahalogenated 1,3-ditelluraetanes according to Scheme 14. These compounds are soluble in DMF with adduct formation, but are not soluble in other common solvents. With AsF_5 in SO_2 , only $Te_4[AsF_6]_2$ can be detected (13).

The synthesis of a C=Te double bond for the first time encouraged us to search for other molecules with such a group. Some of these might even be more stable. From what we know thus far the stability of C-chalcogen double bonds decreases from O to Te and from F to CF_3 , but increases when F or CF_3 is replaced by CF_3E (E = S, Se). So the chances of synthesizing molecules of the type $(CF_3E)_2C=Te$ or probably even $(CF_3Te)_2C=Te$ should be reasonable.

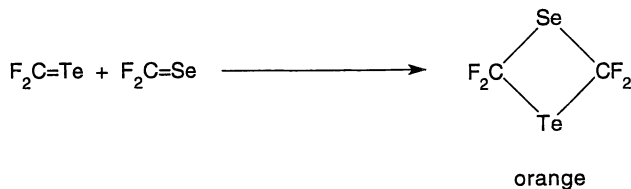
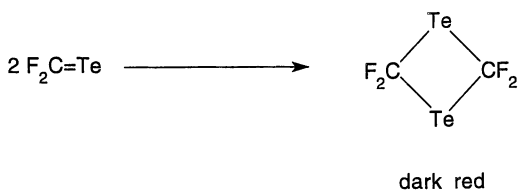
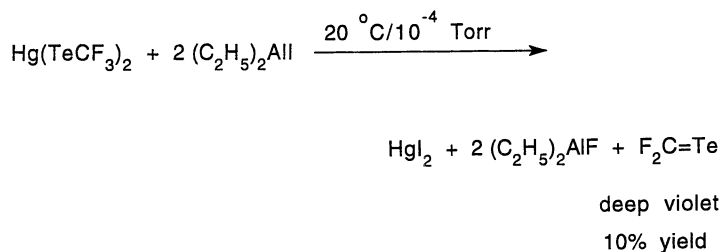


Preparation of F₂C=Se:



M=B, n=3 (8); M=(CH₃)₃Sn, n=1 (9); M=(CH₃)₂Al, n=1 (10)

Scheme 11



Scheme 12

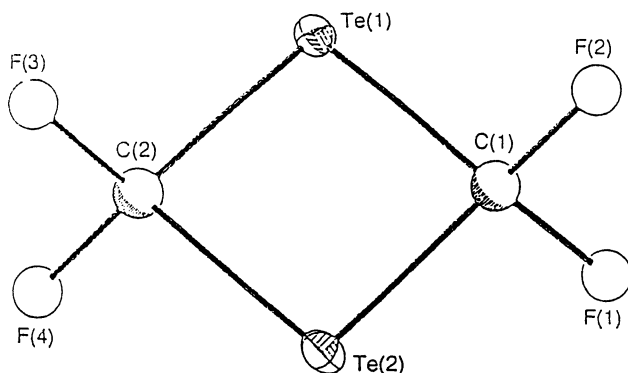
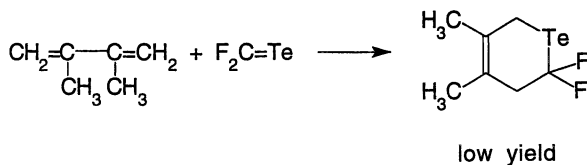
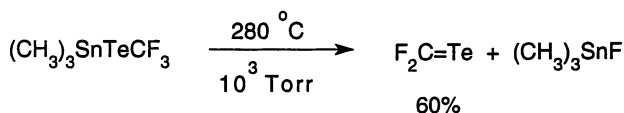
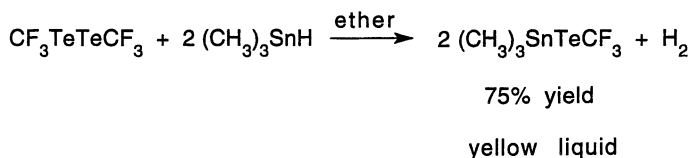
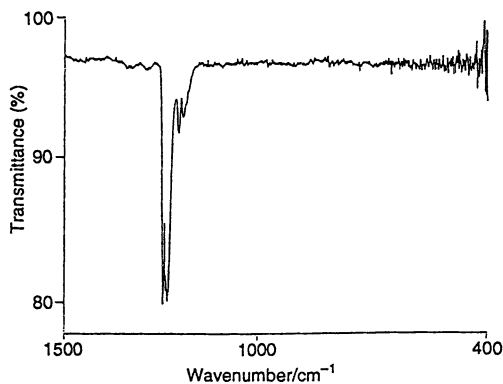
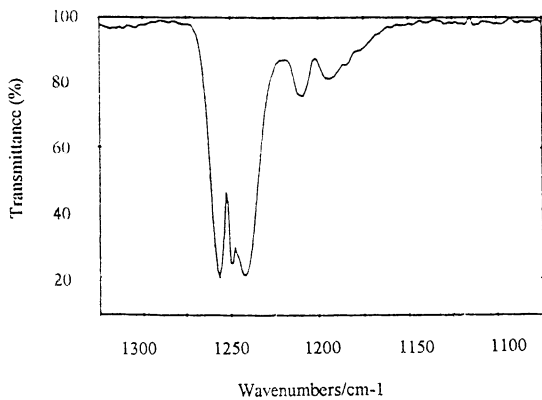
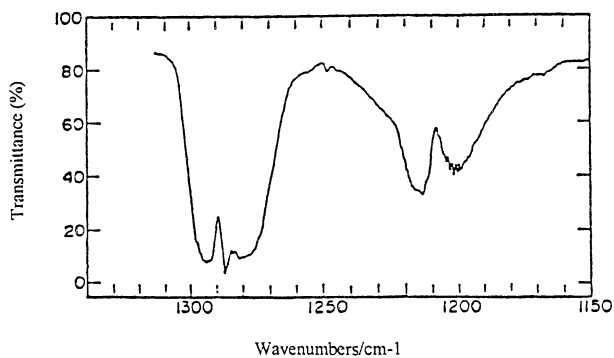


Figure 5. The crystal structure of tetrafluoro-1,3-ditelluraetane. Average bond lengths (in Å over two independent molecules in the unit cell): C-F 1.359 (10), Te-C 2.191 (11); angles (°): C-Te-C 78.9 (4), Te-C-Te 101.2 (4), F-C-F 105.3 (10), Te-C-F 112.7 (5).



Scheme 13

Figure 6a. IR gas phase spectrum of $F_2C=Te$. $TeCF_2$  $SeCF_2$ Figure 6b. Comparison of IR band contours of $F_2C=Te$ with $F_2C=Se$.

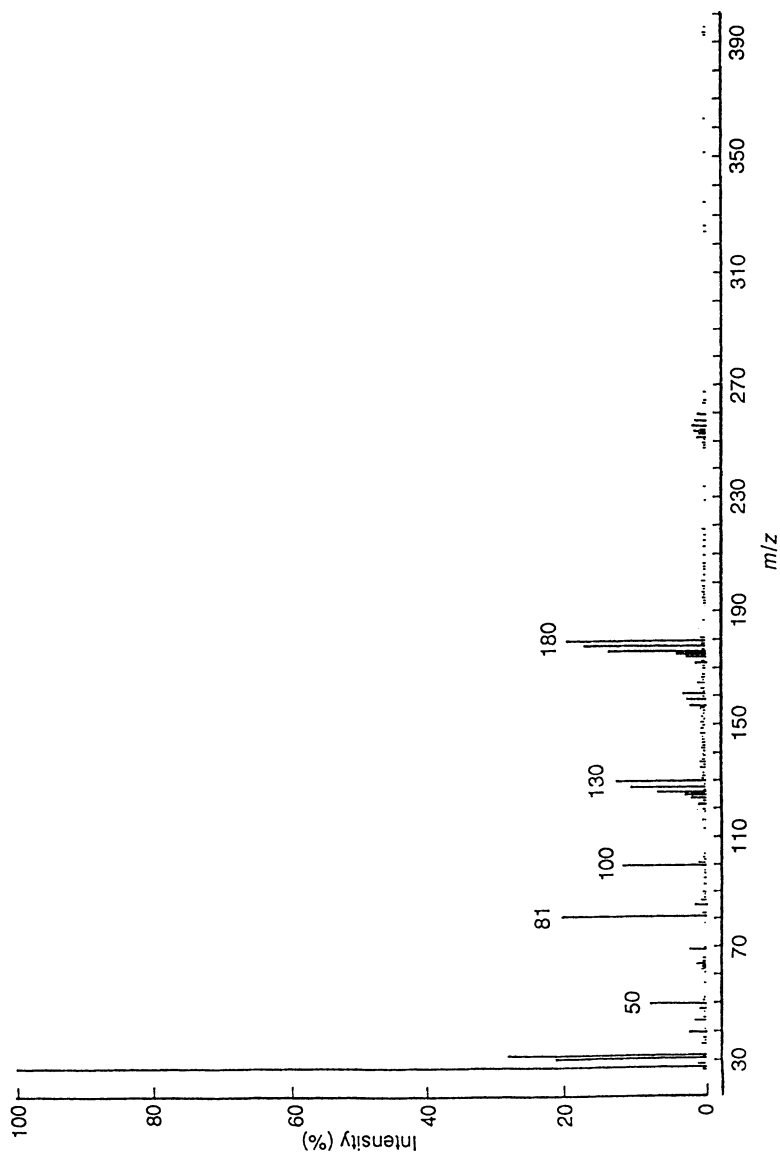
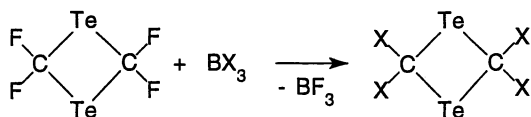
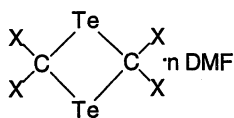


Figure 7. Mass spectrum of $F_2C=Te$.



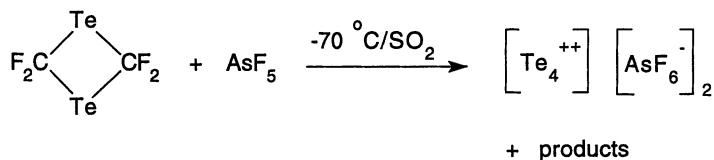
X = Cl, Br

Soluble only in $(\text{CH}_3)_2\text{NC}(\text{O})\text{H}$ (DMF) forming complexes



X = Cl, n = 0.5

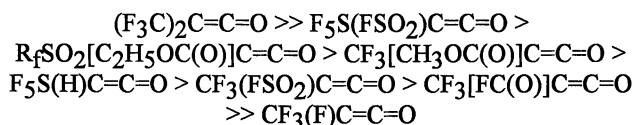
X = Br, n = 1



Scheme 14.

Fluorine-Containing Ketenes and Thioketenes

A ketene results when the carbonyl function becomes a ligand to a carbene. Dihalogenated and perfluoroalkyl-substituted ketenes exhibit characteristic and peculiar chemical properties. The stability of dihalogenoketenes can tentatively be arranged as follows: $F_2C=C=O > Cl_2C=C=O > Br_2C=C=O \gg FCIC=C=O$, and similarly the other fluorine-containing ketenes show the following scale of stability:



The normally electrophilic character of the ketene group is increased by introducing two electronegative groups, making both $(CF_3)_2C=C=O$ and $F_2C=C=O$ stable and pronounced electrophiles. What is going to happen if the less electronegative CF_3S group becomes a substituent? Will $(CF_3S)_2C=C=O$ become less stable and more reactive? To answer these questions the molecule had to be synthesized. This was achieved by three routes following known literature procedures as given in Scheme 15.

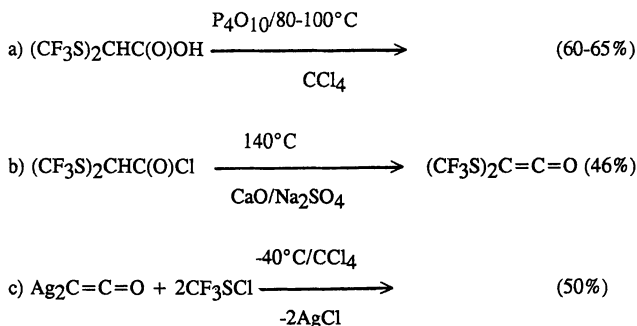
The starting materials for reactions a) and b) are synthesized as shown in Scheme 16. $(CF_3S)_2C=C=O$ is a colorless liquid which is stable up to at least 100°C. When the compound is heated at 200°C in a Carius tube, dimerization takes place, giving two isomers according to Scheme 17. Both isomers were separated by preparative gas chromatography. Photolysis of $(CF_3S)_2C=C=O$ in CCl_4 for 72 h gave $(CF_3S)_2C=C(SCF_3)_2$ and CO in low yields only. This reaction has already been mentioned. When the ketene or its acetal was treated with ozone, oxidation took place according to Scheme 18 (14).

Attempts to prepare $(CF_3S)_2C=C=S$ by treating $(CF_3S)_2C=C=O$ or its precursors with P_4S_{10} in toluene at 145°C yielded ring compounds shown in Scheme 19 (15).

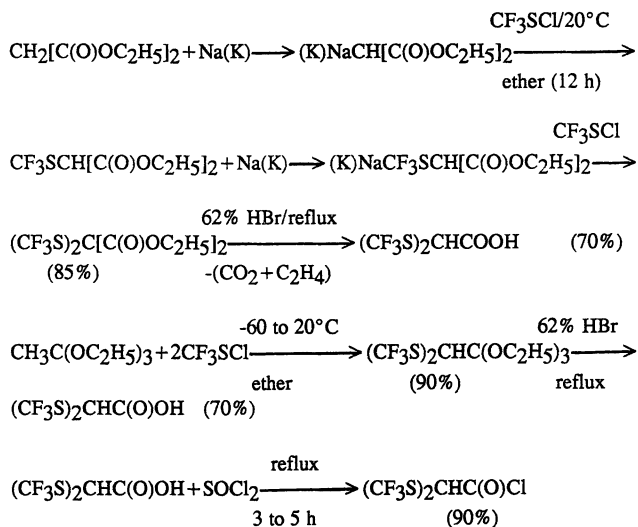
Fluorine-Containing Sulfines, Isocyanates, and Sulfinylamines

When $=S=O$ becomes a ligand to X_2C , sulfines (thiocarbonyl-S-oxides) are formed. Their stability increases in the order $F < CF_3 < CF_3S$; that means $F_2C=S=O$ is less stable than $(CF_3)_2C=S=O$ and $(CF_3S)_2C=S=O$. Stability and reactivity of perfluorinated ketenes and sulfines compare rather well. With CO as a ligand to XN, isocyanates are obtained. Their chemistry and stability is well known and shows that CF_3SNCO is more stable than CF_3NCO and $FNCO$ (16).

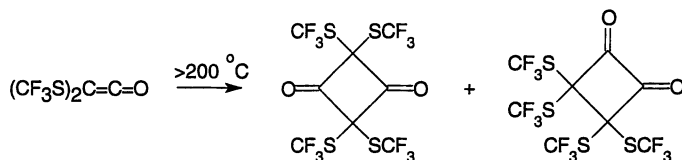
Similarly, with $S=O$ as a ligand to XN, compounds of the type XNSO are obtained. Again the reactivity of FNSO (17-19) is higher than the reactivity of F_3CNSO (20-22) and F_3CSNSO (23). In agreement with these facts, the reactions of F_3CNSO or FNSO with water gave no stable intermediates which could be isolated or fully characterized. Therefore hydrolysis of F_3CSNSO was studied in detail to elucidate whether stable products result.



Scheme 15

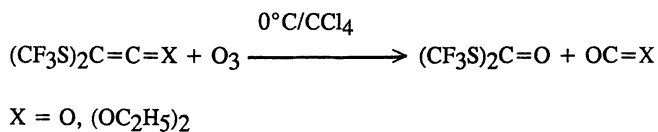


Scheme 16

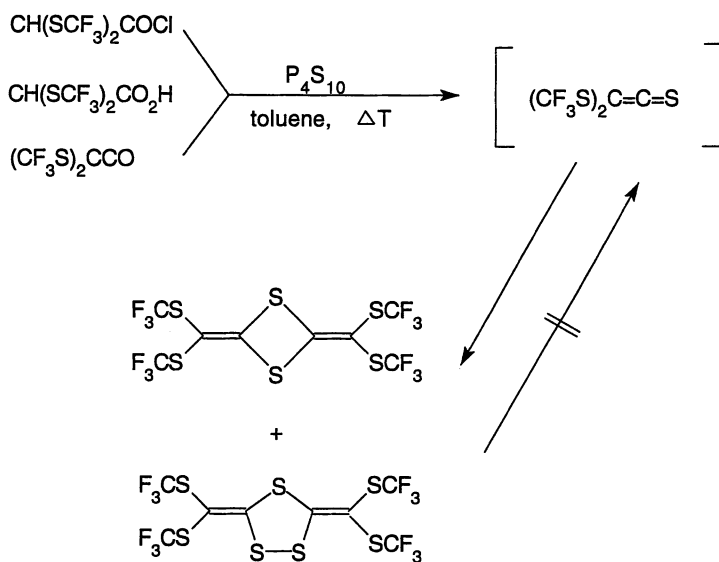


Separation by gas chromatography [parameters:
 3.0 m (i.d. = 6 mm) OV 101 10% on Chromosorb P AW
 45 - 60 mesh, 95 °C, He flow: 80 mL/min

Scheme 17

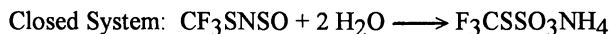


Scheme 18

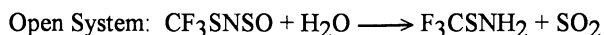


Scheme 19

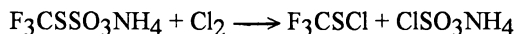
Hydrolysis of F_3CSNSO yielded colorless crystals which were characterized as the first representative of a perfluoroorganothiosulfonate R_fSSO_2OR . In a stoichiometric reaction carried out in a sealed Carius tube, one mole of F_3CSNSO reacted with two moles of water to form ammonium trifluoromethylthiosulfonate as the sole product, according to



The ammonium salt melts at $195^\circ C$ and can be stored in a dry atmosphere for a few days at room temperature without decomposition. When the hydrolysis was carried out in an open system, the corresponding amine F_3CSNH_2 and sulfur dioxide were detected.

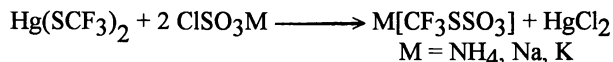


In addition to the measurement of the 1H -, ^{14}N -, ^{19}F -, ^{13}C -, ^{17}O -NMR (Table II), IR, and Raman spectra, which agree very well with the nature of the compound, $CF_3SSO_3NH_4$ was also treated with a stoichiometric amount of chlorine. The expected cleavage of the characteristic sulphur-sulphur bond provided further evidence for the proposed thiosulfonate molecular structure, in full agreement with the behavior of the corresponding organothiosulfonates (24). Stoichiometric amounts of

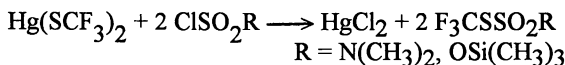


the well known products were isolated and their identities confirmed by spectroscopic investigations and elemental analyses.

An alternative route to trifluoromethylthiosulfonate is the reaction between ammonium chlorosulfonate and $Hg(SCF_3)_2$ in acetonitrile according to



Separation of the salt-like compounds from $HgCl_2$ was laborious, as both products are soluble in polar solvents. However, covalent derivatives of the type F_3CSSO_2R were prepared by reacting the mercurial with covalent derivatives of chlorosulfonic acid. These reactions were carried out in CCl_4 , a solvent in which the reactants and products, except $HgCl_2$, are soluble.



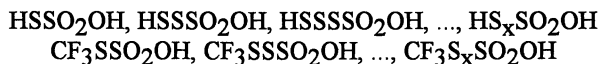
Thus, the *N,N*-dimethylamino and trimethylsiloxy derivatives of trifluoromethylthiosulfonic acid were prepared and characterized by spectroscopic methods (Table II). The ^{29}Si -NMR shift of the trimethylsilylester allowed us to estimate the acidity of the corresponding acid by a known correlation (25) of $\delta(^{29}Si)$ -values of the various trimethylsilylesters with the acidity of their parent acids. The acidity of

Table II. NMR spectra (solvent) of Trifluoromethylthiosulfonates

	$F_3CSSO_3NH_4$	$F_3CSSO_3SiMe_3$	F_3CSSO_3H	$F_3CSSO_2N(CH_3)_2$
1H standard: TMS	$\delta = 5.9(1:1:t)$ (D_3CCN) $^1J(^1H, ^{14}N) = 51$ Hz	$\delta = 0.48(s)$ ($CCl_4/CDCl_3$)	$\delta = 9.92(s)$ ($CDCl_3$)	$\delta = 2.99(s)$ ($CDCl_3$)
^{14}N standard: H_3CNO_2	$\delta = 352.6$ (quintet) $^1J(^{14}N, ^1H) = 51$ Hz	---	---	---
^{13}C standard: TMS	$\delta = 127.7(q)$ (D_3CCN) $^1J(^{13}C, ^{19}F) = 310.7$ Hz	$\delta(F_3C) = 127.12(q)$ $^1J(^{13}C, ^{19}F) = 312.8$ Hz $\delta = 0.081(m)$ $^1J(^{13}C, ^1H) = 121.43$ Hz ($CDCl_3$)	$\delta = 126.95(s)$ ($CDCl_3$) $^1J(^{13}C, ^{19}F) = 312.4$ Hz	$\delta(CF_3) = 128.21(q)$ $^1J(^{13}C, ^{19}F) = 312.9$ Hz $\delta(CH_3) = 38.49(q)$ $^1J(^{13}C, ^1H) = 141.1$ Hz ($DCCl_3$)
^{17}O standard: H_2O	$\delta = 239.1(s)$ (D_3CCN) $\omega = 70$ Hz	$\delta(S=O) = 408(s)$ ($CDCl_3$) $\omega = 100$ Hz $\delta(S-O-Si) = 368(s)$ $\omega = 200$ Hz	$\delta = 209$ ($D_3CCN/ext.$)	$\delta = 203.7(s)$ ($DCCl_3$)
^{19}F standard: $FCCl_3$	$\delta = -38.5(s)$ (D_3CCN)	$\delta = -39.9(s)$ (D_3CCN)	$\delta = -39.0(s)$ ($CCl_4/CDCl_3$)	$\delta = -37.7(s)$ ($DCCl_3$)
^{29}Si standard: TMS	---	$\delta = 41.9(m)$ ($CDCl_3$) $^2J(^{29}Si, ^1H) = 6.97$ Hz	---	---

trifluoromethylthiosulfonic acid is extrapolated to be similar to the acidities of trifluoromethylsulfonic and perchloric acid.

It is known that HSSO_2OH is only the first member of a homologous series of polysulfane monosulfonic acids which can be generated by the reaction of H_2S_x with SO_3 , whereas $\text{CF}_3\text{SSO}_3\text{H}$ should be the first member of a second homologous series as shown below:



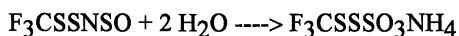
In analogy to the insertion of SO_3 into the S-H bond of H_2S with formation of HSSO_2OH (26), CF_3SH reacts with SO_3 forming a colorless liquid which was characterised (Table II) as trifluoromethylthiosulfonic acid according to



The free acid is extremely sensitive and decomposes at room temperature to $\text{F}_2\text{C}=\text{S}$ and fluorosulfonic acid.

It is noteworthy that all of the ^{19}F -NMR resonances of the trifluoromethylthiosulfonates $\text{F}_3\text{CS}-\text{SO}_2\text{R}$ are in a narrow region of -38.5 ± 1.5 ppm, without great influence from the inductive effect of different substituents R. It is possible to assign the characteristic, but coupled, S-S stretching frequencies in this type of compound by comparing the IR and Raman data (Table IV). The frequencies are very similar in the region of around 430 wavenumbers, and the S-S stretching vibration appears as a strong peak in the Raman and a weak peak in the infrared spectra.

Due to the oxidizing nature of SO_3 and the reducing properties of CF_3SSH , the second member of the homologous series $\text{F}_3\text{CS}_x\text{SO}_2\text{OH}$, where $x = 2$, cannot be obtained via insertion because side reactions are dominant. An alternative route to the first derivative of $\text{F}_3\text{CSSSO}_2\text{OH}$ is hydrolysis of CF_3SSNSO obtained from CF_3SSCl and $(\text{CH}_3)_3\text{SiNSO}$ (27). In analogy to the reaction of CF_3SNSO , CF_3SSNSO reacts stoichiometrically with two moles of water, forming the ammonium salt of trifluoromethylsulphenylthiosulfonic acid as the sole product with the characteristic NMR data as shown in Table III. It may be possible to convert this salt to other ionic



and covalent derivatives of $\text{F}_3\text{CSSSO}_2\text{OH}$ providing a new and interesting chemistry.

Conclusions

It has been shown that one can successfully plan and carry out syntheses by incorporating either fluorine or parahalogen substituent groups in the chemistry of certain functional groups including carbenes, nitrenes, carbonyls, thiocarbonyls, selenocarbonyls, tellurocarbonyls, ketenes, thioketenes, sulfines, isocyanates, and sulfinylamines. In certain cases a decrease in stability is observed upon going from F to CF_3 and CF_3S , while in other cases the instability of all derivatives precludes a

Table III. NMR spectra (solvent) of F₃CSSO₃NH₄

¹ H;	¹⁹ F;	¹³ C;	¹⁷ O;
standard: TMS	standard: FClCl ₃ (D ₃ CCN)	standard: TMS (D ₃ CCN)	standard: H ₃ CNO ₂ (D ₃ CCN)
δ=6.0(1:1:1 t)	δ=-45.2(s)	δ=130.21(q)	δ=222.1(s)

Table IV. Assignments of S-S vibrations

compound	wavelength/cm ⁻¹
F ₃ CSSO ₃ NH ₄	434
F ₃ CSSO ₃ SiMe ₃	432
F ₃ CSSO ₃ H	430
F ₃ CSSO ₂ N(CH ₃) ₂	430
F ₃ CSSSO ₃ NH ₄	381

trend from being established. The chemistry describe herein will hopefully encourage the search for other molecules via the element displacement principle.

Acknowledgment

Dedicated to Prof. Jean'ne M. Shreeve on the occasion of her 60th birthday.

Literature Cited

- (1) Haas, A. *Pure Appl. Chem.* **1991**, *63*, 1577.
- (2) Schlosser, K. *J. Mol. Struct.* **1982**, *95*, 221.
- (3) Dorra, M.; Haas, A., *J. Fluorine Chem.*, in press; Dorra, M. PhD-Thesis, Ruhr-Universität Bochum **1992**.
- (4) Bielefeld, D.; Haas, A. *Chem. Ber.* **1982**, *116*, 1257.
- (5) Haas, A.; Mischo, Th. *Can. J. Chem.* **1989**, *67*, 1902.
- (6) Blutfuß, W.; Mews, R. *J. Chem. Soc., Chem. Commun.* **1979**, 35.
- (7) Boese, R.; Haas, A.; Heß, Th. *Chem. Ber.* **1992**, *125*, 581.
- (8) Haas, A.; Koch, B.; Welcman, N. *Z. Anorg. Allg. Chem.* **1976**, *427*, 114.
- (9) Grobe, J.; Le Van, D.; Welzel, J. *J. Organomet. Chem.* **1988**, *3*, 153; and references therein.
- (10) Darmady, A.; Haas, A.; Koch, B. *Z. Naturforsch.* **1980**, *B35*, 526.
- (11) Haas, A.; Limberg, Ch. *J. Chem. Soc., Chem. Commun.* **1991**, 1378.
- (12) Haas, A.; Limberg, Ch. *Chimia* **1992**, *46*, 78.
- (13) Haas, A.; Limberg, Ch., *J. Chem. Soc., Dalton Trans.*, in press; Limberg, Ch. PhD-Thesis, Ruhr-Universität Bochum **1992**.
- (14) Haas, A.; Praas, H.-W. *Chem. Ber.* **1992**, *125*, 571.
- (15) Haas, A.; Praas, H.-W. *J. Fluorine Chem.*, in press.
- (16) Haas, A. *New Pathways in Inorganic Chemistry*, Cambridge University Press **1968**, 87.
- (17) Veerbeek, W.; Sundermeyer, W. *Angew. Chem.* **1969**, *81*, 331.
- (18) Nachbaur, E.; Kosmus, W.; Krannich, H.; Sundermeyer, W. *Monatsh. Chem.* **1978**, *109*, 1211.
- (19) Eysel, H. H. *J. Mol. Struct.* **1970**, *5*, 275.
- (20) Lustig, M. *Inorg. Chem.* **1966**, *5*, 1317.
- (21) Leidinger, W.; Sundermeyer, W. *Chem. Ber.* **1982**, *115*, 2892.
- (22) De Marco, R. A.; Shreeve, J. M. *J. Fluorine Chem.* **1971**, *1*, 269.
- (23) Haas, A.; Schott, P. *Chem. Ber.* **1968**, *101*, 3407.
- (24) Bunte, H. *Ber. Dtsch. Chem. Ges.* **1874**, *7*, 646.
- (25) Marsmann, H. G.; Horn, H. G. *Z. Naturforsch.* **1972**, *27*, 1448.
- (26) Schmidt, M.; Bauer, A.; Rampf, H. *Angew. Chem.* **1958**, *70*, 399.
- (27) Brosius, A.; Haas, A. *Chem. Ber.*, in press.

RECEIVED November 25, 1993

Chapter 8

Functionalization of Pentafluoro- λ^6 -sulfanyl (SF₅) Olefins and Acetylenes

Rolf Winter and Gary L. Gard

Portland State University, Portland, OR 97207-0751

In this review, the synthesis of SF₅-olefins and acetylenes and their conversion to compounds with new functional groups are described. It will be seen that there are only few reactions that allow the introduction of an SF₅-group, and that there are also only few reactions which lead to derivatives of unsaturated compounds. The chemical transformations of these simple unsaturated compounds into a number of useful and exciting products will be described.

The outstanding chemical stability of sulfur hexafluoride is to some degree carried over to its organic derivatives. Various methods are at hand to effect such a derivatization, e.g., treatment of disulfides, mercaptans or sulfides with fluorine (1), electrochemical fluorination (2), oxidation of aromatic disulfides with silver(II)fluoride (3). SF₅X (X = Cl, Br, SF₅) adds across multiple bonds and forms adducts. Furthermore, tetrafluorosulfur ylides (F₄S=CR₁R₂) add HF to form SF₅-compounds; however, as most of these ylides are formed from SF₅-compounds, this method is only of limited value (4). The simple organic derivatives can undergo further reactions; in particular, the primary addition products of SF₅X and alkenes or alkynes can be dehydrohalogenated to yield alkenes or alkynes.

Over 70 different compounds that contain both the SF₅-substituent and a double or triple bond were synthesized in the last thirty years and are listed in Table I. The high thermal, radiative and chemical stability of the pentafluorothio group make these compounds attractive as replacements for compounds that contain a trifluoromethyl group. The electronegativity value of the SF₅-group appears to be very high; by examining the ¹³C n.m.r. chemical shifts of a number of fluorosulfones, a Pauling electronegativity of 3.62 is found (5). It is, however, comparatively more difficult to introduce this group into a molecule than a CF₃-

Note: A common name for the SF₅ group is pentafluorothio and will be used throughout the text.

0097-6156/94/0555-0128\$08.00/0
© 1994 American Chemical Society

Table I. SF₅ Alkenes Derivatives

Compound (Two-Carbon Alkenes)	IR(C=C) (CM ⁻¹)	Bp (°C)	Reference
1. SF ₅ CH=CH ₂	---	41	(27)
2. SF ₅ CH=CHF	---	---	(29)
3. SF ₅ CH=CHCl	1615	65-67	(20)
4. SF ₅ C(Cl)=CH ₂	1616	64	(40)
5. SF ₅ CH=CF ₂	1748	28.1	(32,72)
6. <i>cis/trans</i> SF ₅ CF=CHF	---	---	(17)
7. SF ₅ CH=CFCl			(48)
8. SF ₅ CF=CF ₂	1786	19	(27,31,72)
9. SF ₅ C(Cl)=CF ₂	1721	---	(40)
10. SF ₅ CH=CHBr	1611	86±2	(20b)
11. SF ₅ C(Br)=CH ₂	---	86	(20)
12. <i>E/Z</i> -SF ₅ CH=CFP(O)(OH) ₂	1649	66(mp)	(61)
13. <i>cis/trans</i> SF ₅ C(Br)=CHCl		50/52mm	(20)
14. <i>E</i> -SF ₅ CF=CFP(O)(OH) ₂	---	101(mp)	(61)
15. <i>cis/trans</i> SF ₅ C(Br)=CH(Br)	1573	55±1/48mm	(20b)
16. SF ₅ CF=CFI	1672	48	(43)
17. SF ₅ C(Br)=CH(SF ₃)	1610	---	(22)
18. (SF ₃) ₂ C=CF ₂	1706	88	(33,34)

Continued on next page

Table I. Continued

Compound		IR(C=C)		
(Three-Carbon Alkenes)		(CM⁻¹)	Bp(°C)	Reference
1.	SF ₅ CH ₂ CH=CH ₂	---	80-82	(27)
2.	<i>cis/trans</i> SF ₅ CH=CHCH ₃	1663	80-82	(27)
3.	<i>cis</i> -SF ₅ CH=CHOCH ₃	1672	50/20mm	(20)
4.	<i>trans</i> -SF ₅ CH=CHOCH ₃	1639	115	(20)
5.	SF ₅ CH=C(Cl)CH ₃	1653	92	(27)
6.	SF ₅ CH ₂ C(Cl)=CH ₂	1640	59/158mbar	(42)
7.	SF ₅ CH=C(CH ₃)Br	1643	109±2	(23)
8.	SF ₅ C(CF ₃)=CF ₂	1722	47	(32,49)
9.	SF ₅ CF ₂ C(Cl)=CF ₂	---	---	(41)
10.	<i>E/Z</i> -SF ₅ CH=C(CF ₃)Br	1630/1637	93±1	(22,23)

Compound		IR		
(Four-Carbons)		(C=C)	Bp(°C)	Reference
1.	SF ₅ CH=C(CH ₃) ₂	1668	102-106	(33)
2.	SF ₅ CH ₂ CHFCH=CH ₂	---	---	a
3.	SF ₅ CH ₂ CH(Cl)CH=CH ₂	---	---	(27)
4.	SF ₅ CH=CHCH=CHCl	---	---	(20)
5.	SF ₅ C(CH ₃)=C(Cl)OCH ₃	---	40-45/20mbar	(24)
6.	SF ₅ CH=C(Br)C≡CH	1620 sh. at 1590	---	(26b)
7.	SF ₅ CF=CFCH ₂ CH ₂ I	---	---	(29)
8.	(SF ₅ CF=CF ₂) ₂	---	---	(52)

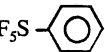
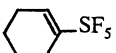
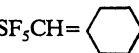
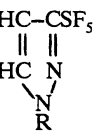
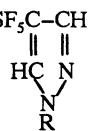
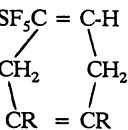
a See M. Tremblay (8) reference in the cited literature.

Table I. Continued

	Compound (Five or More Carbons)	IR (C=C)	Bp(°C)	Reference
1.	$\text{SF}_5\text{C}(\text{CH}_3)=\text{C}(\text{Cl})\text{OC}_2\text{H}_5$	---	45/20mbar	(24)
2.	$E/Z\text{-SF}_5\text{CH}=\text{CFP}(\text{O})(\text{OEt})_2$	1655/1630	---	(61)
3.	$\text{SF}_5\text{CF}=\text{CFP}(\text{O})(\text{OEt})_2$	1666	38°/0.04mm	(60)
4.	$[\text{SF}_5\text{CF}=\text{CFPMe}_3]^+\text{BF}_4^-$	1660	159°(mp)	(43)
5.	$E/Z\text{-SF}_5\text{CH}=\text{CFP}(\text{O})(\text{OSiMe}_3)_2$	1660/1640	---	(61)
6.	$\text{SF}_5(\text{CF}_2)_4\text{CH}_2\text{OC}(\text{O})\text{CH}=\text{CH}_2$	---	---	a
7.	$\text{SF}_5\text{CF}=\text{CFP}(\text{O})(\text{OSiMe}_3)_2$	1665	72°/0.1mm	(60)

a See J.C. Hansen and P.M. Savu (7) reference in the cited literature.

SF₅ Cyclic, Heterocyclic, Aromatic Derivatives

	Compound (Mono SF₅)	IR(C=C) (cm⁻¹)	Bp(°C)	Reference
1.		---	72.0/48mm (X=H) ^a	(3,20)
2.		---	161°	(27)
3.	$\text{SF}_5\text{CH}=\text{C}_6\text{H}_{11}$ 	---	62°C/15mm	(33)
4.	$\text{HC}-\text{CSF}_5$ 	$\text{SF}_5\text{C}-\text{CH}$ 	---	68-69°(mp) (R=H) (20) --- (R=C(O)N(CH ₃) ₂)
5.	$\text{SF}_5\text{C}=\text{C}-\text{H}$ 	1686(C=C) 1652(CH=C-S)	48-50/10mm (R=H) 65°/4mm (R=CH ₃)	(20)

Continued on next page

Table I. Continued

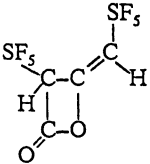
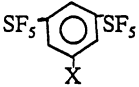
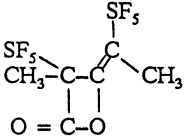
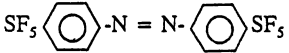
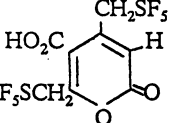
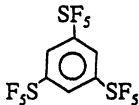
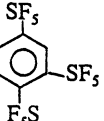
SF₅ Cyclic, Heterocyclic, Aromatic Derivatives, cont'd.

6.		---	197-198°(mp)(R=H) (21)	
		---	78-78.5 (mp)(R=CH ₃ C(O))	
		---	200-201 (mp)	
		---	(R=C ₆ H ₅ NHC(O)) 116-117 (mp)(R=NH ₂)	
7.		---	120°	b
8.		1890/1865	---	(X=CO) (26)
		1750	137°C(mp)	(X=P(C ₆ H ₅) ₃)

a Numerous derivatives with X = *m*-NO₂, *p*-NO₂, *m*-NH₂, *p*-NH₂, *m*-OH, *p*-OH, *m*-CO₂H, *p*-CO₂H, *m*-CH=CH₂, etc.

b See Reference Banks et al (7) in the cited literature.

Table I. Continued

Compound (poly SF ₆)	Compound (poly SF ₆)	IR(C=C) (cm ⁻¹)	Bp(°C)	Reference
1.		---	---	(73)
2.		---	88/1.6mm (X=NO ₂) --- (X=NH ₂) 80.7-81.5°(mp) (X=NH ₂ ·HCl)	(3)
3.		---	---	(74)
4.		---	163-164°(mp)	(3)
5.		---	---	(35)
6.		---	126-127°(mp)	(25)
7.		---	6°	(25)

Continued on next page

Table I. Continued

SF₅ Alkyne Derivatives

	Compound	IR(C≡C) (cm⁻¹)	Bp(°C)	Reference
1.	SF ₅ C≡CH	2118	6°C	(20,21)
2.	SF ₅ C≡CLi	---	---	(25)
3.	SF ₅ C≡CCH ₃	2661	65-70°C	(27)
4.	SF ₅ C≡C-C≡CH	2260	57.6°	(26)
5.	SF ₅ C≡C-Cl	---	-69°	(25)
6.	SF ₅ C≡C-CF ₃	2295	14.4°	(22)
7.	SF ₅ C≡C-Br	---	-65°	(25)
8.	(CH ₃) ₃ SiC≡CSF ₅		-8.5°C (mp) 96.9°	(25)
9.	SF ₅ CH=C(Br)C≡CH	2120 (C≡C) 1620, sh. at 1590 (C=C)	---	(26)
10.	SF ₅ C≡C-Ag	2062	---	(20)
11.	SF ₅ C≡C-I	---	-52°(mp)	(25)
12.	SF ₅ C≡CSF ₅	2220	51°	(22)
13.	IMg(C≡CSF ₅)	---	---	(25)
14.	SF ₅ C≡C-C≡CSF ₅	2180	105°	(26b)
15.	Co ₂ (CO) ₆ (HC≡C-SF ₅)	---	47°(mp)	(25)
16.	Hg(C≡CSF ₅) ₂	---	---	(25)
17.	Co ₂ (CO) ₆ ((CH ₃) ₃ SiC≡C-SF ₅)	---	135°(mp)	(25)
18.	Co ₂ (CO) ₅ (HC≡C-SF ₅) ₂	---	74°(mp)	(25)
19.	Co ₂ (CO) ₆ (SF ₅ C≡CSF ₅)	---	149°(mp)	(25)
20.	Co ₂ (CO) ₄ (HC≡C-SF ₅) ₃	---	108°(mp)	(25)
21.	C ₆ H ₅ HgC≡CSF ₅		100°(mp)	(25)

group, or generally, C_nF_{2n+1} -group, and also rather more expensive. It is envisioned that SF_5 -compounds could be useful dielectrics, replacements for fluorochlorohydrocarbons, very resistant polymers, fuel cell electrolytes with advantageous properties, blood substitutes, surfactants, high energy materials (explosives and rocket fuels (6)) or pesticides. In several cases, these expectations are seen to be fulfilled (7).

In order to allow for ready access to these compounds, it was necessary to devise acceptably simple syntheses of both SF_5Cl and SF_5Br , which form an SF_5-C bond by addition across double and triple bonds. The use of S_2F_{10} has been described, either alone (8) or as a mixture with iodine (9); product mixtures were obtained with olefins and only selected olefins yielded any SF_5 -compounds at all.

The Synthesis of Pentafluorothio Halides (SF_5X)

Pentafluorothio chloride can be obtained by several different methods, the oldest one being first heating SF_4 with cesium fluoride (at ca $150^\circ C$), potassium fluoride ($300^\circ C$) or silver fluoride ($300^\circ C$) and then treating the intermediate MSF_5 with chlorine ($M = Cs$ ca. 75% yield, $K = 5-10\%$, $Ag = 22\%$) (10). The less expensive KF can be used instead at lower temperature ($200-225^\circ C$) in a more cumbersome process and yields are also apparently very good (ca 80%) (11). The easiest method consists of allowing a frozen equimolar mixture of SF_4 and ClF in the presence of a small amount of CsF to attain room temperature slowly (12). Care has to be taken that the ClF is completely free of ClF_3 (ClF is prepared by heating ClF_3 and Cl_2). This can be achieved through low temperature distillation at $-140^\circ C$; otherwise, dangerous explosive reactions can occur. The yield is almost quantitative.

The compound SF_5Br was first obtained by heating a mixture of Br_2 , BrF_5 and SF_4 (10% yield) (13), then by heating Br_2 and S_2F_{10} ($<150^\circ C$, up to 80% yield) (14), or by heating a mixture of preformed BrF and SF_4 in the presence of CsF (15).

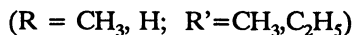
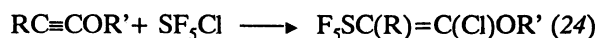
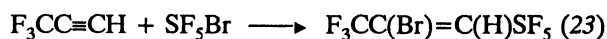
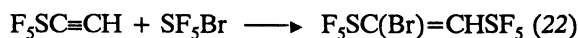
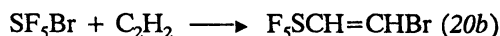
The Addition of SF_5 -Halides to Multiple Carbon-Carbon Bonds

The products that result from the addition of SF_5X to multiple bonds can usually be predicted when one considers the relative stabilities of intermediate radicals. Phenomenologically, the addition of SF_5Cl passes through the stablest intermediate SF_5 -containing radical (only the incorporation of SF_5 in the radical species will maintain the chain reaction). When the addition to either one of two sites results in intermediate radicals of comparable stability, product mixtures are obtained. The addition of SF_5Cl appears to be reversible and is in accord with a radical mechanism as was shown by Tedder (16). The addition of SF_5Br to *cis* and *trans* 1,2-difluoroethene leads to almost identical ratios of *threo* and *erythro* products, which is again in accord with a free radical mechanism (17). The reversibility of SF_5 addition is a consideration, particularly in photochemical reactions, where complicated product mixtures, S_2F_{10} , SF_4 and fluorinated

products may be formed (18). The existence of SF₅-radicals is confirmed through their observation at low temperature by either electron spin resonance or infrared spectroscopy. The radicals were generated by ultraviolet irradiation of SF₅X (X = F, Cl, Br) or concomitant matrix deposition of SF₄ and fluorine that had passed through a microwave discharge (19).

Addition to Acetylenes

The addition of SF₅X to acetylenes has been exploited in but a few cases, e.g.,



Treatment of the primary adducts with base (usually KOH) leads to alkynes (F₅SC≡CH, F₅SC≡CSF₅, F₅SC≡CCF₃, F₅SC≡CCH₃). The acetylene F₅SC≡CH forms salts (Li⁺, Hg²⁺, Mg²⁺, Ag⁺) which can be halogenated or trimethylsilylated (25). Pyrazoles are formed with diazomethane (20) or substituted diazomethanes (21). This acetylene also trimerizes to either 1,2,4- or 1,3,5-tris pentafluorothiobenzene depending on the experimental conditions (25). The symmetric compound is obtained upon irradiation of the acetylene, while the asymmetric compound results from the oxidative (bromine) decomposition of the complex Co₂(CO)₄(HC≡CSF₅)₃, in which the three acetylene units are positioned to result in 1,2,4-substitution in the six-membered ring. A complex Ni(CO)₂(F₅SC≡CCF₃), in which CO can be replaced by triphenyl phosphine (26a), is also formed from F₅SC≡CCF₃ and nickel tetracarbonyl. SF₅ containing diacetylenes (SF₅C≡C-C≡CSF₅, SF₅C≡C-C≡CH) have also been reported (26b).

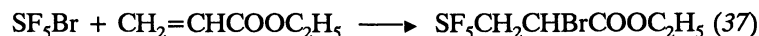
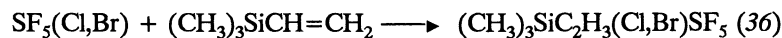
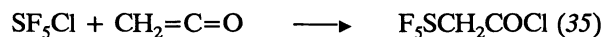
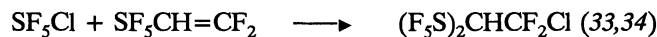
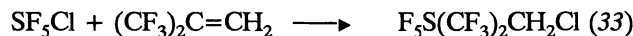
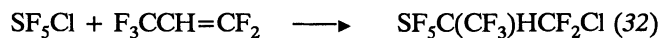
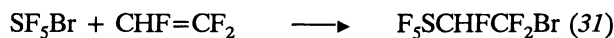
Addition to Olefins and the Preparation of SF₅-Alkenes

With the exception of the addition of pentafluorothio halides to acetylenes, which leads directly to alkenes, other members of this group are obtained mostly through SF₅X addition to alkenes, followed by dehydrohalogenation. Usually, the addition is uni-directional, with one product being formed in excess. Mixtures are obtained, exemplarily, with perfluoropropylene and trifluorochloroethene (27) or trifluoroethylene (28) or 1,1-difluoro-2-chloroethene (29). In this laboratory, it was also found that SF₅Br will add to β-acetoxy ethyl acrylate to give a mixture of α-bromo-β-SF₅-β-acetoxy propionate and α-SF₅-β-bromo-β-acetoxy propionate, the latter being in excess (29).

The reaction of SF_5X to alkenes often has to be moderated by working in the gas phase (ethylene and SF_5Br), at low temperature and in high dilution in an inert solvent (SF_5Br and vinyl acetate in CCl_3F , $-110^\circ C$) (29), or at low temperature in the gas phase with irradiation (isobutylene and SF_5Cl) (33). These reaction conditions are necessary because XF might be added instead of SF_5X , accompanied by SF_4 expulsion, and polymerization of the olefin or both.

The requirements for the olefins are not severe as electron-poor double bonds will not react; maleic anhydride is completely inert to the reactive SF_5Br at $100^\circ C$. Electron-rich double bonds (1,3-butadiene, vinyl acetate, β,β -bis-ethoxy ethyl acrylate) are so reactive that it is difficult to obtain any SF_5X adducts (instead XF addition products are formed) (27,29).

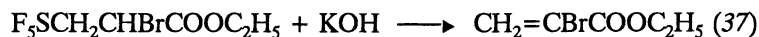
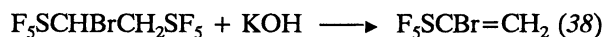
The following reactions exemplify the scope of such addition reactions.



Treatment of suitable primary adducts with base (usually aqueous KOH) results in the formation of the respective alkenes (27,15):



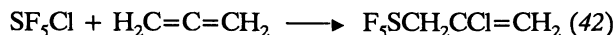
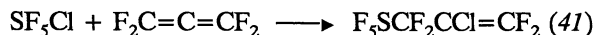
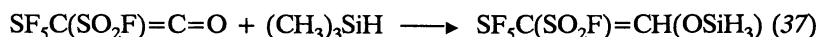
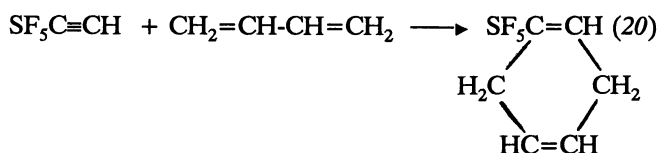
Only in exceptional cases are difficulties encountered (HSF_5 elimination):



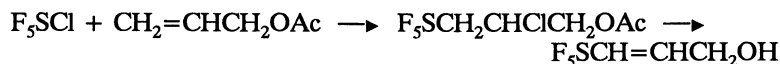
In a second pathway, other reagents (halogens, CF_3OCl , dienes and alkoxydes) can be added to SF_5 -alkynes or alkenes. In the first case, an alkene results from either free radical, nucleophilic, or cycloaddition to the multiple bond; in the second case, elimination will lead to an alkene.



The *Z*-isomer is obtained by nucleophilic addition of CH_3OH to $\text{SF}_5\text{C}\equiv\text{CH}$ (20a).



Allyl acetate very slowly reacts with SF_5Cl under forcing conditions; the product loses hydrogen chloride when subjected to base treatment and is hydrolyzed concurrently to an allyl alcohol (37):

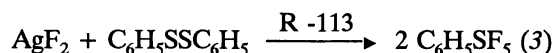


Furthermore, unexpected eliminations may occur (37):



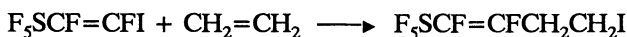
Additional Methods for Preparing SF_5 Alkenes

Aromatic disulfides can be oxidized with the aid of AgF_2 . This was reported for aromatic systems (3):



The recent synthesis of *E*- $\text{F}_5\text{SCF}=\text{CFI}$ (43) (through a phosphonium salt) offers a new method for obtaining olefins and SF_5 -substituted 1,3-butadiene derivatives. This is analogous to the photochemical addition reactions of

trifluoroiodoethylene (44) to olefins. Ethylene adds to $F_5SCF=CFI$ as follows:



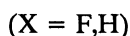
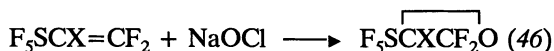
Gas chromatography-mass spectroscopy indicates two compounds with the molecular weight 344 which seem to be the *E*- and *Z*-product, produced probably by photochemical isomerization during the reaction (29).

Reactions of SF_5 -Olefins

The reactions of pentafluorothio olefins are broad, with cycloadditions being rare; 1- SF_5 -1,3-cyclohexadiene can be dehydrogenated to $C_6H_5SF_5$ (20). Additions of halogens and pseudohalogens take place easily; nucleophilic and electrophilic additions or nucleophilic substitutions may occur (20,21).

Bromine addition, under the action of light, was described for $SF_5CH=CH_2$ (20), $SF_5CH=CHBr$ (21), and $SF_5CH=CHCl$ (20), leading to the respective polybromo compounds. In the case of $SF_5CH=CF_2$, an exceptional reaction took place and $F_5SCHBrCF_3$ was formed. This product was transformed into the SF_5 -ketone $F_5SC(O)CF_3$ (45). Chlorine also adds to $SF_5CH=CF_2$ (40) and $SF_5CBr=CH_2$ (29) with irradiation. Chlorine monofluoride was added to $SF_5CH=CF_2$, and trifluoromethyl hypochlorite to $SF_5CH=CH_2$ (40).

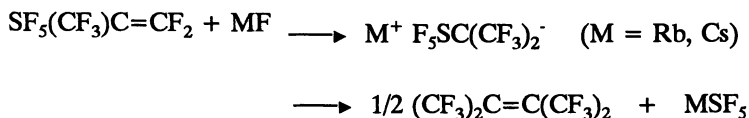
Nucleophilic additions were observed in several instances:



$F_5SCH=CHOCH_3$ can be converted with sodium methoxide in methanol to the dimethyl acetal $F_5SCH_2CH(OCH_3)_2$ (20,39). The same reagent will convert 1-bromo-1- SF_5 -ethylene to $SF_5CHBrCH_2OCH_3$ (37).

Electrophilic reactions are not usually observed, e.g., it was not possible to obtain a haloacetate from $F_5SCH=CH_2$ under the same conditions (acetic acid, bromine, mercury acetate) where perfluoroalkyl-substituted ethylenes are known to yield haloacetates. An exception is the rather easy (47) addition of SO_3 to $F_5SCH=CF_2$, although a significant amount of by-product is formed, one of which is formed in an intricate reaction that leads to the degradation of the SF_5 -group (48).

As with other perfluoro olefins, it is found that certain pentafluorothio olefins will form perfluoro carbanions. This is either deduced from the isolation of products which are formed through their intermediacy or through direct observation. One general feature of such SF_5 -anionic species in solution seems to be a yellow color, as well as the substantial low-field ^{19}F n.m.r. shift of all sulfur bonded fluorine resonances (they appear at 80-110 ppm, instead of 50-80 ppm in the neutral species). With the olefin $SF_5(CF_3)C=CF_2$ and metal fluorides the following reactions are observed:



The pentafluoro sulfates that are formed crystallize well and are suitable for crystallographic analysis (49).

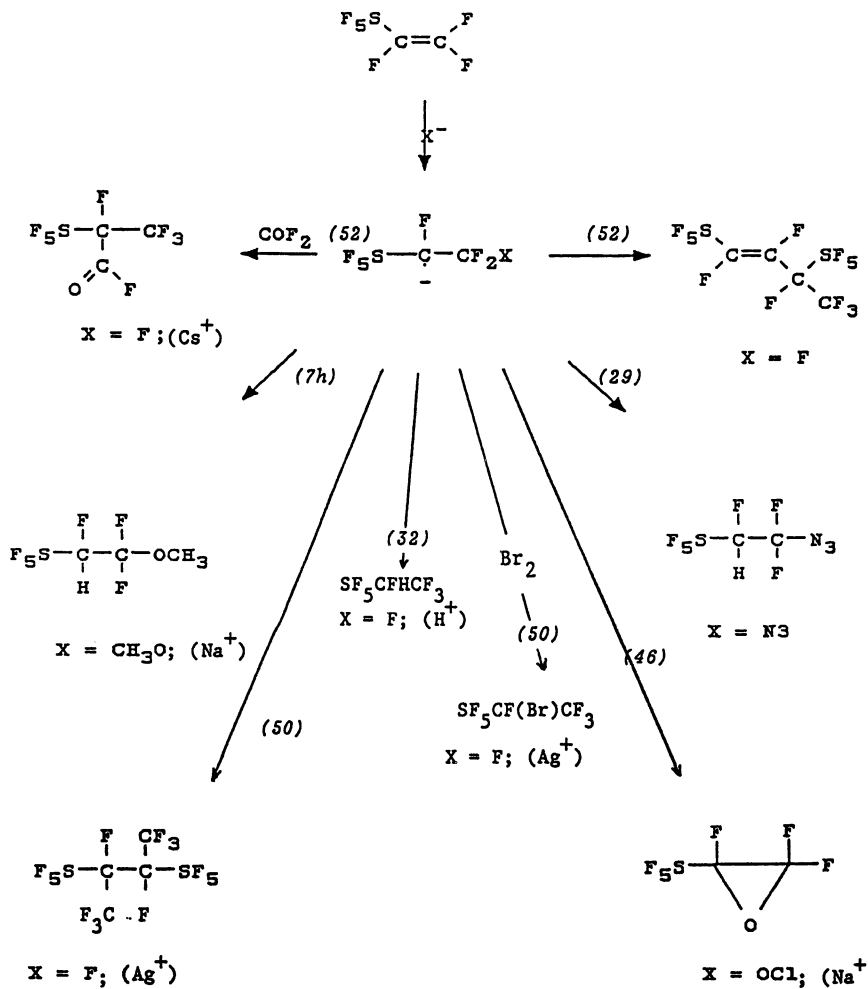
The Reactions of $\text{F}_5\text{SCF}=\text{CF}_2$

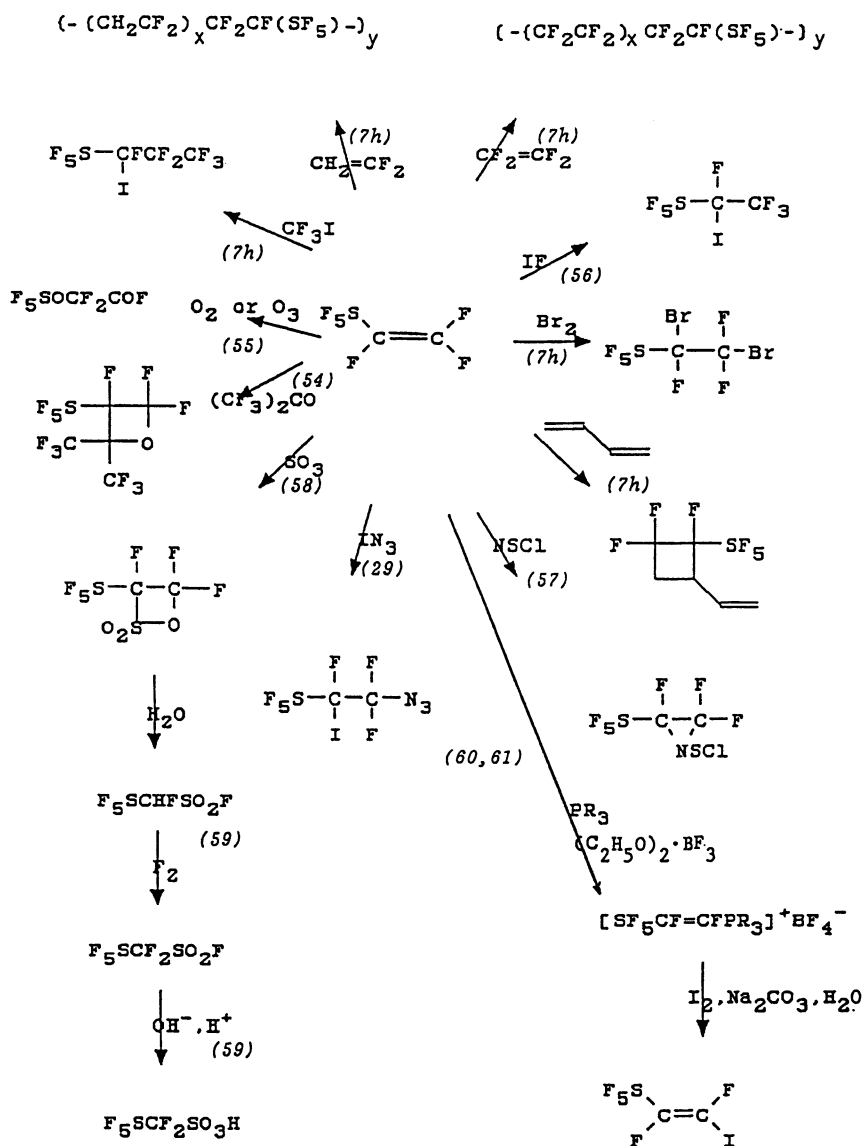
An array of reactions is encountered with perfluorovinyl sulfurpentafluoride (Schemes 1 and 2). In general, intermediate addition products formed via an anionic pathway have not been isolated, exceptions being the adducts $\text{Ag}[\text{CF}(\text{SF}_5)\text{CF}_3] \cdot \text{CH}_3\text{CN}$ (50) and $\text{M}^+[\text{F}_5\text{SC}(\text{SO}_2\text{F})\text{COX}]^-$ ($\text{X} = \text{F}, \text{OCH}_3, \text{M}^+ = \text{Ag}, \text{Na}, \text{Cs}$) (51). Reaction of $\text{F}_5\text{SCF}=\text{CF}_2$ with cesium fluoride results in a telomeric material, while reaction with tris(dimethylamino)sulfonium difluorotrimethylsilicate ("TASF") the dimer was obtained (52). In this case, vinylic substitution (in trans position) occurred, while with methoxide (7h), hypochlorite (46), azide and fluoride plus COF_2 (52) saturated adducts were formed (Scheme 1). The observed result with azide is different when compared to the behavior of perfluoropropylene which leads to vinylic substitution and to an azacyclobutene (53). The ketene $\text{F}_5\text{S}(\text{SO}_2\text{F})\text{C}=\text{C}=\text{O}$, if considered as an alkene, shows a pronounced tendency toward nucleophilic addition; adducts with bases are perfectly stable and can be isolated, crystallized, and subjected to further chemical transformation.

The addition of neutral species is extended to the cycloaddition of 1,3-butadiene (7h) and $(\text{CF}_3)_2\text{CO}$ (54), as well as the addition of Br_2 (18), CF_3I (18), Cl_2 (27), O_2 or O_3 (55), IF (56) (a mixture of I_2 and IF_3), NSCl (57), IN_3 (29) and SO_3 (58) (Scheme 2). Halogen addition leads to extensive cleavage of the SF_5 -group (7a). The addition of oxygen did not result in the expected epoxide but rather to the insertion of oxygen in the sulfur-carbon bond (55). This represents the only anomalous reaction if one compares the parallel reactions of perfluoropropene. The sultone that is obtained by addition of SO_3 has proven very useful in preparing other SF_5 -compounds, in particular, the SF_5 -derivative of triflic acid ($\text{SF}_5\text{CF}_2\text{SO}_3\text{H}$) (59). Another significant result is represented by the synthesis of the phosphonium tetrafluoroborates of $\text{SF}_5\text{CF}=\text{CF}_2$ with PR_3 ($\text{R} = n\text{-C}_4\text{H}_9$, has proven most advantageous) and of phosphonates from $\text{SF}_5\text{CF}=\text{CF}_2$ and $\text{SF}_5\text{CH}=\text{CF}_2$ (60,61). The chief advantage of the phosphonium salts lies in their convertibility to the iodide $E\text{-F}_5\text{SCF}=\text{CFI}$. The iodide should be useful for the synthesis of SF_5 -substituted butane derivatives by photochemical addition of olefins, or perhaps by generating a metal organic intermediate followed by reaction with alkyl halides.

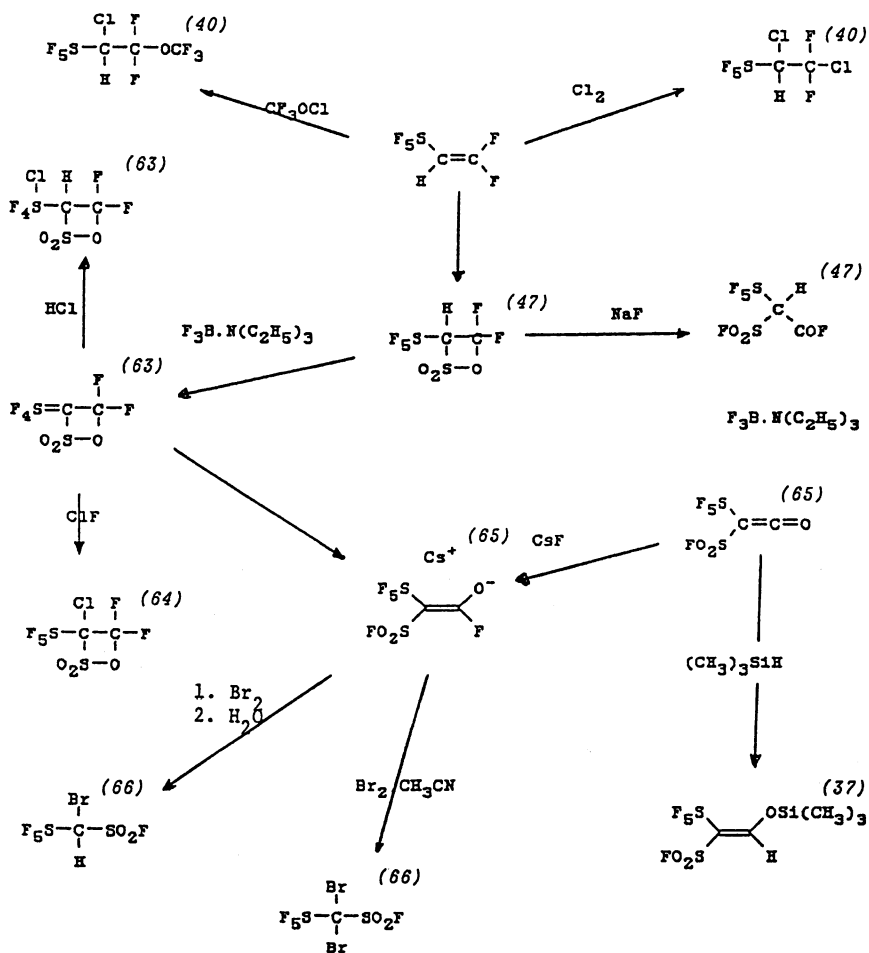
The $\text{SF}_5\text{CH}=\text{CF}_2$ olefin also has a manifold, although less explored, chemical transformability (Scheme 3). In addition to forming the sultone,

$\text{SF}_5\text{CH}(\text{CF}_2)\text{OSO}_2$ (47), an interesting side product is isolated, $\text{F}_4\text{SCH}(\text{CF}_2\text{OSO}_2\text{F})\text{SO}_2\text{O}$ (48). The crystal structure of $\text{SF}_5\text{CH}(\text{CF}_2)\text{OSO}_2$ is





Scheme 2



Scheme 3

known (62). The pertinent references for the reactions shown in Scheme 3 are listed for each reaction product.

Structural Studies of Gases and Solids

The structures of organic derivatives of sulfur hexafluoride have been determined by mostly three means: X-ray crystallography, electron diffraction and microwave spectroscopy. In general, no striking features are uncovered. The S-F bond length in SF₆ is 1.5623(4) Å (67) while in a number of SF₅-unsaturated compounds $d(\text{S-F})_{\text{axial}} \approx 1.54\text{--}1.58 \text{ \AA}$, $d(\text{S-F})_{\text{equatorial}} \approx 1.57\text{--}1.59 \text{ \AA}$ and $d(\text{S-C}) \approx 1.73\text{--}1.79 \text{ \AA}$ (68). With the compound [NH(C₂H₅)₃][F₅SC(SO₂F)COOCH₃] the anion showed some interesting bond lengths and angles changes when compared to neutral compounds (69). For example, in this salt the SF₅C distance was found to be 1.770(4) Å, the FSO₂-C distance 1.679(4) Å. In neutral compounds the SF₅-C distance would be expected to be 1.79-1.90 Å and the FSO₂-C distance 1.79-1.80 Å. Gas phase structures have been determined for SF₅C≡CH, SF₅CH=CH₂ and SF₅CF=CF₂ (68). Crystal structures were also determined for Co₂(CO)₆(F₅SC≡CSF₅) (70), Co₂(CO)₄(HC≡CSF₅)₃ (25) and [SF₅CF=CFP(CH₃)₃]⁺ [BF₄]⁻ (71).

Literature Cited:

1. Clifford, A.F.; El-Shamy, H.K.; Emel us, H.J.; Haszeldine, R.N. *J. Chem. Soc.* **1953**, 2372.
2. Haszeldine, R.N.; Nyman, L. *J. Chem. Soc.* **1956**, 2684. Baba, H.; Kodaira, K.; Nagase, S.; Abe, T. *Bull. Chem. Soc. Japan* **1977**, *50*, 2809. Baba, H.; Kodaira, K.; Nagase, S.; Abe, T. *Bull. Chem. Soc. Japan* **1978**, *51*, 1891. Abe, T.; Nagase, S.; Baba, H. *Bull. Chem. Soc. Japan* **1976**, *46*, 3845. Abe, T.; Nagase, S.; Kodaira, K.; Baba, H. *Bull. Chem. Soc. Japan* **1970**, *43*, 1812.
3. Sheppard, W.A. *J. Am. Chem. Soc.* **1962**, *84*, 3064.
4. Winter, R.; Gard, G.L. *J. Fluorine Chem.* **1991**, *52*, 57.
5. Castro, V.; Boyer, J.L.; Canselier, J.P.; Terjeson, R.J.; Mohtasham, J.; Peyton, D.H.; Gard, G.L. *Magn. Res. Chem.* **1990**, *28*, 998 and private communication with J.P. Canselier (1990).
6. Sitzmann, M.E.; Gilligan, W.H.; Ornellas, D.L.; Thrasher, J.S. *J. Energ. Mat.* **1990**, *8*, 353.
7. Woolf, C.; Gard, G.L. U.S. Patent 3448121, **1969**. Terjeson, R.J.; Gard, G.L. *J. Fluorine Chem.* *35*, 653. Gilbert, E.E.; Gard, G.L. U.S. Patent 3475453, **1969**. Tullock, C.W. U.S. Patent 3228981, **1966**. Ray, N.H. British Patent 941393, **1963**. Ray, N.H.; Roberts, H.L. U.S. Patent 3086048, **1963**. Sherratt, S. British Patent 929900, **1963**. Banks, R.E.; Barlow, M.G.; Haszeldine, R.N.; Morton, W.D. *J. Chem. Soc. Perkins I* **1974**, 1266. Hansen, J.C.; Savu, P.M. European Patent 0444822AI, **1992**.

8. Emel us, H.J.; Packer, K.J. *J. Chem. Soc.* **1962**, 771 (reaction of S_2F_{10} with SO_2 to give F_5SOSO_2F). Emel us, H.J.; Packer, K.J. *J. Chem. Soc.* **1962**, 3183 (reaction with olefins and benzene; $CF_3CF(SF_5)CF_2SF_5$ and $SF_5CHClCH_2SF_5$). Cohen, B.; McDiarmid, A.G. *Chem. Ind. (London)* **1962**, 1866. Tremblay, M. *Can. J. Chem.* **1965**, *46*, 219 (describes reactions with olefins). Czerepinski, R.; Cady, G.H. *J. Am. Chem. Soc.* **1968**, *90*, 3954 (describes the reaction of S_2F_{10} with oxalyl fluoride). Kovacina, T.A.; Berry, A.D.; Fox, W.B. *J. Fluorine Chem.* **1976**, *7*, 430 (describes the synthesis of SF_5Br from S_2F_{10}).
9. Hutchinson, J. *J. Fluorine Chem.* **1973/74**, *3*, 429.
10. Tullock, C.W.; Coffman, D.D.; Muetterties, E.L. *J. Am. Chem. Soc.* **1964**, *86*, 357.
11. Bekker, R.A.; Dyatkin, B.L.; Knunyants, I.L. *Bull. Akad. Nauk USSR. Ser. Khim.* **1970**, 2575.
12. Schack, C.J.; Wilson, R.D.; Warren, M.G. *J. Chem. Soc. Chem. Comm.* **1969**, 1110.
13. Merrill, C.I.; Cady, G.H. *Chem. Abstr.* **1964**, *60*, 6463.
14. Cohen, B.; McDiarmid, A.G. *Inorg. Chem.* **1965**, *4*, 1782.
15. Christe, K.O.; Curtis, E.C.; Schack, C.J.; Roland, A. *Spectrochim. Acta* **1977**, *A33*, 69. Wessel, J.; Kleemann, G.; Seppelt, K. *Chem. Ber.* **1983**, *116*, 2399.
16. Sidebottom, H.W.; Tedder, J.M.; Walton, J.C. *Trans. Faraday Soc.* **1969**, *65*, 2103.
17. Berry, A.D.; Fox, W.B. *J. Org. Chem.* **1978**, *43*, 365.
18. See reference 7, Banks, R.E.; et al.
19. Smardzewski, R.R.; Fos, W.B. *J. Fluorine Chem.* **1976**, *7*, 456. Morton, J.R.; Preston, K.F. *Chem. Phys. Lett.* **1973**, *18*, 98. Hasegawa, A.; Williams, F. *Chem. Phys. Lett.* **1977**, *45*, 275.
20. Hoover, F.W.; Coffman, D.D. *J. Org. Chem.* **1964**, *29*, 3567. Canich, J.; Ludvig, M.M.; Paudler, W.W.; Gard, G.L.; Shreeve, J.M. *Inorg. Chem.* **1985**, *24*, 3668. Terjeson, R.J.; Canich, J.; Gard, G.L. *Inorg. Synth.* **1990**, *27*, 329.
21. Neunhoeffer, H.; Canich, J.M.; Ludvig, M.M.; Paudler, W.W.; Shreeve, J.M.; Gard, G.L. Abstract, 39th NW Regional ACS Meeting, **1984**, Moscow, ID.
22. Berry, A.D.; De Marco, R.A.; Fox, W.B. *J. Am. Chem. Soc.* **1979**, *101*, 737.
23. Wang, Q.C.; White, H.F.; Gard, G.L. *J. Fluorine Chem.* **1979**, *13*, 455.
24. P tter, B.; Seppelt, K. *Inorg. Chem.* **1982**, *21*, 3147. P tter, B.; Kleemann, G.; Seppelt, K. *Chem. Ber.* **1984**, *119*, 3255.
25. Wessel, J.; Hartl, H.; Seppelt, K. *Chem. Ber.* **1986**, *119*, 453.
26. Berry, A.D.; De Marco, R.A. *Inorg. Chem.* **1982**, *21*, 457. Kovacina, A.; De Marco, R.A.; Snow, A.W. *J. Fluorine Chem.* **1982**, *21*, 261.
27. Case, J.R.; Ray, N.H.; Roberts, H.L. *J. Chem. Soc.* **1961**, 2070, 2066.
28. Banks, R.E.; Haszeldine, R.N.; Morton, W.D. *J. Chem. Soc., Dalton Trans.* **1969**, 1947. Here it is found that SF_5Cl will add to trifluoroethylene (CCl_4 , benzoyl peroxide, $150^\circ C$) to give a 95:5 mixture of SF_5CHFCF_2Cl and SF_5CF_2CHFCI .
29. In-house work done at Portland State University.
30. Merrill, C.; Ph.D. Dissertation, University of Washington, Seattle, 1961.
31. Steward, J.; Kegley, L.; White, H.F.; Gard, G.L. *J. Org. Chem.* **1969**, *34*, 760.

32. De Marco, R.A.; Fox, W.B. *J. Fluorine Chem.* **1978**, *12*, 137.
33. Grelbig, T.; Krügerke, T.; Seppelt, K. *Z. Anorg. Allg. Chem.* **1987**, *544*, 74.
34. Gerhardt, R.; Seppelt, K. *Chem. Ber.* **1989**, *122*, 463. Gerhardt, R.; Grelbig, T.; Buschmann, J.; Luger, P.; Seppelt, K. *Angew. Chem. Int. Ed. Engl.* **1988**, *27*, 1534.
35. Coffman, D.D.; Tullock, C.W. U.S. Patent 3102903, **1963**. Coffman, D.D.; Tullock, C.W. *Chem. Abstr.* **1964**, *60*, 1599c. Kleemann, G.; Seppelt, K. *Chem. Ber.* **1979**, *112*, 1140.
36. Berry, A.D.; Fox, W.B. *J. Fluorine Chem.* **1975**, *6*, 175. The composition of the adducts is only determined through elemental analysis; ref. 3 states that such adducts may also be obtained by adding silanes to $\text{SF}_5\text{CH}=\text{CH}_2$.
37. Winter, R. Ph.D. Dissertation, Portland State University, **1990**.
38. Berry, A.D.; Fox, W.B. *J. Fluorine Chem.* **1976**, *7*, 449.
39. Winter, R.; Gard, G.L.; Willett R. *Inorg. Chem.* **1989**, *28*, 2499.
40. Terjeson, R.; Gupta, R.; Sheets, R.; Gard, G.L.; Shreeve, J.M. *Rev. de Chimie Miner.* **1986**, *23*, 1.
41. Witucki, E.F. *J. Fluorine Chem.* **1982**, *20*, 807.
42. Wessel, J.; Kleemann, G.; Seppelt, K. *Chem. Ber.* **1983**, *116*, 2399.
43. Wessolowski, H.; Rösenthaller, G.-V.; Winter, R.; Gard, G.L. *Z. Naturforsch.* **1991**, *46b*, 123.
44. Park, J.D.; Seffl, R.J.; Lacher, J.R. *J. Am. Chem. Soc.* **1956**, *78*, 59.
45. De Marco, R.A.; Fox, W.B. *J. Org. Chem.* **1982**, *47*, 3772.
46. Winter, R.; Gard, G.L. *J. Fluorine Chem.* **1990**, *50*, 141.
47. Terjeson, R.J.; Mohtasham, J.; Gard, G.L. *Inorg. Chem.* **1998**, *27*, 2916.
48. Gerhardt, R.; Kuschel, R.; Seppelt, K. *Chem. Ber.* **1992**, *125*, 557.
49. Bittner, J; Fuchs, J.; Seppelt, K. *Z. Anorg. Allg. Chem.* **1988**, *557*, 182.
50. Nofle, R.E.; Fox, W.B. *J. Fluorine Chem.* **1977**, *9*, 219.
51. Winter, R.; Gard, G.L. *Inorg. Chem.* **1988**, *27*, 4329. Winter, R.; Gard, G.L. *J. Fluorine Chem.* **1991**, *52*, 73.
52. DeBuhr, R.; Howbert, J.; Canich, J.M.; White, H.F.; Gard, G.L. *J. Fluorine Chem.* **1982**, *20*, 515. Gard, G.L.; Mews, R. work done at Universität Bremen and Portland State University.
53. Knunyanz, I.L. *Chem. Abstr.* **1960**, *54*, 20804d.
54. Gard, G.L.; Woolf, C. U.S. Patent 3448121, **1969**.
55. Marcellis, A.W.; Eibeck, R.E. *J. Fluorine Chem.* **1975**, *5*, 71.
56. Gard, G.L.; Woolf, C. *J. Fluorine Chem.* **1971/72**, *1*, 487.
57. Hare, M.; Gard, G.L.; Winter, R.; Lork, A.; Mews, R.; Stohrer, W.-D. *J. Chem. Soc. Chem. Comm.* **1992**, 898.
58. Canich, J.; Ludvig, M.M.; Gard, G.L.; Shreeve, J.M. *Inorg. Chem.* **1984**, *23*, 4403.
59. Gard, G.L.; Waterfeld, A.; Mews, R.; Mohtasham, J.; Winter, R. *Inorg. Chem.* **1990**, *29*, 4588.
60. Wessolowski, H.; Rösenthaller, G.-V.; Winter, R.; Gard, G.L. *Z. Naturforsch.* **1991**, *46b*, 126.
61. Wessolowshi, H.; Rösenthaller, G.-V.; Winter, R.; Gard, G.L. *Phosphorus, Sulfur and Silicon* **1991**, *60*, 201.

62. Pressprich, M.R.; Willett, R.D.; Terjeson, R.J.; Winter, R.; Gard, G.L. *Inorg. Chem.* **1990**, *29*, 3058.
63. Winter, R.; Peyton, D.H.; Gard, G.L. *Inorg. Chem.* **1989**, *28*, 3766.
64. Winter, R.; Gard, G.L. *J. Fluorine Chem.* **1991**, *52*, 57.
65. Winter, R.; Gard, G.L. *Inorg. Chem.* **1988**, *27*, 4329.
66. Winter, R.; Gard, G.L. *J. Fluorine Chem.* **1991**, *52*, 73.
67. Kelly, H.M.; Fink, M.J. *Chem. Phys.* **1982**, *77*, 1813.
68. SF₅C≡CH: Császár, A.G.; Hedberg, K.; Terjeson, R.J.; Gard, G.L. *Inorg. Chem.* **1987**, *26*, 955. SF₅C≡CH, SF₅CH=CH₂, SF₅CF=CF₂: Zylka, P.; Christen, D.; Oberhammer, H.; Gard, G.L.; Terjeson, R.J. *J. Mol. Str.* **1991**, *249*, 285. Weiss, I.; Oberhammer, H.; Seppelt, K.; Gard, G.L.; Winter, R. *J. Mol. Str.* **1992**, *269*, 197.
69. Winter, R.; Gard, G.L.; Mews, R.; Noltemeyer, M. *J. Fluorine Chem.* **1993**, *60*, 109.
70. Damerius, R.; Leopold, D.; Schulze, W.; Seppelt, K. *Z. Anorg. Allg. Chem.* **1989**, *578*, 110.
71. Ron, G.; Willett, R.; Wessolowski, G.-V.; Röschenthaler, G.-V.; Winter, R.; Gard, G.L. *Eur. J. Solid State Inorg. Chem.* **1992**.
72. Mohtasham, J.; Terjeson, R.J.; Gard, G.L. *Inorg. Syn.* **1992**, *29*, 33.
73. Krügerke, T.; Buschmann, J.; Kleemann, G.; Luger, P.; Seppelt, K. *Angew. Chem., Int. Ed. Engl.* **1987**, *26*, 799.
74. Bittner, J.; Seppelt, K. *Chem. Ber.* **1990**, *123*, 2187.

RECEIVED November 10, 1993

Chapter 9

Fluoro-Sulfur Anions

Transition States, Intermediates, and Reagents

R. Mews

Institut für Anorganische und Physikalische Chemie, Universität
Bremen, Leobenerstrasse NW2, D-28334 Bremen, Germany

The addition of fluoride ions to lower coordinated sulfur derivatives and sulfur-nitrogen species with SN double bonds leads to a number of unusual fluoro anions. The stability of those anions depends on the fluoride ion donor (CsF, TASF); especially with $TAS^+ [(Me_2N)_3S^+]$ as a counterion, isolable anions are generated, which might be regarded as stabilized transition states of S_N2 reactions. A second approach to NS anions is the Si - N bond cleavage of silicon-nitrogen-sulfur derivatives. Useful reagents for further syntheses are generated from this approach.

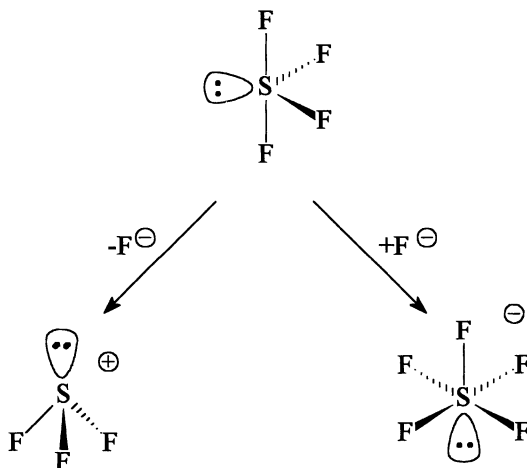
Fluorinated sulfur anions and cations were often postulated as intermediates in sulfur chemistry and systematic investigations to generate, stabilize, and isolate these reaction intermediates were started in our group some time ago (1). With the availability of new and more effective fluoride ion donors, e.g. $(Me_2N)_3S^+Me_3SiF_2^-$ (TASF) (2), $Me_4N^+F^-$ (3), or $[(Me_2N)_3P]_2N^+F^-$ (4), much progress has been achieved in the chemistry of fluorinated anions of the maingroup elements, especially during the last few years.

Fluorosulfuranide Anions

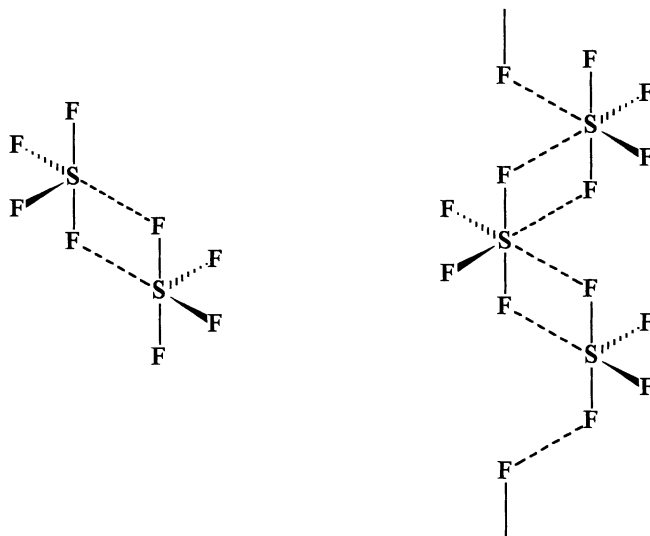
Sulfur tetrafluoride is known to act as both a fluoride ion donor and acceptor. Bartlett and Robinson were the first to show that fluoro Lewis acids abstract F^- under formation of the trifluorosulfonium ion SF_3^+ (5), similar results were obtained independently by Seel and Detmer (6). Structure determinations were reported later by Bartlett's group (7).

Fluoride ion acceptor properties of SF_4 were first suggested by Tullock *et al.* (8); Christe and coworkers established the existence of the SF_5^- ion by IR spectroscopy (9), and Seppelt *et al.* recently succeeded in solving the crystal structure of $Rb^+SF_5^-$ (10).

0097-6156/94/0555-0148\$08.00/0
© 1994 American Chemical Society

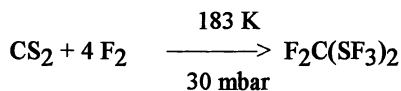


These intrinsic donor-acceptor properties of SF_4 should lead to intermolecular interactions in the condensed phase, resulting either in self-ionization or association. For the liquid state, several models are discussed in the literature. Seel and Gombler concluded from NMR-investigations that SF_4 forms dimers or polymers with axial fluorines acting as bridges (11)



These associates are too unstable to be isolated; therefore, no structural information is available. Perfluoro alkyl derivatives, e.g., CF_3SF_3 , show similar behavior (11).

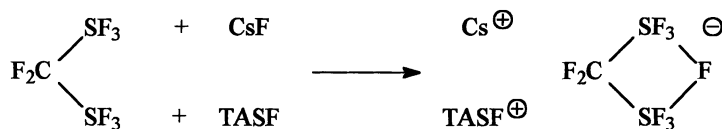
In α , ω -bis(trifluorosulfur)alkanes $F_3S-(CF_2)_nSF_3$ a comparable, but intramolecular interaction between the two SF_3 groups might be expected, even in the gas phase. This interaction should depend on the number, n , of bridging atoms. The first member of this series, $F_3S-CF_2-SF_3$ (12-14), is easily prepared by direct fluorination of CS_2 at low temperature and low pressure (14):



The gas phase structure of $F_2C(SF_3)_2$ (Fig. 1) was determined by electron diffraction (15). The two SF_3 -groups show the expected pseudo trigonal bipyramidal structure with a difference in the bond lengths of 10 pm between the axial [$d(SF_a) = 166.4$ (4) pm] and the equatorial bonds [$d(SF_e) = 156.2$ (4) pm]. Within the limits of experimental error they are the same as in F_3CSF_3 [$d(SF_e) = 156.5$ (8) pm; $d(SF_a) = 165.5$ (5)] (16). Especially interesting in the structure of $F_2C(SF_3)_2$ is the small SCS angle of 108.2 (5) $^\circ$; this results in a very short non bonded contact $F_1 \cdots S'$ ($F_1' \cdots S$) = 266 pm between a sulfur and one axial fluorine of the opposite SF_3 -group. As can be seen from the Newman projection in Figure 1, the sulfur centers are attacked by these bridging fluorines in the equatorial plane, as in the model suggested from the NMR data of liquid SF_4 or CF_3SF_3 (11).

Similar to SF_4 , CF_3SF_3 acts as a fluoride ion donor towards strong Lewis acids (AsF_5 , SbF_5) (17,18). Under the same conditions, $F_2C(SF_3)_2$ forms only monocations even with a large excess of Lewis acid, due to a strong interaction of the two sulfur centers (19).

The classical fluoride ion donor in fluorine chemistry is CsF ; however, for the generation and stabilization of anions, ionic fluorides with large organic counterions, e.g., Me_4N^+ (3) or $[(Me_2N)_3P]_2N^+$ (4) seem to be more useful. In "TAS-fluoride" $(Me_2N)_3S^+Me_3SiF_2^-$ (2) the fluoride is stabilized as the $Me_3SiF_2^-$ anion. Due to the very weak SiF bonds [$d(SiF) = 176$ pm] it is an extremely useful fluoridating agent (20). Fluoride ions will be transferred to all acceptors better than Me_3SiF . In the investigation described herein, CsF and $TASF$ were used exclusively. Both reagents form only monoanions with $F_2C(SF_3)_2$ (21):



According to the X-ray structure determination (Fig. 2), the two sulfur centers are symmetrically bridged by a fluoride ion; this distance $d(SF_{br}) = 211.7$ (1) pm is much longer than $d(SF(2))/d(SF(4)) = 170.0$ (2) pm and $d(SF(3)) = 160.7$ (2) pm.

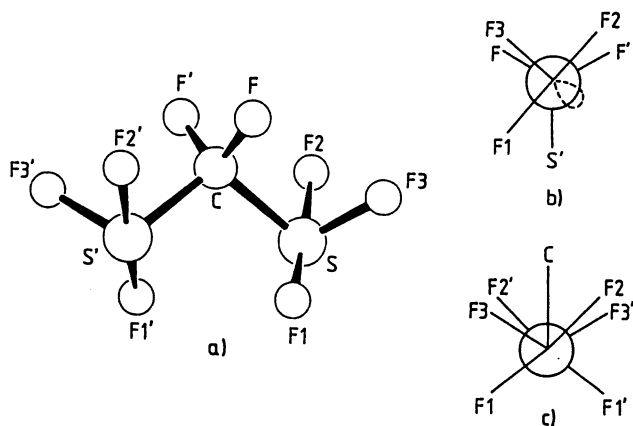


Figure 1. (a) Gas phase structure of $F_2C(SF_3)_2$ (15)
 (b) Newman projection along one CS bond
 (c) Newman projection along the S...S' direction

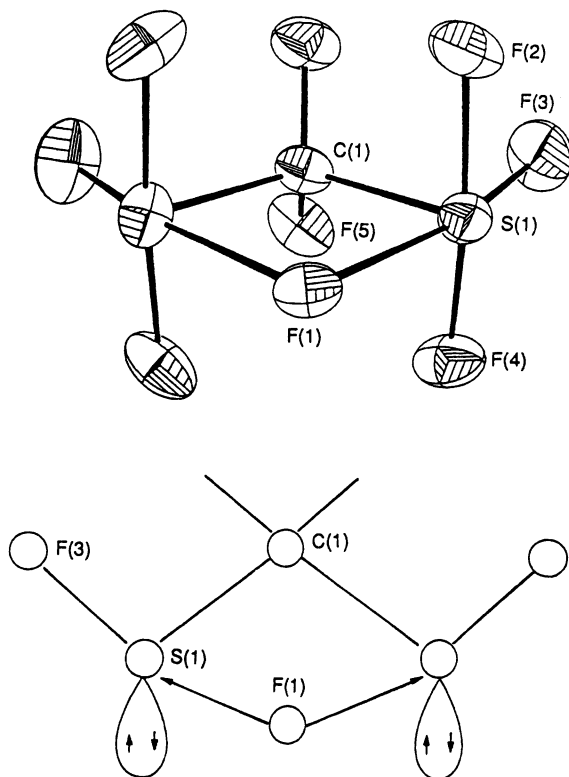
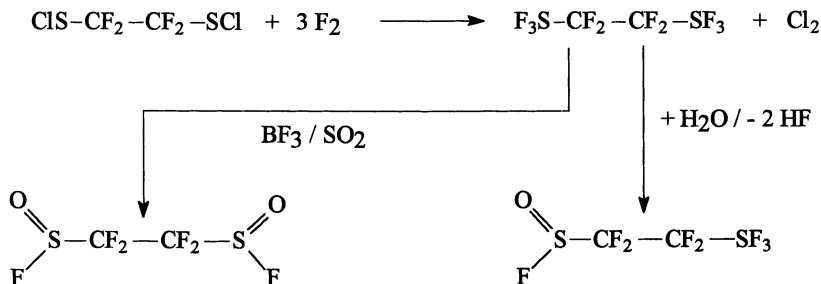


Figure 2. X-Ray structure of the $[F_2C(SF_3)_2F]^-$ anion (21).

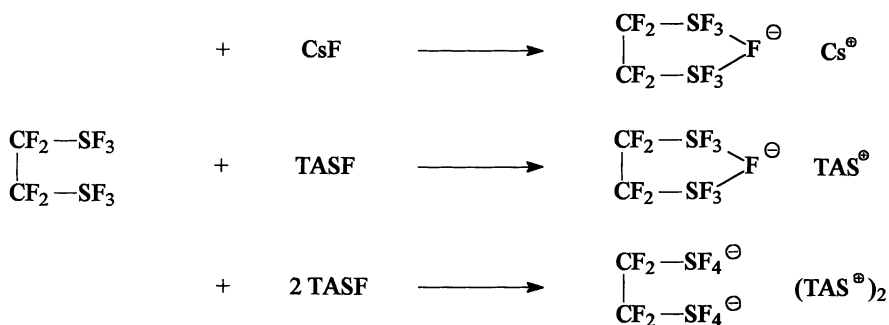
Despite the almost ideal pseudo square pyramidal geometry (according to the bond angles around the sulfur atoms), the difference in SF bond lengths between "axial" and "equatorial" bonds in the anion is similar to that in the parent neutral molecule. Here also the incoming (bridging) fluoride attacks the pseudo trigonal bipyramidal centers in the equatorial plane, almost exactly bisecting the "C(1) -S- lone pair" angle.

From the direct fluorination of $(\text{CF}_2\text{SCl})_2$ (22) 1,2-bis(trifluorosulfur)perfluoroethane was isolated in 83% yield (23):



When compared to the methane derivative, the ethane derivative is much more sensitive against moisture. Since the mutual interaction of the SF_3 groups should have a stabilizing effect, this indicates a lower interaction between the SF_3 groups in the ethane than in the methane derivative.

The compound $(-\text{CF}_2\text{-SF}_3)_2$ reacts with AsF_5 and SbF_5 to give stable salts with monocations, e.g., $[(-\text{CF}_2\text{-SF}_3)_2\text{F}]^+\text{MF}_6^-$. With CsF only monoanions are formed, while with excess TASF even a dianion precipitates in quantitative yield from CH_3CN solution (24).

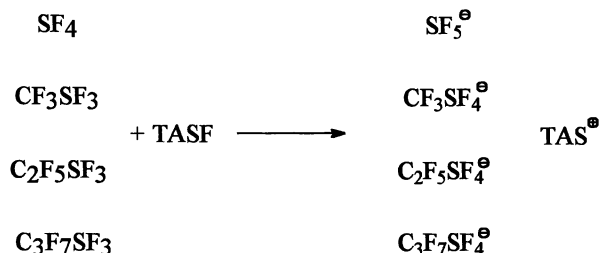


This indicates that TASF is superior to CsF in its fluoride donor property. It also indicates that towards TASF both $-\text{CF}_2\text{-SF}_3$ groups react independently.

Crystals of the Cs salt which were suitable for an X-ray structure determination (Fig. 3) were obtained from CH_3CN solution. The salt crystallizes with one molecule of the solvent (25).

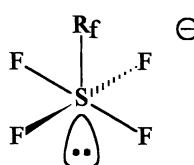
Due to the bridging of the fluoride, a five-membered $\text{C}_2\text{S}_2\text{F}$ ring is formed with significantly different $\text{F}(1) - \text{S}(1)$ (222.8 pm) and $\text{F}(1) - \text{S}(2)$ (206.7 pm) distances. Although the geometry around the sulfur centers is almost pseudo octahedral, the remaining SF distances are very different ($\Delta = "d(\text{SF}_a)" - "d(\text{SF}_e)" = 10$ pm), resembling the situation in a pseudo trigonal bipyramid. With the approach of the fluoride ion, negative charge is transferred to the sulfur centers, resulting in a lengthening of the SF bond distances.

The structures of $\text{CF}_2(\text{SF}_3)_2$, $[\text{CF}_2(\text{SF}_3)_2\text{F}]^-$ and $[(-\text{CF}_2-\text{SF}_3)_2\text{F}]^-$ establish four experimental points (two from the last structure) on the reaction coordinate for the nucleophilic attack of F^- on pseudo pentacoordinated sulfur (IV) centers. This transition state is attained in the fluorosulfuranide anions (23, 26):



The ^{19}F -NMR-data for the perfluoroalkyl derivatives indicate an apical position for the R_F groups (See Table I):

Table I. ^{19}F -NMR data of fluorosulfuranide anions

	F	CF_3	C_2F_5	C_3F_7	
		59.8	15.7	{35.0}	32.4
	44.8	20.0		12.0	$^2J_{(\text{FF})} / ^3J_{(\text{FF})}$ [Hz]

The perfluoroethyl and -isopropyl derivatives readily decompose. Possible decomposition mechanisms are β -fluoride transfer from carbon to sulfur under formation of perfluoroalkenes and SF_5^- or heterolytic cleavage of the C-S bond to give R_F^- and SF_4 as the primary products (26).

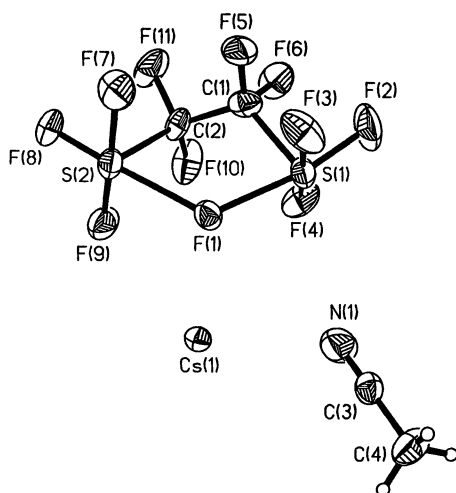
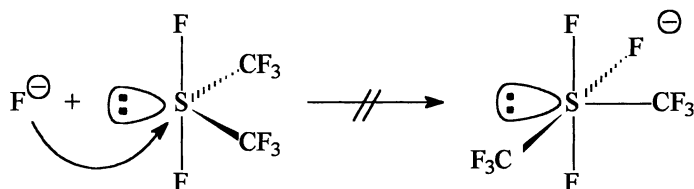


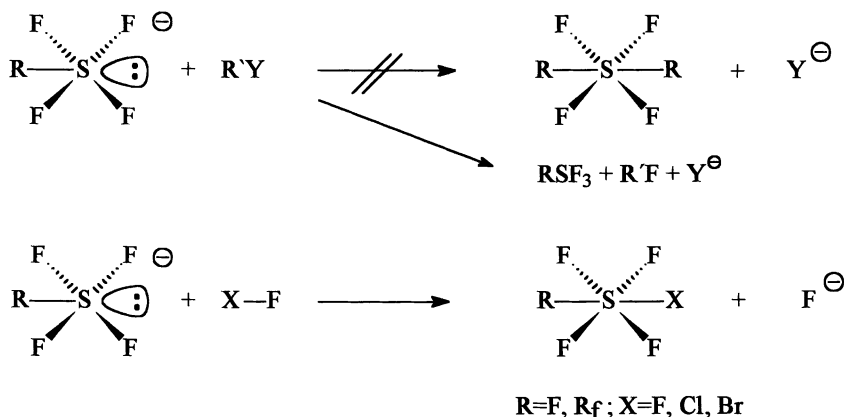
Figure 3. X-ray structure of $\text{Cs}^+ [(-\text{CF}_2-\text{SF}_3)_2\text{F}]^- \cdot \text{CH}_3\text{CN}$.

Although CF_3 groups seem to increase the F^- acceptor properties of sulfur centers, $(\text{CF}_3)_2\text{SF}_2$ surprisingly does not interact with F^- .



A possible explanation for this behavior is, that in anions the CF_3 group avoids the energetically unfavorable 3c-4e-bond system (26).

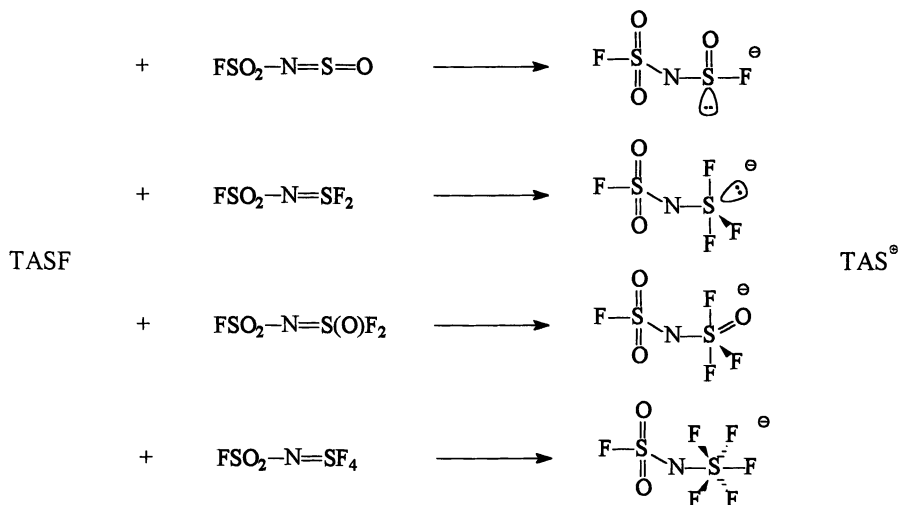
The chemistry of the sulfuramide ions is rather disappointing. No examples are yet known for a successful use as a nucleophile:



They react as fluorinating agents, thus only with oxidizing agents is the RSF_4 -moiety preserved (27,28).

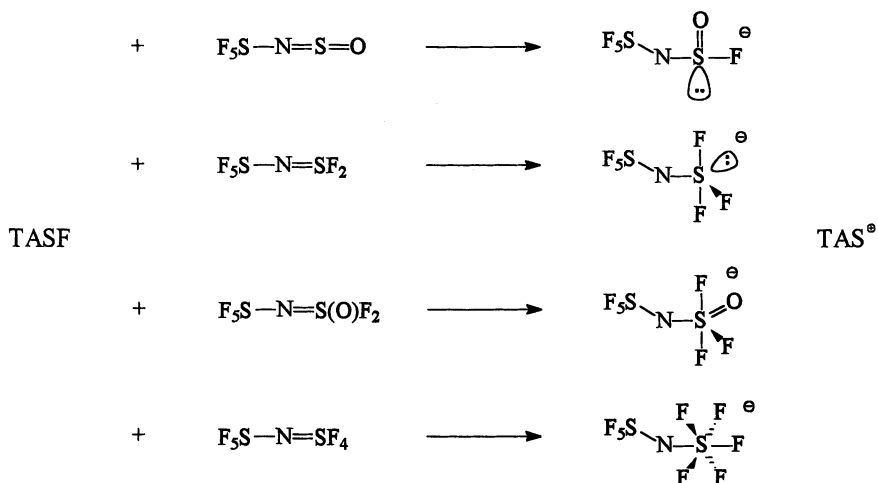
Fluorinated Sulfuramide Anions

Sulfur nitrogen double bond systems with electron-withdrawing substituents will add fluoride ions under formation of fluorosulfuramide anions (29-31). Especially interesting are the inorganic fluorosulfonyl and pentafluorosulfanyl derivatives, but *N*-perfluoroalkyl derivatives also react:

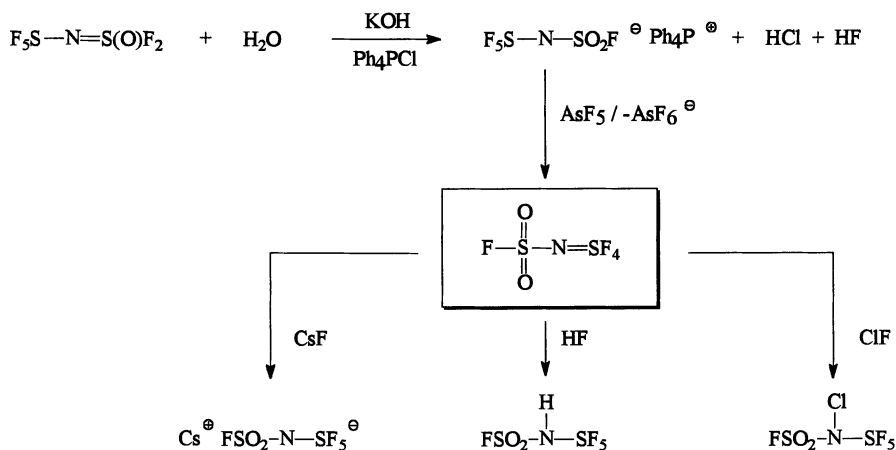


In these examples, the FSO₂ groups (with sulfur (VI) and coordination number 4) are connected to both sulfur (IV) and sulfur (VI) centers with different coordination numbers. Previously, only fluorosulfuramide anions were described in the literature with sulfur (VI) and coordination number 4 or 6, e.g. (FSO₂)₂N⁻ (32), FSO₂NSF₅⁻ (33), (SF₅)₂N⁻ (34), and NSF₂-NSO₂F⁻ (35).

The reaction of pentafluorosulfanyl imino derivatives with TASF is similar to that of the FSO₂ species and results in the formation of stable salts:



The first isolation of the $F_5S-N-SO_2F^-$ -anion resulted from the hydrolysis of $F_5SNSO_2F_2$ in the presence of large cations (33):

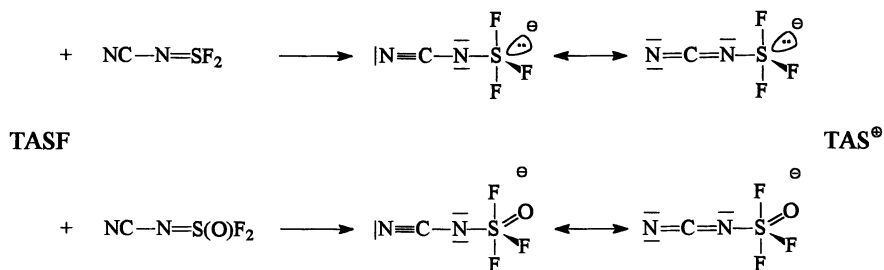


In this anion two kinetically rather inert sulfur centers are present. Arsenic pentafluoride exclusively abstracts F^- from the pentafluorosulfanyl group (36), while an excess of AsF_5 leads to the formation of rather labile $\text{FSO}_2\text{NSF}_3^+\text{AsF}_6^-$ (31). The tetrafluorosulfur imide is a useful starting material for introducing the $\text{FSO}_2-\text{N}-\text{SF}_5$ group, either via the Cs-salt, the free amine or the *N*-chloroamine (31).

Addition of Fluoride Ions to Bifunctional SN Systems

As seen before, sulfur-nitrogen double bond systems readily add F^- at the sulfur center. If this sulfur center competes with other functional groups, e.g. $-\text{CN}$, $-\text{C}(\text{O})\text{R}$ (with multiply bonded carbon), $-\text{SiR}_3$ (with a center having the possibility of coordination expansion), when different reactive sites are in the same molecule, then fluoride ion addition by TASF might answer the question of relative acceptor properties of these different groups. With TASF as fluoride ion donor NMR spectroscopic investigations in homogeneous solution are possible. With this method the site of primary attack and reaction mechanisms might be elucidated.

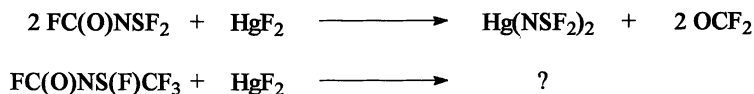
TASF reacts with NC-NSF_2 (37,38) and NC-NS(O)F_2 (39,40) in quantitative yield to give remarkably stable, colorless salts (41):



F^- is added exclusively to the sulfur centers. Structure determinations will show, whether these anions might be regarded as *N*-cyano trifluorosulfur- and -oxotrifluorosulfur salts, respectively, or as trifluorosulfur / oxotrifluorosulfur carbodiimide salts. The NMR spectra of these *N*-cyano derivatives fit well into the series of other trifluorosulfur- and oxotrifluorosulfur amide anions as well as into the system of pentacoordinated sulfur(VI)- and pseudo-pentacoordinated sulfur(IV) derivatives, as shown in Table II (30, 36, 41-46) and Table III (30, 41, 47-50).

Oxotrifluorosulfur imide anions RNS(O)F_3^- are isoelectronic with the tetrafluorosulfurimides RN=SF_4 . Similar structures are expected with the substituent *R* in an axial position and inequivalent axial bonded fluorine substituents F_a, F'_a (see Table II). This inequivalence of F_a and F'_a has been established, e.g., for $\text{CH}_3\text{N=SF}_4$ (44) and FN=SF_4 (51) by NMR in solution and by gas phase structure determinations. In the NMR experiments of RNS(O)F_3^- only one signal is found for F_a and F'_a due to rapid exchange (either inversion at the nitrogen or rotation around the NS -bond).

In the *N*-acyl fluorosulfur imides $\text{R}_F\text{C(O)NS(F)R}_F$ ($\text{R}_F=\text{F}, \text{CF}_3$) two competing centers for the fluoride ion are also present. Many years ago the reaction of HgF_2 with FC(O)NSF_2 was reported to give $\text{Hg(NSF}_2)_2$ and OCF_2 , with the mercurial serving as a source for pure NSF (52, 53).



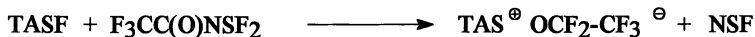
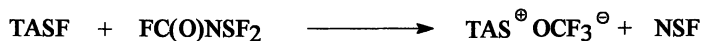
Similarly, FC(O)NS(F)CF_3 was expected to give $\text{Hg}[\text{NS(F)CF}_3]_2$ and from this " CF_3SN " should be generated. But from this reaction no conclusive results were obtained.

Table II: ^{19}F -NMR Data of Pentacoordinated N-S(VI)-F-Species

R	Me	Et	CH ₃	C ₂ F ₅	FSO ₂	(CF ₂)CF	FSO ₂	SF ₅	NC	Me
F _{ax}	63.8	64.5	76.3/ 73.9	76.5/ 75.1	101.8/ 74.4	100.4	100.9	97.8	94.3	76.8
F _{eq}	61.6	61.4	68.3	69.2	66.6	75.2	73.1	77.4	71.9	66.5
$^2J_{\text{FF}}$	220.6	218.4	194.0/ 201.0	194.8/ 200.6	206.0/ 211.0	44.0	151.9	148.1	149.4	163.1
	(42)	(42)	(44)	(45)	(36)	(30)	(50)	(30)	(41)	(46)

Table III: ^{19}F -NMR Data of Pseudo - Pentacoordinated N-S(IV)-F-Species

R/R'	Me/Me	Me/CF ₃	C ₂ F ₅	FSO ₂	CN	C ₂ F ₅	
SF _{ax}	59.4	66.9	64.0(br)	69.7	66.3	30.0	27.6
SF _{eq}	20.2	4.1	56.0(br)	59.4	48.05	-	-
$^2J_{\text{FF}}$	58.0	32.8	-	47.0	70.2	-	-
$^3J_{\text{FF}}$	-	-	-	-	-	18.0	17.5
	(47,48)	(49)	(30)	(30)	(41)	(30)	(50)



TASF

TAS[⊕]

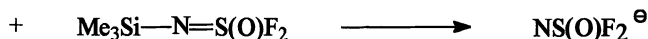
In the reaction of TASF and FC(O)NSF_2 or $\text{F}_3\text{CC(O)NSF}_2$ no intermediates could be detected; the final products were NSF and TAS-perfluoroalkoxides. These results indicate that OCF_2 and $\text{F}_3\text{C-C(O)F}$ are better F^- acceptors than NSF (41).

In contrast to the difluorosulfur imides, reaction of TASF with the corresponding S-trifluoromethyl monofluorosulfur imides leads to reasonably stable anions with pseudo pentacoordinated sulfur (41). It is not unlikely that in both systems the sulfur centers are primarily attacked by F^- under formation of RC(O)NSF_3^- and $\text{RC(O)NSF}_2\text{CF}_3^-$, respectively. There are no profound theoretical investigations on the different stabilities of these two types of anions. Nevertheless, for decomposition to occur fluoride ion transfer from sulfur to carbon is necessary. If this occurs only from an equatorial position, then the difference in stability could be explained.

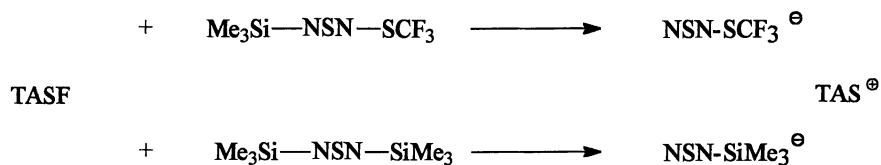
In the reaction of TASF with $\text{R}_3\text{Si-N=S}$ species the primary attack of F^- could occur either at the sulfur or at the silicon atom. Even in low temperature experiments no intermediates were detected; facile cleavage of the Si-N-bond was observed (54, 55).



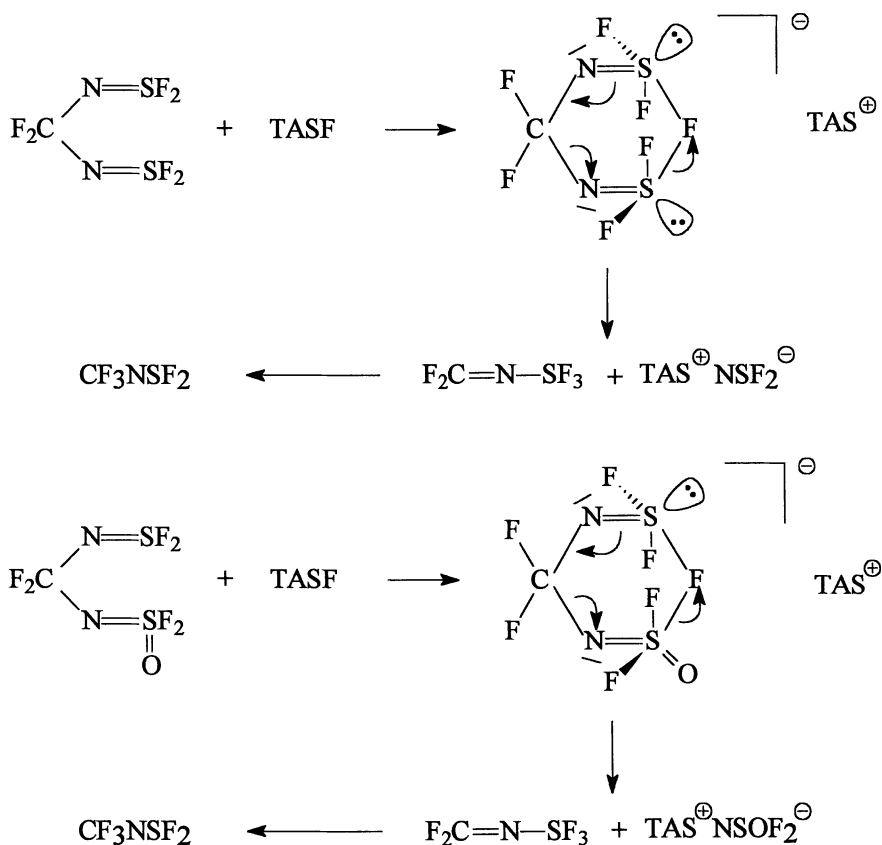
TASF

TAS[⊕]

The NSOF_2^- anion (isoelectronic with NSF_3) is known from the literature to show a broad singlet in the ^{19}F -NMR ($\delta = 77.8$ ppm) (56,57). With TAS^+ as a counterion $^2J(^{14}\text{N-F}) = 17.0$ Hz is observed similar to NSF_3 ($\delta = 70.0$ ppm, $^2J(^{14}\text{N-F}) = 26.4$ Hz (58)).



The primary products of TASF addition to the bifunctional methane derivatives $\text{F}_2\text{C}(\text{NSF}_2)_2$ (38) and $\text{F}_2\text{C}(\text{NSF}_2)\text{NS}(\text{O})\text{F}_2$ (59) are unstable and decompose at temperatures above -30°C to give F_3CNSF_2 and $\text{TASF}^+\text{NSF}_2^-$ or $\text{TASF}^+\text{NS}(\text{O})\text{F}_2^-$, respectively.

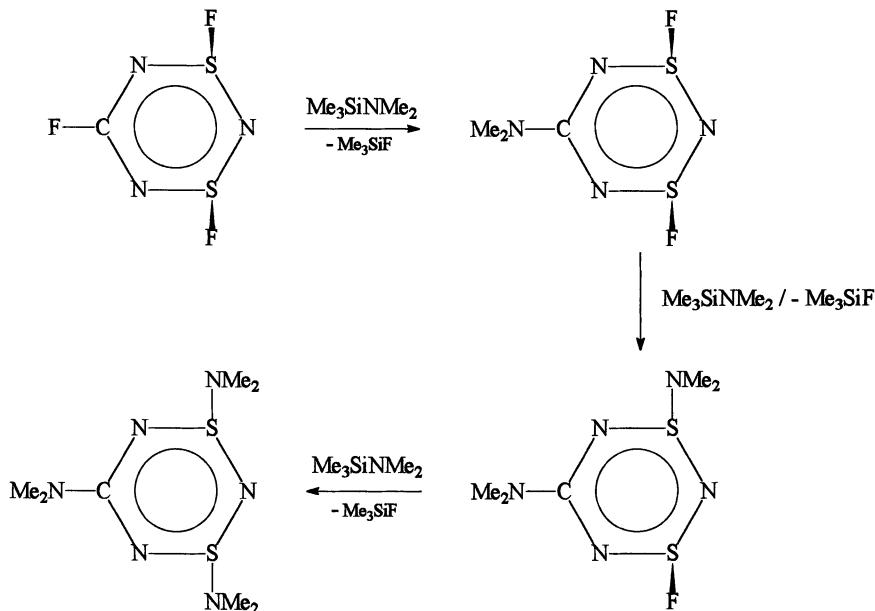


The first step involves the attack of fluoride ion at the sulfur centers. In both systems only one signal is observed for the sulfur-bonded fluorine atoms (with a very broad line in the latter example). In the rapid exchange of F^- between the two sulfur centers, a six-membered $\text{CN}_2\text{S}_2\text{F}^-$ heterocycle with pseudo pentacoordinated sulfur atoms should be the transition state. As with the previously described results, the bridging

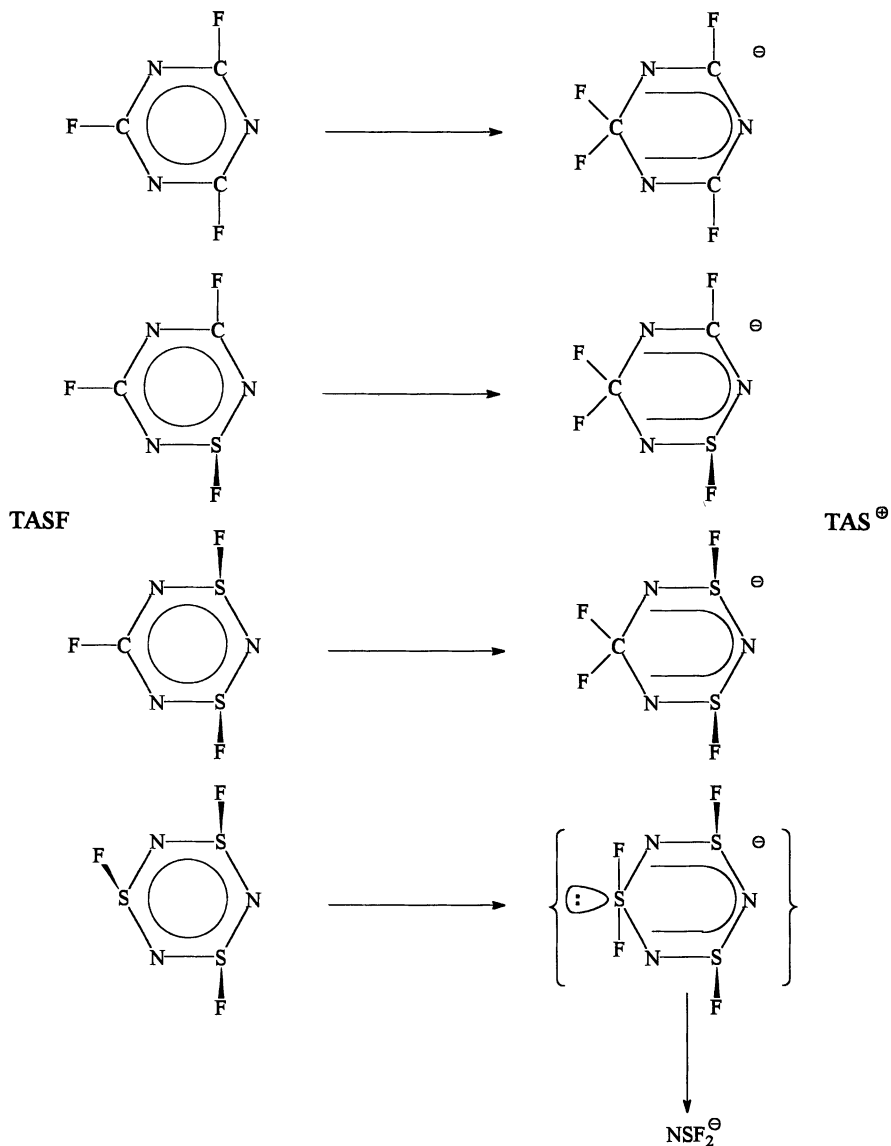
position should be occupied by axial fluorine ligands. The first step in the decomposition will be $F_2C=NSF_3$ and $TAS^+NSF_2^-$ or $TAS^+NS(O)F_2^-$, respectively. $F_2C=NSF_3$ will rearrange via a 1,3-fluorine atom shift to give the thermodynamically more favorable CF_3NSF_2 .

The formation of CF_3NSF_2 and $TAS^+NSOF_2^-$ instead of $CF_3NS(O)F_2$ and $TAS^+NSF_2^-$, does not suggest that the NSF_2 group is a better acceptor than the $NS(O)F_2$ group. Rather it merely indicates that $NSOF_2^-$ is a better leaving group than NSF_2^- . There are several examples in the literature for the decomposition of bis(difluorosulfurimide) derivatives, e.g., $OC(NSF_2)_2$ (60) and $O_2S(NSF_2)_2$ (60) under formation of NSF and $FC(O)NSF_2$ and FSO_2NSF_2 , respectively. Our investigations show that these decompositions might be F^- catalyzed.

Another example of the elucidation of reaction mechanisms comes from the chemistry of thiatriazines. In the reaction of 1,3,5-trifluoro-dithiatriazines with silylamines the CF bond is attacked first. With an excess of silylamine, exchange also occurs at one or both sulfur atoms (61):



Carbon containing fluoro triazines react with TASF to give stable cyclic anions [$(Cs^+C_3N_3F_4^-)$ is known from the literature (62)], with attack occurring exclusively at the carbon. With $(NSF)_3$ the corresponding cyclic anion $N_3S_3F_4^-$ is the primary product, but this readily decomposes to give $TAS^+NSF_2^-$ (63). These cyclic anions might be regarded as stabilized S_N2^- transition states for a nucleophilic attack at the ring systems.



Conclusions

Due to the availability of unusual fluoride ion transfer reagents new pathways for the generation, stabilization, and structural investigation of previously unknown fluorosulfur-, fluorosulfur-nitrogen-, and sulfur-nitrogen anions have been developed. With these tools a "mechanistic-synthetic" chemistry is possible, leading to "stabilized transition states", starting points for further preparative work. This chemistry is not

restricted to sulfur chemistry, as examples from other main group elements have been previously reported e.g., from $>C=O$ (64) and $>C=N-$ systems (65) stable TAS salts have been generated. Structural investigations with TAS^+ as a counterion are often not completely satisfying, since the C_s symmetry of the cation leads to disordering of the anion. Examples are $TAS^+ CF_3-N-C(O)F^-$ or $TAS^+ N(CF_3)_2^-$ (65).

Acknowledgment

I want to thank my coworkers Prof. Dr. U. Behrens, Dr. S.-J. Shen, G. Knitter, Dr. N. Hamou, Dr. W. Heilemann, Dr. T. Meier, Dr. D. Viets, Dr. A. Waterfeld and specially E. Lork for their enthusiastic engagement in this work. The help of Dr. P. G. Watson in preparing this manuscript and support by the University of Bremen (F.N.K.), Deutsche Forschungsgemeinschaft and the Fonds der Chemischen Industrie is gratefully acknowledged.

Literature Cited

- (1) Mews, R. *Adv. Inorg. Chem. Radiochem.* (H.J. Emeleus, A.G. Sharpe, eds.) **1976**, *19*, 185.
- (2) Middleton, W.J. (E.I. du Pont de Nemour & Co), U.S. Patent, **1963**, 3 940 402 (*Chem. Abstr.* **1976**, *85*, 6388); *Org. Synth.* **1985**, *64*, 221.
- (3) Christe, K.O.; Wilson, W.W.; Wilson, R.D.; Bau, R.; Feng, J. *J. Am. Chem. Soc.* **1990**, *112*, 7619.
- (4) Schwesinger, R.; Link, R.; Thiele, G.; Rotter, H.; Honert, D.; Limbach, H.-H.; Männle, F. *Angew. Chem., Int. Ed. Engl.* **1991**, *30*, 1372; *ibid* **1992**, *31*, 850.
- (5) Bartlett, N.; Robinson, P.L. *Chem. Ind. (London)* **1956**, 1351; *J. Chem. Soc.* **1961**, 3417.
- (6) Seel, F.; Detmer, O. *Angew. Chem.* **1958**, *70*, 163; *Z. Anorg. Allg. Chem.* **1959**, *385*, 113.
- (7) Gibler, D.D.; Adams, C.J.; Fischer, M.; Zalkin, A.; Bartlett, N. *Inorg. Chem.* **1972**, *11*, 2325; Mallouk, T.E.; Müller, G.; Brusasco, R.; Bartlett, N. *ibid* **1984**, *23*, 3167.
- (8) Tullock, C.W.; Coffman, D.D.; Muetterties, E.L. *J. Am. Chem. Soc.* **1964**, *86*, 357.
- (9) Christe, K.O.; Curtis, E.C.; Schack, C.J.; Pilipovich, D. *Inorg. Chem.* **1972**, *11*, 1679.
- (10) Bittner, J.; Fuchs, J.; Seppelt, K. *Z. Anorg. Allg. Chem.* **1988**, *557*, 82.
- (11) Gombler, W.; Seel, F. *J. Fluorine Chem.* **1974**, *4*, 333.
- (12) Clifford, A.F.; El-Shamy, H.K.; Emeleus, H.J.; Haszeldine, R.N. *J. Chem. Soc.* **1953**, 2375.
- (13) Shimp, L.A.; Lagow, R.J. *Inorg. Chem.* **1977**, *16*, 2974.
- (14) Waterfeld, A.; Mews, R. *J. Fluorine Chem.* **1983**, *23*, 325.
- (15) Weiss, I.; Oberhammer, H.; Viets, D.; Mews, R.; Waterfeld, A. *J. Mol. Structure* **1991**, *248*, 407.
- (16) Minkwitz, R.; Molsbeck, W.; Oberhammer, H.; Weiss, I. *Inorg. Chem.* **1992**, *31*, 2104.
- (17) Kramar, M.; Duncan, L.C. *Inorg. Chem.* **1971**, *10*, 647

- (18) Pauer, F.; Erhart, M.; Mews, R.; Stalke, D. *Z. Naturforsch. Part B* **1990**, *45*, 271.
- (19) Viets, D.; Mews, R.; Noltemeyer, M.; Schmidt, H.G.; Waterfeld, A. *Chem. Ber.* **1991**, *124*, 1353.
- (20) Heilemann, W.; Mews, R.; Noltemeyer, M.; Dixon, D.; Farnham, W.B. *Heteroatom Chem.*, in press (1993)
- (21) Viets, D.; Heilemann, W.; Waterfeld, A.; Mews, R.; Besser, S.; Herbst-Irmer, R.; Sheldrick, G.M.; Stohrer, W.D. *J. Chem. Soc. Chem. Comm.* **1992**, 1017.
- (22) Krespan, C.G., (E.I. du Pont de Nemour & Co), *U.S.Pat.* **1960/1963**, 3, 099, 688 (*Chem. Abstr.* **1964**, *60*, 1597).
- (23) Viets, D.; Mews R. unpublished results.
- (24) Viets, D.; Heilemann, W.; Mews, R. unpublished results.
- (25) Behrens, U.; Lork, E.; Viets, D.; Mews, R. unpublished results.
- (26) Heilemann, W.; Mews, R.; Pohl, S.; Saak, W. *Chem. Ber.* **1989**, *122*, 427.
- (27) Tullock, C.W.; Coffman, D.D.; Muetterties, E.L. *J. Am. Chem. Soc.*, **1964**, *86*, 357.
- (28) Darragh, J.I.; Haran, G.; Sharp, D.W.A. *J. Chem. Soc. Dalton Trans.* **1973**, 2289.
- (29) Heilemann, W.; Mews, R. *J. Fluorine Chem.* **1991**, *52*, 377.
- (30) Heilemann, W.; Mews, R. *Eur. J. Solid State Inorg. Chem.* **1992**, *29*, 799.
- (31) Meier, T.; Mews, R. unpublished results.
- (32) Ruff, J.K. *Inorg. Chem.* **1965**, *4*, 1446.
- (33) Höfer, R.; Glemser, O. *Z. Naturforsch. Part B.* **1975**, *30*, 1980.
- (34) Waterfeld, A.; Mews, R. *Chem. Ber.* **1983**, *116*, 1674.
- (35) Glemser, O.; Höfer, R. *Z. Naturforsch. Part B* **1979**, *29*, 121.
- (36) Meier, T.; Mews, R. *J. Fluorine Chem.* **1989**, *42*, 81.
- (37) Sundermeyer, W. *Angew. Chem. Int. Ed.* **1967**, *6*, 90;
- (38) Glemser, O.; Biermann, U. *Inorg. Nucl. Chem. Lett.* **1967**, *3*, 223.
- (39) Lustig, M.; Ruff, J.K. *Inorg. Nucl. Chem. Lett.* **1967**, *3*, 531;
- (40) Glemser, O.; Biermann, U.; Hoff, A. *Z. Naturforsch. Part B* **1967**, *22*, 893.
- (41) Lork, E.; Mews, R. unpublished results.
- (42) Meier, T.; Mews, R. *Angew. Chem. Int. Ed.* **1985**, *24*, 344.
- (43) Meier, T.; Mews, R. *J. Fluorine Chem.*, in press (1993)
- (44) Günther, H.; Oberhammer, H.; Mews, R.; Stahl, I. *Inorg. Chem.* **1982**, *21*, 1872.
- (45) Stahl, I.; Mews, R.; Glemser, O. *Angew. Chem. Int. Ed.* **1980**, *19*, 408.
- (46) Glemser, O.; v.Halasz, S.P.; Biermann, U. *Z. Naturforsch. Part B* **1968**, *23*, 1381.
- (47) Demitras, G.C.; Mac Diarmid, A.G. *Inorg. Chem.* **1967**, *6*, 1903.
- (48) Ibbott, D.G.; Janzen, A.F. *Can. J. Chem.* **1972**, *50*, 2428.
- (49) Henle, H.; Mews, R. *Chem. Ber.* **1982**, *115*, 3547.
- (50) Heilemann, W.; Mews, R. unpublished results.
- (51) Des Marteau, D. D.; Eysel, H.H.; Oberhammer, H.; Günther, H. *Inorg. Chem.* **1982**, *21*, 1607.
- (52) Glemser, O.; Mews, R.; Roesky, H.W. *Chem. Ber.* **1969**, *102*, 1523.
- (53) The C-N bond cleavage in FC(O)-NSF₂ by CsF was reported by: Ruff, J.K. *Inorg. Chem.*, **1966**, *5*, 1787

- (54) Heilemann, W.; Mews, R. *Chem. Ber.* **1988**, *121*, 461
- (55) Chen, S.-J.; Cutin, E.; Grotzki, I.; Knitter, G.; Mews, R. unpublished results.
- (56) e.g. Roesky, H.W.; Glemser, O.; Hoff, A.; Koch, W. *Inorg. Nucl. Chem. Lett.* **1967**, *3*, 39;
- (57) Feser, M.; Höfer, R.; Glemser, O. *Z. Naturforsch. Part B*, **1974**, *29*, 916.
- (58) Richert, H.; Glemser, O. *Z. Anorg. Allg. Chem.* **1961**, *304*, 328.
- (59) Glemser, O.; v.Halasz, S.P. *Inorg. Nucl. Chem. Lett.* **1968**, *4*, 191.
- (60) Biermann, U.; Glemser, O. *Chem. Ber.* **1967**, *100*, 3795.
- (61) Chen, S.-J.; Mews, R. unpublished results.
- (62) Chambers, R.D.; Philot, P.D.; Russel, P.L. *J. Chem. Soc. Perkin Trans.* **1977**, *14*, 1605.
- (63) Chen, S.-J.; Heilemann, W.; Maggiulli, R.; Mews, R. unpublished results.
- (64) Farnham, W.B.; Smart, B.E.; Middleton, W.J.; Calabrese, J.C.; Dixon, D.A. *J. Am. Chem. Soc.* **1985**, *107*, 4565; Dixon, D.A.; Farnham, W.B.; Smart, B.E. *Inorg. Chem.* **1990**, *29*, 3954.
- (65) Hamou, N.; Erhart, M.; Behrens, U.; Lork, E.; Mews, R. unpublished results.

RECEIVED July 1, 1993

Chapter 10

Quest for an Aromatic Silicon Species An Unusual Geometry around Silicon in a 10-Si-5 Siliconate

Suman K. Chopra¹, Chester D. Moon², and J. C. Martin

Department of Chemistry, Vanderbilt University, Nashville, TN 37235

Several hypervalent 10-Si-5 compounds containing a tridentate ligand system suitable for stabilizing three-center four-electron (3c-4e) hypervalent bonds have been synthesized. Normally 10 electron hypervalent main group species that have five ligands attached to the central atom exhibit a trigonal bipyramidal (TBP) geometry about the central atom. However, in our attempts to synthesize a hypervalent silicon species in which the silicon atom is contained within an aromatic ring, we obtained a compound whose X-ray crystal structure revealed a rectangular pyramidal geometry about silicon. The geometry of this unique structure is explained in terms of stabilizing factors associated with hypervalent bonding.

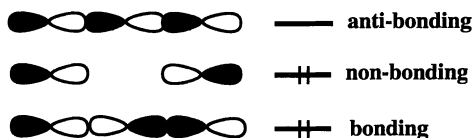
For many years chemists used Lewis' octet rule to explain the stability of molecules. However, this rule did not explain the stability of compounds such as PCl_5 and SF_4 , both of which contain a central atom with 10 electrons formally associated with it. Throughout the years chemists explained the stability of such electron rich species by invoking the use of *d*-orbitals to accommodate the expansion of the valence octet resulting in sp^3d hybridization (1). However, subsequent studies (2-4) of such electron rich species showed inconsistencies in the electron distributions expected in sp^3d hybridization.

In 1969, Musher (5) termed such electron rich species as hypervalent. Musher suggested that the three-center four-electron (3c-4e) bond could be viewed as a linear combination of an atomic *p*-orbital from each of the three atoms involved in the hypervalent bond. The combination of these orbitals leads to three molecular orbitals that approximate hypervalent bonding. The orbital diagram indicates two of

¹Current address: Colgate Palmolive Company, 909 River Road, Piscataway, NJ 08855

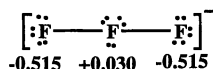
²Current address: Manufacturing Technology Laboratory, Reynolds Metals Company, 3326 East 2nd Street, Muscle Shoals, AL 35661

the four electrons in the hypervalent bond reside in a nonbonding orbital. Such an arrangement places most of the electron density on the terminal sites of the 3c-4e bond resulting in a charge separation with partial negative charge at the terminal atoms and partial positive charge at the central atom.



Orbital Diagram for Hypervalent Bonding

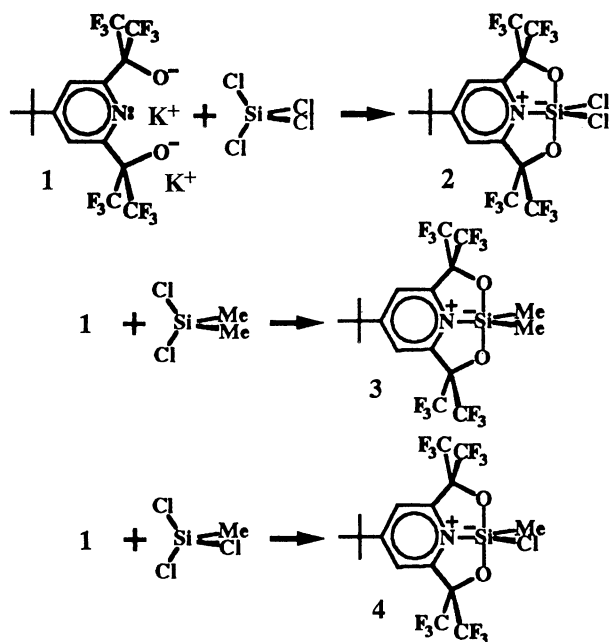
Calculations performed on the hypervalent 10-F-2 (*6*) trifluoride anion (*7*) are consistent with the bonding diagram. This hypervalent species consists of a 3c-4e bond that has a partial negative charge of -0.515 at each terminal fluorine and a partial positive charge of 0.030 at the central fluorine. This charge separation indicates that the formal octet expansion is distributed over the three atoms of the hypervalent bond.



Calculated Charges for the 10-F-2 Trifluoride Anion

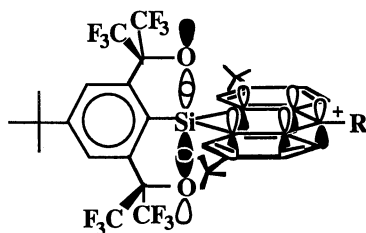
For the past several years, our research efforts have focused on the syntheses of stable hypervalent compounds. Our success has stemmed from the design of various ligand systems that stabilize the charge separation of the hypervalent bond (*8-10*). One such ligand system is compound **1**. This compound consists of 4-*tert*-butylpyridine substituted with the potassium salt of hexafluoroisopropanol at the 2 and 6 position (*11*). Treatment of **1** with tetrachlorosilane produces dichlorosiliconate **2**. Compound **2** contains the hypervalent O-Si-O bond. The tridentate ligand system stabilizes this bond by placing two electronegative CF₃ groups adjacent to the terminal oxygen atoms. These electronegative groups serve to stabilize the partial negative charge on the oxygen atoms. The nitrogen center in **2** also serves to charge compensate the structure so that it is overall neutral. The corresponding siliconates **3** and **4** are formed by the reactions of **1** with dichlorodimethylsilane and methyltrichlorosilane, respectively, as shown in Scheme 1.

In terms of preparing an aromatic silicon species, the strategy was to prepare further siliconates where the silicon atom would actually be part of a 9-silaanthracene. If the methylene carbon (10-position) of the silaanthracene was then made cationic by formal removal of a proton, the silicon atom might end up in a cyclic array of



Scheme 1

p-orbitals containing six electrons. The orbital diagram below shows such a cyclic array of orbitals with four electrons coming from the anthracene ring system and two electrons coming from the bonding molecular orbital of the hypervalent bond centered on silicon, cf. bis(ipso)aromaticity proposed for the $4n + 2\pi$ system containing a pentavalent trigonal bipyramidal (TBP) carbon atom (12). It was not known *a priori* whether the energy match between the bonding molecular orbital of the hypervalent bond and the pi framework of the anthracene ring would be close enough. Therefore, it was also deemed important to attempt the synthesis of the corresponding anionic derivative in case the energy match should be better with the antibonding molecular orbital of the hypervalent bond. All six electrons for aromaticity would then come from the *p*-orbitals on the carbon atoms.



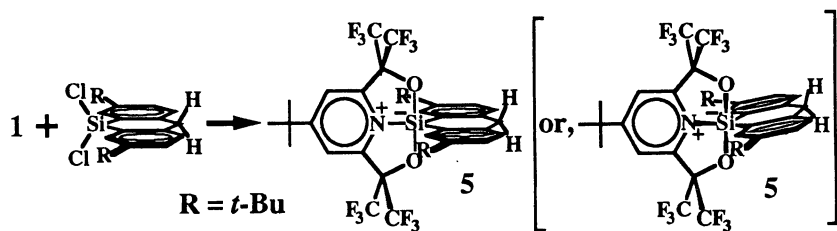
Experimental Section

4-(*t*-Butyl)- $\alpha,\alpha,\alpha',\alpha'$ -tetrakis(trifluoromethyl)-2,6-pyridinedimethanolato-(2)- $N_1,O\alpha,O\alpha'$ -dichloro Siliconate, 2. Tetrachlorosilane (0.25 mL, 2.2 mmol) was added to the dipotassium salt **1** (1.00 g, 1.84 mmol) in THF (15 mL) at $-40\text{ }^\circ\text{C}$. The reaction mixture was stirred for 15 - 20 min. The solvent was then removed, and the KCl was filtered by dissolving the reaction mixture in Et₂O. Compound **2** was then recrystallized from Et₂O/hexane (0.68 g, 1.2 mmol, 65%); ¹⁹F NMR (THF-*d*₈) δ -74.45 (s); ¹H NMR (THF-*d*₈) δ 8.42 (s, 2, 3,5 HPy), 1.50 (s, 9, *t*-Bu). Anal. (C₁₅H₁₁NO₂F₁₂C₁₂Si) C, H, N.

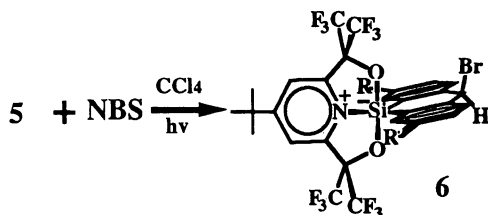
4-(*t*-Butyl)- $\alpha,\alpha,\alpha',\alpha'$ -tetrakis(trifluoromethyl)-2,6-pyridinedimethanolato-(2)- $N_1,O\alpha,O\alpha'$ -dimethyl Siliconate, 3. Dichlorodimethylsilane (0.25 mL, 2.1 mmol) was added to the dipotassium salt **1** (1.00 g, 1.84 mmol) in THF (5 mL) at $-78\text{ }^\circ\text{C}$. The reaction mixture was stirred for 1 h. The solvent was then removed, and the KCl was filtered by dissolving the reaction mixture in Et₂O. Compound **3** was then recrystallized from Et₂O/hexane (0.70 g, 1.3 mmol, 73 %); ¹⁹F NMR (THF-*d*₈) δ -75.21 (s); ¹H NMR (THF-*d*₈) δ 8.28 (s, 2, 3,5 HPy), 1.52 (s, 9, *t*-Bu), 0.32 (s, 3, Me). Anal. (C₁₇H₁₇NO₂F₁₂Si) C, H, N.

4-(*t*-Butyl)- $\alpha,\alpha,\alpha',\alpha'$ -tetrakis(trifluoromethyl)-2,6-pyridinedimethanolato-(2)- $N_1,O\alpha,O\alpha'$ -methylchloro Siliconate, 4. Methyltrichlorosilane (0.30 mL, 2.6 mmol) was added to the dipotassium salt **1** (1.00 g, 1.84 mmol) in THF (7 mL) at $-78\text{ }^\circ\text{C}$. The reaction mixture was stirred for 1 h. The solvent was then removed, and the KCl was filtered by dissolving the reaction mixture in Et₂O. Compound **4** was then recrystallized from Et₂O/hexane (0.61 g, 1.1 mmol, 61 %): mp 146.5-147.5 $^\circ\text{C}$; ¹⁹F NMR (THF-*d*₈) δ -74.4 (q, 6, *J* = 9.3 Hz), -76.9 (q, 6, *J* = 9.3 Hz); ¹H NMR (THF-*d*₈) δ 8.22 (s, 2, 3,5 HPy), 1.52 (s, 9, *t*-Bu), 0.60 (s, 3, CH₃). Anal. (C₁₆H₁₄NO₂F₁₂ClSi) C, H, N.

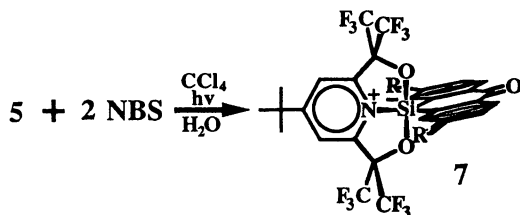
4-(*t*-Butyl)- $\alpha,\alpha,\alpha',\alpha'$ -tetrakis(trifluoromethyl)-2,6-pyridinedimethanolato-(2)- $N_1,O\alpha,O\alpha'$ -methylenedi-2,1-(2,7-di-*t*-butylphenylene) Siliconate, 5. 2,7-Di-*t*-butyl-9,9-dichloro-9,10-dihydro-9-silaanthracene (2.71 g, 7.17 mmol) (**13**) was dissolved in THF (10 mL), and the resulting solution was added dropwise to the dipotassium salt **1** (3.99 g, 7.18 mmol) in THF (20 mL) at $-78\text{ }^\circ\text{C}$. The reaction mixture was stirred overnight at room temperature. The solvent was then removed on a vacuum line, and the KCl was removed by dissolving the reaction mixture in Et₂O. Compound **5** was then recrystallized from THF/hexane (4.25 g, 5.51 mmol, 76.8 %): mp 279.5 - 280.5 $^\circ\text{C}$; ¹⁹F NMR (THF-*d*₈) δ -74.37 (s); ¹H NMR (THF-*d*₈) δ 8.43 (s, 2, 3,5 HPy), 7.23 (dd, 2, *J* = 7.9, 1.8 Hz, para to Si), 7.17 (d, 2, *J* = 7.9 Hz, ortho to CH₂), 7.11 (d, 2, *J* = 1.8 Hz, ortho to Si), 4.16 (s, 2, CH₂), 1.56 (s, 9H, *t*-Bu), 1.18 (s, 18H, *t*-Bu). Anal. (C₃₆H₃₇NO₂F₁₂Si) C, H, N.



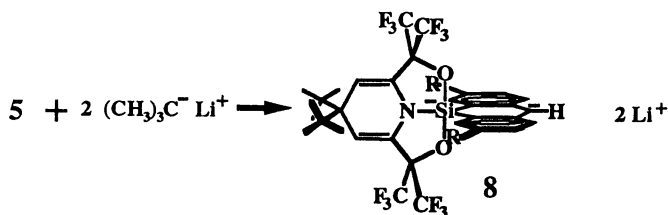
4-(*t*-Butyl)- $\alpha,\alpha,\alpha',\alpha'$ -tetrakis(trifluoromethyl)-2,6-pyridinedimethanolato-(2)- $N_1,O\alpha,O\alpha'$ -bromomethylenedi-2,1-(2,7-di-*t*-butylphenylene) Siliconate, 6. Siliconate 5 (0.63 g, 0.82 mmol) and *N*-bromosuccinimide (0.15 g, 0.84 mmol) were dissolved in CCl_4 (20 mL), and the reaction mixture was irradiated with a UV tungsten light for 1.5 h. The solvent was then removed on a vacuum line, and 6 was crystallized from THF/hexane (0.66 g, 0.78 mmol, 95 %). ^{19}F (CDCl_3) δ -74.8 (s); ^1H (CDCl_3) δ 8.26 (s, 2, 3,5 HPy), 7.46 (d, 2, $J = 8.2$ Hz, ortho to CHBr), 7.34 (dd, 2, $J = 8.2, 2.1$ Hz, para to Si), 6.81 (d, 2, $J = 2.1$ Hz, ortho to Si), 6.67 (s, 1, CHBr), 1.58 (s, 9, *t*-Bu), 1.15 (s, 18, *t*-Bu). Anal. ($\text{C}_{36}\text{H}_{36}\text{NO}_2\text{F}_{12}\text{BrSi}$) C, H, N.



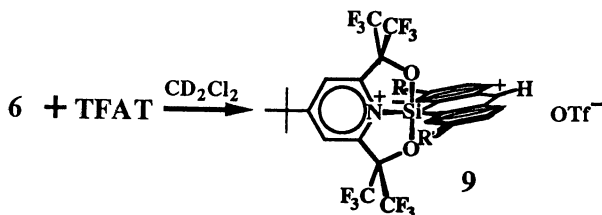
4-(*t*-Butyl)- $\alpha,\alpha,\alpha',\alpha'$ -tetrakis(trifluoromethyl)-2,6-pyridinedimethanolato-(2)- $N_1,O\alpha,O\alpha'$ -ketodi-2,1-(2,7-di-*t*-butylphenylene) Siliconate, 7. A mixture of siliconate 5 (0.40 g, 0.53 mmol) and *N*-bromosuccinimide (0.38 g, 2.1 mmol) in CCl_4 (10 mL) was irradiated with a UV tungsten light for 3 h. The solvent was then removed on a vacuum line. Excess *N*-bromosuccinimide was filtered by dissolving the reaction mixture in hexane, and compound 7 was crystallized from hexane (0.36 g, 0.46 mmol, 87 %). ^{19}F NMR (CDCl_3) δ -75.14 (s); ^1H NMR (CDCl_3) δ 8.32 (d, 2, $J = 8.4$ Hz, ortho to $\text{Ph}_2\text{C}=\text{O}$), 8.28 (s, 2, 3,5 HPy), 7.48 (dd, 2, $J = 8.4, 2.1$ Hz, para to Si), 6.82 (d, 2, $J = 2$ Hz, ortho to Si), 1.59 (s, 9, *t*-Bu), 1.18 (s, 18, *t*-Bu); mass spectrum FAB m/z 787 (M^+). Anal. ($\text{C}_{36}\text{H}_{35}\text{NO}_3\text{F}_{12}\text{Si}$) C, H, N.



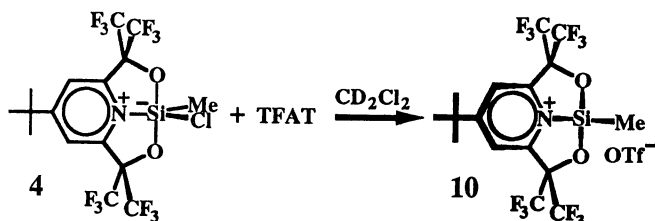
Dilithium Salt of 4,4'-Bis-(*t*-butyl)- $\alpha,\alpha,\alpha',\alpha'$ -tetrakis(trifluoromethyl)-2,6-dihydropyridinedimethanolato-(2-)- $N_1,O\alpha,O\alpha'$ -methinedi-2,1-(2,7-*t*-butylphenylene) Siliconate Dianion, 8. *t*-Butyl lithium (0.35 mL, 1.7 M, 0.6 mmol) in pentane was added to siliconate 5 (0.20 g, 0.26 mmol) at $-78\text{ }^\circ\text{C}$. The reaction mixture was slowly brought to room temperature (2 h). Siliconate 8 was recrystallized from hexane/pentane (0.15 g, 0.18 mmol, 68%): mp $254\text{--}256\text{ }^\circ\text{C}$; ^{19}F NMR (Et_2O) δ -75.9 (s); ^{19}F NMR (THF) δ -75.39 (br s); ^1H NMR (Et_2O) δ 7.27 (d, 2, $J = 2.2$ Hz, ortho to Si), 6.82 (dd, 2, $J = 8.4, 2.2$ Hz, para to Si), 6.55 (d, 2, $J = 8.4$ Hz, ortho to CHPh_2), 5.07 (s, 2, 3,5 HPy), 4.59 (s, 1, CHPh_2), 1.11 (s, 18, *t*-Bu), 1.05 (s, 18, *t*-Bu); ^1H NMR (THF) δ 7.17 (d, 2, $J = 2.2$ Hz), 6.67 (dd, 2, $J = 9, 2$ Hz), 6.36 (d, 2, $J = 9$ Hz), 5.02 (s, 2, 3,5 HPy), 4.50 (s, 1, CH), 1.11 (s, 18, *t*-Bu), 1.05 (s, 18 *t*-Bu). Anal. ($\text{C}_{40}\text{H}_{45}\text{NO}_2\text{F}_{12}\text{SiLi}_2$) C, H, N.



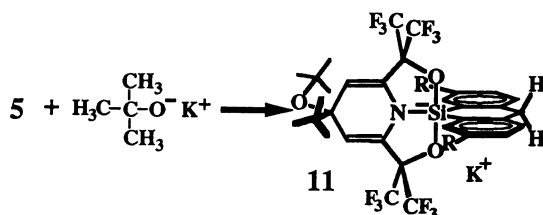
Triflate Salt of 4-(*t*-Butyl)- $\alpha,\alpha,\alpha',\alpha'$ -tetrakis(trifluoromethyl)-2,6-pyridine-dimethanolato-(2-)- $N_1,O\alpha,O\alpha'$ -hydrogencarbon(+)-di-2,1-(2,7-di-*t*-butylphenylene) Siliconate, 9. Siliconate 9 was prepared by removing bromide from 6 by reaction with trifluoroacetyl triflate (TFAT) at $-78\text{ }^\circ\text{C}$. ^{19}F NMR (CD_2Cl_2) δ -74.92 (s, 12), -78.7 (s, 3). ^1H NMR (CD_2Cl_2) δ 9.54 (s, 1), 8.48 (d, 2, $J = 8.3$ Hz), 8.45 (s, 2, 3,5 HPy), 7.80 (dd, 2, $J = 8.3, 1.85$ Hz), 7.23 (s, 2), 1.62 (s, 9, *t*-Bu), 1.27 (s, 18, *t*-Bu). Anal. ($\text{C}_{37}\text{H}_{36}\text{NSO}_5\text{F}_{15}\text{Si}$) C, H, N.



Triflate Salt of 4-(*t*-Butyl)- $\alpha,\alpha,\alpha',\alpha'$ -tetrakis(trifluoromethyl)-2,6-pyridine-dimethanolato-(2-)- $N_1,O\alpha,O\alpha'$ -methyl Siliconate, 10. The chlorine in 4 was removed with TFAT to form the cationic siliconate 10 with OTf^- as the counterion. ^{19}F NMR (CD_2Cl_2) δ -74.44 (br s, 6), -76.04 (br s, 6), -77.58 (s, 3, OTf^-); 1H NMR (CD_2Cl_2) δ 8.23 (s, 2, Py), 1.51 (s, 9, *t*-Bu), 0.5 (s, 3, Me).



Potassium Salt of 4-(*t*-Butyl)-4-(*O-t*-Butyl)- $\alpha,\alpha,\alpha',\alpha'$ -tetrakis(trifluoromethyl)-2,6-dihydropyridinedimethanolato-(2-)- $N_1,O\alpha,O\alpha'$ -methylenedi-2,1-(2,7-*t*-butylphenylene) Siliconate, 11. The siliconate 11 was prepared by the reaction of 5 with potassium *t*-butoxide in THF. ^{19}F NMR (THF) δ -75.02 (q, 6, $J = 9.5$ Hz), -75.44 (q, 6, $J = 9.5$ Hz); 1H NMR (THF) δ 7.70 (s, 1, ortho to Si), 7.50 (s, 1, ortho to Si), 7.05 (m, 4, para to Si and ortho to CH_2), 5.05 (s, 2, Py), 4.05 (s, 2, CH_2), 1.25 (s, 9, *t*-Bu), 1.22 (s, 9, *t*-Bu), 1.21 (s, 9, *t*-Bu), 1.10 (s, 9, *t*-Bu).



Crystal Data for Siliconate 6. All measurements were made on a Rigaku AFC6S diffractometer with graphite monochromated Cu K α radiation. A colorless prism of C₃₆H₃₆NO₂F₁₂BrSi was mounted on a glass fiber. Final lattice parameters as obtained from a least-squares refinement using the setting angles of 25 carefully centered reflections are given in Table I. Based on the systematic absences of 0kl: k \neq 2n, h0l: l \neq 2n, and hk0: h \neq 2n, and the successful solution and refinement of the structure, the space group was determined to be: *Pbca* (#61).

Table I. Summary of Crystal Data and Data Collection Conditions for Siliconate 6

Empirical Formula	C ₃₆ H ₃₆ F ₁₂ O ₂ NBrSi
Formula Weight	850.66
Crystal Color, Habit	colorless, prism
Crystal Dimensions, mm	0.4 X 0.4 X 0.2
Crystal System	orthorhombic
No. Reflections Used for Unit	
Cell Determination, (2 θ range, deg)	60.3 - 78.4
Space Group	<i>Pbca</i> (#61)
a, Å	20.835 (2)
b, Å	20.419 (5)
c, Å	18.365 (2)
V, Å ³	7813 (4)
Z	8
d_{calc} , g/cm ³	1.446
Radiation	Cu K α (graphite monochromated)
μ (CuK α), cm ⁻¹	25.46
θ Scan Peak Width at Half-height	0.33
F ₀₀₀	3456
Scan Width, deg	(1.05 + 0.30 tan θ)
2 θ max, deg	120.2
No. of Measured Reflections	6416
Function Minimized	$\Sigma w (F_o - F_c)^2$
Least-squares Weights	4F _o ² / σ^2 (F _o ²)
p-factor	0.03
Anomalous Dispersion	All non-hydrogen atoms
No. Observations (I > 3.00s(I))	2956
No. Variables	478
Reflection/Parameter Ratio	6.18
Residuals: R; R _w	0.051; 0.059
Goodness of Fit Indicator	1.92
Max Shift/Error in Final Cycle	1.12

The data were collected at a temperature of 20 ± 1 °C using the ω - 2θ scan technique to a maximum 2θ value of 120.2° . Omega scans of several intense reflections, made prior to data collection, had an average width at half-height of 0.33° with a take-off angle of 6.0° . Scans of $(1.05 + 0.30 \tan \theta)^\circ$ were made at a speed of $8.0^\circ/\text{min}$ (in omega). The weak reflections [$I < 10.0\sigma(I)$] were rescanned (maximum of 3 rescans), and the counts were accumulated to assure good counting statistics. Stationary background counts were recorded on each side of the reflection. The ratio of peak counting time to background counting time was 2:1. The diameter of the incident beam collimator was 0.5 mm and the crystal to detector distance was 200.0 mm.

A total of 6416 reflections was collected. The intensities of three representative reflections which were measured after every 150 reflections remained constant throughout data collection indicating crystal and electronic stability (no decay correction was applied). The linear absorption coefficient for Cu $K\alpha$ is 25.5 cm^{-1} . An empirical absorption correction, based on azimuthal scans of several reflections, was applied which resulted in transmission factors ranging from 0.82 to 1.00. The data were corrected for Lorentz and polarization effects.

Solution and Refinement of the Structure of Siliconate 6. All calculations were performed using the TEXSAN (14) crystallographic software package of Molecular Structure Corporation. The structure was solved by a combination of the Patterson method and direct methods (15). The non-hydrogen atoms were refined anisotropically. The final cycle of full-matrix least-squares refinement (16) was based on 2956 observed reflections [$I > 3.00\sigma(I)$] and 478 variable parameters and converged to $R = 0.051$ and $R_w = 0.059$. The maximum and minimum peaks on the final difference Fourier map corresponded to 0.46 and $-0.61 \text{ e}^-/\text{\AA}^3$, respectively.

Results and Discussion

Although our attempts to synthesize an aromatic silicon species failed (17), we were able to obtain the X-ray crystal structure for compound 6. Upon examination of the molecular structure, we found that the geometry about silicon was rectangular pyramidal instead of the expected TBP geometry (see Figures 1-3 and Tables II-III). We attribute the unusual geometry about silicon to factors that stabilize hypervalent bonding. Most 10 electron, hypervalent main group compounds usually exhibit TBP geometry with the terminal atoms of the hypervalent bond located at the apical positions. Therefore, stabilization of hypervalent bond is possible by placing electronegative groups at the apical positions thus stabilizing the partial negative charge at the terminal atoms of the hypervalent bond. Also, placing electropositive groups at the equatorial positions of the TBP geometry stabilizes partial positive charge on the central atom of the hypervalent bond through σ -donation.

We hypothesize that the rectangular pyramidal geometry in 6 is caused by the positively charged nitrogen being unstable in the equatorial position of the TBP. As the nitrogen atom donates its lone electron pair to form the bond with silicon, it

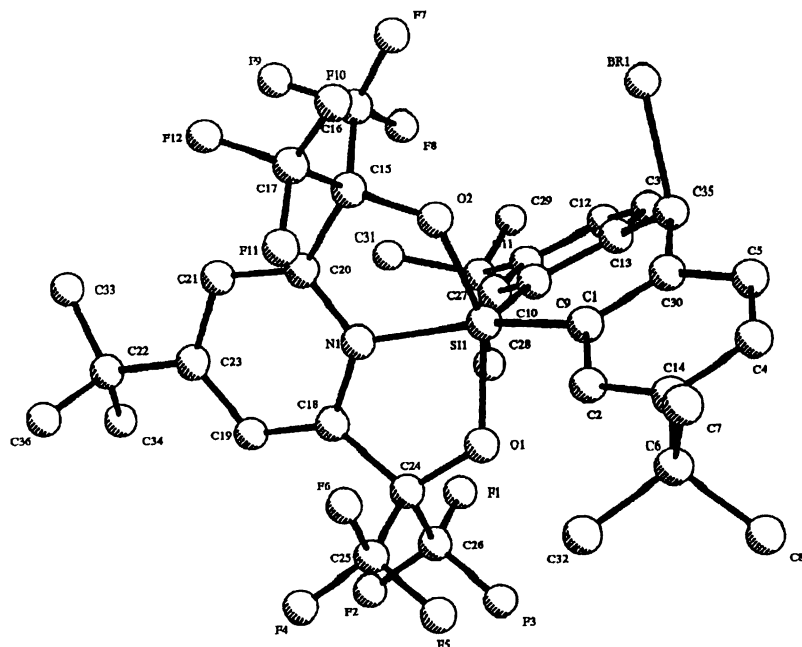


Figure 1. Ball and stick representation of siliconate **6** (View 1). Hydrogen atoms are omitted for clarity.

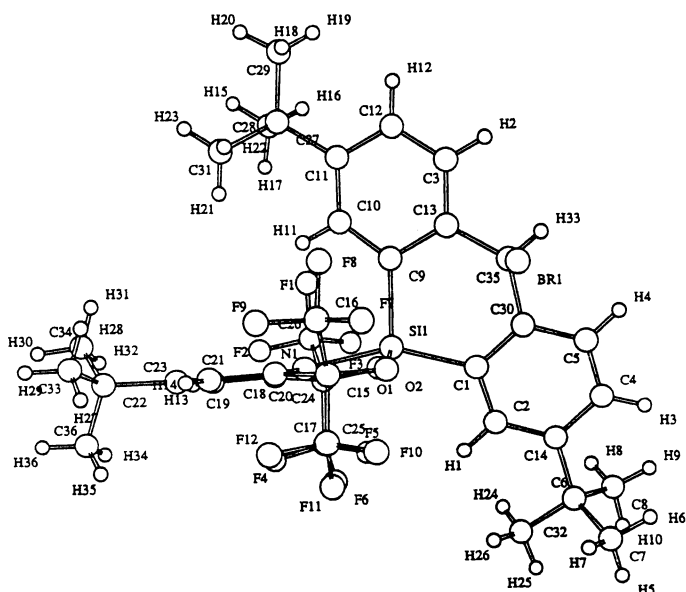


Figure 2. Ball and stick representation of siliconate **6** (View 2).

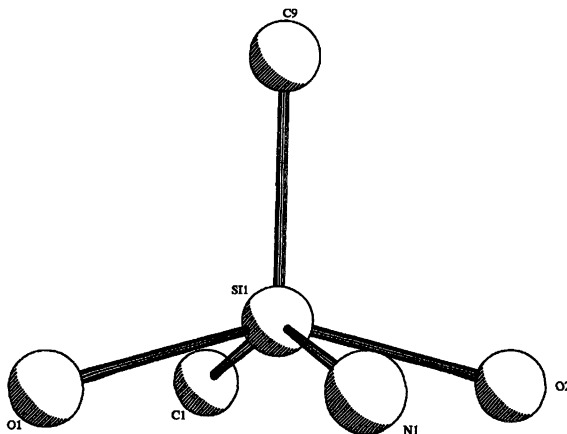


Figure 3. Ball and stick representation of siliconate **6** showing only atoms bonded to silicon.

becomes effectively more electronegative. With this increase in electronegativity, the nitrogen atom would prefer to be in an apical position of the TBP. We believe the nitrogen attempts to migrate to an apical position as in a Berry pseudorotation (18). However, due to the geometrical constraints of the molecule, this distortion from TBP geometry stops at the rectangular pyramidal geometry. A least squares plane calculation from the crystal structure data reveals that C1, O1, O2, and N1 have mean distances from a calculated plane that are not statistically different from zero. This fact as well as the selected bond distances and angles shown in Tables II and III clearly indicate that the geometry about silicon is rectangular pyramidal.

Table II. Selected Bond Angles (Deg) of Siliconate **6**

atom	atom	atom	angle	atom	atom	atom	angle
O1	Si1	O2	147.0 (2)	O2	Si1	C1	93.8 (2)
O1	Si1	N1	79.7 (2)	O2	Si1	C9	103.5 (2)
O1	Si1	C1	91.7 (2)	N1	Si1	C1	152.1 (3)
O1	Si1	C9	106.6 (3)	N1	Si1	C9	103.7 (3)
O2	Si1	N1	80.3 (2)	C1	Si1	C9	104.2 (3)

Table III. Selected Bond Lengths (Å) of Siliconate **6**

atom	atom	distance	atom	atom	distance
Br1	C35	2.008 (6)	Si1	N1	1.928 (5)
Si1	O1	1.760 (4)	Si1	C1	1.858 (6)
Si1	O2	1.752 (4)	Si1	C9	1.870 (6)

A very closely related distortion of a TBP phosphorus center to a rectangular pyramidal geometry has been recently reported (19). This example employs a 5-coordinate phosphorus center in a tridentate ligand. Electronegativity effects from two additional fluorine atoms cause a distortion similar to that which we observe in 6. Another highly relevant study, which also tries to join aromaticity and hypervalency, is the computational study of the $C_5H_5SF_3$ molecule, 1,1,1-trifluorothiabenzene, recently reported by Xie, Schaefer, and Thrasher (20). In this study, two different structures of almost equal energy were found. One of these structures is TBP in shape with an axial carbon substituent, while the other is rectangular pyramidal. The differences between these structures was explained with the concepts of aromaticity, directional repulsive effects of π bonds, apicophilicity of substituent groups in TBP systems, and Bent's rule.

A small number of other rectangular (or square) pyramidal, five-coordinate main group species have been previously reported, with the most recent example being a germanium(IV) anion from J. G. Verkade's laboratory (21). In addition to further examples with neutral pentavalent main group centers (22,23), most of the other known examples have originated from R. R. Holmes' laboratory and are spirocyclic compounds (24-29). Specific examples of rectangular pyramidal, tetravalent silicon anions include reports from Holmes (30) and D. Schomburg (31). The silicon anion 6 is unique in that the rectangular pyramidal geometry is stabilized by multiple five- and six-membered rings. As pointed out by Verkade and co-worker (21), all previous examples are stabilized by multiple four- and five-membered rings, whereas their new rectangular pyramidal germanium(IV) anion is stabilized by a combination of six- and seven-membered rings. Although the crystal structures of compounds 2, 5, 7, and 9 were not determined, an examination of the expected distribution of electron density within these molecules reveals that they will most likely be rectangular pyramidal as well.

Acknowledgments

Parts of this work were supported by the National Science Foundation (CHE-8910896) and others by the Department of Health and Human Services (GM 36844-06). The authors would like to thank Prof. J. S. Thrasher for helpful discussions.

Literature Cited

- (1) Huheey, J. E. *Inorganic Chemistry*, 3rd ed.; Harper & Row: New York, 1983; p 118.
- (2) Riedel, E. F.; Willett, R. D. *J. Am. Chem. Soc.* **1975**, *97*, 701.
- (3) Jones, C. W. *J. Chem. Phys.* **1975**, *62*, 4343.
- (4) Reed, A. E.; Weinhold, F. *J. Am. Chem. Soc.* **1986**, *108*, 3586.
- (5) Musher, J. I. *Angew. Chem., Int. Ed. Engl.* **1969**, *8*, 54.
- (6) The *N-X-L* classification scheme characterizes species in terms of the number (*N*) of formal valence shell electrons about an atom *X* and the number of ligands (*L*) bonded to *X*. Perkins, C. W.; Martin, J. C.; Arduengo, A. J., III; Lau, W.; Alegria, A.; Kochi, J. K. *J. Am. Chem. Soc.* **1980**, *102*, 7753.

- (7) Cahill, P. A.; Dykstra, C. E.; Martin, J. C. *J. Am. Chem. Soc.* **1985**, *107*, 6359.
- (8) Chopra, S. K.; Martin, J. C. *J. Am. Chem. Soc.* **1990**, *112*, 5342.
- (9) Stevenson, W. H.; Martin, J. C. *J. Am. Chem. Soc.* **1985**, *107*, 6352.
- (10) Stevenson, W. H.; Scott, W.; Martin, J. C.; Farnham, W. B. *J. Am. Chem. Soc.* **1985**, *107*, 6340.
- (11) Taylor, S. L.; Lee, D. Y.; Martin, J. C. *J. Org. Chem.* **1983**, *48*, 4156.
- (12) Forbus, T. R., Jr.; Martin, J. C. *J. Am. Chem. Soc.* **1979**, *101*, 5057.
- (13) Chopra, S. K.; Martin, J. C., unpublished result.
- (14) TEXSAN-Texray Structure Analysis Package, Molecular Structure Corporation, 1985.
- (15) Beurkans, P. T. *Dirdif: Direct Methods for Difference Structure Factors*; Crystallography Laboratory: Toernooiveld, Nijmegen, Netherlands, 1984.
- (16) Least Squares

$$\text{Function Minimized: } \Sigma w(|F_o| - |F_c|)^2$$

$$w = 4 F_o^2/\sigma^2(F_o)^2$$

$$\sigma^2(F_o)^2 = [S^2 (C+R^2B)+pF_o^2]^2/L_p^2$$

$$S = \text{Scan Rate}$$

$$C = \text{Total Integrated Peak Count}$$

$$R = \text{Ratio of Scan Time to Background Counting Time}$$

$$B = \text{Total Background Count}$$

$$L_p = \text{Lorentz-Polarization}$$

- (17) Chopra, S. K.; Martin, J. C., unpublished result; ^{13}C NMR (CD_2Cl_2): δ C-10 in **5** 40.60 ($J = 126.6$ Hz), C-10 in **6** 55.46 ($J = 99.81$ Hz), and C-10 in **9** 63.66 ($J = 97.57$ Hz).
- (18) Berry, R. S. *J. Chem. Phys.* **1960**, *32*, 933.
- (19) Arduengo, A. J., III; Breker, J.; Davidson, F.; Kline, M. *Heteroat. Chem.* **1993**, *4*, 213.
- (20) Xie, Y.; Schaefer, H. F., III; Thrasher, J. S. *J. Mol. Struct. (Theochem)* **1991**, *234*, 247.
- (21) Ye, M.; Verkade, J. G. *Inorg. Chem.* **1993**, *32*, 2796 and references therein.
- (22) Davis, R. V.; Wintergrass, D. J.; Janakiraman, M. N.; Hyatt, E. M.; Jacobson, R. A.; Daniels, L. M.; Wroblewski, A.; Padmakumari Amma, J.; Das, S. K.; Verkade, J. G. *Inorg. Chem.* **1991**, *30*, 1330.
- (23) Das, S. K.; Amma, P. Kumari; Vaidyanathaswamy, R.; Weydert, J.; Verkade, J. G. *Phosphorus Sulfur* **1987**, *30*, 301.
- (24) Holmes, R. R. *Pentacoordinated Phosphorus*; ACS Monograph 175; American Chemical Society: Washington, DC, 1980.
- (25) Holmes, R. R. *Pentacoordinated Phosphorus*; ACS Monograph 176; American Chemical Society: Washington, DC, 1980.
- (26) Day, R. O.; Holmes, J. M.; Sau, A. C.; Holmes, R. R.; Deiters, J. A.; Devillers, J. R. *J. Am. Chem. Soc.* **1982**, *104*, 2127.
- (27) Day, R. O.; Holmes, R. R. *Inorg. Chem.* **1980**, *19*, 3609.
- (28) Clark, T. E.; Day, R. O.; Holmes, R. R. *Inorg. Chem.* **1979**, *18*, 1668.

- (29) Brown, R. K.; Day, R. O.; Husebye, S.; Holmes, R. R.; *Inorg. Chem.* **1978**, *17*, 3276.
- (30) Holmes, R. R.; Day, R. O.; Chandrasekhar, V.; Harland, J. J.; Holmes, J. M. *Inorg. Chem.* **1985**, *24*, 2016.
- (31) Schomburg, D. Z. *Naturforsch.* **1983**, *38B*, 938.

RECEIVED January 24, 1994

Chapter 11

Reaction of SiH_4 with UF_6 and/or HF below 25 °C

A Fourier Transform IR Study

Walter V. Cicha¹, John H. Wang, and Jane Covey

Crisla Technologies Research and Development, 225–15 Innovation
Boulevard, Saskatoon, Saskatchewan S7N 2X8, Canada

Reactions carried out between uranium hexafluoride (UF_6) and silane (SiH_4) with $0.13 \leq \text{UF}_6/\text{SiH}_4 \leq 5.2$ in the temperature range -196 to +25 °C commence in less than 30 minutes and reach completion in 2 to 5 days, depending on the exact reagent ratio. The progress of the reactions is monitored using FT-IR spectroscopy. The reaction between 2 mole equivalents of UF_6 and SiH_4 results in the final products SiH_2F_2 , SiHF_3 , SiF_4 , H_2 , and the solid “ $\text{U}_2\text{F}_9 \cdot 2$ ”. Hydrofluoric acid (HF) fluorinates SiH_4 completely to SiF_4 under very similar conditions and at a similar reaction rate, with the three partially fluorinated silanes forming only as detectable reaction intermediates. Results are presented that indicate UF_6 reacts with SiH_3F but not with SiH_2F_2 nor SiHF_3 , and the possible mechanisms involved in the UF_6 - SiH_4 and HF- SiH_4 systems are contrasted. Plausible equilibria describing the UF_6 - SiH_4 system are given, and evidence indicating the active role of surface catalysis is provided.

The chemical and physical properties of silane and many of its simple derivatives, such as the fluorosilanes ($\text{SiH}_{4-x}\text{F}_x$, with $x = 1-4$), have been studied extensively over the last decade as a result of their importance in the semiconductor industry (1). Ongoing interest in these molecules is indicated by the recent influx of reports dealing with theoretical and/or experimental studies of their fundamental properties (1a,2). Numerous vibrational spectroscopy studies of these compounds have been reported in the literature, both in the gaseous (2c,3) and condensed (matrix) states (3b,4) The

¹Current address: Central Research and Development, DuPont, Experimental Station, Wilmington, DE 19880–0262

controlled (stepwise) fluorination of SiH_4 is, accordingly, a topic of some importance. The reactions of F_2 and SiH_4 both in the gas phase and in an Ar matrix (with and without UV photolysis) have been reported (5) as has the matrix reaction between SiH_4 and HF (6). Whereas at ambient temperature no reaction was observed between SF_6 and SiH_4 in the gas phase, the reaction between WF_6 and SiH_4 was reported to yield SiHF_3 , SiF_4 and H_2 as the volatile species during a tungsten chemical vapor deposition (W-CVD) study done at 300 °C (7).

Interest in the physics and chemistry of UF_6 has been high for nearly fifty years owing to its critical role in the nuclear fuel cycle (8), which lends the system UF_6 - SiH_4 added significance. The initial study of this system was published in 1979 by Catalano and coworkers, who reported that no reaction between the two gases occurred below 130 °C, which they coined the "turn on" temperature (9). They investigated the thermal reaction in the range 25-157 °C, using IR spectroscopy as evidence to support their conclusions. However, their experimental IR data was not included in either paper. They reported that no reaction was initiated in 25 minutes even at 100 °C, while at the highest temperature studied the reaction went to 100% completion after 6 hours. The reaction was reported to be 5-90% complete in the temperature range 130-145 °C within 25 minutes. The primary focus of the 1979 paper (9a) was an investigation of the matrix infrared photochemical reaction between the two species in question. The conclusions reached were later refuted by an independent group of researchers (10); unfortunately, the latter study did not mention the thermal chemistry between the respective species.

A re-investigation of the thermal chemistry between SiH_4 and UF_6 in the temperature range -196 to +25 °C, employing diverse reaction conditions and two independent gas-handling systems, is presented here. FT-IR spectroscopy is employed as the primary analytical tool for gauging the progress of the reactions.

Experimental Methods

Chemicals. Natural UF_6 was provided by Cameco Corporation's Port Hope Conversion Facility in Ontario. The UF_6 gas (90-95% pure) was purified at -50 and 0 °C by evolving any volatile impurities (predominantly HF) under vacuum in three freeze-thaw cycles at each temperature. The purity of the gas following this treatment was determined to be in excess of 99% using FT-IR spectroscopy.

SiH_4 (99.999%) was purchased from Matheson and the gas was bled in directly out of the cylinder during preliminary experiments. It was purified (after prolonged storage) for follow-up experiments by removing any non-condensable volatiles in vacuo at -196 °C in three freeze-thaw cycles.

HF (99.9%) was purchased from Matheson and was used without further purification. ClF_3 (99%) was purchased from Air Products and was also employed without further purification. U.H.P. N_2 and U.H.P. He gas (both >99.999%) were purchased from Alphagaz Liquid Air.

Reactions. Multiple reactions were carried out between i) UF_6 and SiH_4 ; ii) UF_6 ,

SiH₄, SiH_{4-x}F_x (1 < x < 4), and HF; and iii) SiH₄ and HF. The experimental conditions employed are given in Table I. The UF₆/SiH₄(U/Si) ratios used in the study ranged from an 8-fold excess of SiH₄ to a greater than 5-fold excess of UF₆.

Apparatus and General Procedure. The majority of the experiments were carried out using a vacuum line constructed of Monel tubing (0.64, 0.97 and 1.27 cm O.D.), Monel Swagelok fittings, 316 stainless steel valves and Teflon-FEP reaction tubes (0.97 or 1.27 cm O.D., 15-20 cm long) - this line is referred to as "metal/Teflon" in Table I. ClF₃ was used to passivate (react with and thus remove any adsorbed impurities such as H₂O, while creating a fluorinated surface layer on the reactor walls) (11) the entire assembly at ambient temperature (50-300 torr - at least three cycles prior to each experiment) before the system was preconditioned with either UF₆ or HF, depending on which was to be used in the given reaction. The same passivating agent was used to treat the Monel gas handling system in the previously reported investigation of this system (9a). UF₆ and then SiH₄ or SiH₄ and then HF were condensed at -196 °C into a Teflon-FEP reaction tube and allowed to warm up to ambient temperature. The segment of the line used to transfer the UF₆ was heated to approximately 60 °C to accommodate more efficient movement of the dense gas. The volatile products (at ambient temperature) were collected on-line into a 316 stainless steel IR cell of 10 cm path length equipped with Viton O-rings and AgCl optical windows (25 x 4 mm). The cell was passivated and preconditioned in a fashion similar to the rest of the reaction manifold. The volatile intermediate products from each reaction were frozen back into the reactor while the final volatile products were removed in vacuo following the recording of their spectra. *Caution: SiH₄ and ClF₃ made a highly exothermic and sometimes explosive mixture in the presence of minute amounts of unidentified impurities and consequently should not be condensed together!* Manipulation of all solid products occurred in a dry N₂ box (< 0.1 ppm moisture).

An alternate reaction cell was constructed from Monel and 316 stainless steel. Optical windows of CaF₂ and KCl were incorporated into the reactor, which allowed direct mixing of the reagent gases at ambient temperature as well as the recording of FT-IR spectra in situ (the line labeled as "metal" in Table I). Viton O-rings, fluorocarbon grease and Teflon tape were used at the various connections to ensure vacuum-tight seals. The reaction cell was approximately 2 cm in diameter and 250 cm long. The reactant gases were mixed at the two entrance ports located at each end of the cell and an MKS baratron manometer located at the center of the cell monitored the total gas pressure. All data were collected and stored automatically using Paragon 500 software on a PC-based data acquisition system. The gas manifold used to carry the reagent gases to the cell was also constructed of Monel and 316 stainless steel, as were the two feed tanks used to premix each reagent gas with helium. The reagent/He mixture was introduced to the cell via a series of nozzles at both ends of the cell. Both the cell and the manifold were passivated with a minimum of 30 torr ClF₃ for no less than 30 minutes prior to each experiment.

FT-IR spectra of the gaseous products from the metal Teflon line were recorded on a Bruker IFS66 FT-IR spectrometer, operating with a spectral resolution

Table I. Summary of Initial Experimental Conditions Employed for Reactions between UF₆ and SiH₄

Reaction #	P(UF ₆) ^a Torr	P(UF ₆) ^b mmol	P(SiH ₄) Torr	SiH ₄ ^c mmol	HF mmol	U/Si molar ratio	Temperature (°C)	Gas Handling Apparatus
1a	<100	0.27	211	0.18	-	1.5	-196 to +20	metal/Teflon
1b	<100	0.34 ^d	211 ^d	0.18	-	1.9	-196 to +20	metal/Teflon
2	<100	0.4	342	0.30	-	1.4	-196 to +20	metal/Teflon
3	<100	1.8	756	0.75	-	2.4	-196 to +20	metal/Teflon
4	<100	1.3	260	0.26	-	5.2	-196 to +20	metal/Teflon
5	<100	1.4	269	0.27	-	5.0	-196 to +20	metal/Teflon
6	<100	1.2	3540	3.1	-	0.4	-196 to +22	metal/Teflon
6-HF	<100	1.2 ^d	3540 ^d	3.1	2.3	0.4	-196 to +22	metal/Teflon
7	<100	0.32	2200	0.60	-	0.5	-196 to +20	metal/Teflon
8	<100	0.51	1740	1.01	-	0.5	-196 to +20	metal/Teflon
9a ^e	1	N.A.	8	N.A.	-	0.13	+25	metal
9b ^e	1	N.A.	8	N.A.	-	0.13	+25	metal

a Initial amount of UF₆ exceeds maximum pressure at ambient temperature (<100 Torr) - molar fraction of UF₆ consequently condensed.

b Based on mass.

c Based on ideal behavior of gas.

d Not corrected for reagent consumed during first stage of reaction.

e 7 Torr of He carrier gas was also employed.

of 2 cm⁻¹. PC-run OPUS software (versions 1.2 and 1.3) was employed to collect and store the spectral data. Spectra of the gases mixed in the all-metal line were recorded using an Analect FX-65 FT-IR spectrometer operating with a spectral resolution of 4 cm⁻¹. All FT-IR spectra were recorded at ambient temperature.

The Mikroanalytisches Laboratorium of Beller in Göttingen, Germany was employed for the microanalysis of the solid products isolated.

Vapor Phase FT-IR Studies

The System UF₆-SiH₄. Of the eleven distinct reactions that were carried out between UF₆ and SiH₄ (experimental data listed earlier in Table I), the FT-IR spectra of three will be discussed here in detail, namely reactions 1a, 1b and 4, as these are the most telling examples of the system's behavior. The IR spectrum of the more volatile starting material, SiH₄, is well-known and its reported band positions are given in Table II, along with those of the other four possible species of the type SiH_{4-x}F_x. In addition, the FT-IR spectrum of SiH₄ handled in our previously passivated (with ClF₃) apparatus was recorded, and is shown in Figure 1. The band positions are in good agreement with the literature.

The spectral views of the volatile species from reaction 1a given in Figure 2 indicate that a reaction has occurred, as distinct bands due to species other than SiH₄ are present. Si-H stretching vibrations are expected in the spectral region shown at the right while the left region is host to Si-H bending modes, Si-F stretching and bending modes as well as any U-F stretching modes (3a). Recorded 35 minutes after allowing the reaction mixture to warm up to ambient temperature, spectrum A in Figure 2 shows weak albeit distinct signs of bands due to SiF₄ (~1030 cm⁻¹), SiHF₃ (2316, 990-1005 cm⁻¹), SiH₂F₂ (2250, 980-990, ~730 cm⁻¹) and perhaps SiH₃F (~990, ~730 cm⁻¹ - additional bands at ~2205 and ~950-960 cm⁻¹ should however also be present for this species). The starting materials SiH₄ (bandcenters at ~2180-2190 and 900-940 cm⁻¹) and UF₆ (ν₃ fundamental at ~630 cm⁻¹) (3a) are also present, indicating an incomplete reaction. Due to band overlap and large variance among absorption coefficients, it is difficult to unambiguously assign the presence of SiH₃F when both SiH₂F₂ and SiH₄ are also present. Furthermore, it is not possible to assign all of the fundamental bands (in the studied spectral range) for any of the product species except SiF₄, nor is the relative abundance of each species apparent. However, the band complexity in the ~870-1030 cm⁻¹ region suggests that at least three of the fluorosilanes are present. After 20 hours at ambient temperature (spectrum B), the intensity of the SiH₄ bands markedly decreased while that of the SiHF₃, SiF₄ and especially SiH₂F₂ bands increased significantly. The distinct new band at 2205 cm⁻¹ and the very high intensity of the bands in the region ~2200-2260 cm⁻¹ suggest that the presence of SiH₃F is more likely here than in spectrum A. After 5 days at ambient temperature (spectrum C), the same trend is seen to continue (with the exception that SiH₃F is again not very apparent), but the UF₆ is now fully exhausted while a small amount of SiH₄ still remains. This suggested that a UF₆/SiH₄

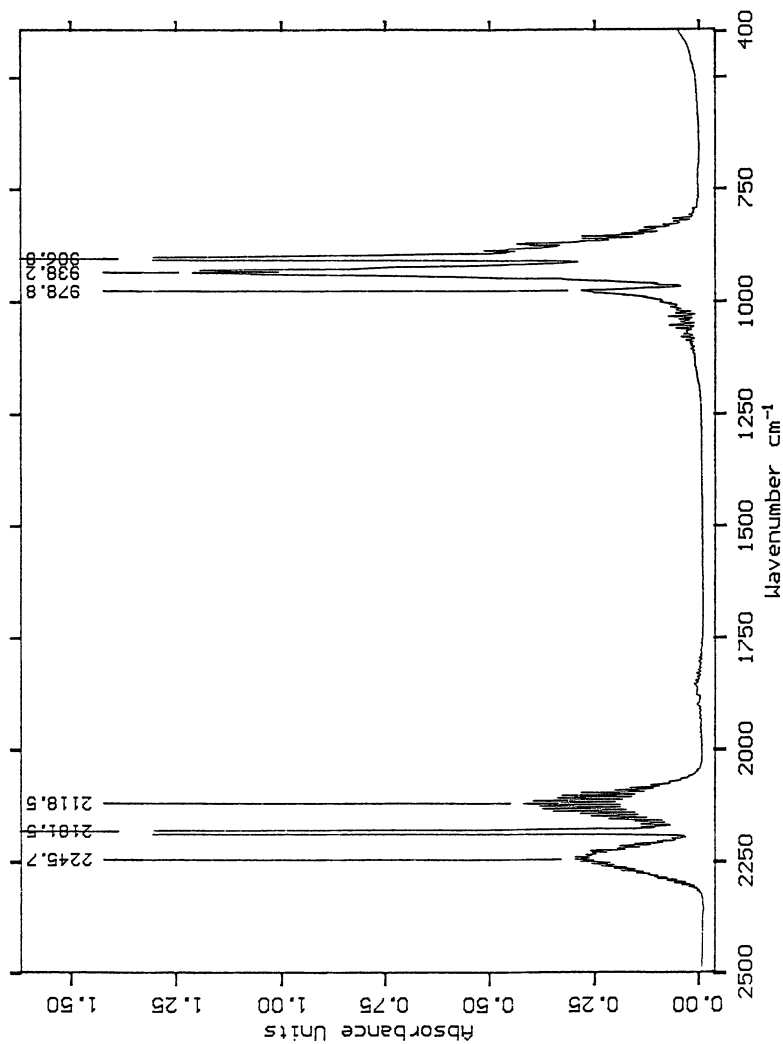


Figure 1. FT-IR spectrum of SiH₄ (from 2500 to 400 cm⁻¹, 38 torr).

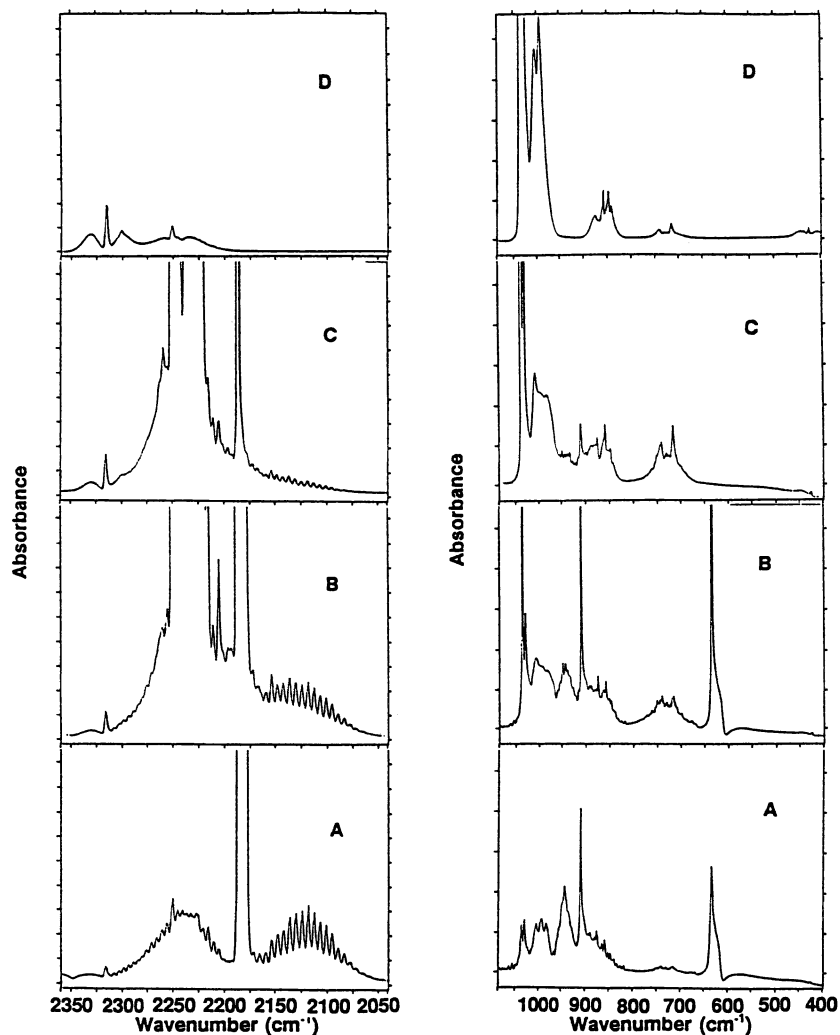


Figure 2. FT-IR spectral views of the vapor phase products from the UF_6 - SiH_4 reactions 1a and 1b (from 2360 to 2041 and from 1085 to 400 cm^{-1}). Spectra 2A-2C were recorded during reaction 1a; 2A: 0.55 hours, 57 torr; 2B: 20 hours, 56 torr; 2C: 120 hours, 41 torr. Spectrum 2D was recorded during reaction 1b, 24 hours following the second addition of UF_6 (see text), 16 torr.

ratio of more than 1.5 was needed to fully consume both reagents, i.e., this was not the required "redox equivalence" ratio.

Spectrum D in Figure 2 confirmed the above hypothesis. It was recorded 24 hours following the introduction of an additional 0.4 mole equivalents of UF_6 to the reaction 1a product, making the overall reaction 1b stoichiometry 1.9:1 (or approximately 2:1) in favor of UF_6 . It is evident from the spectrum that all of the SiH_4 has now been consumed while no UF_6 remains, indicating that an approximate 2:1 stoichiometry best describes the completed reaction. This was supported by reactions 2 (UF_6 consumed while some SiH_4 remained) and 3 (SiH_4 consumed while some unreacted UF_6 remained), having respective U/Si ratios of 1.4 and 2.4. The compounds SiF_4 , SiHF_3 , SiH_2F_2 and a tiny amount of HF (a very weak, rotationally revolved signal centered at $\sim 3950\text{ cm}^{-1}$, a region not shown here) (3a) are unequivocally the only species present in spectrum D. HF was absent from spectrum C but interestingly was present in comparably small amounts in spectra A and B, suggesting its reaction with the $\text{SiH}_{4-x}\text{F}_x$ species. The absence of UF_6 in the presence of some HF in spectrum D suggests that the reaction of SiH_4 with UF_6 may actually be a little bit faster than with HF. The role of HF in the system will be discussed in more detail later. The relative simplicity of the bandform in the $950\text{--}1005\text{ cm}^{-1}$ region here compared to that in spectra A - C supports the presence of SiH_3F among the reaction 1a products. Furthermore, the absence of the third band in this region at $\sim 980\text{ cm}^{-1}$ (observed in spectra A - C) suggests that this band corresponds to SiH_3F , which implies that due to band overlap and variance in absorption coefficients, the *apparent* frequencies in this spectral region for the mixture of two or all three partially fluorinated silanes ($\text{SiHF}_3 + \text{SiH}_2\text{F}_2$: ~ 1004 and 992 cm^{-1} ; $\text{SiHF}_3 + \text{SiH}_2\text{F}_2 + \text{SiH}_3\text{F}$: ~ 1004 , 992 , and 980 cm^{-1}) are slightly different than reported in the literature (see Table II) for the individual species. In summary, the overall effect of adding more UF_6 to the product of reaction 1a was to produce a greater amount of SiF_4 and SiHF_3 at the expense of most of the SiH_2F_2 and all of the SiH_3F and SiH_4 .

Reactions 4 and 5 were carried out to determine whether an excess of UF_6 would yield SiF_4 as the sole fluorosilane product. The spectra of the volatile products from reaction 4 are shown in Figure 3. Here (as in reaction 5) it is evident that the effect of excess UF_6 is quite insignificant, as the final products from the reaction (after 2 days, at which point all of the SiH_4 was consumed) seen in spectrum C are again SiF_4 , SiHF_3 and SiH_2F_2 , as well as unreacted UF_6 and a significant amount of HF, the latter's relative abundance increasing with time. This further suggested that the rate of reaction of SiH_4 with UF_6 was comparable to its reaction rate with the HF being produced, although some of the resulting HF may have been due to a very slow but gradual leakage of moist air into the previously leak-tested IR cell, resulting in the production of minute amounts of HF and UO_2F_2 from the reaction of H_2O with the excess UF_6 (12). A very weak, broad band at $\sim 940\text{ cm}^{-1}$ (the region of the $\text{O}=\text{U}=\text{O}$ stretching band) (3a, 13) in the spectra of the empty IR cell after a series of experiments did in fact indicate the deposition of a thin film of

Table II. Compilation of Previously Reported Fundamental IR Vibrational Frequencies (cm^{-1}) for SiH_4-xF_x ($0 \leq x \leq 4$)

SiH_4 (T_d) ^{a,b,c}	SiH_3F (C_{3v}) ^{a,b,d}	SiH_2F_2 (C_{2v}) ^{a,d}	SiHF_3 (C_{3v}) ^{a,b,d}	SiF_4 (T_d) ^{a,b,d}
2183-2192 (417)	2206, 2209 (35)	2250 (159)	2315-2321 (71)	
	2206, 2196 (340)	2246 (61)		1030-1032 (828)
	991 (213)	982 (142)	998-999 (612)	
	943-956, 961 (224)	981 (339)		
910-913 (534)	872, 875 (104)	903 (14)	856-859 (101)	
	729 (140)	870 (100)	844-846 (48)	
		730 (164)	425 (86)	
		322 (22)	306-307 (30)	389 (176)

a Ref. 2c.

b Ref. 3.

c The relative intensities given in brackets were experimentally determined (Ref. 2c).

d The relative intensities given in brackets were predicted from theory (Ref. 2c).

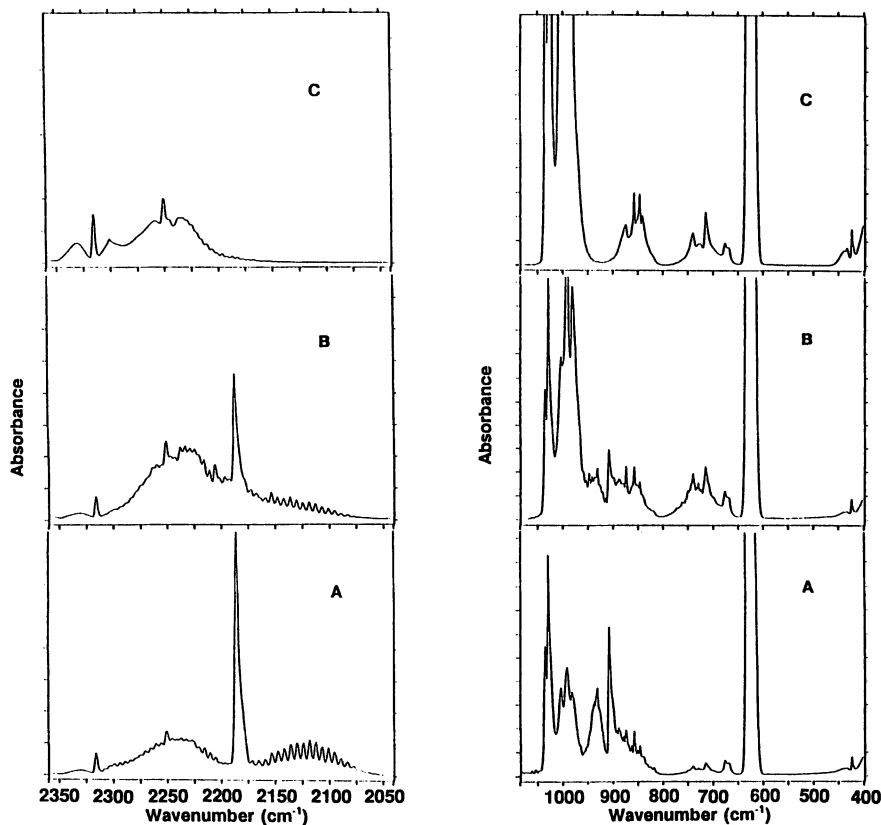


Figure 3. FT-IR spectral views of the vapor phase products from the $\text{UF}_6\text{-SiH}_4$ reaction 4 (from 2360 to 2041 and from 1085 to 400 cm^{-1}). 3A: 1.5 hours, 53 torr; 3B: 27 hours, 55 torr; 3C: 51 hours, 58 torr.

UO₂F₂ on the AgCl optical windows. Surprisingly, it appeared that the relative abundance of SiH₂F₂ here compared to that in the reaction 1b product was slightly greater than that of SiHF₃, while they were both relatively greater than that of SiF₄. This suggested that perhaps kinetics, more than the exact reagent ratio, dictates the fluorosilane product distribution. Furthermore, the relatively lesser amounts of the more fluorinated silanes (SiHF₃ and especially SiF₄) in the presence of excess of UF₆ here compared to the reaction 1 system (where the UF₆ was totally consumed) implies that a reaction between the intermediate product HF and the partially fluorinated silanes may be responsible for the majority of the SiF₄ formed, while the fluorosilanes themselves are a result of the reaction between UF₆ and SiH₄. This will be expanded upon later.

As complements to reactions 4 and 5, reactions 6, 7 and 8 involved an excess of SiH₄ (see Table I). In addition to unreacted SiH₄, SiHF₃, SiH₂F₂, debatably SiH₃F and a relatively smaller amount of SiF₄ were present in each case after ~ 2 days. Allowing the fluorosilane reaction mixture to sit 4 additional days at ambient temperature resulted in a noticeable decrease in the abundance of SiH₂F₂ and questionably SiH₃F. The level of SiH₄ also marginally decreased. The increased intensity of the bands due to SiHF₃ (at 2316 cm⁻¹ and less so 425 cm⁻¹) was the most significant change, especially in the absence of any change in the amount of SiF₄ present. As there was no sign of UF₆ in the reactor after 2 days in any of these reactions with excess SiH₄, a fluorine source other than UF₆ or HF (latter also absent) was likely responsible for the slight but nevertheless significant change in the product composition witnessed after the additional 4 days. A reaction with the fluorinated surface of the FEP-Teflon reactor and/or stainless steel IR cell is one explanation for the observed behavior and this aspect of the system's chemistry will be briefly discussed later. Alternatively, rearrangement equilibria between the assorted fluorosilanes would also result in the observed effect, but this is less likely. The absence of HF from any of the spectra in these three reactions is consistent with the low U/Si ratio used. Together with the trends seen in the previously discussed spectra, these observations support the existence of nontrivial, statistically and kinetically controlled equilibria between the respective species in this system.

A non-condensable (at -196 °C) gas was formed in varying amounts in reactions 1-8, and its cumulative amount in reaction 6 was measured to correspond to approximately 1 mole equivalent of the SiH₄ that had reacted, taking into account that the reagents are consumed according to an approximate stoichiometry of 2UF₆:SiH₄ (see above). However, owing to the ~ 5 atmospheres of initial gas pressure in the Teflon-FEP reactor used in this reaction, it is possible that some of the non-condensable gas diffused out of the reactor over the 6 days at ambient temperature, which was in fact suggested by the reduced pressure of the SiH_{4-x}F_x species that remained. Thus, the measured amount of non-condensable gas produced per mole SiH₄ used is a minimum estimate. The only reasonable candidate for this species is H₂ (bp: -253 °C), whose presence is consistent with the active role of HF in this system. H₂ has been reported previously as one of the products in the high temperature reaction of WF₆ with SiH₄ (7). In light of the redox equivalence ratio of

$\sim 2\text{UF}_6:\text{SiH}_4$ that was determined, the presence of <2 mole equivalents of H_2 (based on SiH_4) in the final product agrees with the presence of partially fluorinated silanes (2 mole equivalents of H_2 would be expected if the SiH_4 was fully converted to SiF_4). It is of considerable interest that the previous report (9) of this reaction occurring above $130\text{ }^\circ\text{C}$ did not mention H_2 as a final product - HF together with the entire fluorosilane series $\text{SiH}_{4-x}\text{F}_x$ ($x = 1-4$) were unequivocally identified as the vapor phase products of the completed reaction while only SiH_3F and HF were said to result from any reactions that did not go to completion. It is consequently noteworthy that SiH_3F was not present among the vapor phase products in any of the reactions 1-8 carried out here that went to completion. Furthermore, it is possible that any H_2 which may have formed as an intermediate in the previously reported high temperature reaction (9) went on to react with any unconsumed UF_6 . However, it should be noted that there is some uncertainty in the literature regarding the exact temperature at which UF_6 and H_2 commence reacting, with the majority of studies reporting this temperature at or above $225\text{ }^\circ\text{C}$ (13b,13c).

To this point, the discussion has focused on experiments undertaken in Teflon-FEP reactors used in conjunction with a metal gas-handling system (reactions 1-8), referred to as experiment series A from now on. To verify the observed results, two additional experiments (reactions 9a and 9b) were run on a significantly different and completely independent gas handling system, as described earlier in the Experimental Section. A few key differences were present between these experiments and those discussed earlier: i) the gases were allowed to mix directly at $25\text{ }^\circ\text{C}$, as opposed to first condensing them at $-196\text{ }^\circ\text{C}$ and then allowing them to warm, a situation which resulted in both reagents initially co-existing in the solid phase - some solid UF_6 initially remained even at ambient temperature in the latter case (owing to its relatively low vapor pressure of < 100 torr); ii) a significantly lower total reagent gas pressure of 9 torr was employed, and iii) the design of the reactor combined with the low pressure led to a much greater surface area/gas pressure ratio here. In preparation for reaction 9a, the reactor was thoroughly preconditioned with UF_6 after it was passivated with ClF_3 . This required passing UF_6 through the system until it no longer adsorbed to the reactor walls, as indicated by the intensity of its ν_3 fundamental band at $\sim 625\text{-}630\text{ cm}^{-1}$ and a constant pressure remaining in the reaction chamber for at least 30 minutes. A fresh batch of UF_6 and SiH_4 were then introduced simultaneously. Judging from the decrease in intensity of the ν_3 UF_6 band and the formation of weak bands at $\sim 990\text{ cm}^{-1}$ due to one or more of the $\text{SiH}_{4-x}\text{F}_x$ species ($x = 1-3$), a reaction commenced in less than 10 minutes. After a total of 15 minutes, all of the UF_6 was consumed. A significant decrease in the SiH_4 intensity was not noticeable owing to the small U/Si ratio employed (0.13), nor was there any sign of SiF_4 in the spectrum. However, there is little doubt that a reaction had occurred, with its relative rapidity being at least in part a result of the low gas pressures utilized.

Before reaction 9b was carried out, the reactor was thoroughly preconditioned with ClF_3 . When SiH_4 was added, a reaction took place between it and the fluorinated reactor walls, as indicated by the appearance of a weak band due to SiF_4 at

1030 cm⁻¹ after less than five minutes. Evidence for such a wall reaction was not seen earlier in the spectrum of SiH₄ (see Figure 1) that was recorded prior to carrying out experiment series A. Multiple batches of SiH₄ were then introduced into the reactor, until the intensity of the SiF₄ band remained constant for more than half an hour, indicating no further surface reaction. UF₆ and SiH₄ were then introduced into the evacuated cell simultaneously (as in reaction 9a). Within 25 minutes, the intensity of the SiF₄ band in the spectrum was noticeably increased, while very weak bands due to SiH₂F₂ and/or SiH₃F also formed. The intensity of the UF₆ band had also decreased accordingly, again indicating that UF₆ and SiH₄ do undergo reaction with each other at these conditions (regardless of the exact apparatus or its preconditioning treatment), supporting the results obtained in experiment series A.

Reactions on Reactor Walls. Following the study of reactions 9a and 9b, it became apparent that the fluorinated surfaces of the reactors' walls may play some role in the mechanism of the chemical reactions between SiH₄ and UF₆. Three experiments were carried out to shed more light on the nature of the suspected surface effect: i) an FT-IR spectrum of SiD₄ handled in a non-fluorinated system was recorded and then compared to its spectrum recorded in the same fluorinated system as used for experiment series A - SiD₄ was employed to eliminate band overlap of the broad Si-H bending mode (centered at ~ 915 cm⁻¹) of SiH₄ with the very weak bands due to a minute amount of fluorosilanes, which may have prevented their observation in Figure 1; ii) an IR cell (and gas handling system) preconditioned with ClF₃ and then UF₆ was exposed to SiH₄ to further test for the latter's potential reaction with UF₆ on the cell walls, and iii) an IR cell (and gas handling system) preconditioned with SiH₄ was exposed to UF₆ to test for a possible competing reaction of the latter with the silanated surface.

Figure 4 compares the spectral view of SiD₄ obtained in an unfluorinated system (A) to that recorded in one previously fluorinated with ClF₃ (B). The region shown is host to Si-F stretching modes and/or Si-H bending modes. The former spectrum was recorded within ten minutes of charging the prefluorinated IR cell with the SiD₄, and shows extremely weak bands due to SiF₄ and one or more of the species SiD_{4-x}F_x (the absorbance of the SiD₄ fundamental bands at the pressure employed is well in excess of the 7 absorbance unit cut-off) - no sign of these bands is present in the unfluorinated cell's spectrum A. The intensity of the fluorosilane bands remained unchanged over the next two hours, probably due to the relatively small surface area/gas pressure ratio present in the cell. In any case, the degree of reaction that SiD₄ underwent with the fluorinated walls of the IR cell and/or gas handling system was negligible in this instance.

The second experiment consisted of first passivating the IR cell with two batches of ~ 50 torr ClF₃ (15 minutes each) and then conditioning it with two more batches of an approximately equivalent pressure of UF₆ (20 minutes each). 15 torr of SiH₄ was then introduced into the evacuated cell and allowed to reside there for 70 minutes, during which time FT-IR spectra were recorded at regular intervals. After 17 minutes, all four possible fluorosilanes were present in the IR cell (apparent relative

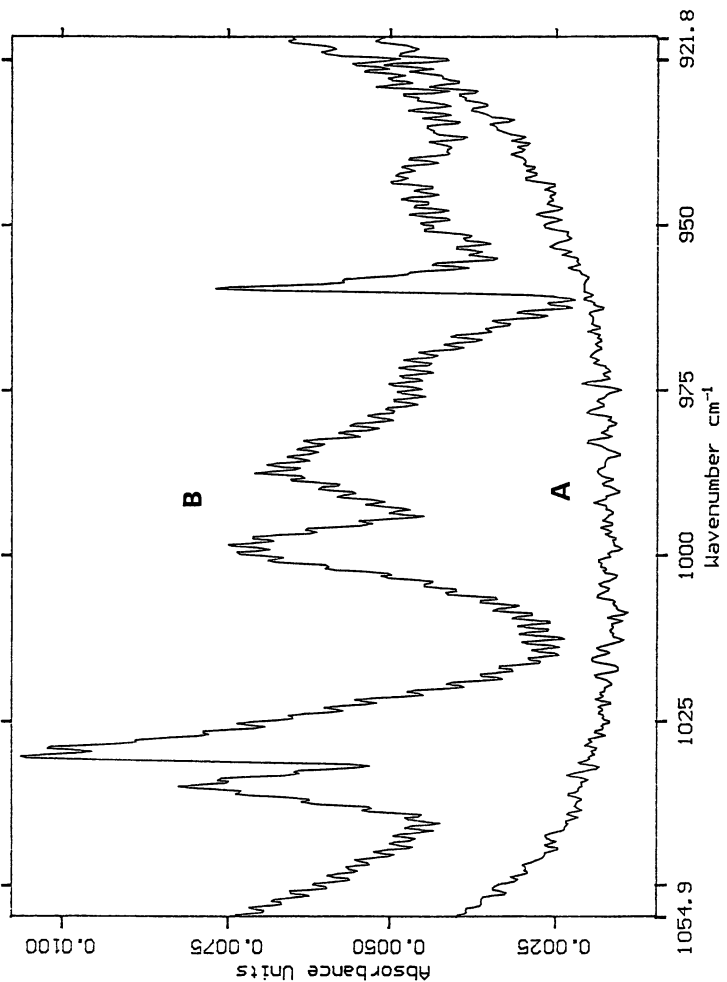


Figure 4. FT-IR spectra of SiD₄ recorded in a fluorinated and in an unfluorinated system (from 1055 to 922 cm⁻¹). 6A: unfluorinated, 66 torr; 6B: fluorinated 77 torr.

abundance $\text{SiH}_3\text{F} > \text{SiH}_2\text{F}_2 > \text{SiHF}_3 > \text{SiF}_4$), in addition to a much greater amount of SiH_4 and a very minute amount of HF. Over the next 53 minutes, the bands all appeared to increase in intensity proportionally to their relative abundance after 17 minutes, i.e., the absolute difference in abundance between the species was much greater after 70 than after 17 minutes. This suggested that the distribution of the fluorosilanes was statistically and kinetically governed in agreement with observations made in previous sections. The relative abundance of the fluorosilanes also implied that UF_6 and perhaps weaker oxidizers of the type UF_{6-x} , $x < 2$ (13a) were indeed the adsorbed species which reacted with the SiH_4 , based on the similar IR band distribution seen for the vapor phase products of reaction 4 (excess SiH_4 also present). A very small amount of HF was also present, and the intensity of its band pattern was seen to slightly increase with time. This further suggested that UF_6 , rather than HF, prefers to react with SiH_4 . The IR data are also consistent with the earlier hypothesis that HF rather than UF_6 converts the partially fluorinated silanes to SiF_4 . It would consequently appear that the rate of HF production in this totally surface catalyzed reaction is greater than its rate of consumption, as would be expected. It should be noted that the wall surface involved in this experiment consisted of stainless steel and AgCl, whereas Teflon-FEP was the primary surface material involved in experiment series A.

The last experiment designed to study the role of the reactor/IR cell walls in the system involved preconditioning the IR cell with SiH_4 , evacuating it in vacuo for 30 minutes, and then introducing 20 torr of UF_6 into it. An IR spectrum of the gas was recorded after 10 minutes and is shown in Figure 5. In addition, to an intense UF_6 band at 626 cm^{-1} , bands due to SiF_4 , SiHF_3 and SiH_2F_2 are also present, indicating a reaction of UF_6 with surface-adsorbed SiH_4 . In fact, the spectrum is very similar to spectrum D in Figure 2, except for the presence of UF_6 and a relatively smaller amount (surprisingly) of SiF_4 found in the present spectrum. No significant change in the spectrum was observed after three additional hours. A small amount of HF (slightly greater than in spectrum D, Figure 2) was also present in the spectrum, which became increasing noticeably over the three hours. As excess UF_6 was present, minor leaks in the IR cell may have contributed to the abundance of HF, as discussed earlier. Its prime source would however be expected to be the reaction of UF_6 with the adsorbed SiH_4 , which again implies that this reaction is preferred to the reaction of HF with the latter species. Furthermore, it is interesting to note that even the presence of an obviously large excess of UF_6 does not entirely fluorinate the fluorosilanes SiH_2F_2 and SiHF_3 to SiF_4 , which is consistent with the outcome of the earlier discussed reactions 4 and 5, and further suggests that it is HF and not UF_6 that is directly responsible for the formation of SiF_4 in this system.

Based on the above observations, it is very difficult to conclude which (if either) of the two distinct surface catalysis pathways is dominant in the bulk reaction between SiH_4 and UF_6 ; there is however little doubt that the walls of both gas handling systems employed in this study contributed to catalyze the observed reactions. The degree to which their progress was affected by this "surface effect" as well as the mechanisms involved are currently poorly understood and are the subject of continuing focused study in our laboratory.

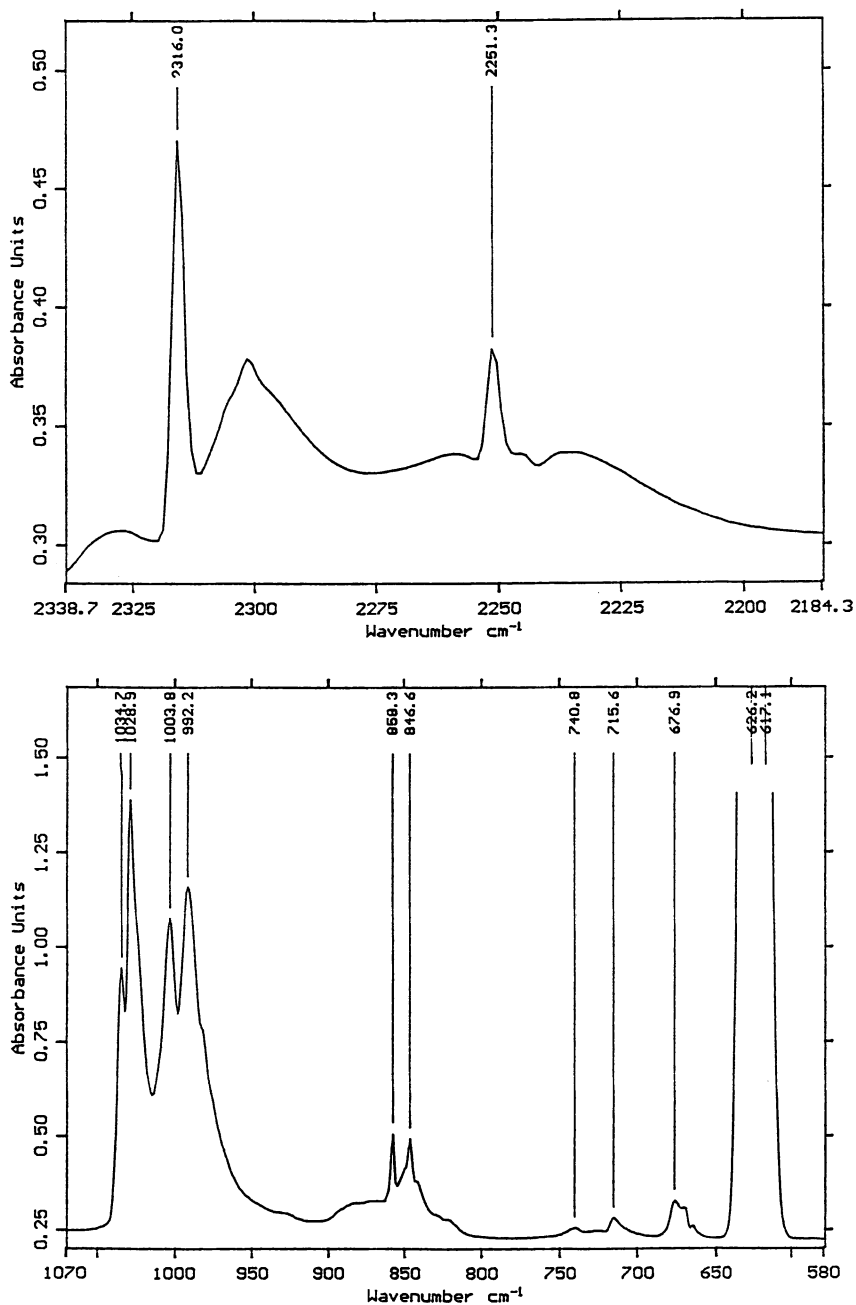


Figure 5. FT-IR spectral views of UF₆ (20 torr) recorded in an IR cell that was previously conditioned with SiH₄ (from 2339 to 2184 and from 1070 to 580 cm⁻¹).

The System UF₆-SiH₄-HF. In reactions 1-8, the initial UF₆:SiH₄ ratio used appeared to dictate whether HF was present among the vapor phase products. A ratio in excess of ~ 2:1 (redox equivalence ratio) led to the presence of HF among the final products, while a lower ratio resulted in the presence of HF only during the initial stages of the reaction, with it being fully consumed when the UF₆ was used up. The formation of H₂ was also observed in all of the reactions undertaken, implying the active role of HF as an intermediate reagent. Since the expected reaction of UF₆ with trace amounts of moisture in the system could also lead to the formation of HF (see section above), the exact role of HF in this system could not yet be ascertained. Consequently, HF was added in 4 stages to the product of reaction 6, after the reaction had reached completion (6 days at room temperature). The resulting reaction will be referred to as 6-HF in the ensuing discussion, as it is in Table I.

The addition of 1 mole equivalent of HF (in four nearly equivalent portions) (14) during experiment 6-HF led to the production of ≥ 0.7 mole equivalents of H₂. This is not inconsistent with the relative abundance of the final vapor phase species in the system being SiH₄ > SiF₄ > SiHF₃ ~ SiH₂F₂, as estimated from FT-IR spectra recorded after the HF had completely reacted. The seeming tendency of HF to react with SiH_{4-x}F_x preferentially over SiH₄ (at least in the presence of uranium fluorides, the solid portion of the reaction 6 product), thus resulting in the predominant formation of SiF₄ in experiment 6-HF, is consistent with many of the observations already made during the previous sections. Further detailed discussion of the role of HF will be given in the next section.

A weak but distinctly shaped bandform centered at ~ 2900 cm⁻¹ (due to the formation of HCl) (15) was seen in many of the spectra recorded during experiment 6-HF as well as during the other experiments involving only SiH₄ and UF₆. There are three possible sources of HCl in this system: i) from the reaction of the IR cell's AgCl optical windows with an aggressive hydrogen source; ii) as an impurity in one or more of the reagents employed, and iii) from the reaction of a hydrogen source with any Cl adsorbed to the reactor walls during previous passivation of the system with ClF₃. IR spectra recorded of HF (various pressures) also showed significant amounts of HCl and the amount of the impurity slowly increased with the time that the HF spent in the IR cell. This suggested that HF was undergoing some reaction with the cell walls to produce the HCl. AgCl is known to be unaffected by HF under mild conditions (16), and thus a combination of the possible HCl sources ii) and iii) stated above are most likely in this case. A yellowish film was noticed to form on the AgCl windows after repeated experimental runs. UO₂F₂, which is light yellow in color (13a), is a likely component of this by-product as its bands were identified in the spectra of the empty IR cell recorded after multiple experiments (discussed in earlier section). HCl may also have been initially present as an impurity with HF in the lecture bottle. Moreover, detectable traces of HCl were present in product gas mixtures that did not contain HF. It has been reported (7) that the reaction between SiH₄ and powdered AgCl at 22 °C will go to 5% completion with the formation of primarily HCl and SiH₃Cl, suggesting that SiH₄ may also have undergone a very

minor side reaction with the AgCl optical windows here. The other expected by-product species would most likely be unstable in the highly fluorinating environment employed. However, exposure of SiD₄ to both a passivated and a clean system (including AgCl optical windows) failed to show any distinct sign of DCl in the expected IR region (3*a*), suggesting that the reaction of SiH(D)₄ with any Cl source must be a very minor contributor of H(D)Cl. In any case, H(D)Cl would be expected to be a relatively inert species in these systems.

The System SiH₄-HF. HF was added to SiH₄ using the same techniques and apparatus employed during reactions 1-8. It was introduced in three stages, with the products again monitored by PVT measurements and FT-IR spectroscopy. The amount of reagent gases used and non-condensable gas (H₂) produced at each stage and in total are summarized in Table III. Figure 6 shows spectral views of the product from the reaction 51 minutes following the first addition of HF (spectrum A) as well as 4 days later (spectrum B). In addition to unreacted HF and SiH₄, bands due to SiF₄, SiH₂F₂ and probably SiH₃F are present in spectrum A. An extremely weak band due to SiHF₃ is also seen at 2315 cm⁻¹. The very weak band pattern in the range 3000-2750 cm⁻¹ is again due to HCl while the slightly stronger band pattern at ~ 3100 cm⁻¹ is a silane combination band. From the intensity of the HF band, it was estimated that approximately 60-65% of the HF was consumed at this point. There is no sign of HF in spectrum B. There is a very slight increase in the abundance of SiH₂F₂, SiF₄ and perhaps SiH₃F, but the increase in the quantity of SiHF₃ is much more dramatic. Only bands due to SiH₄ decrease in intensity, in contrast with the previous section's observation that HF appears to react preferably with SiH_{4-x}F_x species rather than with SiH₄. The near absence of SiHF₃ and the presence of SiF₄ in spectrum A combined with the presence of both species in spectrum B indicate that the conversion rate of SiHF₃ to SiF₄ in the presence of HF is the fastest step among the system's equilibria; this is consistent with the earlier hypothesis that solely HF is directly responsible for the production of SiF₄ in the UF₆-SiH₄ system. From Table III it is apparent that the amount of H₂ produced was approximately equivalent to the initial amount of each reagent, in agreement with the spectral data.

The addition of a second equivalent batch of HF to the reactor, now containing silane as well as the assorted fluorosilanes, led to the consumption of more SiH₄, all of the SiHF₃ and most of the other two fluorosilanes. The resulting species was SiF₄, which is more or less consistent with trends discussed earlier. However, after an additional 2 days of reaction, all of the intermediate fluorosilanes were formed again, albeit in significantly smaller quantities than were present after the first addition - the SiF₄ band intensity remained unchanged. The HF was completely consumed as well at this point and more SiH₄ was understandably used up. Based on the amount of H₂ produced in this process, it can be estimated that between 15 and 25% of the SiH₄ was consumed after the first addition of HF, which, according to the initial HF/SiH₄ ratio used, is approximately equal to the amount that should have been consumed during experiment 6-HF in the previous section. The latter amount however was somewhat smaller (as was the H₂ quantity produced), suggesting that presence of the

Table III. Summary of Data from Study of the System SiH_4 -HF (-196 to +20 °C) ^a

	HF Addition #1	HF Addition #2	HF Addition #3	Totals
Reaction duration	4 days	3 days	4 days	11 days
SiH_4 (mmol)	0.20	see text	see text	0.20
HF added (mmol)	0.21	0.21	0.44	0.86
H_2 produced (mmol)	0.18	0.15	0.15	0.48
HF/ SiH_4 ^b	1.00	1.00	2.20	4.20
H_2 / SiH_4 ^b	0.90	0.75	0.75	2.40

^a Vapors are treated as ideal gases.^b Initial amount of SiH_4 .

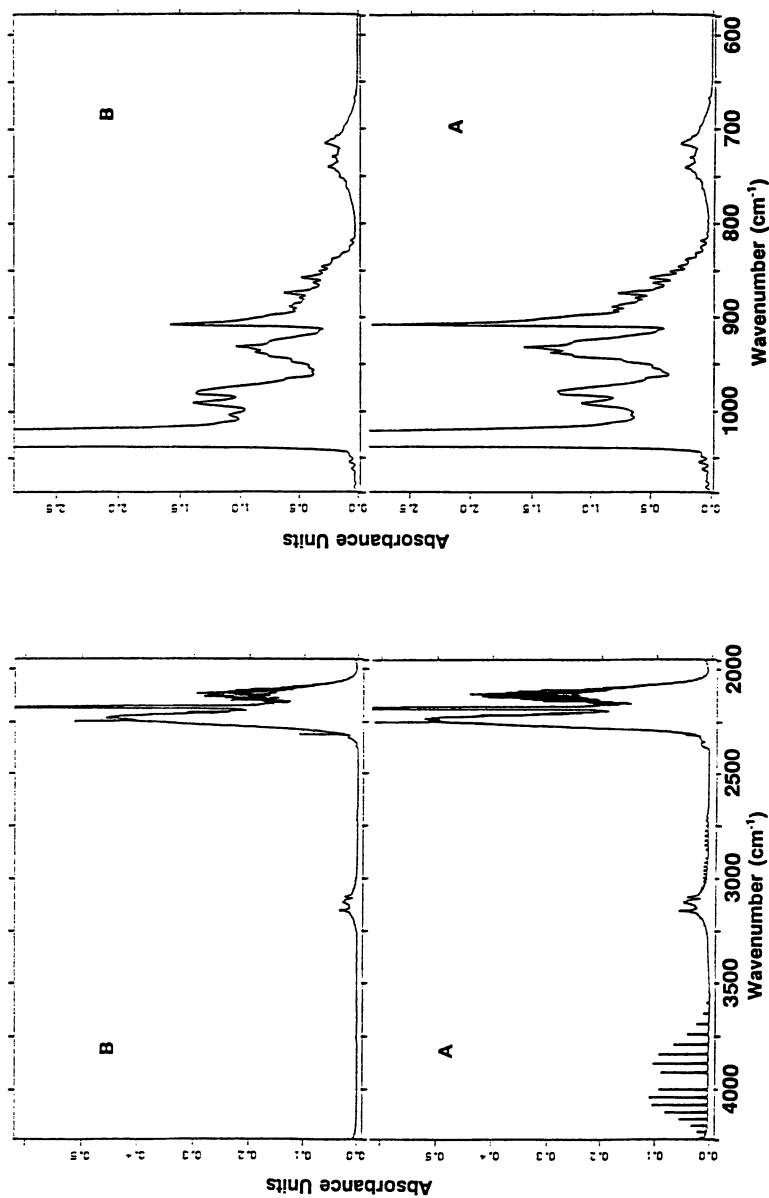


Figure 6. FT-IR spectral views of the system HF-SiH₄ (from 4241 to 1960 and from 1087 to 580 cm⁻¹). 6A: 51 minutes, 70 torr; 6B: 4 days, 38 torr.

solid uranium fluoride product may have somehow perturbed the reactivity of the HF added. This is supported by the slightly different progress of the sequential fluorination within the two contrasting silane/fluorosilane mixtures, and may also help explain why HF was present as a product in reactions 4 and 5 (excess UF₆) ~ 2 days following their commencement. The latter effect may alternatively be explained by the tendency of HF to adhere to UF₆ (18), thus impeding the former's reactivity with the intermediate product species SiH_{4-x}F_x. However, the pressure data must be treated with caution due to the previously mentioned possibility of gas diffusing out through the Teflon-FEP walls (although the total cell pressure during the HF-SiH₄ reactions did not exceed 1000 torr).

Figure 7 shows the spectrum recorded 1 day after the third and final batch of HF was added to the silane/fluorosilane mixture. SiH₄ and all of the intermediate fluorosilanes are now consumed, with the predominant band at ~ 1030 cm⁻¹ being due to SiF₄. The large amount of SiF₄ present results in at least four overtone/combination bands, at ~ 2050, 1830, 1290, and 1190 cm⁻¹. The bands at approximately 2350 and 670 cm⁻¹ are due to external CO₂ (3a) in the IR sampling chamber while the identities of the weak bands at ~900 and 780 cm⁻¹ are still unknown. A very noticeable amount of unreacted HF is also present, and the overall reaction between SiH₄ and HF is best described by the expected pathway:



The slight overall excess of HF used (~5%) is in reasonable agreement with the 15% excess indicated by the intensity of the HF band in the Figure 7 spectrum. The total 2.4 mole equivalents of H₂ measured as a product is on the low side, probably due to accumulated random error in the measurements combined with the likely systematic error mentioned earlier.

The experiments discussed in this section indicate that a ≥ 4:1 ratio of HF to SiH₄ fully fluorinates the latter to SiF₄ after a few days at room temperature, via the intermediate formation of the three partially fluorinated silanes. This is unlike the fluorination of SiH₄ by UF₆ where SiH₂F₂ and SiHF₃ were present together with SiF₄ as the final fluorinated silane derivatives (even in the presence of excess UF₆). This clearly suggests that UF₆ does not further fluorinate SiH₂F₂ nor SiHF₃ but that it does react with SiH₃F (although this latter deduction is strictly based on the fact that SiH₃F was the only fluorosilane absent from the final product of the reaction between SiH₄ and UF₆ and carries with it the consequent assumption that the rate of reaction between HF and the three intermediate fluorosilanes is comparable) (19). In light of these results, the presence of HF as a final product from reactions 4 and 5 (see Table I) is somewhat puzzling and may be due to still poorly understood factors, as mentioned earlier. The next section will discuss the nature of the solid uranium fluoride products in order to gain better insight into the equilibria involved in the UF₆-SiH₄ system.

Solid Products. The microanalytical data for the solid products from reactions 4 and

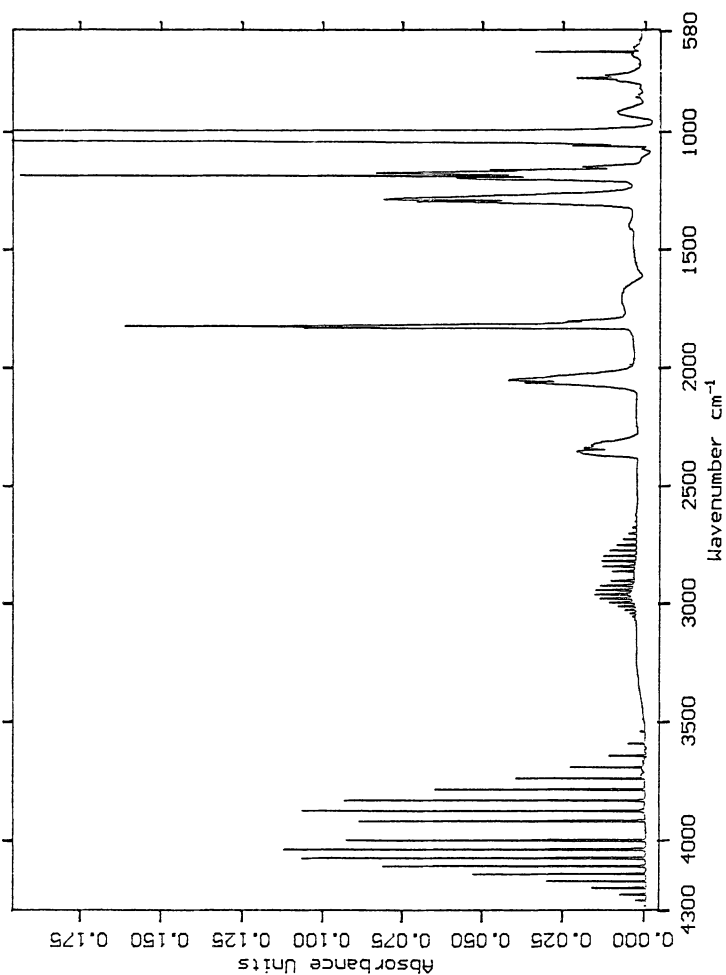
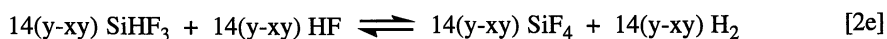
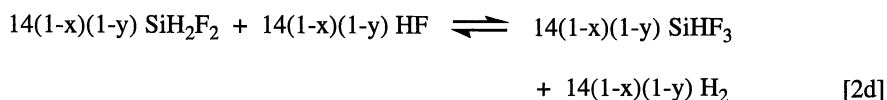
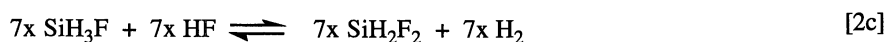
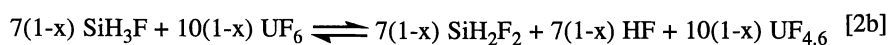
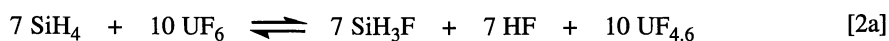


Figure 7. FT-IR spectrum of products from the reaction between SiH_4 and excess HF (from 4300 to 580 cm^{-1}); 1 day after 3rd HF addition (see text), 48 torr.

6 (see Table I) are listed in Table IV. These reactions involved the two extreme initial U/Si reagent ratios used. The F:U ratio of 4.6 determined in both cases suggests that the solids were a mixture of UF₄ and UF₅ and/or one or more of the other intermediate uranium fluorides of the type U_xF_{4x+1} (13a,20), with UF₅ slightly dominating. Not unexpectedly, this ratio ranged from 4.55 to 4.60 for the other solid product samples that were analyzed, independent of the initial reagent stoichiometry. The khaki green color of the solids was indicative of a mixture of UF₅ (usually reported to be yellow, although other colors have been observed) (13a,20,21) and UF₄ (emerald green in color) being present in significant majority over the intermediate fluorides, which are reported to be black (13a,20). One must however exercise caution when relying on color as an indicator of the composition of the solid products, especially since it is not obvious how UF₆ could have been reduced to a mixture of 40% UF₄ and 60% UF₅; it would seem more likely that one intermediate fluoride with the corresponding composition would have resulted. Unfortunately, we have not yet succeeded at recording meaningful IR or Raman spectra of these solids. In any case, the composition of the solid products suggests that the reducing strength of SiH₄ toward UF₆ under these conditions was insufficient to fully convert it to UF₄, although it is apparently greater than that of HCl, where the F:U ratio of the solid products was determined (via microanalysis) to fall in the range 4.8-4.9 under very similar experimental conditions (18).

Together with the results discussed in the previous sections, the composition of the solid product(s) supports the following series of equilibria as best approximating the behavior of the UF₆-SiH₄ system (22):



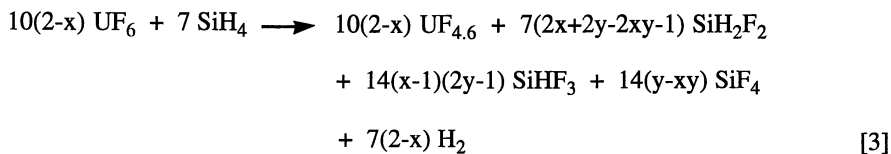
In Equation 2b, it is implied that the reactivity of SiH₃F towards “UF_{4.6}” is insignificant compared to its reaction with UF₆. It should be apparent from the above equations that the theoretical range for the initial U/Si ratio required to consume both UF₆ and SiH₄ in the reaction is between 1.4 and 2.8 (the corresponding theoretical range for the expected H₂/Si ratio is between 1 and 2). However, the experimental value is closer to 2, as indicated by the results from reaction 1b. Results from reaction 1a and reaction 3 additionally imply that the actual ratio is greater than 1.5 and less than 2.4. Consequently, the best approximate value for x in the above equations is 0.6. By summing up the equilibria in Equations 2a-e, the overall reaction describing

Table IV. Summary of Microanalytical Data

Reaction	U/Si	Wt. % U	Wt. % F	Wt. % X ^a	F/U
4	5.2	73.28	27.00	-0.28	4.62
6	0.4	72.77	26.60	0.63	4.58

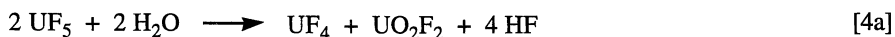
^a X = 100% - Wt. % (F + U).

the system can be explicitly stated



Equation 3 clearly shows that for x values of ~ 0.6 , a significant portion of the product will consist of only partially fluorinated silanes due to an inadequate amount of HF being produced in Equations 2a and 2b, which is in accordance with the experimental findings. It also follows from Equation 3 that $y \leq 0.5$ (in accordance with its physical definition given in reference 22), since otherwise unreacted HF would be present among the final products. A more accurate estimate of y and the consequent relative amounts of SiH_2F_2 , SiHF_3 and SiF_4 in the final product cannot be obtained from these equilibria, as the exact affinity of HF for the former two fluorosilanes is presently unknown.

The weight percent due to elements other than U or F in the two analyzed products is quite insignificant (especially in reaction 4) in light of the expected error limit ($\sim 0.3\%$ per element) of the analyses. The slightly greater discrepancy in the second set of analytical data listed in Table IV may be due to the presence of trace amounts of moisture which escaped through efforts at its complete elimination. This would have introduced oxygen into the solid product in the form of UO_2F_2 according to one or both of the following reaction pathways: (12,13)



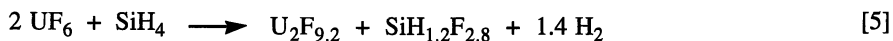
The more likely hydrolysis pathway is Equation 4a, as the introduction of any trace moisture to the system would be expected during the manipulation of the solid product rather than during its preparation. Also, the elimination of any unreacted UF_6 from the product was ensured by either adding excess SiH_4 to the reactor immediately prior to the isolation of the remaining solid or by evolving it in vacuo at ambient temperature with all the other volatile species. Thus, it follows from Equation 4a that approximately 5 mole % of the analyzed solid product from reaction 6 was composed of UO_2F_2 .

Conclusions

Contrary to work reported in the literature stating that SiH_4 and UF_6 do not undergo thermal reaction at temperatures below 130°C (9), evidence has been presented here for a reaction between the two species commencing at or below ambient temperature in less than 30 minutes and reaching completion within 2 to 5 days. The system was studied over a wide range of initial reagent ratios using two independent gas handling

systems, with all of the results obtained being consistent with the above conclusion. In contrast, the previously reported study employed one gas handling system and a U/Si ratio that ranged from 0.8 to 1.2 (the total reactor pressure ranged from 70 to 90 torr) (9b). It is possible, but unlikely, that differences between the primary materials of construction of the gas handling systems used here (316SS, Teflon-FEP and Monel) and in the previous study (Monel) contributed to the respective differences in reactivity, especially since the behavior of the two additional materials introduced here is known to be very comparable to that of Monel (23).

The reaction between a 2:1 mixture of UF₆ and SiH₄, respectively, led to the complete consumption of both reagents. Based on the experimental data gathered, this reaction may be expressed as



The moiety "SiH_{1.2}F_{2.8}" is actually comprised of the three fluorosilanes SiH₂F₂, SiHF₃ and SiF₄, as identified by FT-IR spectroscopy in the final vapor phase product (24). Their relative abundance is presently still unknown, as it cannot be determined with any precision from the IR spectra.

Two other significant conclusions can be made from this study: i) the observed reaction between SiH₄ and UF₆ was most likely surface catalyzed and ii) UF₆ and HF show fundamentally different reactivity towards partially fluorinated silane derivatives. Evidence for the first conclusion was obtained from reactions involving either SiH₄ or UF₆ and reactor walls preconditioned with UF₆ or SiH₄, respectively, which proceeded in a very similar fashion to the bulk reactions between the two species. The latter reactions proceeded at or below ambient temperature whether the two species were mixed directly in the gas phase or first condensed together at -196 °C before warming up to ambient temperature, which supports the apparently active role of the reactor walls in the system's chemistry.

Whereas the completed reaction between UF₆ and SiH₄ led to the formation of the fluorosilanes SiH₂F₂, SiHF₃ and SiF₄, the reaction of HF with SiH₄ resulted in SiF₄ as the sole silane derivative. This implied that UF₆ reacted with SiH₄ and most likely with SiH₃F but not with SiH₂F₂ and SiHF₃, while HF reacted with SiH₄ and all three partially fluorinated silanes (its reaction with SiHF₃ is debatably the fastest step) to form SiF₄ as the final product. This in turn suggests that the reducing power of SiH₄ toward UF₆ was significantly diminished upon the substitution of each hydride (H is more electronegative than Si) (25) by a highly electronegative fluorine atom, resulting in the non-reactivity of SiH_{4-x}F_x (x = 2,3) towards the highly oxidizing UF₆. This also helps explain why UF₆ was incompletely reduced to the species "UF_{4.6}", and implies that this moiety is a single species rather than a mixture of fluorides. Conversely, the reactivity of the much more ionic HF with the Si-H bond in the series SiH_{4-x}F_x (0 ≤ x ≤ 3) would be expected to gradually increase as the number of fluorine atoms increased if an ionic substitution mechanism was involved, due to the simultaneous increase in electropositivity of the Si atom. However, the high enthalpies of deprotonation (2e,2f) for the species SiH_{4-x}F_x (0 ≤ x ≤ 3) of 1450-

1560 kJ·mol⁻¹ (decreasing with increasing x) and HF (1550 kJ·mol⁻¹) suggest the involvement of a gas phase free radical mechanism (it is noteworthy that SiH₂F₂ and SiHF₃ behave as slightly stronger acids than HF in the gas phase). Based on the relatively small difference between the Si-H bond strengths in SiH₄ compared to SiHF₃ (41 kJ·mol⁻¹ greater for latter) (26), it is likely that this is only one of the factors contributing to the observed lack of reactivity between UF₆ and SiH_{4-x}F_x (x = 2,3); steric hindrance and a synergistic stabilization of the two fluorosilanes resulting from F-F interactions (2e) may be among the others. Further work focused at better understanding the mechanisms involved in this system is ongoing.

Acknowledgements

The invaluable assistance with many of the technical aspects of this work that was provided by Mr. Brian C. Olson and Mr. Tuan Chau is greatly appreciated. We also thank Dr. Dennis G. Garratt and Dr. Ken Falk for many helpful discussions.

Literature Cited

- (a) Ignacio, E. W.; Schlegel, H. B. *J. Chem. Phys.* **1990**, *92*, 5404; (b) Gordon, M. S.; Gano, D. R.; Binkley, J. S.; Frisch, M. J. *J. Am. Chem. Soc.* **1986**, *108*, 2191; (c) Gordon, M. S.; Truong, T. N.; Bonderson, E. K. *J. Am. Chem. Soc.* **1986**, *108*, 1421; (d) Schlegel, H. B. *J. Phys. Chem.* **1984**, *88*, 6255; (e) Matsuda, A.; Yagii, K.; Kaga, T.; Tanaka, K. *Jpn. J. Appl. Phys.* **1984**, *L576*, 23; (f) Koinuma, H.; Manako, T.; Natsuki, H.; Fujioka, H.; Fueki, K. *J. Non-Cryst. Solids* **1985**, *7*, 801.
- (a) Ignacio, E. W.; Schlegel, H. B. *J. Phys. Chem.* **1992**, *96*, 1620; (b) Koshi, M.; Kato, S.; Matsui, H. *J. Phys. Chem.* **1991**, *95*, 1223; (c) Dixon, D. A. *J. Phys. Chem.* **1988**, *92*, 86; (d) Moffat, H. K.; Jensen, E. F.; Carr, R. W. *J. Phys. Chem.* **1991**, *95*, 145; (e) Rodriguez, C. F.; Hopkinson, A. C. *Can. J. Chem.* **1992**, *70*, 2234; (f) Smith, B. J.; Radom, L. *J. Phys. Chem.* **1991**, *95*, 10549.
- (a) Nakamoto, K. *Infrared and Raman Spectra of Inorganic and Coordination Compounds*, 4th ed.; Wiley-Interscience: New York, 1986 (and references therein); (b) Simpson, J. In *Inorganic Chemistry Series 2. Main Group Elements, Groups IV and V*; Sowerby, D. B., Ed.; Butterworths: London, 1975; Vol. 2, pp 1-51 (and references therein); (c) Robiette, A. G.; Cartwright, G. J.; Hoy, A. R.; Mills, I. M. *Mol. Phys.* **1971**, *20*, 541; (d) Newman, C.; O'Loane, J. K.; Polo, S. R.; Wilson, M. K. *J. Chem. Phys.* **1956**, *25*, 855; (e) Newman, C.; Polo, S. R.; Wilson, M. K. *Spectrochim. Acta* **1959**, *10*, 793; (f) Burger, H.; Biedermann, S.; Ruoff, A. *Spectrochim. Acta* **1971**, *27A*, 1687.
- (a) Wilde, R. E.; Srinivasan, T. K. K.; Harral, R. W.; Sankar, S. G. *J. Chem. Phys.* **1971**, *55*, 5681; (b) Fournier, R. P.; Savoie, R.; The, N. D.; Belzile, R.; Cabana, A. *Can. J. Chem.* **1972**, *50*, 35.
- McInnis, T. C.; Andrews, L. *J. Phys. Chem.* **1992**, *96*, 5276.
- Davis, S. R.; Andrews, L. *J. Chem. Phys.* **1987**, *86*, 3765.
- Kobayashi, N.; Goto, H.; Suzuki, M. Proceedings of the VIth VLSI Conference, Materials Research Society, Pittsburgh, PA. 1991.

8. (a) Whitehead, C. *Chemistry in Britain* **1990**, 1161; (b) *Uranium Enrichment*; Villani, S., Ed.; Springer-Verlag: Berlin, 1979; (c) Becher, F. S.; Kompa, K. L. *Nuclear Technology* **1982**, 58, 329; (d) Horsley, J. A.; Rabinowitz, P.; Stein, A.; Cox, D. M.; Brickman, R. O.; Kaldor, A. *IEEE Journal of Quantum Electronics* **1980**, QE-16, 412; (e) Greenland, P. T. *Contemporary Physics* **1990**, 31, 405.
9. (a) Catalano, E.; Barletta, R. E.; Pearson, R. K. *J. Chem. Phys.* **1979**, 70, 3291; (b) Pearson, R. K. University of California (Lawrence Livermore Laboratory) Internal Document #17969, November, 1978.
10. Jones, L. H.; Ekberg, S. A. *J. Chem. Phys.* **1979**, 71, 4764.
11. Christe, K. O.; Wilson, R. D.; Schack, C. J. *Inorg. Nucl. Chem. Lett.* **1975**, 11, 161.
12. Sherrow, S. A.; Hunt, R. D. *J. Phys. Chem.* **1992**, 96, 1095.
13. (a) Brown, D. *Halides of the Lanthanides and Actinides*; Wiley-Interscience: London, 1968; (b) Katz, J. J.; Rabinowitch, E. *The Chemistry of Uranium - Part I*; McGraw-Hill: New York, 1951; (c) Galkin, N. P.; Sudarikov, B. N.; Veryatin, U. D.; Shishkov, Yu. D.; Maiorov, A. A. In *Technology of Uranium*; Galkin, N. P.; Sudarikov, B. N., Eds.; Israel Program for Scientific Translation: Jerusalem, 1966.
14. SiH_4 and $\text{SiH}_{4-x}\text{F}_x$ species were present together prior to the additions; the HF equivalents added are based on the quantity of SiH_4 present as estimated from the $\sim 2\text{U/Si}$ equivalence ratio determined earlier.
15. *Gases and Vapors - A Special Collection of Infrared Spectra*; Craver, C. V., Ed.; The Coblenz Society: Kirkwood, U.S.A., 1980.
16. Dove, M. F. A.; Clifford, A. F. In *Chemistry in Nonaqueous Ionizing Solvents*; Jander, G.; Spandau, H.; Addison, C. C., Eds.; Pergamon Press: New York, 1971; Vol. 2, Part 2.
17. Vanderwielen, A. J.; Ring, M. A. *Inorg. Chem.* **1972**, 11, 246.
18. Cicha, W. V.; Covey, J. unpublished results.
19. We have not been able to locate a supplier of pure SiH_3F to allow confirmation of this deduction.
20. Weigel, F. In *The Chemistry of the Actinides*, 2nd ed.; Katz, J. J.; Seaborg, G. T.; Morss, L. R., Eds.; Chapman and Hall: London, 1986 (and references therein).
21. Asprey, L. B.; Paine, R. T. *J. Chem. Soc., Chem. Commun.* **1973**, 920.
22. In Equations 2d and 2e, (1-y) and y represent the fraction of available HF which reacts with SiH_2F_2 and SiHF_3 , respectively.
23. Granec, J.; Lozano, L. In *Inorganic Solid Fluorides: Chemistry and Physics*; Hagenmuller, P., Ed.; Academic Press: Orlando, 1985.
24. The overall F:H ratio of the fluorosilane products in Equation 4 was based on the analyzed F:U ratio of the solid product and consequently is only an approximate value, due to the experimental error in determining the reaction stoichiometry (it is not possible to accurately determine the quantity of each individual species from the IR spectra, for reasons mentioned earlier).
25. Cotton, F. A.; Wilkinson, G. *Advanced Inorganic Chemistry*, 5th ed.; John Wiley & Sons: New York, 1988; p 275.
26. *Handbook of Chemistry and Physics*, 71st ed.; Lide D. R., Ed.; CRC Press: Boca Raton, 1990-1991.

RECEIVED August 23, 1993

Chapter 12

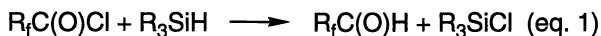
Fluorinated Aldehydes and Their Polymers

William B. Farnham and Stephen G. Zane

Central Research and Development, DuPont, Experimental Station,
Wilmington, DE 19880-0328

Fluorinated aldehydes are prepared in high yield by reaction of readily available acid chlorides with trialkylsilanes in the presence of Pd/C catalyst. Since no solvent is used, simple separation from by-product chlorosilane provides pure aldehyde. Previously reported syntheses are inconvenient, not easily amenable to scale-up, or require separate dehydration steps. Polymerization reactions of these aldehydes are described. Aluminum and titanium alkoxides initiate polymerization by a coordination mechanism. With selected examples, polymerization and appropriate end-capping affords soluble, high molecular weight polyacetal stable to ca. 300 ° C.

We have found that fluorinated aldehydes can be prepared conveniently and in high yield by reaction of readily available fluorinated acid chlorides with trialkylsilanes in the presence of a supported palladium catalyst (eq. 1) (1). Previously reported laboratory methods for preparing fluorinated



aldehydes are inconvenient, not amenable to scale-up, or require additional steps to liberate aldehyde from the corresponding hydrate or hemiacetal. By comparison with triethylsilane, sterically demanding triisopropylsilane provides advantages in selectivity, yield and catalyst lifetime. In a typical reaction, triisopropylsilane is charged into a cooled reaction vessel containing palladium on carbon. A fluorinated acid chloride is then added dropwise, and the ensuing exothermic reaction is usually controlled at 25 - 30 °C by means of an external bath. Conversions are readily monitored by GC. Although the fluorinated aldehyde usually phase-separates as the

reaction proceeds, product isolation is carried out most conveniently by separation of the phases at ca. -20 °C to 0 °C after vacuum transfer of volatile components. Small quantities of triisopropylsilane or chlorosilane byproduct can be removed by washing the fluorocarbon product with petroleum ether. All operations are carried out in an atmosphere of dry nitrogen. Solvents are deliberately avoided during the reduction process to limit side reactions and to facilitate product purification. Representative examples are provided in Table I. Some of the acid chlorides are commercially available. Others were prepared from trifluorovinyl ether ester precursor, $\text{CF}_2=\text{CFOCF}_2\text{CF}(\text{CF}_3)\text{OCF}_2\text{CF}_2\text{CO}_2\text{CH}_3$, by standard functional group manipulations in combination with a new, catalyzed addition reaction of selected alcohols and trifluorovinyl ethers (2,3). Tetrafluoroethylene is a convenient starting material for one example (4).

Table I. Representative Fluorinated Aldehyde Preparations

$$\text{R}_f\text{C}(\text{O})\text{Cl} + (\text{i-Pr})_3\text{SiH} \xrightarrow{\text{Pd/C}} \text{R}_f\text{C}(\text{O})\text{H} + (\text{i-Pr})_3\text{SiCl}$$

Rf	isolated yield (%) ^a
C ₇ F ₁₅ -	90
CF ₂ =CFOCF ₂ CF(CF ₃)OCF ₂ CF ₂ -	57
CF ₃ CH ₂ OCF ₂ CHFOCF ₂ CF(CF ₃)OCF ₂ CF ₂ -	80
CF ₃ CF ₂ CF ₂ OCF(CF ₃)-	63
CF ₃ CH ₂ OCF ₂ CF ₂ -	62
CF ₃ CF ₂ CF ₂ -	60

a) Isolated yields are based upon acid chloride.

Aldehyde purity can be of critical importance: some of the reactions of fluorinated aldehydes are adversely affected by the presence of small amounts of precursor acid chloride or aldehyde hydrate. For example, some of the catalysts used for polymerization (*vide infra*) are effectively deactivated by small amounts (0.1-0.5%) of aldehyde hydrate. We have not examined medium effects in the silane/acid chloride reaction, but the high reactivity of the fluorinated aldehydes can lead to unexpected results. For example, fluorinated aldehydes and acid chlorides condense rapidly in THF to afford esters of the form $\text{R}_f\text{C}(\text{O})\text{OCHClR}'_f$. In contrast, this reaction is very slow in CHCl_3 . Fortunately, esters of this type are usually not significant products under our preferred reduction conditions. The aldehydes described here are quite reactive and can undergo spontaneous

polymerization. These undesired events can be minimized by monomer storage in Teflon® FEP vessels at -20 °C to -30 °C.

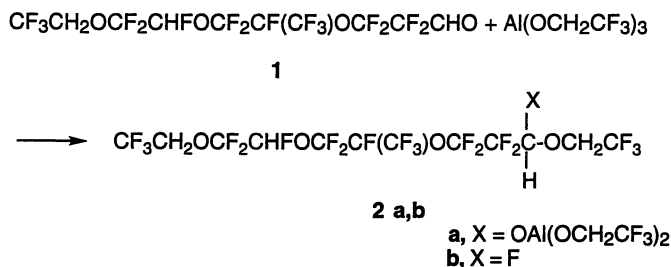
The literature on fluorinated aldehydes and their polymers, although relatively sparse, has been reviewed (5). A reading of this review and the original literature citations reveals that much remains to be learned about this area: most of the polymerization studies were carried out with CF₃CHO which offers difficult handling problems along with rather intractable polymer. Some mechanistic speculation has been advanced but critical evaluation appears minimal. Longer chain or substituted fluorinated aldehydes have received less attention.

We have begun a study of fluorinated aldehyde polymerization reactions and have examined initiation by anionic species, neutral electron-pair donors, and various main group species. Polymerization reactions were carried out on small scale (0.4 to 5 g) in carefully washed and dried glass vessels using a dry box for all operations except for finishing steps of end-capping procedures and the handling of materials such as Cl₂ and SF₄. We have focused on titanium and aluminum catalyst systems containing alkoxy ligands because they appear to offer a good opportunity for architectural control. Many of these polymer-forming systems appear to be living (6), and afford high molecular weight polymer. Soluble polymer obtained with selected aldehydes has been subjected to NMR, light scattering, and size-exclusion analyses. The facility with which the polyacetal species depolymerize depends upon the R_f group, solvent, temperature and identity of the growing or "capped" end. For example, aldehyde **1** (neat) is rapidly converted to polymer with catalytic quantities of TAS Me₃SiF₂. Without end-capping, this material slowly dissolves in THF but easily reverts to monomer. However, it is converted to stable, high mw (400,000) elastomer (T_g = -53 °C) on treatment with excess perfluoroalkylfluorosulfate. As judged by GPC, the molecular weight distribution obtained is skewed toward the low molecular weight side, and it is not clear whether deficiencies are greater in the end-capping or propagation reactions.

Initiated with AlCl₃, the polyacetal produced from **1** initially appears stable in solution, but increasing amounts of monomer were observed after several days' storage. On initiation with Al(OCH₂CF₃)₃ and end-capping by treatment with SF₄, aldehyde **1** provides high molecular weight (ca. 10⁶) polymer exhibiting thermal stability to about 250 °C. End-capping with SF₄ suffers some deficiencies, including color formation in the polymer and a significant proportion of lower molecular weight material. We have found that an alternative end-capping procedure which involves treatment with PCl₃, followed by chlorination (after removal of excess PCl₃) affords more uniform distribution of molecular weight, colorless polymer and higher thermal stability (300 °C). GPC (polystyrene standards) analysis indicates a weight average molecular weight of ca. 9.3 x 10⁵ for this material. Since the calibration standards do not resemble the fluorinated polyacetal very closely, and since some of the samples elute near the total exclusion volume of the linear column set used for the size-exclusion analyses, light-scattering measurements were undertaken and provided an alternate molecular weight estimate of 400,000. As measured by a thermal field flow fractionation method (TFFF), intrinsic viscosity values [η] were in accord with

expectation for high molecular weight material: 1.6 (PCl_3/Cl_2 end-capping) and 3.3 (diethylaminosulfur trifluoride end-capping, but with some product fractionation prior to analysis) (7). These values, obtained from preliminary, small-scale reactions, support our conclusion that very high molecular weight polyacetals are accessible from fluorinated aldehydes. Although circumstantial, they also indicate that processes equivalent to chain transfer to monomer are relatively slow (6).

With aluminum (and titanium) alkoxides, the polymerization process appears to be a rare example of coordination polymerization of a fluorinated monomer. The (RO) ligand of RO-M is transferred to the carbonyl carbon of the incoming aldehyde producing a new ligand for the metal. The first-formed species in these reactions have been prepared by alternate reaction schemes (e.g., **2a**). With the exception of their likely involvement in higher aggregates (dimers, etc. of $\text{Al}(\text{OR})_3$), characterization is straightforward, and their operability as active polymerization catalysts has been demonstrated. For example, treatment of a THF solution of aluminum tris(trifluoroethoxide) with one molar equivalent of aldehyde **1** in THF provided the adduct **2a** as the dominant species. This was demonstrated by ^{19}F NMR analysis (distinguishable trifluoroethoxy groups) and conversion of **2a** to **2b** by treatment with SF_4 .



Scheme 1

Current efforts are focused on improved control of molecular weight and on developing alternative end-capping procedures for use with our several classes of initiators. We are also investigating the properties of these unique fluoropolymers.

Experimental Section

Preparation of $\text{C}_7\text{F}_{15}\text{CHO}$. Catalyst 10% Pd/C (200 mg) was placed in a 3-necked round-bottomed flask and cooled at $0\text{ }^\circ\text{C}$. Triisopropylsilane (3.32 g, 21 mmol) was added, followed by perfluorooctanoyl chloride (7.9 g, 18.2 mmol). The mixture was allowed to warm to room temperature and was then controlled at $25\text{--}27\text{ }^\circ\text{C}$ during the exothermic reaction. After 3 hr, GC analysis showed an aldehyde/acid chloride ratio = 94/6. Another 0.26 mL of

silane was added and stirring was continued for 1 hr. Vacuum transfer gave a liquid which was chilled at $-25\text{ }^{\circ}\text{C}$. The resulting solid was shaken with petroleum ether, chilled at $-25\text{ }^{\circ}\text{C}$, and separated again. In this way, 6.48 g of product was obtained, mp ca. $-5\text{ }^{\circ}\text{C}$. ^{19}F NMR: -81.3 (t of t's, $J=9.8, 2.3$), -121.8 (m), -122.3 (m), -123.0 (m), -123.7 (m), -125.4 (t of m's, with $J_{\text{FCCH}}=3$ Hz), -126.5 (m).

Preparation of $\text{CF}_3\text{CH}_2\text{OCF}_2\text{CHFOCF}_2\text{CF}(\text{CF}_3)\text{OCF}_2\text{CF}_2\text{CHO}$. A 3-necked round-bottomed flask equipped with an addition funnel was charged with 10% Pd/C (1.2 g) and cooled to $0\text{ }^{\circ}\text{C}$. Triisopropylsilane (11.0 g, 70 mmol) was added in one portion and $\text{CF}_3\text{CH}_2\text{OCF}_2\text{CHFOCF}_2\text{CF}(\text{CF}_3)\text{OCF}_2\text{CF}_2\text{COCl}$ (30 g, 57 mmol) was added dropwise over a 10 min period. The mixture was allowed to warm to ca. $25\text{ }^{\circ}\text{C}$, and the exotherm was controlled by a cool water bath. Conversion of the acid chloride was substantially complete at this stage. The last few percent was converted to product by addition of 0.3 g Pd/C and 1.8 g triisopropylsilane and stirring for 48 hr. The product was removed at 0.1 mm while maintaining the reaction vessel at ca. $40\text{--}50\text{ }^{\circ}\text{C}$. The lower layer was isolated after chilling at $-25\text{ }^{\circ}\text{C}$, and additional washing with petroleum ether gave 16.5 g of a colorless liquid. ^1H NMR (THF- d_8): 9.64 (m), 6.72 (d of m's, $J=52$), 4.62 (q, $J=8$). ^{19}F NMR: -74.80 (t, $J=8$, CF_3CH_2), -80.0 (m, CF_3), -81.7 to -85.3 (overlapping AB patterns, OCF_2), -89.95 and -90.64 (AB patterns, $J=145$, OCF_2), -127.91 (apparent quartet, $J=2.5$, CF_2CHO), -144.7 (apparent t, $J=21$, CF), -145.9 (d of m's, $J=52$, CHF). IR (CCl_4) featured bands at 1768 cm^{-1} (C=O) and $1240\text{--}1150\text{ cm}^{-1}$ (CF). GC/MS showed highest mass fragment of $m/z=471.9844$. Calcd. for $\text{C}_{10}\text{H}_3\text{F}_{15}\text{O}_4$ (M-H, F)= 471.9791 .

Polymerization of $\text{CF}_3\text{CH}_2\text{OCF}_2\text{CHFOCF}_2\text{CF}(\text{CF}_3)\text{OCF}_2\text{CF}_2\text{CHO}$ with TAS Me_3SiF_2 . A catalyst solution was prepared by treating TAS Me_3SiF_2 [tris(dimethylaminosulfonium) trimethyldifluorosilicate] (10 mg) with 10 drops of 1,1,2,2,3,3-hexafluorocyclopentane. One drop of the catalyst solution was added to the title aldehyde (0.50 g) and the mixture was manipulated with a spatula. After 18 hr, perfluoroallylfluorosulfate (1.0 mL) was added and the mixture was stirred for 1.5 hr. 1,1,2-trichloro-1,2,2-trifluoroethane (10 mL) was added, and stirring was continued for ca. 1.5 hr to afford a viscous solution. After an additional 1.5 hr, the volatiles were removed and the product was washed with CH_2Cl_2 to give 0.46 g of white waxy solid. TGA showed a 10% weight loss between $150\text{ }^{\circ}\text{C}$ and $230\text{ }^{\circ}\text{C}$, then a more rapid loss. DSC featured a T_g at $-53\text{ }^{\circ}\text{C}$. Size exclusion analysis showed: $M_w = 395,000$; $M_n = 33,500$. ^{19}F NMR (THF- d_8): -75.0 (s (br), CF_3CH_2), -80.0 and -80.2 (CF_3 + part of OCF_2), -82.5 to -87.0 (overlapping signals, OCF_2), -90.8 (s (br), OCF_2), -121 to -126 and -132 to -139 (overlapping collection of AB patterns for CF_2CH), -145.0 (s (br), CF), and -146 (d of m's (br), CHF). ^1H NMR (THF- d_8): 6.5 (d of m's, $J=52$ Hz, CHF), 5.8 and 5.4 (br, overlapping signals), 4.5 (br m, CH_2CF_3).

Polymerization of $\text{C}_7\text{F}_{15}\text{CHO}$ with $\text{CF}_3\text{CH}_2\text{OTiL}_3$. A mixture of triethanolaminetitanium isopropoxide (9.29 g, 36.7 mmol) and toluene (100 mL) was treated with trifluoroethanol (7.34 g, 73.4 mmol) and was stirred for 67 hr. The resulting suspension was evaporated, and the solid was triturated with ether and filtered to give 10.08 g of a white powder, mp 177--

180 °C. ^{19}F NMR ($\text{CD}_2\text{Cl}_2/25\text{ °C}$): -76.5 (t, $J=9$), ^1H NMR: 4.70 (q, $J=10$ Hz), 4.57 (m, CH_2), and 3.30 (m, CH_2). Spectral features were temperature- and concentration-dependent.

A sample of $\text{C}_7\text{F}_{15}\text{CHO}$ (400 mg) was treated with the title titanate (4 mg). The resulting mixture gelled and then became a crumbly white solid. TGA showed the onset of weight loss at ca. 65 °C.

Polymerization of $\text{CF}_3\text{CH}_2\text{OCF}_2\text{CHFOCF}_2\text{CF}(\text{CF}_3)\text{OCF}_2\text{CF}_2\text{CHO}$ with $\text{Al}(\text{OCH}_2\text{CF}_3)_3$. Aluminum tris(trifluoroethoxide) was prepared by treatment of a toluene solution of triethylaluminum (0.38 M) with three equivalents of trifluoroethanol at -25 °C. After gas evolution was complete, the reaction mixture was allowed to stand at room temperature. When precipitation of the product appeared to be well-advanced (1-2 hr), the reaction mixture was cooled at -25 °C for 18 hr before collecting the solid product. From 1.76 mmol of Et_3Al and 0.528 g trifluoroethanol was obtained 435 mg of a white solid, mp 171-172 °C. ^1H NMR (THF- d_8): 4.1 (q, $J=8$). ^{19}F NMR (THF- d_8): -77.0 (br s), trace signals at -76.3 and -77.7.

A sample of the title aldehyde (0.50 g) in a glass vial was treated with aluminum trifluoroethoxide (0.2 mg). The resulting solution formed a clear hard gel which was allowed to stand for 18 hr. ^{19}F NMR analysis showed that the product readily reverts to the starting aldehyde in THF- d_8 . The sample was treated with toluene (15 mL) and SF_4 (0.5 mL) and stirred for 2 hr. Excess SF_4 was removed in a stream of N_2 , and the remaining mixture was heated to reflux for 1.75 hr. After standing for 18 hr, the supernatant was decanted and the remaining solid was dried to give 0.42 g. ^{19}F NMR (THF- d_8): -75.0 (s (br), CF_3), -80.0 and -80.5 (overlapping s (br), CF_3 and OCF_2), -82.5 to -87.0 (overlapping m's, OCF_2), -90.8 (s (br), OCF_2), -124 and -136 (br m's, CF_2), -144.0 to -146.5 (overlapping m's, CF and CHF). TGA showed only 1-2% weight loss up to 260 °C. Size exclusion analysis of the crude solid showed a major peak with peak molecular weight = 1×10^6 and a minor amount (2%) of an unidentified, low-mw material with a retention volume similar to the starting aldehyde.

Polymerization of $\text{CF}_3\text{CH}_2\text{OCF}_2\text{CHFOCF}_2\text{CF}(\text{CF}_3)\text{OCF}_2\text{CF}_2\text{CHO}$ with $\text{Al}(\text{OCH}_2\text{CF}_3)_3$ / End-Capping with PCl_3 ; Cl_2 . The title aldehyde (0.60 g) was treated with ca 0.2 mg of $\text{Al}(\text{OCH}_2\text{CF}_3)_3$ and the solution allowed to stand at 25 °C for 18 hr. The resulting solid disk was cut into small pieces with a sharpened spatula and treated with PCl_3 (2 mL) and trichlorotrifluoroethane (6 mL) and heated at reflux for 2 hr. Glyme (5 mL) was added and reflux was continued for 2 hr. Volatiles were removed under a stream of nitrogen, and the residue was rinsed with dichloromethane (6 mL). The product was treated with trichlorotrifluoroethane (10 mL) and Cl_2 (0.25 mL of liquid, collected at -78 °C) and stirred for 18 hr at 25 °C, then heated at reflux for 1.5 hr. Most of the solvent was removed by distillation, and the remainder was removed under a stream of nitrogen. Product was rinsed with dichloromethane and dried to give 0.53 g of a white solid. ^{19}F NMR showed the expected signals for polymer along with those due to a small amount (1 or 2%) of hydrated aldehyde. TGA showed a 1 to 2% weight loss between 200 and 300 °C, then a major loss beginning at 300 °C. Size exclusion analysis (polystyrene standards) showed the peak mol. wt. at 1.3×10^6 , $M_w = 930,000$; and $M_n = 100,000$. The molecular weight estimate obtained by light scattering analysis was 400,000.

Acknowledgment

Note: This chapter is contribution number 6535

Literature Cited

1. Reactions of hydrocarbon acid chlorides with silicon hydrides in the presence of palladium have been reported (Citron, J. D., *J. Org. Chem.* **1969**, *34*, 1977). Significant reactivity differences are usually found in comparisons of hydrocarbon- and fluorocarbon-substituted carbonyl substrates, and the fluorinated aldehydes discussed in this chapter further exemplify this trend.
2. Hung, M. H.; Farnham, W. B.; Feiring, A. E.; Rozen, S. *J. Am. Chem. Soc.* **1993**, *115*, 8954.
3. Feiring, A. E.; Wonchoba, E. R. *J. Org. Chem.* **1992**, *57*, 7014.
4. Krespan, C. G.; Van-Catledge, F. A.; Smart, B. E. *J. Am. Chem. Soc.* **1984**, *106*, 5544.
5. Neeld, K. and Vogl, O. J. *Polymer Science: Macromolecular Reviews*, **1981**, *16*, 1-40.
6. Our criteria for "livingness" are admittedly circumstantial and operational at this stage: treated with additional monomer, un-capped polymer continues the polymerization process. One example of a block copolymer (with different R_f groups) has been achieved using Al(OCH₂CF₃)₃ initiation. For a short discussion and proposal for ranking of living polymerization systems, see Matyjaszewski, K. *Macromolecules* **1993**, *26*, 1787.
7. We thank J. J. Kirkland of this department for these measurements and for useful discussion. See Kirkland, J. J.; Rementer, S. W.; Yau, W. W. *J. Appl. Polym. Sci.* **1989**, *38*, 1383 for a discussion of TFFF.

RECEIVED November 4, 1993

Chapter 13

Synthesis and Chemistry of Perfluoro Macrocycles

Perfluoro Crown Ethers and Cryptands

Richard J. Lagow, Tzuhn-Yuan Lin, Herbert W. Roesky,
Wayne D. Clark, Wen-Huey Lin, Jennifer S. Brodbelt,
Simin D. Maleknia, and Chien Chung Liou

Department of Chemistry, The University of Texas at Austin,
Austin, TX 78712

Perfluoro macrocycles are a new development in organic and inorganic chemistry which has occurred in the last five years. The synthesis of perfluoro crown ethers and perfluorocryptands forecast the synthesis of many more perfluoro macrocycles in the next few years. The most surprising development to date with these new very chemically and thermally stable macrocycles has been the findings that they coordinate anions rather than cations and that they are extremely biocompatible materials. Perfluoro macrocycles have the potential for development as a new class of very thermally stable oxygen carriers which reversibly bind oxygen.

A recent breakthrough in our laboratory has involved the synthesis of perfluorinated crown ethers and cryptands. We have previously reported the synthesis of the first perfluoro crown ethers, perfluoro [18]crown-6, perfluoro [15]crown-5 and perfluoro [12]crown-4 (1).

Perfluoro Crown Ethers

Perfluoro crown ethers have been synthetically inaccessible by conventional reactions of fluorocarbons and outside the capability of synthesis by fluorination using selective fluorination reagents. Examples of this potentially useful class of macrocycles have been prepared recently in our laboratory. These syntheses have been initially accomplished using the broadly applicable technique for controlling reactions of elemental fluorine (the La Mar process) developed in our laboratory. The reactions were conducted in the previously described cryogenic fluorination reactor (2).

Perfluoro crown ethers are very thermally and chemically stable. The reactions to produce perfluoro macrocycles are all illustrated in Figure 1. There are potential applications of such perfluoro macrocycles in biomedical

0097-6156/94/0555-0216\$08.18/0
© 1994 American Chemical Society

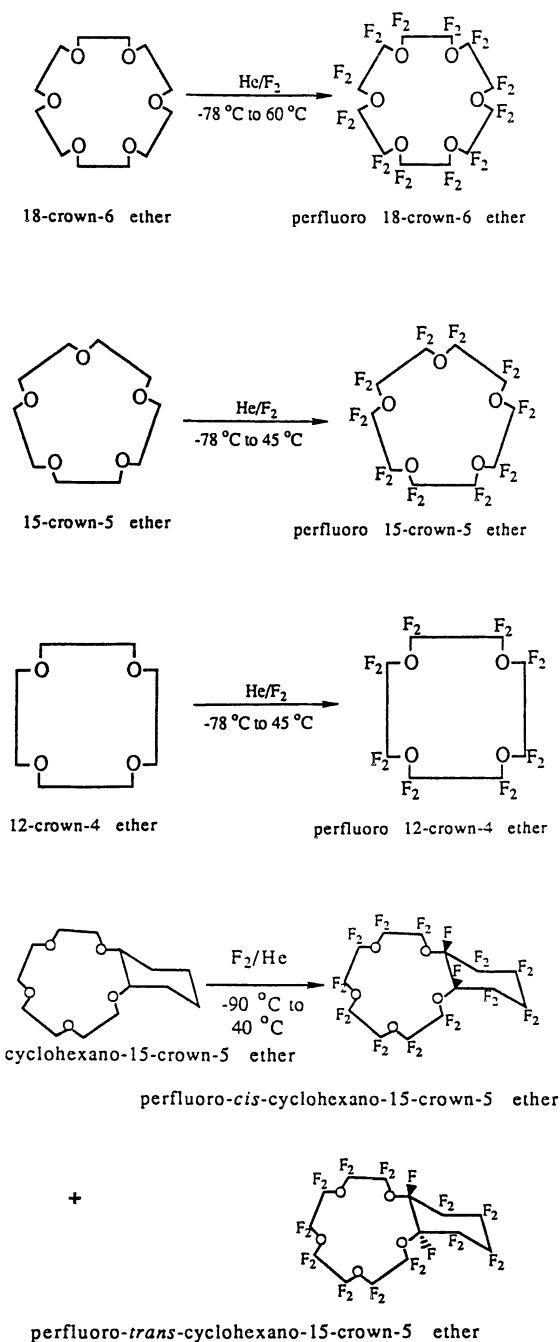
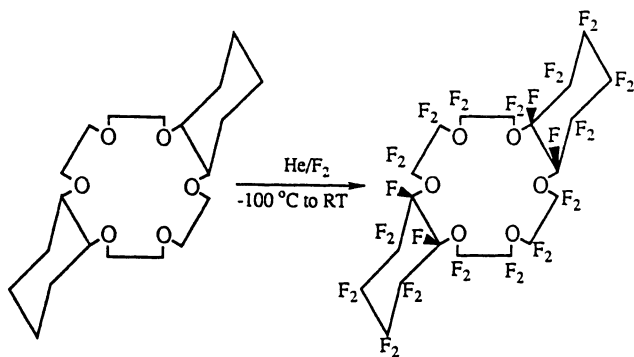
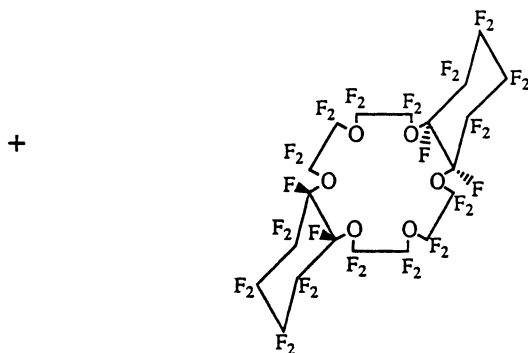
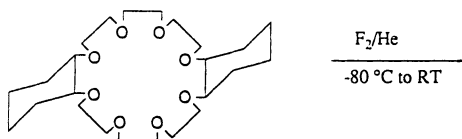
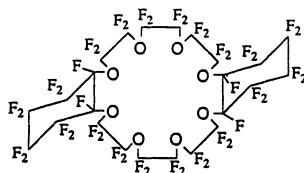


Figure 1. Reaction scheme for all compounds.
Continued on next page.

perfluoro-*cis-syn-cis*-dicyclohexano-18-crown-6 etherperfluoro-*cis-anti-cis*-dicyclohexano-18-crown-6 ether

dicyclohexano-24-crown-8 ether



perfluorodicyclohexano-24-crown-8 ether

Figure 1. *Continued.*

and catalytic chemistry. Properties and characterization of perfluoro [15]crown-5 and perfluoro [12]crown-4 are shown in Table I.

Perfluoro [15]Crown-5 Ether. Perfluoro crown ethers (1,3) are becoming very important as the molecules of choice for many ^{19}F NMR imaging applications (4) in humans and is particularly effective in brain and spinal diagnostics when administered to the cerebrospinal fluid compartment. Synthesis scale up for perfluoro [15]crown-5 (1-3) and plans for commercialization are underway while research is being conducted on other biological applications of these new compounds (5). In collaboration with Air Products, excellent brain imaging scans have been obtained by infusing perfluoro [15]crown-5 in the spinal fluids. Toxicology reports on these are very favorable; essentially no toxic effects physiologically were found in several studies involving different animals. There are some pharmaceutical companies actively negotiating to obtain licensing on perfluoro [15]crown-5 on which a composition of matter patent (3) has been obtained by our laboratory.

Perfluoro [18]Crown-6 Ether. The perfluoro [18]crown-6 ether analog has approximate C_2 symmetry, unlike [18]crown-6 which has C_1 symmetry (6), as illustrated with a view looking through the cavity of the molecule in Figure 2. The folding or puckering of the ring is seen in Figure 3.

The effects of perfluorinating [18]crown-6 show up very well in the shortened C-O bonds and lengthened C-C bonds. The average C-O bond length in perfluoro [18]crown-6 [1.376 (7) Å] is 0.034 Å shorter than the average C-O bond length in [18]crown-6 [1.411 (8) Å]. On the other hand, the perfluoro analog exhibits an average C-C bond length [1.539 (3) Å] that is 0.032 Å longer than the average value [1.507 (2) Å] in the nonfluorinated crown. The C-F bonds [average 1.334 (2) Å] are normal for disubstituted paraffinic C-F bonds (7). Bond angles at O and C are also affected considerably by the H/F exchange. The COC angles change from an average 113.5° to $121.1 (5)^\circ$ and the OCC angles change from 109.8° to $107.1 (2)^\circ$.

The distances between O atoms across the cavity (and related by the pseudo-2-fold axis) range from 4.416 (2) - 5.528 (2) Å. This is considerably more circular than [18]crown-6 which has a range of 4.27-6.97 Å. In [18]crown-6, two H atoms project into the cavity, such that their interatomic distance is only 3.04 Å. Figure 2 illustrates that not just one pair of F atoms but two pairs project into the cavity resulting in F-F distances of 3.012 Å and 2.932 Å. Figure 3 illustrates the packing. The closest intermolecular contacts are between F atoms, the shortest of which is 2.845 (2) Å.

Perfluoro cis-syn-cis- and cis-anti-cis-Dicyclohexyl[18]Crown-6 Ether. Very recently we have synthesized perfluoro crown ethers from the hydrocarbon dibenzo crown ether (see Figure 8) (10). We have prepared two interesting isomers of perfluorodicyclohexyl[18]crown-6 ethers (10), the cis-syn-cis and cis-anti-cis isomers. Their structures have also been established by X-ray crystallography.

Table I. Properties and Characterization of Perfluoro [15]Crown-5 and Perfluoro [12]Crown-4^a

	[15]Crown 5	[12]Crown-4
Boiling Point (°C)	146	118
IR (vapor phase) (cm ⁻¹)	1250(s)	1260(vs)
	1228(vs)	1188(vs)
	1158(vs)	1160(vs)
	745(m)	1080(m)
		825(m)
		745(br)
NMR (neat liquid)	¹⁹ F--91.8(s) ppm	¹⁹ F--90.0(s) ppm
	(ext. CFCl ₃)	(ext. CFCl ₃)
	¹³ C δ114.9(s)	¹³ C δ114.9(s)
Mass spectrum	580(C ₁₀ F ₂₀ O ₅ , M ⁺)	445(C ₈ F ₁₅ O ₄ , M ^{+-F})

^aSatisfactory elemental analyses (C,F) were obtained.

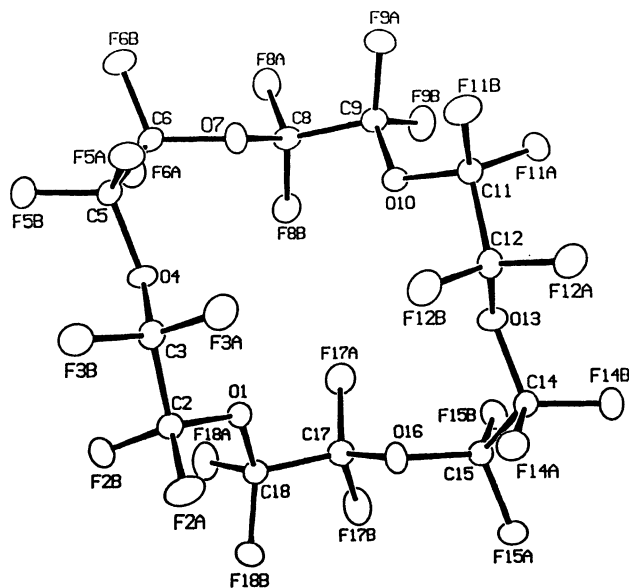


Figure 2. ORTEP drawing of perfluoro [18]crown-6 viewed through the cavity. Thermal ellipsoids are drawn at the 35% probability level.

The single crystals of each isomer were grown from the gas phase through condensation to a cold surface at 1 atm pressure (8). X-ray structures (9) show that the isomers have distinctly different solid state structures. The syn- isomer has a twisted-bent elliptical ring structure with two cyclohexano groups located at two ends while the anti- isomer has an elliptical ring structure with two cyclohexano groups symmetrically distributed on two sides (see Figures 4-7 for X-ray structures).

Perfluorocryptands

We have also reported the first perfluorocryptand molecule, the perfluorocryptand[2.2.2] (see Figure 9) (11). The perfluorocryptand is a very stable, inert, high boiling clear oil. While hydrocarbon crown ethers coordinate cations, both the perfluoro crown ethers and the new perfluorocryptand coordinate anions. Two manuscripts have recently appeared in collaboration with Professor Jennifer S. Brodbelt in which both perfluoro crown ethers and perfluorocryptands tenaciously encapsulate O_2 and F^- (11-12).

The perfluorocryptand[2.2.2] compound is expected to have a number of interesting applications. Aside from the possibility of acting as a perfluoro "host" for certain types of "guest" species, perfluorocryptand[2.2.2] has shown potential as a very clean, high mass compound for use as a mass spectral marker material (13). The compound is expected to be biologically inert (in contrast to the hydrocarbon analog), and as in the case of the perfluoro crown ether compounds, may be useful in fluorocarbon biological and medical applications where physiologically inert or oxygen carrying fluids are required. The ^{19}F NMR of the perfluorocryptand[2.2.2] is shown in Figure 10.

The basicities of the crown systems would be expected to decrease with an increased amount of fluorine substitution in the molecule. This trend is seen in the partially fluorinated cyclams (14) and is continued to the perfluoro crown ethers (1,15). The coordination chemistry, organometallic chemistry, and reaction chemistry of perfluorocryptands are being explored in collaboration with Professor Jean-Marie Lehn. Lehn provided the original hydrocarbon samples and suggested this project to us many years before we had developed the direct fluorination capability to the extent required to effect this synthesis. In addition, we have underway a collaborative project with Professor Leland C. Clark, Jr., in which we are exploring the physiological and biological properties of the new perfluorocryptand. The physiological applications of perfluorocryptand[2.2.2] will be published elsewhere.

Gas-Phase Reactions of Perfluoro Macrocyces

The coordination capabilities of perfluorinated macrocycles have generated considerable interest based on the properties of crown ethers and related macrocycles as model hosts in the field of molecular recognition (16-17). Numerous studies have described aspects of host-guest complexation of hydro crown ethers with a variety of model guests, including alkali metal ions and ammonium ions (18). Thus, the perfluorinated macrocycles provide an

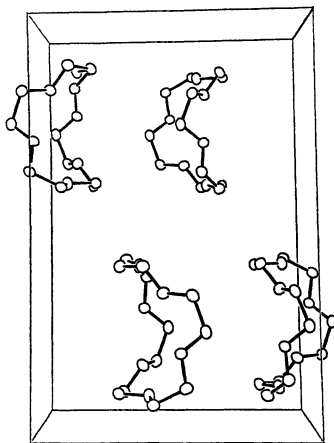


Figure 3. Packing diagram of perfluoro [18]crown-6 with F atoms removed as viewed along the a -axis. The c -axis is vertical and the b -axis is horizontal.

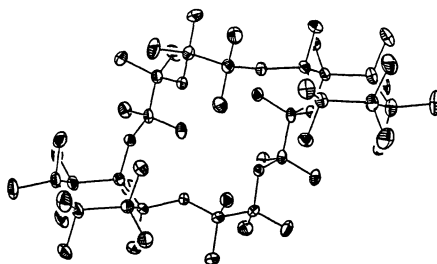


Figure 4. Single crystal X-ray structure of perfluoro -cis-syn-cis-dicyclohexyl[18]crown-6 ether.

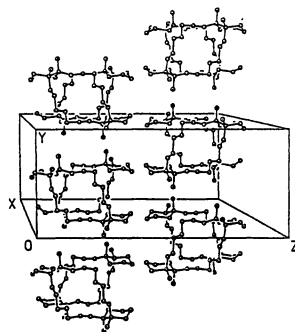


Figure 5. Unit cell packing of perfluoro-cis-syn-cis-dicyclohexyl-[18]crown-6 ether.

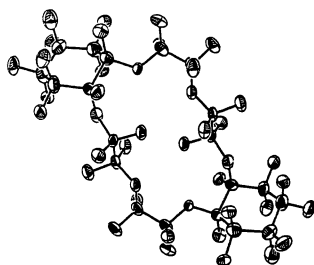


Figure 6. Single crystal X-ray structure of perfluoro-cis-anti-cis-dicyclohexyl[18]crown-6 ether.

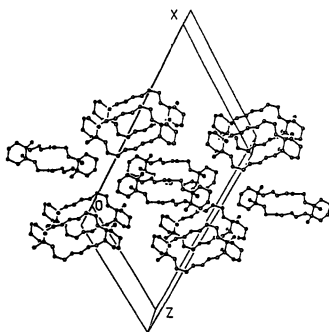


Figure 7. Unit cell packing of perfluoro-cis-anti-cis-dicyclohexyl[18]crown-6 ether.

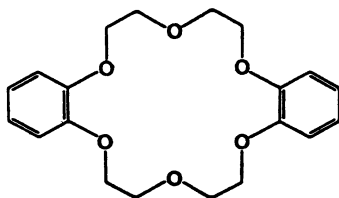


Figure 8. The dibenzo crown ether hydrocarbon starting material.

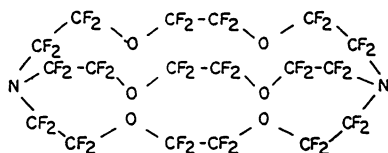


Figure 9. The perfluorocryptand[2.2.2].

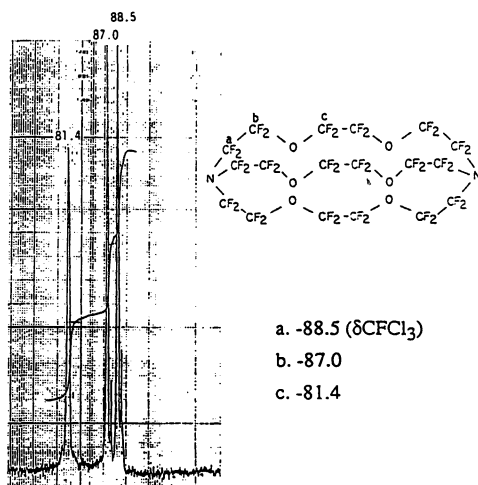


Figure 10. The ¹⁹F NMR of the perfluorocryptand[2.2.2]

intriguing structural analog to the hydrogenated macrocycles. Studies of these novel model hosts may reveal new insight into the structural and thermodynamic factors which mediate selective complexation. Recently, studies of host-guest chemistry in the solvent-free environment of the gas phase has opened a new frontier for the investigation of molecular recognition (11,12,19-22). Complexation may be evaluated in the absence of solvation effects, and thus the intrinsic binding properties of model hosts can be examined. Three studies of the gas-phase ion chemistry of perfluoro macrocycles are reviewed in the following section.

The high oxygen-carrying capacity of some perfluorocarbons makes them viable as artificial blood components (23), and yet to date the mechanism of oxygen binding to fluoro ethers is not well understood. Thus, it was of considerable interest to probe the ability of perfluoro macrocycles to bind molecular oxygen and other small molecules in the gas phase in order to obtain new information about the binding affinities of these compounds (11). For these studies, each perfluoro macrocycle was admitted into the source of a triple quadrupole mass spectrometer. Argon was introduced into the source manifold at $2-3 \times 10^{-6}$ torr to aid in the production of thermal electrons for electron capture negative ionization. The desired reagent gas (CO , N_2 , CO_2 , air for O_2) was added to attain a total source pressure of 1-2 torr. The ethers examined included perfluoro [12]crown-4, perfluoro [15]crown-5, perfluoro [18]crown-6, perfluorinated 4,7,13,16,21,24-hexaoxa-1,10-diazabicyclo[8.8.8]hexacosane (cryptand), their hydro crown analogs, and one acyclic perfluoro ether, perfluoro-triethylene glycol dimethyl ether.

Each perfluoro macrocycle was ionized to form M^- then allowed to react with O_2 to successfully form $(\text{M} + \text{O}_2)^-$ adducts (11). Ion/molecule reactions involving an acyclic perfluoro ether and hydrogenated crown ethers were also examined to determine whether the cyclic and/or perfluoro nature of the macrocycles played a role in the formation of the $(\text{M} + \text{O}_2)^-$ adducts. Neither the perfluoro acyclic analog nor hydrogenated crown ethers reacted with O_2 to form $(\text{M} + \text{O}_2)^-$ adduct ions. This result confirmed that the macrocyclic nature of the perfluoro crown ethers enhanced their ability to bind O_2 .

Additionally, the ability of the perfluoro crown ethers to form complexes with CO , N_2 , CO_2 , and Ar, species with similar sizes and some similar chemical and physical properties as O_2 , was examined. Adducts with these species were not observed (11). Thus, the tendency of the perfluoro crown ethers to form adducts exhibited striking selectivity for O_2 only.

Structural details of the perfluoroether adduct ions, $(\text{M} + \text{O}_2)^-$, were probed via collisionally activated dissociation (CAD) of the mass-selected ions (11). Figure 11 illustrates the 40 eV CAD spectra of the perfluoro 15-crown-5 $(\text{M} + \text{O}_2)^-$ adduct (m/z 612), showing two series of fragment ions. One is a series of losses of $(\text{C}_2\text{F}_4\text{O})_n$, analogous to the series of losses observed from the M^- ion, resulting in fragment ions at m/z 148, 264, 380, and 496. This trend indicates that the O_2 is bound to the perfluoro crown ether strongly enough to be retained after the adduct ion is activated and implies that the binding interaction must be at least as strong as the C-C and C-O bonds that are cleaved during the competing dissociation processes in which $\text{C}_2\text{F}_4\text{O}$ units are

expelled. The C-C and C-O bond energies for these perfluoro crown ethers have been estimated as 84 and 98 kcal/mole, respectively. Additionally, a series of fragment ions corresponding to loss of $[n(C_2F_4O) + O_2]$ units is seen as m/z 232, 348, and 464, where $n = 3, 2, 1$, the same fragment ions produced from CAD of the non-complexed molecular ion as shown in Figure 12.

Direct loss of O_2 is not a significant dissociation channel using any collisional activation conditions (for 10-120 eV kinetic energy collisions, the percentage of the total fragment ion abundance due to O_2 loss is 0 - 10%). This result suggests that the O_2 -crown ether complex is not a loosely bound adduct, but instead a species in which stronger bonding forces are involved than those associated with a single weak ion/dipole electrostatic interaction. An adduct species in which O_2 is cradled by four electronegative fluorine atoms is feasible. In general, O-F bonds are not stronger than 50 kcal/mole, so a complex containing a single F- O_2 binding interaction is not supported.

It was also timely to examine the ability of perfluoro macrocycles to react with fluoride in the gas phase (12). It has been shown recently from crystallographic studies that a fluoride ion may be held in the cavity of a fluorinated macrocyclic vinyl polymer (24), and thus it was of interest to investigate the possibility of forming related fluoride complexes in the gas phase. Fluoride/macrocyclic adducts were successfully generated in the gas phase by ionization of a mixture of a macrocycle and a fluorinated reagent such as CHF_3 admitted simultaneously into the ion source. Moderately abundant $(M + F)^-$ adducts (relative abundance = 10% compared to M^-) are formed by reaction of F^- with the macrocyclic molecules. The CAD spectrum of the $(M + F)^-$ adduct of perfluoro [15]crown-5, shown in Figure 13, is similar to the CAD spectrum for the molecular anion M^- of perfluoro [15]crown-5 shown in Figure 12, with the exception that each fragment ion is shifted to a higher mass by 19 amu (due to the fluorine addition). The series of ions incorporating the additional fluorine is the only type of fragment observed, indicating that the fluorine is *always* retained by the ionic portion during dissociation. The most abundant dissociation processes involve loss of two or three C_2F_4O units. The direct loss of F^- from the $(M + F)^-$ adduct is not observed. This result suggests a very strong crown ether-fluoride binding interaction. For example, the fluoride ion may attack the least nucleophilic carbon position and promote ring opening, resulting in a branched monocyclic structure with a covalently bound fluorine. A mechanism depicting this proposed pathway is shown in Scheme 1.

In the third gas-phase study (24), a new type of cluster ion consisting of a perfluorinated macrocycle (M) associated with multiple ether molecules was generated in the source of a triple quadrupole mass spectrometer. The clusters have the general formula $(M - F + nEther)^+$ where $n = 1, 2, 3, \dots$ depending on the type of ether. The ethers which promoted the most extensive clustering were highly strained cyclic ethers such as ethylene oxide and ethylene sulfide, whereas the perfluoro macrocycles attached only one unit of the acyclic ether analogs, such as dimethyl ether. Collisionally activated dissociation of the cluster ions revealed that the ether units were eliminated sequentially, indicating that the ether molecules are attached separately around the perfluoro

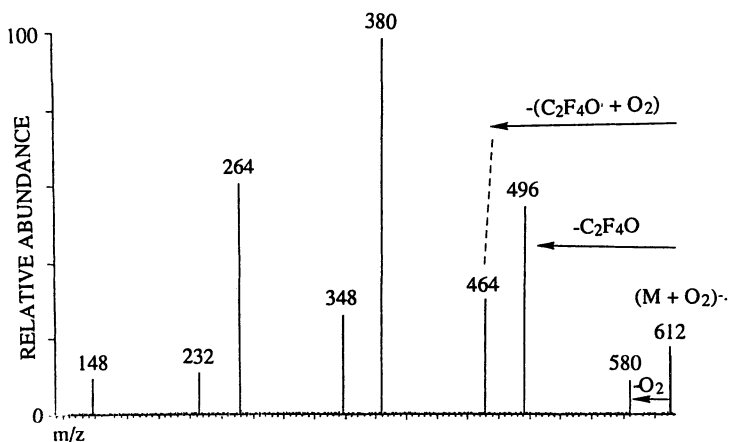


Figure 11. Collisionally activated dissociation mass spectra of the $(M + O_2)^-$ ion of perfluoro [15]crown-5 acquired with a triple quadrupole mass spectrometer.

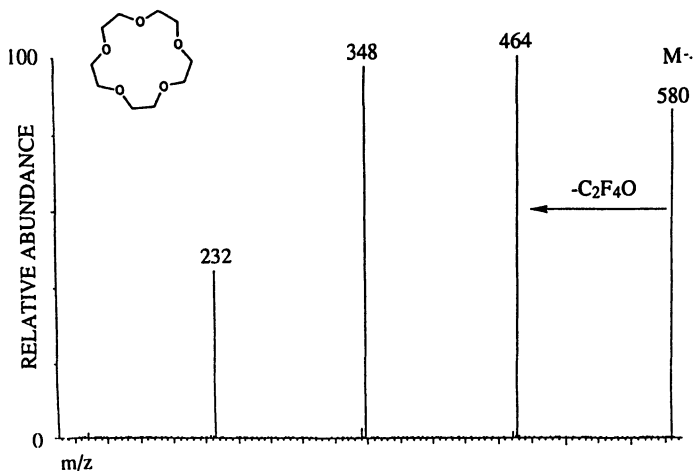


Figure 12. Collisionally activated dissociation mass spectra of the M^- ion of perfluoro [15]crown-5 acquired with a triple quadrupole mass spectrometer.

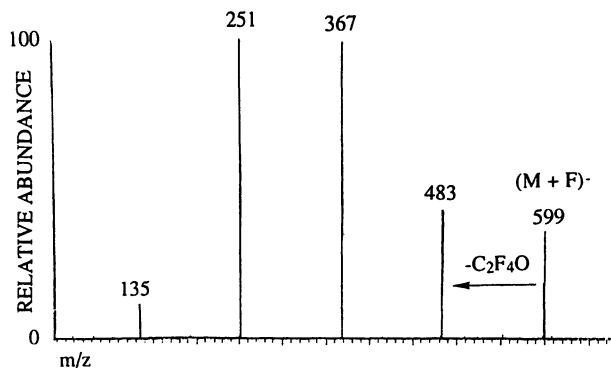
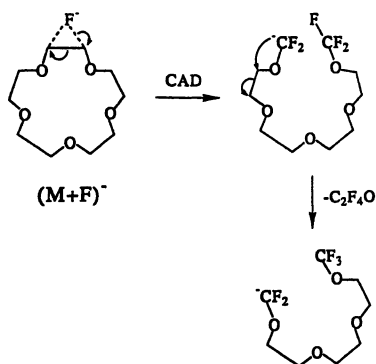


Figure 13. Collisionally activated dissociation mass spectra of the $(M + F)^-$ ion of perfluoro [15]crown-5 acquired with a triple quadrupole mass spectrometer.



Scheme 1. Proposed mechanism for dissociation of the $(M + F)^-$ adduct.

macrocyclic ion. The nature of the binding interactions in these novel types of cluster assemblies is still under investigation.

The ability to form and characterize new types of macrocyclic ion complexes involving perfluoro ethers holds great promise for future studies of host-guest complexation in the gas phase. Comparisons to the gas-phase chemistry of hydrogenated macrocycles may allow further insight into the influence of thermochemical and structural properties on the binding interactions of host molecules. All of the perfluoro crown ethers and perfluorocryptands to date have been found to coordinate O_2^- and F^- as well as some other anions (24).

Mass Spectrometric Characterization by Collisionally Activated Dissociation

The structures of the perfluoro macrocycles were further characterized by CAD mass spectrometric techniques. CAD is a method in which a mass-selected ion undergoes energetic collisions with a neutral target gas, resulting in fragmentation of the ion by structurally diagnostic pathways (25). The acquisition of characteristic CAD spectra is especially important for the interpretation of the gas-phase macrocyclic complexation studies described earlier. For the CAD spectra discussed in this section, a Finnigan MAT TSQ-70 triple stage quadrupole mass spectrometer was operated in both negative and positive ionization modes at a source temperature of 80 °C. For the negative ionization mode, methane or argon was introduced into the source at 1.2 torr to aid in the production of thermal electrons to promote electron capture negative ionization.

Each perfluorinated crown ether produced $(M - F)^+$ ions under positive chemical ionization conditions, likely as a result of elimination of HF from an initial $(M + H)^+$ ion (26). These positive ions dissociate via two routes upon collisional activation. They may eliminate units of C_2F_4O or they may eliminate $(C_2F_2O_2 + nC_2F_4O)$ where $n = 0, 1, 2, \dots$. In the negative ion mode, the perfluoro crown ethers produce abundant anions, M^- , which dissociate by a characteristic series of losses (26). For example, a typical CAD spectrum for perfluoro [15]crown-5 is shown in Figure 12. In general, the molecular radical anion of each perfluoro crown ether dissociates by loss of $n(C_2F_4O)$ units ($n = 1, 2, 3$).

The perfluorinated 4,7,13,16,21,24-hexaoxa-1,10-diazabicyclo[8.8.8]-hexacosane (cryptand) dissociates by several pathways that are analogous to those noted for the crown ethers: elimination of nC_2F_4O units are predominant, where $n = 1, 2, 3$, resulting in ions at m/z 908, 792, and 676 (26). Additionally, losses of two or three C_2F_4O units in conjunction with C_4F_9N elimination are observed as fragment ions at m/z 559 and 443. These latter fragments are evidence of cleavage at the nitrogen bridge.

The CAD spectra of the molecular anions of two perfluoro dicyclohexyl crown ethers, the [18]crown-6 and [24]crown-8 ethers, also show characteristic fragmentation patterns (26). The CAD spectrum for the first one is shown in Figure 14. For these substituted perfluoro crown ethers, the molecular anions do not dissociate via simple loss of C_2F_4O units as was observed for the other

macrocycles. Instead, elimination of $C_6F_{11}^{\cdot}$ (cyclohexyl ring) is a predominant process and may then be coupled with losses of $n(C_2F_4O)$. The first process may be rationalized as a radical-initiated ring cleavage, followed by a fluorine transfer to the cyclohexyl ring via a four-membered transition state. The resulting fragment ion is presumably acyclic. This fragment ion then proceeds to dissociate by consecutive losses of C_2F_4O units. For the [18]crown-6 ether shown in Figure 14, losses of up to three units of C_2F_4O are observed in conjunction with loss of C_6F_{11} (formation of m/z 391, 507, 623, 739). Additionally, loss of $3(C_2F_4O)$ is observed coupled to the loss of both C_6F_{11} , the first cyclohexyl ring, and C_4F_6 , the second cyclohexyl ring, resulting in formation of m/z 229. For the analogous [24]crown-8 system, this latter pathway is coupled instead to the loss of $4(C_2F_4O)$ units.

Discussion

Two large scale syntheses using solvent reactors of a new design recently developed (27) by Lagow and associates at Exflur Research Corporation have made possible the synthesis of kilogram quantities of perfluoro macrocycles in near quantitative yield. For example, two kilograms of the promising ^{19}F NMR agent perfluoro [15]crown-5 have been recently prepared for a biomedical industrial firm interested in NMR imaging.

Perfluorinated derivatives of hydrocarbon compound usually exhibit different properties than their hydrocarbon analogues. The perfluoro crown ethers are markedly more volatile than the hydrocarbon products. One would expect the dimensions of the pocket size to change and both modeling and crystal structures clearly establish that the pockets are smaller and the crown ether rings are slightly more bent. As observed in the gas phase studies, perfluoro crown ethers and cryptands all coordinate O_2^- , F^- and several other such anions. We have a collaboration with Jean-Marie Lehn at Louis Pasteur University in Strasbourg to explore this anion work on a macroscopic scale. Interestingly, sometime before this discovery, Jean-Marie Lehn had predicted during visits to the Lagow laboratory perhaps as early as 1975 that anions rather than cations would be the most favorable species to encapsulate in perfluorinated crown ethers (28). Although a crystal structure of an encapsulated species is not yet in hand from Professor Lehn's group, perfluoro crown ethers and cryptands are indeed very weak bases; if there is any base character at all. It would also appear that electron density from the anion is transferred to the binding sites in the crown ether. One would suspect that the binding occurs at the oxygen atoms. As indicated by the fragmentation thermodynamics, there is a 40-60 kcal interaction binding the anion to the macrocycle. Lehn's insight at such an early date was indeed remarkable.

Whether the perfluoro macrocycles are also capable of binding cations is still not certain. Two talented collaborators on this project have not been successful in obtaining cationic complexes with the alkali metals. One complication was that the perfluoro macrocycles are not soluble in common organic solvents. On the other hand, both organometallic compounds and organic species as well as these perfluoro macrocycles are soluble in

chlorofluoro solvents such as Freon 113, $F_2ClC-CF_2Cl$. It is also quite possible that the base character of such perfluoro macrocycles is nonexistent.

The single crystal X-ray diffraction studies of [18]crown-6 ether indicate that the ring is puckered in a manner so that the oxygen site are exposed and projected toward a metal coordinate site. In view of the possibility of a rigid conformation existing in the solution at lower temperature, the ^{19}F spectrum of perfluoro [18]crown-6 in $CFCl_3$ has been monitored at $-85^\circ C$. Only one singlet peak was observed. This fact reveals that the molecule is quite flexible in the solution. The energy barrier associated with the conformational change would be extremely low.

Three crystal structures of perfluoro crown ethers containing the [18]crown-6 ether skeleton are reported. Comparisons of these structures show that the perfluoro [18]crown-6 ether and the *cis-syn-cis*-dicyclohexyl-isomer have similar conformations of the ether ring skeleton (29). Figure 15 shows the superposition of the carbon and oxygen atoms of the perfluoro *-cis-syn-cis*-dicyclohexyl[18]crown-6 ether (solid lines) onto the equivalent atoms of perfluoro [18]crown-6 ether (dashed lines) illustrating the similar configuration of the perfluoro ether rings of the two structures. The perfluorocyclohexyl groups may not be the dominating steric factor which controls the conformation of their ether ring skeleton. Distances between oxygen atoms and the center of the molecule, and between adjacent oxygen atoms in both isomer are given in Table II and Table III.

Although perfluoro [18]crown-6 has a melting point of $34^\circ C$ in a sealed capillary, the solid compound has a substantial vapor pressure; it can be sublimed easily and moves on a vacuum line. Perfluoro [18]crown-6 has a marked propensity to form large and beautiful single crystals. Crystals weighing at least one half gram which have the appearance of sparkling zircons are obtained routinely. Both the perfluoro [15]crown-5 and [12]crown-4 species are clear liquids with properties favorable for several biomedical applications.

As previously discussed, perfluoro [15]crown-5 has great potential as a ^{19}F NMR imaging agent (4). This crown ether has only one fluorine resonance making very sharp pictures during brain scans and spinal scans of animals possible. Perfluoro [15]crown-5 is also used successfully as an oxygen carrier in collaborative studies between our group and Dr. Leland Clark's laboratory. Work at Air Products has established that the perfluoro crown ethers are nontoxic in animals and are therefore very different from hydrocarbon crown ethers.

As previously indicated, a sample of over two kilograms in size of perfluoro [15]crown-5 has been made by new technology at Exfluor Research Corporation in Austin, Texas (27). With new reaction technology the yields are on this substance are in the high ninety percent range and large quantities are possible. This opens the possibility of preparing any of the materials in this manuscript on a commercial scale.

The perfluorocryptand[2.2.2] compound is expected to have interesting applications, and we await with great interest further studies of its reaction chemistry.

The synthetic breakthroughs which have been responsible for these macrocycles open the possibility of preparation of many novel crown ether

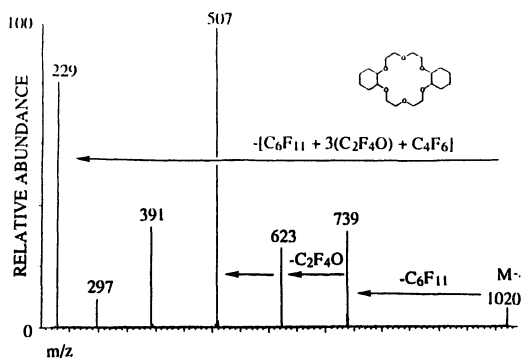


Figure 14. Collisionally activated dissociation mass spectra of the M^+ ion of perfluoro dicyclohexyl[18]crown-6 acquired with a triple quadrupole mass spectrometer.

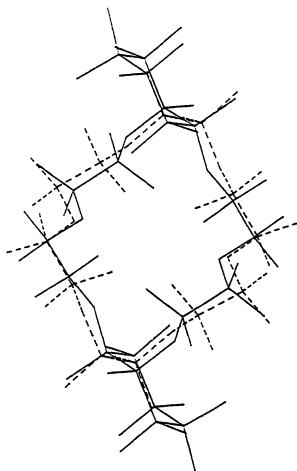
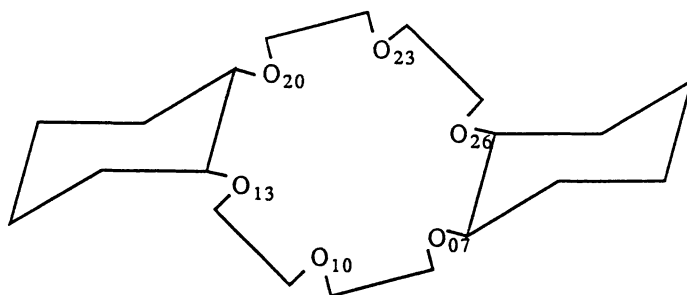


Figure 15. The superposition of the carbon and oxygen atoms of the perfluoro -cis-syn-cis-dicyclohexyl[18]crown-6 ether (solid lines) onto the equivalent atoms of perfluoro [18]crown-6 ether (dashed lines) illustrating the similar configuration of the perfluoro ether rings of the two structures.

Table II. Distances Between Oxygen Atoms and the Center of the Molecule, and Between Adjacent Oxygen Atoms in Perfluoro -cis-syn-cis-Dicyclohexyl-[18]Crown-6 Ether



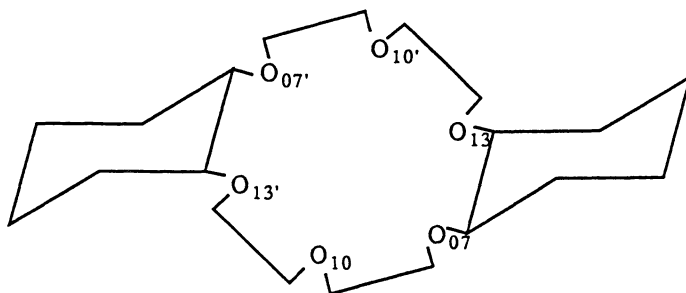
Perfluoro -cis-syn-cis-Dicyclohexyl[18]crown-6 ethers

<u>Oxygen Atoms</u>	<u>Distance to center of molecule</u>
O ₀₇	2.536 Å
O ₁₀	2.129 Å
O ₁₃	3.177 Å
O ₂₀	2.543 Å
O ₂₃	2.141 Å
O ₂₆	3.181 Å

Distances between adjacent oxygen atoms

O ₁₃ -O ₂₀	2.662 Å
O ₂₀ -O ₂₃	2.713 Å
O ₂₃ -O ₂₆	2.665 Å
O ₂₆ -O ₀₇	2.667 Å
O ₀₇ -O ₁₀	2.707 Å
O ₁₀ -O ₁₃	2.667 Å

Table III. Distances Between Oxygen Atoms and the Center of the Molecule, and Between Adjacent Oxygen Atoms in Perfluoro-cis-anti-cis-Dicyclohexyl-[18]Crown-6 Ether



Perfluoro -cis-anti-cis-Dicyclohexyl[18]crown-6 ethers

<u>Oxygen Atoms</u>	<u>Distance to center of molecule</u>
O ₀₇	3.156 Å
O ₁₀	2.403 Å
O ₁₃	3.332 Å

Distances between adjacent oxygen atoms

O ₁₃ -O ₀₇	2.702 Å
O ₀₇ -O ₁₀	3.525 Å
O ₁₀ -O ₁₃	2.727 Å

systems as well as the synthesis of the entire series of perfluorocryptands. Such high stability ligands will be much less subject to chemical attack, much less prone to thermal degradation, and as such offer unique properties as ligands.

Acknowledgment

We are grateful for support of this work by the Air Force Office of Scientific Research (F49620-92-J-O104), U.S. Department of Energy (DE-FG05-91ER12119), and NATO (Grant 87006). We also (RJL) acknowledge an Alexander von Humboldt Award (1992).

Literature Cited

- (1) Lin, W. H.; Bailey, W. I., Jr.; Lagow, R. J. *J. Chem. Soc., Chem. Commun.* **1985**, 1550.
- (2) Margrave, J. L.; Lagow, R.J. *Prog. Inorg. Chem.* **1979**, *26*, 161.
- (3) Lin, W. H.; Lagow, R. J. U.S. Patent 4 570 005, 1986.
- (4) Schweighardt, F. K.; Rubertone, J. A. U.S. Patent 4 838 274, 1989.
- (5) Lin, T. Y.; Clark, L. C., Jr.; Lagow, R. J. to be published.
- (6) Dunitz, J. D.; Seiler, P. *Acta Cryst.* **1974**, *B30*, 2739.
- (7) International Tables for X-ray Crystallography, Vol. III, p 275.
- (8) This was accomplished during the purification process using preparatory gas chromatography.
- (9) Data for perfluoro cis-syn-cis- and cis-anti-cis-dicyclohexyl[18]crown-6 were collected at -75 °C on a Nicolet R3 diffractometer with Mo K α radiation ($\lambda = 0.7107 \text{ \AA}$) using a graphite monochromator. Perfluoro cis-syn-cis-dicyclohexyl[18]crown-6 is monoclinic, space group C2/c, with a 27.051 (2), b = 10.087 (1), c = 23.526 (3) \AA , $\beta = 100.920 (8)^\circ$, V = 6303.5 (11) \AA^3 , with $\rho(\text{calc}) = 2.15 \text{ g cm}^{-3}$ for Z = 8. The structure was solved by direct methods and refined by full-matrix least-squares to R = 0.042, wR = 0.044 using 3959 reflections with $F_o > 4(\sigma(F_o))$. Perfluoro -cis-anti-cis-dicyclohexyl[18]crown-6 is also monoclinic, space group C2/c, with a = 32.211 (5), b = 6.0477 (6), c = 18.828 (3) \AA , $\beta = 124.782 (9)^\circ$, V = 3012.4 (8) \AA^3 , with $\rho(\text{calc}) = 2.25 \text{ g cm}^{-3}$ for Z = 4. The molecule lies around a crystallographic inversion center. The structure was solved by direct methods and refined by full-matrix least-squares to R = 0.096, wR = 0.11 using 1832 reflections with $F_o > 4(\sigma(F_o))$.
- (10) Lin, T. Y.; Lagow, R. J. *J. Chem. Soc., Chem. Commun.* **1991**, 12.
- (11) Brodbelt, J.; Maleknia, S. D.; Lin, T. Y.; Lagow, R. J. *J. Am. Chem. Soc.* **1991**, *113*, 5913.
- (12) Brodbelt, J.; Maleknia, S. D.; Lin, T. Y.; Lagow, R. J. *J. Chem. Soc., Chem. Commun.* **1991**, 1705.
- (13) Maleknia, S. D.; Clark, W. D.; Lagow, R. J. Presented at the 36th ASMS Conference on Mass Spectrometry and Allied Topics, San Francisco, CA, June 1988.
- (14) Shinkai, S.; Torigoe, K.; Manabe, O.; Kajiyama, T. *J. Am. Chem. Soc.* **1987**, *109*, 4458.

- (15) Lin, W. H.; Bailey, W. I., Jr.; Lagow, R. J. *Pure Appl. Chem.* **1988**, *60*, 473.
- (16) (a) Lehn, J. *Angew. Chem., Int. Ed. Engl.* **1988**, *27*, 89. (b) Cram, D. *Science* **1988**, *240*, 760.
- (17) (a) Hiroaka, M. *Crown Compounds*; Kodansha Scientific, Tokyo, 1978. (b) Izatt, R.M.; Christensen, J. S. *Progress in Macrocyclic Chemistry*; Wiley, New York, NY, 1979; Vol. 1.
- (18) Pederson, C. J. *J. Am. Chem. Soc.* **1970**, *92*, 391.
- (19) Maleknia, S.; Brodbelt, J. *J. Am. Chem. Soc.* **1992**, *114*, 4295.
- (20) Liou, C. C.; Brodbelt, J. *J. Am. Chem. Soc.* **1992**, *114*, 6761.
- (21) Liou, C. C.; Brodbelt, J. *J. Am. Soc. Mass Spectrom.* **1992**, *3*, 543.
- (22) Zhang, H.; Chu, I.; Leming, S.; Dearden, D. A. *J. Am. Chem. Soc.* **1991**, *113*, 7415.
- (23) Reiss, J.; LeBlanc, M. *Angew. Chem., Int. Ed. Engl.* **1978**, *17*, 621.
- (24) Brodbelt, J. S.; Liou, C. C.; Maleknia, S. D.; Lin, T. Y.; Lagow, R. J. to be published.
- (25) Busch, K. L.; Glish, G. L.; McLuckey, S. A. *Techniques and Applications of Tandem Mass Spectrometry*; VCH, 1988.
- (26) Maleknia, S.; Liou, J.; Brodbelt, J. *Org. Mass Spectrom.* **1991**, *26*, 997.
- (27) Bierschenk, T. R.; Juhlke, T. J.; Kawa, H.; Lagow, R. J. U.S. Patent 5 093 432, 1992.
- (28) Private communication from Jean-Marie Lehn to RJL.
- (29) Lin, T. Y.; Lynch, V. M.; Lagow, R. J. unpublished results.

RECEIVED October 1, 1993

Chapter 14

Alkali Metal Polyhydrogen Fluorides Useful Halogen-Exchange Media

Richard E. Fernandez¹ and Joseph S. Thrasher²

¹DuPont Specialty Chemicals, Jackson Laboratory, DuPont,
Deepwater, NJ 08023

²Department of Chemistry, The University of Alabama, P.O. Box 870336,
Tuscaloosa, AL 35487-0336

Alkali metal polyhydrogen fluoride systems, $MF \cdot nHF$ where $M = K, Rb, Cs$ or mixtures thereof and $n = 0.5 - 3$ are versatile fluorination media for halogen exchange reactions. The chemical and physical properties of these systems will be discussed as well as their applicability towards fluorocarbon synthesis.

Alkali metal fluorides are well known as traditional halogen exchange or nucleophilic substitution reagents (1-5). Typically polar aprotic solvents such as *N,N*-dimethylformamide, *N,N*-dimethylacetamide, acetonitrile, tetrahydrofuran, glymes, etc. are required. In addition, crown ethers are often added to increase the solubility of the alkali metal fluorides and thereby the halogen exchange reaction rate. The order of reactivity is $Cs > Rb > K > Na$ for the alkali metals and $1^0 > 2^0$ for the electrophilic carbon center.

From an industrial point of view these traditional halogen exchange media present a number of severe limitations. First, alkali metal fluorides, especially cesium fluoride, are expensive and are generally not recovered. Crown ethers are also expensive and difficult to recover in addition to being toxic. Recovery and disposal problems are also of concern with any of the aforementioned aprotic solvents. And perhaps the most severe limitation of all is the fact that these halogen exchange media can only be used in a batch mode of operation.

The Concept

While it is known that alkali metal bifluorides are poor traditional halogen exchange reagents they should be good "solvents" for alkali metal fluorides. If we consider the simplest case where the cations of the solvent and solute are the same then the "n" value, the molar ratio of HF to alkali metal cation, describes the system. Hence a value of "n" < 1 describes a basic or nucleophilic system, a value of "n" = 1 describes a "neutral" system, and a value of "n" > 1 describes an acidic system. The "free

¹Corresponding author

0097-6156/94/0555-0237\$08.00/0
© 1994 American Chemical Society

In Inorganic Fluorine Chemistry; Thrasher, J., et al.;
ACS Symposium Series; American Chemical Society: Washington, DC, 1994.

fluoride" concentration or the melt basicity can be readily controlled by HF addition/removal. And since polyhydrogen fluorides are always in thermal equilibrium with the metal fluoride and HF, temperature can be used as a control as well.



Thus the alkali metal polyhydrogen fluorides are "participatory solvents," able to generate, *in situ*, the required reagents for traditional alkali metal fluoride halogen exchange. Further the solubilized alkali metal chloride product from the halogen exchange reaction should be easily regenerated to the alkali metal fluoride by addition of HF and removal of HCl.

It was of interest to apply this concept to the synthesis of CFC alternatives, and as such the reaction sequence can be written as a repetitive loop between equations 2 and 3, the organic reaction and the inorganic or regeneration reaction, respectively. Before moving to experimental results it is informative to examine both

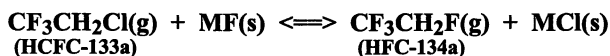


the thermodynamics and literature precedents for these two reactions.

Thermodynamics and Early References

The utility of alkali metal fluorides in halogen exchange reactions has already been documented. It is also a well-established fact that cesium is most effective and lithium least effective for the transformation of an R-Cl bond to an R-F bond. This is largely due to the minimization of the difference in lattice energies between MF and MCl coupled with the increased R-X bond strength (3,6). A pertinent example is the reaction of HCFC-133a to HFC-134a as shown in Table I (7-11) where the $\log_{10}K_p$ values clearly show the advantage of the larger cation.

Table I. Organic Reaction



MF	ΔH°_r , kJ/mole	ΔG°_r , kJ/mole	$\text{Log}_{10}K_p$
HF	24.8	24.5	-4.3
LiF	54.7	51.2	-9.0
NaF	10.3	7.7	-1.3
KF	-22.1	-23.2	4.1
RbF	-31.7	-32.7	5.7
CsF	-42.2	-42.4	7.4

For the inorganic regeneration reaction (eq 3) the situation is not so clear. Nowhere in the literature is it documented which alkali metal chloride can be most easily or efficiently converted to the corresponding alkali metal fluoride. A similar thermodynamic analysis for this reaction as shown in Table II (8,11) indicates a preference for the smaller cation. This is in contrast to the requirement of the organic

Table II. Inorganic Reaction - Alkali Metal Fluoride Regeneration

$$\text{MCl(s)} + \text{HF(g)} \rightleftharpoons \text{MF(s)} + \text{HCl(g)}$$

MCl	ΔH°_r , kJ/mole	ΔG°_r , kJ/mole	$\text{Log}_{10}K_p$
LiCl	-28.4	-25.3	4.4
NaCl	16.0	18.3	-3.2
KCl	48.4	49.2	-8.6
RbCl	57.9	58.6	-10.3
CsCl	68.4	68.4	-12.0

reaction for a larger cation. However, one must also consider the formation of polyhydrogen fluorides during the regeneration reaction if more than one equivalent of HF is used. As shown in Table III (8,9,11) for the alkali metal bifluorides, the regeneration reaction is then more favored in all cases, which can be rationalized by the well-known exothermicity of the reaction between alkali metal fluorides and hydrogen fluoride (bifluoride formation). While these data suggest larger cations could be used, the trend of favoring the smaller cation still predominates. One should bear in mind that these very approximate thermodynamic calculations are for room temperature gas-solid reactions and as such should only be used as a guide. To obtain more quantitative values one must include corrections for temperature, phases, heats of solution, etc. Unfortunately, the data required to make these corrections are not readily available.

Table III. Inorganic Reaction - Alkali Metal Bifluoride Regeneration

$$\text{MCl(s)} + 2 \text{HF(g)} \rightleftharpoons \text{MHF}_2\text{(s)} + \text{HCl(g)}$$

MCl	ΔH°_r , kJ/mole	ΔG°_r , kJ/mole	$\text{Log}_{10}K_p$
LiCl	-81.3	-36.9	6.5
NaCl	-56.4	-14.1	2.5
KCl	-41.8	-0.3	0.1
RbCl	-34.5	6.2	-1.1
CsCl	-28.2	9.5	-1.7

On the other hand, literature references dating as early as 1869 have shown that alkali metal chlorides can be converted to alkali metal fluorides in the presence of HF. Gore (12) described the reaction between the chlorides of lithium, sodium, potassium, and ammonium as strong in action with effervescence and solution. Fredenhagen (13) has shown that potassium fluoride can be produced in quantitative yield from the reaction of potassium chloride with excess hydrogen fluoride. Hood and Woyski (14) gave the first indication that the regeneration reaction could be carried out more efficiently at room temperature rather than at elevated temperatures. For example, they reported that sodium chloride reacted with anhydrous hydrogen fluoride at room temperature to form solvated sodium fluoride, while no reaction was observed at 200 °C.

Results - Organic Reaction

We have found that alkali metal polyhydrogen fluoride melts possess a wide range of synthetic utility including substitution reactions, HF addition reactions, and HX elimination reactions (15-17). The utility of a specific melt is governed primarily by the cation and the value of "n" of the melt. Generally, Cs/K mixtures are more effective than pure Cs melts, which are better than pure K melts, which are in turn better than Cs/Na melts. Sodium bifluoride does not melt but decomposes on heating to sodium fluoride and hydrogen fluoride. The value of "n" of a melt determines its melting point and HF vapor pressure at a given temperature. This value is also useful in generalizing the kinds of reactivity towards organics that a specific melt possesses. If it is desired to affect a halogen exchange, i.e. fluoride for chloride, then values of "n" in the range of 0.5 to 1.5 are usually most effective. If it is desired to affect the addition of HF to an olefinic species, then values of "n" greater than 1.5 are usually most effective. If it is desired to affect the elimination of HX to form an olefinic species, then values of "n" less than 0.5 are usually most effective. It should be noted that optimization of the desired transformation depends on the cation, value of "n," temperature and most importantly on the properties of the organic substrate. Optimum reaction conditions to effect a substitution reaction on one substrate may give predominantly elimination products when a different substrate is used. Table IV

Table IV. Substitution and Addition Reactions

Substrate	Cation	"n"	Temp (°C)	Product	Conversion	Selectivity
CF ₃ -CH ₂ Cl	Cs/K	0.8	300	CF ₃ -CH ₂ F	100 %	96 %
CF ₃ -CH ₂ Cl	Cs	1.0	300	CF ₃ -CH ₂ F	98 %	99 %
CH ₂ Cl-CH ₂ Cl	Cs	1.0	204	CH ₂ F-CH ₂ F	90 %	70 %
CHF ₂ -CCl ₂ H	Cs	1.0	204	CHF ₂ -CF ₂ H	23 %	15 %
CFH=CCl ₂	K	21.0	160	CFH ₂ -CFCl ₂	32 %	96 %
CCl ₂ =CCl ₂	Cs	1.4	300	CF ₃ -CCl ₂ H	100 %	51 %
				CF ₃ -CHFCl		12 %
				CF ₃ -CF ₂ H		6 %

illustrates this point. Mechanistically it is reasonable to assume that the reaction of tetrachloroethylene to HCFC-123, HCFC-124 and HFC-125 is really a series of HF additions and HCl eliminations, i.e. the well-known addition/elimination pathway. This is shown in Figure 1 below. CFC-1111, HCFC-123, HCFC-123a, HCFC-124 and HFC-125 are the observed products in this reaction when starting with tetrachloroethylene, and their presence lends credence to this hypothesis.

Results - Inorganic or Regeneration Reaction

As mentioned earlier, the inorganic or regeneration reaction (eq. 3) has very little specific literature precedent. If one assumes that the regeneration reaction takes place through the intermediate heterobihalide anion FHCl^- (18-26), then it is possible to carry out a Born Haber cycle calculation such as that shown in Figure 2 in order to ascertain in which direction the heterobihalide anion might decompose. Using standard thermochemical data (6,27-29), a remarkable dependence on the choice of the cation is observed. $\Delta H_{D1} - \Delta H_{D2}$ turns out to be negative only when $M = \text{Li}$ and Na ; the values for $\Delta H_{D1} - \Delta H_{D2}$ are given in parentheses following the respective alkali metal (see Figure 2).

Although this analysis indicates that the transformation in equation 3 should be favored for sodium over potassium and cesium, there are several other factors to be considered. First, as was pointed out for the previous thermodynamic analyses, no allowances have been made for entropy changes (25) nor differing heats of solution for MF and MCl in a fused salt medium (30). In fact, these effects must be important as it is well-known that the solvolysis of each of the chlorides LiCl, NaCl, KCl, RbCl, and NH_4Cl by HF generates a solution of the respective fluoride (31,32). Bulkier cations would also be favored based on the fundamental stabilization of a complex anion as a salt by the use of a bulky cation (6,27). With this uncertainty, it was of interest to broadly determine the optimum conditions for equation 3 with respect to cation or mixtures of cations, cation concentration, and percent conversion. Other interests included studying the reaction equilibria, kinetics, mechanisms, and phase behavior.

Statistical Design I. In order to optimize the conversion of MCl to MF we chose to use a statistically designed experimental approach. This approach is particularly useful when a large number of variables are involved over a rather large reaction space. Essentially a statistically designed experiment is produced by defining the reaction space with variables that may have some bearing on a desired result. This result must be quantifiable and is referred to as the response surface. The completed "experiment" then describes the response of interest as a function of the variables, i.e. a surface in "n" dimensional space.

As physical variables temperature was varied between room temperature and 500 °C and pressure from 1 to 20 atmospheres. As compositional variables the cation was varied from 100% cesium to 100% potassium to mixtures including sodium, and the HF/cation ratio was varied between one and twelve. The response surface would then be % conversion.

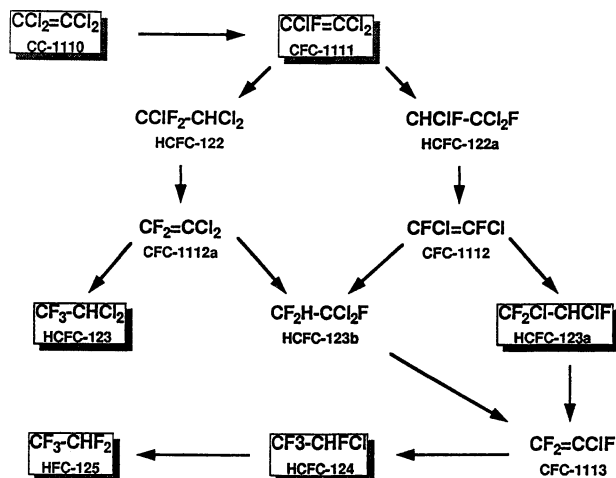


Figure 1. Proposed mechanistic pathway for the reaction of tetrachloroethylene with a CsF·nHF melt. All of the products shown in the boxes were observed spectroscopically.

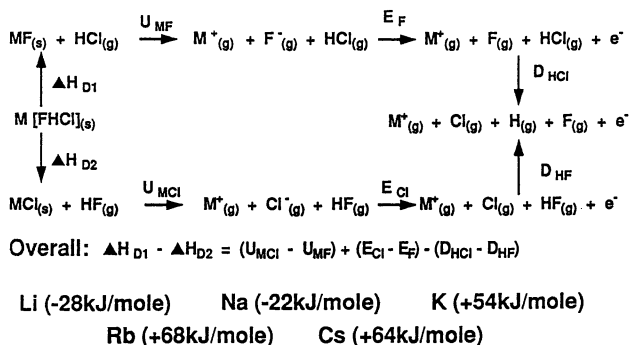


Figure 2. Born-Haber Cycle for the formation/decomposition of M[FHCl].

A set of 50 runs or reactions made up the first statistical design. The reactions were run starting with 100% MCl as a solid in either a sealed, evacuated Monel or Inconel autoclave (static method) or a nickel boat in an inert gas (N₂) purged nickel tube reactor (dynamic method). The autoclave or tube reactor was brought to the desired temperature and a preweighed amount of anhydrous HF was added in one portion to the autoclave or metered through the tube reactor with the aid of a mass flow controller. The autoclave was held at the desired temperature for 30 minutes with stirring, and the pressure was monitored. The volatile contents of the autoclave were then vented into an aqueous potassium hydroxide solution of known concentration. The effluent from each tube reaction was also scrubbed with an aqueous potassium hydroxide solution of known concentration. Following the addition of HF, each tube reaction was purged for 30 minutes with dry nitrogen with the effluent again going to the scrubber. The liquid and/or solid remaining in the autoclave or boat was then dissolved in another aqueous potassium hydroxide solution of known concentration. All solutions were quantitatively analyzed for chloride and fluoride by specific ion electrodes and/or ion chromatography. The percent conversion was then calculated from these data for each run with the chloride concentration remaining in the solid being the primary basis for % conversion. Several experiments were run in the opposite direction, i.e. starting with 100% MF, in order to assure that equilibrium conditions had been established.

Results. The results or response surfaces for several specific cases - starting with 100% CsCl, KCl, and NaCl, respectively - are shown as 3-dimensional plots in Figures 3-5. In each figure, % conversion is plotted as both a function of temperature and the HF to metal chloride mole ratio. These results indicate that high conversions of metal chloride to metal fluoride (bifluoride) are possible for all three alkali metal chlorides. When the three figures are considered together the trends on going from cesium to sodium are obvious with the highest conversions being favored by a) the larger cation, b) lower temperatures, and c) higher HF to metal chloride mole ratio. It is interesting to note that again we see trends contrary to thermodynamic predictions. Also noteworthy is the trough like feature on each plot in the 300 to 400 °C range. This is a real phenomenon and may represent the transition between a MCl to MHF₂ pathway to a direct MCl to MF pathway as MHF₂ salts are unstable at elevated temperatures.

Statistical Design II. The second statistically designed experiment was focused on the more realistic case where a simulated "spent" melt (from the organic reaction) was regenerated with HF. This "spent" melt would be expected to only be partially depleted to the metal chloride, the bulk remaining as the metal polyhydrogen fluoride solvent. The first statistically designed experiment indicated that lower temperatures were most beneficial. The temperature in this experimental design was fixed at 150 °C as a compromise between the preferred higher temperature of the organic reaction and the preferred lower temperature of the inorganic regeneration reaction. Obviously, substantial cost savings could be realized by minimizing the difference between the two reaction temperatures, if this process were commercialized. The compositional variables in these experiments were mole fraction of MX as metal chloride (varied from 0.1 to 0.4), mole fraction of M as potassium (varied from 0.2 to

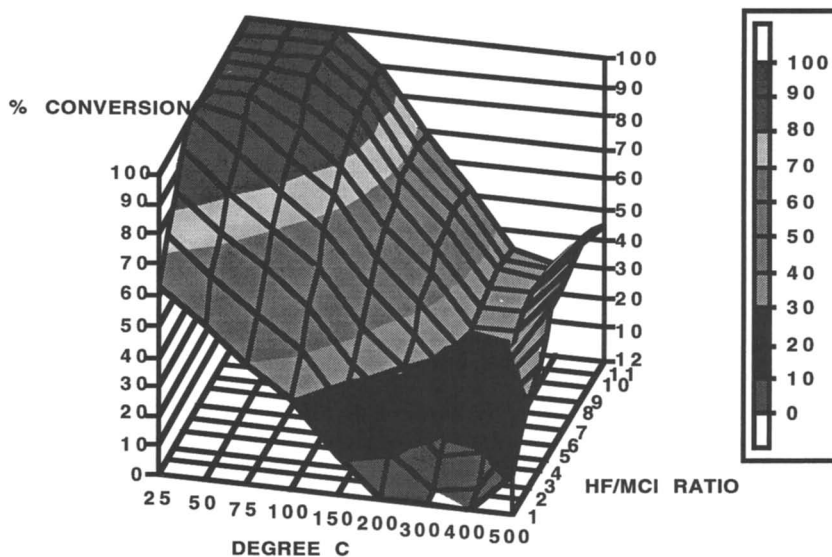


Figure 3. Statistical design I results after starting with 100% cesium chloride.

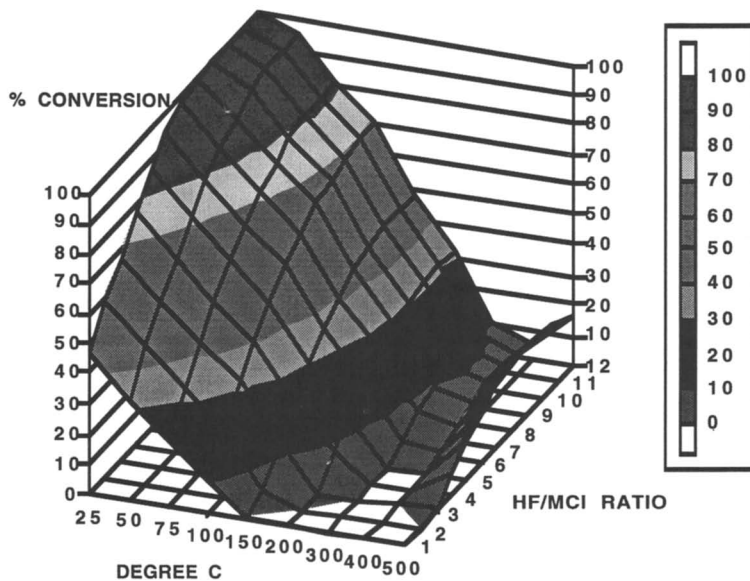


Figure 4. Statistical design I results after starting with 100% potassium chloride.

1.0 with the remaining M being cesium), and the HF to metal cation ratio "n" (varied from 1.0 to 5.5). Again the response surface was % conversion of the dissolved metal chloride to the metal fluoride or polyhydrogen fluorides.

All 27 trials in this statistically design experiment were run in the Monel autoclave as previously described above (static method). Pressure was allowed to vary, but was monitored. The effect of pressure from added nitrogen was also examined in some reactions.

Results. Figure 6 displays a contour plot of % conversion as a function of the mole fraction of potassium and the HF to total cation mole ratio "n" at a constant temperature of 150 °C. Again, very high conversions of MCl to MF can be obtained at all mole fractions of potassium when between 4.5 and 5.5 mole equivalents of HF are used.

Removal of Excess HF. Once the regeneration has been carried out, the resulting melt has a value of "n" \approx 5.0, i.e. much too high to recycle directly to the organic reaction. Therefore, it was necessary to study the thermal stability of these high "n" melts in order to determine the best way to return the melt to the desired "n" value of 0.8 - 1.0. For these studies a Cahn Instruments C-1100 pressure balance was utilized. This equipment allows thermogravimetric analyses (TGA) to be carried out in a stream of anhydrous hydrogen fluoride. A schematic diagram of the experimental setup is shown in Figure 7.

In a typical experiment, a known amount of alkali metal fluoride is placed in the sample pan. The sample chamber of the balance is then heated to 500 °C while purging with dry nitrogen in order to dry the sample. This step is complete when a constant weight is obtained for the sample. After drying, the sample is heated at the desired reaction temperature while the nitrogen purge is replaced with an anhydrous hydrogen fluoride purge. The sample weight is continuously monitored by the computer. When a maximum weight is attained and noted, the hydrogen fluoride purge is replaced with a dry nitrogen purge. The weight loss is then followed and recorded *versus* time. Repeating this experiment at several different temperatures allows a plot of isotherms of stability to be determined as a function of the value of "n" with time. An example of this type of plot is shown for potassium fluoride in Figure 8.

The effect of different cations or mixtures of cations on the thermal stability of various melts at a given temperature can be compared and contrasted. The plot shown in Figure 9 compares the thermal stability of a cesium-, a potassium-, and a cesium/potassium polyhydrogen fluoride based melt at 150 °C. As expected, the cesium melt is the most stable (top line), the potassium melt the least stable (bottom line), and the cesium/potassium melt of intermediate stability (middle line).

Additional information on the freezing points (33), vapor pressures (34), densities/viscosities (35), solubilities (36), phase diagrams (33,37), and thermal stabilities (38) of the alkali metal fluoride-hydrogen fluoride systems is available in the literature. This information is useful when developing halogen exchange chemistry around these systems. We are in the process of measuring similar data for the ternary system cesium fluoride-potassium fluoride-hydrogen fluoride. For example, one can

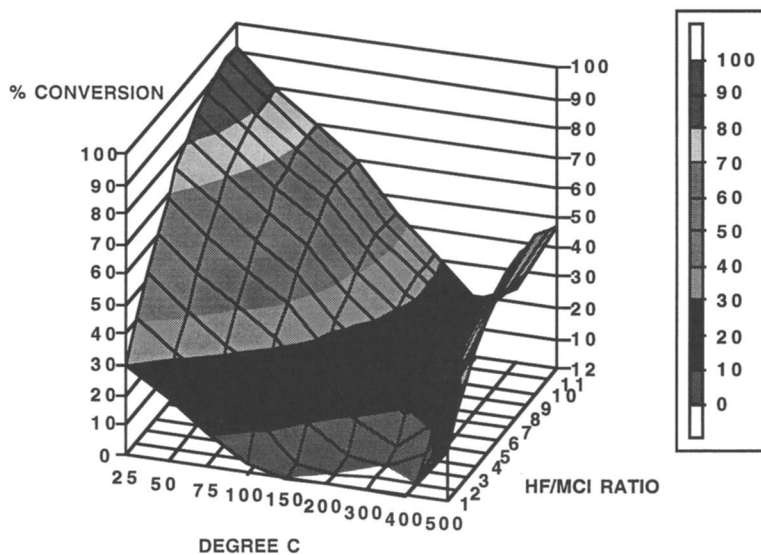


Figure 5. Statistical design I results after starting with 100% sodium chloride.

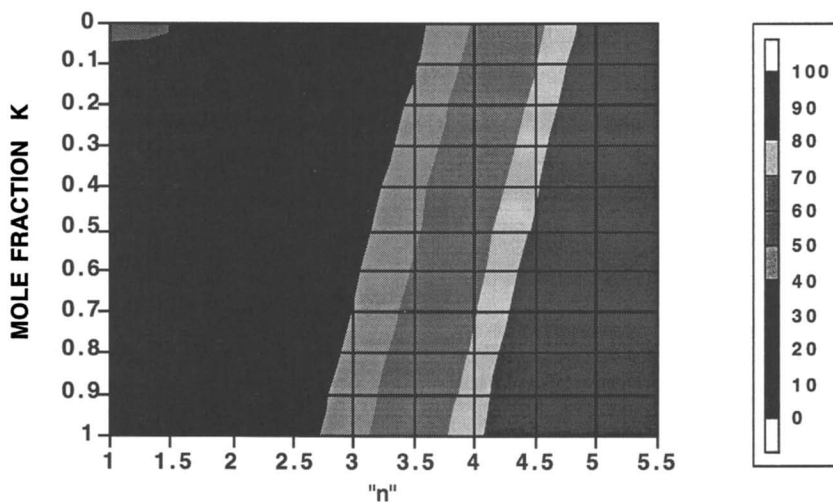


Figure 6. Statistical design II results after starting with a mole fraction of 0.2 chloride.

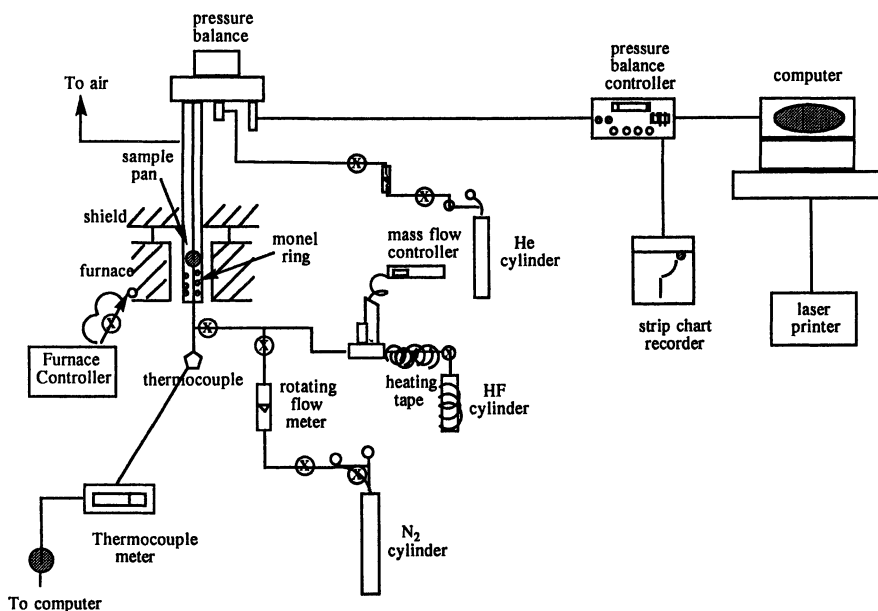


Figure 7. Experimental setup for TGA studies utilizing a Cahn Instruments C-1100 pressure balance.

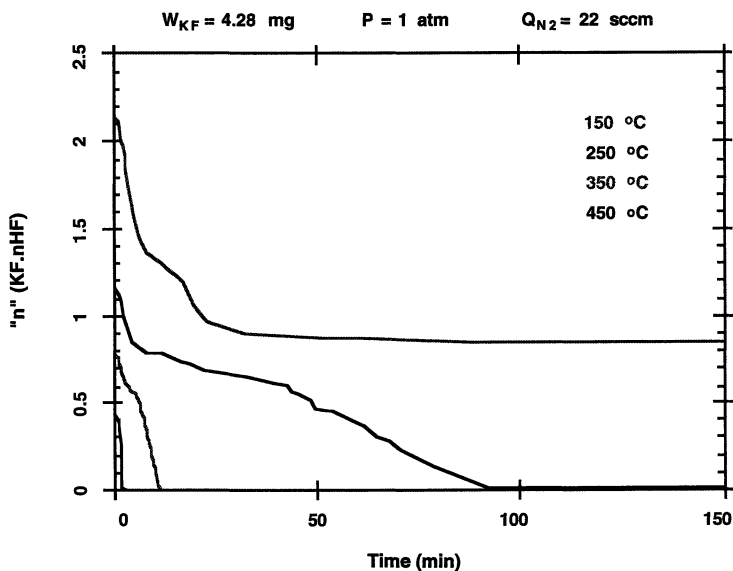


Figure 8. Thermal stability of $\text{KF}\cdot n\text{HF}$ versus temperature.

gain insight into the ternary phase diagram not only through experimentation, but also by careful examination of all available binary phase diagram information (33,37,39). The results of these studies will be the subject of a later publication.

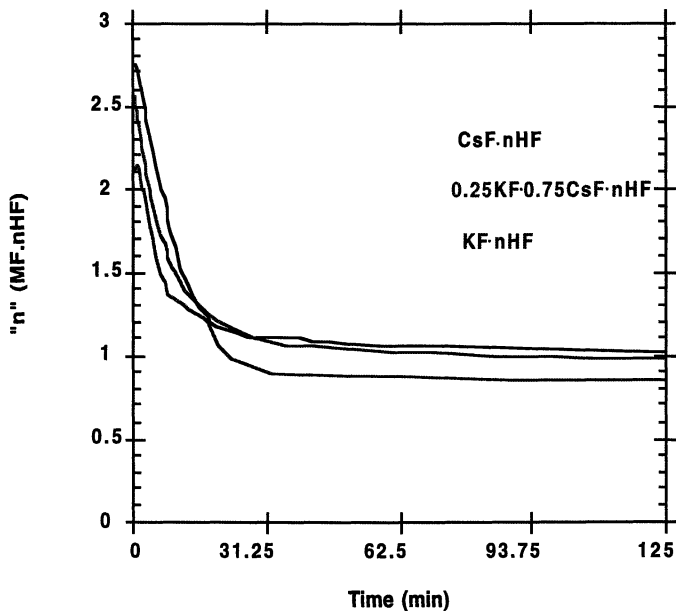


Figure 9. A comparison of the thermal stability of CsF·nHF, 0.25KF·0.75CsF·nHF, and KF·nHF at 150 °C.

Conclusions

Alkali metal polyhydrogen fluoride melts are tunable, participatory solvents for halogen exchange, HF addition, and HX elimination reactions. High conversions with excellent selectivities to the desired fluorocarbon products are possible with the appropriate melt. The resulting alkali metal chlorides can be easily regenerated with anhydrous hydrogen fluoride in a separate step.

Acknowledgments

We gratefully acknowledge the assistance of John F. Kook, John E. Miller and R. Bertram Diemer of the Du Pont Company and Liang Hu, H. P. Sampath Kumar, Jian Sun, Jeff Choron and Carl Williams all of the University of Alabama.

Literature Cited

1. Wilkinson, J. A. *Chem. Rev.* **1992**, *92*, 505 and reference therein.
2. Meshri, D. T. In *Fluorine: The First Hundred Years (1886-1986)*; Banks, R. E.; Sharp, D. W. A.; Tatlow, J. C., Eds.; Elsevier: New York, 1986; Chapter 10.
3. Chambers, R. D. *Fluorine in Organic Chemistry*; John Wiley & Sons: New York, 1973 and references therein.
4. Hudlicky, M. *Chemistry of Organic Fluorine Compounds: A Laboratory Manual with Comprehensive Literature Coverage*, 2nd (revised) ed.; Ellis Horwood: Chichester, 1976 and references therein.
5. Young, J. A. *Fluorine Chem. Rev.* **1967**, *1*, 359.
6. Steudel, R. *Chemistry of the Non-Metals*; Walter de Gruyter: Berlin, 1977; Chapter 5.
7. Buckley, G. S.; Rodgers, A. S. *J. Phys. Chem.* **1983**, *87*, 126.
8. *J. Phys. Chem. Ref. Data* **1985**, *14*, Suppl. 1.
9. *J. Phys. Chem. Ref. Data* **1982**, *11*, Suppl. 2.
10. Chen, S. S.; Rodgers, A. S.; Chao, J.; Wilhoit, R. C.; Zwolinski, B. J. *J. Phys. Chem. Ref. Data* **1975**, *4*, 441.
11. Barin, I. *Thermochemical Data of Pure Substances*; VCH Publishers: New York, 1988.
12. Gore, G. *J. Chem. Soc.* **1869**, *22*, 368.
13. Fredenhagen, H. *Z. Anorg. Allg. Chem.* **1939**, *242*, 23.
14. Hood, G. C.; Woyski, M. M. *J. Am. Chem. Soc.* **1951**, *73*, 2738.
15. Cassel, W. R.; Fernandez, R. E.; Mader, F. W. U.S. Patent 4 990 701, 1991.
16. Cassel, W. R.; Fernandez, R. E.; Mader, F. W. U.S. Patent 4 990 702, 1991.
17. Fernandez, R. E.; Gumprecht, W. H.; Kaplan, R. B. U.S. Patent 5 045 634, 1991.
18. Evans, J. C.; Lo, G. Y-S. *J. Phys. Chem.* **1966**, *70*, 543.
19. Ault, B. S. *J. Phys. Chem.* **1979**, *83*, 837.
20. Fujiwara, F. Y.; Martin, J. S. *J. Am. Chem. Soc.* **1974**, *96*, 7625.
21. Evans, J. C.; Lo, G. Y-S. *J. Chem. Phys.* **1966**, *70*, 11.
22. Smart, R. St. C.; Sheppard, N. *J. Chem. Soc., Chem. Commun.* **1969**, 468.
23. Smart, R. St. C.; Sheppard, N. *Proc. Roy. Soc. Lond.* **1971**, *320A*, 417.
24. Fujiwara, F. Y.; Martin, J. S. *J. Phys. Chem.* **1972**, *56*, 4091.
25. Salthouse, J. A.; Waddington, T. C. *J. Chem. Soc., A* **1964**, 4664.
26. King, D. L.; Herschbach, D. R. *Faraday Discuss. Chem. Soc.* **1973**, *55*, 331.
27. Douglas, B. E.; McDaniel, D. H.; Alexander, J. J. *Concepts and Models of Inorganic Chemistry*, 2nd ed.; John Wiley & Sons: New York, 1983; p 229.
28. *CRC Handbook of Chemistry and Physics*; Weast, R. C., Ed.; CRC Press: Boca Raton, Florida, 1986; pp D-100 - D-114.

29. Greenwood, N. N.; Earnshaw, A. *Chemistry of the Elements*; Pergamon Press: Oxford, 1984; pp 94-97.
30. Thompson, N. R. ; Tittle, B. In *Halogen Chemistry*; Gutmann, V., Ed.; Academic Press: New York, 1967; Vol. 2.
31. Dove, M. F. A.; Clifford, A. F. In *Chemistry in Nonaqueous Ionizing Solvents*; Jander, G.; Spandau, H.; Addison, C. C., Eds.; Pergamon Press: New York, 1971; Vol. 2, Pt. 2, pp 119-300 and references therein.
32. Jache, A. W. In *Fluorine-Containing Molecules: Structure, Reactivity, Synthesis, and Applications*; Liebman, J. F.; Greenberg, A.; Dolbier, Jr., W. R., Eds.; VCH Publishers: New York, 1988; Chapter 9.
33. Cady, G. H. *J. Am. Chem. Soc.* **1934**, *56*, 1431.
34. Yusova, Y. L.; Alabyshev, A. F. *Russ. J. Phys. Chem.* **1962**, *36*, 1506.
35. Semerikova, I. A.; Alabyshev, A. F. *Russ. J. Phys. Chem.* **1962**, *36*, 1507.
36. Cady, G. H. *J. Phys. Chem.* **1952**, *56*, 1106.
37. Winsor, R. V.; Cady, G. H. *J. Am. Chem. Soc.* **1948**, *70*, 1500.
38. Opalovsky, A. A.; Fedorov, V. E.; Fedotova, T. D. *J. Thermal Anal.* **1970**, *2*, 373.
39. Sangster, J.; Pelton, A. D. *J. Phys. Chem. Ref. Data* **1987**, *16*, 509.

RECEIVED November 24, 1993

Chapter 15

New and Revisited Transition Metal Chemistry of Fluoro-olefins and Fluorodienes

Russell P. Hughes¹, Owen J. Curnow¹, Peter R. Rose¹,
Xiaoming Zheng¹, Erin N. Mairs¹, and Arnold L. Rheingold²

¹Chemistry Department, Burke Laboratory, Dartmouth College,
Hanover, NH 03755–3564

²Chemistry Department, University of Delaware, Newark, DE 19716

Organometallic chemistry of three classes of fluorinated ligands is reported. New Ru(II) complexes, $[\text{Ru}(\text{C}_5\text{Me}_5)(\text{acac})(\text{C}_2\text{F}_4)]$ (acac = acetylacetonate, and substituted analogues), containing η^2 -tetrafluoroethylene are described. Dynamic ^{19}F NMR studies show unprecedentedly low barriers to propeller rotation of the C_2F_4 ligands. The first complex, $[\text{Ru}(\text{C}_5\text{Me}_5)\text{Cl}(\text{C}_4\text{F}_6)]$, containing an η^4 -hexafluoro-butadiene ligand is reported; it exists as two conformational isomers, one of which has been characterized by X-ray crystallography. Hexafluorobutadiene reacts with $[\text{RhCl}(\text{PPh}_3)_3]$ to afford initially a five-coordinate hexafluororhodacyclopentene complex, which is extraordinarily sensitive to water and undergoes facile hydrolysis to generate an α -ketone complex. In contrast, hexafluorobutadiene reacts with $[\text{RhCl}(\text{PMe}_3)_3]$ to afford a six-coordinate hexafluororhodacyclopentene complex, *mer*- $[\text{RhCl}(\text{PMe}_3)_3(\text{C}_4\text{F}_6)]$, which reacts with water to give a β -ketone complex. Finally, the first successful synthesis of a complex containing an η^5 -pentafluorocyclopentadienyl ligand is described. The ruthenocene, $[\text{Ru}(\text{C}_5\text{Me}_5)(\text{C}_5\text{F}_5)]$, is prepared by flash vacuum pyrolysis of the corresponding η^5 -pentafluorophenoxide complex, with extrusion of CO.

Organometallic compounds with perfluorinated ligands have been known since the earliest days of the renaissance of the field in the 1950s, and advances in the field have been reviewed by a number of authors (1-6). This paper will deal with recent work in our group in three principal areas which illustrate the kinds of bonding trends, structural preferences, and reaction chemistry encountered in fluorocarbon-transition metal chemistry: a new class of ruthenium-tetrafluoroethylene complexes which exhibit unusually low barriers to propeller rotation of the olefin; new metallacyclic complexes, derived from hexafluorobutadiene, which exhibit facile hydrolytic activation of CF_2 groups; and the first successful synthesis of a transition metal complex containing an η^5 -pentafluorocyclopentadienyl ligand.

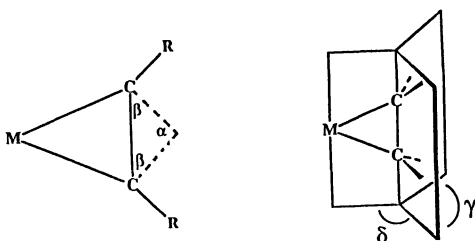
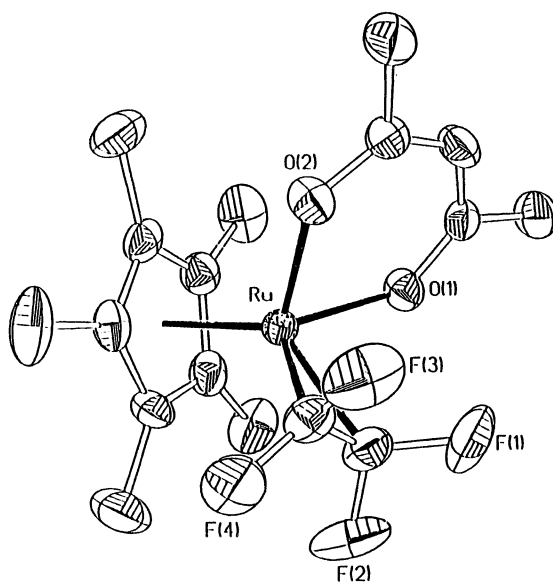
0097-6156/94/0555-0252\$08.00/0
© 1994 American Chemical Society

Tetrafluoroethylene Complexes with Metallacyclopropane Structures, but with Low Activation Barriers to Olefin Rotation.

The d^8 -rhodium(I) complex **1** is often used as a paradigm for illustrating the differences between the bonding of the hydrocarbon olefin, ethylene, and its fluorinated analogue, tetrafluoroethylene, to transition metal centers. The molecular structure of **1** shows a more metallacyclopropane interaction for the C_2F_4 ligand than for the C_2H_4 (**7**), and while the activation barrier for propeller rotation of the C_2H_4 ligand can be measured using NMR techniques to be 13.6 ± 0.6 kcal mol⁻¹ [57 kJ mol⁻¹] (**8**), the rate of rotation of C_2F_4 is so slow on the NMR timescale so as not to result in any broadening of the ^{19}F resonances in **1** even at $100^\circ C$. This latter observation, taken with many other analogous observations of apparently static behavior in other d^8 and d^{10} complexes of C_2F_4 (**1**) has led to the assumption that propeller rotation of C_2F_4 should invariably have a high activation barrier. It is sometimes assumed that the observation of a metallacyclopropane structure should necessarily mean a high barrier to propeller rotation, but this is not the case, as the metallacyclopropane structure is simply one extreme of a continuum of bonding possible within the Dewar-Chart-Duncanson model of the transition-metal olefin bond (**9**). Theoretical studies of conformational preferences and rotational barriers in metal-olefin complexes suggested clearly that the lowest barriers to propeller rotation of olefins should occur in d^6 complexes (**9**), and led to our attempts to make tetrafluoroethylene complexes of d^6 metal centers.

Prior to embarking on a study of d^6 -complexes we revisited one d^8 compound of C_2F_4 , the acetylacetonato (acac) complex **2**. The 56 MHz ^{19}F NMR spectrum was reported to exhibit an apparent single environment for all 4 F atoms, (**10**) possibly indicative of facile propeller rotation, yet its molecular structure is consistent with a metallacyclopropane Rh- C_2F_4 interaction like that proposed in **1** (**11**). We found that the ^{19}F NMR spectrum of this compound at 282 MHz ($CDCl_3$; $20^\circ C$) can be simulated as an AA'BB'X pattern [$\nu_A = -115.1$, $\nu_B = -116.1$ ppm rel. $CFCl_3$; $J_{AA'} = J_{BB'} = -2.4$, $J_{AB} = J_{A'B'} = 104.3$, $J_{AB'} = J_{BA'} = -56.6$, $J_{RhA} = 9.6$, $J_{RhB} = 3.3$ Hz], confirming that rotation is slow on the NMR time scale. A small chemical shift difference is probably the reason for the single F environment reported for the dipivalomethane analogue of this acac complex (**12**).

Our synthetic approach to d^6 complexes of C_2F_4 started with the well known tetrameric complex $[RuCp^*Cl]_4$ ($Cp^* = C_5Me_5$) (**13**), which was shown to react with C_2F_4 to afford the crystallographically characterized dimer complex **3** (**14**). This compound proved too insoluble for the required variable temperature NMR studies, and so mononuclear β -diketonate analogues **4a-c** were prepared by reaction of **3** with the appropriate thallium salt (**15**). The molecular structure of **4a** was determined crystallographically, and an ORTEP is shown in Figure 1. The key bond and dihedral angles associated with the Ru- C_2F_4 subunit, also shown in Figure 1, were found to be almost identical with those found in **1**, clearly indicating that a metallacyclopropane description of the bonding was quite appropriate for **4a** (**15**). The ^{19}F NMR spectrum of **4a** showed two broad resonances which sharpened into an AA'XX' pattern at low temperatures, but which coalesced into a single peak at about $100^\circ C$, with $\Delta G^\ddagger = 55 \pm 2$ kJ mol⁻¹. This behavior is consistent with propeller rotation, or with a dissociation/recombination process for ^{19}F site-exchange. However, clear support for the former mechanism is provided by the variable temperature ^{19}F NMR spectrum of **4b**, which shows the expected four resonances of an AGMX pattern at low temperature, and coalescence to two resonances at $100^\circ C$ with $\Delta G^\ddagger = 53 \pm 3$ kJ mol⁻¹. Dissociation/recombination would scramble all four ^{19}F environments, whereas propeller rotation only accomplishes a pairwise interchange of mutually trans-fluorines ($F_1 \rightarrow F_3, F_3 \rightarrow F_1$; $F_2 \rightarrow F_4, F_4 \rightarrow F_2$). That the latter process occurs without any pseudorotation at the metal is confirmed by the observation that **4c** exhibits fluorine



RuCp*(C₂F₄)(acac) RhCp(C₂H₄)(C₂F₄)

d(C-F)	1.349(7)	1.351(3)
d(C-M)	2.047(6)	2.024(2)
d(C-C)	1.395(9)	1.405(7)
α	73.9°	74.3°
β	53.0°	52.8°
δ	114.5°	114.3°
γ	131.0°	131.4°

Figure 1. ORTEP of **4a** and comparison of its structural features with those of **1 (7)**. Definition of angles α , β , δ , and γ , is provided in reference (36).

site exchange analogous to that observed for **4a**, without any corresponding site exchange of diastereotopic methyl groups within the isopropyl groups in the ^1H NMR spectrum over the same temperature range (16). The only remaining explanation for the observed site exchange of fluorines is that of propeller rotation of the tetrafluoroethylene ligand. The activation barriers for C_2F_4 rotation are at the low end of those usually found for ethylene rotation in d^8 and d^{10} complexes, and are unprecedentedly low for tetrafluoroethylene.

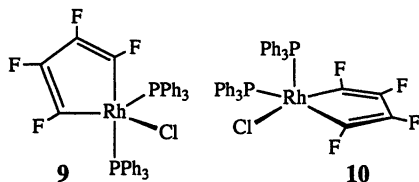
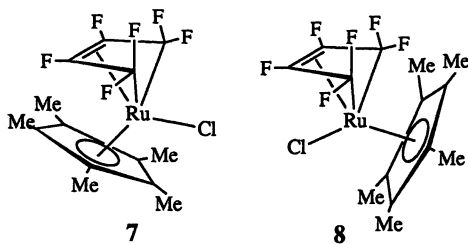
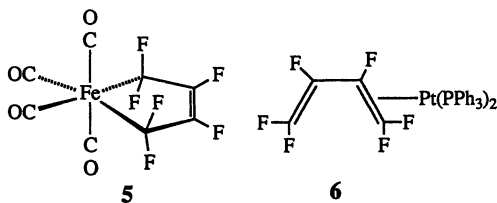
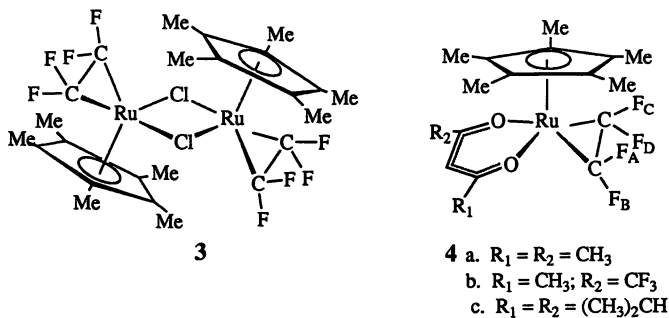
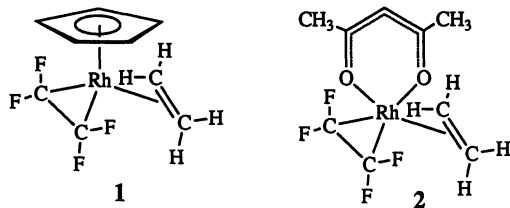
It remains to be seen whether other d^6 complexes containing C_2F_4 can be prepared, and whether the facility of propeller rotation in these compounds proves to be a general phenomenon. It is noteworthy that the lack of facile propeller rotation of C_2F_4 in d^8 and d^{10} complexes may contribute to the lack of reactivity of C_2F_4 in these compounds towards insertion into metal-carbon bonds. Whether such insertion proves to be more facile in d^6 systems remains to be explored.

New and Revisited Transition Metal Chemistry of Hexafluorobutadiene.

Compared to the abundant chemistry of its hydrocarbon analogue, 1,3-butadiene, that of hexafluorobutadiene is remarkably sparse. Two well characterized complexes containing this ligand have been reported prior to our work. In contrast to butadiene itself, which binds to the tricarbonyliron fragment in the well-known η^4 -diene mode, hexafluorobutadiene reacts with iron carbonyl to afford the fluorinated metallacyclopentene complex **5** (17), which has been characterized unambiguously by X-ray crystallography (18). The driving force for this mode of reactivity may well be the formation of stronger metal-carbon σ -bonds to fluorinated carbon atoms, and the gem-difluoro effect which arises from the exothermicity associated with the pyramidalization of a planar CF_2 group (19). In addition to **5** the only other complex containing hexafluorobutadiene appears to be the η^2 -diene complex of platinum(0), **6**, which has been characterized spectroscopically (20). Examples of reaction chemistry of hexafluorobutadiene are also few: the insertion of hexafluorobutadiene into a Co-H bond to give allylic complexes of cobalt has been reported (21), and some early reports of defluorination reactions involving rhodium are revisited below.

We were intrigued that no examples of η^4 -hexafluorobutadiene complexes had been reported, and buoyed by our success at binding C_2F_4 to d^6 centers, we carried out the reaction of hexafluorobutadiene with the tetrameric reagent $[\text{RuCp}^*\text{Cl}]_4$. The reaction proceeds smoothly to give two isomeric products **7** and **8**, which differ only in the exo/endo conformation of the diene ligand. The isomer **7** appears to be the more thermodynamically stable, and a single crystal X-ray diffraction study has confirmed the conformation of the η^4 -diene (22). An ORTEP is shown in Figure 2, together with a schematic diagram showing relevant distances and angles. There is extensive pyramidalization at the terminal CF_2 groups, and the C-C bond distances in the coordinated diene are consistent with the valence bond description shown in the line drawing of **7**. This type of coordination is analogous to that found previously in the tricarbonyliron compound containing η^4 -bound perfluoro-1,3-cyclohexadiene (23). The chemistry of complexes **7** and **8** is under ongoing investigation in our group.

We were puzzled by an early report that reaction of hexafluorobutadiene with Wilkinson's compound, $[\text{RhCl}(\text{PPh}_3)_3]$, in hot benzene solution, afforded a tetrafluorometallacyclopentadiene complex, with apparent loss of one PPh_3 ligand and two fluorines! While the proposed structures **9** or **10** would require four different fluorine and two different phosphorus environments, the ^{19}F NMR spectrum of this compound showed only three ^{19}F resonances in a 2:1:1 ratio, leading to the assumption that two fluorines in the ring were accidentally isochronous. Unfortunately no ^{31}P NMR data were reported. In addition, the IR spectrum of this compound showed two bands at 1739 and 1672 cm^{-1} , which were attributed to the two fluorinated double bonds in the ring.



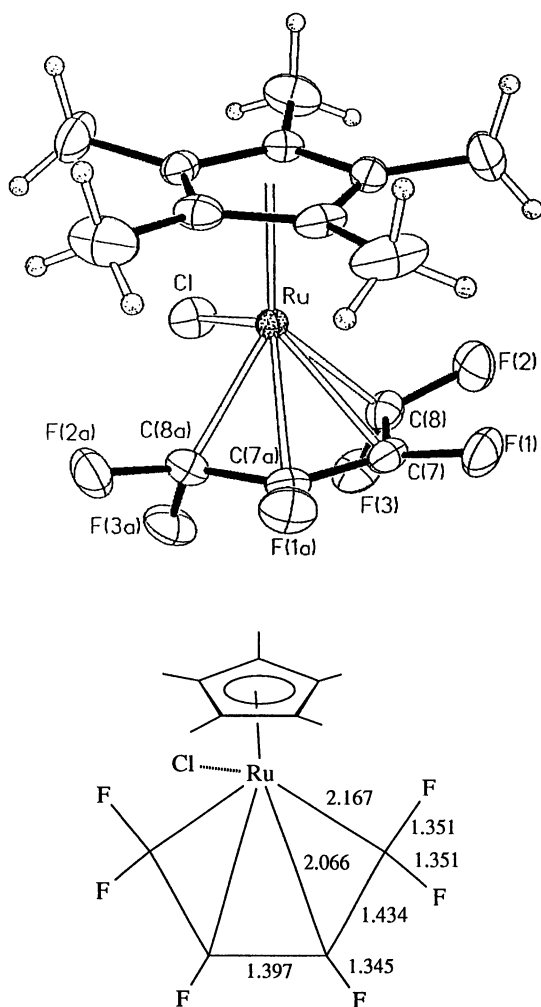


Figure 2. ORTEP of **7**, with a schematic representation of some key bond distances (in Å). There is a crystallographic plane of symmetry relating the two halves of the molecule.

The apparent cleavage of two C–F bonds, and loss of two fluorines to an unspecified fate intrigued us, and we re-investigated this reaction. Repetition under the literature conditions afforded 60–70% yields of yellow crystalline material with almost identical ^{19}F NMR and IR data to those reported in the literature. Subjection of single crystals of this compound for X-ray crystallographic analysis revealed the true structure of the compound as **11**, in which the hexafluorobutadiene had been converted into a tetrafluorometallacyclopentenone ligand. The interpretation of the 1:1:2 pattern in the ^{19}F NMR spectrum is now clear, and the IR bands can be reassigned as 1672 ($\nu_{\text{C}=\text{O}}$) and 1734 ($\nu_{\text{C}=\text{C}}$) cm^{-1} . An ORTEP of the structure of **11** is shown in Figure 3, together with a schematic drawing containing key bond distances (24).

Clearly one CF_2 group in hexafluorobutadiene has undergone conversion to a ketone. We regarded water as the most likely reagent for this transformation, with formation of the C=O and 2 equivalents of HF providing the thermodynamic compensation for cleavage of 2 C–F bonds, but careful drying of solvents and reagents still resulted in formation of good yields (60%) of **11**. Only when the internal glass surfaces of the reaction vessel were silylated was formation of **11** suppressed; in its place was formed the metallacyclopentene complex **12**, containing a metallacyclic ring analogous to that found in the iron complex **5**. Characterization of **12** was accomplished spectroscopically using ^{19}F and ^{31}P NMR. When solutions of **12** were transferred to unsilylated glass vessels, or when water was added to dry solutions of **12**, conversion to **11** was rapid.

We reasoned that the loss of the third triphenylphosphine might be sterically driven, and that the presence of a vacant coordination site in **12** might be important in facilitating its conversion to **11**. Consequently we carried out the corresponding reaction of hexafluorobutadiene with the analogous rhodium complex $[\text{RhCl}(\text{PMe}_3)_3]$. In this reaction a clean conversion to the metallacyclic complex **13** was observed. This product was characterized spectroscopically and by a single crystal X-ray diffraction study (24). An ORTEP and key bond distances are shown in Figure 4. The complex contains a metallacyclopentene ring analogous to that found in **12**, but with pseudo-octahedral coordination around rhodium and retention of all three PMe_3 ligands meridionally bound in the coordination sphere. Complex **13** shows no tendency to react with water at room temperature but on heating hydrolysis did occur to give a mixture of two isomeric complexes **14** and **15**. Isomer **15** could be crystallized from the mixture and its structure was confirmed by X-ray crystallography (24). An ORTEP and key bond distances are shown in Figure 5. The metallacyclic ring is isomeric with that observed in **11**, with the ketone function β to the metal rather than α .

Thus we conclude that in a 5-coordinate system such as **12** hydrolysis of an α - CF_2 in the metallacycle is extraordinarily facile; notably, subsequent hydrolysis of the second CF_2 group is much slower, and certainly does not occur at 60°C. In the 6-coordinate complex **13** the additional phosphine on the metal shuts down facile hydrolysis of an α - CF_2 in the hexafluorometallacyclopentene ring, but under more forcing conditions hydrolysis occurs at the β -position. Some mechanistic speculation as to the possible role of a vacant coordination site on rhodium is presented in Scheme 1. The transition metal chemistry of hexafluorobutadiene is clearly significantly different from that of its hydrocarbon analogue, and is under continuing investigation in our group.

The Pentafluorocyclopentadienyl Ligand.

While there are thousands of examples of transition metal complexes containing the cyclopentadienyl ligand and its substituted analogues, there are few examples of compounds containing pentachloro-, pentabromo-, and pentaiodo-cyclopentadienyl ligands (25). The absence of the pentafluorocyclopentadienyl ligand from this group is

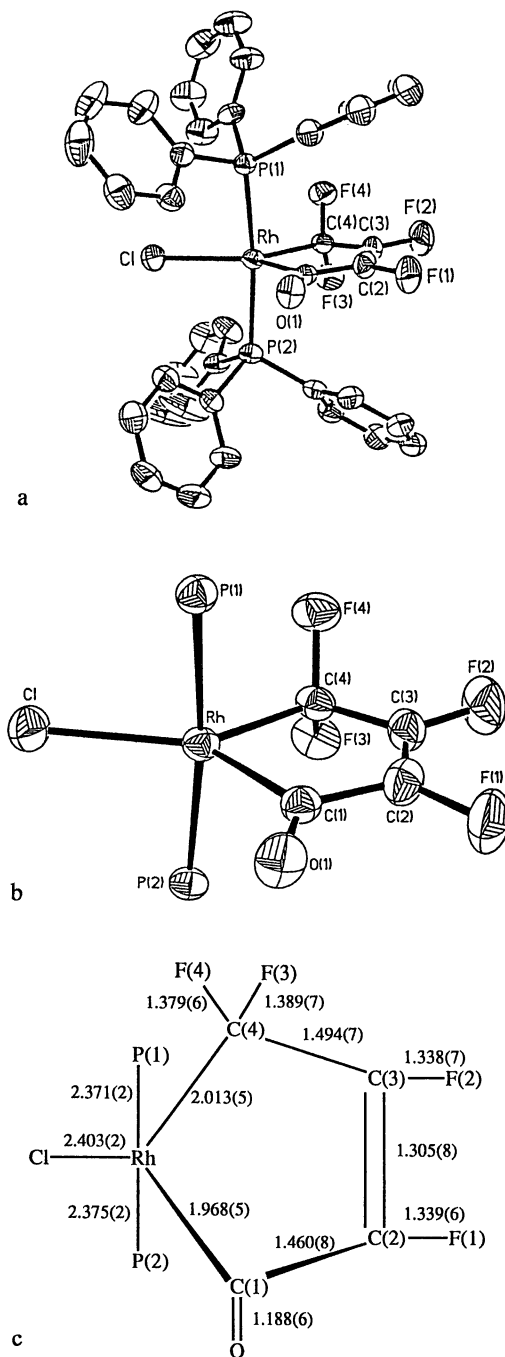


Figure 3. a) ORTEP of **11**; b) ORTEP of **11** with phenyl groups omitted from the PPh₃ ligands; c) a schematic representation of some key bond distances (in Å).

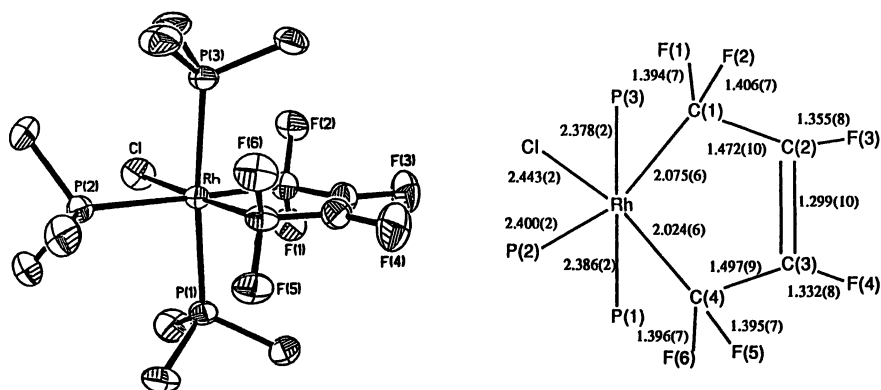


Figure 4. ORTEP of **13**, with a schematic representation of some key bond distances (in Å).

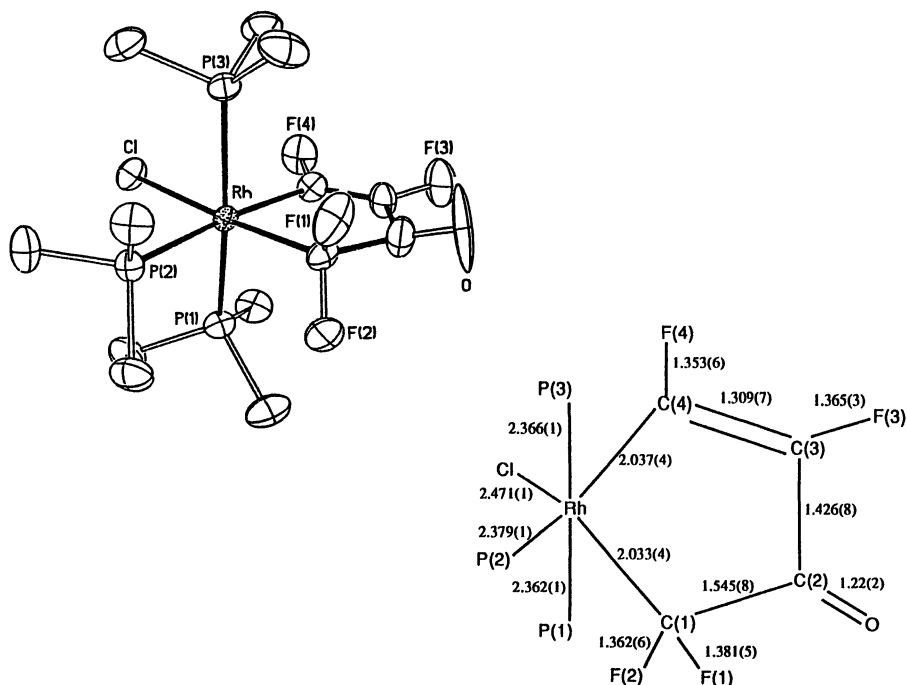
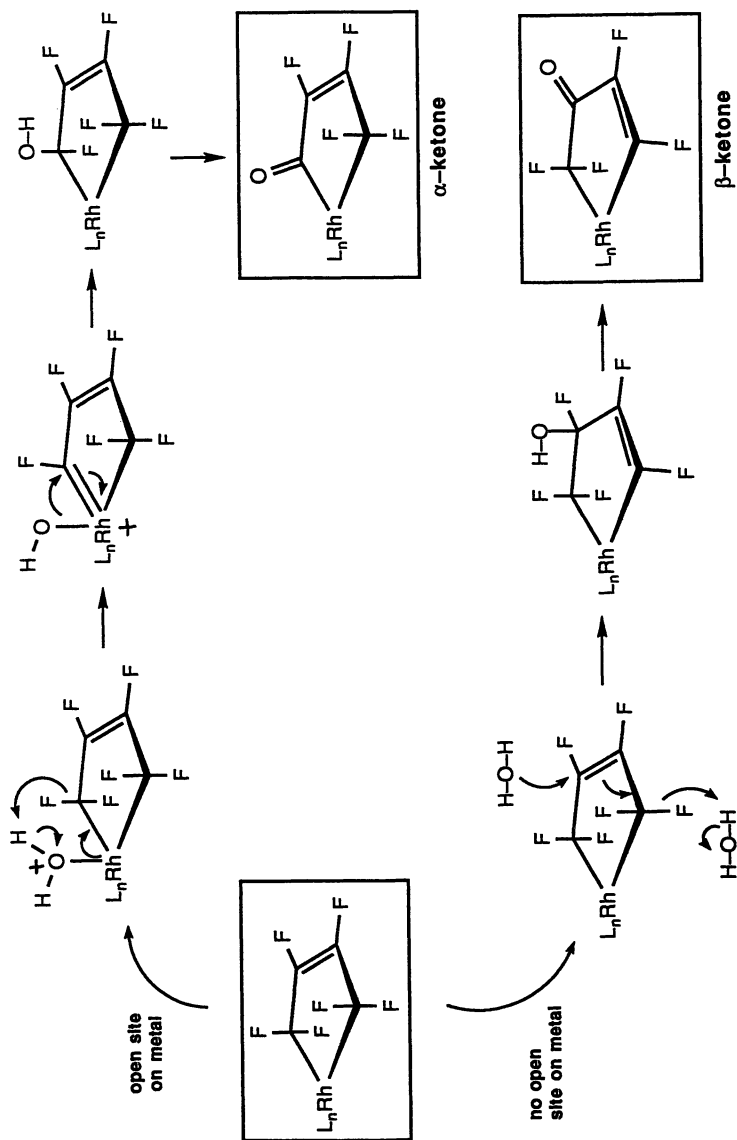


Figure 5. ORTEP of **15**, with a schematic representation of some key bond distances (in Å).



Scheme 1. Some possible mechanisms for formation of α and β -ketone functionality by reaction of hexafluorocyclopentene rings with water.

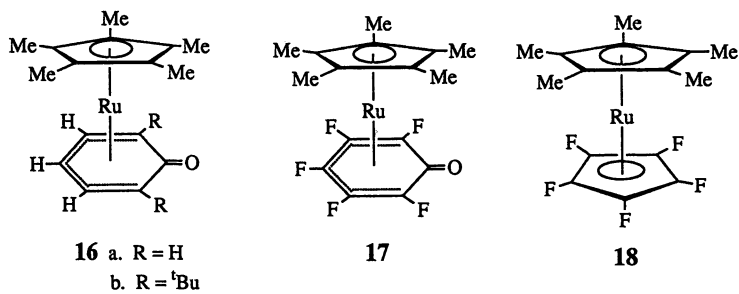
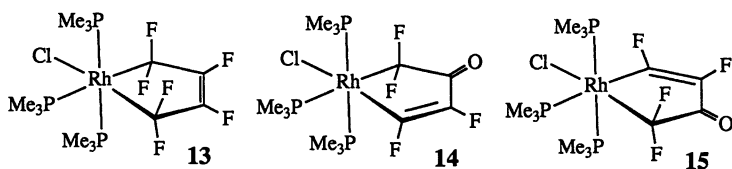
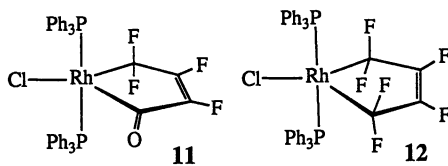
noteworthy, especially in view of the considerable effort that has gone into attempts to synthesize this missing member of the family. One might expect that the perfluorocyclopentadienyl ligand might impart enhanced thermal stability, and significantly different physical and chemical properties to its transition metal complexes, as compared to its hydrocarbon analogue. In fact, only one example of a complex containing a monofluorocyclopentadienyl ligand, monofluoroferrocene, has been characterized with any degree of certainty (26,27); although (monofluorocyclopentadienyl)tricarbonylmanganese has also been reported, no ^{19}F NMR data were given (28).

The most sustained efforts to prepare pentafluorocyclopentadienyl-transition metal compounds came in the 1980s, following the elegant synthesis of the pentafluorocyclopentadienyl anion (29). Remarkably, attempts to bind this anion to transition metal centers via metathesis reactions with transition metal halides were unsuccessful (30). Other routes involving the 5H-pentafluorocyclopentadiene and its 5-bromo analogue also met with no success (31), leading to suggestions that η^5 -pentafluorocyclopentadienyl ligands bound to transition metals were perhaps unstable (30).

Our alternative approach to this fascinating ligand was stimulated by recent observations that the affinity of the $[\text{RuCp}^*]^+$ fragment for binding to arene rings allows the η^5 -phenoxide complexes **16** to be prepared (32, 33). We were quickly able to establish that the pentafluorophenoxide analogue **17** could be generated easily, and could be characterized by its 2:2:1 pattern in the ^{19}F NMR spectrum and the characteristic C=O stretch at 1620 cm^{-1} in its IR spectrum (34). Attempts to extrude CO from this molecule by extended reflux or photolysis in various solvents failed to do so. However, when subjected to flash vacuum pyrolysis (FVP) at 770°C complex **17** underwent extrusion of CO, to give a 20% yield of white crystalline **18**, in which the presence of the pentafluorocyclopentadienyl ring was confirmed by a combination of mass spectrometric, and ^1H , ^{19}F , and ^{13}C NMR spectroscopic data. (34). Complex **18** melts in air without decomposition at 235°C . Its ^{19}F NMR spectrum appears as a sharp singlet at $\delta -213.2$ ppm to high field of CFCl_3 . The $^{13}\text{C}\{^1\text{H}\}$ NMR spectrum of the pentafluorocyclopentadienyl ring can be simulated successfully as an ABB'CC'X system, with $\text{X} = ^{13}\text{C}$, and a small isotopic perturbation of the chemical shift of the unique fluorine (A) compared to the other four ring fluorines (35). Unfortunately, despite repeated attempts, we have been unable to obtain a crystal structure of **18**, due to an end for end disorder problem. Attempts to circumvent this problem by preparing the ethyltetramethylcyclopentadienyl analogue of **18** were fruitless; while the compound was easily prepared by the same method, its crystals showed identical disorder problems. Attempts to prepare other derivatives are underway.

This successful synthesis of the pentafluorocyclopentadienyl ligand, albeit by an unorthodox route, demonstrates clearly that complexes of this ligand can be prepared, and that they are likely to be thermally stable, thus re-opening the synthetic challenge to develop suitable general syntheses of complexes of this ligand.

The work outlined here shows that there are still many interesting discoveries to be made in the organometallic chemistry of fluorinated ligands. The synthesis of new ligands, evaluation of their effects on the chemical and physical properties of organometallic compounds, and investigation of their chemical reactivity, continue to present significant intellectual challenges.



Acknowledgments.

We are grateful to the Air Force Office of Scientific Research (Grant AFOSR-91-0227) and the National Science Foundation for generous support of our research. Generous loans of precious metal salts from Johnson Matthey Aesar/Alfa are gratefully acknowledged.

Literature Cited.

- Hughes, R. P. *Adv. Organomet. Chem.*, **1990**, *31*, 183.
- Stone, F. G. A. *Pure Appl. Chem.*, **1972**, *30*, 551.
- Bruce, M.; Stone, F. G. A. *Prep. Inorg. React.*, **1968**, *4*, 177.
- Treichel, P. M.; Stone, F. G. A. *Adv. Organomet. Chem.*, **1964**, *1*, 143.
- Morrison, J. A. *Adv. Inorg. Chem. Radiochem.*, **1983**, *27*, 293.
- Brothers, P. J.; Roper, W. R. *Chem. Rev.*, **1988**, *88*, 1293.
- Guggenberger, L. J.; Cramer, R. *J. Am. Chem. Soc.*, **1972**, *94*, 3779.
- Cramer, R.; Kline, J. B.; Roberts, J. D. *J. Am. Chem. Soc.*, **1969**, *91*, 2519.
- Albright, T. A.; Hoffman, R.; Thibeault, J. C.; Thorn, D. L. *J. Am. Chem. Soc.* **1979**, *101*, 3801.
- Parshall, G. W.; Jones, F. N. *J. Am. Chem. Soc.* **1965**, *87*, 5356.
- Evans, J. A.; Russell, D. R. *J. Chem. Soc. Chem. Commun.* **1971**, 197.
- Jarvis, A. C.; Kemmitt, R. D. W. *J. Organomet. Chem.* **1974**, *81*, 415.
- Fagan, P. J.; Ward, M. D.; Caspar, J. C.; Krusic, P. J. *J. Am. Chem. Soc.* **1988**, *110*, 2981. Fagan, P. J.; Ward, M. D.; Calabrese, J. C. *ibid*, **1989**, *111*, 1698.
- Curnow, O. J.; Hughes, R. P.; Rheingold, A. L. unpublished results.
- Curnow, O. J.; Hughes, R. P.; Rheingold, A. L. *J. Am. Chem. Soc.* **1992**, *114*, 3153.
- Curnow, O. J.; Hughes, R. P.; Mairs, E. N. unpublished results.
- Hunt, R. L.; Roundhill, D. M.; Wilkinson, G. *J. Chem. Soc. (A)*, **1967**, 982.
- Hitchcock, P. B.; Mason, R. *J. Chem. Soc. Chem. Commun.*, **1967**, 242.
- Smart, B. E. In *"The Chemistry of Functional Groups, Supplement D,"* (S. Patai and Z. Rappoport, eds), **1983**, Chapter 14, John Wiley & Sons, New York.
- Green, M.; Osborn, R. B. L.; Rest, A. J.; Stone, F. G. A. *J. Chem. Soc. (A)*, **1968**, 2525.
- Sasaoka, S. -I.; Joh, T.; Tahara, T.; Takahashi, S. *Chem. Lett.*, **1989**, 1163.
- Hughes, R. P.; Rose, P. R.; Zheng, X.; Rheingold, A. L. unpublished results.
- Churchill, M. R.; Mason, R. *Proc. Roy. Soc. A*, **1967**, *301*, 433.
- Hughes, R. P.; Rose, P. R.; Rheingold, A. L. unpublished results.
- For a recent compilation of such compounds, see: Winter, C. H.; Han, Y. -H.; Heeg, M. J. *Organometallics* **1992**, *11*, 3169.
- Hedberg, F. L.; Rosenberg, H. *J. Organomet. Chem.* **1971**, *28*, C14.
- Popov, V. I.; Lib, M.; Haas, A. *Ukr. Khim. Zh. (Russ. Ed.)* **1990**, *56*, 1115.
- Cais, M.; Narkis, N. *J. Organomet. Chem.* **1965**, *3*, 269.
- Paprott, G.; Seppelt, K. *J. Am. Chem. Soc.* **1984**, *106*, 4060.
- Paprott, G.; Lehmann, S.; Seppelt, K. *Chem. Ber.* **1988**, *121*, 727.
- Paprott, G.; Lenz, D.; Seppelt, K. *Chem. Ber.* **1984**, *117*, 1153.
- Koelle, U.; Wang, M. H.; Raabe, G. *Organometallics* **1991**, *10*, 2573.
- Loren, S. D.; Champion, B. K.; Heyn, R. H.; Tilley, T. D.; Bursten, B. E.; Luth, K. W. *J. Am. Chem. Soc.* **1989**, *111*, 4712.
- Curnow, O. J.; Hughes, R. P. *J. Am. Chem. Soc.*, **1992**, *114*, 5895.
- Curnow, O. J.; Hughes, R. P. unpublished results. We are grateful to Professor David Lema for suggesting this spin system for a successful simulation.
- Ittel, S.D.; Ibers, J.A. *Adv. Organomet. Chem.*, **1976**, *14*, 33.

RECEIVED February 24, 1994

Chapter 16

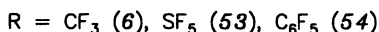
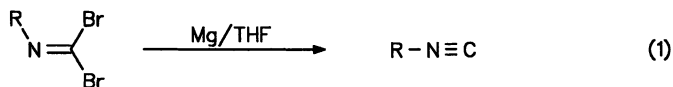
Organometallic Chemistry of Fluorinated Isocyanides

Dieter Lentz

Institut für Anorganische und Analytische Chemie, Freie Universität
Berlin, Fabeckstrasse 34–36, D–14195 Berlin, Germany

Studies of many complexes of trifluoromethyl isocyanide have demonstrated that in contrast to common isocyanides this ligand is a very strong π -accepting ligand. This has been confirmed by vibrational spectroscopic studies of $\text{Cp}^*\text{Mn}(\text{CO})_2\text{L}$ and $\text{Cp}^*\text{Mn}(\text{CO})(\text{CNCF}_3)\text{L}$ complexes and the structural data of *trans*- $(\text{CO})_4\text{Cr}(\text{CNCF}_3)(\text{CNCH}_3)$ which allows direct comparison of a fluorinated and nonfluorinated isocyanide ligand. As a consequence of these ligand properties structures can be realized which are not possible with other isocyanide ligands or carbonyl ligands. $\text{Ru}_3(\text{CO})_{11}(\mu_2\text{-CNCF}_3)$ adopts the $\text{Fe}_3(\text{CO})_{12}$ structure with one bridging isocyanide and one bridging carbonyl ligand whereas $\text{Ru}_3(\text{CO})_{12}$ has only terminal ligands. Even more surprising is the isolation and structural characterization of $\text{Os}_3(\text{CO})_{11}(\mu_2\text{-CNCF}_3)_2$, a derivative of the hypothetical $\text{Os}_3(\text{CO})_{13}$. The partially fluorinated methyl isocyanides have ligand properties in between CNCH_3 and CNCF_3 showing a lower π acceptor to σ donor ratio than CNCF_3 . Only a few complexes of trifluorovinyl and pentafluorophenyl isocyanide have been prepared thus far. The coordinated fluorinated isocyanide ligands can be used to build up other ligands like the *N*-trifluoromethyl formimidoyl ligand or carbene ligands.

Isocyanides are versatile ligands in transition metal chemistry (1). In general they are regarded as good σ donor ligands, and several thousand complexes containing isocyanide ligands have been prepared (1) even of isocyanides which are unknown or unstable as free molecules like $(\text{CO})_5\text{Cr}(\text{CNCN})$ (2), $(\text{CO})_5\text{Cr}(\text{CNCCL}_3)$ (3), $\mu_3\text{-}[(\text{CO})_5\text{Cr}(\text{CN-C})]\text{Co}_3(\text{CO})_9$ (4).



The first fluorinated isocyanide, trifluoromethyl isocyanide, was synthesized by Makarov et al. (5). Its chemistry, however, remained unexplored until a high yield

synthesis from *N*-(trifluoromethyl)dibromomethanimine (6) became available. This new synthesis has allowed the study of the transition metal chemistry of this powerful π accepting ligand.

Although CNCF_3 is extremely unstable in the condensed phase, as it tends to polymerize below its boiling point of -80°C , it can be stored at liquid nitrogen temperature and handled on conventional vacuum line systems.

According to the photoelectron spectra (7) replacement of the methyl group in an isocyanide by the strong electron-withdrawing trifluoromethyl group results in an increase of the ionization energy of the lone electron pair on carbon and the π electrons by 1.3 eV and 2.1 eV, respectively. If one assumes a similar π to π^* splitting which is justified by almost equal $\text{C}\equiv\text{N}$ bond lengths of 117.1(3) pm for CNCF_3 (8) and 116.6(1) pm for CNCH_3 (9) and $\text{C}\equiv\text{N}$ stretching frequencies in both isocyanides, then both the HOMO and the LUMO in CNCF_3 are significantly lower in energy than in methyl isocyanide. Therefore, trifluoromethyl isocyanide should have a higher π acceptor/ σ donor ratio when compared to methyl isocyanide. In addition, trifluoromethyl isocyanide has a much lower dipole moment of only 1.06 D which is much closer to the value of CO [0.1 D (10)] than the value 3.8 D of methyl isocyanide (11).

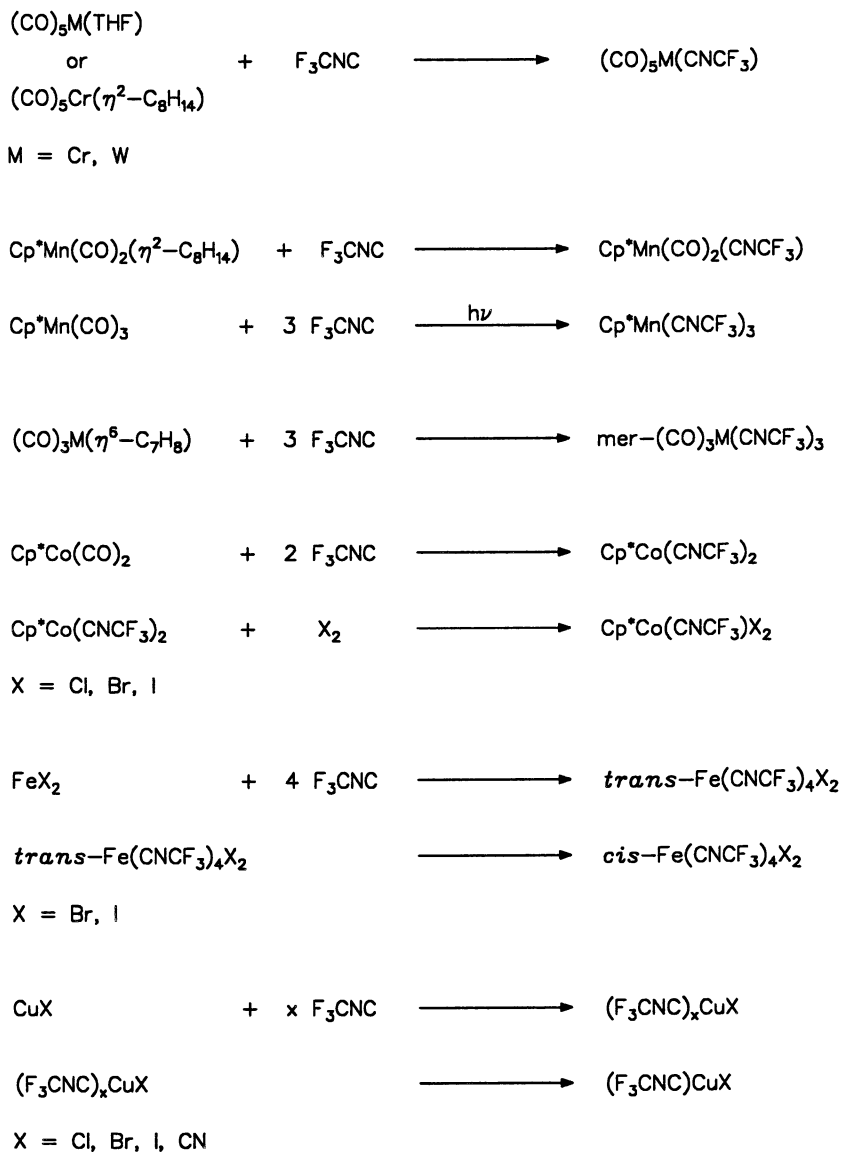
Mononuclear Trifluoromethyl Isocyanide Complexes

In order to prove this assumption, several trifluoromethyl isocyanide complexes with metals in low oxidation states have been synthesized, and their spectroscopic data, reactivity and structures have been studied.

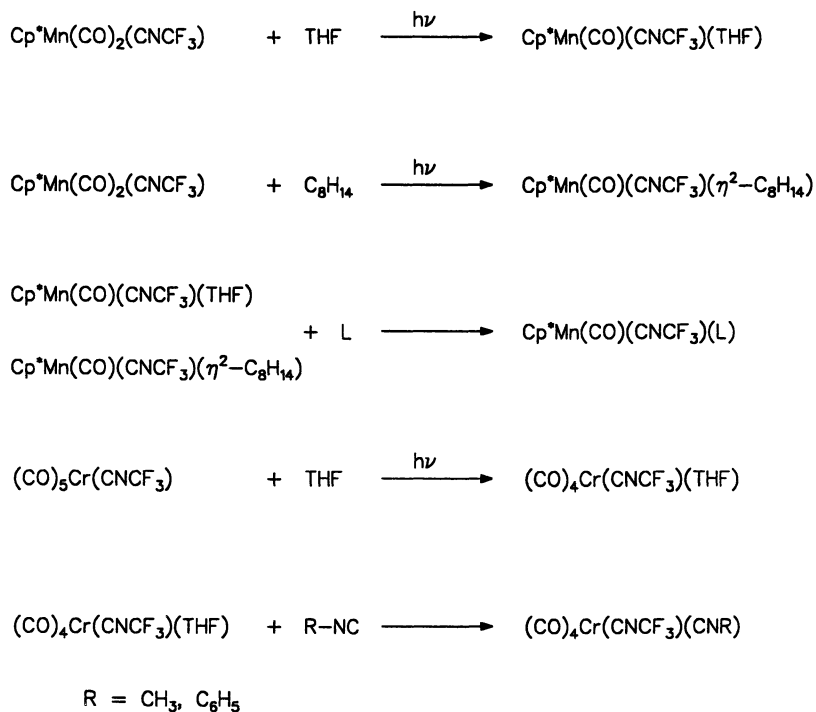
Many trifluoromethyl isocyanide complexes have been synthesized by ligand substitution reactions. Due to the instability of CNCF_3 in the condensed phase, mild reaction conditions and reactive metal complexes have to be chosen as starting materials (Scheme I). The first trifluoromethyl isocyanide complexes $(\text{CO})_5\text{M}(\text{CNCF}_3)$ ($\text{M} = \text{Cr}, \text{W}$) were obtained by replacement of a tetrahydrofuran or a *cis*-cyclooctene ligand in $(\text{CO})_5\text{CrL}$ ($\text{L} = \text{THF}, \text{C}_8\text{H}_{14}$) (12). $\text{Cp}^*\text{Mn}(\text{CO})_2(\text{CNCF}_3)$ was prepared by a similar method (13), whereas the synthesis of $\text{Cp}^*\text{Mn}(\text{CNCF}_3)_3$ required photolytic replacement of the carbonyl ligands. Reaction of the more reactive $\text{Cp}^*\text{Co}(\text{CO})_2$ with trifluoromethyl isocyanide yielded $\text{Cp}^*\text{Co}(\text{CNCF}_3)_2$ which can be oxidized easily to $\text{Cp}^*\text{Co}(\text{CNCF}_3)_2\text{X}_2$ ($\text{X} = \text{Cl}, \text{Br}, \text{I}$) using halogens (14). Metal halides like FeX_2 or CuX were used to synthesize $\text{Fe}(\text{CNCF}_3)_4\text{X}_2$ (15) ($\text{X} = \text{Br}, \text{I}$) and $(\text{F}_3\text{CNC})_x\text{CuX}$ (16) ($\text{X} = \text{Cl}, \text{Br}, \text{I}$). The iron complexes were obtained from diethyl ether solutions as the *trans* isomer which tended to isomerize to the *cis* compound in dichloromethane solution (15). With an excess of the isocyanide, soluble copper complexes of unknown composition and structure were formed. $(\text{F}_3\text{CNC})\text{CuX}$, which is insoluble in non-coordinating solvents crystallized on standing at ambient temperature.

The first evidence for the unique π accepting ability of the CF_3NC ligand came from the spectroscopic and structural data of $(\text{CO})_5\text{M}(\text{CNCF}_3)$ ($\text{M} = \text{Cr}, \text{W}$) (12, 17, 18). However, the vibrational spectroscopic data of these complexes are complicated due to strong coupling of the CO vibrations with the NC vibration. The structure determination of the chromium complex by electron diffraction (17) indicated a strongly bent isocyanide ligand but could not give detailed information on the metal carbon distances.

A simpler situation was found in half-sandwich complexes of the type $\text{Cp}^*\text{Mn}(\text{CO})_2\text{L}$ ($\text{L} = \text{CNCF}_3, \text{CNCH}_3, \text{CO}, \text{CS}$) (13), $\text{Cp}^*\text{Mn}(\text{CO})(\text{CNCF}_3)\text{L}$ ($\text{L} = \text{CO}, \text{CS}, \text{CNCH}_3, \text{CNC}_6\text{H}_5, \text{PET}_3, \text{PPh}_3, \text{PF}_3$) (19) and $[\text{C}_6\text{H}_3(\text{CH}_3)_3]\text{Cr}(\text{CO})(\text{CNCF}_3)\text{L}$ ($\text{L} = \text{CO}, \text{CNCH}_3$) (20) that were synthesized according to Scheme II.



Scheme I



Scheme II

The low energy CN modes for the complexes $\text{Cp}^*\text{Mn}(\text{CNCF}_3)_3$ (13) and $[\text{C}_6\text{H}_3(\text{CH}_3)_3]\text{Cr}(\text{CNCF}_3)_3$ (20) prove that the lowest frequency vibrations between 1700 and 2100 cm^{-1} have to be assigned to the NC modes and not the CO modes.

Table I. Vibrational spectroscopic data of manganese half-sandwich complexes containing the trifluoromethyl isocyanide ligand

L =	CO	CNCH ₃	CS
$\text{Cp}^*\text{Mn}(\text{CO})_2\text{L}$			
$\nu(\text{CO}) \text{ cm}^{-1}$	2010, 1918	1940, 1893	1996, 1945
$\nu(\text{CN}) \text{ cm}^{-1}$		2105	
$k(\text{CO}) \text{ Ncm}^{-1}$	15.45	14.83	15.68
$\text{Cp}^*\text{Mn}(\text{CO})(\text{CNCF}_3)\text{L}$			
$\nu(\text{CO}) \text{ cm}^{-1}$	2007, 1945	1939	1988
$\nu(\text{CN}) \text{ cm}^{-1}$	1810	1762, 2129	1831
$k(\text{CO}) \text{ Ncm}^{-1}$	15.77	15.1	15.9

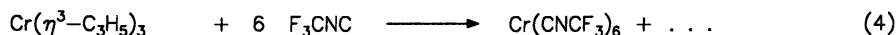
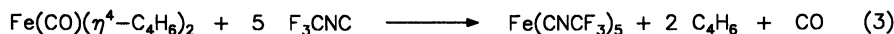
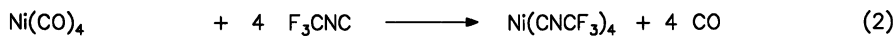
Information about the π acceptor/ σ donor ratio of the ligands can be obtained from the CO stretching frequency force constants in the various complexes (Table I) which correlates with the electron density in the π^* orbitals of the carbonyl ligand. Small CO stretching force constants, k_{CO} , are observed for good σ donating ligands, whereas strong π accepting ligands such as CS or CNCF_3 exhibit large k_{CO} .

The relative strength of the metal to carbon bonds in mixed carbonyl trifluoromethyl isocyanide complexes is reflected in their ligand substitution chemistry, too. Photolysis of $\text{Cp}^*\text{Mn}(\text{CO})_2(\text{CNCF}_3)$ or $(\text{CO})_5\text{Cr}(\text{CNCF}_3)$ in THF (Scheme II) results in the replacement of only a carbonyl ligand by a solvent molecule. No replacement of the isocyanide ligand took place as was demonstrated by the products of the reaction of these complexes with other ligands such as methyl isocyanide, which allowed for the syntheses of mixed substituted complexes. These complexes make possible a detailed comparison of the bonding of the fluorinated and nonfluorinated isocyanide and the carbonyl ligand as they contain all of the ligands in one molecule.

The structure determination of *trans*-(CO)₄Cr(CNCH₃)(CNCF₃) (21) by X-ray crystallography (Figure 1) gives information about the different metal carbon bond lengths. The shortest metal carbon bond observed is the one to the trifluoromethyl isocyanide ligand which is about 20 pm shorter than that to the methyl isocyanide ligand. It is even significantly shorter than those to the carbonyl ligands. In addition, the trifluoromethyl isocyanide ligand is strongly bent in contrast to an almost linear methyl isocyanide ligand.

The synthesis of homoleptic complexes is very difficult due to the instability of trifluoromethyl isocyanide in the condensed phase. The complexes $\text{Ni}(\text{CNCF}_3)_4$ (22), $\text{Fe}(\text{CNCF}_3)_5$, $\text{Fe}_2(\text{CNCF}_3)_9$ (23) and $\text{Cr}(\text{CNCF}_3)_6$ (24) have been synthesized from $\text{Ni}(\text{CO})_4$, $\text{Fe}(\text{CO})(\eta^4\text{-C}_4\text{H}_6)_2$ and $\text{Cr}(\eta^3\text{-C}_3\text{H}_5)_3$, respectively. All of these homoleptic complexes are stable, volatile materials. The compound $\text{Fe}(\text{CNCF}_3)_5$, which presumably has a trigonal bipyramidal structure like $\text{Fe}(\text{CO})_5$ (25) and $\text{Fe}(\text{CNR})_5$ (R = Et, *i*-Pr, *t*-Bu) (26), is nonrigid on the NMR time scale exhibiting a single resonance for the CNCF_3 ligands even at -100 °C. $\text{Fe}(\text{CNCF}_3)_5$ tends to

dimerize forming $\text{Fe}_2(\text{CNCF}_3)_9$ (23). The crystal structure determination of $\text{Cr}(\text{CNCF}_3)_6$ (24) revealed the expected almost octahedral coordination sphere at the chromium.



However, four crystallographically independent CNCF_3 ligands are found that differ mainly in the order of bending at the isocyanide nitrogen atom.

Dinuclear Trifluoromethyl Isocyanide Complexes and Cluster Compounds

Due to its strong π accepting ability, the trifluoromethyl isocyanide ligand tends to occupy the bridging position in dinuclear complexes and clusters even if the analogous carbonyl derivative has only terminal ligands as in $[\text{CpM}(\text{CO})_3]_2$ ($\text{M} = \text{Mo}, \text{W}$) (27) or $\text{M}_3(\text{CO})_{12}$ ($\text{M} = \text{Ru}, \text{Os}$) (28,29).

Addition of trifluoromethyl isocyanide onto the metal-metal triple bond of $[\text{CpM}(\text{CO})_2]_2$ (Scheme III) results in the formation of $\text{Cp}_2\text{M}_2(\text{CO})_4(\eta^2\text{-}\mu_2\text{-CNCF}_3)$ ($\text{M} = \text{Mo}, \text{W}$; $\text{Cp} = \text{C}_5\text{H}_5, \text{C}_5\text{Me}_5$) (30) which according to the spectroscopic data possess structures similar to that of the phenyl isocyanide derivative (31). When an excess of CNCF_3 is used two different isomeric products are obtained depending on the reaction conditions. The red isomer $[\text{CpM}(\text{CO})_2(\mu_2\text{-CNCF}_3)]_2$ (Figure 2) which is formed at 0°C has two symmetrical trifluoromethyl isocyanide bridges. It can be converted into the violet isomer $[\text{Cp}(\text{CO})_2\text{M}(\mu\text{-F}_3\text{C-N=C=C=N-CF}_3)\text{M}(\text{CO})_2\text{Cp}]$ by dissolving the compound in dichloromethane at ambient temperature or by running the reaction at ambient temperature (30,32).

Unlike $[\text{CpMo}(\text{CO})_3]_2$ (27), $\text{Mo}_2\text{Cp}_2(\text{CO})_5(\text{CNCH}_3)$ (33), and $[\text{CpMo}(\text{CO})_2(\text{CN-}i\text{-Bu})]_2$ (34) $[\text{Cp}^*\text{Mo}(\text{CO})_2(\mu_2\text{-CNCF}_3)]_2$ (30) has bridging ligands. These bridging positions are occupied by the trifluoromethyl isocyanide ligands. Carbon molybdenum bond distances of 207.9(5) and 230.8(6) pm indicate a small asymmetry in these bridges. As the molecule has a crystallographic center of symmetry, the pentamethylcyclopentadienyl ligands are exactly in a trans position. This centrosymmetric structure is maintained in solution as indicated by two infrared absorptions for the terminal CO ligands at 1945 and 1919 cm^{-1} and a single band for the bridging isocyanide ligand at 1610 cm^{-1} . The violet isomer $[\text{Cp}(\text{CO})_2\text{Mo}(\mu\text{-F}_3\text{C-N=C=C=N-CF}_3)\text{Mo}(\text{CO})_2\text{Cp}]$ (32) (Figure 2) has a bridging diazabutatriene ligand (dimeric isocyanide) that is coordinated to one molybdenum center by the nitrogen atoms and the other molybdenum center by the carbon atoms C4 and C4' forming a five-membered and a three-membered metallacycle, respectively. Although a formal electron count results in 19 and 17 electrons at the molybdenum centers, the compound is diamagnetic indicating delocalized electron systems in the rings. $\text{Cl}_2(i\text{-BuNC})_4\text{Nb}(\mu\text{-}i\text{-BuNCCN-}i\text{-Bu})\text{NbCl}_4$ (35) is the only other example of a dimeric isocyanide functioning as a ligand. The reductive coupling of coordinated isocyanides has been studied in detail in recent years by Lippard et al. (36) and Fillipou et al. (37).

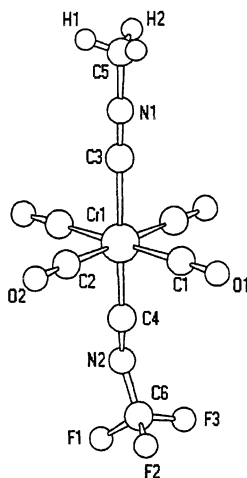
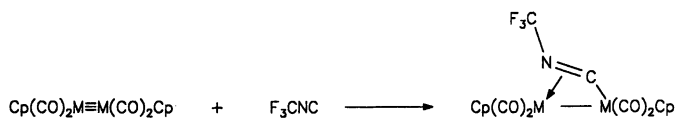
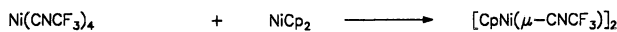
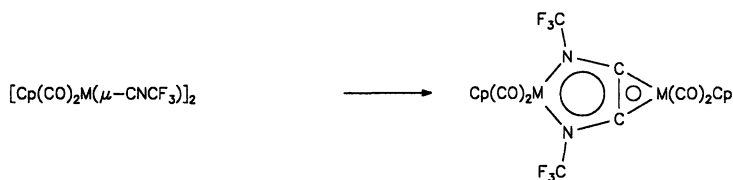
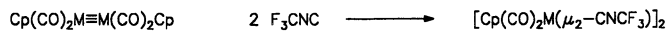


Figure 1. SCHAKAL plot of *trans*-(CO)₄Cr(CNCH₃)(CNCF₃). Cr1-C1 188.2 (5), Cr1-C2 189.8 (5), Cr1-C3 201.7 (5), Cr1-C4 181.4 (6) pm, C3-N1-C5 179.7 (3), C4-N2-C6 141.2 (7) °. (Reproduced with permission from ref. 21. Copyright 1990 VCH.)



M = Mo, W

Cp = C₅H₅, C₅Me₅



Scheme III

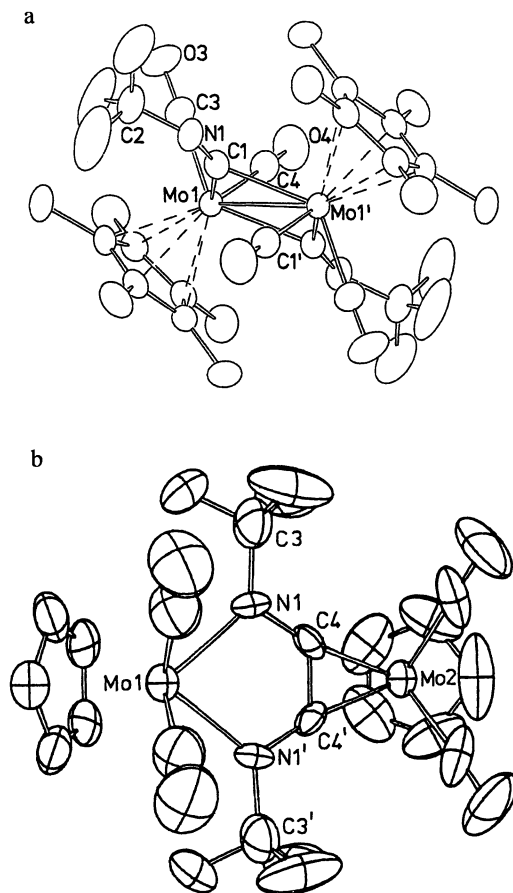


Figure 2. Molecular structure of $[\text{Cp}^*\text{Mo}(\text{CO})_2(\mu_2\text{-CNCF}_3)]_2$ (a) (Reproduced with permission from ref. 30. Copyright Elsevier 1986.) and $[\text{Cp}(\text{CO})_2\text{Mo}(\mu\text{-F}_3\text{C-N=C=C=N-CF}_3)\text{Mo}(\text{CO})_2\text{Cp}]$ (b). (Reproduced with permission from ref. 32. Copyright 1984 VCH.)

$\text{Fe}_3(\text{CO})_{10}(\text{L})(\mu_2\text{-CNCF}_3)$ (L = CO, PMe_3 , PEt_3 , $\text{P}(\text{OMe})_3$, $\text{P}(\text{OEt})_3$, and CN-*t*-Bu) (Scheme IV) have been synthesized by replacement of a carbonyl or acetonitrile ligand in the suitable starting material by CNCF_3 (38). The structures of $\text{Fe}_3(\text{CO})_{10}(\text{L})(\mu_2\text{-CNCF}_3)$ [L = CO, PMe_3 , $\text{P}(\text{OMe})_3$] (38) have been determined by X-ray crystallography (Figure 3). They all have a bridging CNCF_3 ligand, a bridging CO ligand, and the phosphine or phosphite in equatorial positions. The $\text{P}(\text{OMe})_3$ derivatives exist as a mixture of two positional isomers. Isomer I bears the phosphite ligand at a bridged iron atom, whereas in isomer II this ligand is coordinated at the unbridged iron atom. Like $\text{Fe}_3(\text{CO})_{12}$, all of these compounds are fluxional on the NMR time scale at ambient temperature; however, they are the only derivatives of $\text{Fe}_3(\text{CO})_{12}$ for which it has been possible to observe the low-temperature limiting spectra which correspond to the solid state structures. This fluxionality has been studied in detail (38) but the exchange mechanism is still under discussion (39).

Unlike $\text{Fe}_3(\text{CO})_{12}$ and its derivatives $\text{Ru}_3(\text{CO})_{12}$ (28) and $\text{Os}_3(\text{CO})_{12}$ (29) have approximately D_{3h} symmetry with only terminal ligands. This changes drastically if the trifluoromethyl isocyanide ligand is introduced. Replacement of the labile acetonitrile ligand in $\text{Ru}_3(\text{CO})_{11}(\text{CH}_3\text{CN})$ (Scheme IV) by CNCF_3 yields $\text{Ru}_3(\text{CO})_{11}(\mu_2\text{-CNCF}_3)$ which according to the X-ray crystal structure determination has a bridging CNCF_3 and CO ligand (Figure 4). In addition, small amounts of $\text{Ru}_3(\text{CO})_{10}(\mu_2\text{-CNCF}_3)_2$ and the cluster degradation product $\text{Ru}_2(\text{CO})_6(\mu_2\text{-CNCF}_3)_3$ are obtained (40).

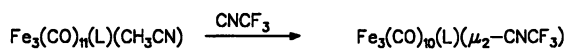
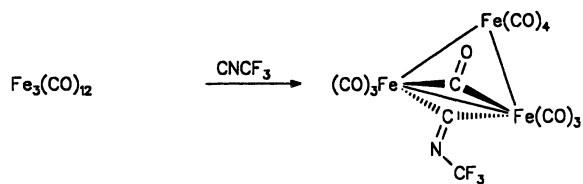
Attempts to synthesize the corresponding osmium compounds (Scheme V) yielded $\text{Os}_3(\text{CO})_{11}(\mu_2\text{-CNCF}_3)_2$ (41), a stabilized derivative of the unknown complex $\text{Os}_3(\text{CO})_{13}$, and a possible structural model for the ligand addition products of other reactions with $\text{M}_3(\text{CO})_{12}$ clusters. On heating $\text{Os}_3(\text{CO})_{11}(\mu_2\text{-CNCF}_3)_2$ loses carbon monoxide quantitatively yielding $\text{Os}_3(\text{CO})_{10}(\mu_2\text{-CNCF}_3)_2$. Even more surprising is the fact that if $\text{Os}_3(\text{CO})_{10}(\text{CH}_3\text{CN})_2$ is used as the starting material $\text{Os}_3(\text{CO})_{10}(\text{CH}_3\text{CN})(\mu_2\text{-CNCF}_3)_2$ and $\text{Os}_3(\text{CO})_9(\text{CH}_3\text{CN})(\mu_2\text{-CNCF}_3)_2$ (Figure 5) are isolated besides the expected $\text{Os}_3(\text{CO})_{10}(\mu_2\text{-CNCF}_3)_2$ (42). Thus the unique property of the trifluoromethyl isocyanide ligand to form very strong bridges between metal atoms allows structures that cannot be found with other ligands.

Heating of $\text{Fe}_3(\text{CO})_{10}(\text{L})(\mu\text{-CNCF}_3)$ in *n*-heptane (Scheme VI) resulted in loss of two CO ligands and a change in the bonding mode of the isocyanide ligand, which according to the crystal structure determination of $\text{Fe}_3(\text{CO})_8[\text{P}(\text{OMe})_3](\eta^2\text{-}\mu_3\text{-CNCF}_3)$ functions as a $\eta^2\text{-}\mu_3$ -bridging ligand (43) (Figure 6). The isocyanide ligand is oriented perpendicular to one iron-iron bond with the carbon atom coordinated to all three iron atoms [Fe2-C4 174.6(4), Fe1-C4 199.6(4), Fe3-C4 201.3(4) pm] and the nitrogen atom coordinated to Fe1 and Fe3 [Fe1-N1 200.2(4), Fe3-N1 197.9(4) pm]. The isocyanide functions as a six electron donor ligand resulting in an expansion of the C-N bond to 130.9(6) pm. This type of coordination resembles that of a small molecule (isocyanide) at a metal surface making this compound possibly an interesting model for elementary steps in catalysis in accordance with earlier suggestions (44). Indeed an enhanced reactivity is observed even with molecular hydrogen (see below).

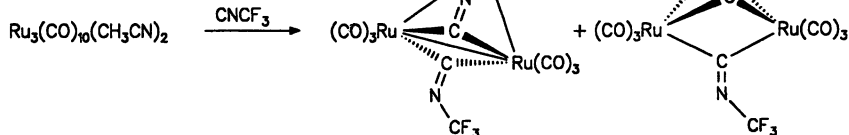
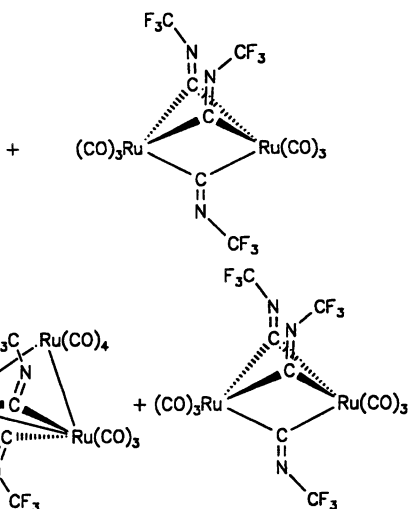
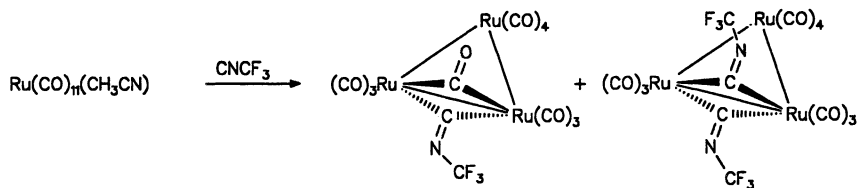
Reactions of the Coordinated Trifluoromethyl Isocyanide Ligand

As mentioned, $[\text{CpM}(\text{CO})_2(\mu_2\text{-CNCF}_3)]_2$ (M = Mo, W) shows dimerization of the coordinated bridging CNCF_3 ligands forming diazabutatriene ligands (see above). This dimerization process is thus far limited to these dinuclear complexes.

In pioneering work Chatt et al. studied the reaction of several isocyanide complexes with nucleophiles yielding carbene complexes (45). We have studied the reaction of $(\text{CO})_5\text{Cr}(\text{CNCF}_3)$ and $\text{Cp}^*\text{Co}(\text{CNCF}_3)_2$ with nucleophiles. The reaction



L = CO, PMe₃, PEt₃, P(OMe)₃, P(OEt)₃, CN-*t*-Bu



Scheme IV

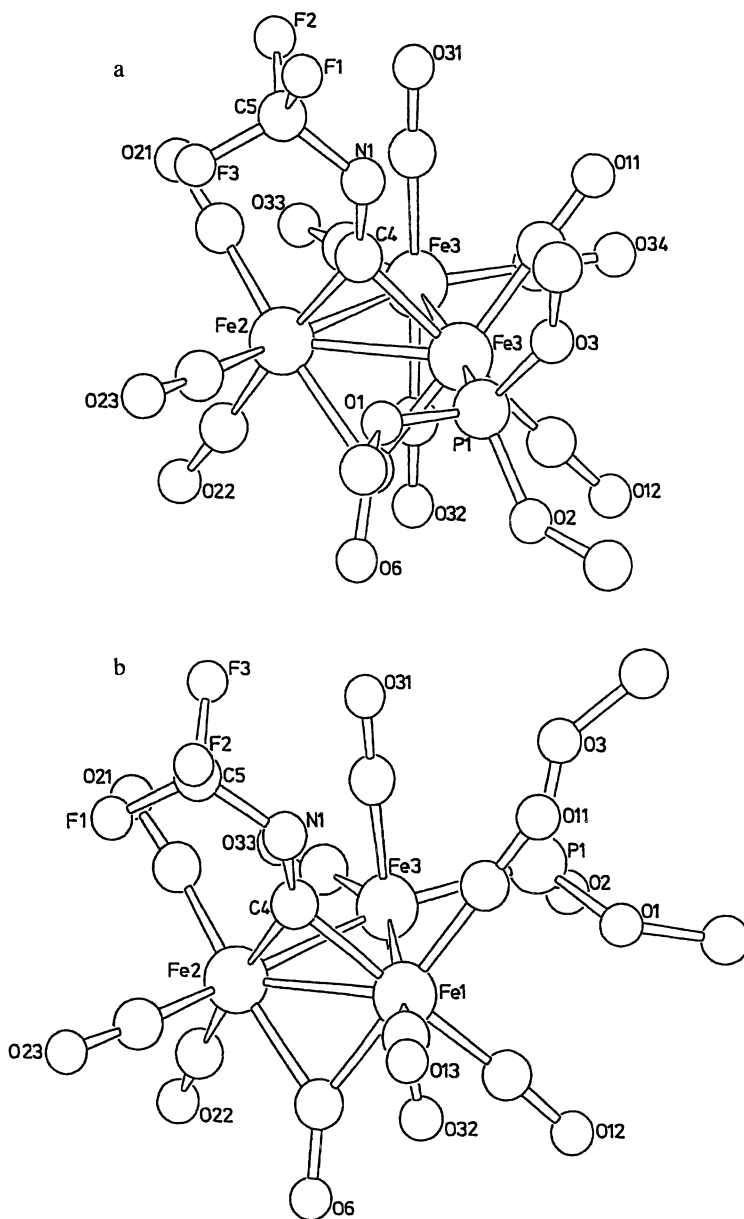


Figure 3. Molecular structure of $\text{Fe}_3(\text{CO})_{10}(\mu_2\text{-CNCF}_3)[\text{P}(\text{OMe})_3]$, isomer I (a) and isomer II (b). (Reproduced with permission from ref. 38. Copyright 1991 ACS.)

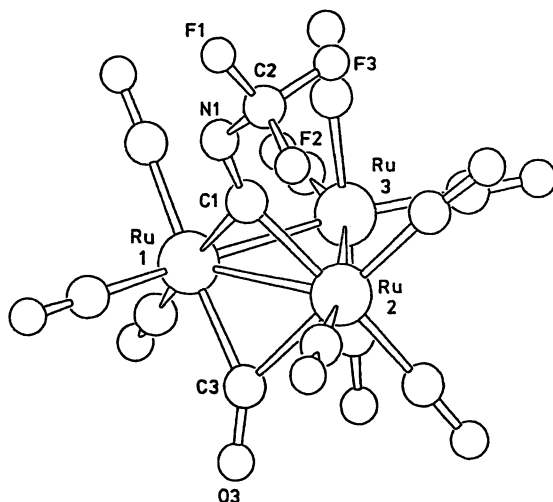
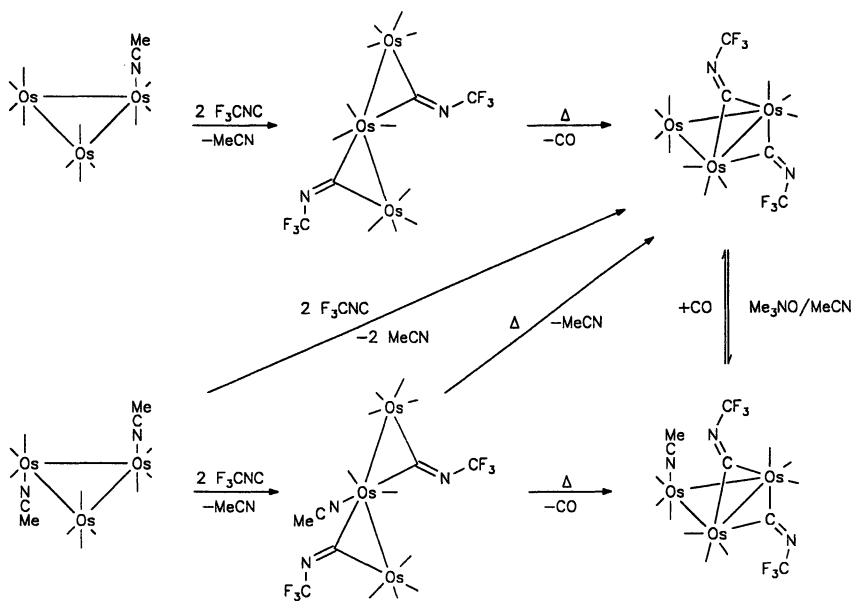


Figure 4. Molecular structure of $\text{Ru}_3(\text{CO})_{11}(\mu_2\text{-CNCF}_3)$. (Reproduced with permission from ref. 40. Copyright 1991 VCH.)



Scheme V

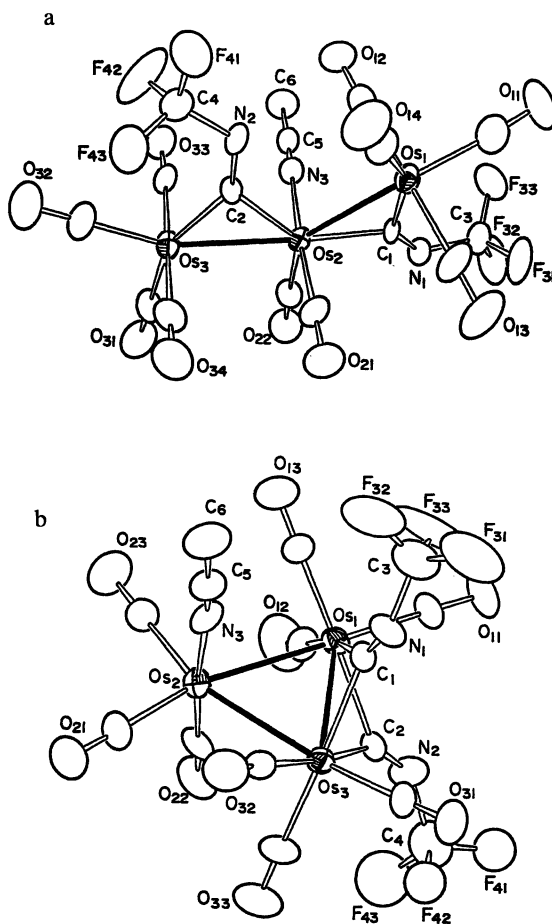


Figure 5. Molecular structures of $\text{Os}_3(\text{CO})_{10}(\text{CH}_3\text{CN})(\mu_2\text{-CNCF}_3)_2$ (a) and $\text{Os}_3(\text{CO})_9(\text{CH}_3\text{CN})(\mu_2\text{-CNCF}_3)_2$ (b). (Reproduced with permission from ref. 42. Copyright 1992 ACS.)

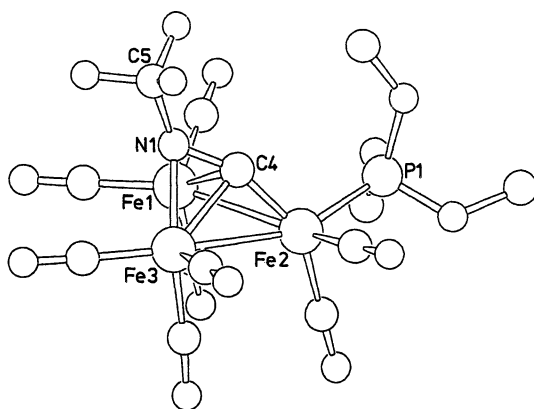
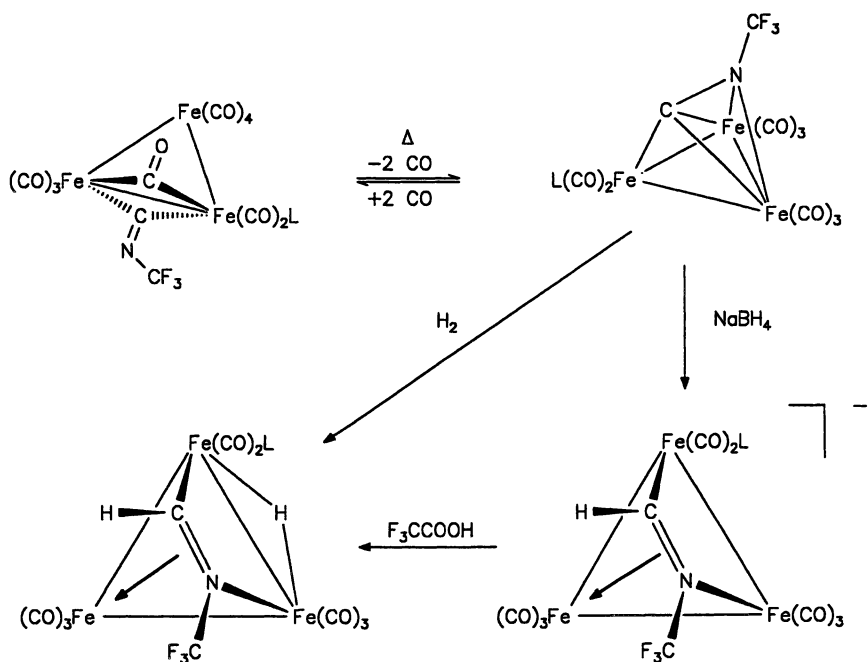
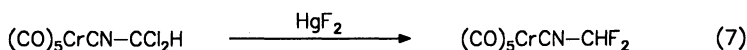
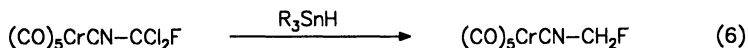
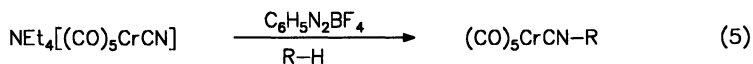


Figure 6. Molecular structure of $\text{Fe}_3(\text{CO})_8[\text{P}(\text{OMe})_3]\eta^2\text{-}\mu_3\text{-CNCF}_3$. (Reproduced with permission from ref. 43. Copyright 1991 VCH.)

of the chromium complex (Scheme VII) with various amines yields carbene complexes by a nucleophilic attack at the isocyanide carbon followed by HF elimination and a second nucleophilic attack at the formimidoyl carbon atom (46). The reaction of the cobalt complex (Scheme VIII) is less straightforward. The final product results from a complete change of one trifluoromethyl isocyanide ligand, whereas the other trifluoromethyl isocyanide ligand is converted into a *N*-trifluoromethyl formimidoyl ligand (47). A possible reaction mechanism is outlined in Scheme VIII. The first nucleophilic attack occurs at the isocyanide carbon atom resulting in a carbene complex. HF elimination gives rise to a N=CF₂ group which can be further attacked by secondary amine and by water. Ring closure to form the metallacycle accompanied by H migration to the isocyanide carbon atom yields the final product whose structure has been elucidated by X-ray crystallography (48).

Fluoromethyl and Difluoromethyl Isocyanide

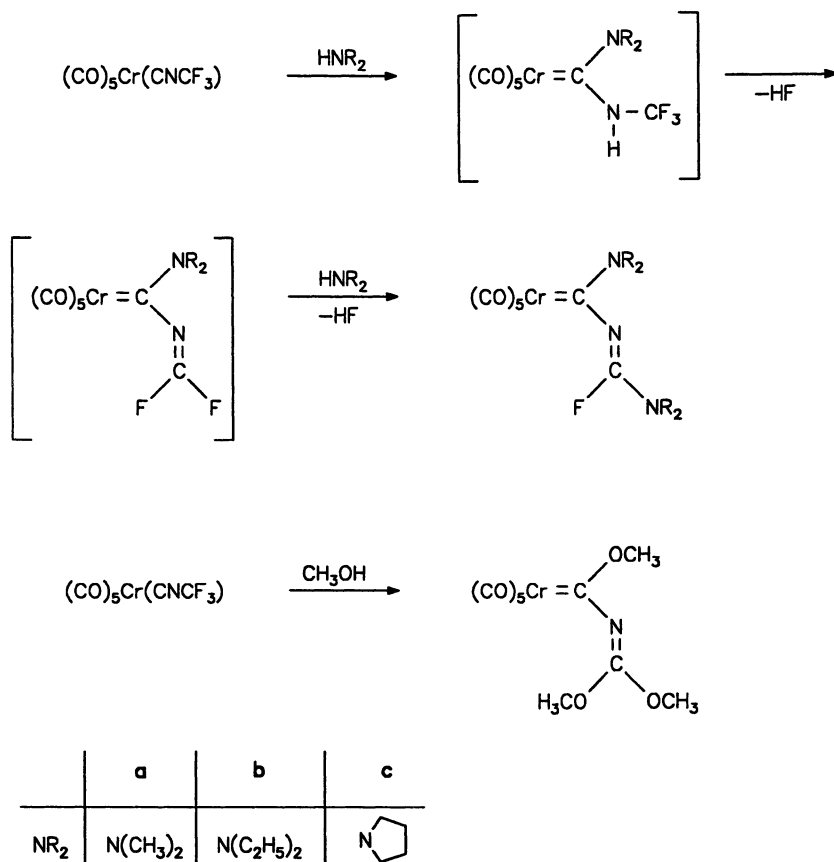
The synthesis of H₂FC-NC and HF₂C-NC suffers from the lack of a suitable fluoroorganic starting material. Therefore, an indirect method for their synthesis has to be found. As demonstrated by Fehlhammer et al. (3) pentacarbonyl(cyano)chromate can be alkylated in a radical pathway.



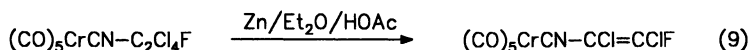
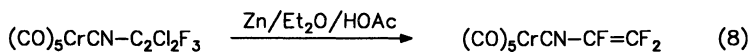
By using either CH₂Cl₂ or CHFCl₂ the desired starting materials can be obtained in moderate yields (3). These can be converted to the fluoromethyl and difluoromethyl isocyanide complexes by reduction with tributyltin hydride or halogen exchange with mercuric fluoride, respectively (48). The vibrational and ¹³C NMR spectroscopic data indicate a decreasing π accepting/σ donor ratio on lowering the number of fluorine atoms at the methyl carbon atom. Attempts to obtain the free isocyanide by flash vacuum pyrolysis were unsuccessful for fluoromethyl isocyanide, whereas difluoromethyl isocyanide could be obtained and spectroscopically characterized (49). However, this pyrolysis gave only an impure product which contains HCN as a major impurity and more importantly HCC-CN and HCC-NC as minor impurities. This finding led to the discovery, synthesis and microwave spectroscopic characterization of ethynyl isocyanide (50) and its detection in interstellar space by radio astronomy (51).

Trifluorovinyl Isocyanide

The synthesis of trifluorovinyl isocyanide again requires the organometallic detour as suitable fluoroorganic starting materials are not available.



Scheme VII



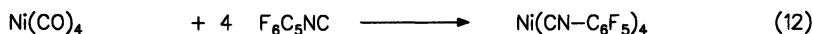
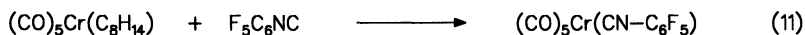
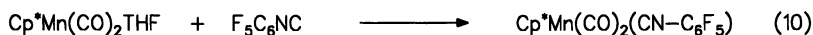
Radical alkylation of $\text{NEt}_4[(\text{CO})_5\text{Cr}(\text{CN})]$ in 1,2-dichloro-1,1,2-trifluoroethane yields $(\text{CO})_5\text{Cr}(\text{CN}-\text{CF}-\text{CF}_2\text{Cl})$ which can be converted to the trifluorovinyl isocyanide complex by dechlorination with zinc (52).

According to the X-ray crystal structure determination (Figure 7) the chromium atom is coordinated almost octahedrally by five carbonyl ligands and the trifluorovinyl isocyanide ligand. The chromium carbon distance to the isocyanide ligand is slightly longer than the distances to the carbonyl ligands.

Flash vacuum pyrolysis of the complex at 240 °C yields the free isocyanide which has been characterized by ^{19}F NMR, IR and mass spectroscopy (52). The isocyanide function can be unambiguously detected by a strong infrared absorption at 2111 cm^{-1} and the coupling of the geminal fluorine atom with the nitrogen isotope ^{14}N (nuclear spin 1) of about 10 Hz.

Pentafluorophenyl Isocyanide

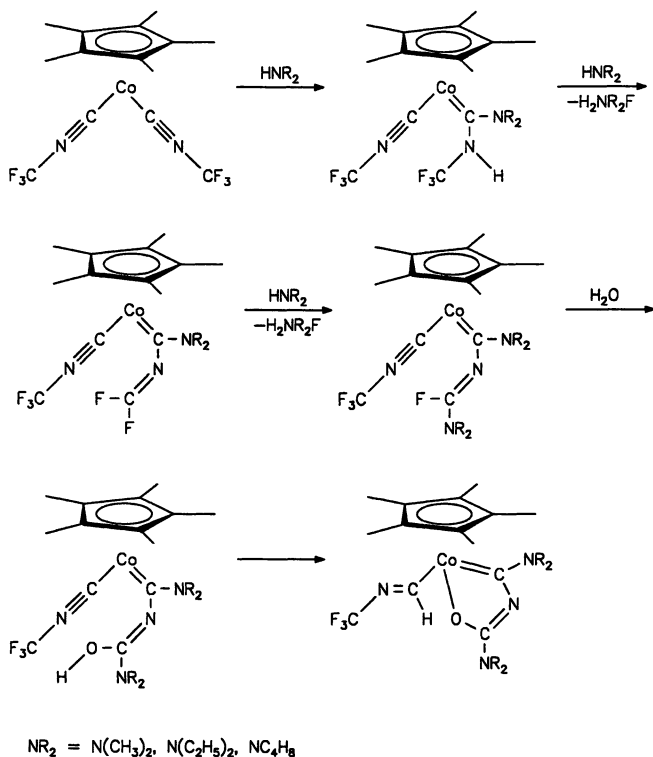
The synthesis of pentafluorophenyl isocyanide follows the pathway established for CNC_3F_3 (6) and CNSF_5 (53). Debromination of $\text{F}_5\text{C}_6\text{-N}=\text{CBr}_2$ with magnesium give moderate yields of $\text{F}_5\text{C}_6\text{-NC}$ melting at 13 °C under decomposition (54).



Its structure has been elucidated by X-ray crystallography at 115 K (55). Only the three complexes $\text{Ni}(\text{CNC}_6\text{F}_5)_4$ (56), $(\text{CO})_5\text{Cr}(\text{CNC}_6\text{F}_5)$ (56) and $\text{Cp}^*\text{Mn}(\text{CO})_2(\text{CNC}_6\text{F}_5)$ (54) have been synthesized so far. The spectroscopic data indicate that the fluorinated aryl isocyanide ligand has a lower π acceptor/ σ donor ratio than the trifluoromethyl isocyanide ligand. This is supported by the X-ray crystallographic results of $\text{Cp}^*\text{Mn}(\text{CO})_2(\text{CNC}_6\text{F}_5)$ (54) which reveal a slightly longer Mn-C bond to the isocyanide carbon atom in comparison to the carbonyl carbon atoms.

Conclusion

Fluorinated isocyanides of the alkyl, aryl and alkenyl series can now be synthesized either by direct methods or the organometallic detour. Among these trifluoromethyl isocyanide has unique properties as it is an extremely strong π accepting ligand with a strong preference for the bridging position in dinuclear complexes and cluster compounds. Although many complexes have been synthesized containing this carbonyl-like ligand and our understanding in the ligand properties has increased during recent years, there remains many open questions and possibilities to make use of these ligand properties. The chemistry of the other fluorinated isocyanides is still



Scheme VIII

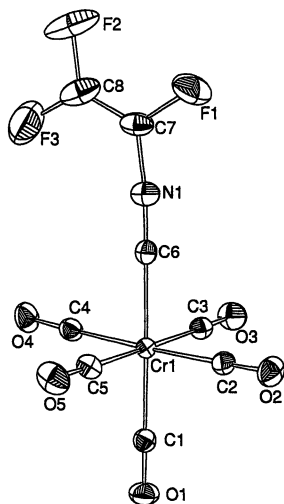


Figure 7. Molecular structure of $(\text{CO})_5\text{Cr}(\text{CN}-\text{CF}=\text{CF}_2)$. (Reproduced with permission from ref. 52. Copyright 1992 The Royal Society of Chemistry.)

at the beginning. Fluoroethynyl isocyanide is still missing and it is a challenge to find a synthesis for this presumably unstable molecule either in the free state or as a ligand on a metal.

Note Added in Proof

G. Simonneaux et al. (57) published the synthesis and complexation to ruthenium(II) and iron(III) *meso*-tetraphenylporphyrins of two new fluorinated alkyl isocyanides, 2-monofluoroethyl isocyanide and 2,2,2-trifluoroethyl isocyanide. A new synthesis of trifluoroethyl isocyanide, pentafluoroethyl isocyanide and heptafluoropropyl isocyanide from R-N=CF₂ (R = CF₃, C₂F₅, C₃F₇) using triphenyl phosphine has been reported (58). Geometries and HOMO and LUMO energies of fluorinated vinyl isocyanides have been calculated (59). Pentacarbonyl chromium complexes of both isomers of the first fluorinated diisocyanide, 1,2-diisocyano-1,2,3,3,4,4-hexafluoro cyclobutane have been isolated from a [2+2] cycloaddition reaction of pentacarbonyl(trifluorovinyl isocyanide) chromium. The structure of the *cis* isomer has been elucidated by X-ray crystallography (60).

Acknowledgment

This research was supported by the Deutsche Forschungsgemeinschaft, the Fonds der Chemischen Industrie, and the Graduiertenkolleg "Synthese und Strukturaufklärung niedermolekularer Verbindungen" der TU und FU Berlin. This review article contains several, in part still unpublished, results collected by my coworkers mentioned in the references, whose enthusiastic cooperation I gratefully acknowledge.

Literature Cited

1. Singleton, E.; Oosthuizen, H. E. *Adv. Organomet. Chem.* **1983**, *22*, 209; Bonati, F.; Mingheti, G. *Inorg. Chim. Acta* **1974**, *9*, 95.
2. Christian, G.; Stolzenberg, H.; Fehlhammer, W. P. *J. Chem. Soc., Chem. Comm.* **1982**, 184.
3. Fehlhammer, W. P.; Degel, F.; Beck, G. *Chem. Ber.* **1987**, *120*, 461.
4. Fehlhammer, W. P.; Degel, F.; Stolzenberg, H. *Angew. Chem., Int. Ed. Engl.* **1981**, *20*, 214.
5. Makarov, S. P.; Englin, M. A.; Videiko, A. F.; Nikolaeva, T. V. *Zh. Obsh. Khim.* **1967**, *37*, 2781.
6. Lentz, D. *J. Fluorine Chem.* **1984**, *24*, 523.
7. Bock, H.; Dammel, R.; Lentz, D. *Inorg. Chem.* **1984**, *23*, 1535.
8. Christen, D.; Ramme, K.; Haas, B.; Oberhammer, H.; Lentz, D. *J. Chem. Phys.* **1984**, *90*, 4020.
9. Halonen, L.; Mills, I. M. *J. Mol. Spectrosc.* **1978**, *73*, 494.
10. Burrus, C. A. *J. Chem. Phys.* **1958**, *28*, 427.
11. Ghosh, N.; Trambarulo, R.; Gordy, W. *J. Chem. Phys.* **1961**, *21*, 308.
12. Lentz, D. *Chem. Ber.* **1984**, *117*, 415.
13. Lentz, D.; Kroll, J.; Langner, C. *Chem. Ber.* **1987**, *120*, 803.
14. Lentz, D.; Pötter, B. *J. Organomet. Chem.* **1987**, *336*, 393.
15. Lentz, D. unpublished results.
16. Lentz, D.; Marschall, R. unpublished results.
17. Oberhammer, H.; Lentz, D. *Inorg. Chem.* **1985**, *24*, 1271.
18. Beach, D. B.; Jolly, W. L.; Lentz, D. *Inorg. Chem.* **1985**, *24*, 1892.
19. Lentz, D.; Marschall, R. *Chem. Ber.* **1989**, *122*, 1223.

20. Lentz, D.; Marschall, R. *Z. Anorg. Allg. Chem.* **1991**, *593*, 181.
21. Lentz, D.; Pötter, B.; Marschall, R.; Brüdgam, I.; Fuchs, J. *Chem. Ber.* **1990**, *123*, 257.
22. Lentz, D. *Chem. Ber.* **1985**, *118*, 560.
23. Lentz, D. *J. Organomet. Chem.* **1989**, *377*, 305.
24. Lentz, D. *J. Organomet. Chem.* **1990**, *381*, 205.
25. Cotton, F. A.; Danti, A.; Waugh, J. S.; Fesseden, R. W. *J. Chem. Phys.* **1958**, *29*, 1427.
26. Basset, J.-M.; Berry, D. E.; Barker, G. K.; Green, M.; Howard, J. A. K.; Stone, F. G. A. *J. Chem. Soc., Dalton Trans.* **1980**, 80.
27. Gould, R. O.; Barker, J.; Kilner, M. *Acta Crystallogr.* **1988**, *C44*, 461; Adams, R. D.; Collins, D. M.; Cotton, F. A. *Inorg. Chem.* **1974**, *13*, 1086; Wilson, F. C.; Shoemaker, D. P. *Naturwissenschaften* **1956**, *43*, 57; Wilson, F. C.; Shoemaker, D. P. *J. Chem. Phys.*, **1957**, *27*, 809.
28. Mason, R.; Rae, A. I. *J. Chem. Soc. A.* **1968**, 778; Churchill, M. R.; Hollander, F. J.; Hutchinson, J. P. *Inorg. Chem.* **1977**, *16*, 2655.
29. Corey, E. R.; Dahl, L. F. *Inorg. Chem.* **1962**, *1*, 521.
30. Lentz, D.; Brüdgam, I.; Hartl, H. *J. Organomet. Chem.* **1986**, *299*, C38; Lentz, D.; Lönnewitz, B. unpublished results.
31. Adams, R. D.; Katahira, D. A.; Yang, L. W. *Organometallics* **1982**, *1*, 231.
32. Lentz, D.; Brüdgam, I.; Hartl, H. *Angew. Chem., Int. Ed. Engl.* **1984**, *23*, 525.
33. Adams, R. D.; Brice, M.; Cotton, F. A. *J. Am. Chem. Soc.* **1973**, *95*, 6594.
34. Coville, N. J. *J. Organomet. Chem.* **1981**, *281*, 337.
35. Cotton, F. A.; Roth, W. J. *J. Am. Chem. Soc.* **1983**, *105*, 3734.
36. Carnahan, E. M.; Lippard, S. J. *J. Am. Chem. Soc.* **1990**, *112*, 3230; Vrtis, R. N.; Rao, C. P.; Warner, S.; Lippard, S. J. *J. Am. Chem. Soc.* **1988**, *110*, 2669; Vrtis, R. N.; Rao, C. P.; Bott, S. G.; Lippard, S. J. *J. Am. Chem. Soc.* **1988**, *110*, 7564; Bianconi, P. A.; Vrtis, R. N.; Rao, C. P.; Williams, I. D.; Engler, M. P.; Lippard, S. J. *Organometallics* **1987**, *6*, 1968; Bianconi, P. A.; Warner, S.; Lippard, S. J. *Organometallics* **1986**, *5*, 1716 and cited references.
37. Filippou, A. C.; Grünleitner, W. *J. Organomet. Chem.* **1990**, *393*, C10 and cited references.
38. Lentz, D.; Marschall, R. *Organometallics* **1991**, *10*, 1487; Brüdgam, I.; Hartl, H.; Lentz, D. *Z. Naturforsch.* **1984**, *39b*, 721.
39. Mann, B. E. *Organometallics* **1992**, *11*, 481; Johnson, B. F. G.; Parisini, E.; Roberts, Y. V. *Organometallics* **1993**, *12*, 233.
40. Lentz, D.; Marschall, R.; Hahn, E. *Chem. Ber.* **1991**, *124*, 777.
41. Adams, D. R.; Chi, Y.; DesMarteau, D. D.; Lentz, D.; Marschall, R. *J. Am. Chem. Soc.* **1992**, *114*, 1909.
42. Adams, R. D.; Chi, Y.; DesMarteau, D. D.; Lentz, D.; Marschall, R.; Scherrmann, A., *J. Am. Chem. Soc.* **1992**, *114*, 10822.
43. Lentz, D.; Marschall, R. *Chem. Ber.* **1991**, *124*, 497.
44. Chini, P. *Inorg. Chim. Acta Rev.* **1968**, *2*, 31; Johnson, B. F. G.; Lewis, J. *Pure Appl. Chem.* **1975**, *44*, 43; Muettterties, E. L. *Bull. Soc. Chim. Belg.* **1975**, *84*, 959; Muettterties, E. L. *Science* **1977**, *196*, 839; Muettterties, E. L. *Chem. Rev.* **1979**, *79*, 91; Muettterties, E. L. *Pure Appl. Chem.* **1982**, *54*, 83; Ugo, R. *Catal. Rev. Sci. Eng.* **1975**, *11*, 225.
45. Badley, E. M.; Chatt, J.; Richards, R. L.; Sim, G. A. *J. Chem. Soc., Chem. Commun.* **1969**, 1322; see also ref. 1 and Crociani, B. in *Reactions of Coordinated Ligands* (Bratermann, P. S., Ed.), Plenum Press: New York, 1986; Beck, G.; Fehlhammer, W. P. *Angew. Chem., Int. Ed. Engl.* **1988**, *27*, 1344; Fehlhammer, W. P.; Beck, G. *J. Organomet. Chem.* **1989**, *369*, 105; Fehlhammer, W. P.; Beck, G. *Chem. Ber.* **1989**, *122*, 1907.
46. Lentz, D.; Marschall, R. *Chem. Ber.* **1990**, *123*, 751.

47. Lentz, D.; Marschall, R. *Chem. Ber.* **1990**, *123*, 467.
48. Lentz, D.; Preugschat, D. *J. Organomet. Chem.* **1992**, *436*, 185.
49. Lentz, D.; Preugschat, D. 10th Winter Fluorine Conference, St. Petersburg, Florida, **1991**.
50. Krüger, M.; Dreizler, H.; Preugschat, D.; Lentz, D. *Angew. Chem., Int. Ed. Engl.* **1991**, *30*, 1644.
51. Kawaguchi, K.; Ohishi, M.; Ishikawa, S.-I.; Kaifu, N. *Astrophys. J.* **1992**, *386*, L51.
52. Lentz, D.; Preugschat, D. *J. Chem. Soc., Chem. Comm.* **1992**, 1523.
53. Thrasher, J. S.; Madappat, K. V. *Angew. Chem., Int. Ed. Engl.* **1989**, *28*, 1256.
54. Lentz, D.; Graske, K.; Preugschat, D. *Chem. Ber.* **1988**, *121*, 1445.
55. Lentz, D.; Preugschat, D. *Acta Crystallogr.* **1993**, *C49*, 52.
56. Lentz, D.; Preugschat, D. unpublished results.
57. Gèze, C.; Legrand, N.; Bondon, A.; Simonneaux, G. *Inorg. Chim. Acta* **1992**, *195*, 73.
58. Krumm, B.; Kirchmeier, R. L.; Shreeve, J. M. ACS 11th Winter Fluorine Conference, St. Petersburg, Florida, **1993**.
59. Madappat, K. V.; Thrasher, J. S.; Preugschat, D.; Lentz, D. ACS 11th Winter Fluorine Conference, St. Petersburg, Florida, **1993**.
60. Lentz, D.; Preugschat, D. ACS 11th Winter Fluorine Conference, St. Petersburg, Florida, **1993**.

RECEIVED June 23, 1993

Chapter 17

Synthetic, Structural, and Reactivity Studies of Organocobalt(III) Compounds Containing Fluorinated Alkyl Ligands

Paul J. Toscano, Elizabeth Barren, Holger Brand, Linda Konieczny,
E. James Schermerhorn, Kevin Shufon, and Stephen van Winkler

Department of Chemistry, State University of New York at Albany,
Albany, NY 12222

The synthesis and NMR (^1H , ^{13}C , and ^{19}F) spectral and X-ray structural characterization of fluoroalkyl bis(dimethylglyoximato)-cobalt(III) complexes are described. A discussion on the effect of fluorine substitution on the NMR spectral properties as well as on structural parameters relevant to electron-donating and steric properties of the fluorinated alkyl ligands is presented.

Bis(dimethylglyoximato)cobalt(III) complexes, also known trivially as the cobaloximes, have been well-studied as models for reactions involving the cleavage of the Co-C bond relevant to the mechanism of action of cobalamin-dependent enzymes (1-7). In addition, these compounds have received significant attention with regard to the elucidation of the factors that affect Co-C bond energies (8-11) and ground-state stabilities (1-3). A typical, neutral, pseudo-octahedral low-spin Co(III) cobaloxime, $\text{LCo}(\text{DH})_2\text{X}$ (where DH is the monoanion of dimethylglyoxime), is depicted in Figure 1. The cobaloximes are notable for their ability to accommodate a variety of neutral (L) and formally anionic (X) ligands (1-3). The anionic ligands span a wide range of traditional "inorganic" ligands, such as halides and pseudohalides, as well as covalently coordinated alkyl ligands containing substituents of differing electron-donating properties. These compounds also often readily form crystals that are suitable for single-crystal X-ray diffraction studies (2,3).

The synthesis and characterization of cobaloximes that have fluorine-containing alkyl ligands, especially those with fluorine substituents at the carbon atom ($\alpha\text{-C}$) attached to the cobalt ion, are the topic of this report. As noted above, the cobaloximes have been intensely examined spectroscopically and numerous high quality solid-state structural investigations have been previously accomplished (1-3). We have been interested in exploiting these properties of the cobaloxime system in order to assess the effect of fluorine substitution on spectroscopic and structural parameters of this class of compounds.

Synthesis of α -Fluorinated Organocobaloxime Complexes

Introduction of Fluoroalkyl Ligands via Fluorinated Aliphatic Alkyl Halides. Organocobaloximes, $\text{LCo}(\text{DH})_2\text{R}$ containing functionalized aliphatic alkyl (R) ligands that do not have α -fluorine ($\alpha\text{-F}$) atom substituents, are prepared in

0097-6156/94/0555-0286\$08.00/0
© 1994 American Chemical Society

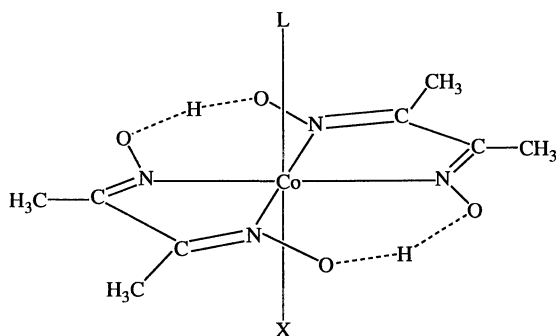


Figure 1. Schematic representation of a neutral $\text{LCo}(\text{DH})_2\text{X}$ cobaloxime.

general via reduction of $\text{LCo}^{\text{III}}(\text{DH})_2\text{Cl}$ to the anionic $\text{Co}(\text{I})$ complex $[\text{LCo}^{\text{I}}(\text{DH})_2]^-$ with excess NaBH_4 in strongly basic methanol (12-14) followed by addition of an alkyl halide or tosylate, where L is most often pyridine (py). However, if the R ligand to be introduced contains α -F atoms, this method can fail to provide pure products due to side reactions induced by the fluorine substitution. We will examine these problems briefly.

Although $\text{pyCo}(\text{DH})_2\text{CF}_3$ was reportedly prepared via the usual $[\text{pyCo}^{\text{I}}(\text{DH})_2]^-$ methods with CF_3I (15,16), it was later shown that partial replacement of F by H occurred under the reaction conditions (17). In our hands, we isolated a mixture of $\text{pyCo}(\text{DH})_2\text{CF}_3/\text{pyCo}(\text{DH})_2\text{CHF}_2$ in the ratio of 7.5:1 (18). We have observed similar results when $[\text{pyCo}^{\text{I}}(\text{DH})_2]^-$ interacts with ClCHF_2 ; an inseparable mixture of $\text{pyCo}(\text{DH})_2\text{R}$ (R = CHF_2 and CH_2F) was isolated. A further problem arises in the case of fluorinated alkyl moieties, such as CF_2CF_3 and especially $\text{CF}(\text{CF}_3)_2$, for which the alkylating reagents and product complexes are easily decomposed by excess borohydride reducing agent. In these cases, significant Co-C bond cleavage as well as facile decomposition of the alkylating agent occur unless large excesses of alkyl halide are employed (19).

We have found that these undesirable reactions can be avoided by decreasing the molar amount of NaBH_4 to 0.25 equivalents per cobalt complex. The desired $\text{pyCo}(\text{DH})_2\text{CF}_3$ then could be obtained using CF_3Br in one step, free from $\text{pyCo}(\text{DH})_2\text{CHF}_2$ (18). This procedure is superior to $\text{Co}(\text{II})$ methods (17,20,21) in that lengthy preparative and chromatographic steps can be avoided, less alkylating agent is required, and CF_3Br can be substituted for the costlier CF_3I . In addition, the complexes $\text{pyCo}(\text{DH})_2\text{R}$ (R = CF_2CF_3 and $\text{CF}(\text{CF}_3)_2$) (19) were readily isolated in modest yields using the respective alkyl iodides as alkylating agents. While alkyl chlorides can usually be utilized for alkylations of reduced $\text{Co}(\text{I})$ species (1), it appears that alkyl bromides or iodides must be utilized when the amount of borohydride reducing agent is limited. We have found that ClCHF_2 does not react with $[\text{pyCo}^{\text{I}}(\text{DH})_2]^-$ under the modified reaction conditions, although alkylation accompanied by defluorination occurred when excess NaBH_4 was employed (*vide supra*).

No special precautions are required for the preparation of organocobaloximes containing alkyl ligands with fluorine substitution at the β or further removed positions of the alkylating reagent. Thus, $\text{pyCo}(\text{DH})_2\text{R}$ (R = for example CH_2CF_3 (22) or $\text{CH}_2\text{C}_6\text{F}_5$) is readily prepared by the standard reduction of $\text{pyCo}^{\text{III}}(\text{DH})_2\text{Cl}$ to $[\text{py}^{\text{I}}\text{Co}(\text{DH})_2]^-$ followed by addition of the appropriate alkyl halide (12,13). We have also found that the complex with R = CH_2F can be obtained in poor to modest yields in the same manner using ClCH_2F with no substitution of F by H during the reaction.

It is interesting to note that we observed little or no formation of $\text{pyCo}(\text{DH})_2\text{X}$ (X = Br or I) in the above interaction of $[\text{pyCo}^{\text{I}}(\text{DH})_2]^-$ with fluoroalkyl halides. For example, prior studies have demonstrated that the nucleophile $[\text{Mn}(\text{CO})_5]^-$ reacts with highly fluorinated alkyl iodides to give $\text{Mn}(\text{CO})_5\text{I}$ rather than $\text{Mn}(\text{CO})_5\text{R}$ (23,24). These results were interpreted as arising from attack of the nucleophile at iodine due to a reversal of polarity in the C-I bond caused by the electronegative fluorine substituents. In the cobaloxime case, we suggest that a single electron transfer process may account for the isolation of the organocobalt complexes.

Introduction of Fluorine-Containing Ligands Via Highly Fluorinated Olefins. It is known that $[\text{pyCo}^{\text{I}}(\text{DH})_2]^-$ will substitute readily the halogen of vinyl and styryl halides (26). On the other hand, $[\text{pyCo}^{\text{I}}(\text{DH})_2]^-$ reacts with $\text{CH}_2=\text{CHZ}$

(Z = a strong electron-withdrawing group, such as CN or CO₂Me) under basic conditions to give pyCo(DH)₂CH₂CH₂Z by nucleophilic addition followed by subsequent protonation during workup (27). In the case of F₂C=CFX (X = F, Cl, Br, I), highly electron withdrawing substituents as well as potential leaving groups are present. Thus, we were interested in systematically establishing the manner in which the Co(I) nucleophile would interact with F₂C=CFX olefins under the usual high pH reaction conditions.

For X = F, only pyCo(DH)₂CF₂CF₂H was formed via an apparent nucleophilic addition to the fluoro-olefin followed by protonation during workup (28). This result is analogous to those observed for the interaction of other Co(I) systems with F₂C=CF₂ (29,30).

When X = Cl, the nucleophilic addition complex pyCo(DH)₂CF₂CFCIH is the major product in good yields (25); addition occurs at the terminus that has two fluorine atoms in accord with previous investigations involving the interaction of traditional main group nucleophiles with F₂C=CFCl (28). However, trace amounts of pyCo(DH)₂CF=CF₂ and pyCo(DH)₂Cl were observed in the crude product by ¹H NMR spectroscopy. These impurities were removed easily via recrystallization (25). The identity of the product as pyCo(DH)₂CF₂CFCIH was further confirmed by its independent synthesis from the reaction of BrCF₂CFCIH with [pyCo^I(DH)₂]⁻ under conditions of limiting NaBH₄. This latter preparation again illustrates the preference of the cobalt anion for Br over Cl under these reaction conditions (*vide supra*).

On the other hand, when X = Br (25) or I, the major isolated complex was found to be pyCo(DH)₂CF=CF₂; only a minor amount of pyCo(DH)₂CF₂CFXH was evident for X = Br with essentially none for X = I. The amount of pyCo(DH)₂X (X = Br or I) in the crude product depended upon the addition rate of F₂C=CFX (25); faster additions produced more of the undesired halogeno complex. We found that the addition of gaseous F₂C=CFBr was easier to control than addition of liquid F₂C=CFI. Thus, F₂C=CFBr was the preferred reagent for preparation of pyCo(DH)₂CF=CF₂, which could be obtained in pure form after fractional recrystallization (25). The difference in the nature of the products obtained as a function of X in F₂C=CFX is most likely a manifestation of competing nucleophilic addition and electron transfer reaction pathways (25).

Substitution of the Pyridine Ligand of the Fluoroalkyl Cobalt Complexes. Most of the above discussion has been concerned with cobaloximes in which the neutral ligand was pyridine. We and others have found previously that the pyridine ligand of LCo(DH)₂R (where R = CF₃ (17), CF₂CF₃, CF(CF₃)₂ (19), CF=CF₂, CF₂CFCIH) can be replaced by H₂O utilizing the ion-exchange resin-assisted technique. In the case of fluoroalkyl cobaloximes, the substitution reactions are very slow; for example, completion of ligand exchange requires *ca.* two weeks for R = CF₃ and *ca.* four weeks for R = CF(CF₃)₂ at ambient temperature. Higher reaction temperatures cause significant decomposition. The slow ligand exchange rates are consistent with the poor electron donating properties of the fluoroalkyl ligands and the dissociative nature of the reaction mechanism for substitution (17,31,32). The aquo ligand in H₂OCo(DH)₂R can be easily substituted by a variety of two electron donor (L) ligands in CH₂Cl₂ solution to give LCo(DH)₂R in nearly quantitative yields.

Characterization of the Fluoroalkyl Cobaloximes by NMR Spectroscopy.

^1H NMR Spectroscopy. The ^1H NMR spectra of the organofluorocobaloximes are relatively unremarkable being rather typical for cobaloximes (3), although the spectra are useful for structural characterization of this class of compounds. For example on first inspection, the ^1H NMR spectra of $\text{pyCo}(\text{DH})_2\text{CF}_2\text{CFCIH}$ and $\text{pyCo}(\text{DH})_2\text{CF}=\text{CF}_2$ have similar chemical shifts for the oxime methyl resonances (25). However, the oxime methyl groups for the CF_2CFCIH complex give rise to two closely spaced singlets (δ 2.19 and 2.17) due to the magnetic anisotropy caused by the asymmetric center in the alkyl ligand. On the other hand for the $\text{CF}=\text{CF}_2$ compound, the oxime methyl resonance is a single sharp line at δ 2.20. The CF_2CFCIH complex, of course, also contains a resonance at δ 6.15 for the alkyl ligand. This peak can be easily overlooked since it is split into a doublet of doublet pattern by the three magnetically inequivalent fluorine nuclei and only integrates to one proton (33,34).

The oxime methyl resonances for $\text{pyCo}(\text{DH})_2\text{R}$ ($\text{R} = \text{CF}_3, \text{CF}_2\text{CF}_3, \text{CF}(\text{CF}_3)_2, \text{CF}=\text{CF}_2$) fall in the chemical shift range of δ 2.20 to 2.24 (18,19,25). These shifts are downfield from their hydrocarbyl analogs, which is in accord with the poor electron-donating properties of the fluoroalkyl ligands (3). The α -H resonances of the py ligand are ca. 0.08 to 0.10 ppm upfield from the chemical shifts for the hydrocarbyl analogs (18,19,25), which is again in agreement with previous observations that this resonance moves further upfield as the electron-donating power of the alkyl ligand decreases (3).

^{13}C NMR Spectroscopy. The ^{13}C chemical shift of the γ -C of coordinated pyridine in $\text{pyCo}(\text{DH})_2\text{R}$ has previously been demonstrated to reflect the electron-donating ability of the *trans*-alkyl ligand (3); the poorer the electron-donation by the R group, the further downfield that this shift occurs. Not surprisingly, the highly α -fluorinated alkyl ligands are among the poorer ligands at electron-donation as judged by this NMR indicator (Table I).

Table I. ^{13}C Chemical Shifts for the γ -C of $\text{pyCo}(\text{DH})_2\text{R}$

R	δ	R	δ
$\text{CH}(\text{CN})\text{Cl}$	138.60 ^a	$\text{CF}_2\text{CF}_2\text{H}$	138.37
CF_2CF_3	138.60	CH_2CN	138.25 ^a
$\text{CF}(\text{CF}_3)_2$	138.54	CH_2CF_3	138.03 ^b
CH_2NO_2	138.48 ^b	$\text{CH}=\text{CH}_2$	137.72 ^a
CF_3	138.44	CH_3	137.48 ^b
$\text{CF}=\text{CF}_2$	138.39	CH_2CH_3	137.34 ^a
CF_2CFCIH	138.37	$\text{CH}(\text{CH}_3)_2$	137.21 ^a

^aRef. 35. ^bRef. 3

The ^{13}C chemical shift of the ester carbon of coordinated $\text{P}(\text{OCH}_3)_3$ is likewise sensitive to electron-donation by the *trans* R ligand (3). A plot of the pyridine γ -C chemical shifts vs. the trimethyl phosphite ester carbon chemical shifts

gives a good linear correlation except for large R groups. These deviations likely originate from lengthening of the Co-C bond distance in the $P(OCH_3)_3$ complex relative to the py complex due to increased steric interactions between the alkyl ligand and the equatorial ligands. The $CF(CF_3)_2$ point is exceptionally distant from the least-squares line for sterically small ligands (19). This result is presumably due to the very large size of this perfluorinated alkyl ligand.

^{19}F NMR Spectroscopy. The ^{19}F NMR chemical shifts of the perfluoroisopropyl ligand of $LCo(DH)_2[CF(CF_3)_2]$ and their correlations to ligand (L) cone angles, pK_a of L, Hammett substituent constants for substituents on L, as well as their general relationship to the steric bulk of L, have been thoroughly discussed (36) and will be only briefly presented here. Importantly, the ^{19}F chemical shifts for the Co-CF moiety occur considerably further upfield than for *d*-block transition metal complexes having strongly π -accepting ligands, such as CO (37-40). In fact, the $\delta[^{19}F(Co-CF)]$ values for the cobaloximes are strikingly close to those reported for d^{10} metal complexes (41-43) in which the $CF(CF_3)_2$ group is believed to be strongly carbanionic. This upfield shift suggests that there is increased electron density on the perfluoroisopropyl ligand due to strong electron withdrawal and/or that the metal-to-ligand bonding has considerable ionic character. In general as the electron-donating ability of the *trans* L ligand increases (steric bulk of L held constant), the $\delta[^{19}F(Co-CF)]$ chemical shifts move further upfield as expected under this interpretation.

Similar observations with regard to chemical shifts are obtained for the α -F resonances for the CF_3 , CF_2CF_3 , and CF_2CFClH complexes as well. In the latter case in particular (25), the α -F resonances are significantly upfield from the analogous resonances in $(CO)_5M(CF_2CFClH)$ ($M = Mn$ or Re) complexes (33,34,44,45). Again, this suggests that there is increased electron density on the alkyl ligand in the cobaloxime complexes due to the high electronegativity of the fluorine substituents.

Finally, we note as a general observation for the fluorinated alkyl cobaloximes that ^{19}F NMR resonances for the α -F atoms generally are broadened due to incomplete averaging of coupling to the quadrupolar ^{59}Co ($I = 7/2$) nucleus. This broadening is evident for the $CF=CF_2$ complexes as well, where the F atom on the carbon atom attached to cobalt is severely broadened and the F atom *trans* to the cobalt is slightly broadened (25).

Structural Studies of the Fluorinated Alkyl Cobaloximes.

Background. It has long been recognized that fluoroalkyl transition metal complexes generally are more stable than their hydrocarbyl analogs (46,47). While this effect may be due in part to kinetic factors such as suppression of decomposition pathways, a shortening of the M-C bond in the α -fluorinated derivatives has been noted in relevant X-ray and electron diffraction studies (48-53). The increased stability of the fluoroalkyl compounds, as well as the bond length diminution and other properties (54), have been interpreted as arising from ionic-covalent resonance (electrostatic) effects, as well as from partial double bonding character of the M-C bond and rehybridization of the σ orbital on the carbon atom attached to the metal (46-54). Although diffraction studies could shed some light on the latter suggestions, there have been few direct structural comparisons of alkyl metal complexes in which the effect on structural parameters of fluorine for hydrogen substitution has been probed (48-53). The cobaloxime system appeared to be a good candidate for such studies since nearly two hundred cobaloxime structures have been determined previously (2,3), thus facilitating interpretations of structural changes as a function of fluorine substitution.

LCo(DH)₂CF₃. Structural data for LCo(DH)₂CF₃ (L = py, MeOH, and P(OMe)₃) are collected in Table II, as well as comparisons to LCo(DH)₂CH₃ (L = py, H₂O, and P(OMe)₃). Although ¹³C NMR chemical shifts suggest that the CF₃ ligand is a much poorer electron-donor than CH₃, Co-L distances are only slightly shorter, if at all, for related compounds. The α and d values for the most part imply that CH₃ and CF₃ are similar in steric bulk.

Table II. Bonding Parameters for LCo(DH)₂R

L/R	Co-L(Å)	Co-R(Å)	d (Å) ^a	α (°) ^b
py/CH ₃ ^c	2.068(3)	1.998(5)	0.04	3.2
py/CF ₃ ^d	2.043(3)	1.949(4)	0	3.0
H ₂ O/CH ₃ ^e	2.058(3)	1.990(5)	0	-4.0
MeOH/CF ₃	2.021(4)	1.934(5)	-0.03	-4.9
P(OMe) ₃ /CH ₃ ^e	2.256(4)	2.014(14)	0.10	10
P(OMe) ₃ /CF ₃	2.258(4)	1.957(16)	0.01	1.2

^aDisplacement of the Co atom out of the N₄-donor plane; positive values indicate towards L. ^bInterplanar angle between DH ligands; positive values indicate bending away from L. ^cRef. 55. ^dRef. 18. ^eRef. 3.

On the other hand, bonding parameters involving the alkyl ligand are of more interest. The results for pyCo(DH)₂CF₃ (Figure 2) are representative for this type of complex (18). The Co-R bond length decreases significantly by *ca.* 0.05 Å relative to the CH₃ complex as was expected (46). The Co-C-F angles open up to 115.3(4)^o (avg.), while the F-C-F angles are compressed to 102.9(4)^o (avg.). The C-F distances in the ligand were of normal length (1.327(7) Å). The elongation of the CF₃ tetrahedron coupled with the normal C-F bond lengths suggest that the shortening of the Co-C bond in LCo(DH)₂CF₃ is probably best ascribed to ionic/covalent resonance effects, rather than to rehybridization or hyperconjugation. That is, the Co-C bonding has a strong ionic component, which is in agreement with the NMR results that suggest that the electron density on the fluoroalkyl group is high (*vide supra*).

LCo(DH)₂CF₂CF₃. Bonding parameters for the complexes LCo(DH)₂R (L = 4-[NH=C(OMe)]py, R = CH₂CH₃; L = 4-CNpy, R = CH₂CF₃; L = py, R = CF₂CF₃) are collected in Table III. The structural comparison of compounds having differently substituted pyridine ligands is justified by the large data base of cobaloxime structures (2,3). The structure of pyCo(DH)₂CF₂CF₃ is depicted in Figure 3.

A shortening of the Co-N(py) bond is observed as fluorine substitution increases. However, the Co-C bond length remains about the same throughout the series perhaps because the CF₃ group prevents closer approach. While one must not overlook packing forces, some support for this notion can be derived from the large negative d and α values for the CF₂CF₃ derivative. There is again a pronounced elongation of the tetrahedron about the carbon atom attached to cobalt and the C-C bond length of the alkyl ligand is very short (1.417(14) Å). These results are

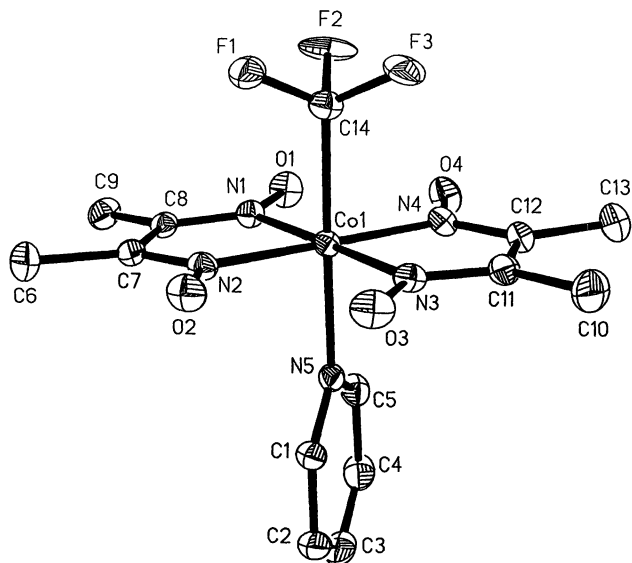


Figure 2. ORTEP view of the structure of $\text{pyCo}(\text{DH})_2\text{CF}_3$.

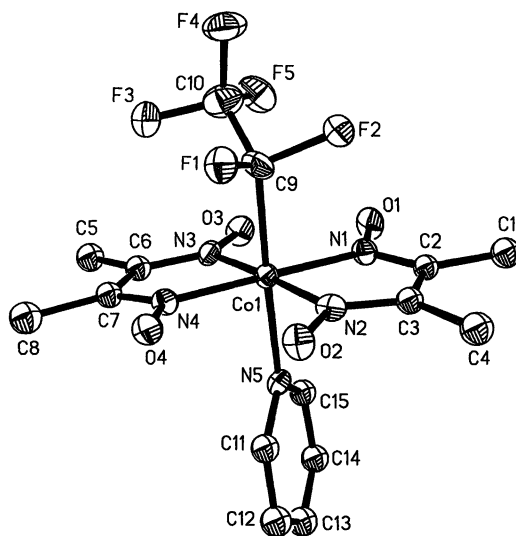


Figure 3. ORTEP view of the structure of $\text{pyCo}(\text{DH})_2\text{CF}_2\text{CF}_3$.

consistent with a significant ionic contribution to the bonding of the alkyl ligand to the cobalt.

Table III. Bonding Parameters for X-pyCo(DH)₂R

R	Co-L(Å)	Co-R(Å)	<i>d</i> (Å) ^a	<i>α</i> (°) ^a
CH ₂ CH ₃ ^b	2.081(3)	2.035(5)	0.05	9.1
CH ₂ CF ₃ ^c	2.041(2)	2.010(3)	0.01	1.0
CF ₂ CF ₃ ^d	2.024(6)	2.013(3)	-0.04	-8.8

^aSame definitions as in Table II. ^bX = NH=C(OMe); Ref. 56.

^cX = CN; Ref. 22. ^dX = H.

LCo(DH)₂CF(CF₃)₂. The structures of LCo(DH)₂CF(CF₃)₂ (L = py (Figure 4) and P(C₆H₅)₃) have been thoroughly discussed previously (19,36) and will be summarized here. The extreme steric bulkiness of the CF(CF₃)₂ group is manifested by large negative *d* and *α* values in each complex. Bonding parameters within the alkyl ligand again can be reconciled with ionic character in the Co-C bond, in accord with the ¹⁹F NMR studies of complexes containing the CF(CF₃)₂ ligand (*vide supra*).

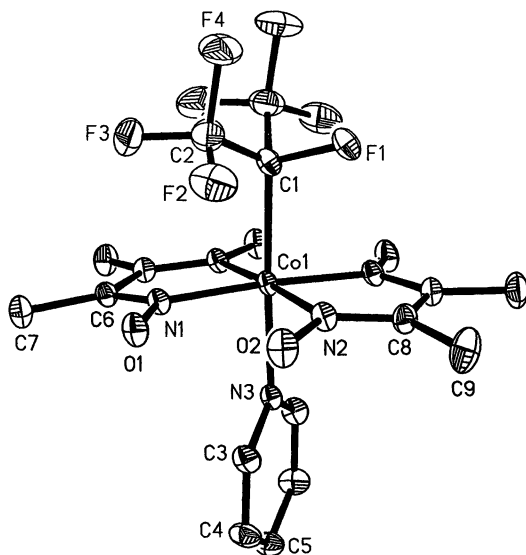


Figure 4. ORTEP view of the structure of pyCo(DH)₂CF(CF₃)₂.

Conclusions

Synthetic methods have been devised that lead to moderate to good yields of α -fluorinated alkyl cobaloximes. NMR studies and structural comparisons to the nonfluorinated analogs suggest that there is a significant ionic character in the bonding of the fluorinated alkyl ligands to the cobalt center.

Literature Cited

1. Toscano, P. J.; Marzilli, L. G. *Prog. Inorg. Chem.* **1984**, *31*, 105.
2. Randaccio, L.; Bresciani-Pahor, N.; Zangrando, E.; Marzilli, L. G. *Chem. Soc. Rev.* **1989**, *18*, 225.
3. Bresciani-Pahor, N.; Forcolin, M.; Marzilli, L. G.; Randaccio, L.; Summers, M. F.; Toscano, P. J. *Coord. Chem. Rev.* **1985**, *63*, 1.
4. Anderson, R. J.; Ashwell, S.; Dixon, R. M.; Golding, B. T. *J. Chem. Soc., Chem. Commun.* **1990**, 70.
5. Grate, J. H.; Grate, J. W.; Schrauzer, G. N. *J. Am. Chem. Soc.* **1982**, *104*, 1588.
6. Tada, M.; Nakamura, T.; Matsumoto, M. *J. Am. Chem. Soc.* **1988**, *110*, 4647.
7. Finke, R. G.; Schiraldi, D. A.; Mayer, B. J. *Coord. Chem. Rev.* **1984**, *54*, 1.
8. Ng, F. T. T.; Rempel, G. L.; Mancuso, C.; Halpern, J. *Organometallics* **1990**, *9*, 2762.
9. Halpern, J. *Polyhedron* **1988**, *7*, 1483.
10. Koenig, T. W.; Hay, B. P.; Finke, R. G. *Polyhedron* **1988**, *7*, 1499.
11. Toscano, P. J.; Seligson, A. L.; Curran, M. T.; Skrobitt, A. T.; Sonnenberger, D. C. *Inorg. Chem.* **1989**, *28*, 166.
12. Trogler, W. C.; Stewart, R. C.; Epps, L. A.; Marzilli, L. G. *Inorg. Chem.* **1974**, *13*, 1564.
13. Bulkowski, J.; Cutler, A.; Dolphin, D.; Silverman, B. *Inorg. Synth.* **1980**, *20*, 131.
14. Schrauzer, G. N. *Inorg. Synth.* **1968**, *11*, 61.
15. Schrauzer, G. N.; Windgassen, R. J. *J. Am. Chem. Soc.* **1966**, *88*, 3738.
16. Schrauzer, G. N.; Ribeiro, A.; Lee, L. P.; Ho, R. K. Y. *Angew. Chem., Int. Ed. Engl.* **1971**, *10*, 807.
17. Brown, K. L.; Yang, T.-F. *Inorg. Chem.* **1987**, *26*, 3007 and references therein.
18. Toscano, P. J.; Konieczny, L.; Liu, S.; Zubieta, J. *Inorg. Chim. Acta* **1989**, *166*, 163.
19. Toscano, P. J.; Brand, H.; Liu, S.; Zubieta, J. *Inorg. Chem.* **1990**, *29*, 2101.
20. Roussi, P. F.; Widdowson, D. A. *J. Chem. Soc., Perkin Trans. 1* **1982**, 1025.
21. Roussi, P. F.; Widdowson, D. A. *J. Chem. Soc., Chem. Commun.* **1979**, 810.
22. Bresciani-Pahor, N.; Calligaris, M.; Randaccio, L.; Marzilli, L. G.; Summers, M. F.; Toscano, P. J.; Grossman, J.; Liotta, D. *Organometallics* **1985**, *4*, 630.
23. McClellan, W. R. *J. Am. Chem. Soc.* **1961**, *83*, 1598.
24. Beck, W.; Hieber, W.; Tengler, H. *Chem. Ber.* **1961**, *94*, 862.
25. Toscano, P. J.; Barren, E. *J. Chem. Soc., Chem. Commun.* **1989**, 1159.
26. Dodd, D.; Johnson, M. D.; Meeks, B. S.; Titchmarsh, D. M.; Duong, K. N. V.; Gaudemer, A. *J. Chem. Soc., Perkin Trans. 2* **1976**, 1261.
27. Schrauzer, G. N.; Windgassen, R. J. *J. Am. Chem. Soc.* **1967**, *89*, 1999.
28. Chambers, R. D.; Mobbs, R. H. *Adv. Fluorine Chem.* **1965**, *4*, 50.
29. Mays, M. J.; Wilkinson, G. *Nature* **1964**, *203*, 1167.
30. Mays, M. J.; Wilkinson, G. *J. Chem. Soc.* **1965**, 6629.

31. Charland, J.-P.; Attia, W. M.; Randaccio, L.; Marzilli, L. G. *Organometallics* **1990**, *9*, 1367.
32. Stewart, R. C.; Marzilli, L. G. *J. Am. Chem. Soc.* **1978**, *100*, 817.
33. Bruce, M. I.; Jolly, P. W.; Stone, F. G. A. *J. Chem. Soc. A* **1966**, 1602.
34. Wilford, J. B.; Stone, F. G. A. *Inorg. Chem.* **1965**, *4*, 93.
35. Zangrando, E.; Bresciani-Pahor, N.; Randaccio, L.; Charland, J.-P.; Marzilli, L. G. *Organometallics* **1986**, *5*, 1938.
36. Toscano, P. J.; Brand, H.; Geremia, S.; Randaccio, L.; Zangrando, E. *Organometallics* **1991**, *10*, 713.
37. King, R. B.; Kapoor, R. N.; Houk, L. W. *J. Inorg. Nucl. Chem.* **1969**, *31*, 2179.
38. Burns, R. J.; Bulkowski, P. B.; Stevens, S. C. V.; Baird, M. C. *J. Chem. Soc., Dalton Trans.* **1974**, 415.
39. Stanley, K.; Zelonka, R. A.; Thomson, J.; Fiess, P.; Baird, M. C. *Can. J. Chem.* **1974**, *52*, 1781.
40. King, R. B.; Bond, A. *J. Am. Chem. Soc.* **1974**, *96*, 1334.
41. Burch, R. R.; Calabrese, J. C. *J. Am. Chem. Soc.* **1986**, *108*, 5359.
42. Lange, H.; Naumann, D. *J. Fluorine Chem.* **1984**, *26*, 1.
43. Lange, H.; Naumann, D. *J. Fluorine Chem.* **1984**, *26*, 435.
44. Treichel, P. M.; Pitcher, E.; Stone, F. G. A. *Inorg. Chem.* **1962**, *1*, 511.
45. Wilford, J. B.; Treichel, P. M.; Stone, F. G. A. *J. Organomet. Chem.* **1964**, *2*, 119.
46. Kemmitt, R. D. W.; Russell, D. R. In *Comprehensive Organometallic Chemistry*; Wilkinson, G., Stone, F. G. A., Abel, E. W., Eds.; Pergamon Press: Oxford, U. K., 1982; Chapter 34.3.2.2.
47. Bruce, M. I.; Stone, F. G. A. *Prep. Inorg. React.* **1968**, *4*, 177.
48. Bennett, M. J.; Mason, R. *Proc. Chem. Soc., London* **1963**, 273.
49. Churchill, M. R.; Fennessey, J. P. *J. Chem. Soc., Chem. Commun.* **1966**, 695.
50. Seip, H. M.; Seip, R. *Acta Chem. Scand.* **1970**, *24*, 3431.
51. Beagley, B.; Young, G. G. *J. Mol. Struct.* **1977**, *40*, 295.
52. Bennett, M. A.; Chee, H.-K.; Robertson, G. B. *Inorg. Chem.* **1979**, *18*, 1061.
53. Bennett, M. A.; Chee, H.-K.; Jeffery, J. C.; Robertson, G. B. *Inorg. Chem.* **1979**, *18*, 1071.
54. Hall, M. B.; Fenske, R. F. *Inorg. Chem.* **1972**, *11*, 768.
55. Bigotto, A.; Zangrado, E.; Randaccio, L. *J. Chem. Soc., Dalton Trans.* **1976**, 96.
56. Marzilli, L. G.; Summers, M. F.; Ramsden, J. H., Jr.; Bresciani-Pahor, N.; Randaccio, L. *J. Chem. Soc., Dalton Trans.* **1984**, 511.

RECEIVED March 16, 1993

Chapter 18

Perfluorovinyl and Perfluoroaryl Zinc and Cadmium Reagents

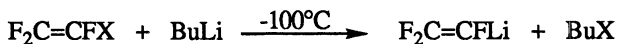
Preparation, Stability, and Reactivity

Donald J. Burton

Department of Chemistry, University of Iowa, Iowa City, IA 52242

F-Vinyl iodides and bromides react directly with cadmium or zinc metal to stereospecifically produce the corresponding F-vinyl cadmium and zinc reagents. These vinyl cadmium and zinc reagents exhibit excellent thermal stability (> 100°C) and do not couple with F-vinyl halides. Metathesis with Cu(I) salts gives the analogous F-vinyl copper reagents. The F-vinyl copper reagents readily undergo stereospecific alkylation, coupling and acylation reactions. They also add stereospecifically *syn* to F-2-butyne to produce F-dienyl copper reagents. Acylation of the dienyl copper reagent gives a dienyl ketone which spontaneously undergoes electrocyclicization to a pyran derivative. The F-vinyl zinc reagents couple to aryl iodides in the presence of Pd⁰ and provide useful stereoselective routes to α,β,β-trifluorostyrenes and 1-arylperfluoropropenes. Similar Pd⁰ catalyzed coupling of the F-vinyl zinc reagent with 1-iodoperfluoroolefins provides a stereospecific route to F-dienes. Reaction of bromopentafluorobenzene with cadmium metal gives the analogous F-aryl cadmium reagent, which readily undergoes metathesis with Cu(I) salts to give the F-aryl copper reagent essentially quantitatively. The F-aryl copper reagent also adds stereospecifically *syn* to F-2-butyne to give a vinyl copper reagent which is easily alkylated, arylated or acylated.

The low thermal stability of perfluoroalkenyl lithium and Grignard reagents has restricted their application for the synthesis of the fluorinated vinyl derivatives. Their preparation must be carried out at low temperatures and scale up processes are difficult. In addition, since both the preparation and reaction of these thermally labile organometallics must be accomplished at low temperatures, only reactive substrates can be utilized in functionalization reactions.



X = H, Cl, Br, I

0097-6156/94/0555-0297\$08.00/0
© 1994 American Chemical Society

In Inorganic Fluorine Chemistry; Thrasher, J., et al.;
ACS Symposium Series; American Chemical Society: Washington, DC, 1994.

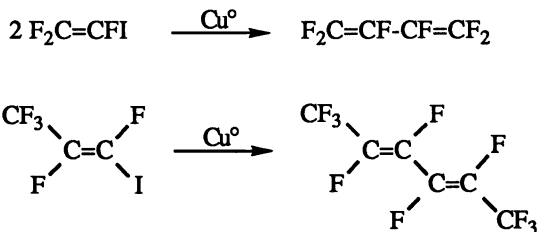
Therefore, we have attempted to develop a general route to stable \underline{E} -vinyl organometallic compounds that would: (a) possess thermal stability at room temperature or above; (b) possess functionalization (or exchange) capability; and (c) be formed in one step (one-pot) from readily accessible precursors. The above properties would permit these reagents to be prepared with minimal experimental difficulty, easily scaled up, and readily utilized in preparative transformations to stereospecifically yield polyfunctionalized materials.

Thus, our initial attention focused on \underline{E} -vinyl copper reagents. Miller (*1*) had reported the preparation of the stable copper reagent, E - $CF_3CF=C(CF_3)Cu$, from E - $CF_3CF=C(CF_3)Ag$. Although the generality of this approach was seriously limited by the regioselectivity and stereoselectivity of AgF addition to \underline{E} -alkynes, the thermal stability of the vinyl copper reagent prompted us to develop a more general route to this class of fluorinated organometallics.

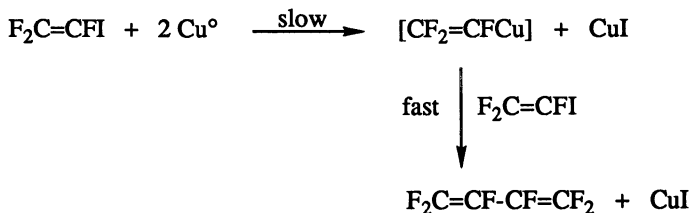
Initial Approaches

Our initial strategy was to utilize \underline{E} -vinyl halides as precursors. Many of these compounds are readily available or easily prepared. Also, we anticipated that the formation of the organometallic reagent from the vinyl halide would occur stereospecifically, thus permitting preparation of the appropriate E - or Z -organometallic by proper choice of the E - or Z -vinyl halide.

Unfortunately, when either iodotrifluoroethene or Z -1-iodopentafluoropropene was reacted with copper metal (activated by various reported procedures), only diene products were detected. No vinyl copper reagent was observed in these reactions.



Apparently, the slow step in diene formation is the formation of the vinyl copper reagent followed by rapid coupling of the vinyl copper reagent with additional vinyl halide.



Consequently, it is necessary to generate the vinyl copper reagent in the absence of vinyl halide to preclude coupling reactions (diene formation).

Perfluorovinyl Cadmium Reagents. In order to achieve the formation of the \underline{E} -vinyl copper reagent in the absence of \underline{E} -vinyl halide, we turned to the formation of a \underline{E} -vinyl organometallic reagent that does not readily couple with vinyl halides. We

initially selected \bar{E} -vinyl cadmium reagents to study for the following reasons: (a) in the formation of \bar{E} -aryl cadmium reagents from bromopentafluorobenzene and cadmium metal, we had not observed the formation of any \bar{E} -biphenyl (coupled product); and (b) ^{111}Cd and ^{113}Cd NMR active isotopes in the organometallic compound would allow us to monitor formation of the organometallic reagent by ^{19}F and ^{113}Cd NMR and assist in the structural assignments of the mono and bis reagent.

As expected, \bar{E} -vinyl bromides and iodides readily reacted with cadmium metal in DMF to give stable \bar{E} -vinyl cadmium reagents (mixture of mono and bis reagents) (2). In general, the vinyl iodides reacted at room temperature (mild exotherm) and the vinyl bromides required mild heating (RT-60°C). With E - and Z -vinyl halides (including diene precursors) stereospecificity was preserved in formation of the \bar{E} -vinyl cadmium reagent.

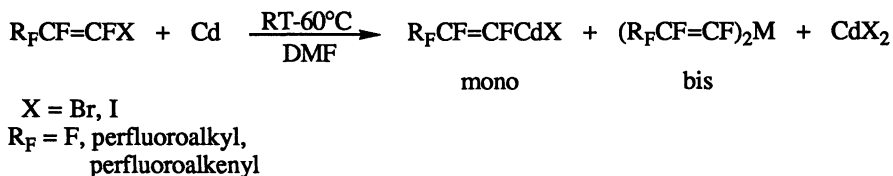


Table I summarizes typical examples of \bar{E} -vinyl cadmium reagents.

Table I. Preparation of Alkenyl Cadmium Reagents from \bar{E} -Vinyl Halides and Cadmium

Olefin	Cadmium Reagent ^a	Yield ^b
$\text{CF}_2=\text{CFI}$	$\text{CF}_2=\text{CFCdX}$	99
$Z\text{-CF}_3\text{CF}=\text{CFI}$	$Z\text{-CF}_3\text{CF}=\text{CFCdX}$	96
$E\text{-CF}_3\text{CF}=\text{CFI}$	$E\text{-CF}_3\text{CF}=\text{CFCdX}$	92
$Z\text{-CF}_3(\text{CF}_2)_4\text{CF}=\text{CFI}$	$Z\text{-CF}_3(\text{CF}_2)_4\text{CF}=\text{CFCdX}$	95
$\text{CF}_3\text{CF}=\text{CICF}_3^c$	$\text{CF}_3\text{CF}=\text{C}(\text{CF}_3)\text{CdX}^d$	91
$\text{CF}_3\text{CF}=\text{C}(\text{Ph})\text{CF}=\text{CFBr}^e$	$\text{CF}_3\text{CF}=\text{C}(\text{Ph})\text{CF}=\text{CFCdX}^f$	61
$E\text{-CF}_3\text{C}(\text{Ph})=\text{CFI}$	$E\text{-CF}_3\text{C}(\text{Ph})=\text{CFCdX}$	77

^a Mixture of mono and bis reagent; $\text{X} = \text{halogen or another } \bar{E}\text{-alkenyl group.}$

^b ^{19}F NMR yield vs. PhCF_3 .

^c E/Z mixture; $E/Z = 39/61$

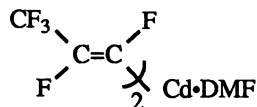
^d $E/Z = 37/63$

^e $E, Z:Z, Z = 90/10$

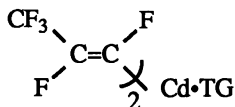
^f $E, Z:Z, Z = 90/10$

Reproduced with permission from ref. 2. Copyright Elsevier 1986.

The thermal stability of these vinyl cadmium reagents is remarkable. A solution of $Z\text{-CF}_3\text{CF}=\text{CFCdX}$ in dry DMF was stable for > 30 days at room temperature and lost only 25% activity at 123°C after 1.5 hours. The mono and bis cadmium reagents are involved in a Schlenk equilibrium; the bis reagent being the more volatile reagent. Thus, a short-path vacuum distillation of the reaction mixture followed by recrystallization from $\text{CH}_2\text{Cl}_2/\text{pentane}$ (1:5) permits isolation of the bis reagent as a low-melting solvate (white solid). Thus, the DMF and triglyme (TG) solvates were isolated from $\text{F}_2\text{C}=\text{CFI}$ and $Z\text{-CF}_3\text{CF}=\text{CFI}$ (3).



m.p. 77-80°C



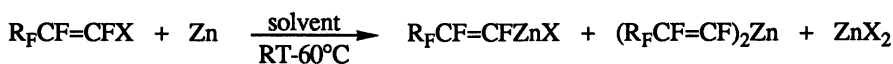
m.p. 64-65°C



m.p. 20-25°C

As noted above, ^{113}Cd NMR readily distinguishes the mono and bis reagents. Thus, for $\text{F}_2\text{C}=\text{CFCdX}$ ($X = \text{halogen or } -\text{CF}=\text{CF}_2$), the mono reagent appears in the ^{113}Cd NMR spectrum as a doublet of doublet of doublets, whereas the bis reagent appears as a triplet of triplet of triplets. Similarly, $Z\text{-CF}_3\text{CF}=\text{CFCdX}$ ($X = \text{halogen or } -\text{CF}=\text{CF}_2$) shows a doublet of doublets for the mono reagent and a triplet of triplets for the bis reagent in the ^{113}Cd spectrum (coupling to vinylic fluorines). These spectra and multiplicities are readily observable even in reaction mixtures and can be utilized to determine the mono-bis ratio directly.

Perfluorovinyl Zinc Reagents. Success in the formation of E -vinyl cadmium reagents (without coupling to vinyl halides) prompted us to examine formation of the corresponding zinc reagents. Thus, we found that zinc metal reacted readily with a



$X = \text{Br, I}$

$\text{R}_F = \text{F, perfluoroalkyl}$
perfluoroalkenyl

mono

bis

variety of E -vinyl iodides and bromides to stereospecifically produce the corresponding mono and bis zinc reagents (4) - again **without** formation of any symmetrical diene. Unfortunately, zinc has no useful NMR active isotopes (like Cd); thus NMR could not be utilized to unequivocally assign mono and bis zinc reagents. However, in most cases the mono and bis zinc reagents were distinguishable by ^{19}F NMR. Thus, by enhancement of the signal for the mono reagent on addition of the appropriate zinc halide at the expense of the signal for the bis reagent, the mono/bis ratio could be determined.



bis

$X = \text{Br, I}$

mono

Table II summarizes typical E -vinyl zinc reagents prepared from zinc metal and E -vinyl halides.

Table II. Preparation of Vinyl Zinc Reagents from *E*-Vinyl Halides and Zinc Metal

$R_FCF=CFX + Zn \xrightarrow{\text{solvent/RT}} R_FCF=CFZnX + (R_FCF=CF)_2Zn + ZnX_2$				
Vinyl Halide	Solvent ^a	Zinc Reagent ^b	Mono:Bis	Yield ^c
CF ₂ =CFI	DMF	CF ₂ =CFZnX	80:20	79%
	DMAc		84:16	97%
	MG			60%
	TG		68:32	95%
	TetG		67:33	85%
CF ₂ =CFBr	DMF	CF ₂ =CFZnX	95:5	72%
CF ₂ =CBr ₂	DMF	CF ₂ =CBrZnX	68:32	97%
Z-CF ₃ CF=CFI	THF	Z-CF ₃ CF=CFZnX	68:32	98%
	TG		65:35	96%
	DMF		74:26	100%
	CH ₃ CN		81:19	90%
<i>E</i> -CF ₃ CF=CFI	TG	<i>E</i> -CF ₃ CF=CFZnX	59:41	100%
Z-CF ₃ CF ₂ CF=CFI	TG	Z-CF ₃ CF ₂ CF=CFZnX		90%
Z-CF ₃ (CF ₂) ₄ CF=CFBr	DMF	Z-CF ₃ (CF ₂) ₄ CF=CFZnX		77%
Z-CF ₃ (CF ₂) ₄ CF=CFI	TG	Z-CF ₃ (CF ₂) ₄ CF=CFZnX		74%
CF ₃ C(Ph)=CFBr ^d	DMF	CF ₃ C(Ph)=CFZnX ^d		94%
CF ₃ C(Ph)=CBr ₂	DMF	CF ₃ C(Ph)=CBrZnX ^e		95%
<i>E</i> -CF ₃ C(Ph)=CFI	THF	<i>E</i> -CF ₃ C(Ph)=CFZnX	67:33	78%
Z-CF ₃ (C ₆ F ₅)C=CFI	THF	Z-CF ₃ (C ₆ F ₅)C=CFZnX	57:43	86%
CF ₃ CF=C(Ph)CF=CFBr ^f	DMF	CF ₃ CF=C(Ph)CF=CFZnX ^f		71%
<i>E</i> -CF ₃ CH=CFI	TG	<i>E</i> -CF ₃ CH=CFZnX	67:33	89%
<i>E</i> -CF ₃ CF=C(CF ₃)I	TG	<i>E</i> -CF ₃ CF=C(CF ₃)ZnX	80:20	75%

^a MG = monoglyme, TG = triglyme, TetG = Tetraglyme.

^b Mixture of mono and bis reagent; X = halogen or another *E*-vinyl group.

^c ¹⁹F NMR yield vs. PhCF₃.

^d *E/Z* mixture; *E/Z* = 59/41

^e *E/Z* = 67/33

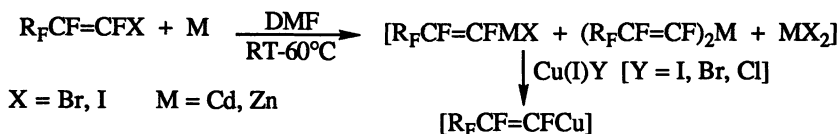
^f *E, Z:Z, Z* = 90:10

Reproduced with permission from ref. 4. Copyright Elsevier 1987.

In contrast to the \bar{E} -vinyl cadmium reagents, the \bar{E} -vinyl zinc reagents can be prepared in a variety of amide, etheral, and nitrile solvents such as DMF, DMAC (*N,N*-dimethylacetamide), MG (monoglyme), TG (triglyme), TetG (tetraglyme), THF, and CH_3CN (cf. Table II). The ability to form the \bar{E} -vinyl zinc reagents in etheral solvents is often important in functionalization reactions, since the functionalized derivative can react with amide solvents (5).

The \bar{E} -vinyl zinc reagents exhibit excellent thermal stability. For example, $Z\text{-CF}_3\text{CF}=\text{CFZnX}$ in TG showed < 10% loss of activity after one month at room temperature and < 5% loss of activity after three days at 65°C. Thus, these reagents can be prepared on a large scale and stored for extended periods of time without any significant change in activity of the stock solution.

Perfluorovinyl Copper Reagents. The \bar{E} -vinyl cadmium and zinc reagents outlined previously, could be readily prepared from \bar{E} -vinyl halides without significant formation of dienes. Subsequent metathesis of the \bar{E} -vinyl cadmium and zinc reagents in DMF with Cu(I) halides stereospecifically gives a solution of a stable \bar{E} -vinyl



copper reagent (6). Since no \bar{E} -vinyl halide remains after formation of the intermediate \bar{E} -vinyl cadmium or zinc reagents, no coupling results and the \bar{E} -vinyl copper reagent survives. The stereochemical integrity is retained throughout the synthetic sequence and the \bar{E} -vinyl copper reagent can be readily formed in either the *E*- or *Z*-configuration from the appropriate *E*- or *Z*- \bar{E} -vinyl halide or diene. Table III summarizes some typical \bar{E} -vinyl copper reagents prepared *via* this methodology.

Table III. Preparation of Vinylcopper Reagents

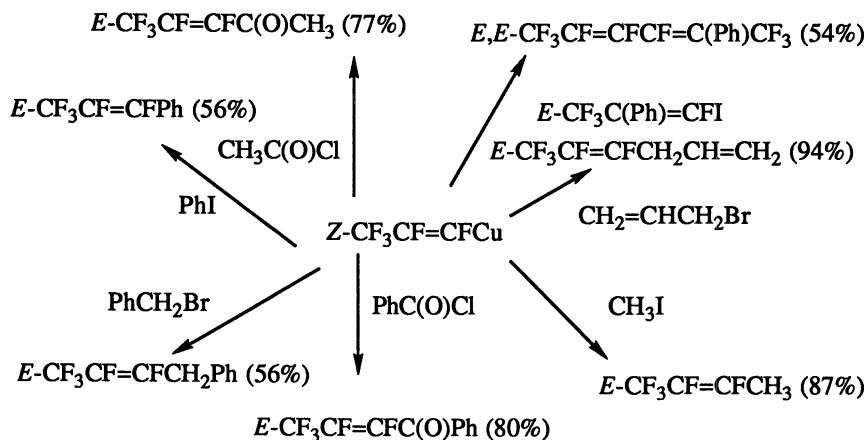
olefin	M	$\text{R}_F\text{CF}=\text{CFCu}$	% yield ^a
$\text{CF}_2=\text{CFI}$	Cd	$\text{CF}_2=\text{CFCu}$	99%
$\text{CF}_2=\text{CFBr}$	Zn	$\text{CF}_2=\text{CFCu}$	72%
$Z\text{-CF}_3\text{CF}=\text{CFI}$	Cd	$Z\text{-CF}_3\text{CF}=\text{CFCu}$	92%
$Z\text{-CF}_3\text{CF}=\text{CFI}$	Zn	$Z\text{-CF}_3\text{CF}=\text{CFCu}$	76%
$E\text{-CF}_3\text{CF}=\text{CFI}$	Cd	$E\text{-CF}_3\text{CF}=\text{CFCu}$	83%
$Z\text{-CF}_3(\text{CF}_2)_4\text{CF}=\text{CFI}$	Cd	$Z\text{-CF}_3(\text{CF}_2)_4\text{CF}=\text{CFCu}$	87%
$Z\text{-CF}_3\text{CCl}=\text{CFI}$	Cd	$Z\text{-CF}_3\text{C(Ph)}=\text{CFCu}$	78%
$\text{CF}_3\text{C(Ph)}=\text{CFBr}$	Zn	$\text{CF}_3\text{C(Ph)}=\text{CFCu}$	84%
$E/Z = 59/41$		$E/Z = 59/41$	
$\text{CF}_3\text{CF}=\text{C(Ph)CF}=\text{CFBr}$	Zn	$\text{CF}_3\text{CF}=\text{C(Ph)CF}=\text{CFCu}$	63%
$E/Z = 90/10$		$E/Z = 90/10$	

^aOverall ^{19}F NMR yield based on starting olefin.

Reproduced from ref. 6. Copyright American Chemical Society, 1986.

The *E*-vinyl copper reagents exhibit excellent stability at room temperature in the absence of moisture and/or oxygen. At higher temperatures (> 50°C) they undergo rapid decomposition.

The *E*-vinyl copper reagents participate in a variety of alkylation, coupling and acylation reactions as illustrated in Scheme I.

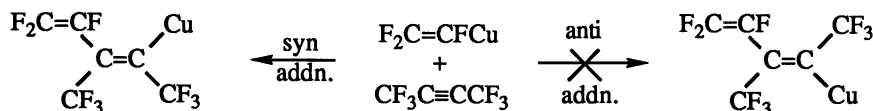


Scheme I

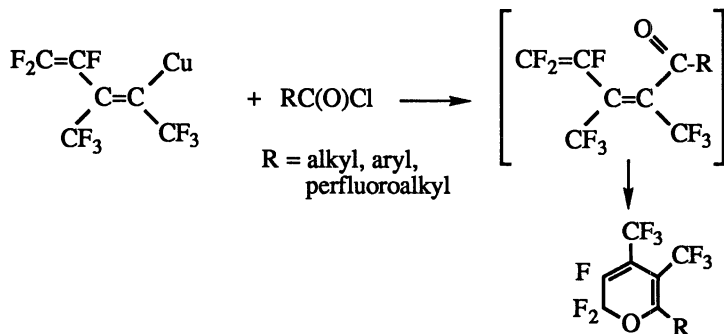
Reproduced from ref. 6. Copyright American Chemical Society, 1986.

Stereospecific Addition of *E*-Vinyl Copper Reagents to *E*-Alkynes

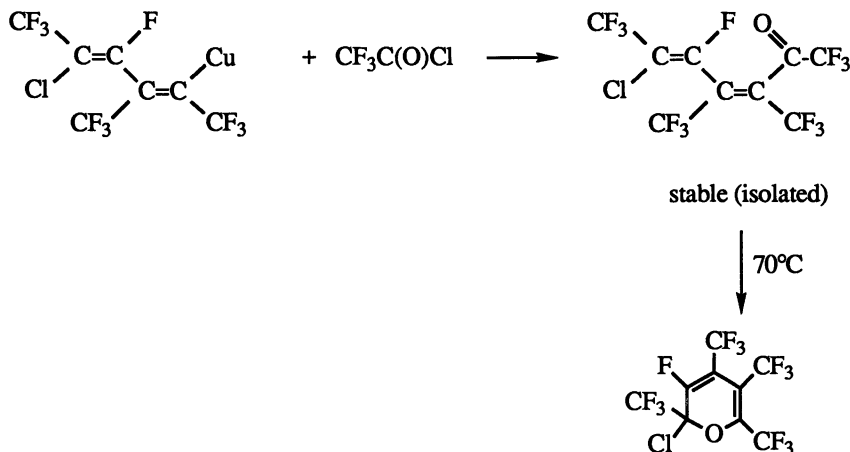
Similar to their hydrocarbon analogues, the *E*-vinyl copper reagents add to alkynes. Although either *syn* or *anti* addition is possible, only *syn* addition was detected in the



addition of trifluorovinyl copper to *E*-2-butyne (3). When the copper/alkyne adduct is acylated, the corresponding dienyl ketone is **not** detected. Instead, the electrocyclicization product is isolated.



If the *E*-vinyl copper reagent contains two bulky groups at the β -position, the electrocyclization process is not spontaneous and the dienyl ketone can be isolated. Subsequent heating of the dienyl ketone to 70°C promotes electrocyclization of the ketone to the heterocyclic product (3).

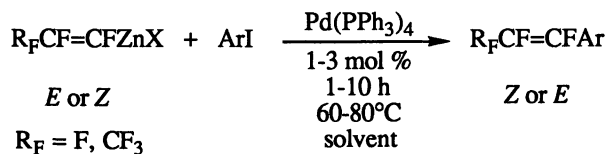


Palladium-Catalyzed Coupling Reactions of *E*-Vinyl Zinc Reagents

[A]: With Aryl Iodides

Pd^0 coupling reactions generally occur under mild conditions, with minimal side reactions and proceed with regiochemical and/or stereochemical control.

E-Vinyl zinc reagents readily react with aryl iodides in the presence of 1-3 mol % $\text{Pd}(\text{PPh}_3)_4$ to give excellent yields of 1-aryl-perfluoroolefins (7).



When $\text{R}_F = \text{F}$, the α,β,β -trifluorostyrenes are formed in good to excellent yields. Both electron-withdrawing and electron-releasing groups on the aryl ring can be utilized successfully. With 1,4-diiodobenzene, the bis-substituted compound is formed. Table IV summarizes typical preparations of trifluorovinyl styrenes *via* this methodology.

When $\text{R}_F = \text{CF}_3$, the Pd^0 coupling reaction with aryl iodides proceeds with 100% retention of configuration with *Z*- $\text{CF}_3\text{CF}=\text{CFZnX}$ and > 92% retention of configuration with *E*- $\text{CF}_3\text{CF}=\text{CFZnX}$. Table V illustrates typical examples with *Z*- and *E*- $\text{CF}_3\text{CF}=\text{CFZnX}$.

Table IV. Isolated Yields of α,β,β -Trifluorostyrenes

$\text{CF}_2=\text{CFZnX} + \text{ArI} \xrightarrow[\text{1-10 h, 60-80}^\circ\text{C}]{\text{Pd(PPh}_3)_4, \text{1-3 Mol \%}}$		$\text{CF}_2=\text{CFAr}$
α,β,β -Tifluorostyrene	Solvent	Isolated Yield, %
$\text{C}_6\text{H}_5\text{CF}=\text{CF}_2$	DMF	74
<i>o</i> - $\text{NO}_2\text{C}_6\text{H}_4\text{CF}=\text{CF}_2$	DMF	73
<i>p</i> - $\text{MeOC}_6\text{H}_4\text{CF}=\text{CF}_2$	THF	61
<i>o</i> - $(\text{CH}_3)_2\text{CHC}_6\text{H}_4\text{CF}=\text{CF}_2$	THF	70
2,5- $\text{Cl}_2\text{C}_6\text{H}_3\text{CF}=\text{CF}_2$	DMF	75
<i>o</i> - $\text{CF}_3\text{C}_6\text{H}_4\text{CF}=\text{CF}_2$	TG ^a	73
<i>m</i> - $\text{NO}_2\text{C}_6\text{H}_4\text{CF}=\text{CF}_2$	TG ^a	81
<i>p</i> - $\text{ClC}_6\text{H}_4\text{CF}=\text{CF}_2$	DMF	77
<i>p</i> - $\text{CF}_2=\text{CFC}_6\text{H}_4\text{CF}=\text{CF}_2$ ^b	DMF	56

^aTG = triglyme. ^bRoom temperature for 2 days.

Reproduced from ref. 7. Copyright American Chemical Society, 1988.

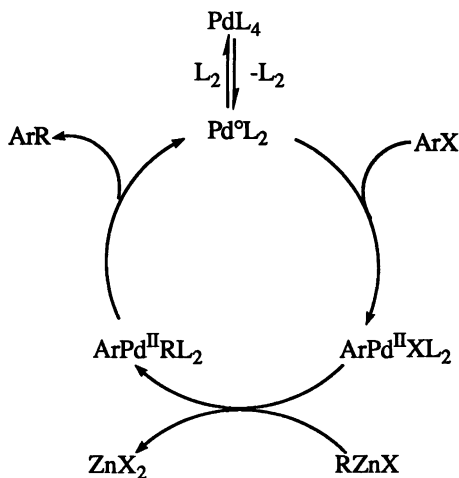
Table V. Isolated Yields of *E*-1-Arylperfluoropropenes and *Z*-1-Arylperfluoropropenes^a

$\text{CF}_3\text{CF}=\text{CFZnX} + \text{ArI} \xrightarrow[\text{1-10 h, 60-80}^\circ\text{C}]{\text{Pd(PPh}_3)_4, \text{1-3 Mol \%}}$		$\text{CF}_3\text{CF}=\text{CFAr}$
<i>E</i> or <i>Z</i>		<i>Z</i> or <i>E</i>
1-Arylperfluoropropene		Isolated Yield, %
<i>E</i> - $\text{C}_6\text{H}_5\text{CF}=\text{CFCF}_3$		80
<i>E</i> - <i>p</i> - $\text{CH}_3\text{C}_6\text{H}_4\text{CF}=\text{CFCF}_3$		65
<i>E</i> - <i>p</i> - $\text{ClC}_6\text{H}_4\text{CF}=\text{CFCF}_3$		61
<i>E</i> - <i>m</i> - $\text{NO}_2\text{C}_6\text{H}_4\text{CF}=\text{CFCF}_3$		80
<i>Z</i> - $\text{C}_6\text{H}_5\text{CF}=\text{CFCF}_3$ ^b		82
<i>Z</i> - <i>p</i> - $\text{CH}_3\text{C}_6\text{H}_4\text{CF}=\text{CFCF}_3$ ^c		70
<i>Z</i> - <i>p</i> - $\text{ClC}_6\text{H}_4\text{CF}=\text{CFCF}_3$ ^b		74

^aAll preparations were conducted in triglyme with yellow $\text{Pd(PPh}_3)_4$ prepared in our laboratory. ^b*Z/E* = 97/3. ^c*Z/E* = 92/8.

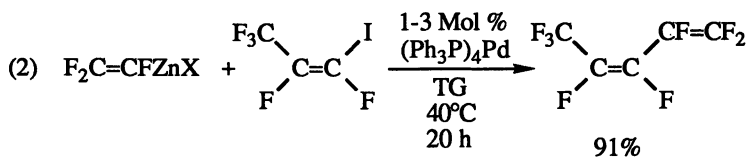
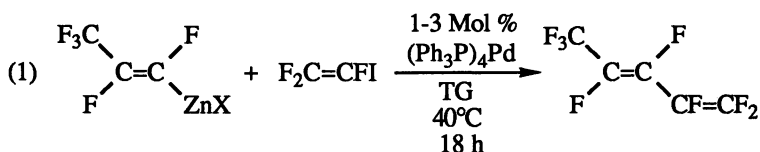
Reproduced from ref. 7. Copyright American Chemical Society, 1988.

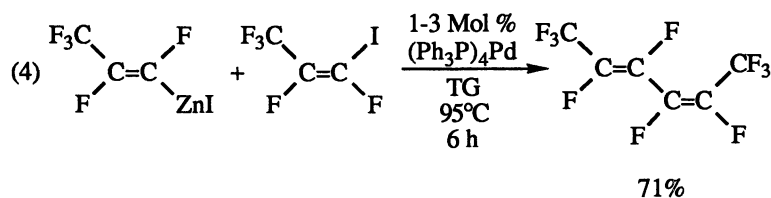
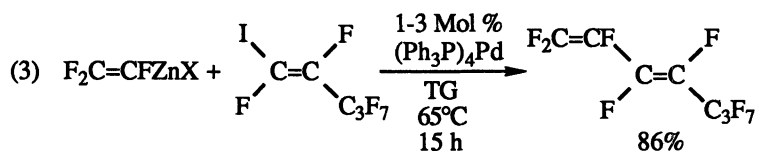
The mechanism of the Pd⁰ coupling presumably proceeded *via* the typical oxidative addition of the aryl iodide to Pd⁰ to give a palladium (II) intermediate. Subsequent metathesis of the Pd (II) intermediate with the *E*-vinyl zinc reagent followed by reductive elimination gave the aryl-substituted olefin and regenerated the Pd⁰ catalyst as summarized below for a typical palladium catalysis cycle.



[B]: With Perfluorovinyl Iodides

Previous work in our laboratory demonstrated that *E*-vinyl iodides could undergo oxidative addition to Pd⁰. Thus, utilization of the palladium catalysis cycle (with R_FCF=CF- in place of Ar-) would provide a useful, stereospecific route to *E*-dienes. Thus, we found that the following dienes could be stereospecifically prepared *via* this approach (8).

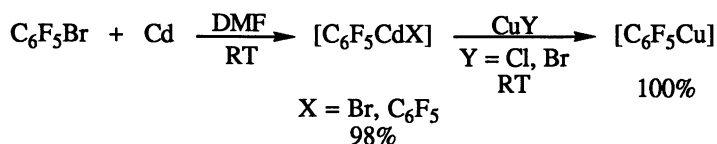




Perfluoro Aryl Copper Reagents

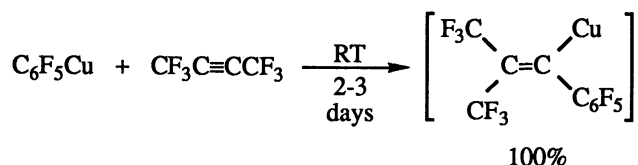
A previous report from our laboratory has demonstrated that F -aryl cadmium reagents could be readily formed at room temperature *via* reaction of cadmium powder with bromopentafluorobenzene (9).

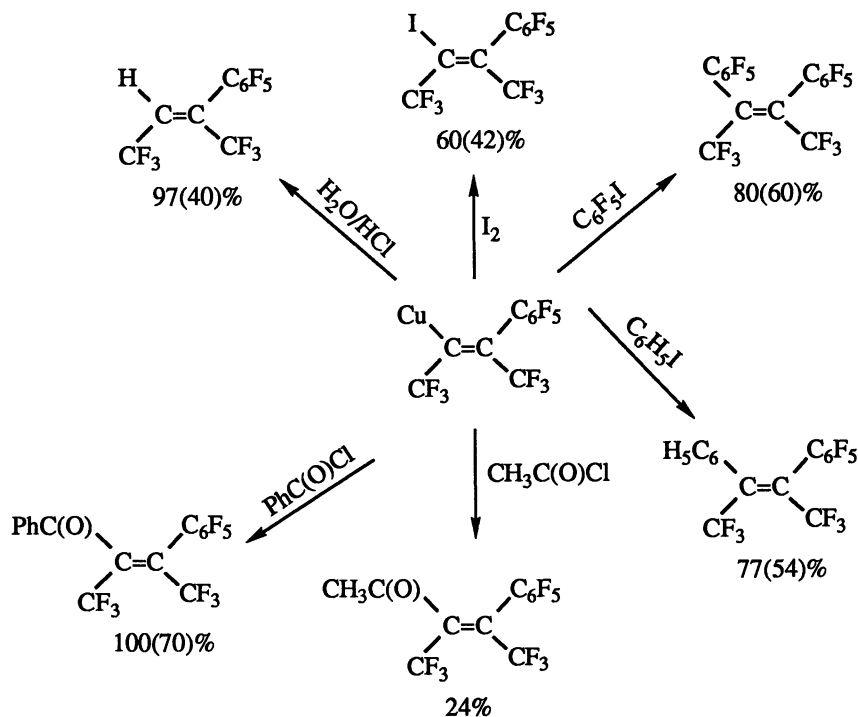
The facile metathesis reaction of F -vinyl cadmium reagents with Cu(I) salts suggested that the F -aryl copper reagent could be similarly prepared *via* metathesis of the F -aryl cadmium reagent. Indeed, this method works very well as summarized below (10):



Similar to the F -vinyl copper reagents, we have found that the F -aryl copper reagent also adds stereospecifically *syn* to F -2-butyne. The addition is slow (2-3 days) at room temperature but can be accomplished within a few hours at 40-60°C (10).

The alkyne addition adduct can be protonated, halogenated, arylated and acylated to give reasonable yields of highly substituted fluoroolefins as outlined in Scheme II (yields in parentheses are based on $\text{C}_6\text{F}_5\text{Br}$).





Scheme II

Acknowledgments. We thank the National Science Foundation and the Air Force Office of Scientific Research for support of this work.

Literature Cited

- (1) Miller, W.T. Abstracts of the 9th International Symposium on Fluorine Chemistry, Avignon, France, p O 27.
- (2) Burton, D.J.; Hansen, S.W. *J. Fluorine Chem.* **1986**, *31*, 461.
- (3) Hansen, S.W. Ph.D. Thesis, University of Iowa.
- (4) Hansen, S.W.; Spawn, T.D.; Burton, D.J. *J. Fluorine Chem.* **1987**, *35*, 415.
- (5) Spawn, T.D.; Burton, D.J. *Bull. Soc. Chim. Fr.* **1986**, (6), 876.
- (6) Burton, D.J.; Hansen, S.W. *J. Am. Chem. Soc.* **1986**, *108*, 4229.
- (7) Heinze, P.L.; Burton, D.J. *J. Org. Chem.* **1988**, *53*, 2714.
- (8) Nakamura, A. University of Iowa, unpublished results.
- (9) Heinze, P.L.; Burton, D.J. *J. Fluorine Chem.* **1985**, *29*, 359.
- (10) MacNeil, K. Ph.D. Thesis, University of Iowa.

RECEIVED April 6, 1993

Chapter 19

Organic and Main-Group Chemistry of the 2,4,6-Tris(trifluoromethyl)phenyl Substituent

Kinetic Stabilization through Steric and Electronic Effects

Frank T. Edelmann

Institut für Anorganische Chemie, Universität Göttingen,
Tammannstrasse 4, D-37077 Göttingen, Germany

The organic and main group chemistry of the 2,4,6-tris(trifluoromethyl)phenyl substituent (= R_F) is reviewed. This unique ligand combines steric bulk with the possibility of electronic stabilization. In organic RF chemistry steric hindrance is an important factor guiding the reactivity of various substrates. Low coordination numbers around main group elements are effectively stabilized through the formation of short metal-fluorine interactions. Among other RF-derived substituents the thiolate anion R_FS⁻ promises to be a useful ligand for transition metals.

During the past ten years the "Classical Double-Bond Rule" has been widely overcome through the successful preparation of stable species containing multiple bonds between heavier main group elements. The key principle leading to major achievements in this area of modern main group chemistry is kinetic stabilization (1). It involves the use of sterically demanding substituents which protect the low-coordinate main group elements and thus inhibit dimerization or polymerization as well as attack of other reagents. A typical example is the diphosphene system. Simple substituted diphosphene derivatives, RP=PR (R = alkyl, aryl) are usually highly unstable. Early attempts to isolate these materials were frustrated by the formation of oligomerization products (i.e. cyclopolyphosphines, (RP)_n) (2). Kinetic stabilization and hence formation of a stable monomer was achieved by introducing the very bulky 2,4,6-tri(*t*-butyl)phenyl (= "supermesityl" or Mes*) substituent (3). *Yoshifuji's* successful preparation of Mes*P=PMes* marks the beginning of vigorous research activities in the field of low-coordinate main group compounds. Dicoordination around heavy main group elements has become a familiar sight in

0097-6156/94/0555-0309\$08.00/0
© 1994 American Chemical Society

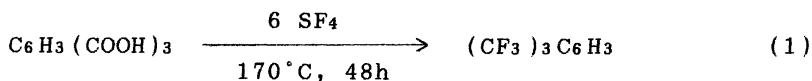
inorganic chemistry. Besides the diphosphene homologues $R-P=As-R$ (4), $R-As=As-R$ (5) and $R-P=Sb-R$ (6) the isolation of stable compounds containing $P=C$ (7), $Si=Si$ (8), $Si=N$ (9) and $Si=P$ (10) multiple bonds has been reported. Kinetic stabilization allowed the synthesis of numerous monomeric germylenes (11) and stannylenes (12). Even phosphalkynes, $R-C\equiv P$ (13-15), (and to a lesser extent arsaalkynes, $R-C\equiv As$ (16)) have become a well investigated class of compounds. A substantial number of sterically demanding ligands has been successfully employed. The wide range of bulky substituents includes *t*-butyl, neopentyl, $-CH_2SiMe_3$, $-CH(SiMe_3)_2$, $-C(SiMe_3)_3$, mesityl, 2,4,6-tri(*i*-propyl)phenyl, 2,4,6-tri(*t*-butyl)phenyl and pentamethylcyclopentadienyl. The bis(trimethylsilyl)methyl substituent, $-CH(SiMe_3)_2$, has also been found to be extremely useful for the realization of very low coordination numbers around *f*-elements. Tricoordinate homoleptic alkyls of the type $M[CH(SiMe_3)_2]_3$ have been reported for uranium(III) (17) and several lanthanide elements (18). Bulky amido ligands such as $-N(SiMe_3)_2$, $-N(SiMe_2Ph)_2$ and $-NMe_2(BMe_2)$ have been used in the preparation of dicoordinate *d*-transition metal derivatives (19).

During the past three years the game has become even more exciting through the appearance of a new player: 2,4,6-tris(trifluoromethyl)phenyl (= R_f). This substituent is not just another sterically demanding ligand. It adds a new dimension to steric bulk: Electronic stabilization. Due to the possibility of forming short metal-fluorine contacts to the *ortho*- CF_3 groups of R_f , an additional stabilizing effect is imposed on low-coordinate main group elements. It is the combination of steric and electronic stabilization which makes 2,4,6-tris(trifluoromethyl)phenyl truly unique among all other bulky substituents reported so far. The chemistry of the 2,4,6-tris(trifluoro-methyl)phenyl substituent has recently been compiled in a review article (20). In addition to some important earlier results this article therefore focusses on some new developments in this area.

Preparation of the Starting Materials: R_fH and R_fLi

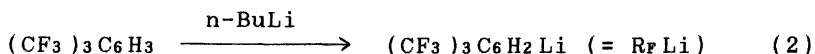
The earliest reports on the parent fluorocarbon, 1,3,5-tris(trifluoromethyl)benzene (= R_fH), date back to 1947, when *McBee* and *Leech* described its synthesis via fluorination of 1,3,5- $(CCl_3)_3C_6H_3$ (21). 1,3,5-Tris(trifluoromethyl)benzene was "rediscovered" by *Chambers* et al., who reported the first simple synthesis of R_fH (22). It was obtained in 33% yield by fluorination of commercially available benzene-1,3,5-tricarboxylic acid with SF_4 at elevated temperatures. Reinforcement of the original reaction conditions subsequently led to a significant improvement of the product yield. A 90-95% isolated yield of 1,3,5-tris(trifluoromethyl)benzene is reproducibly

obtained when benzene-1,3,5-tricarboxylic acid is heated with excess SF₄ at 170°C for 48 h (23) (Equation 1):



The physical and spectroscopic properties of 1,3,5-(CF₃)₃C₆H₃ have been determined (21-24). Since various fluoro-carbons are known to be rather toxic (25), R_FH should be handled with great care until the physiological properties have been studied more thoroughly.

Derivatization of 1,3,5-tris(trifluoromethyl)benzene generally starts with ring metalation using *n*-butyllithium as described by Chambers et al. in 1987 (22) (Equation 2):



The formation of 2,4,6-tris(trifluoromethyl)phenyllithium (= R_FLi) occurs readily in diethylether at reflux temperature. Quenching of the reaction mixture with CH₃OD after 1 h resulted in the formation of the mono-deuterated derivative in 90% yield. However, isolated yields of main group compounds derived from the R_FLi intermediate are often considerably lower. The metalation reaction works equally well on a mmol-scale or with 0.1 - 0.2 mol of 1,3,5-tris(trifluoromethyl)benzene. It has been found very convenient to prepare R_FLi *in situ* and use the resulting solutions in diethylether/hexane without any further purification for subsequent reactions. It is, however, possible to isolate a pure crystalline diethylether adduct, [R_FLi·Et₂O]₂ (26). Evaporation of the 1,3,5-(CF₃)₃C₆H₃/*n*-BuLi solutions to dryness and recrystallization of the oily residue from hexane yields colorless crystals of [R_FLi·Et₂O]₂ in moderate yield. Curiously, very pure [R_FLi·Et₂O]₂ has been obtained during attempts to prepare (R_F)₂Ca and (R_F)₂Ba (27). Treatment of *in situ* prepared R_FLi with either anhydrous CaCl₂ or BaI₂ resulted in the formation of yellow solutions, from which [R_FLi·Et₂O]₂ was isolated as the only product by crystallization from hexane. **Caution:** Solid [R_FLi·Et₂O]₂ decomposes violently upon contact with protic solvents like ethanol or acetone and even occasional explosions have been reported. The crystalline compound should only be prepared in small quantities and always be handled with great care! The dimeric nature of [R_FLi·Et₂O]₂ was revealed by a low-temperature X-ray structure determination (26) (Figure 1).

This structure is already a striking example of electronic stabilization in R_F chemistry: The dimers are

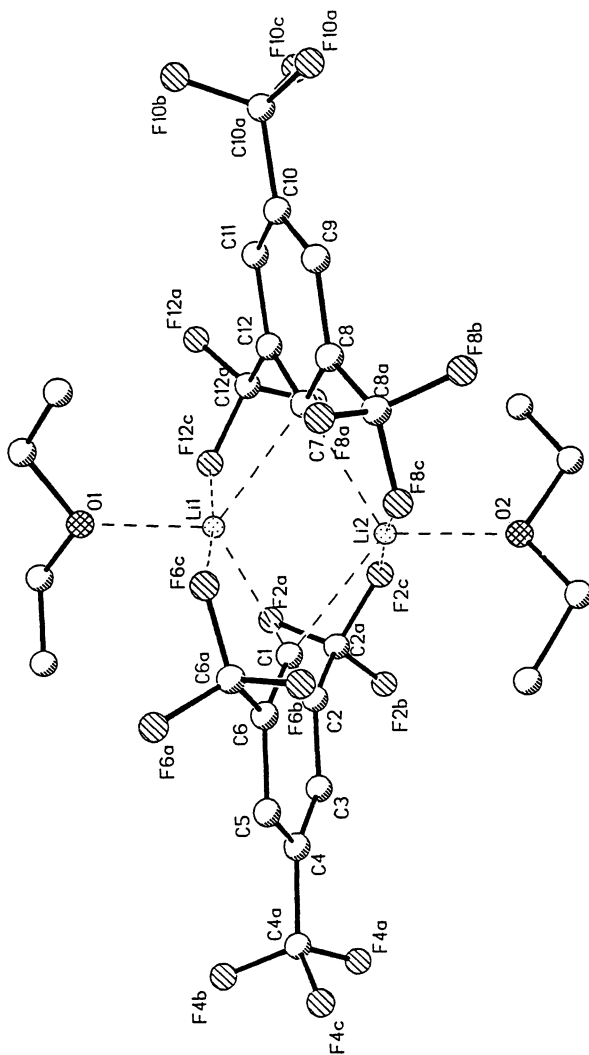


Figure 1. Molecular structure of dimeric $[\text{RfLi}\cdot\text{Et}_2\text{O}]_2$.

held together by lithium-fluorine interactions. The coordination environment around lithium is that of a distorted trigonal bipyramid. Each lithium atom is coordinated by the *ipso*-carbon atoms of the phenyl rings, two fluorine atoms from *ortho*-CF₃ groups and an oxygen atom of a diethylether ligand. Obviously the four Li-F interactions have to be considered the main stabilizing factor in the dimeric [R_fLi·Et₂O]₂ molecule. Attempts to eliminate lithium fluoride from R_fLi and to trap the resulting diradical intermediate using furan have failed (22). Solid R_fLi showed a remarkable thermal stability when heated in a sealed tube at 90°C. Addition of furan in a similar experiment did not yield an isolable trapping product.

Apparently no attempts have been made to isolate R_f derivatives of the heavier alkaline metals, R_fM (M = Na, K, Rb, Cs), although these organometallics are anticipated to exhibit interesting structural properties. Other attempts to derivatize 1,3,5-tris(trifluoromethyl)benzene have failed so far, because the three CF₃ groups strongly deactivate the phenyl ring toward electrophilic substitution. Accordingly, no reaction was observed with acetyl chloride and anhydrous AlCl₃ (28).

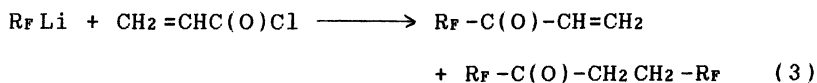
Organic Chemistry with R_f

A number of carbon-carbon bond formation reactions have been studied in detail by *Chambers* (22) and *Filler* (28). Some of these transformations show that significant steric hindrance is imposed by the 2,4,6-tris(trifluoromethyl)phenyl substituent. Steric effects became especially apparent in the failure of several attempts to prepare the acetophenone derivative R_fC(O)CH₃ and the related vinyl ketone R_fC(O)CH=CH₂ (28). The elusive 2,4,6-tris(trifluoromethyl)acetophenone is apparently formed when R_fLi is treated with acetyl chloride. Initially formed R_fC(O)CH₃ undergoes rapid hydrogen-metal exchange with unreacted R_fLi and the resulting lithium enolate reacts with another equivalent of acetyl chloride to give the 1,3-diketone R_fC(O)-CH₂C(O)CH₃ as the only isolable product. This 1,3-diketone appears to be an interesting compound in itself as a chelating ligand for transition metals, but so far no experiments in that direction have been reported.

Other attempts to prepare 2,4,6-tris(trifluoromethyl)acetophenone have also been met only with very limited success (28): 1) No reaction was observed when 1,3,5-tris(trifluoromethyl)-benzene was treated with acetyl chloride in the presence of anhydrous AlCl₃ (*vide supra*). 2) The secondary alcohol R_fCH(OH)CH₃ can be prepared from R_fLi and acetaldehyde. However, it was found impossible to oxidize this alcohol with Jones reagent (Cr^{VI}). Although IR spectra showed some evidence

for the formation of carbonyl-containing species, the ketone could not be isolated. 3) A general route to ketones involves treatment of lithium carboxylates with alkyl or aryl lithium reagents. The carboxylic acid $R_f\text{COOH}$ (*vide infra*) cleanly reacts with methyllithium to give the corresponding lithium salt, but the subsequent reaction with excess CH_3Li did not lead to the formation of 2,4,6-tris(trifluoromethyl)acetophenone. The non-reactivity of $R_f\text{COOLi}$ towards methyllithium was attributed to severe steric hindrance in the requisite tetrahedral intermediate $R_f\text{C}(\text{OLi})_2\text{CH}_3$.

The case of 2,4,6-tris(trifluoromethyl)acetophenone has been discussed in some detail in order to demonstrate that sometimes R_f chemistry can be quite different from that of less sterically hindered aromatic compounds. Similar problems as in the case of $R_f\text{C}(\text{O})\text{CH}_3$ were encountered in an attempted preparation of a related aryl vinyl ketone, $R_f\text{C}(\text{O})\text{CH}=\text{CH}_2$ (28). When $R_f\text{Li}$ was reacted with acryloyl chloride, $\text{CH}_2=\text{CH}-\text{COCl}$, a mixture of two ketones was obtained. One of them seemed to be $R_f\text{C}(\text{O})\text{CH}=\text{CH}_2$. The other ketone, $R_f\text{C}(\text{O})\text{CH}_2\text{CH}_2R_f$, resulted from a Michael addition between $R_f\text{C}(\text{O})\text{CH}=\text{CH}_2$ and the strong nucleophile $R_f\text{Li}$ (Equation 3).



In view of these results it is not surprising that even more sterically hindered carbonyl derivatives of R_f are also not accessible (22). An attempted synthesis of $(R_f)_2\text{CO}$ from $R_f\text{Li}$ and dimethyl carbonate gave the methyl ester of 2,4,6-tris(trifluoromethyl)benzoic acid instead (25% yield). Similarly, treatment of $R_f\text{Li}$ with oxalyl dichloride did not yield the desired benzil derivative. In this reaction a 45% yield of 2,4,6-tris(trifluoromethyl)-2-oxoethanoic acid, $R_f\text{C}(\text{O})\text{COOH}$, was obtained (22). All these experiments clearly demonstrate that in organic R_f chemistry steric hindrance is an important factor guiding the reactivity of various substrates.

In contrast to the unsuccessful syntheses of various R_f -derived ketones, the preparation of 2,4,6-tris(trifluoromethyl)benzoic acid is simple and straightforward (22,28,29). It can be obtained in 80% yield by reaction of $R_f\text{Li}$ with carbon dioxide and subsequent acidification. Pure crystalline $R_f\text{COOH}$ melts at 190-191°C and has a pK_a of 3.0, rendering it more acidic than mesitoic acid (pK_a 3.8). The CF_3 groups in $R_f\text{COOH}$ are very stable against hydrolysis. Prolonged heating (24h) with either concentrated NaOH or 96% H_2SO_4 led to a near quantitative recovery of unreacted $R_f\text{COOH}$ (28). 2,4,6-Tris(trifluoromethyl)benzoic acid deserves some interest because the carboxyl group is expected to be in a perpendicular arrangement with respect to the aromatic ring. Thus

conjugation between the two π -systems is expected to be negligible. Verification of this hypothesis through X-ray analyses seems highly desirable.

Again, due to steric hindrance, $R_F\text{COOH}$ was reported to be very resistant to attack by thionyl chloride. Only a small yield (10-15%) of $R_F\text{C(O)Cl}$ was obtained after heating the mixture at 70°C for 48 h (28). In our hands the yield of acid chloride was 32% (29). Pure $R_F\text{C(O)Cl}$ is a beautifully crystalline, low melting (39°C) solid which is quite resistant to hydrolysis. It is interesting to note that the corresponding acid fluoride, $R_F\text{C(O)F}$, was obtained earlier by a different route (25,30). 2,4,6-Tris(trifluoromethyl)benzoyl fluoride was prepared in 78% yield by fluorination of benzene-1,2,3,5-tetracarboxylic acid with SF_4 . $R_F\text{C(O)F}$ served as a useful starting material in the synthesis of 2,4,6-tris(trifluoromethyl)aniline, $R_F\text{NH}_2$, which is not accessible by more conventional routes. The preparation of $R_F\text{NH}_2$ involves conversion of the acid fluoride to the amide and subsequent Hoffmann conversion to the amine (overall yield 56%) (25,30). The chemistry of $R_F\text{NH}_2$ is largely undeveloped and certainly merits further attention.

The methyl ester $R_F\text{COOCH}_3$ was obtained serendipitously in 25% yield from $R_F\text{Li}$ and dimethyl carbonate (*vide supra*) (22). Normal acid-catalyzed esterification of $R_F\text{COOH}$ was found to be unsuccessful (28). A similar behavior was reported earlier for mesitoic acid. Once again steric crowding by the *ortho* substituents was made responsible for the non-ability to form a tetrahedral transition state required for the ester formation. The problem can be circumvented by "steric acceleration", i.e. formation of a sterically less crowded linear acylium ion. In the case of $R_F\text{COOH}$ the corresponding acylium ion $R_F\text{CO}^+$ is significantly destabilized by structure C of the resonance hybrid. Nevertheless, generation of $R_F\text{CO}^+$ from $R_F\text{COOH}$ and 96% H_2SO_4 and subsequent reaction with ethanol allowed the preparation of ethyl ester $R_F\text{COOC}_2\text{H}_5$ in low yield (28). Alternatively, the acylium ion can be generated via a mixed anhydride of $R_F\text{COOH}$ and trifluoroacetic acid, $R_F\text{C(O)OC(O)CF}_3$. Thus, the highly crowded phenolic ester $R_F\text{C(O)OC}_6\text{H}_2(\text{CH}_3)_3$ -2,4,6 was prepared in 44% yield by heating a mixture of $R_F\text{COOH}$, 2,4,6-trimethylphenol and trifluoroacetic anhydride (28).

No further reactions of $R_F\text{COOH}$ have been reported and no metal salts or complexes have been fully characterized. Thus far the derivative chemistry of $R_F\text{C(O)Cl}$ also remains largely unexplored. Originally it was anticipated that $R_F\text{C(O)Cl}$ would be the ideal starting material for the synthesis of the hitherto unknown phosphalkyne $R_F\text{C}\equiv\text{P}$. Initial experiments have shown however, that the preparation of this material is not straightforward and further studies are required. The only definite result so far is the formation of a lithium diacylphosphide, $\text{Li}^+R_F\text{C(O)PC(O)R}_F^-$, from $R_F\text{C(O)Cl}$ and $\text{LiP}(\text{SiMe}_3)_2$ (31).

Yellow crystalline $\text{Li}^+\text{RfC}(\text{O})\text{PC}(\text{O})\text{Rf}^-$ was obtained in 24% yield and fully characterized by spectroscopic methods. Although this diacylphosphide anion seems to be an attractive chelating ligand for transition metals, the reactivity of $\text{Li}^+\text{RfC}(\text{O})\text{PC}(\text{O})\text{Rf}^-$ towards metal halides has not yet been investigated. The only initial experiment showed that $\text{Li}^+\text{RfC}(\text{O})\text{PC}(\text{O})\text{Rf}^-$ did not react with $(\text{C}_5\text{Me}_5)\text{TiCl}_3$, but further work is required to investigate the ligand properties of the $\text{RfC}(\text{O})\text{PC}(\text{O})\text{Rf}^-$ anion.

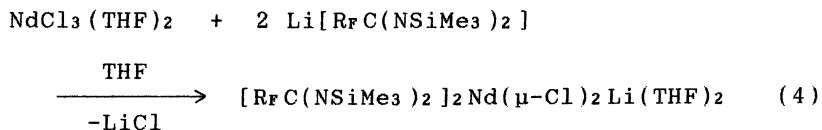
Another potentially interesting ligand for transition metals is the recently reported dithiocarboxylate anion RfCSS^- (32). Treatment of *in situ* prepared RfLi with excess carbon disulfide results in the formation of a red-brown solution, from which RfCSSH can be isolated after acidification (55% yield). Pure 2,4,6-tris(trifluoromethyl)dithiobenzoic acid forms a dark red oily liquid. Orange crystalline $[\text{C}_5\text{H}_{10}\text{NH}_2]^+\text{RfCSS}^-$ has been prepared by neutralizing the free acid with piperidine in pentane solution (32). The coordination chemistry of the RfCSS^- anion still awaits further investigation.

Yet another anion formally derived from 2,4,6-tris(trifluoromethyl)benzoic acid has already been proven to be a useful chelating ligand. The very highly substituted benzamidinate anion $[\text{RfC}(\text{NSiMe}_3)_2]^-$ has been synthesized in one step by adding RfLi to bis(trimethylsilyl)carbodiimide (33).

$\text{Li}[\text{RfC}(\text{NSiMe}_3)_2]$ is obtained in 80% yield in the form of large, colorless, transparent crystals after recrystallization from hexane. The presence of two bulky trimethylsilyl substituents in addition to the CF_3 groups is responsible for the high solubility of the lithium benzamidinate derivative in unpolar solvents such as pentane or hexane. $\text{Li}[\text{RfC}(\text{NSiMe}_3)_2]$ is also quite volatile and slowly sublimates at room temperature under moderate vacuum. The $[\text{RfC}(\text{NSiMe}_3)_2]^-$ anion represents the limit of steric saturation. Accordingly $\text{Li}[\text{RfC}(\text{NSiMe}_3)_2]$ does not react with Me_3SiCl to give the fully silylated benzamidine derivative $\text{RfC}(=\text{NSiMe}_3)[\text{N}(\text{SiMe}_3)_2]$. The 2,4,6-tris(trifluoromethyl)-*N,N'*-bis(trimethylsilyl)benzamidinate anion exhibits interesting ligand properties in coordination compounds with lanthanide and actinide elements (33). As part of a general study on f-element complexes containing bulky chelating ligands, we have demonstrated that silylated benzamidinate anions of the type $[\text{RC}_6\text{H}_4\text{C}(\text{NSiMe}_3)_2]^-$ can be regarded as "steric cyclopentadienyl equivalents" (33). The cone angle of the silylated benzamidinate is comparable with that of cyclopentadienyl and virtually all different types of f-element cyclopentadienyl complexes have analogues in the benzamidinate chemistry of these elements. Typical examples are compounds like $[\text{RC}_6\text{H}_4\text{C}(\text{NSiMe}_3)_2]_3\text{Ln}$ (34), $[\text{RC}_6\text{H}_4\text{C}(\text{NSiMe}_3)_2]_3\text{UCl}$ (33), $[\text{RC}_6\text{H}_4\text{C}(\text{NSiMe}_3)_2]_3\text{UMe}$ (35) or $[\text{RC}_6\text{H}_4\text{C}(\text{NSiMe}_3)_2]_2\text{Ln}(\text{THF})_2$ (36), which correspond to the well-known f-element cyclopentadienyl complexes Cp_3Ln ,

Cp_3UCl , Cp_3UMe and $\text{Cp}_2\text{Ln}(\text{THF})_2$ (37). The introduction of *ortho* substituents in the phenyl ring should significantly increase the steric bulk of the benzamidinate anions. It was therefore anticipated that the reactivity of the sterically demanding $[\text{RfC}(\text{NSiMe}_3)_2]^-$ anion would resemble that of the pentamethylcyclopentadienyl ligand. The experimental results have revealed that this is exactly the case. Towards lanthanide and actinide ions the sterically demanding $[\text{RfC}(\text{NSiMe}_3)_2]^-$ ligand behaves just like Cp^* . Given uranium and thorium as an example, Marks et al. have shown that UCl_4 and ThCl_4 react with two or more equivalents of a Cp^* transfer reagent to give exclusively $\text{Cp}^*_2\text{UCl}_2$ and $\text{Cp}^*_2\text{ThCl}_2$ resp. as the only isolable products (38). Trisubstitution, i.e. formation of Cp^*_3UCl or Cp^*_3ThCl , was not observed. A striking similarity was found for the analogous reactions of $\text{Li}[\text{RfC}(\text{NSiMe}_3)_2]$ with UCl_4 and ThCl_4 . In both cases the disubstituted products $[\text{RfC}(\text{NSiMe}_3)_2]_2\text{AcCl}_2$ ($\text{Ac} = \text{U, Th}$) were isolated. There was no evidence for the formation of trisubstituted derivatives $[\text{RfC}(\text{NSiMe}_3)_2]_3\text{AcCl}$. The actinide benzamidinate complexes $[\text{RfC}(\text{NSiMe}_3)_2]_2\text{UCl}_2$ and $[\text{RfC}(\text{NSiMe}_3)_2]_2\text{ThCl}_2$ have been fully characterized by X-ray crystallography (33). The ligand environment in these formally six-coordinate actinide complexes is very similar as in the bent metallocenes $\text{Cp}^*_2\text{AcCl}_2$ ($\text{Ac} = \text{U, Cl}$) (Figure 2).

Further evidence for the steric similarity between Cp^* and the bulky benzamidinate ligand $[\text{RfC}(\text{NSiMe}_3)_2]^-$ came from lanthanide chemistry. Until very recently, Cp^* was the only ligand known to form complexes of the general type $\text{L}_2\text{Ln}(\mu\text{-Cl})_2\text{Li}(\text{THF})_2$, in which lanthanide and lithium ions are bridged by two halide ligands to give a four-membered ring system (39). Substitution reactions of anhydrous lanthanide trichlorides with LiCp^* in THF solution usually yield complexes of the composition $\text{Cp}^*_2\text{Ln}(\mu\text{-Cl})_2\text{Li}(\text{THF})_2$. The coordination of lithium halide illustrates the tendency of the lanthanide ions to adopt high formal coordination numbers. A very similar complex was synthesized by using the "steric Cp^* equivalent" $[\text{RfC}(\text{NSiMe}_3)_2]^-$. Treatment of anhydrous neodymium trichloride with two equivalents of $\text{Li}[\text{RfC}(\text{NSiMe}_3)_2]$ gave exclusively the disubstituted product $[\text{RfC}(\text{NSiMe}_3)_2]_2\text{-Nd}(\mu\text{-Cl})_2\text{Li}(\text{THF})_2$ (40) (Equation 4).



Once again the X-ray structure determination revealed a striking analogy between the neodymium benzamidinate and the bent metallocene derivative $\text{Cp}^*_2\text{Nd}(\mu\text{-Cl})_2\text{Li}(\text{THF})_2$ (Figure 3).

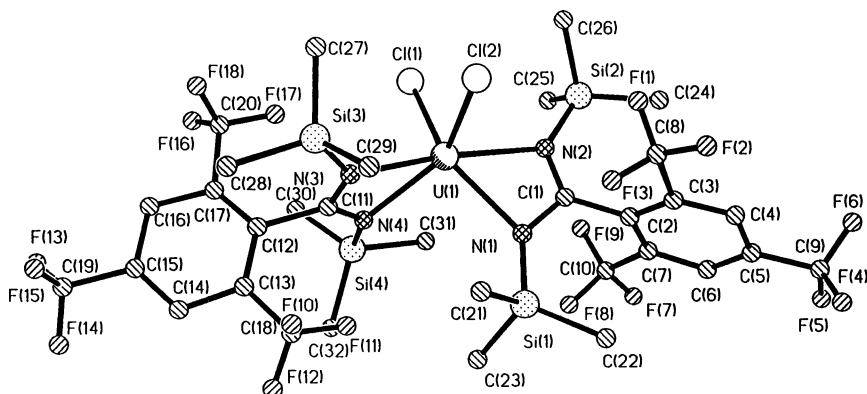


Figure 2. Molecular structure of $[RfC(NSiMe_3)_2]_2UCl_2$.

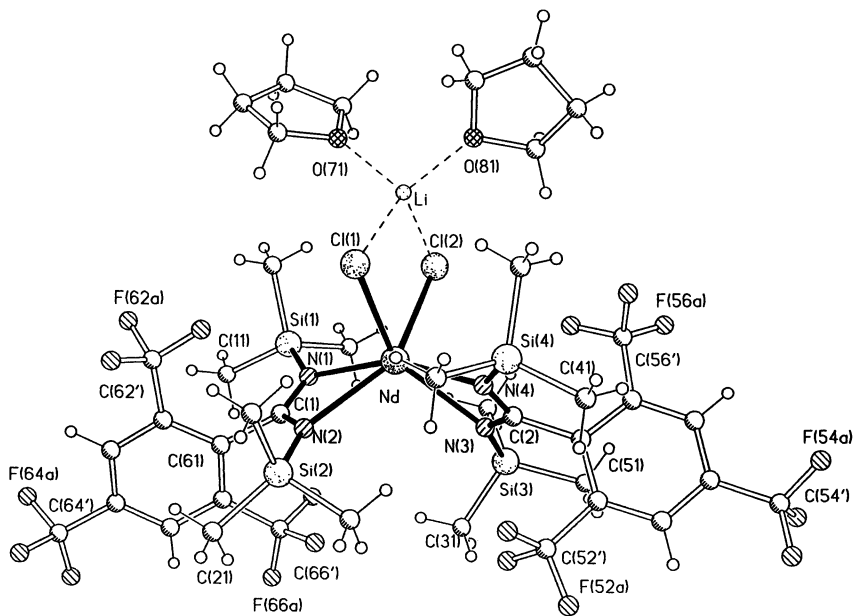


Figure 3. Molecular structure of $[RfC(NSiMe_3)_2]_2-Nd(\mu-Cl)_2Li(THF)_2$.

The most recent addition to the family of organic R_F derivatives is 2,4,6-tris(trifluoromethyl)benzyl alcohol, R_FCH₂OH (41). This seemingly unspectacular compound was prepared by a standard procedure from R_FLi and (CH₂O)_n. R_FCH₂OH was isolated in low yield (15%) as a low-melting crystalline solid. What makes R_FCH₂OH interesting is its unusual crystal structure. Six R_FCH₂OH molecules are connected via hydrogen bridges. The resulting hexameric array resembles the chairconformation of a "supercyclohexane" (Figure 4).

The unexpected structure of R_FCH₂OH clearly demonstrates that more work is needed to elucidate the molecular structures of "simple" organic R_F derivatives.

Metal Derivatives containing R_F and R_FS Ligands

Main group metal derivatives containing R_F, R_FO and R_FS ligands have been the main topic of the first review article on R_F chemistry (20). Therefore only a few of these results will be mentioned here in addition to some new developments in that area. Perhaps the most significant result in R_F chemistry was the synthesis of the first diaryl plumblyene, (R_F)₂Pb (42). Bright yellow, crystalline (R_F)₂Pb can be prepared by reacting PbCl₂ with two equivalents of R_FLi in diethyl ether/hexane solution. In contrast to previously reported reactions of PbCl₂ with aryllithium or aryl Grignard reagents, the formation of (R_F)₂Pb is very clean and no disproportionation is observed. An X-ray crystal structure analysis revealed that (R_F)₂Pb is monomeric in the solid state. This compound is another good example for the electronic stabilization of low-coordinate main group elements induced by the R_F substituent. Four intramolecular Pb-F contacts contribute to the unusual stability of the diarylplumblyene (Figure 5).

Disappointingly, but not surprisingly (inert pair effect!), (R_F)₂Pb is very reluctant to undergo oxidative addition reactions (32). So far it was not possible to prepare any lead(IV) derivatives containing R_F ligands (e.g. (R_F)₂PbCl₂ or (R_F)₂Pb(SPh)₂). However, it was found that (R_F)₂Pb can serve as a useful starting material in the preparation of unsolvated lead(II) thiolates. The reaction of (R_F)₂Pb with two equivalents of 2,4,6-tris(trifluoromethyl)benzenethiol, R_FSH, in hexane solution provided bright yellow crystalline (R_FS)₂Pb in high yield (42). The only by-product in this reaction is the volatile fluorocarbon 1,3,5-tris(trifluoromethyl)benzene. Thus the method appears to be an elegant way of making lead(II) alkoxides or thiolates and deserves further elucidation. Unsolvated (R_FS)₂Pb has so far resisted all attempts to obtain suitable single crystals for an X-ray analysis. In one occasion repeated crystallization from toluene produced large, yellow block-like crystals. An X-ray structure determination

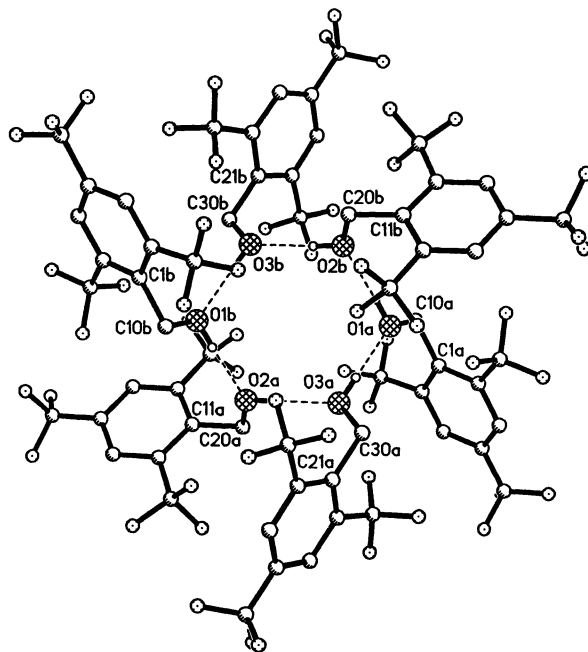


Figure 4. Molecular structure of hexameric $[R_fCH_2OH]_6$.

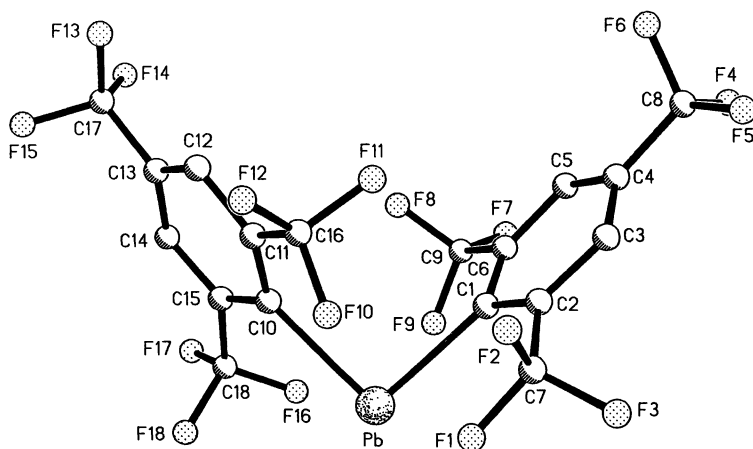


Figure 5. Molecular structure of $(R_f)_2Pb$.

revealed that this material was a new compound resulting from contamination of the original lead(II) thiolate with small amounts of oxygen. This resulted in the formation of the unusual oxygen-centered lead thiolate cluster $Pb_5O(SR_f)_8$ (43) (Figures 6 and 7).

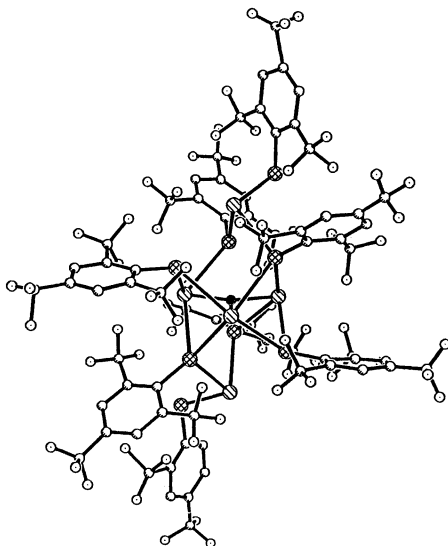


Figure 6. Molecular structure of $Pb_5O(SRf)_5$.

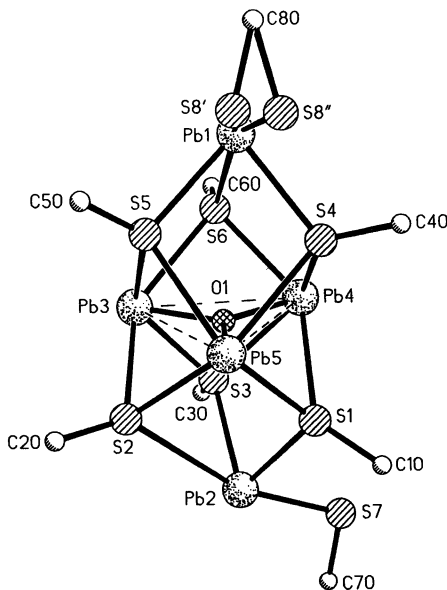


Figure 7. Coordination polyhedron in $Pb_5O(SRf)_5$ showing two loosely coordinated toluene molecules (Rf substituents omitted for clarity; disorder at sulfur atom $S8$).

Generally the chemistry of metal complexes containing R_fS ligands is already fairly extensive. Starting point is 2,4,6-tris(trifluoromethyl)benzenethiol, R_fSH , which was first described by *Chambers et al.* in 1987 (22). R_fSH is isolated as an oily liquid with a pungent odor. The acidity of R_fSH is so high that it forms a stable ammonium thiolate. $NH_4^+R_fS^-$ is obtained in high yield as a white precipitate when R_fSH is treated with $HN(SiMe_3)_2$ in hexane solution (32). The colorless crystals of $NH_4^+R_fS^-$ are highly volatile and sublime readily at room temperature. Various main group and transition metal derivatives of R_fSH have been prepared either from the free thiol or via the readily available alkaline metal thiolates. Unsolvated $NaSR_f$ and KSR_f are easily prepared by deprotonation of R_fSH with $NaN(SiMe_3)_2$ or $KN(SiMe_3)_2$ in toluene solution (ca. 90% yield). The remarkable polymeric crystal structures of their THF adducts have already been discussed in detail (20). A ladder-shaped polymeric structure was also reported for the related thallium thiolate $[TlSR_f \cdot 0.5 \text{ dioxane}]_n$ (44).

$TlSR_f$ can be prepared in 80% yield by a metathetical reaction of $NaSR_f$ with Tl_2CO_3 in acetonitrile solution. A more convenient synthesis which produces analytically pure $TlSR_f$ in 87% yield involves treatment of $TlOEt$ with free R_fSH . $TlSR_f$ forms a colorless crystalline precipitate when the reaction is carried out in hexane. Similarly, the previously described lead(II) thiolate $Pb(SR_f)_2$ can be prepared by reacting $PbCl_2$ with $NaSR_f$ in a molar ratio of 1:2 (45). The solvated species $Pb(SR_f)_2 \cdot THF$ was obtained by recrystallization from THF and structurally characterized by X-ray crystallography.

In contrast to the mono-THF adduct $Pb(SR_f)_2 \cdot THF$, the corresponding thiolates of zinc(II) and manganese(II) crystallize with two additional THF ligands. $Mn(SR_f)_2 \cdot 2THF$ is best prepared by reacting $Mn[N(SiMe_3)_2]_2 \cdot THF$ with two equivalents of R_fSH . While the lead and zinc derivatives are air-stable, the colorless manganese complex is easily oxidized by traces of oxygen. The isomorphous molecular structures of $Zn(SR_f)_2 \cdot 2THF$ and $Mn(SR_f)_2 \cdot 2THF$ have been determined by X-ray diffraction.

Acknowledgments

Special thanks are due to Professor Herbert W. Roesky for his generous support of this work and for stimulating my interest in fluorine chemistry. Various contributions have been made by a number of talented co-workers, whose names appear in the list of references. The work carried

out at Göttingen was financially supported by the Fonds der Chemischen Industrie, the Deutsche Forschungsgemeinschaft and the Dr. Otto Röhm-Gedächtnisstiftung. I am also grateful to Dr. Sally Brooker, Professor John W. Gilje, Professor Kenton H. Whitmire, Dr. Dietmar Stalke and Dr. Hansjörg Grützmacher for helpful discussions and valuable contributions. Special thanks are also due to Mr. Klaus Keller who prepared all the SF₄ and 1,3,5-tris(trifluoromethyl)benzene used for these studies.

References

1. Cowley, A.H. *Acc. Chem. Res.* **1984**, *17*, 386 and references therein.
2. Köhler, H.; Michaelis, A. *Ber. Dtsch. Chem. Ges.* **1877**, *10*, 807.
3. Yoshifuji, M.; Shima, I.; Inamoto, N. *J. Am. Chem. Soc.* **1981**, *103*, 4587.
4. Cowley, A.H.; Lasch, J.G.; Norman, N.C.; Pakulski, M. *J. Chem. Soc. Chem. Commun.* **1983**, 881.
5. Couret, C.; Escudie, J.; Madule, Y.; Ranaivonjatovo, H.; Wolf, J.-G. *Tetrahedron Lett.* **1983**, *24*, 2769.
6. Romanenko, V.D.; Klebanski, E.O.; Markovskii, L.N. *Zh. Obshch. Khim.* **1985**, *55*, 2141.
7. Appel, R.; Knoll, F.; Ruppert, I. *Angew. Chem.* **1981**, *93*, 771; *Angew. Chem. Int. Ed. Engl.* **1981**, *20*, 731.
8. R. West, *Pure Appl. Chem.* **1984**, *56*, 163.
9. Hesse, M.; Klingebiel, U. *Angew. Chem.* **1986**, *98*, 638; *Angew. Chem. Int. Ed. Engl.* **1986**, *25*, 649.
10. Smit, C.N.; Lock, F.M.; Bickelhaupt, F. *Tetrahedron Lett.* **1984**, *25*, 3011.
11. Lange, L.; Meyer, B.; du Mont, W.-W. *J. Organomet. Chem.* **1987**, *329*, C17.
12. Veith, M.; Recktenwald, O. *Top. Curr. Chem.* **1982**, *104*, 57.
13. Regitz, M.; Binger, P. *Angew. Chem.* **1988**, *100*, 1541; *Angew. Chem. Int. Ed. Engl.* **1988**, *27*, 1484 and references therein.
14. Nixon, J.F. *Chem. Rev.* **1988**, *88*, 1327.
15. M. Regitz, *Chem. Rev.* **1990**, *90*, 191.
16. Märkl, G.; Sejpka, H. *Angew. Chem.* **1986**, *98*, 286; *Angew. Chem. Int. Ed. Engl.* **1986**, *25*, 264.
17. van der Sluys, W.G.; Burns, C.J.; Sattelberger, A.P. *Organometallics* **1989**, *8*, 855.
18. Hitchcock, P.B.; Lappert, M.F.; Smith, R.G. Bartlett, R.A.; Power, P.P. *J. Chem. Soc. Chem. Commun.* **1988**, 1007.
19. Power, P.P.; *Comments Inorg. Chem.* **1989**, *8*, 177.
20. Edelmann, F.T. *Comments Inorg. Chem.* **1992**, *12*, 259.
21. McBee, E.T.; Leech, R.E. *Ind. Eng. Chem.* **1947**, *39*, 394.
22. Carr, G.E.; Chambers, R.D.; Holmes, T.F.; Parker, D.G. *J. Organomet. Chem.* **1987**, *325*, 13.
23. Scholz, M.; Roesky, H.W.; Stalke, D.; Keller, K.; Edelmann, F.T. *J. Organomet. Chem.* **1989**, *366*, 73.

24. Takahashi, K.; Yoshino, A.; Hosokawa, K.; Muramatsu, H. *Bull. Chem. Soc. Jpn.* **1985**, *58*, 755.
25. *Synthesis of Fluoroorganic Compounds*, Knunyants, I.L.; Yakobson, G.G., Eds.; Springer-Verlag: Berlin Heidelberg New York Tokio, 1985.
26. Stalke, D.; Whitmire, K.H. *J. Chem. Soc. Chem. Commun.* **1990**, 833.
27. Buijink, J.-K.; Edelmann, F.T. *unpublished*.
28. Filler, R.; Gnanndt, W.K.; Chen, W.; Lin, S. *J. Fluor. Chem.* **1991**, *52*, 99.
29. Bertel, N. *Ph.D. Thesis*, Universität Göttingen **1989**.
30. Burmakov, A.I.; Alekseeva, L.A.; Yagupolskii, L.M. *Zh. Org. Khim.* **1970**, *6*, 144.
31. Scholz, M. *Ph.D. Thesis*, Universität Göttingen **1990**.
32. Edelmann, F.T. *unpublished*.
33. Wedler, M.; Knösel, F.; Noltemeyer, M.; Edelmann, F. *J. Organomet. Chem.* **1990**, *388*, 21.
34. Wedler, M.; Knösel, F.; Pieper, U.; Stalke, D.; Edelmann, F.T.; Amberger, H.-D. *Chem. Ber.* **1992**, *125*, 2171.
35. Wedler, M.; Knösel, F.; Edelmann, F.T.; Behrens, U. *Chem. Ber.* **1992**, *125*, 1313.
36. Wedler, M.; Noltemeyer, M.; Pieper, U.; Schmidt, H.-G.; Stalke, D.; Edelmann, F.T. *Angew. Chem.* **1990**, *102*, 941; *Angew. Chem. Int. Ed. Engl.* **1990**, *29*, 894.
37. *Comprehensive Organometallic Chemistry*, Stone, F.G.A.; Wilkinson, G.; Abel, E.W., Eds.; Pergamon Press: London, 1982; Vol. 3.
38. Fagan, P.J.; Manriquez, J.M.; Maatta, E.A.; Seyam, A.M.; Marks, T.J. *J. Am. Chem. Soc.* **1981**, *103*, 6650.
39. Evans, W.J. *Adv. Organomet. Chem.* **1985**, *24*, 131.
40. Recknagel, A.; Knösel, F.; Gornitzka, H.; Noltemeyer, M.; Edelmann, F.T.; Behrens, U. *J. Organomet. Chem.* **1991**, *417*, 363.
41. Bohnen, F.M.; Herbst-Irmer, R.; Edelmann, F.T. *unpublished*.
42. Brooker, S.; Buijink, J.-K.; Edelmann, F.T. *Organometallics* **1991**, *10*, 25.
43. Brooker, S.; Edelmann, F.T. *unpublished*.
44. Labahn, D.; Pohl, E.; Herbst-Irmer, R.; Stalke, D.; Roesky, H.W.; Sheldrick, G.M. *Chem. Ber.* **1991**, *124*, 1127.

RECEIVED April 12, 1993

Chapter 20

Reaction of Nonmetal Fluorides with Some Platinum Metal Complexes

R. W. Cockman^{1,2}, E. A. V. Ebsworth^{1,3}, J. H. Holloway⁴, H. Murdoch¹,
N. Robertson^{1,5}, and P. G. Watson^{1,6}

¹Department of Chemistry, Edinburgh University, West Mains Road,
Edinburgh EH9 3JJ, Scotland

²BP Chemicals Ltd., P.O. Box 21, Bo'ness Road, Grangemouth FK3 9XH,
Scotland

³Durham University, Old Shire Hall, Old Elvet, Durham DH1 3HP,
United Kingdom

⁴Department of Chemistry, The University, Leicester LE1 7RH,
United Kingdom

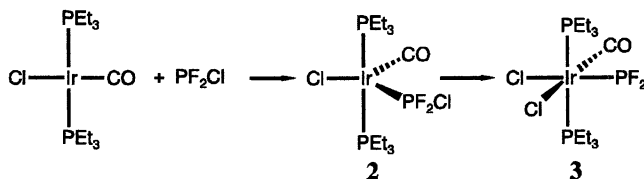
⁵Institut für Anorganische und Analytische Chemie, Freie Universität
Berlin, Fabeckstrasse 34–36, D–14195 Berlin, Germany

⁶Institut für Anorganische und Physikalische Chemie, Universität
Bremen, Leobenerstrasse NW2, D–28334 Bremen, Germany

XeF₂ reacts with [M(CO)X(PEt₃)₂], **1** (M = Rh, Ir; X = Cl, Br, I) to give the *cis*-addition product, [M(CO)F₂X(PEt₃)₂], characterised by NMR spectroscopy; *cis*- and *trans*-[Ir(DPPE)₂F₂]⁺ have been obtained and characterised similarly. With complexes of 6-coordinated Ir(III), reaction below 300K only occurs where, formally, F₂ can be added to a ligand (such as PF₂ or PH₂). [Ir(CO)₃(PEt₃)₂]⁺ and related species react with XeF₂ to form novel fluoroacyl complexes of Ir(III), eg [Ir(CO)₂(COF)F(PEt₃)₂]⁺, **9**; reactions of **9** with silyl compounds and with Lewis acids are discussed. Complexes **1** react with SF₄ to form [M(CO)FX(PEt₃)₂(SF₃)]; two distinct fluxional processes have been observed in the SF₃-groups. Analogous SeF₃ derivatives are formed from **1** and SeF₄; with TeF₄, the rhodium complexes form [Rh(CO)X(PEt₃)₂(TeF₃)]⁺[TeF₅]⁻.

Reactions between non-metal fluorides and transition metal complexes have not been extensively studied. Powerfully oxidising fluorides such as BrF₃ usually give fluoroanions of highly-oxidised metals. Molecules such as PF₃ normally act as electron-pair donors; the PF₃ bonds are not active in oxidative addition. For example, (I) PF₂Cl reacts with *trans*-[Ir(CO)Cl(PEt₃)₂] at low temperatures as a simple donor to form a complex of 5-coordinated Ir(I), **2**; at 270K this complex rearranges by adding P-Cl across the Ir(I) centre to form a PF₂-complex of six-coordinated Ir(III), **3**

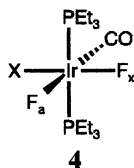
0097-6156/94/0555-0326\$08.00/0
© 1994 American Chemical Society



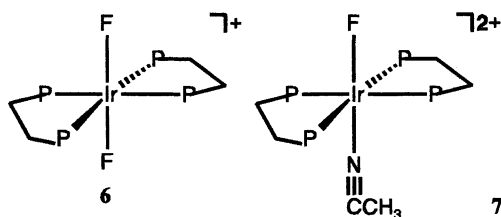
In view of current interest in fluorochemistry, we have explored the reactions of a wider range of non-metal fluorides with complexes of low-valent transition metal complexes, and we here describe reactions between some phosphine complexes of Ir(I) and Rh(I) and XeF₂, SF₄, SeF₄ and TeF₄.

Reactions of XeF₂.

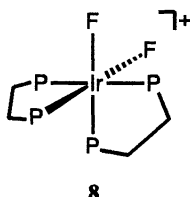
We find that XeF₂ reacts with bis-phosphine complexes of 4-coordinated Ir(I) by oxidative addition. (2) With *trans*-[Ir(CO)X(PEt₃)₂] (X = Cl, Br, I) reaction is smooth at 240K in CH₂Cl₂; there is one major product, [Ir(CO)F₂X(PEt₃)₂], **4** as established by the ¹⁹F and ³¹P-¹H NMR spectra.



Small amounts of two isomeric monofluorides [Ir(CO)FX₂(PEt₃)₂], and of the trifluoride, [Ir(CO)F₃(PEt₃)₂], **5** are also formed; none of these is present at a level greater than 10% of **4**. The ¹⁹F NMR spectrum of **4** shows two doublets of triplets of equal intensity; the NMR parameters are collected in Table I. The assignments of the F resonances are based on three observations: the resonances most sensitive to X are assigned to F_x; in the spectrum of [Ir(CO)F₃(PEt₃)₂], the resonance due to F_x is twice as intense as that due to F_a; finally, in the spectrum of [Ir(¹³CO)F₂(PEt₃)₂(SF₃)] the resonance assigned to F_a by analogy with the assignments proposed here shows the large ²J(FC) associated with F *trans* to CO. [Ir(CO)F₂X(PEt₃)₂] is stable at room temperature in solution. Analogous derivatives have been obtained with iridium complexes of other phosphines and with rhodium. The rhodium complexes are less thermally stable, and amounts of the mono- and trifluorides increase with time at room temperature. There is no direct evidence as to the mechanism of addition. However, results obtained (**3**) with [Ir(DPPE)₂]⁺ (DPPE = Bis-(diphenylphosphinoethane)) suggest that the addition may not be concerted. This cation reacts smoothly with XeF₂ in CD₂Cl₂ at 240K to give a single product whose simple NMR spectra (¹⁹F resonance, quintet, δ -522.2; ³¹P-¹H, triplet δ 8.8, ²J(PF) = 18Hz) show that it must be the complex **6** below, formed by *trans* addition:



In CH_3CN the main product is a related species, **7** (^{19}F , δ -495.1, quintet; ^{31}P - $\{^1\text{H}\}$, δ 11.0, doublet, $^2\text{J}(\text{PF}) = 20\text{Hz}$). The analogous complex with *cis*-fluorine ligands, **8**, has been obtained by treating $[\text{Ir}(\text{DPPE})_2\text{S}_2]^+$ with XeF_2 in CD_2Cl_2 .

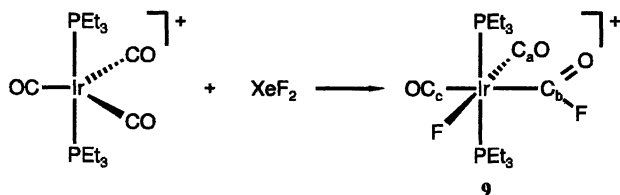


8

The complex second-order ^{19}F and ^{31}P - $\{^1\text{H}\}$ NMR spectra have been analysed as arising from the spin system $\text{AA}'\text{X}_2\text{X}_2'$, with a ^{19}F chemical shift of δ -345.6. Reaction at 180K with an equimolar ratio of reactants suggests that the initial product may have been $[\text{Ir}(\text{DPPE})_2\text{F}(\text{SSF})]^+$, but the intermediate has not been identified conclusively.

Reactions of XeF_2 with Complexes of 5-coordinated Ir(I)

We find that XeF_2 reacts with $[\text{Ir}(\text{CO})_3(\text{PEt}_3)_2]^+$ in CH_2Cl_2 to form the very unusual fluoroacyl complex **9** below (4-5):



9

The product has been characterised by single crystal X-ray crystallography and by its ^{19}F , ^{13}C - $\{^1\text{H}\}$ and ^{31}P - $\{^1\text{H}\}$ NMR spectra; the NMR parameters are given in Table II. The ^{13}C data were obtained from a sample containing about 10% ^{13}C in the CO groups; the large values of $^2\text{J}(\text{FC})$ and $^3\text{J}(\text{FC})$ are noteworthy, conforming to the general pattern of large couplings between *trans* nuclei, though it is unusual to find so large a 3-bond FC coupling. We have observed analogous reactions between XeF_2 and $[\text{Ir}(\text{CO})_3\text{L}_2]^+$ where $\text{L} = \text{PMe}_3$, PMe_2Ph , PEt_2Ph and $\text{P}(\text{EtPh})_2$, though the fluoroacyl complex formed in the last of these reactions was not stable at room temperature. We did not detect the formation of fluoroacyl complexes where $\text{L} = \text{PMePh}_2$, PPh_3 or $\text{P}(\text{Cyclohexyl})_3$. It seems that the most important property of the phosphine ligand is its basicity (δ): complexes of the most basic phosphines react most readily to give fluoroacyl complexes, as would be expected if electron density at Ir(I) were important in the reaction. The failure of the tricyclohexylphosphine complex to react suggests that the very bulky phosphines (**7**) block the reaction. Among other complexes of 5-coordinated Ir(I), $[\text{Ir}(\text{CO})(\text{PMe}_3)_4]^+\text{Cl}^-$ reacts with XeF_2 to give $[\text{Ir}(\text{COF})(\text{PMe}_3)_4]^+\text{Cl}^-$, which is stable at room temperature. Here, as in **9**, the values of $^2\text{J}(\text{PF})$ and $^3\text{J}(\text{PF})$ are large. Reaction between

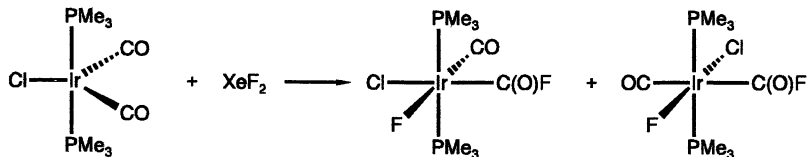
Table I. NMR Data for *cis*-[F₂M(CO)X(PEt₃)₂]

M	X	Chemical shifts/ppm		Coupling Constants/Hz						
		$\delta(P)$	$\delta(F_a)$	$\delta(F_x)$	$^1J(MF_a)$	$^1J(MF_x)$	$^1J(MP)$	$^2J(F_aF_x)$	$^2J(PF_a)$	$^2J(PF_x)$
Rh	F	31.3	-318.8	-512.2	102	205	77	89	24	18
	Cl	30.0	-324.0	-445.5	103	182	75	115	24	20
	Br	8.1	-329.1	-429.4	103	176	74	123	24	21
	I	30.5	-337.5	-393.6	102	177	73	131	24	23
Ir	F	6.9	-288.5	-470.6	-	-	-	96	31	18
	Cl	6.1	-299.1	-488.7	-	-	-	115	29	18
	Br	4.7	-303.2	-392.0	-	-	-	130	31	22
	I	3.2	-313.8	-364.6	-	-	-	143	33	21

Table II. NMR Data for [Ir(CO)₂(COF)F(PEt₃)₂]

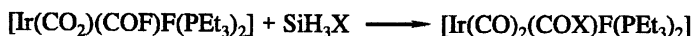
Chemical Shifts/ppm					
δP	δF_M	δF_b	δC_a	δC_b	δC_c
2.85	-393.8	132.4	151.0	153.4	162.6
Coupling Constants/Hz					
$^1J(F_bC_b)$	$^2J(PC_a)$	$^2J(PC_b)$	$^2J(PC_c)$	$^2J(F_M C_a)$	$^2J(F_M C_b)$
424	7	9	7	62	9
$^2J(F_M C_c)$	$^2J(PF_M)$	$^3J(F_b C_a)$	$^3J(F_b C_c)$	$^3J(F_M F_b)$	
15	32	7	48	14	

$[\text{Ir}(\text{CO})_2\text{Cl}(\text{PMe}_3)_2]$ and XeF_2 is more complicated; at 250K two fluoroacyl species are formed:



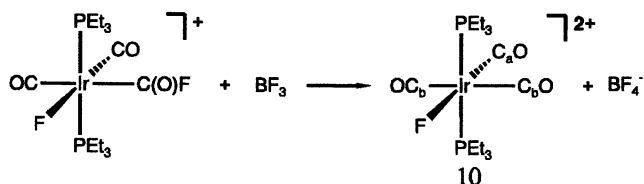
We believe that they differ in the stereochemical relationships of the ligands in the equatorial plane, but we have no conclusive evidence at this point.

These fluoroacyl complexes have some potential as synthetic intermediates. Silyl compounds can sometimes be used to replace fluoride by other functional groups; we find that **9** reacts with SiH_3X ($\text{X} = \text{CN}, \text{NCO}, \text{NCS}$) to give novel acyl complexes:



The products are unstable at room temperature, but they have been fully characterised by NMR spectroscopy, using ^{13}C N and ^{15}N CS. With $\text{X} = \text{CN}$, the ^{19}F spectrum shows that the acyl fluoride has been displaced and the IrF retained; the formation of large quantities of silyl fluoride suggests that $-\text{COF}$ has been converted into COCN . The ^{13}C O spectrum shows that the product still contains three different CO environments; with ^{13}C N, two of the ^{13}CO peaks showed new doublet splittings assigned to $^1\text{J}(\text{CNCO})$ and $^3\text{J}(\text{CNCO})$ respectively. On warming to room temperature the resonances due to this species disappeared. The initial decomposition product gave a triplet IrF resonance, which appeared as a triplet of doublets when ^{13}C N was used. We conclude that initial decomposition involves elimination of CO from the COCN ligand. When $\text{X} = \text{NCS}$, the analogous product was formed at 195K and characterised similarly; with ^{15}N CS, one ^{13}CO resonance showed an additional doublet splitting of 7Hz, confirming the presence of NCS bound to CO. The reaction with SiH_3NCO was more complicated, but the spectrum of the isocyanato-species could be identified at low temperature.

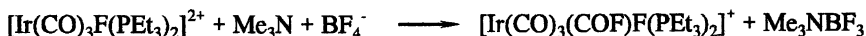
9 reacts smoothly and cleanly with BF_3 ; the Lewis acid abstracts the acyl fluoride, leaving a tris-carbonyl cation of $\text{Ir}(\text{III})$, **10**:



The product was characterised by single-crystal X-ray crystallography and by its NMR spectra. The two mutually *trans* CO-groups are equivalent; the $\text{Ir}-\text{C}$ bond lengths are the same within error, and the ^{13}C NMR spectrum shows two resonances in the ratio 2:1, the peak due to the acyl fluoride is absent in the ^{19}F NMR spectrum.

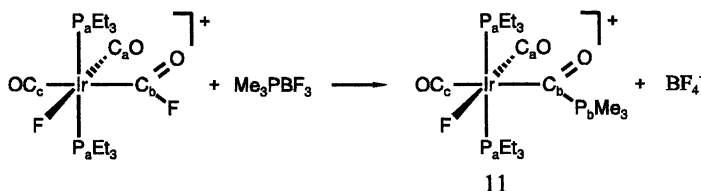
Though the abstraction of fluoride by BF_3 is commonplace, the formation of a dication of Ir(III) containing so many π -acceptor ligands is unusual.

The reactions of **10** bear on the mechanism of the original reaction between XeF_2 and $[\text{Ir}(\text{CO})_3(\text{PEt}_3)_2]^+$. When the tetrafluoroborate salt of **10** is allowed to react with Me_3N , **9** is regenerated, with Me_3NBF_3 . This is in effect the reverse of the process by which **10** is formed:



There is no evidence at all for fluorination of the carbonyl group *trans* to F. It is possible that F migrates from Ir to C, leaving a vacant coordination site which is then filled by F^- ; it is even possible that the reaction involves BF_4^- and **10** ion pairs, in which attack at BF_4^- by Me_3N leads to transfer of F^- to **10**.

The reaction between **10** and Me_3P is more remarkable. At 240K, **9** is regenerated, with the adduct Me_3PBF_3 , just as in the reaction between **10** and Me_3N . At 260K, however, the peaks of a new species dominate the spectra. From its ^{19}F , $^{13}\text{C}\{-^1\text{H}\}$ and $^{31}\text{P}\{-^1\text{H}\}$ NMR spectra we have identified it as **11**, a most unusual dication derived from **9** in which F_a has been replaced by Me_3P :



The ^{19}F spectrum shows a doublet of narrow triplets in the IrF region. The $^{31}\text{P}\{-^1\text{H}\}$ spectrum shows two doublets, one twice as strong as the other. The stronger, in the region of the spectrum associated with Et_3P bound to Ir(III), was assigned to P_a ; the weaker, considerably displaced from the region associated with Me_3P bound to Ir(III), is assigned to P_b . No P_aP_b coupling was detected, confirming that P_b was not bound to the metal; *cis*-PP couplings in complexes of Ir(III) are normally in the range 10-25Hz. In the $^{13}\text{C}\{-^1\text{H}\}$ spectrum, P_b showed coupling of 49Hz to C_b and 27Hz to C_c . These values are consistent with the proposed structure. Although $^1\text{J}(\text{PC})$ is a little low, it lies within the range expected for these couplings. (8) In particular, the relatively large value of $^3\text{J}(\text{PC})$ is in keeping with the large values of analogous couplings in the other acyl complexes described here, and in marked contrast to the absence of resolved $\text{J}(\text{PC})$ and $\text{J}(\text{PP})$. We obtained **11** as an oil that decomposed at room temperature.

The reactions between **10** and Lewis bases are consistent with the suggestion that XeF_2 reacts with $[\text{Ir}(\text{CO})_3(\text{PEt}_3)_2]^+$ as XeF^+ and F^- , initial attack being of XeF^+ on the metal; this would explain why the reaction is helped by basic phosphines. We have now shown that F^- will attack at one of the mutually *trans* CO-carbon atoms in **10**.

Reactions of XeF_2 with Complexes of 6-coordinated Ir(III)

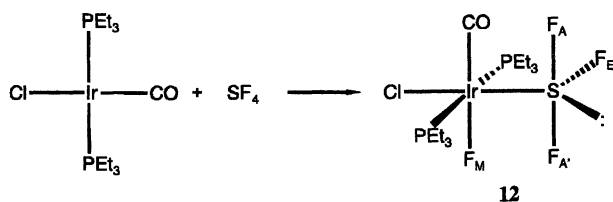
We have explored the reactions between XeF_2 and a number of complexes of the type $[\text{Ir}(\text{CO})\text{XYZ}(\text{PEt}_3)_2]$. In general the coordination-sites around the metal are

unaffected at temperatures up to 300K, when the systems usually start to decompose. Reactions that are well-defined involve fluorination of unsaturated ligands or ligands that can be oxidised or fluorinated. We have successfully prepared $[\text{Ir}(\text{CO})\text{Cl}_2(\text{PEt}_3)_2(\text{PF}_4)]$ (*9*) from **3**, and $[\text{Ir}(\text{CO})\text{Br}_2(\text{PEt}_3)_2(\text{PF}_2\text{H}_2)]$ (*10*) has been obtained from the corresponding PH_2 -complex and XeF_2 , though the latter product is unstable except at very low temperatures. However, our attempts to fluorinate coordinated I, CCH, CN, S and S_2 have not led to products that could be characterised, though in the last case there was evidence for the formation of a very unstable complex $[\text{Ir}(\text{DPPE})_2\text{F}(\text{SSF})]^+$ at low temperatures.

Reactions of YF_4 (Y = S, Se, Te) with $[\text{M}(\text{CO})\text{X}(\text{PEt}_3)_2]$ (M = Rh, Ir)

In preliminary experiments, we found that NF_3 , normally considered relatively unreactive, reacted at 250K with complexes of 4-coordinated Rh(I) or Ir(I) to form a large number of products containing F bound to a metal centre with two phosphine ligands. The mixtures had such complicated NMR spectra that we could not unravel them, but this ready reaction made us explore reactions of $[\text{M}(\text{CO})\text{X}(\text{PEt}_3)_2]$ with other non-metal fluorides.

Though SF_6 was found not to react up to 300K, SF_5Cl reacted readily at 200K to give a mixture of products including one with four complicated F resonances of equal intensity. The other products could be understood as derived from addition of ClF across the metal centre with some disproportionation; thus it appeared that the metal had extracted ClF from SF_5Cl , and our novel product might be derived from the reaction of the resulting SF_4 . Treatment of $[\text{Ir}(\text{CO})\text{Cl}(\text{PEt}_3)_2]$ with SF_4 confirmed this; there is ready reaction at very low temperature to give a single complex $[\text{Ir}(\text{CO})\text{ClF}(\text{PEt}_3)_2(\text{SF}_3)]$, **12** (*11*):



The product is identified by its ^{19}F and ^{31}P - $\{^1\text{H}\}$ NMR spectra. Because this is a derivative of $\text{S}(\text{IV})$, the lone pair at S and the coordinative asymmetry at Ir means that in principle we might expect to observe three distinct SF resonances. At 200K the ^{19}F spectrum contains four resonances of equal intensity (see Figure 1). The two at highest frequency, in the general region associated with axial fluorines in SF_3 derivatives, are assigned to F_A and F_A' . That at intermediate frequency is assigned to F_E , while the resonance at very low frequency is assigned to F_M . The three SF resonances are sharp and show well-resolved detail which can be analysed in terms of coupling to the other SF nuclei, to IrF and to two P nuclei. The IrF resonance is somewhat broadened at this temperature, and appears as a triplet of doublets; the ^{31}P - $\{^1\text{H}\}$ spectrum is second-order, because the relative chemical shift between the

two P nuclei is not large compared with ${}^2J(\text{PP})$, and all we have obtained from it is the value of ${}^2J(\text{PP})$.

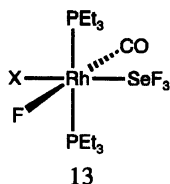
The way in which the ${}^{19}\text{F}$ NMR spectrum changes with temperature shows that at least two different exchange-processes are involved. As the solution is warmed above 240K, the two resonances assigned to F_A and $F_{A'}$ start to broaden, though they retain structure up to 270K. That due to F_E remains sharp, but the centre lines merge to give it a basic triplet pattern, while the resonance due to F_M sharpens into a triplet of narrow quartets and the ${}^{31}\text{P}\{-{}^1\text{H}\}$ spectrum becomes a doublet of quartets, losing its second order character. At 290K the peaks due to F_A and $F_{A'}$ have coalesced into a single broad line. At higher temperatures the peak due to F_E begins to broaden and lose structure, though at 306K the couplings ${}^3J(\text{FF})$ and ${}^3J(\text{PF})$ are still well-resolved. The peaks due to F_E and F_A coalesce at 304K and at that temperature all couplings involving fluorine bound to sulphur have been lost. There must be at least two and probably three processes involved in this fluxional system. We believe that the process responsible for merging F_A and $F_{A'}$ involves rotation or rocking of the SF_3 group about the Ir-S bond. The two axial fluorine sites are only distinct if they do not lie in the P-Ir-P plane. Since the Et_3P groups are bulky, it is likely that they will not lie in this plane; in the crystal structure of the analogous $[\text{Ir}(\text{CO})\text{Cl}_2(\text{PEt}_3)_2(\text{PF}_4)]$ the axial F-P-F plane lies between the P-Ir-P and the Cl-Ir-CO planes. However, rotation of F-S-F through the Cl-Ir-S plane would lead to effective equivalence. Under these conditions, coupling between F_E and the two axial fluorines becomes equal. It must be by chance that all three $\text{SF}\text{-IrF}$ couplings are equal. The process that leads to equivalence of axial and equatorial fluorines is likely to have an intermolecular component, since all couplings between the fluorine nuclei bound to sulphur and Ir^P or Ir^F are lost. However, the retention of SF couplings across Ir at 306K when the peak due to F_E has broadened suggests that there may well be an intramolecular component, perhaps a pseudorotation, as well. In marked contrast to the ready observation of F sites bound to 5-coordinated sulphur at temperature up to 270K, all fluorines in $[\text{Ir}(\text{CO})\text{Cl}_2(\text{PEt}_3)_2(\text{PF}_4)]$ are seen as equivalent in the ${}^{19}\text{F}$ and ${}^{31}\text{P}\{-{}^1\text{H}\}$ spectra down to 180K, and have only been partly resolved at 135K.

This fluxional behaviour is influenced by the other ligands in the complex, and by their geometric relationship. In the series $[\text{Ir}(\text{CO})\text{FX}(\text{PEt}_3)_2(\text{SF}_3)]$ coalescence temperatures rise in the order $\text{F} < \text{Cl} < \text{Br} < \text{I}$, we have been able to study the difluoride because it is formed in certain reaction systems. When X is NCO or NCS we have observed the formation of isomers and other products, and it is clear that when CO or NCY is *trans* to SF_3 the fluxional process is much faster. It is tempting to relate this to π -acceptor properties of ligands, but the effect may be principally steric, through influence on the conformation of the phosphine ligands. Changing these has a more dramatic effect on the spectra. In $[\text{Ir}(\text{CO})\text{FX}(\text{L})_2(\text{SF}_3)]$, where L is a tertiary phosphine, similar spectra are obtained when L is PEt_3 , PEt_2Ph , PMe_2Ph and PPh_3 ; where $\text{L} = \text{PEtPh}_2$, two isomers are formed, one with F *trans* to CO and the other with F *trans* to X, while the complex with $\text{L} = \text{PPh}_3$ reacts reluctantly with SF_4 , and when $\text{L} = \text{P}(\text{Cyclohexyl})_3$ no SF_3 complex is formed. When $\text{L} = \text{PMe}_3$ however, the ${}^{19}\text{F}$ and ${}^{31}\text{P}\{-{}^1\text{H}\}$ NMR spectra of the SF_3 complex are quite different. At 180K the ${}^{19}\text{F}$ spectrum shows that F_A and $F_{A'}$ are equivalent; there is only one resonance in the highest frequency region of the spectrum, a sharp doublet (${}^2J(\text{FF})$) of triplets

($^3J(\text{PF})$) of doublets ($^3J(\text{FF})$). This resonance is twice as intense as those due to F_E and F_M , both of which are well-resolved. The chemical shift of F_M , δ -382.3 is in the region associated with F *trans* to X rather than to CO (see Table III), so it may be that the geometry of this product is slightly different from that of its PEt_3 analogue. However, we have not observed such clear equivalence of F_A and $F_{A'}$ in any of the isomeric species with other phosphine ligands whose spectra we have studied. As the temperature is raised, the resonances due to F_A and F_E broaden and collapse, and coalesce at 300K; at this temperature couplings between SF and the IrF and P nuclei are retained, showing that here at least, coalescence of F_A and F_E is due to an intramolecular process.

We have studied the reactions of SF_4 with analogous complexes of rhodium. In general the results are similar, though the rhodium complexes are less stable and the initial reactions less simple, leading to the formation of more isomeric products. Fluxional processes are also similar, and are affected by ligand and by stereochemistry in the same sort of way.

Reactions of SeF_4 . Reaction of SeF_4 with $[\text{Rh}(\text{CO})\text{X}(\text{PEt}_3)_2]$ ($X = \text{Cl}, \text{Br}, \text{I}, \text{NCS}, \text{NCO}$) in CD_2Cl_2 occurred at 195K to produce mixtures of complexes, the most abundant of which were **13**, analogous to **12**:



These were identified by their ^{19}F and $^{31}\text{P}\{-^1\text{H}\}$ NMR spectra. Both sets of spectra were very similar to those observed for **12** except that the three highest-frequency resonances, assigned to F_A , $F_{A'}$ and F_E came at much lower values than for **12**. The resonance due to F_E also showed ^{77}Se satellites at approximately 4% of the intensity of the main resonance ($^1J(\text{SeF}) = 580 - 600\text{Hz}$). We also observed resonances at δ 56.1 and δ 13.0, which from their multiplet structures and by analogy with TeF_5^- (**13**) we assign to SeF_5^- .

Fluxional behaviour of the SeF resonances is similar to that observed in the SF_3 complexes, but because of problems with the low volatility of SeF_4 and of working with fluoroplastic tubes we were not able to obtain solutions free of HF, so our studies of these systems is not complete. However, there was an important difference between the S and Se complexes. In the Se species, the resonance due to RhF on warming to ambient temperature, broadened with the resonances assigned to SeF_5^- . This implies that an intermolecular exchange occurs at these relatively high temperatures between RhF and SeF_5^- . The original spectrum was obtained when the solution was recooled to 195K, showing that the exchange was reversible.

The minor resonances observed have all been identified as isomers or products of halide-exchange. These complexes were much less thermally stable than their S-analogues; indeed the species where $X = \text{I}$ or NCS decomposed in solution at 210K.

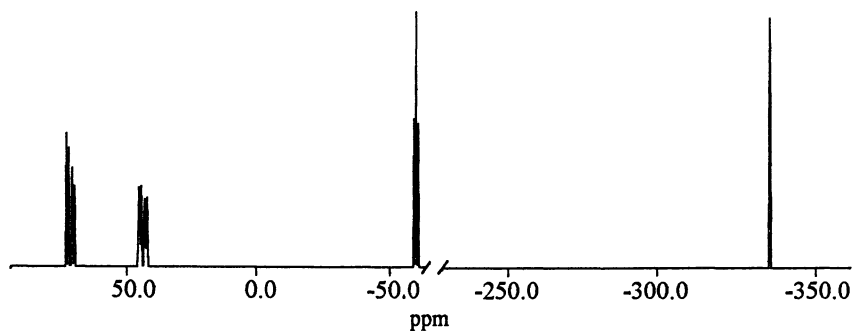
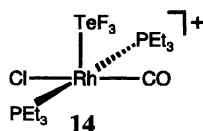


Figure 1
 $^{19}\text{F}\{-^1\text{H}\}$ NMR Spectrum of 11.

Table III. NMR Data for $[\text{Ir}(\text{CO})\text{FX}(\text{PEt}_3)_2(\text{SF}_3)]$ at 180K

X	Chemical Shifts/ppm						
	F _A	F _{A'}	F _E	F _M	P _A	P _B	
Cl	75.5	45.2	-66.8	-334.9	7.6	0.3	
Br	74.4	44.8	-66.1	-344.1	3.6	-3.6	
I	72.8	41.7	-67.6	-356.2	-1.6	-8.7	
X	Coupling constants/Hz						
	$^2\text{J}(\text{PP})$	$^2\text{J}(\text{F}_\text{A}\text{F}_\text{A}')$	$^2\text{J}(\text{F}_\text{A}\text{F}_\text{E})$	$^2\text{J}(\text{F}_\text{A}'\text{F}_\text{E})$	$^2\text{J}(\text{F}_\text{A}\text{F}_\text{M})$	$^2\text{J}(\text{F}_\text{A}'\text{F}_\text{M})$	$^2\text{J}(\text{F}_\text{E}\text{F}_\text{M})$
Cl	340.0	179.7	58.8	80.6	3.6	9.6	n.o.
Br	336.0	182.8	58.0	78.9	3.5	10.0	n.o.
I	331.0	183.2	60.0	80.3	3.5	10.0	n.o.

Reactions of TeF₄. Reaction of [Rh(CO)Cl(PEt₃)₂] with TeF₄ in 1:2 molar ratio occurred rapidly at 195K producing a single complex which we identify as [Rh(CO)Cl(PEt₃)₂(TeF₃)]⁺[TeF₅]⁻ **14**. (14)



The ³¹P-¹H} NMR spectrum showed only one resonance, a doublet of triplets of narrow doublets (δ 27.1, ¹J(RhP) = 92Hz, ³J(PF) = 16Hz & ³J(PF) = 3Hz). The value of ¹J(RhP) is very dependant upon the geometry and oxidation state of the rhodium and a value of 92Hz is in keeping with square pyramidal Rh(III). The ¹⁹F NMR spectrum consisted of four resonances in the ratio 2(F_a):1(F_b):4(F_c):1(F_d). The second and third of these are due (13) to [TeF₅]⁻; F_a is assigned to two equivalent axial fluorines and F_d to the equatorial fluorine of a coordinated TeF₃ group that is rotating or rocking rapidly on the NMR timescale, as in the trimethylphosphine-SF₃ complexes of Ir. The ¹³C-¹H} NMR spectrum of **14** enriched with ¹³CO showed one resonance in the CO-region, a doublet (¹J(RhC) = 71Hz) of triplets (²J(PC) = 9Hz) of doublets (³J(F_dC) = 8Hz). The structure assigned is consistent with the NMR spectra and with our observations of the behaviour of the SF₃ and SeF₃ complexes described here. In the sulphur complexes there is no evidence of exchange of fluorine bound to the metal; in the selenium derivatives there is evidence for exchange of F between the metal and SeF₅⁻, but the main product contains 6-coordinate Rh with a well-defined Rh-F bond. It seems that TeF₄ is a Lewis acid of sufficient strength to remove F⁻ from the metal.

Where X = Br and NCS, similar spectra were obtained, indicating that similar complexes were formed. The chemical shifts were slightly different, confirming that X remained bound to rhodium. On warming, the only changes observed in the ¹⁹F NMR spectra were coalescence of the two TeF₅⁻ resonances. Coalescence occurred at different temperatures for each complex, (X = Cl, 275K; Br, 240K; NCS, 265K). This indicates that there is a significant ion-pairing in these systems.

Preliminary experiments with [Ir(CO)X(PEt₃)₂] suggest that analogous TeF₃-complexes are formed at low temperatures, but that they are short-lived and decompose even at low temperatures.

Acknowledgments

We acknowledge with thanks financial support from S. E. R. C. to R. W. C., N. R. and P. G. W., and from the University of Edinburgh to HM. We are most grateful for helpful discussions with Professor D. W. H. Rankin from the University of Edinburgh.

Literature Cited

- 1 Ebsworth, E. A. V.; McManus, N. T.; Rankin, D. W. H.; Whitelock, J. D. *Angew. Chem., Int. Ed. (Engl.)*, **1981**, *20*, 801.
- 2 Cockman, R. W.; Ebsworth, E. A. V.; Holloway, J. H.; Watson, P. G.; Wynd, A. J. In Preparation.

- 3 Cockman, R. W.; Ebsworth, E. A. V. Unpublished work.
- 4 Blake, A. J.; Cockman, R. W.; Ebsworth, E. A. V.; Holloway, J. H. *J. Chem. Soc., Chem. Commun.*, **1986**, 1622.
- 5 Ebsworth, E. A. V.; Robertson, N.; Yellowlees, L. J. In Press.
- 6 Rahman, M. A.; Liu, H. Y.; Prock, A.; Giering, W. P. *Organometallics*, **1987**, *6*, 650.
- 7 Tolman, C. A. *Chem. Rev.*, **1977**, *77*, 3.
- 8 *Phosphorus-31 NMR Spectroscopy in Stereochemical Analysis*; Verkade, J. K.; Quin, L. D., Eds.; Methods in Stereochemical Analysis 8; VCH: Deerfield Beach, Fl., **1986**.
- 9 Ebsworth, E. A. V.; Holloway, J. H.; Pilkington, N. J.; Rankin, D. W. H. *Angew. Chem., Int. Ed. (Engl.)*, **1984**, *23*, 630.
- 10 Blake, A. J.; Cockman, R. W.; Ebsworth, E. A. V.; Henderson, S. G. D.; Holloway, J. H.; Pilkington, N. J.; Rankin, D. W. H. *Phosphorus and Sulfur*, **1987**, *30*, 143.
- 11 Cockman, R. W.; Ebsworth, E. A. V.; Holloway, J. H. *J. Amer. Chem. Soc.*, **1987**, *109*, 2194.
- 12 Darragh, J. I.; Hossain, S. F.; Sharp, D. W. A. *J. Chem. Soc., Dalton Trans.*, **1975**, 218.
- 13 Morris, R. J.; Moss, K. C.; *J. Fluorine Chem.*, **1979**, *13*, 991.
- 14 Ebsworth, E. A. V.; Holloway, J. H.; Watson, P. G. *J. Chem. Soc., Chem. Commun.*, **1991**, 1443.

RECEIVED February 17, 1994

Chapter 21

Large Polyfluorinated Anions Used To Generate Coordinative Unsaturation in Cations

Paul K. Hurlburt, Dawn M. Van Seggen, Jeffrey J. Rack,
and Steven H. Strauss

Department of Chemistry, Colorado State University,
Fort Collins, CO 80523

The search for anions that are larger and more weakly coordinating than BF_4^- , PF_6^- , etc. has led to the study of species such as $\text{B}(\text{OTeF}_5)_4^-$, $\text{Zn}(\text{OTeF}_5)_4^{2-}$, $\text{Pd}(\text{OTeF}_5)_4^{2-}$, $\text{Ti}(\text{OTeF}_5)_6^{2-}$, $\text{Nb}(\text{OTeF}_5)_6^-$, and $\text{Sb}(\text{OTeF}_5)_6^-$. The pentafluorooxotellurate (OTeF_5) groups do not transfer a fluoride ion to cationic electrophiles. However, the $\text{B}(\text{OTeF}_5)_4^-$ ion has been found to transfer an intact OTeF_5^- anion to H^+ , Ag^+ , SiR_3^+ , and $\text{Fe}(\text{porphyrin})^+$. On the other hand, the $\text{Nb}(\text{OTeF}_5)_6^-$ and $\text{Sb}(\text{OTeF}_5)_6^-$ anions are much more stable in the presence of cationic electrophiles, probably because their oxygen atoms are not as accessible to the electrophiles as those in the $\text{B}(\text{OTeF}_5)_4^-$ anion. These OTeF_5 based anions have allowed unusual complexes to be isolated and structurally characterized, including $[\text{Ag}(\text{CO})]^+$, $[\text{Ag}(\text{CO})_2]^+$, $[\text{Ag}(\text{CH}_2\text{Cl}_2)_2]^+$, and $[\text{Ag}(\text{CH}_2\text{Cl}_2)_3]^+$.

It is now widely recognized that under certain circumstances the classical "noncoordinating" anions ClO_4^- , SO_3CF_3^- , SO_3F^- , BF_4^- , PF_6^- , AsF_6^- , and SbF_6^- can coordinate to metal ions from all regions of the periodic table. This chemistry has been the subject of a number of reviews (1-4). Here we will focus on polyfluorinated anions that are larger and even more weakly coordinating than those mentioned above. These anions are derivatives of the OTeF_5 group, and include $\text{B}(\text{OTeF}_5)_4^-$, $\text{Zn}(\text{OTeF}_5)_4^{2-}$, $\text{Pd}(\text{OTeF}_5)_4^{2-}$, $\text{Ti}(\text{OTeF}_5)_6^{2-}$, $\text{Nb}(\text{OTeF}_5)_6^-$, and $\text{Sb}(\text{OTeF}_5)_6^-$.

Cationic Complexes and Coordinative Unsaturation

In a seminal piece of work, Rosenthal reviewed structural and spectroscopic data that proved unequivocally that anions which are noncoordinating in aqueous solution, such as ClO_4^- , NO_3^- , and BF_4^- , "are found to be coordinating where water has been excluded" (5). He concluded the paper by stating, "It is clear that the notion of the non-coordinating anion should be put to rest alongside the notion of the non-coordinating solvent." It would therefore be more meaningful as well as more precise

0097-6156/94/0555-0338\$08.00/0
© 1994 American Chemical Society

to use the relative terms "weakly coordinating solvent" and "weakly coordinating anion."

Many coordination chemists are concerned with enhancing the chemical reactivity of metal complexes, whether for catalysis, for the synthesis of new complexes, or for examining the binding of extremely weak donors. One measure of reactivity is Lewis acidity. In what ways can it be enhanced using larger and more weakly coordinating anions? Let us consider an isolated, coordinatively unsaturated cationic complex, $[L_{n-1}M]^+$. In solution, the vacant coordination site would behave like the coulombic version of a vacuum, i.e., its potential to attract a pair of electrons is extremely large. What can fill the void? The four most important possibilities are (i) the solvent can coordinate to the metal ion and can fill the vacant site, (ii) the counterion (X^-) can fill the site, (iii) one of the ancillary ligands can become bidentate, and (iv) bridges can be formed by two ancillary ligands. Therefore, a truly vacant coordination site may be impossible to achieve at a cationic center in solution, even if the solvent and the counterion are very weakly coordinating.

This line of reasoning leads to the conclusion that what is normally referred to as a vacant coordination site in a cationic complex is, in most cases, an extremely weak, extremely labile metal-ligand bond. (We are not considering coordinatively unsaturated transition states or extremely short-lived intermediates in this discussion. Our focus is on whether *persistent* vacant coordination sites ever exist in cationic complexes in solution.) Perhaps the term "vacant coordination site" should be replaced with "virtual coordination site" or "latent coordination site." It follows that the weakest cation-ligand interaction possible in a given solvent is a cation-solvent bond. Therefore, weakening the M-X bond becomes the primary goal of those seeking the closest thing to coordinative unsaturation for a cationic center in a given solvent. Whether one can achieve situation (i) in weakly coordinating, low dielectric solvents will depend in large part on the availability of new anions that are larger and more weakly coordinating than those in common use. It will also depend on the hardness of the cationic center: what may be the least coordinating anion for a hard metal center may not be the least coordinating anion for a soft metal center.

Ideal Properties for Weakly Coordinating Anions

An optimal set of properties for weakly coordinating anions includes low overall charge and a high degree of charge dispersion. Ideally, all new weakly coordinating anions should have a 1- charge, but in some cases a species with a 2- charge may have certain advantages and can be tolerated (one advantage, for example, is a lower equivalent mass). The charge should be dispersed over the entire anion, so that no individual atom or group of atoms bears a local concentration of charge. Obviously, this suggests that the larger the anion (the more atoms it contains), the more diffuse the charge and the more weakly coordinating it will be. Alternatively, a large anion with localized charge on atoms that are sterically inaccessible could also prove useful. An equally important property is the presence of only very weakly basic sites on the periphery of the anion. Thus, anions with only hydrogen atoms or fluorine atoms available for binding to the cation should be more weakly coordinating than anions

with accessible oxygen atoms or chlorine atoms: several studies have shown that BF_4^- and PF_6^- are more weakly coordinating than, for example, ClO_4^- or SO_3CF_3^- (6-8).

Perhaps the most important property is the kinetic stability, if not the thermodynamic stability, of the anion. There are two potential problems to be avoided. First, some very large weakly coordinating anions could dissociate into smaller, more strongly coordinating fragments. Rapid fluoride ion abstraction by electrophiles is known to be a problem even with small anions such as BF_4^- , PF_6^- , and SbF_6^- (8). Second, the stability of a weakly coordinating anion with respect to oxidation will determine whether it can be used as a counterion for the most electrophilic cations, many of which will also be strong oxidants. The well-known tendency of BPh_4^- to undergo chemical and electrochemical oxidation is a case in point (9). Recent examples of larger, more stable, and more weakly coordinating anions include fluorinated derivatives of BPh_4^- such as $\text{B}(\text{C}_6\text{F}_5)_4^-$ and $\text{B}(3,5\text{-C}_6\text{H}_3(\text{CF}_3)_2)_4^-$ (10), $\text{CB}_{11}\text{H}_{12}^-$ and related carborane anions (11,12), and heteropolyanions (Keggin ions) such as $\text{PW}_{12}\text{O}_{40}^{3-}$ (13). Our own work, which is described below, has involved polyfluorinated anions based on the OTeF_5 group.

Anions Based on the OTeF_5 Group

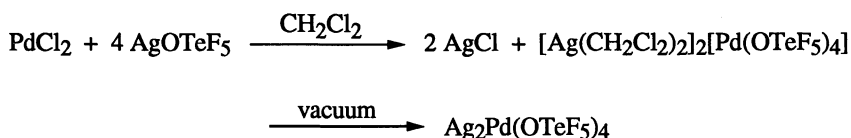
Pentafluorooxotellurate, or teflate, has been used for some time as a hard and very electronegative substituent for main group elements (14). Most notable is the recent low-temperature generation of $\text{Kr}(\text{OTeF}_5)_2$, one of only a handful of krypton compounds and the first one with Kr-O bonds (15). The structure of the free teflate anion is a slightly distorted octahedron, with Te-O and average Te-F bond distances of 1.786 (3) and 1.853 (3) Å, respectively, and an average O-Te-Feq bond angle of $95.2(2)^\circ$ (16). Therefore, teflate is nearly isostructural and isodimensional with SbF_6^- ($\text{Sb-F (av)} = 1.844(8)$ Å in KSbF_6 (17)). Nearly all teflate compounds are prepared using the strong acid HOTeF_5 (14).

As discussed above, a major disadvantage of fluoroanions such as BF_4^- , PF_6^- , etc. is the potential for fluoride ion abstraction by electrophiles. This is *not* a problem for the teflate anion, however. There is no evidence for fluoride ion or fluorine atom loss from free or bound OTeF_5^- at temperatures below 200°C .

In an effort to obtain larger and more weakly coordinating anions, several $\text{M}(\text{OTeF}_5)_n^{m-}$ complexes ($n = 4, 6$; $m = 1, 2$) have been studied (18-22). It was anticipated that having the negative charge dispersed over a large number of fluorine atoms would diminish the interaction of any given fluorine atom and a cationic metal center. In an effort to further minimize cation-anion interactions, the soft monovalent cations Ag(I) and Tl(I) were chosen for initial studies. An additional reason for choosing these particular cations is that the set of $\text{Ag}_m\text{M}(\text{OTeF}_5)_n$ and $\text{Tl}_m\text{M}(\text{OTeF}_5)_n$ salts would then be available as metathesis reagents for the introduction of the $\text{M}(\text{OTeF}_5)_n^{m-}$ anions.

$\text{M}(\text{OTeF}_5)_4^{2-}$. A subset of these anions ($\text{M} = \text{Zn}$ (20) and Pd (19)) will be considered first. Their Ag(I) salts have proven to be the most interesting. Crystalline $\text{Ag}_2\text{Zn}(\text{OTeF}_5)_4$ binds 2 equivalents of carbon monoxide at 22°C and pressures < 1 atm (AgOTeF_5 takes up only one equivalent and AgSbF_6 does not form a complex

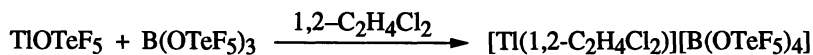
with CO under these conditions) (20). Another interesting example is $\text{Ag}_2\text{Pd}(\text{OTeF}_5)_4$, which is formed from PdCl_2 and AgOTeF_5 as follows (19):



The double salt $\text{Ag}_2\text{Pd}(\text{OTeF}_5)_4$ absorbs up to 2 equiv of dichloromethane vapor in the solid state. Both a 1:1 ($\text{Ag}:\text{CH}_2\text{Cl}_2$) and a 1:2 complex can be formed. The 1:2 complex has an equilibrium vapor pressure of dichloromethane above the crystals of ~350 torr, which is nearly the vapor pressure of neat dichloromethane at 22°C. The structure of the 1:2 complex is shown in Figure 1. Each Ag(I) ion in this centrosymmetric complex is coordinated to two bidentate dichloromethane ligands. The Ag–Cl bond distances range from 2.775 (2) to 2.882 (2) Å. These distances are much shorter than the sum of van der Waals radii for Ag and Cl atoms, 3.45 ± 0.05 Å (23). Considering that the chlorine atom ligands do not bear a full negative charge, the Ag–Cl bonds are quite short: they can be compared with Ag–Cl distances involving a terminal chloride ion, 2.512 (1) Å in $\text{Ag}(\text{diphos})\text{Cl}$ (24), chloride ions that bridge Ag(I) and Pt(II) ions, 2.408 (8) and 2.724 (8) Å in $\text{Ag}_2\text{Pt}_2\text{Cl}_4(\text{C}_6\text{F}_5)_4$ (25), and an octahedral array of chloride ions, 2.77512 (5) Å in AgCl (26).

Note that each Ag(I) ion in $[\text{Ag}(\text{CH}_2\text{Cl}_2)_2]_2[\text{Pd}(\text{OTeF}_5)_4]$ is bonded to two of the oxygen atoms of the $\text{Pd}(\text{OTeF}_5)_4^{2-}$ counterion. Evidently, steric hindrance does not prevent Ag–O bond formation. In order to gauge the strength of the cation-anion interaction in $[\text{Ag}(\text{CH}_2\text{Cl}_2)_2]_2[\text{Pd}(\text{OTeF}_5)_4]$, equivalent conductances were measured for $\text{Ag}_2\text{Pd}(\text{OTeF}_5)_4$, AgOTeF_5 , and related compounds in dichloromethane and 1,2-dichloroethane (19). The results suggest that a much higher proportion of Ag(I) ions are dissociated from $\text{Pd}(\text{OTeF}_5)_4^{2-}$ than from OTeF_5^- , so it is the former anion that is the more weakly coordinating. The results also require that specific solvation of Ag(I) ions (i.e., coordination to Ag(I) ions) must be stronger with 1,2-dichloroethane than with dichloromethane, a conclusion that was corroborated by ^{13}C NMR experiments (19).

$\text{B}(\text{OTeF}_5)_4^-$. A logical extension of the chemistry described above was the exploration of the $\text{B}(\text{OTeF}_5)_4^-$ anion as a very bulky and less coordinating alternative to BF_4^- . It was thought that the relatively short B–O bonds might prevent strong B–O–M bridges from forming. Several compounds have been structurally characterized, including $[\text{Tl}(\text{mes})_2][\text{B}(\text{OTeF}_5)_4]$ (18), $[\text{Tl}(1,2\text{-C}_2\text{H}_4\text{Cl}_2)][\text{B}(\text{OTeF}_5)_4]$ (22d), $\text{AgB}(\text{OTeF}_5)_4$ (22c), and $[\text{Ag}(\text{CO})][\text{B}(\text{OTeF}_5)_4]$ (20). In the two Tl(I) compounds, the only cation-anion interactions are relatively long Tl–F secondary bonds. In the compound $[\text{Tl}(\text{mes})_2][\text{B}(\text{OTeF}_5)_4]$, which contains two η^6 -mesitylene ligands for each Tl(I) ion, the four closest Tl–F contacts are made with two borate counterions and are 3.17 (1), 3.25 (1), 3.47 (1), and 3.83 (1) Å (18). The last two distances are longer than the sum of van der Waals radii for thallium and fluorine, 3.42 ± 0.08 Å (23). The compound $[\text{Tl}(1,2\text{-C}_2\text{H}_4\text{Cl}_2)][\text{B}(\text{OTeF}_5)_4]$ was prepared as follows (22d):



The presence of a simple chelating bidentate 1,2-dichloroethane ligand instead of two η^6 -mesitylene ligands leads to a greater number of Tl–F contacts. In this case, four anions donate nine fluorine atoms, and the distances range from 2.950 (5) to 3.981 (8) Å. For comparison, the Tl–F distances in TlF, which possesses a very distorted Rock Salt structure, range from 2.25 (2) to 3.90 (2) Å (27). Another relevant comparison can be made with Tl(PF₆)(C₉H₂₁N₃), in which the Tl(I) ion has an N₃F₃ donor set (28). In this compound, the Tl–F distances are 3.23 (1), 3.27 (1), and 3.54 (1) Å.

In both AgB(OTeF₅)₄ and in [Ag(CO)][B(OTeF₅)₄], however, there are Ag–O–B bridges, indicating that the borate anion can coordinate more strongly under some circumstances. In the structure of [Ag(CO)][B(OTeF₅)₄] (the first isolable silver carbonyl), which is shown in Figure 2, there are two Ag–O bonds (Ag–O1 = 2.324 (6) Å, Ag–O2 = 2.436 (7) Å) and four Ag–F contacts (not shown) which range in distance from 2.959 (6) to 3.076 (8) Å (20). The Ag(I) ion in AgB(OTeF₅)₄ is bonded to O1 (2.500 (5) Å) and O2 (2.601 (5) Å) from one borate anion and more weakly bonded to O3' (2.756 (5) Å) from another (22*b*). Six Ag–F contacts, 2.644 (5)–3.017 (5) Å, round out the coordination sphere of the cation. Differences in ionic radii may explain why Tl(I) does not coordinate to B(OTeF₅)₄[–] oxygen atoms. The six-coordinate radii of Ag(I) and Tl(I) are 1.15 and 1.50 Å, respectively (29). Clearly, the oxygen atoms are sterically less accessible than the fluorine atoms, and the larger Tl(I) ion may not be able to form Tl–O–B bridge bonds without requiring a severe distortion of the borate anion.

Similar bridge bonds to the oxygen atoms of the borate anion may explain how cationic electrophiles abstract a teflate anion from B(OTeF₅)₄[–]. For example, attempts to prepare [Fe(TPP)][B(OTeF₅)₄], [Fe(OEP)][B(OTeF₅)₄], or [SiPh₃][B(OTeF₅)₄] by metathesis reactions between Fe(TPP)Cl, Fe(OEP)Cl, or SiClPh₃ and AgB(OTeF₅)₄ or TlB(OTeF₅)₄, or between SiHPh₃ and [CPh₃][B(OTeF₅)₄], led only to the isolation of Fe(TPP)(OTeF₅), Fe(OEP)(OTeF₅), or SiPh₃(OTeF₅) (TPP = tetraphenylporphyrinate dianion; OEP = octaethylporphyrinate dianion) (22*c*). The putative cations [Fe(TPP)]⁺, [Fe(OEP)]⁺, and [SiPh₃]⁺ were not observed. Presumably, intermediates such as [(TPP)Fe–O(TeF₅)–B(OTeF₅)₃] are involved in these reactions. Control experiments proved that OTeF₅[–] did not readily dissociate from B(OTeF₅)₄[–]: there was no isotope exchange, even after weeks, when [TBA][¹⁷OTeF₅] was mixed with [TBA][B(¹⁶OTeF₅)₄] in dichloromethane at 22°C (TBA = tetrabutylammonium cation). The presence of an electrophile was definitely required to effect the exchange. For example, ¹⁷O NMR experiments showed that complete isotope exchange occurred within 1 h when H¹⁷OTeF₅ or Ag¹⁷OTeF₅ were mixed with [TBA][B(¹⁶OTeF₅)₄] (22*b*). Therefore, despite the large size and diffuse charge of the B(OTeF₅)₄[–] anion, its usefulness as a weakly coordinating anion is limited: it too easily fragments into OTeF₅[–] and B(OTeF₅)₃ in the presence of strong electrophiles.

We have also succeeded in isolating hygroscopic, thermally labile crystals of [Ag(CO)₂][B(OTeF₅)₄], and have determined that it contains two-coordinate, roughly linear [Ag(CO)₂]⁺ complex ions (30). This was the first structural evidence for a simple two-coordinate M(CO)₂ complex of any metal, although manometric and

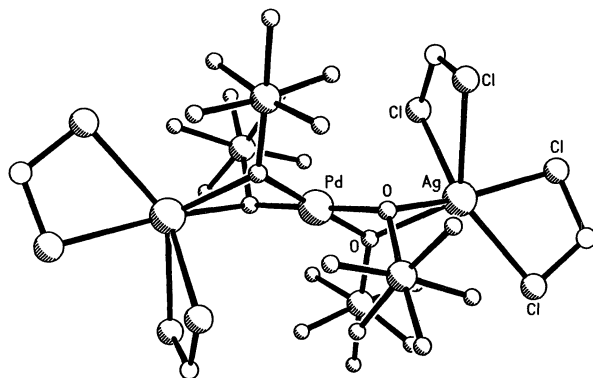


Figure 1. Structure of the centrosymmetric $[\text{Ag}(\text{CH}_2\text{Cl}_2)_2]_2[\text{Pd}(\text{OTeF}_5)_4]$ formula unit. The unlabeled open spheres are carbon atoms, the unlabeled large highlighted spheres are tellurium atoms, and the unlabeled small highlighted spheres are fluorine atoms. Hydrogen atoms have been omitted for clarity. Selected distances (\AA): Ag–Cl, 2.775 (2)–2.882 (2); Ag–O, 2.404 (5), 2.532 (4). (Reproduced with permission from ref 21. Copyright 1993 ACS.)

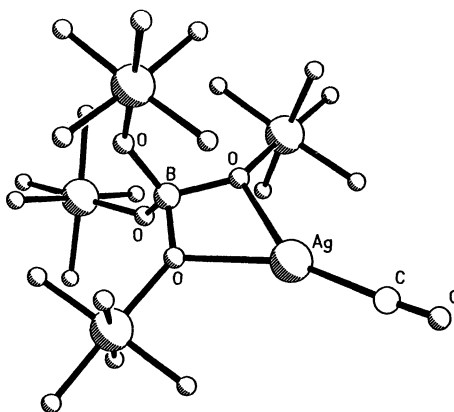


Figure 2. Structure of the $[\text{Ag}(\text{CO})][\text{B}(\text{OTeF}_5)_4]$ formula unit. The unlabeled large highlighted spheres are tellurium atoms and the unlabeled small highlighted spheres are fluorine atoms. Selected distances (\AA) and angles (deg): Ag–C, 2.10 (1); C–O, 1.077 (16); Ag–O, 2.324 (6), 2.436 (7); Ag–C–O, 176 (1). (Reproduced with permission from ref 21. Copyright 1993 ACS.)

spectroscopic data have suggested the existence of solvated $[\text{Ag}(\text{CO})_2]^+$ (31) and $[\text{Au}(\text{CO})_2]^+$ (32) ions in highly acidic media, $[\text{Au}(\text{CO})_2]^+$ ions in the solid state (33), and neutral $\text{M}(\text{CO})_2$ species in carbon monoxide matrices (34). The triclinic ($P\bar{1}$) unit cell of $[\text{Ag}(\text{CO})_2][\text{B}(\text{OTeF}_5)_4]$ contains two symmetry related pairs of $\text{B}(\text{OTeF}_5)_4^-$ anions at general positions, one symmetry related pair of $[\text{Ag}(\text{CO})_2]^+$ cations at general positions, and two $[\text{Ag}(\text{CO})_2]^+$ cations at inversion centers. Figure 3 shows a view of one of the $[\text{Ag}(\text{CO})_2]^+$ ions and its four closest counterions.

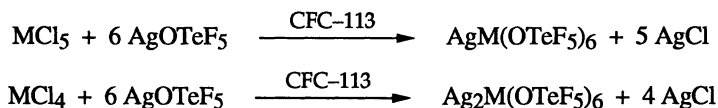
Despite our success in crystallizing $[\text{Ag}(\text{CO})_2][\text{B}(\text{OTeF}_5)_4]$, it is not suitable for detailed spectroscopic study because it decomposes at room temperature, as does $[\text{Ag}(\text{CO})][\text{B}(\text{OTeF}_5)_4]$, by the following reaction:



However, we have found that the salts $\text{Ag}_2\text{Zn}(\text{OTeF}_5)_4$ and $\text{Ag}_2\text{Ti}(\text{OTeF}_5)_6$ (see below) form more stable 1:1 and 1:2 (Ag:CO) adducts when subjected to pressures of CO that are < 1 atm. The values of $\nu(\text{CO})$ for $[\text{Ag}(\text{CO})]_2[\text{Zn}(\text{OTeF}_5)_4]$ and $[\text{Ag}(\text{CO})]_2[\text{Ti}(\text{OTeF}_5)_6]$ are 2203 and 2207 cm^{-1} , respectively, while $\nu_{\text{asym}}(\text{CO})$ for $[\text{Ag}(\text{CO})_2]_2[\text{Zn}(\text{OTeF}_5)_4]$ and $[\text{Ag}(\text{CO})_2]_2[\text{Ti}(\text{OTeF}_5)_6]$ are both 2198 cm^{-1} . All of these values are much higher than in free CO (2143 cm^{-1}), an indication of an increase in C–O bond order upon coordination to Ag(I). We propose that discrete, two-coordinate, linear $[\text{Ag}(\text{CO})_2]^+$ cations are also present in $[\text{Ag}(\text{CO})_2]_2[\text{Zn}(\text{OTeF}_5)_4]$ and $[\text{Ag}(\text{CO})_2]_2[\text{Ti}(\text{OTeF}_5)_6]$. Raman spectroscopy may confirm this prediction, but so far fluorescence has prevented adequate spectra from being recorded.

Since π -backbonding normally decreases $\nu(\text{CO})$, it is sensible to conclude that there is little or no π -backbonding in $[\text{Ag}(\text{CO})_2]^+$. This conclusion is not in conflict with the fact that $\nu_{\text{asym}}(\text{CO})$ for $[\text{Au}(\text{CO})_2]^+$, 2236 cm^{-1} (33a), is higher by 38 cm^{-1} than our value of 2198 cm^{-1} for $[\text{Ag}(\text{CO})_2]^+$. Some might argue, based on the $\nu(\text{CO})$ values, that π -backbonding must be less in $[\text{Au}(\text{CO})_2]^+$ than in $[\text{Ag}(\text{CO})_2]^+$ and therefore π -backbonding is not negligible in $[\text{Ag}(\text{CO})_2]^+$. We believe, however, that the higher value for the gold compound is the result of stronger Au–C σ -bonding, not less π -backbonding. This must be the case since the CO ligands in $[\text{Au}(\text{CO})_2][\text{Sb}_2\text{F}_{11}]$ are not labile (33a), and hence are more strongly bound than the CO ligands in $[\text{Ag}(\text{CO})_2][\text{B}(\text{OTeF}_5)_4]$.

$\text{M}(\text{OTeF}_5)_6^{m-}$. We have investigated a class of even larger, polyfluorinated complex anions and have found that they are (i) much less coordinating, (ii) much more stable in the presence of electrophiles, and (iii) much more solubilizing in weakly coordinating solvents than either $\text{B}(\text{OTeF}_5)_4^-$ or $\text{Pd}(\text{OTeF}_5)_4^{2-}$ (22a,b). The anions include $\text{Nb}(\text{OTeF}_5)_6^-$ and $\text{Ti}(\text{OTeF}_5)_6^{2-}$, which had been prepared previously as their TBA^+ (35) or Cs^+ (36) salts, respectively. We have prepared these and other Ag^+ salts by mixing either MCl_5 ($\text{M} = \text{Nb}, \text{Ta}, \text{Sb}$) or MCl_4 ($\text{M} = \text{Ti}, \text{Zr}, \text{Hf}$) with six equivalents of AgOTeF_5 in 1,1,2-trichlorotrifluoroethane (CFC-113):



The compound $[\text{Ag}(\text{CH}_2\text{Cl}_2)_3]_2[\text{Ti}(\text{OTeF}_5)_6]$ was obtained by recrystallization of $\text{Ag}_2\text{Ti}(\text{OTeF}_5)_6$ from dichloromethane. Its structure, shown in Figure 4, consists of centrosymmetric $\text{Ti}(\text{OTeF}_5)_6^{2-}$ anions that bridge two symmetry related $[\text{Ag}(\text{CH}_2\text{Cl}_2)_3]^+$ cations. To within experimental error, the anion has an octahedral TiO_6 core, and the geometry of the OTeF_5 groups is normal. Three bidentate dichloromethane ligands coordinate to silver in the $[\text{Ag}(\text{CH}_2\text{Cl}_2)_3]^+$ cation. The $\text{Ag}-\text{Cl}$ bond distances range from 2.656 (3) to 3.049 (4) Å (22*b*), which is a greater range of values than was found in $[\text{Ag}(\text{CH}_2\text{Cl}_2)_2]_2[\text{Pd}(\text{OTeF}_5)_4]$.

The most significant feature of the structure is the absence of $\text{Ag}-\text{O}$ bonds, which are present in $[\text{Ag}(\text{CH}_2\text{Cl}_2)_2]_2[\text{Pd}(\text{OTeF}_5)_4]$, $\text{AgB}(\text{OTeF}_5)_4$, and $[\text{Ag}(\text{CO})][\text{B}(\text{OTeF}_5)_4]$. Instead, each $[\text{Ag}(\text{CH}_2\text{Cl}_2)_3]^+$ cation is only *extremely weakly coordinated* to the $\text{Ti}(\text{OTeF}_5)_6^{2-}$ anion by two $\text{Ag}-\text{F}$ contacts of 3.029 (8) and 3.033 (6) Å. The relative strength of anion binding to Ag^+ is also evident in the number of dichloromethane molecules coordinated to Ag^+ : three in $[\text{Ag}(\text{CH}_2\text{Cl}_2)_3]_2[\text{Ti}(\text{OTeF}_5)_6]$ but only two in $[\text{Ag}(\text{CH}_2\text{Cl}_2)_2]_2[\text{Pd}(\text{OTeF}_5)_4]$. Thus, with this new class of octahedral anions, we should be able to more effectively "decouple" cations from their counterions.

In contrast with the $\text{B}(\text{OTeF}_5)_4^-$ anion, $\text{Nb}(\text{OTeF}_5)_6^-$ does not undergo rapid exchange with labelled OTeF_5^- in the presence of electrophilic cations such as H^+ and Ag^+ . For example, when $[\text{TBA}][\text{Nb}^{16}\text{OTeF}_5)_6]$ and $\text{H}^{18}\text{OTeF}_5$ were mixed in dichloromethane at 22°C, IR spectra showed that isotope scrambling was only 22% complete after 47 h. The presence of a larger cation had an even more dramatic effect: when $\text{AgNb}^{16}\text{OTeF}_5)_6$ and $\text{Ag}^{18}\text{OTeF}_5$ were mixed in dichloromethane at 22°C, *no* exchange was observed after 72 h. The anion $\text{Sb}(\text{OTeF}_5)_6^-$ is even more stable: it does not exchange teflate groups with $\text{H}^{18}\text{OTeF}_5$ even after 168 h. Based on the structure of $[\text{Ag}(\text{CH}_2\text{Cl}_2)_3]_2[\text{Ti}(\text{OTeF}_5)_6]$, we propose that electrophiles such as Ag^+ cannot form bridge bonds to the oxygen atoms of $\text{Nb}(\text{OTeF}_5)_6^-$ and $\text{Sb}(\text{OTeF}_5)_6^-$, and that even H^+ cannot form bridge bonds to the oxygen atoms of $\text{Sb}(\text{OTeF}_5)_6^-$. Without such bridge bonds, abstraction of OTeF_5^- by even the strongest electrophiles will not occur rapidly. Thus, steric hindrance causes a *kinetic* stabilization of $\text{Nb}(\text{OTeF}_5)_6^-$ and $\text{Sb}(\text{OTeF}_5)_6^-$ in the presence of electrophilic cations.

Our new silver salts are freely soluble in weakly coordinating, low dielectric solvents such as chlorinated hydrocarbons and chlorofluorocarbons. For example, the solubility of $\text{Ag}_2\text{Pd}(\text{OTeF}_5)_4$ in dichloromethane at 22°C ($\epsilon \sim 9.1$) is only 0.35 M, while the solubility of $\text{Ag}_2\text{Ti}(\text{OTeF}_5)_6$ is *many* times higher (in fact, its solubility is sufficiently high that measuring it quantitatively has been problematic). An even more striking example of solubilizing ability is evident when comparing solubilities in CFC-113 at 22°C ($\epsilon \sim 2.4$): AgOTeF_5 , insoluble; $\text{AgB}(\text{OTeF}_5)_4$, 0.004 M; $\text{AgNb}(\text{OTeF}_5)_6$, 0.4 M. These data prove that appreciable concentrations of metal ions can be produced in solvents that are even more weakly coordinating than dichloromethane if the counterion is large enough and weakly coordinating enough. Whether salts such as $[\text{Fe}(\text{porphyrin})][\text{Nb}(\text{OTeF}_5)_6]$ and $[\text{SiR}_3][\text{Sb}(\text{OTeF}_5)_6]$ can be isolated and fully characterized remains to be seen. These salts would probably represent the closest thing possible to coordinative unsaturation in cations in a condensed phase.

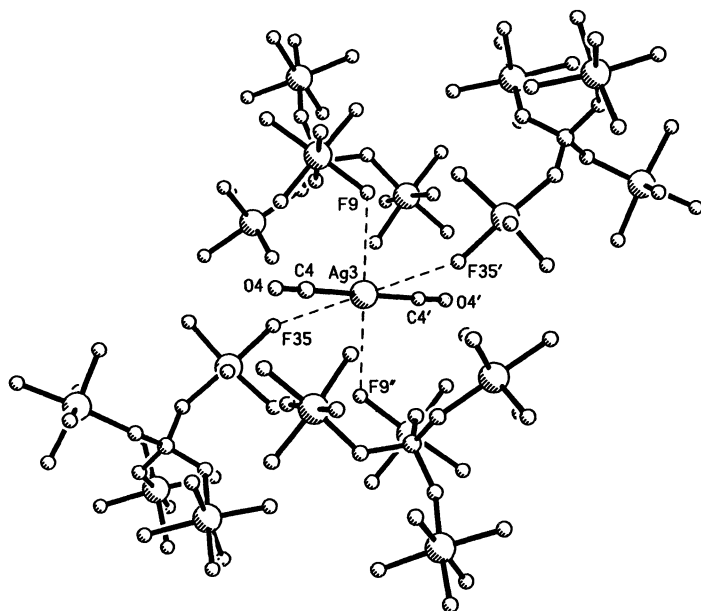


Figure 3. Structure of one of the centrosymmetric $[\text{Ag}(\text{CO})_2]^+$ cations and the four $\text{B}(\text{OTeF}_5)_4^-$ anions that surround it in $[\text{Ag}(\text{CO})_2][\text{B}(\text{OTeF}_5)_4]$. Selected distances (\AA) and angles (deg): $\text{Ag}3\text{-C}4$, 2.14 (3); $\text{C}4\text{-O}4$, 1.08 (4); $\text{Ag}3\text{-F}9$, 2.96 (1); $\text{Ag}3\text{-F}35$, 3.09 (2); $\text{C}4\text{-Ag-C}4'$, 180; $\text{Ag}3\text{-C}4\text{-O}4$, 179 (2). (Reproduced with permission from ref 30. Copyright 1993 ACS.)

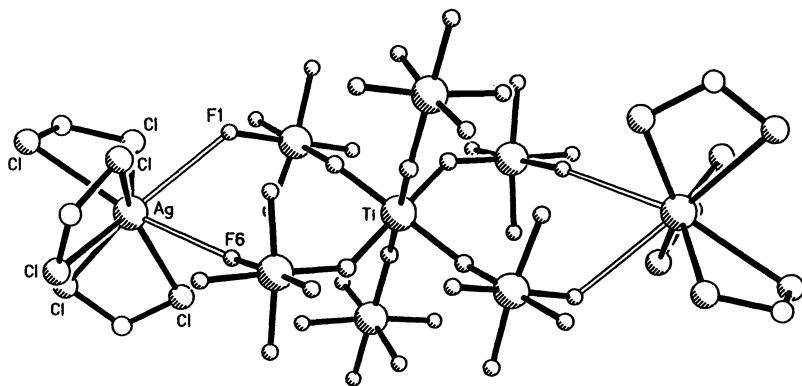


Figure 4. Structure of the centrosymmetric $[\text{Ag}(\text{CH}_2\text{Cl}_2)_3]_2[\text{Ti}(\text{OTeF}_5)_6]$ formula unit. The unlabeled open spheres are carbon atoms, the unlabeled large highlighted spheres are tellurium atoms, and the unlabeled small highlighted spheres are fluorine atoms. Hydrogen atoms have been omitted for clarity. Selected distances (\AA): Ag-Cl , 2.656 (3)-3.049 (4); $\text{Ag-F}1$, 3.029 (8); $\text{Ag-F}6$, 3.033 (6). (Reproduced with permission from ref 21. Copyright 1993 ACS.)

Acknowledgment

Our work in this area has been supported by the Research Corporation, the Alfred P. Sloan Foundation, and the National Science Foundation. We thank Susie M. Miller for experimental assistance. PKH and JJR thank the U.S. Department of Education for fellowship support under the Graduate Assistance in Areas of National Need Program (Grant No. P200A10210).

Literature Cited

1. Gowda, N. M. N.; Naikar, S. B.; Reddy, G. K. N. *Adv. Inorg. Chem. Radiochem.* **1984**, *28*, 255.
2. Lawrance, G. A. *Chem. Rev.* **1986**, *86*, 17.
3. Beck, W.; Sünkel, K. *Chem. Rev.* **1988**, *88*, 1405.
4. Lawrance, G. A. *Adv. Inorg. Chem.* **1989**, *34*, 145.
5. Rosenthal, M. R. *J. Chem. Educ.* **1973**, *50*, 331.
6. (a) Hill, M. G.; Lamanna, W. M.; Mann, K. R. *Inorg. Chem.* **1991**, *30*, 4687. (b) Rhodes, M. R.; Mann, K. R. *Inorg. Chem.* **1984**, *23*, 2053.
7. Bond, A. M.; Ellis, S. R.; Hollenkamp, A. F. *J. Am. Chem. Soc.* **1988**, *110*, 5293.
8. Appel, M.; Schloter, K.; Heidrich, J.; Beck, W. *J. Organomet. Chem.* **1987**, *322*, 77.
9. (a) Fachinetti, G.; Funaioli, T.; Zanazzi, P. F. *J. Chem. Soc., Chem. Commun.* **1988**, 1100. (b) Morris, J. H.; Gysling, H. J.; Reed, D. *Chem. Rev.* **1985**, *85*, 51. (c) Bancroft, E. E.; Blount, H. N.; Janzen, E. G. *J. Am. Chem. Soc.* **1979**, *101*, 3692. (d) Eisch, J. J.; Wilcsek, R. J. *J. Organomet. Chem.* **1974**, *71*, C21. (e) Abley, P.; Halpern, J. *J. Chem. Soc., Chem. Commun.* **1971**, 1238. (f) Williams, J. L. R.; Doty, J. C.; Grisdale, P. J.; Regan, T. H.; Borden, D. G. *J. Chem. Soc., Chem. Commun.* **1967**, 109.
10. (a) Brookhart, M.; Rix, R. C.; DeSimone, J. M.; Barborak, J. C. *J. Am. Chem. Soc.* **1992**, *114*, 5894. (b) Hlatky, G. G. *Paper INOR387 1992*, 204th American Chemical Society National Meeting. (c) Marks, T. J. *Acc. Chem. Res.* **1992**, *25*, 57 and references therein. (d) Pellicchia, C.; Longo, P.; Proto, A.; Zambelli, A. *Makromol. Chem., Rapid Commun.* **1992**, *13*, 265. (e) Taube, R.; Wache, S. *J. Organomet. Chem.* **1992**, *428*, 431. (f) Horton, A. D.; Orpen, A. G. *Organometallics* **1991**, *10*, 3910. (g) Brookhart, M.; Sabo-Etienne, S. *J. Am. Chem. Soc.* **1991**, *113*, 2778. (h) Horton, A. D.; Frijns, J. H. G. *Angew. Chem., Int. Ed. Engl.* **1991**, *30*, 1152. (i) Bochmann, M.; Jaggar, A. J.; Nicholls, J. C. *Angew. Chem., Int. Ed. Engl.* **1990**, *29*, 780. (j) Hlatky, G. G.; Turner, H. W.; Eckman, R. R. *J. Am. Chem. Soc.* **1989**, *111*, 2728. (k) Taube, R.; Krukowka, L. *J. Organomet. Chem.* **1988**, *347*, C9. (l) Turner, H. W. European Patent Appl. 277,004 (assigned to Exxon), 1988. (m) Lin, Z.; Le Marechall, J.-F.; Sabat, M.; Marks, T. J. *J. Am. Chem. Soc.* **1987**, *109*, 4127. (n) Jordan, R. F.; Bajgur, C. S.; Willett, R.; Scott, B. *J. Am. Chem. Soc.* **1986**, *108*, 7410.

11. (a) Jelinek, T.; Baldwin, P.; Scheidt, W. R.; Reed, C. A. *Inorg. Chem.* **1993**, *32*, 0000. (b) Gupta, G. P.; Lang, G.; Young, J. Y.; Scheidt, W. R.; Shelly, K.; Reed, C. A. *Inorg. Chem.* **1987**, *26*, 3022. (c) Shelly, K.; Reed, C. A.; Lee, Y. J.; Scheidt, W. R. *J. Am. Chem. Soc.* **1986**, *108*, 3117.
12. (a) Plešek, J. *Chem. Rev.* **1992**, *92*, 269. (b) Liston, D. J.; Lee, Y. J.; Scheidt, W. R.; Reed, C. A. *J. Am. Chem. Soc.* **1989**, *111*, 6643. (c) Turner, H. W.; Hlatky, G. G. European Patent Appl. 277,003 (assigned to Exxon), 1988. (d) Liston, D. J.; Reed, C. A.; Eigenbrot, C. W.; Scheidt, W. R. *Inorg. Chem.* **1987**, *26*, 2739. (e) Shelly, K.; Finster, D. C.; Lee, Y. J.; Scheidt, W. R.; Reed, C. A. *J. Am. Chem. Soc.* **1985**, *107*, 5955.
13. (a) Siedle, A. R.; Gleason, W. B.; Newmark, R. A.; Skarjune, R. P.; Lyon, P. A.; Markell, C. G.; Hodgson, K. O.; Roe, A. L. *Inorg. Chem.* **1990**, *29*, 1667. (b) Siedle, A. R.; Newmark, R. A.; Sahyun, M. R. V.; Lyon, P. A.; Hunt, S. L.; Skarjune, R. P. *J. Am. Chem. Soc.* **1989**, *111*, 8346. (c) Siedle, A. R.; Newmark, R. A. *J. Am. Chem. Soc.* **1989**, *111*, 2058. (d) Siedle, A. R.; Newmark, R. A. *Organometallics* **1989**, *8*, 1442. (e) Siedle, A. R. *New J. Chem.* **1989**, *13*, 719. (f) Siedle, A. R.; Newmark, R. A.; Gleason, W. B.; Skarjune, R. P.; Hodgson, K. O.; Roe, A. L.; Day, V. W. *Solid State Ionics* **1988**, *26*, 109. (g) Siedle, A. R.; Newmark, R. A.; Brown-Wensley, K. A.; Skarjune, R. P.; Haddad, L. C.; Hodgson, K. O.; Roe, A. L. *Organometallics* **1988**, *7*, 2078. (h) Siedle, A. R.; Markell, C. G.; Lyon, P. A.; Hodgson, K. O.; Roe, A. L. *Inorg. Chem.* **1987**, *26*, 219. (i) Siedle, A. R. U. S. Patent 4,788,308 (assigned to 3M), 1988 (j) Siedle, A. R. U. S. Patent 4,673,753 (assigned to 3M), 1987.
14. (a) Seppelt, K. *Angew. Chem., Int. Ed. Engl.* **1982**, *21*, 877. (b) Engelbrecht, A.; Sladky, F. *Adv. Inorg. Chem. Radiochem.* **1981**, *24*, 189. (c) Seppelt, K. *Acc. Chem. Res.* **1979**, *12*, 211.
15. Sanders, J. C. P.; Schrobilgen, G. J. *J. Chem. Soc., Chem. Commun.* **1989**, 1576.
16. Miller, P. K.; Abney, K. D.; Rappé, A. K.; Anderson, O. P.; Strauss, S. H. *Inorg. Chem.* **1988**, *28*, 2255.
17. Kruger, G. J.; Pistorius, C. W. F. T.; Heyns, A. M. *Acta Cryst.* **1976**, *B32*, 2916.
18. Noirot, M. D.; Anderson, O. P.; Strauss, S. H. *Inorg. Chem.* **1987**, *26*, 2216.
19. Colman, M. R.; Newbound, T. D.; Marshall, L. J.; Noirot, M. D.; Miller, M. M.; Wulfsberg, G. P.; Frye, J. S.; Anderson, O. P.; Strauss, S. H. *J. Am. Chem. Soc.* **1990**, *112*, 2349.
20. (a) Hurlburt, P. K.; Anderson, O. P.; Strauss, S. H. *J. Am. Chem. Soc.* **1991**, *113*, 6277. (b) Hurlburt, P. K.; Rack, J. J.; Dec, S. F.; Anderson, O. P.; Strauss, S. H., Colorado State University, unpublished data.
21. Strauss, S. H. *Chem. Rev.* **1993**, *93*, 927.
22. (a) Van Seggen, D. M.; Hurlburt, P. K.; Anderson, O. P.; Strauss, S. H. manuscript in preparation. (b) Van Seggen, D. M.; Hurlburt, P. K.; Anderson, O. P.; Strauss, S. H. *J. Am. Chem. Soc.* **1992**, *114*, 10995. (c)

- Van Seggen, D. M.; Hurlburt, P. K.; Noiro, M. D.; Anderson, O. P.; Strauss, S. H. *Inorg. Chem.* **1992**, *31*, 1423. (d) Hurlburt, P. K.; Anderson, O. P.; Strauss, S. H. *Can. J. Chem.* **1992**, *70*, 726.
23. (a) Bondi, A. *J. Phys. Chem.* **1964**, *68*, 441. (b) Pauling, L. *The Nature of the Chemical Bond*; Cornell Univ. Press: Ithaca, NY, 1960, p 257.
24. Barrow, M.; Burgi, H.-B.; Camalli, M.; Caruso, F.; Fischer, E.; Venanzi, L. M.; Zambonelli, L. *Inorg. Chem.* **1983**, *22*, 2356.
25. Uson, R.; Fornies, J.; Menjon, B.; Cotton, F. A.; Falvello, L. R.; Tomas, M. *Inorg. Chem.* **1985**, *24*, 4651.
26. Berry, C. H. *Phys. Rev.* **1955**, *97*, 676.
27. Alcock, N. W.; Jenkins, H. D. B. *J. Chem. Soc., Dalton Trans.* **1974**, 1907.
28. Wieghardt, K.; Kleine-Boymann, M.; Nuber, B.; Weiss, J. *Inorg. Chem.* **1986**, *25*, 1309.
29. Shannon, R. D. *Acta Cryst.* **1976**, *A32*, 751.
30. Hurlburt, P. K.; Rack, J. J.; Dec, S. F.; Anderson, O. P.; Strauss, S. H. *Inorg. Chem.* **1993**, *32*, 373.
31. (a) Neppel, A.; Hickey, J. P.; Butler, I. S. *J. Raman Spectrosc.* **1979**, *8*, 57. (b) Souma, Y.; Iyoda, J.; Sano, H. *Osaka Kogyo Gijutsu Shikensho Kiho* **1976**, *27*, 277. (c) Souma, Y.; Iyoda, J.; Sano, H. *Inorg. Chem.* **1976**, *15*, 968.
32. Willner, H.; Aubke, F. *Inorg. Chem.* **1990**, *29*, 2195, and references therein.
33. (a) Willner, H.; Schaeb, J.; Hwang, G.; Mistry, F.; Jones, R.; Trotter, J.; Aubke, F. *J. Am. Chem. Soc.* **1992**, *114*, 8972. (b) Adelhelm, M.; Bacher, W.; Höhn, E. G.; Jacob, E. *Chem. Ber.* **1991**, *124*, 1559.
34. (a) Chenier, J. H. B.; Hampson, C. A.; Howard, J. A.; Mile, B. *J. Phys. Chem.* **1988**, *92*, 2745. (b) Kasai, P. H.; Jones, P. M. *J. Am. Chem. Soc.* **1985**, *107*, 813. (c) *Ibid.*, *J. Phys. Chem.* **1985**, *89*, 1147. (d) McIntosh, D.; Ozin, G. A. *Inorg. Chem.* **1977**, *16*, 51. (e) *Ibid.*, *J. Am. Chem. Soc.* **1976**, *98*, 3167. (f) Huber, H.; Kündig, E. P.; Moskovits, M.; Ozin, G. A. *J. Am. Chem. Soc.* **1975**, *97*, 2097. (g) Ogden, J. S. *J. Chem. Soc., Chem. Commun.* **1971**, 978.
35. Moock, K.; Seppelt, K. *Z. Anorg. Allg. Chem.* **1988**, *561*, 132.
36. Schröder, K.; Sladky, F. *Chem. Ber.* **1980**, *113*, 1414.

RECEIVED May 20, 1993

Chapter 22

Stabilization of Unusual Cations by Very Weakly Basic Fluoro Anions

F. Aubke

Department of Chemistry, The University of British Columbia,
Vancouver, British Columbia V6T 1Z1, Canada

Very weakly basic anions like the sulfonates (SO_3F^- and SO_3CF_3^-) and the fluoroantimonates (SbF_6^- , $\text{Sb}_2\text{F}_{11}^-$, or $\text{Sb}_3\text{F}_{16}^-$) allow the stabilization and study of highly electrophilic cations, both in the respective acid or superacid solutions or in solid, thermally stable compounds. The examples discussed here include main-group cations like a) $(\text{CH}_3)_2\text{Sn}^{2+}$, which is studied by ^{119}Sn Mössbauer spectroscopy and allows the estimation of anion nucleophilicity; or b) the molecular cations O_2^+ , Br_2^+ , and I_2^+ , studied by magnetochemical techniques. Two groups of late transition-metal cations will be included in this review: a) "bare" cations like Ni^{2+} , Pd^{2+} (with $^3\text{A}_{2g}$ ground states), Ag^{2+} , and Au^{2+} , which are studied by ESR and magnetic susceptibility measurements to 4 K; and b) novel cationic coordination complexes like $[\text{Au}(\text{CO})_2]^+$, $[\text{Au}(\text{NCCH}_3)_2]^+$, and $[\text{Pt}(\text{CO})_4]^{2+}$.

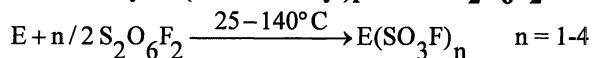
The term "unusual" in the title of this summary is frequently used in chemistry, quite often when minute differences to published precedents are described. Its use here refers to a group of cationic species that exhibit unprecedented and unexpected physical or spectroscopic properties as the result of unconventional coordination geometries, or to new species that point to novel bonding situations and coordination modes as well as to new synthetic applications.

The unusual features discussed below are invariably caused by extremely weakly nucleophilic anions, employed either as counter ions or as weakly coordinated ligands: the fluorosulfate SO_3F^- , the trifluoromethyl sulfate SO_3CF_3^- , and the hexafluoroantimonate(V) SbF_6^- and its poly anions $\text{Sb}_2\text{F}_{11}^-$ and $\text{Sb}_3\text{F}_{16}^-$. The anions are found either as self-ionisation ions in the strong protonic acids HSO_3F or HSO_3CF_3 , or in superacids (*I*) like $\text{HF}\text{-SbF}_5$, and all can function as counter anions or as weakly coordinating mono- or polydentate anionic ligands towards nonmetal and metal ions in solid compounds (*2*). The existence of such a diverse range of cationic compounds or salts is due to the availability of simple and versatile synthetic routes, which will be discussed next.

0097-6156/94/0555-0350\$08.00/0
© 1994 American Chemical Society

Synthetic Routes to Compounds with Weakly Basic Fluoro Anions. The synthetic methods chosen fall into three groups:

(I) Element Oxidation by Bis(fluorosulfonyl)peroxide $S_2O_6F_2$.



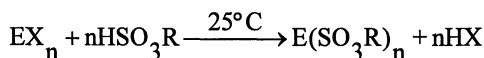
This oxidation reaction forms the corner stone of the work described here. The method is widely applicable to many nonmetals and metals, and may be carried out in the presence or absence of fluorosulfuric acid as ionizing solvent. In many, but not all metal oxidations, the use of HSO_3F is essential. Reversible dissociation of bis(fluorosulfonyl)peroxide into the fluorosulfate radicals (3)



occurs in HSO_3F more readily, and is favored by solvent stabilisation of the radicals formed (4).

(II) Solvolysis Reactions.

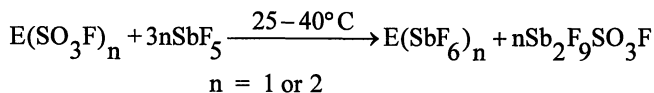
(a) Acidolysis in Protonic Acids



with $X = Cl, Br, O_2CR'$ ($R' = \text{alkyl or aryl}$), etc., and $R = F \text{ or } CF_3$.

A slightly more complex reaction allows the solvolytic conversion of fluorosulfates into trifluoromethyl sulfates (5); however, here the HSO_3F initially formed reacts further with HSO_3CF_3 , present in an excess, to produce a range of volatile materials that do not interfere in the isolation of the binary or ternary trifluoromethyl sulfates. Solvolysis of $RnSnCl_{4-n}$, $R = CH_3$ and $n = 2, 3, \text{ or } 4$, in strong acids is the preferred synthetic route to dimethyltin(IV) salts.

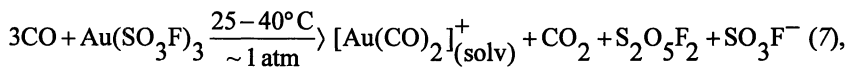
(b) Solvolysis in Liquid Antimony(V) Fluoride



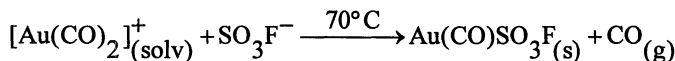
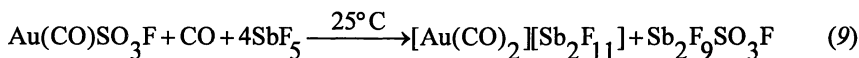
The course of the reaction is best monitored by Raman spectroscopy with respect to the disappearance of SO_3F bands in the product and the formation of volatile $Sb_2F_9SO_3F$ (6). Mild heating is found to reduce the viscosity of SbF_5 and hence speed up the solvolysis. Obviously, depending on the cation, polyanions such as $Sb_2F_{11}^-$ or $Sb_3F_{16}^-$ may form as well.

(III) Carbonylation of Fluorosulfates

(a) Reductive Carbonylation in HSO₃F. The routes leading to gold(I) carbonyl derivatives serve as examples. Extension to Pt(II) carbonyls is feasible (8).



and

**(b) Carbonylation and Solvolysis in Antimony(V) Fluoride**

The synthetic routes may be used in sequence, as exemplified by the stepwise conversion of gold powder to [Au(CO)₂][Sb₂F₁₁]: oxidation of gold by S₂O₆F₂ affords [Au(SO₃F)₃]₂, which needs not to be isolated from the solution in HSO₃F (10); its reductive carbonylation results in the formation and isolation of Au(CO)SO₃F via [Au(CO)₂]⁺ as intermediate, and the solvolysis of Au(CO)SO₃F in SbF₅ in the presence of CO finally leads to [Au(CO)₂][Sb₂F₁₁].

Three points are noteworthy: (i) All synthetic reactions, except for some of the metal oxidations (2), require very mild conditions, which permit working in glass apparatus and allow the isolation of thermally labile products; (ii) All carbonylation reactions proceed quantitatively and have well defined stoichiometries. This facilitates product isolation and allows the use of expensive, isotopically labelled ¹³CO or C¹⁸O for the purpose of a complete vibrational analysis and ¹³C-NMR studies; and (iii) Most starting materials are commercially available, often in a high degree of purity like the metal powders. Of the principal reagents, HSO₃CF₃, technical-grade HSO₃F (11), and SbF₅ are readily purified by repeated distillation. Bis(fluorosulfonyl)peroxide is obtained in very high purity and on a large scale (about 1-2 kg) by a modified version of the method reported by Dudley and Cady (12), the catalytic (AgF₂) fluorination of SO₃.

The synthetic routes summarised briefly are employed in the preparation of compounds that have highly electropositive cations stabilized by very weakly basic fluoroanions. The cations fall into four groups: (i) Main-group organometallic cations exemplified by the dimethyltin(IV) cation, (CH₃)₂Sn²⁺; (ii) Homonuclear, molecular diatomic cations O₂⁺, Br₂⁺, and I₂⁺; (iii) "Bare" or weakly coordinated divalent transition-metal cations; and (iv) Molecular noble-metal cations with CO or NCCH₃ as ligands. These four groups will now be discussed.

The Dimethyltin(IV) Cation and the Scale of Anion Basicity (13). For the dimethyltin(IV) cation, (CH₃)₂Sn²⁺, a linear C-Sn-C grouping is presumed, with bonding involving a 5sp_z hybrid orbital on tin. In polymeric salts with symmetrically bridging polydentate, uni- or dinegative anions, or in anionic complexes of the

type $[(\text{CH}_3)_2\text{SnX}_4]^{2-}$ $X = \text{F}$ or SO_3F , approximately octahedral coordination for tin results. With the methyl groups in trans-octahedral positions, the $5p_x$ and $5p_y$ orbitals are viewed as acceptor orbitals. Electron population in these two p orbitals is proportional to the anion basicity. The underlying structural principle has been confirmed by single-crystal X-ray diffraction in four cases: $(\text{CH}_3)_2\text{SnF}_2$ (14), $(\text{CH}_3)_2\text{Sn}(\text{SO}_3\text{F})_2$ (15), $(\text{CH}_3)_2\text{SnMoO}_4$, even though slight distortions are noted here (16), and more recently in $(\text{CH}_3)_2\text{Sn}(\text{O}_2\text{CH})_2$ (17). In many more cases (18), vibrational and ^{119}Sn Mössbauer spectroscopy have provided strong indirect evidence for the validity of the bonding model. In particular the latter technique has been most informative: strong bonding in the C-Sn-C group involving a Sn sp_z hybrid suggests high s-electron density on tin and will result in high isomer shifts δ (relative to SnO_2), while the highly asymmetric electron distribution in the 5p orbitals gives rise to large quadrupole splittings. As seen in Table I for six relevant examples, the order of decreasing nucleophilicity is:

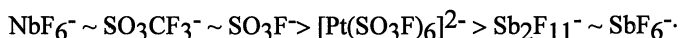


Table I. Selected ^{119}Sn Mössbauer Parameters of Dimethyltin(IV) Salts with Weakly Basic Anions

Compound	ΔE_Q [mm s^{-1}] ± 0.03	δ [mm s^{-1}] ± 0.03	Ref.
$\text{Cs}_2[(\text{CH}_3)_2\text{Sn}(\text{SO}_3\text{F})_4]$	5.50	1.83	18
$(\text{CH}_3)_2\text{Sn}[\text{NbF}_6]_2$	5.51	1.77	19
$(\text{CH}_3)_2\text{Sn}(\text{SO}_3\text{CF}_3)_2$	5.51	1.79	20
$(\text{CH}_3)_2\text{Sn}(\text{SO}_3\text{F})_2$	5.55	1.80	20
$(\text{CH}_3)_2\text{Sn}[\text{Pt}(\text{SO}_3\text{F})_6]$	5.67	1.95	18
$(\text{CH}_3)_2\text{Sn}[\text{Sb}_2\text{F}_{11}]_2$	6.01	2.08	19
$(\text{CH}_3)_2\text{Sn}[\text{SbF}_6]_2$	6.04	2.04	19

The following comments apply here: (i) SbF_6^- and $\text{Sb}_2\text{F}_{11}^-$ appear to be the weakest nucleophiles (19). They become the anions of choice to stabilise highly electrophilic cations. Their ^{119}Sn Mössbauer data are unique: they include the highest isomer shifts for dimethyltin(IV) derivatives, and the largest ΔE_Q values for any tin compound reported to date. (ii) In a number of dimethyltin(IV) derivatives of weak acids the correlation fails. Here strongly coordinated anions are observed, as, e.g., in the case of $(\text{CH}_3)_2\text{SnX}_2$; $X = \text{Cl}$ (21), CN (22), NCS (23), or CO_2CF_3 , recently studied by us. As a consequence, anion bridges become unsymmetrical and the C-Sn-C group is nonlinear. There are also two reports where CH_3CO_2^- (24) or NO_3^- (25) are chelating ligands, again with bent C-Sn-C groups. (iii) A number of anions of very strong protonic acids like OEF_5^- , $E = \text{Se}$ or Te , do not readily form bidentate bridges, even though some examples are known (2) and methyltin(IV) per

chlorates are explosive. They are therefore not ranked in this manner and may well find excellent use as weakly coordinating anions.

The Molecular Cations O_2^+ , Br_2^+ , and I_2^+ . This group comprises the only stable, paramagnetic diatomic main-group cations known. They provide an interesting test case both for our synthetic methods and the stabilisation by suitable, weakly nucleophilic anions. For both $Br_2[Sb_3F_{16}]$ (26) and $I_2[Sb_2F_{11}]$ (27), the molecular structures are known and both are best obtained by oxidation of I_2 or Br_2 by $S_2O_6F_2$ and subsequent solvolysis in liquid SbF_5 (28). $O_2[Mn_2F_9]$, the only O_2^+ salt where a precise molecular structure is known (29), has, just like a number of other O_2^+ -salts, a paramagnetic anion, which complicates a magnetic study. Hence $O_2[AsF_6]$ becomes the material of choice. It is synthesised by UV-photolysis in a quartz bulb (30) to avoid ferromagnetic Monel impurities in the sample, and a detailed ESR study is reported for this salt. The approximate structure is known from powder-diffraction data (31).

Table II: Structural, Spectroscopic and Magnetic Information on $O_2[AsF_6]$, $I_2[Sb_2F_{11}]$, and $Br_2[Sb_3F_{16}]$ and the Corresponding Cations O_2^+ , I_2^+ , and Br_2^+

Data, X denotes O, Br, or I	$O_2[AsF_6]$ or O_2^+ (g)	$Br_2[Sb_3F_{16}]$ or Br_2^+ (g)	$I_2[Sb_2F_{11}]$ or I_2^+ (g)
Shortest $X_2 \cdots X_2$ contact [\AA]	4.0-4.05	6.445	4.29
v. d. Waals radius for X [\AA] (33)	1.52	1.85	1.98
Ground state configuration	$2\Pi_{1/2g}$	$2\Pi_{3/2g}$	$2\Pi_{3/2g}$
Spin-orbit coupling const. λ [cm^{-1}]	185	2820	5125
Diamagnetic corrections 10^{-6} a)	-79	-279	-238
Curie constant	0.34	0.49	-
Weiss constant [K]	-1.90 ± 0.01	-0.74 ± 0.01	-
Curie-Weiss Behav.	60-2	297-4.2	-
Temp. range [K]			
Range of μ_{eff} down to 4 K [μ_B]	1.62-1.39	1.96-1.93	1.81-0.41

a) [$\text{cm}^3 \text{mol}^{-1}$]

The results of a magnetic susceptibility study to 4.2 K are summarised in Table II, together with pertinent structural and spectroscopic information on the three cations. Details have been reported (32) and the results may be summarised as follows: The dibromine cation in $Br_2[Sb_3F_{16}]$ is magnetically dilute and follows Curie-Weiss law over the entire temperature range. The Weiss constant θ is -7.4 ± 0.01 K and the results are consistent with a $2\Pi_{3/2g}$ ground state. The magnetic moment μ_{eff} ranges from 2.04 to 1.93 μ_B between 297 and 4.2 K. In $I_2[Sb_2F_{11}]$

strong antiferromagnetic coupling is observed with a maximum in χ_M at ~ 54 K. It appears that relatively short nonbonding contacts of 4.29 Å are sufficient to allow magnetic interaction between individual cations. For $\text{Br}_2[\text{Sb}_3\text{F}_{16}]$, the shortest $\text{Br}_2 \cdots \text{Br}_2$ contact is 6.445 Å, which appears to be too long for magnetic coupling. Finally for $\text{O}_2[\text{AsF}_6]$, the Curie-Weiss law is obeyed down to 2 K ($\theta = 1.90 \pm 0.01$ K) and weak antiferromagnetic coupling is found at very low temperatures. On account of the ${}^2\Pi_{1/2g}$ ground state, lower magnetic moments between 1.65 and 1.17 μ_B are observed. In addition to spin-orbit coupling, a crystal field splitting due to an orthorhombic site of O_2^+ in the lattice contributes to an estimated separation of the ground state and the nearest excited state of ~ 1480 cm^{-1} (32).

The three examples discussed here suggest that very electrophilic cations may be well separated from each other with magnetic exchange seemingly caused by direct cation \cdots cation contact rather than super-exchange involving the rather large fluoroanion.

The Transition-Metal Cations Ni^{2+} , Pd^{2+} , Ag^{2+} , and Au^{2+} . In order to study their electronic structures and magnetic properties, the corresponding fluorosulfates, $\text{M}(\text{SO}_3\text{F})_2$, are chosen. Only the nickel (34), palladium (35,36) and silver (37) fluorosulfates are known, while the Au^{2+} cation is unknown (38,39). The suggested structures for $\text{M}(\text{SO}_3\text{F})_2$ as well as those of other sulfonates of divalent metals are based on the CdCl_2 layer structure (34) with tridentate-bridging sulfonate groups, resulting in an octahedral environment for the metal and a ${}^3A_{2g}$ ground state for Pd^{2+} and Ni^{2+} . Octahedral coordination is common for Ni^{2+} , but is rare for palladium. So far only three simple binary compounds are known to be paramagnetic with two unpaired electrons: PdF_2 (40) and $\text{Pd}(\text{SO}_3\text{X})_2$ ($\text{X} = \text{F}$ or CF_3) (5,35,36), while most Pd(II) complexes are square planar and diamagnetic. Similarly, binary, paramagnetic silver(II) compounds are limited to AgF_2 (41,42), $\text{Ag}(\text{SO}_3\text{F})_2$ (37), and $\text{Ag}(\text{SO}_3\text{CF}_3)_2$ (43). The former two form a number of cationic and anionic derivatives, as do PdF_2 and $\text{Pd}(\text{SO}_3\text{F})_2$. Both $\text{Ag}(\text{SO}_3\text{F})_2$ (37) and $\text{Pd}(\text{SO}_3\text{F})_2$ (35) are obtained by the oxidation of the corresponding metal by $\text{S}_2\text{O}_6\text{F}_2$ (37) or BrSO_3F (35).

The two binary compounds $\text{Ag}(\text{SO}_3\text{F})_2$ and $\text{Pd}(\text{SO}_3\text{F})_2$ show similar magnetic behaviour. Initial temperature-independent magnetic moments to 80 K had suggested Curie-Weiss behaviour for $\text{Ag}(\text{SO}_3\text{F})_2$ (37), $\text{Pd}(\text{SO}_3\text{F})_2$ (36), and the mixed-valency compound $\text{Pd}(\text{II})[\text{Pd}(\text{IV})(\text{SO}_3\text{F})_6]$ as well (36), in magnetically dilute compounds. This observation is consistent with a ${}^3A_{2g}$ ground state in both Pd(II) compounds (36), and a singly or doubly degenerate ground state for Ag^{2+} (d^9) on account of Jahn-Teller distortions. Only later was it discovered that ferromagnetic coupling is observed below 40 K (44), which is rather uncommon for coordination polymers with molecular, anionic ligands. For the fluorides AgF_2 (45,46), PdF_2 (47), and $\text{Pd}(\text{II})[\text{Pd}(\text{IV})\text{F}_6]$ (48), weak ferromagnetism is suggested as well. In these materials, which are magnetically concentrated, antiferromagnetic ordering appears to dominate. Antiferromagnetism is also found for $\text{Ag}(\text{SO}_3\text{CF}_3)_2$ (43) and $\text{Pd}(\text{SO}_3\text{CF}_3)_2$ (5). The two sulfonates $\text{Ni}(\text{SO}_3\text{F})_2$ and $\text{Ni}(\text{SO}_3\text{CF}_3)_2$ have identical electronic spectra and ligand field parameters at room temperature, consistent with a

$^3A_{2g}$ ground state for Ni^{2+} , and have regular octahedral coordination in both compounds. Their magnetic behaviour down to 50 K is identical, but below this temperature the fluorosulfate shows ferromagnetism, and the trifluoromethyl sulfate antiferromagnetism (49).

Unlike $Ag(SO_3F)_2$, gold(II) fluorosulfate $[Au(SO_3F)_2]_n$ is diamagnetic and best formulated as an oligomeric mixed valency Au(I)Au(II) compound (50). It is obtained by the reduction of dimeric $[Au(SO_3F)_3]_2$ (51), with either CO or a stoichiometric amount of gold powder in fluorosulfuric acid. The solution of diamagnetic, yellow $Au(SO_3F)_2$ in HSO_3F is dark brown, and a highly asymmetric ESR spectrum with three distinctly different g -values and a g_{iso} of 2.3183 is observed in the frozen solutions (50). Partly resolved hyperfine splitting due to four fluorine atoms suggests the spectrum is that of $[Au(SO_3F)_4]^{2-}$, with distortion around Au^{2+} (d^9) caused by Jahn-Teller splitting.

Two alternative approaches lead to substantially different ESR spectra (52):

(i) the reduction of $[Au(SO_3F)_3]_2$ by less than the stoichiometric amount of gold powder produces, in addition to solid $[Au(SO_3F)_2]_n$, a yellow solution of $Au^{2+}_{(solv)}$. The ESR spectrum obtained shows hyperfine splitting due to ^{197}Au , $I = 3/2$, and suggests a nearly square-planar geometry around gold. The g_{iso} value is found to be 2.362. (ii) Controlled, partial pyrolysis of solid $[Au(SO_3F)_3]_2$ proceeds with elimination of SO_3F radicals to $Au(SO_3F)_{3-x}$. The ESR spectrum suggests high axial symmetry for gold. Even though no hyperfine splitting is observed in the solid, g_{iso} is 2.359, nearly identical to the value found for $Au^{2+}_{(solv)}$.

It appears that Au^{2+} is generated as defect in a nearly square-planar Au(III) site in dimeric $[Au(SO_3F)_3]_2$ by reduction or pyrolysis, with the structure strongly influenced by the presence of additional Au(III) with a d^8 configuration in what appears to be an oligomeric species. This is confirmed by following the addition of $[Au(SO_3F)_3]_2$ to monomeric $[Au(SO_3F)_4]^{2-}$ by ESR, where gradually the symmetrical spectrum of $Au^{2+}_{(solv)}$ replaces the unsymmetrical pattern (50).

The ESR data discussed above are summarised in Table III and compared to a spectrum of Ag^{2+} , dissolved in $BrSO_3F$ (53). Here similarly high axial symmetry is suggested, but a lower g_{iso} value of $g = 2.1917$ is found, possibly because of the lower spin-orbit coupling constant for free ions of ~ 1800 for Ag^{2+} vs. $\sim 5000 \text{ cm}^{-1}$ for Au^{2+} (55). Also included in Table III is the previously reported ESR spectrum for $[Au(mnt)_2]^{2-}$ ($mnt = \text{maleonitrile dithiolate}$) (55), which is typical of other previously reported ESR spectra obtained for formally divalent gold(II) compounds, formed with various chelating anionic dithiolate ligands (38,39). A detailed analysis of the ESR spectrum of $[Au(mnt)_2]^{2-}$ indicates that the unpaired electron resides primarily in a ligand-based orbital (55). A similar situation resulting in the formation of radical anions is highly unlikely for SO_3F^- in our system, and it appears that the work discussed here in the light of the ESR spectra observed (50,52) is the first clear identification of the rather elusive Au^{2+} cation.

There may, however, have been a prior, unrecognised encounter of this species. In 1952, Nyholm and Sharpe (57) reported weak, unexplained paramagnetism of the order of $\mu_{eff} \sim 0.5 \mu_B$ in samples of AuF_3 synthesised by the reaction of gold with BrF_3 (58), followed by subsequent pyrolysis of the intermediate $[BrF_2][AuF_4]$

at 180°C. If AuF₃ is prepared by fluorination of Au with F₂, polymeric, diamagnetic AuF₃ forms (59). Similar observations were made during the synthesis of Au(SO₃F)₃ from gold and BrSO₃F (60) via the intermediate Br₃[Au(SO₃F)₄] (10) and its pyrolysis at 100°C. Such samples were sufficiently paramagnetic—estimates indicate about 7% of all gold to be present as Au²⁺ (52)—to permit the measurement of temperature-dependent magnetic susceptibilities between 300 and 100 K (52). Au(SO₃F)₃, made from Au and S₂O₆F₂, is diamagnetic ($\chi_M = 1.46 \times 10^{-6} \text{ cm}^3 \text{ mol}^{-1}$).

Table III. ESR Parameters of Gold(II) and Related Compounds

Complex	T [K]	g ₁	g ₂	g ₃	g _{iso}	Ref.
Au(SO ₃ F) _{3-x}	103	2.093	2.103	2.882	2.359	52
Au ²⁺ _(solv) -HSO ₃ Fa)	103	2.093	2.103	2.890	2.362	52
[Au(SO ₃ F) ₄] ²⁻ -HSO ₃ F	77	2.065	2.234	2.656	2.318	50
[Au(mnt) ₂] ^{2-b)}	133	1.9769	2.0051	2.0023	1.9947	55
[Au(mnt) ₂] ²⁻	-	-	-	-	2.009	56
Ag(SO ₃ F) ₂ -BrSO ₃ F	77	2.072	2.096	2.407	2.407	53

a) Additional data used for spectral simulation in MHz: A₁, 145; A₂, 145; A₃, 120; A_{iso}, 133.7; Q_{ZZ} 46; and Gaussian linewidths L₁ ~ L₂ = 20 G, L₃ = 25 G

b) Sample doped in [Ni(nmt)₂]²⁻, hyperfine parameter [MHz] A₁, 117; A₂, 122; A₃, 124; A_{iso}, 121

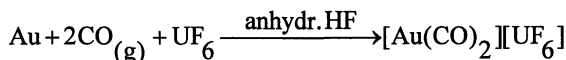
Noble-Metal Carbonyl Derivatives. While many of the results discussed here are very recent, the beginnings go back well into the last century. The synthesis of platinum(II)carbonyl chlorides was reported by Schützenberger in 1870 (61-63). This predates the discovery of Ni(CO)₄ and marks the start of transition-metal carbonyl chemistry. Likewise, the first synthesis of gold(I)carbonyl chloride, Au(CO)Cl, by Manchot and Gall (64) and its independent synthesis by Kharash and Isbell (65) date back into the first half of this century.

The unusual spectroscopic and bonding features of these compounds were soon recognized (66,67), and with thionyl chloride, SOCl₂, a convenient aprotic solvent was discovered (68,69) that allowed both the reductive carbonylation of, e.g., AuCl₃, or the CO-addition to Pd(II) and Pt(II)-halides under mild conditions. With noble-metal halides readily available, the corresponding metal-carbonyl halides became the focus of attention. A number of mono- and dinuclear, neutral and anionic carbonyl halides were subsequently synthesised and studied, with the general consensus that this group of noble-metal compounds was restricted to the halides with the order of thermal stability Cl > Br > I favouring the chlorides, with the fluorides so far unknown (67,69).

The accidental discovery of [Au(CO)₂]⁺_(solv) and Au(CO)SO₃F (7) during attempts to protonate CO in the superacid HSO₃F-Au(SO₃F)₃ (10) provides an

opening in three respects: (i) fluorosulfuric acid, HSO_3F , is a suitable, strongly ionizing reaction medium, which allows the formation of cationic gold carbonyl derivatives near room temperature and at low CO pressure; (ii) binary carbonyl cations, which were unknown as a stable species, and cationic derivatives can form in this medium and are found to be sufficiently thermally stable, once isolated, to allow their study and use in synthetic reactions; and (iii) the most unusual features of these compounds and ions are their CO stretching frequencies, which are well above the value of gaseous CO (2143 cm^{-1}) (70). With decreasing anion basicity, νCO will shift to higher wave numbers, and the thermal stability of compounds increases.

The cation $[\text{Au}(\text{CO})_2]^+$ was initially identified in HSO_3F solution (7). It is seemingly unstable with SO_3F^- as anion, but thermally stable in solid $[\text{Au}(\text{CO})_2][\text{Sb}_2\text{F}_{11}]$ (9). Here νCO_{av} , which was 2232 cm^{-1} for $[\text{Au}(\text{CO})_2]^+(\text{solv})$ (7) is now raised slightly to 2235.5 cm^{-1} (9). The only other example of a $[\text{Au}(\text{CO})_2]^+$ salt reported so far, $[\text{Au}(\text{CO})_2][\text{UF}_6]$ (71), has low thermal stability, insufficient to allow complete characterisation. Its synthesis according to:

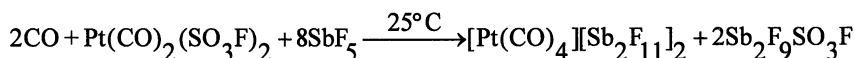


involves again a strong protonic acid, hydrogen fluoride, and points to a feasible alternative to the reductive carbonylation, the oxidation of gold by a suitable hexafluoride. An alternate, very direct route to $[\text{Au}(\text{CO})_2][\text{Sb}_2\text{F}_{11}]$ is also available: the interaction of AuF_3 with an excess of SbF_5 under CO pressure (9).

The facile isolation, thermal stability, and solubility in HSO_3F of $[\text{Au}(\text{CO})_2][\text{Sb}_2\text{F}_{11}]$ permit three interesting applications: (i) With the help of ^{13}C - and C^{18}O -substitution, a complete vibrational assignment, normal coordinate analysis and valence force field calculation are carried out and a useful comparison to the isoelectronic species $[\text{Au}(\text{CN})_2]^-$ and $\text{Hg}(\text{CN})_2$ (72) can now be made (9); (ii) ^{13}C NMR is used both as a diagnostic method to differentiate noble-metal carbonyls from the classical transition-metal carbonyls (9,66), and also to study the CO exchange between $[\text{Au}(^{13}\text{CO})_2]^+$ and $[\text{Au}(^{13}\text{CO})]^+$ in either HSO_3F or $\text{HSO}_3\text{F}-\text{SbF}_5$ (9); and (iii) The ligand-exchange reaction with acetonitrile allows formation of $[\text{Au}(\text{NCCH}_3)_2][\text{SbF}_6]$ (9) and suggests the use of $[\text{Au}(\text{CO})_2][\text{Sb}_2\text{F}_{11}]$ in the synthesis of other AuL_2^+ fluoroantimonates. The molecular structure of $[\text{Au}(\text{NCCH}_3)_2][\text{SbF}_6]$ shows the unusual, perfectly linear alignment of seven atoms for the cation (9).

The high νCO values for $[\text{Au}(\text{CO})_2]^+$ as well as the ^{13}C -NMR chemical shifts suggest the absence of appreciable π -back donation, not only here but also in other noble-metal carbonyl compounds, as in $\text{Ag}(\text{CO})\text{B}(\text{OTeF}_5)_4$ (73) and $[\text{Ag}(\text{CO})_2][\text{B}(\text{OTeF}_5)_4]$ (74), which has very recently been characterised by a low-temperature X-ray diffraction study. Hence the metal-carbon bond in noble-metal carbonyls is viewed as a single bond, strengthened in the case of gold by relativistic effects (75) and polar contributions to the bond. The CO bond becomes a strong triple bond. Support for the importance of polar contribution comes from the observed dependency of thermal stability and νCO_{av} on anion basicity.

Both relativistic effects and polar contributions are expected for cationic Pt(II)-carbonyl derivatives as well. Their recent synthesis has confirmed these expectations. Reductive carbonylation of Pt(SO₃F)₄ in HSO₃F, a strong superacid system (76) leads, depending on reaction conditions, to two isolable products, yellow [Pt(CO)₄][Pt(SO₃F)₆] (8) and, colourless cis-Pt(CO)₂(SO₃F)₂. Solvolysis in SbF₅ in the presence of CO according to



produces a second salt with a square-planar [Pt(CO)₄]²⁺ cation. Both [Pt(CO)₄]-compounds are thermally stable up to 140°C. The average CO stretching frequencies in [Pt(CO)₄][Pt(SO₃F)₆] and in [Pt(CO)₄][Sb₂F₁₁]₂ are at 2251 and 2261 cm⁻¹, the highest so far reported. Force-field calculations, using the method of Cotton and Kraihanzel (77,78), suggest for the latter compound a stretching force constant of 20.6 10² Nm⁻¹. For [Pt(CO)₄][Sb₂F₁₁]₂, the three fundamental CO stretches at 2289 (A_{1g}), 2267 (B_{1g}), observed in the Raman spectrum only, and 2244 cm⁻¹ (E_u), which is only IR active, strongly suggest a square-planar configuration for the cation.

Table IV summarizes average CO stretching frequencies and stretching force constants for this group of carbonyls and related compounds. A higher stretching force constant than found for linear [Au(CO)₂]⁺ (9) and square-planar [Pt(CO)₄]²⁺, is observed only in HCO⁺, where no π-backdonation is possible.

It has become apparent from the observation of νCO above 2200 cm⁻¹ and from stretching force constants above 20 × 10² Nm⁻¹ for [Au(CO)₂]⁺ and [Pt(CO)₄]²⁺, that these binary carbonyl cations differ drastically from classical transition-metal carbonyls with terminal CO groups, where νCO is found in the general range of 2125 to 1850 cm⁻¹ (79, 80) and force constants usually between 15 and 17·10² Nm⁻¹. It is obvious that π-backdonation, which is essential in transition-metal carbonyls (81), must be absent or substantially reduced and that carbon monoxide does not function as a π-acceptor, but rather as a σ-donor in noble-metal carbonyl cations and their cationic derivatives. It is not surprising that other distinguishing features, descriptive or experimental in nature, differ as well for both groups.

On the descriptive side, previously known binary carbonyl cations are usually of the [M(CO)₆]⁺ type with M = Mn, Tc or Re (82). The oxidation state of the metal in these or other ternary cations is 0 or +1, and the ionic charge of the complex does not exceed +1. In addition, far more basic anions are used as counter ions. The effective atomic number rule, which plays an important role in judging stability, structure and reactivity of transition-metal carbonyls, is not valid for the noble-metal carbonyl compounds reported so far. The silver(I) and gold(I) carbonyl derivatives have 14, and the Pt(II) carbonyls have 16 electrons in the metal valence shell.

On the experimental side, just like vibrational spectra, ¹³C-NMR spectra may be used to distinguish the two groups of metal carbonyls. The ¹³C chemical shifts of classical transition-metal carbonyls range from 190 to ~215 ppm (83), while for [Au(¹³CO)₂]⁺, [Au(¹³CO)]⁺, and [Pt(CO)₄]²⁺ shifts of 174, 162 and 130 ppm have

Table IV. Stretching Frequencies and Force Constants of CO in Some Carbonyls and Related Species^{a) b) c)}

Compound	ν_{CO} [cm^{-1}]	f_{r} [10^2 Nm^{-1}]
CO(g)	2143	18.6
CO ⁺	2184	19.3
HCO ⁺ (g)	2184	21.3
W(CO) ₆ (g)	2126	17.2
Cr(CO) ₆ (g)	2119	17.2
[Re(CO) ₆] ⁺ (sol)	2197	18.1
Cu(CO)Cl	2157	18.3
[Cu(CO)][AsF ₆]	2180	19.2
Ag(CO)B(OTeF ₅) ₄	2204	19.6
Au(CO)Br(sol)	2153	
Au(CO)Cl	2170	19.0
Au(CO)SO ₃ F	2196	19.5
[Au(CO) ₂][Sb ₂ F ₁₁]	2235.5	20.1
[Pt(CO) ₄][Sb ₂ F ₁₁] ₂ ^{d)}	2261	22.6

a) Detailed individual references are found in Ref. 9

b) Calculations of f_{r} are according to Jones (72)

c) Unless stated otherwise, spectra are obtained on solids

d) f_{r} is calculated according to Refs. 77 and 78

been observed in HSO₃F (9). Carbon monoxide with a chemical shift of 184 ppm in HSO₃F (9) represents, as for the vibrational spectra, the dividing line between both groups. Finally, preliminary studies by us indicate that both C1s and O1s binding energies in the X-ray photoelectron spectra of [Pt(CO)₄][Sb₂F₄]₂ differ from previously reported data and are shifted to higher rather than to lower energies (84,85) relative to CO.

In addition to the two binary carbonyl cations [Au(CO)₂]⁺ and [Pt(CO)₄]²⁺, which have been characterised by spectroscopic means and are found to contain terminal CO ligands, we have very recently synthesised by reductive carbonylation of Pd(SO₃F)₃ (35,36) in HSO₃F a material of the composition Pd(CO)SO₃F (87). This compound is found by single-crystal X-ray diffraction to contain the planar cyclic cation [Pd₂(μ-CO)₂]²⁺, shown in Fig. 1. The carbonyl groups are nearly symmetrically bridging and the C-O distance is, at 1.133(6) Å, very short, when compared to free CO (1.1281(9) Å) (88). Consequently, the CO stretching frequencies, which are mutually exclusive in the IR and Raman spectra, are, with 1977 and 2017 cm⁻¹, respectively, in a range usually attributed to terminal CO groups (79-81). The stretching force constant of $16.20 \times 10^2 \text{ Nm}^{-1}$ (77,78) is also unexpectedly high. This example shows that the unusual carbonyl bonding extends also to noble-metal compounds with bridging carbonyls. A similar structure has previously been

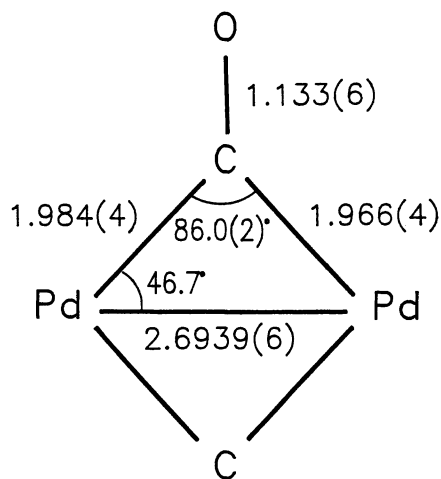


Figure 1. The molecular structure of $[\text{Pd}_2(\mu\text{-CO})_2]^{2+}$ (bond distances in Å).

reported for a palladium carbonyl acetate of the composition $[\text{Pd}_4(\text{CO})_4(\text{O}_2\text{CCH}_3)_4] \cdot 2\text{CH}_3\text{CO}_2\text{H}$ (89,90). However, here the $[\text{Pd}_2(\mu\text{-CO})_2]$ rings are bridged by more strongly coordinated acetate groups, resulting in a rectangular Pd_4 arrangement with alternation short (2.663 Å) and long (2.909 Å) Pd-Pd bonds.

Hence it is more appropriate to view noble-metal carbonyls and their derivatives as coordination complexes of CO rather than as organometallic compounds. A comparison to metal cyanide complexes is far more appropriate, in particular since $[\text{Au}(\text{CO})_2]^+$ and $[\text{Au}(\text{CN})_2]^-$ as well as $[\text{Pt}(\text{CO})_4]^{2+}$ and $[\text{Pt}(\text{CN})_4]^{2-}$ are isoelectronic and isostructural pairs. Strong bonding similarities have been established for the first pair (9). It is unlikely that cationic metal-carbonyl complexes will ever form so many different species as the cyanide complexes, which are known for most transition metals (86). With useful and facile synthetic routes available, further examples of cationic metal carbonyls with similar bonding and spectroscopic features as described here should be prepared and characterised in the future.

Conclusions

When the various, diverse cations discussed in this account are considered, it becomes apparent that none of them contains fluorine, the principle subject of this symposium. Although the cations have taken center-stage throughout, the strong supporting role played by the extremely weakly basic fluoro anions and the principle reagents antimony(V) fluoride, SbF_5 , bis(fluorosulfonyl)peroxide, $\text{S}_2\text{O}_6\text{F}_2$, and fluorosulfuric acid, HSO_3F , must be duly acknowledged.

Acknowledgments

Financial support by the Natural Science and Engineering Research Council of Canada (NSERC) and by the North Atlantic Treaty Organization (NATO) is gratefully acknowledged. Thanks go to my former graduate students Dr. William W. Wilson, Dr. Keith C. Lee, Dr. Patrick Leung, Dr. Walter V. Cicha, and Dr. Roshan M.S. Cader, who laid the foundation, and to my present students Germaine Hwang, Changqing Wang, and Fred Mistry. I am deeply indebted to my colleagues, foremost among them Professor Helge Willner, University of Hannover, my Departmental colleagues Professors F.G. Herring, J.R. Sams, R.C. Thompson, J. Trotter, and Dr. R.S. Rettig, as well as Professor W. Preetz and Dr. H. Homborg, University of Kiel, Germany, and Professor S.H. Strauss, Colorado State University, for making unpublished work available to me, and last but not least Ms. Carolyn Delheij-Joyce, who typed this manuscript.

Literature Cited

1. Olah, G.A.; Prakash, G.K.S.; Sommer, J. *Superacids*; J. Wiley and Sons Inc.: New York, NY, 1985.

2. Aubke, F.; Cader, M.S.R.; Mistry, F. In *Synthetic Fluorine Chemistry*; Olah, G.A.; Chambers, R.D.; Prakash, G.K.S., Eds.; John Wiley and Sons: New York, NY, 1992, pp 43-86.
3. Dudley, F.B.; Cady, G.H. *J. Am. Chem. Soc.* **1963**, *85*, 3375.
4. Cicha, W.V.; Herring, F.G.; Aubke, F. *Can. J. Chem.* **1990**, *68*, 102.
5. Mallela, S.P.; Sams, J.R.; Aubke, F. *Can. J. Chem.* **1985**, *63*, 3305.
6. Wilson, W.W.; Aubke, F. *J. Fluorine Chem.* **1979** *13*, 431.
7. Willner, H.; Aubke, F. *Inorg. Chem.* **1990**, *29*, 2195.
8. Hwang, G.; Bodenbinder, M.; Willner, H.; Aubke, F. *Inorg. Chem.*, submitted.
9. Willner, H.; Schaebis, J.; Hwang, G.; Mistry, F.; Jones, R.; Trotter, J.; Aubke, F. *J. Am. Chem. Soc.* **1992**, *114*, 8972.
10. Lee, K.C.; Aubke, F. *Inorg. Chem.* **1979**, *18*, 389.
11. Barr, J.; Gillespie, R.J.; Thompson, R.C. *Inorg. Chem.* **1964**, *3*, 1149.
12. Dudley, F.B.; Cady, G.H. *J. Am. Chem. Soc.* **1957**, *79*, 513.
13. Mallela, S.P.; Yap, S.; Sams, J.R.; Aubke, F. *Inorg. Chem.* **1986**, *25*, 4327.
14. Schlemper, E.O.; Hamilton, W.C. *Inorg. Chem.* **1966**, *5*, 995.
15. Allen, F.H.; Lerbscher, J.A.; Trotter, J. *J. Chem. Soc. (A)* **1971**, 2507.
16. Sasaki, Y.; Imoto, H.; Nagano, O. *Bull. Chem. Soc. Jpn.* **1984**, *57*, 1417.
17. Mistry, F.; Rettig, S.J.; Trotter, J.; Aubke, F. *Acta Cryst.* **1990**, *C46*, 2091.
18. Mallela, S.P.; Tomic, S.T.; Lee, K.; Sams, J.R.; Aubke, F. *Inorg. Chem.* **1986**, *25*, 2939.
19. Mallela, S.P.; Yap, S.; Sams, J.R.; Aubke, F. *Rev. Chim. Miner.* **1986**, *23*, 572.
20. Yeats, P.A.; Sams, J.R.; Aubke, F. *Inorg. Chem.* **1972**, *11*, 2634.
21. Davies, A.G.; Milledge, H.J.; Puxley, D.C.; Smith, P.J. *J. Chem. Soc. (A)* **1970**, 28, 62.
22. Konnert, J.; Britton, D.; Chow, Y.M. *Acta Cryst.* **1972**, *B28*, 180.
23. Chow, Y.M. *Inorg. Chem.* **1970**, *9*, 794.
24. Lockhart, P.J.; Calabrese, J.C.; Davidson, F. *Organometallics* **1987**, *6*, 2479.
25. Hilton, J.; Nunn, E.K.; Wallwork, S.C. *J. Chem. Soc. Dalton Trans.* **1973**, 173.
26. Edwards, A.J.; Jones, G.R. *J. Chem. Soc. (A)* **1971**, 2318.
27. Davies, C.G.; Gillespie, R.J.; Ireland, P.R.; Sowa, J.M. *Can. J. Chem.* **1974**, *52*, 2048.
28. Wilson, W.W.; Thompson, R.C.; Aubke, F. *Inorg. Chem.* **1980**, *19*, 1489.
29. Müller, B.G. *J. Fluorine Chem.* **1981**, *17*, 409.
30. Shamir, J.; Binenboym, J. *Inorg. Synth.* **1973**, *14*, 39.
31. Naulin, C.; Bougon, R. *J. Chem. Phys.* **1967**, *64*, 4155.
32. Cader, M.S.R.; Thompson, R.C.; Aubke, F. *Can. J. Chem.* **1989**, *67*, 1942.
33. Bondi, M. A. *J. Phys. Chem.* **1964**, *68*, 441.
34. Alleyne, C.S.; O'Sullivan-Mailer, K.; Thompson, R.C. *Can. J. Chem.* **1974**, *52*, 336.
35. Lee, K.C.; Aubke, F. *Can. J. Chem.*, **1977**, *55*, 2473.
36. Lee, K.C.; Aubke, F. *Can. J. Chem.* **1979**, *57*, 2058.
37. Leung, P.C.; Aubke, F. *Inorg. Chem.* **1978**, *17*, 1765.
38. Puddephatt, R.J. *The Chemistry of Gold*, Elsevier: Amsterdam, The Netherlands, 1978.

39. Puddephatt, R.J. In *Comprehensive Coordination Chemistry*; Wilkinson, G. Ed.; Pergamon Press: Oxford, UK, 1987, Vol. 7; p 861.
40. Ruff, O.; Ascher, E. *Z. Anorg. Allg. Chem.* **1929**, *183*, 211.
41. Ebert, M.S.; Rodowskas, E.L.; Frazer, J.C.W. *J. Am. Chem. Soc.* **1933**, *55*, 3056.
42. Ruff, O.; Giese, M. *Z. Anorg. Allg. Chem.* **1934**, *219*, 143.
43. Leung, P.C.; Lee, K.C.; Aubke, F. *Can. J. Chem.* **1979**, *57*, 326.
44. Cader, M.S.R.; Thompson, R.C.; Aubke, F. *Chem. Phys. Letters* **1989**, *164*, 438.
45. Charpin, P.; Plurien, P.; Mériel, P. *Bull. Soc. Fr. Mineral. Cristallogr.* **1970**, *93*, 7.
46. Fischer, P.; Roult, G.; Schwarzenbach, D. *J. Phys. Chem. Solids* **1971**, *32*, 1641.
47. Rao, P.R.; Sherwood, R.C.; Bartlett, N. *J. Chem. Phys.* **1968**, *49*, 3728.
48. Tressaud, A.; Winterberger, N.; Bartlett, N.; Hagenmüller, P. *Compt. Rend. Acad. Sci.* **1976**, *C282*, 1069.
49. Cader, M.S.R., Ph.D. Thesis, University of British Columbia, 1992.
50. Willner, H.; Mistry, F.; Hwang, G.; Herring, F.G.; Cader, M.S.R.; Aubke, F. *J. Fluorine Chem.* **1991**, *52*, 13.
51. Willner, H.; Rettig, S.J.; Trotter, J.; Aubke, F. *Can. J. Chem.* **1991**, *69*, 391.
52. Herring, F.G.; Hwang, G.; Lee, K.C.; Mistry, F.; Phillips, P.S.; Willner, H.; Aubke, F. *J. Am. Chem. Soc.* **1992**, *114*, 1271.
53. Leung, P.C., Ph.D. Thesis, University of British Columbia, 1979.
54. Dunn, T.M. *Faraday Trans.* **1961**, *57*, 1441.
55. Schlupp, R.L.; Maki, A.H. *Inorg. Chem.* **1974**, *13*, 44.
56. Waters, J.H.; Gray, H.B. *J. Am. Chem. Soc.* **1965**, *87*, 2496.
57. Nyholm, R.S.; Sharpe, A.G. *J. Chem. Soc.* **1952**, 3579.
58. Sharpe, A.G. *J. Chem. Soc.* **1949**, 2901.
59. Einstein, F.W.B.; Rao, P.R.; Trotter, J.; Bartlett, N. *J. Chem. Soc. (A)* **1967**, 478.
60. Johnson, W.M.; Dev, R.; Cady, G.H. *Inorg. Chem.* **1972**, *11*, 2260.
61. Schützenberger, P. *Compt. Rend.* **1870**, *70*, 1134.
62. Schützenberger, P. *Compt. Rend.* **1870**, *70*, 1287.
63. Schützenberger, P. *Bull. Chim. France* **1870**, *14*, 97.
64. Manchot, W.; Gall, H. *Chem. Ber.* **1925**, *58B*, 2175.
65. Kharash, M.S.; Isbell, H.S. *J. Am. Chem. Soc.* **1930**, *52*, 2919.
66. Browning, J.; Goggin, P.L.; Goodfellow, R.J.; Norton, M.J.; Rattray, A.J.M.; Taylor, B.F.; Mink, J. *J. Chem. Soc. Dalton Trans.* **1977**, 2061.
67. Calderazzo, F.; Belli Dell'Amico, D. *Pure Appl. Chem.* **1986**, *58*, 561.
68. Calderazzo, F. *Pure Appl. Chem.* **1978**, *50*, 49.
69. Belli Dell'Amico, D.; Calderazzo, F.; Marchetti, F. *J. Chem. Soc. Dalton Trans.* **1976**, 1829.
70. Nakamoto, K. *Infrared Spectra of Inorganic Compounds*; 2nd ed., John Wiley & Sons: New York, NY, 1970; p. 78.
71. Adelhelm, M.; Barker, W.; Höhn, E.G.; Jacob, E. *Chem. Ber.* **1991**, *124*, 1559.
72. Jones, L.H. *Inorganic Vibrational Spectroscopy*; Marcel Dekker: New York, NY, 1971; Vol. 1, p. 122.
73. Hurlburt, P.K.; Anderson, O.P.; Strauss, S.H. *J. Am. Chem. Soc.* **1991**, *113*, 6277.

74. Hurlburt, P.K.; Rack, J.J.; Dec, S.F.; Anderson, O.P.; Strauss, S.H. *Inorg. Chem.* **1993**, *32*, 373.
75. Pyykko, P. *Chem. Rev.* **1988**, *88*, 563.
76. Lee, K.C.; Aubke, F. *Inorg. Chem.* **1984**, *23*, 2124.
77. Cotton, F.A.; Kraihanzel, C.S. *J. Am. Chem. Soc.* **1962**, *84*, 4432.
78. Cotton, F.A.; Kraihanzel, C.S. *Inorg. Chem.*, **1963**, *2*, 533.
79. Braterman, P.S. *Metal Carbonyl Spectra*; Academic Press: New York, NY, 1975.
80. Kettle, S.F.A. *Top. Cur. Chem.* **1977**, *71*, 111.
81. Cotton, F.A.; Wilkinson, G. *Advanced Inorganic Chemistry*, 5th ed.; John Wiley & Sons: New York, 1988; p. 1021.
82. Abel, E.W.; Tyfield, S.P. *Adv. Organomet. Chem.* **1970**, *8*, 117.
83. Mann, B.E. *Adv. Organomet. Chem.* **1974**, *12*, 133.
84. Avazino, S.C.; Bakke, A.A.; Chen, H.-W.; Donahue, C.G.; Jolly, W.L.; Lee, T.H.; Ricco, A.J. *Inorg. Chem.* **1980**, *19*, 1931.
85. Barber, M.; Connor, J.A.; Guest, M.F.; Hall, M.B.; Hiller, I.H.; Meridith, W.N.E. *J. Chem. Soc. Farad. Disc.* **1972**, *54*, 219.
86. Chadwick, B.M.; Sharpe, A.G. *Adv. Inorg. Chem. Radiochem.* **1966**, *8*, 83.
87. Wang, C.; Rettig, S.J.; Trotter, J.; Aubke, F., to be published.
88. Herzberg, G. *Spectra of Dialonic Molecules*; 2nd ed., Van Nostrand: Toronto, 1966; p. 522.
89. Stromnova, T.A.; Kuz'mina, L.G.; Vargaftik, M.N.; Mazo, G. Ya.; Struchkov, Yu.T.; Moiseev, I.I. Trans. from *Izv. Akad. Nauk SSSR, Ser. Khim.* **1978**, *3*, 720.
90. Moiseev, I.I.; Stromnova, T.A.; Vargaftig, M.N.; Mazo, G.Ya.; Kuz'mina, L.G.; Struchkov, Yu.T. *J. Chem. Soc. Chem. Comm.* **1978**, 28.

RECEIVED May 4, 1993

Chapter 23

Synthesis, Structure, and Reactivity of Highly Soluble Organotitanium Lewis Acids

Charles H. Winter and Xiao-Xing Zhou

Department of Chemistry, Wayne State University, Detroit, MI 48202

The synthesis, structure, and reactivity of complexes of the formula $[(\eta^5\text{-C}_5(\text{Si}(\text{CH}_3)_3)_n\text{H}_{5-n})\text{Ti}(\text{acac})_2]^+\text{CF}_3\text{SO}_3^-$ ($n = 2,3$; $\text{acac} = 2,4\text{-CH}_3, \text{CF}_3$, or $t\text{Bu}$ disubstituted acetylacetonates) is described. These species exhibit modest to excellent solubility in alkane and perfluoroalkane solvents. Furthermore, initial reactivity studies are overviewed. These complexes possess varying degrees of hydrolytic stability, depending upon the acetylacetonate substituents, and undergo stepwise hydrolysis to ultimately afford titanium oxide. The course of the hydrolyses is described along with the crystal structures of key intermediates. The results of this work suggest new structures that may be more reactive toward the electrophilic functionalization of organic and fluoroorganic molecules.

The selective functionalization of strong bonds in organic molecules has intrigued and perplexed chemists since the beginning of modern chemistry. Alkanes represent an abundant fraction of petroleum feedstocks and are extremely difficult to transform into more useful products, due to the relative chemical inertness of carbon-hydrogen and carbon-carbon bonds. Although tremendous advances have been made in alkane functionalization strategies, such studies are clearly in their infancy (1,2). Halocarbon activation is usually considered to be easier than alkane activation (e.g., Grignard reagents, lithium-halogen exchange, etc.), but fluorocarbons are the exception, usually being unreactive and difficult to convert to useful products (3-6). Yet, industry is becoming increasingly dependent on fluorocarbon materials for a diverse array of applications, including medicine (4), materials science applications (high-temperature greases, coatings, etc.) (5), and as Freons (5,6). The fluorocarbon issue has even reached the popular press, due to the imminent ban of chlorofluorocarbons as solvents and refrigerants (6). It is clear that increasing use of alkanes and fluorocarbons will require better methods for their functionalization.

These important considerations have not been overlooked by organometallic chemists, since the selective activation of hydrocarbons (7-11) and fluorocarbons (12,13) by transition metals is currently a topic of intense research activity. Intermolecular oxidative addition of alkane C-H bonds has been achieved

0097-6156/94/0555-0366\$08.00/0
© 1994 American Chemical Society

in several middle and late transition metal systems (7-10). Another distinct type of alkane activation has been termed σ -bond metathesis, which has been observed in a number of electrophilic early transition metal, lanthanide, and actinide systems (11). In this process, the C-H bond of an alkane reacts with a metal-carbon bond to produce a new metal-carbon bond with liberation of a new alkane. Reaction of the metal-carbon bonds with electrophiles affords entry into a wide variety of functionalized organic products. Correspondingly less is known about the ability of transition metals to activate carbon-fluorine bonds, although a few transition metal and lanthanide mediated C-F bond cleavage reactions have recently appeared (12,13).

Large-scale industrial alkane activation is usually carried out using acidic zeolite catalysts (14). Protons in the cages of the three-dimensional network act as superacids and promote the isomerization, cracking, and reforming of saturated alkanes. Interaction of the proton with an alkane is thought to form a carbonium ion (R_4CH^+), which is then partitioned into products (15,16). While fluorocarbon activation has not been studied as intensively as alkane functionalization strategies, several intriguing studies (17-19) have demonstrated that antimony pentafluoride and related main group Lewis acids promote a variety of fluorocarbon transformations, including the dimerization and isomerization of fluoroalkenes, addition of aromatics to perfluoroallyl cations, and nucleophilic trapping of perfluoroallyl cations. Significantly, the electrophilic hydrocarbon and fluorocarbon activations outlined above have little analogy in the reactions of homogeneous transition metal complexes.

In the context of the above considerations, we have sought to explore the synthesis of highly electrophilic early transition metal cations whose reactivity toward alkanes and fluorocarbons might resemble that of superacids or antimony pentafluoride (20-25). The approach has been to utilize a transition metal center that is cationic, in its highest oxidation state, and which contains no d electrons. A further requirement is to render such complexes soluble in hexane and other nonpolar solvents to eliminate strongly coordinating solvents that might inhibit the reactivity of the open coordination sites. In this context, we report an overview of the synthesis, structural characterization, and reactivity of complexes of the formula $[(\eta^5-C_5(Si(CH_3)_3)_nH_{5-n})Ti(acac)_2]^+CF_3SO_3^-$ ($n = 2,3$; $acac = 2,4-CH_3, CF_3$, or tBu disubstituted acetylacetonates). These species exhibit modest to excellent solubility in alkane and perfluoroalkane solvents and demonstrate that ionic complexes can be solubilized into even the most nonpolar solvents with the appropriate choice of ligands. Furthermore, initial reactivity studies are described. These complexes possess varying degrees of hydrolytic stability, depending upon the acetylacetonate substituents, and undergo stepwise hydrolysis to ultimately afford titanium oxide. The course of these hydrolyses is described along with the crystal structures of key intermediates. Finally, while no alkane and perfluoroalkane activation processes have been discovered, the results of this work suggest new structures that that may be more reactive toward strong bonds in organic molecules.

Results

Synthesis of Highly Soluble Cationic Organotitanium Lewis Acids. In order to approach the synthesis of highly soluble and electrophilic Lewis acids, we chose to initially concentrate on titanium, since its highest oxidation state, titanium(IV), is the best known and because complexes in this oxidation state are often powerful Lewis acids. Trimethylsilyl-substituted cyclopentadienyl ligands (26,27) were chosen as the solubility-enhancing groups for a variety of reasons,

including ease of synthesis, high lipophilicity, ready access to titanium complexes, and for their simple NMR spectra. Moreover, it had been indicated that complexes containing polysilylated cyclopentadienyl ligands were significantly more soluble in nonpolar solvents than the analogous unsubstituted derivatives (28). Diketonates were selected as ancillary ligands because it was anticipated that the strongly-bound oxygen ligand environment would stabilize an ionic complex. Finally, the triflate counterion was utilized because it tends to be noncoordinating and is a poor fluoride donor (29). This analysis led to complexes of the formula $[(\eta^5\text{-C}_5(\text{Si}(\text{CH}_3)_3)_n\text{H}_{5-n})\text{Ti}(\text{acac})_2]^+\text{CF}_3\text{SO}_3^-$ ($n = 2, 3$; acac = 2,4-CH₃, CF₃, or ^tBu disubstituted acetylacetonates) (30), whose synthesis and chemistry is described below.

Treatment of 1,3-bis(trimethylsilyl)cyclopentadienyltitanium trichloride with silver triflate (1.1 equiv) and an acetylacetonate RCOCH₂COR (2 equiv, R = CH₃, ^tBu, CF₃) in refluxing dichloromethane for 4-10 h afforded the triflate complexes $[(1,3\text{-C}_5(\text{Si}(\text{CH}_3)_3)_2\text{H}_3)\text{Ti}(\text{CH}_3\text{COCHCOCH}_3)_2]^+\text{CF}_3\text{SO}_3^-$ (**1**, 76%), $[(1,3\text{-C}_5(\text{Si}(\text{CH}_3)_3)_2\text{H}_3)\text{Ti}(\text{^tBuCOCHCO^tBu})_2]^+\text{CF}_3\text{SO}_3^-$ (**2**, 71%), and $[(1,3\text{-C}_5(\text{Si}(\text{CH}_3)_3)_2\text{H}_3)\text{Ti}(\text{CF}_3\text{COCHCOCF}_3)_2\text{OSO}_2\text{CF}_3]$ (**3**, 83%; eq 1). Similar reactions using 1,2,4-tris(trimethylsilyl)cyclopentadienyltitanium trichloride and RCOCH₂COR (R = ^tBu, CF₃) afforded $[(1,2,4\text{-C}_5(\text{Si}(\text{CH}_3)_3)_3\text{H}_2)\text{Ti}(\text{^tBuCOCHCO^tBu})_2]^+\text{SO}_2\text{CF}_3^-$ (**4**, 68%), and $[(1,2,4\text{-C}_5(\text{Si}(\text{CH}_3)_3)_3\text{H}_2)\text{Ti}(\text{CF}_3\text{COCHCOCF}_3)_2\text{OSO}_2\text{CF}_3]$ (**5**, 76%). Complexes **3** and **5** rapidly degraded (ca. 1-2 h) upon exposure to moist air, while complexes **1**, **2**, and **4** were indefinitely stable to ambient conditions.

Solid State Structures. The crystal structures of **1**, **3**, and **4** were determined to understand the bonding involved in these complexes. The perspective views are shown in Figures 1-3.

Complex **1** was ionic in the solid state, with the triflate oxygens being >4 Å from titanium (Figure 1). The cyclopentadienyl ligand was bonded to titanium in a pentahapto fashion, with an average titanium-carbon distance of 2.36 Å. The titanium acetylacetonate oxygen distances averaged 1.96 Å (Ti-O(1) 1.951(4), Ti-O(2) 1.958(4), Ti-O(3) 1.971(4), Ti-O(4) 1.969(4) Å). A notable feature was the large empty coordination site that occupied a position trans to the cyclopentadienyl ligand. The angle between the planes of the acetylacetonate ligands (defined by Ti, O(1), O(2) and Ti, O(3), O(4)) was 122°, which indicates the size of the open site.

Complex **3**, by contrast, was molecular in the solid state and existed in an approximately octahedral geometry (Figure 2; hfac fluorines removed for clarity). One diketonate ligand spanned an axial and equatorial site, while the other occupied two equatorial sites. The cyclopentadienyl ligand was bonded in a normal pentahapto fashion, with an average titanium-carbon bond length of 2.38 Å. The three equatorial titanium oxygen bonds (Ti-O(1) 2.007(5), Ti-O(3) 2.052(5), Ti-O(4) 2.027(6) Å) ranged between 2.01-2.05 Å, while the axial Ti-O(2) bond length was 2.168(5) Å. The titanium triflate oxygen distance was 2.018(5) Å. The molecular nature of **3** can be rationalized on the basis of the increased Lewis acidity imparted by the trifluoromethyl substituents.

The structure of **4** was determined in order to probe for distortions that would be the result of steric forces between the ring trimethylsilyl groups and the diketonate tert-butyl groups (Figure 3). The complex adopted an ionic structure, similar to **1**, with no interaction between the triflate and the titanium center. The cyclopentadienyl ligand was bonded to titanium in a pentahapto fashion, with an average titanium-carbon distance of 2.38 Å. The titanium acetylacetonate oxygen distances averaged 1.96 Å (Ti-O(1) 1.999(2), Ti-O(2) 1.952(3), Ti-O(3) 1.925(3), Ti-O(4) 2.015(2) Å). Steric crowding was particularly evident in one of

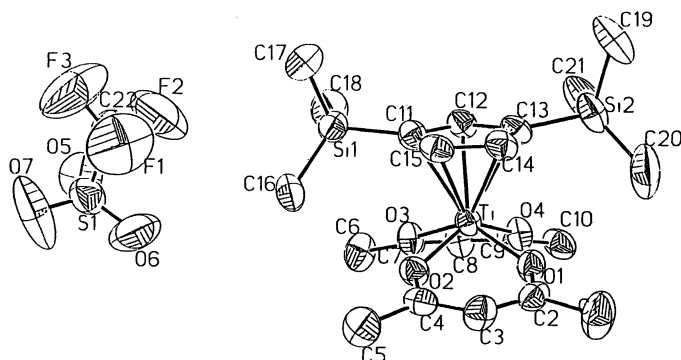
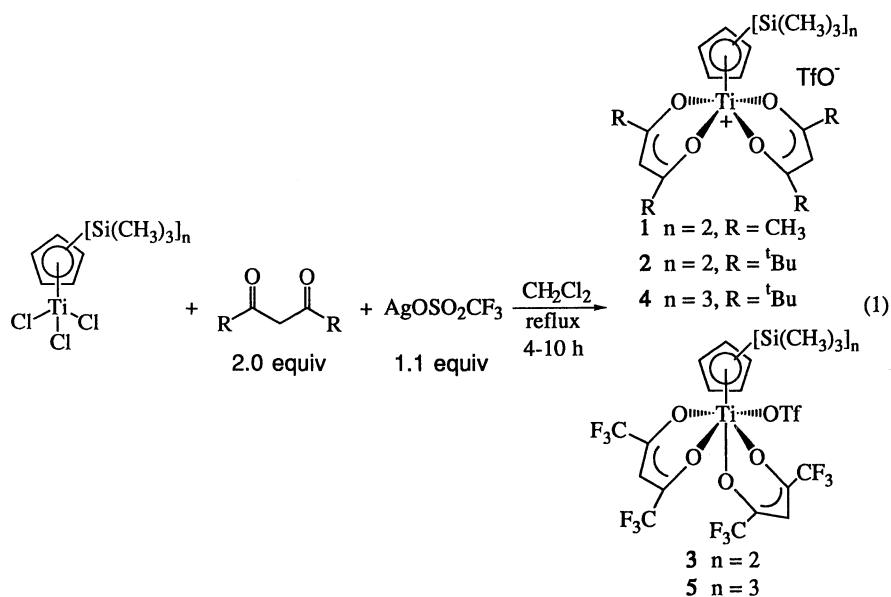


Figure 1. Perspective View of 1 (reproduced from Ref. 22. Copyright 1991, ACS)

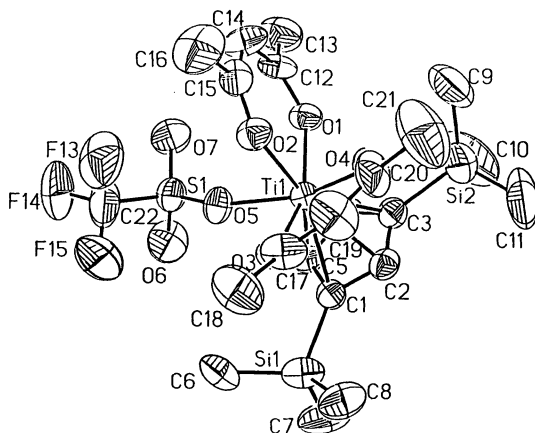


Figure 2. Perspective View of 3 (reproduced from Ref. 22. Copyright 1991, ACS)

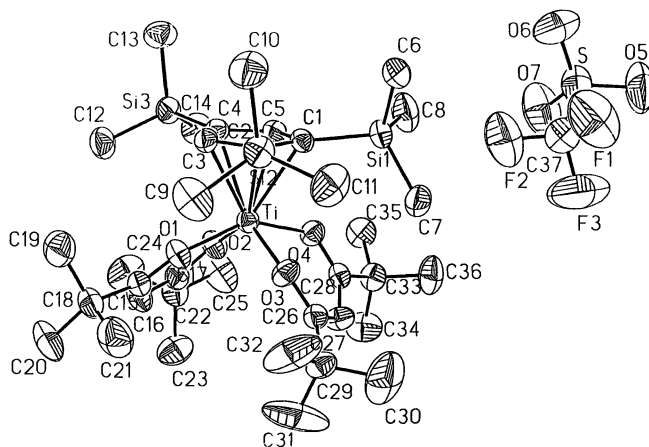


Figure 3. Perspective View of 4

the diketonate ligands, which was severely bent due to trimethylsilyl-tert-butyl crowding.

Since accessibility to an open coordination site was critical to subsequent reactivity studies, the "availability" of the cationic sites in **1** and **4** was explored using models. Figure 4 shows the space filling representations, with the cationic site pointing up in both cases. In complex **1**, an open coordination site clearly exists trans to the cyclopentadienyl ligand and should be available to coordinate Lewis bases. By contrast, the corresponding coordination site in complex **4** is effectively blocked by the tert-butyl groups that are bent away from the cyclopentadienyl ligands. Hence, **4** should be less capable of binding Lewis bases than **1**.

Solubility in Nonpolar Solvents. Table I lists the solubilities of complexes **1-5** in cyclohexane and perfluoromethylcyclohexane. The ionic complexes **1, 2**, and **4** exhibited solubilities of 0.5, 1.5, and 2.5 g/100 mL in cyclohexane, while in the less polar perfluoromethylcyclohexane these values were ~0, 0.03, and 0.06 g/100 mL, respectively. The molecular complexes **3** and **5** were far more soluble than the ionic complexes, as exemplified by their solubilities of 4.9 and >22 g/100mL in cyclohexane and 0.70 and 1.5 g/100 mL in perfluoromethylcyclohexane, respectively. For comparison, 1,3-bis-(trimethylsilyl)cyclopentadienyltitanium trichloride possessed solubilities of 3.7 g/100 mL in cyclohexane and 0.62 g/100 mL in perfluoromethylcyclohexane. Addition of a third trimethylsilyl group leads to a significant increase in solubility, although the diketonate substituents also clearly play a role in solubility enhancement.

Table I. Solubilities^a of **1-5** in Cyclohexane and Perfluoromethylcyclohexane

Complex	Cyclohexane		Perfluoromethylcyclohexane	
	M^b	g/100mL ^c	M^b	g/100mL ^c
1	0.008	0.5	~0.0	~0.0
2	0.020	1.5	0.0004	0.03
3	0.060	4.9	0.0085	0.70
4	0.030	2.5	0.0007	0.06
5	>0.25	>22	0.017	1.5
(1,3-C ₅ (Si-(CH ₃) ₃) ₂ H ₃)-TiCl ₃	0.10	3.7	0.017	0.62

^aSolubilities determined at 23 °C. Solutions were assumed to be saturated if undissolved solid was present after stirring for 0.5 h. ^bSolubilities expressed in mol/L. ^cSolubilities expressed in g/100 mL.

Reaction Chemistry. Our initial goal was to develop highly electrophilic complexes that would react directly with alkanes or fluorocarbons to produce rearranged or functionalized products. Unfortunately, treatment of **1-5** with saturated alkanes and fluorocarbons under a variety of conditions did not lead to any detectable alkane or fluorocarbon activation. Evidently, an oxygen coordination sphere greatly reduces the Lewis acidity of the complexes. However, during the course of these studies, it became apparent that these complexes were exceptionally sensitive to water and that a number of different hydrolysis products were obtained, depending upon the conditions. Since these products would be frequently observed in subsequent chemistry, a careful study of the hydrolysis of **1-5** was initiated. Because of the complexity of the reactions, studies have been largely limited to **1** and **3**.

Hydrolysis of 1. As mentioned previously, complexes bearing alkyl groups on the diketonates were stable to ambient moisture for months, both in the solid state and in solution. However, it became quickly apparent that these complexes were exceptionally water sensitive in the presence of amines and related nitrogen bases. Study of these transformations has revealed a fascinating stepwise hydrolysis.

Treatment of **1** with pyridine in dichloromethane under rigorously anhydrous conditions led to the formation of the pyridine adduct $[(1,3\text{-C}_5(\text{Si}(\text{CH}_3)_3)_2\text{H}_3)\text{Ti}(\text{CH}_3\text{COCHCOCH}_3)_2(\text{NC}_5\text{H}_5)]^+\text{CF}_3\text{SO}_3^-$ (**6**, 96%; Scheme I). Both diketonates were equivalent in the NMR spectra, which suggested that the pyridine was trans to the cyclopentadienyl ligand. No effort was made to rule out fluxional processes, so the exact molecular geometry of **6** has not been conclusively established. Complex **6**, while thermally stable, was hydrolyzed by even traces of water to afford a complex mixture of products. Careful crystallization of the hydrolysis mixture afforded yellow crystals of the dimeric oxo complex $[(1,3\text{-C}_5(\text{Si}(\text{CH}_3)_3)_2\text{H}_3)\text{Ti}(\text{CH}_3\text{COCHCOCH}_3)(\text{O})_2]$ (**7**, 40% based upon the formation of 0.5 mol of **7** from 1.0 mol of **1**). It was subsequently found that simple treatment of **1** with pyridine (5-6 equivs) in wet acetonitrile (ca. 0.5% water) afforded **7** in 86% yield. While **7** was stable toward hydrolysis at ambient temperature, reflux with pyridine (5-6 equivs) in wet acetone or wet acetonitrile afforded the tetrameric oxo complex $[(1,3\text{-C}_5(\text{Si}(\text{CH}_3)_3)_2\text{H}_3)\text{Ti}]_4(\text{O})_6$ (**8**, 31%), with the remainder of the mass balance being titanium dioxide. The structure of **8** is proposed and is based upon the observation of a peak corresponding to the tetramer in the mass spectrum. Complex **8** could be independently prepared in 65% yield by hydrolysis of the triflate complex $[(1,3\text{-C}_5(\text{Si}(\text{CH}_3)_3)_2\text{H}_3)\text{Ti}(\text{OSO}_2\text{CF}_3)_3]$ (vide infra). The extremely high solubility of **8** in hexane precluded the growth of x-ray quality crystals.

The structure of **7** was determined by x-ray crystallography; a perspective view is shown in Figure 5. The molecular geometry consisted of a dimeric planar Ti_2O_2 ring with one cyclopentadienyl and one acetylacetonate ligand bonded to each titanium. The cyclopentadienyl ligands were trans in the dimer. The titanium-oxygen distances for the acetylacetonate ligand were 2.058(4) (Ti-O(1)) and 2.065(3) Å (Ti-O(2)), while the bridging titanium-oxygen distance (Ti-O(3)) was 1.857(3) Å.

When **1** was treated with pyridine (1.5 equiv) in dry diethyl ether or chloroform, addition of water (1.2 equiv) afforded a new complex (**9**) that was converted to **7** over 1-2 hours (Scheme II). ^1H NMR indicated a formulation involving a 1:1:1 ratio of bis(trimethylsilyl)cyclopentadienyl, acetylacetonate, and pyridine ligands. The infrared spectrum did not show O-H absorptions, which ruled out an aquo or hydroxo complex. The oxo-bridged dimer **9** is proposed based on these data and on the facile hydrolysis of **9** to **7**. Other structures for **9** are possible. Unfortunately, the limited thermal and hydrolytic stability of **9** precluded its further characterization.

In confirmation of the modeling predictions outlined above, complex **4** did not form an isolable pyridine complex. In fact, ^1H NMR monitoring of the reaction of **4** with pyridine (5 equivs) in chloroform-d did not show any detectable coordination of the pyridine. However, treatment of **4** with pyridine (5-6 equivs) in refluxing acetonitrile (containing ca. 0.5% water) afforded the dimeric oxo complex $[(1,3\text{-C}_5(\text{Si}(\text{CH}_3)_3)_2\text{H}_3)\text{Ti}(\text{tBuCOCHCOtBu})(\text{O})_2]$ (**77%**). This complex possessed the same gross dimeric structure as **7** (31), but required much more vigorous conditions to effect its synthesis.

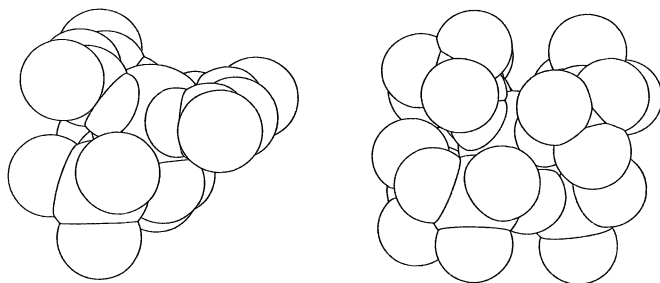
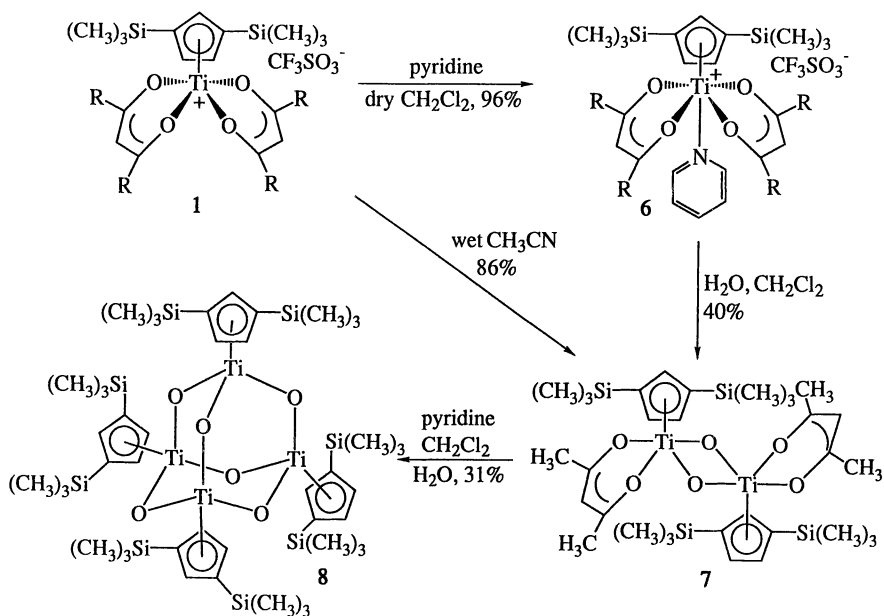


Figure 4. Space Filling Models of 1 and 4



Scheme I. Hydrolysis of 1

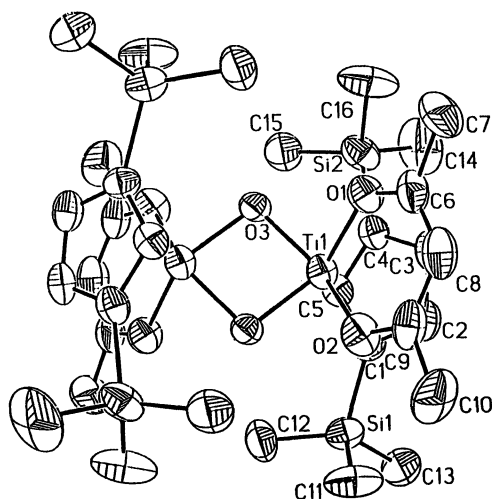
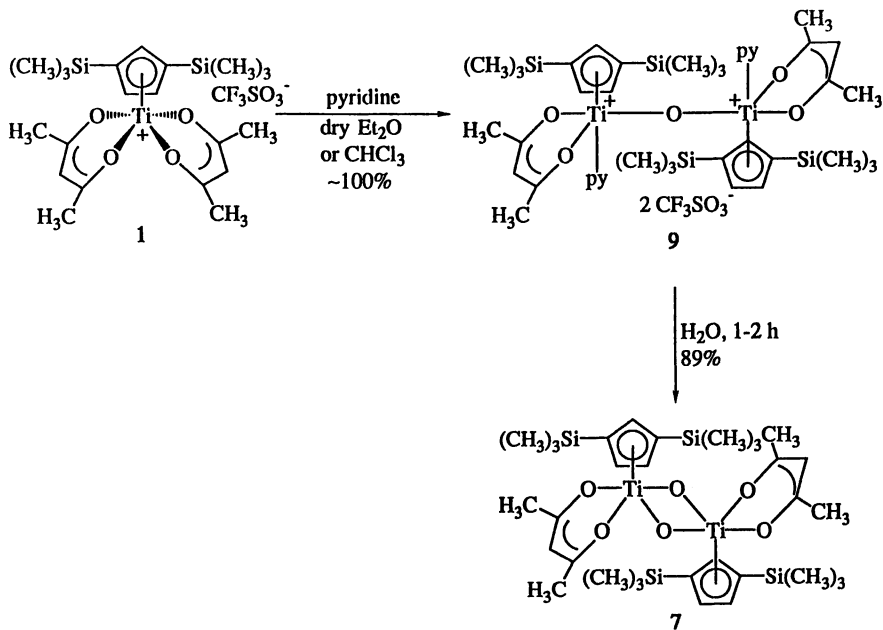


Figure 5. Perspective View of 7



Scheme II. Preparation of 9

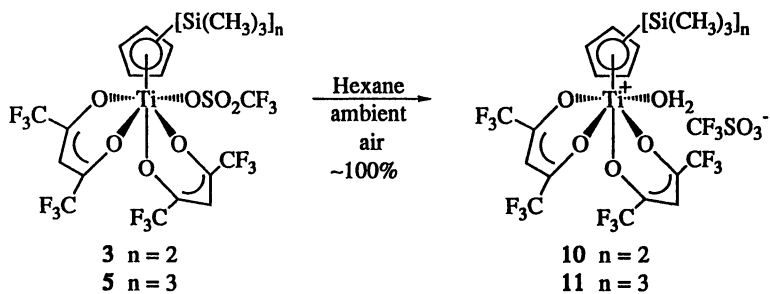
Hence, complex **1** is hydrolyzed in the presence of pyridine to afford the cascade of isolable intermediates $9 \rightarrow 7 \rightarrow 8 \rightarrow \text{TiO}_2$. Several other transient intermediates leading to **9** were detected by NMR monitoring of the hydrolysis of **1** (**31**), but were observed as mixtures and could not be structurally identified. The role of the pyridine is either to deprotonate an intermediate aquo complex or to produce free hydroxide. Either of these scenarios would initiate the hydrolysis sequence and cannot be distinguished based on the available data.

Hydrolysis of 3. Unlike **1**, which required pyridine to promote hydrolysis, complex **3** was hydrolyzed upon exposure to ambient moisture, both in the solid state and in solution. No added base was required. The electron-withdrawing nature of the hexafluoroacetylacetonate ligands makes the titanium center a stronger Lewis acid and therefore more susceptible to hydrolysis. The course of the hydrolysis of **3** is superficially similar to that of **1**, but several major differences are observed that arise from the fluorinated diketonate ligands.

Dissolution of **3** or **5** in hexane, followed by exposure to ambient atmosphere at $-20\text{ }^\circ\text{C}$ for two days afforded quantitative yields of the aquo complexes **10** and **11**, respectively (Scheme III). These reactions were difficult to follow, since both the starting materials and products were deep red and because the water protons were extremely broad in the room temperature ^1H NMR spectra. However, the O-H stretches were clearly observed in the infrared spectrum. For example, **11** showed medium intensity O-H absorptions at 3677, 3554, 3485, 3416, and 3145 cm^{-1} . Fortunately, x-ray quality crystals of **11** were grown and the structure was determined. A perspective view is shown in Figure 6. The cyclopentadienyl ligand was bonded to the titanium in a η^5 -fashion, with an average titanium-carbon distance of 2.41 Å. The equatorial titanium-oxygen distances for the diketonate averaged 2.03 Å (Ti-O(1) 1.996(9), Ti-O(3) 2.047(8), Ti-O(4) 2.041(8) Å), while the axial Ti-O(2) distance was 2.172(8) Å. The titanium-oxygen distance for the coordinated water (Ti-O(8)) was 2.073(7) Å. Interestingly, the aquo ligand occupied an equatorial coordination site. By contrast, the pyridine ligand of **6** was ligated in the axial site trans to the cyclopentadienyl ligand.

Treatment of **3** with wet acetonitrile at room temperature afforded the oxo-bridged dimer $[(1,3\text{-C}_5(\text{Si}(\text{CH}_3)_2\text{H}_3)\text{Ti}(\text{CF}_3\text{COCHCOCF}_3)(\text{O}))_2]$ (**12**, 73%, Scheme IV). The same reaction occurred with diethyl ether or chloroform as solvent; no intermediate hydrolysis products were observed. This is in contrast to the hydrolysis of **1**, where **9** could be isolated and partially characterized. The structure of **12** was evident from the ^1H and ^{13}C NMR spectra and from the mass spectrum, which showed a mass envelope corresponding to the parent ion of the dimer. Furthermore, the crystal structure was determined (**31**). Complex **12** could also be accessed in high yield by exposure of dichloromethane, chloroform, diethyl ether, or acetonitrile solutions of **10** to atmospheric moisture. Finally, hydrolysis of **12** in wet acetone (ca. 0.5% water) at room temperature afforded the tetrameric oxo complex **8** in 43% yield.

The course of hydrolysis for **3** proceeds through the sequence of stable complexes $10 \rightarrow 12 \rightarrow 8 \rightarrow \text{TiO}_2$. The isolation of the aquo complex **10** differentiates the hydrolysis of **3** from that of **1**, where a stable aquo complex was not obtained. Moreover, these hydrolyses ($3 \rightarrow 10 \rightarrow 12 \rightarrow 8$) occur without any added base. This is in contrast to the reactions of **1**, which require a nitrogen base to activate the water. The differences in hydrolytic reactivity between **1** and **3** can be attributed to the electron-withdrawing character of the fluorinated diketonate ligands, which make the titanium center of **3** a much stronger Lewis acid than that of **1**. Hence, the acidity of the aquo ligand in **10** is magnified sufficiently, relative to uncoordinated water, such that water is a strong enough base to deprotonate the



Scheme III. Preparation of the Aquo Complexes **10** and **11**

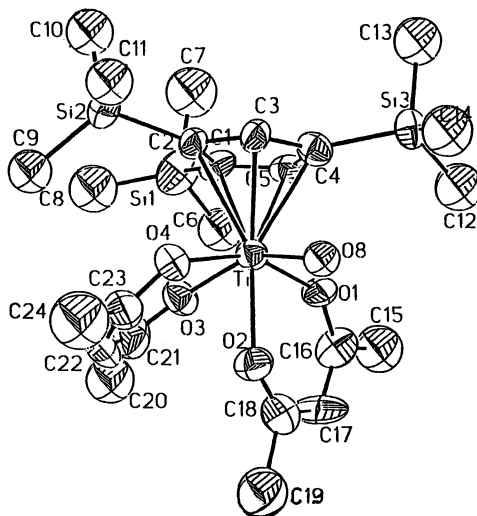


Figure 6. Perspective View of **11**

aquo complex and initiate the hydrolysis cascade. The electron-releasing methyl groups in **1** reduce the Lewis acidity of the titanium center to the point where water is not basic enough to deprotonate an aquo ligand. Moreover, the reduced Lewis acidity of **1**, relative to **3**, is manifested by the preference for softer nitrogen donors over oxygen ligands.

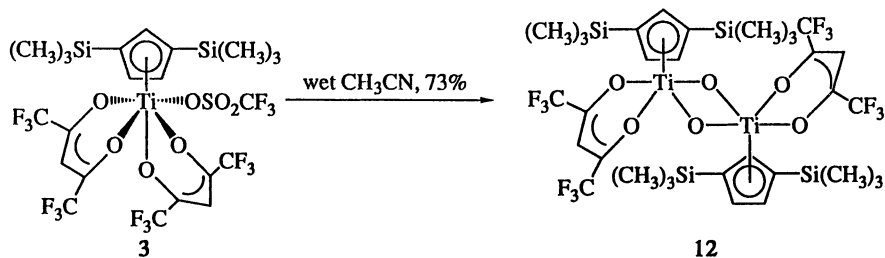
More Reactive Complexes. Because complexes **1-5** did not fulfill the goal of alkane and fluorocarbon activation, it was sought to explore the synthesis of complexes that would be more reactive. The diketonate ligands, in addition to providing oxygen ligation to the titanium with concomitant loss of Lewis acidity, are strongly bonded and have little tendency to dissociate and provide an open coordination site. In response to these considerations, the synthesis and reactivity of the tris(triflate) complex $[(1,3\text{-C}_5(\text{Si}(\text{CH}_3)_2\text{H}_3)\text{Ti}(\text{OSO}_2\text{CF}_3)_3]$ was investigated.

Treatment of $(1,3\text{-C}_5(\text{Si}(\text{CH}_3)_2\text{H}_3)\text{TiCl}_3$ with silver triflate (3 equivs) in dichloromethane for 4 h afforded a complex with the formulation $[(1,3\text{-C}_5(\text{Si}(\text{CH}_3)_2\text{H}_3)\text{Ti}(\text{OSO}_2\text{CF}_3)_3]$ (**13**, 80-90%, Scheme V) (**32**). The empirical formula was determined by microanalysis. ^1H NMR indicated a ca. 60:40 ratio of two isomeric complexes bearing bis(trimethylsilyl)cyclopentadienyl ligands. The presumed isomeric nature of these complexes was supported by reactivity studies, which are outlined in Scheme V. Hence, treatment of **13** with 2,4-pentanedione in dichloromethane afforded the diketonate complex **1** in 80% yield. ^1H NMR monitoring of the reaction with diethyl ether or tetrahydrofuran in dichloromethane- d_2 indicated the quantitative formation of the bis(ether) complexes **14**. Finally, hydrolysis of **13** in dichloromethane afforded the tetrameric oxo complex **8** in 65% yield. These transformations indicated that **13** was significantly more reactive than **1-5**.

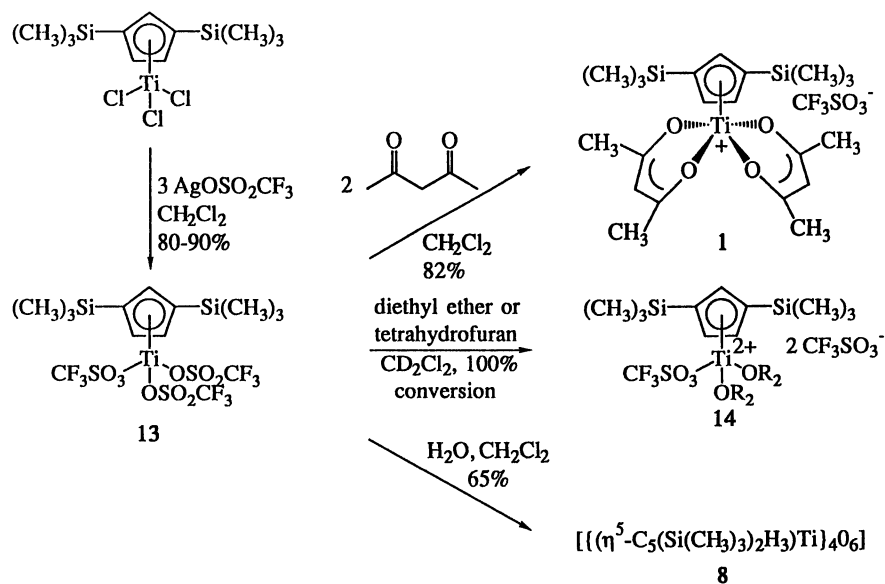
Complex **13** undergoes electrophilic substitution with aromatic substrates. Thus, treatment with benzene in dichloromethane at ambient temperature results in the formation of the diphenyl complex **15** (Scheme VI). Reaction of **13** with pyridine (5-6 equivs) in dichloromethane affords a new complex that is the result of pyridine $\alpha\text{-CH}$ activation. The NMR data clearly show two chemically equivalent coordinated pyridines and pyridine that has lost one of the $\alpha\text{-hydrogens}$. Structure **16** is proposed from the preliminary data. The formation of **15** and **16** was quantitative by ^1H NMR monitoring, but these compounds are reactive and have not been isolated as pure solids. While main group Lewis acids are well known to undergo aromatic substitutions (e.g., mercurations, thallations, etc.) (**33**), relatively little is known about the ability of transition metal complexes to undergo electrophilic aromatic substitution (**34**).

Discussion

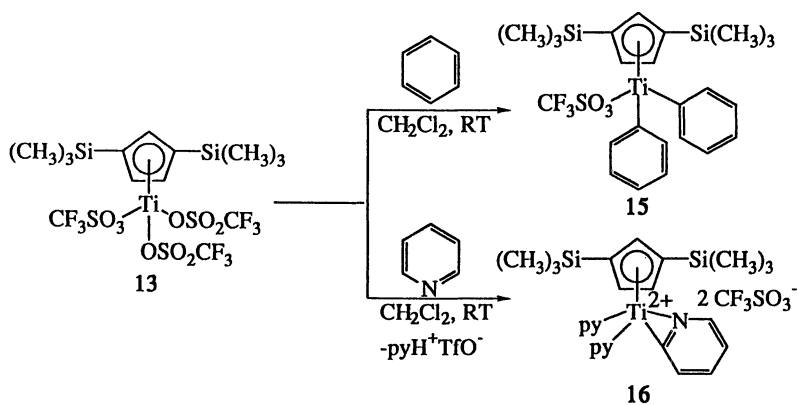
To the best of our knowledge, **1**, **2**, and **4** represent the first examples of cationic transition metal complexes bearing an open coordination site that possess substantial solubilities in alkane and perfluoroalkane solvents. These species are probably tightly ion paired in these media but still appear to be ionic, since the molecular complexes **3** and **5** exhibit considerably higher solubilities. The results of this study provide a rational basis for increasing the solubility of transition metal complexes in nonpolar media through the use of polysilylated cyclopentadienes and substituted acetylacetonates. The fact that the worst case scenario (i.e., cationic complex solubility in cyclohexane and perfluoromethylcyclohexane) is easily achieved implies that simple ligand modification should allow the use of less reactive nonpolar solvents in cases where solvent coordination or reactivity is a problem.



Scheme IV. Preparation of 12



Scheme V. Preparation and Reactions of 13

**Scheme VI.** Electrophilic Aromatic Substitutions with **13**

The structural aspects of 1-5 reveal that the diketone substituents play a critical role in determining the molecular geometries. The alkyl-substituted complexes 1 and 4 exhibit ionic structures in the solid state, with no interactions between the titanium center and the triflate oxygens. Furthermore, an open coordination site is trans to the cyclopentadienyl ring. In 1, this site is capable of binding pyridine to afford a stable complex, while in 4, no evidence for a pyridine adduct could be obtained. The lack of a pyridine complex derived from 4 can be attributed to steric blocking of the open coordination site by the tert-butyl groups of the diketone ligand. In contrast to 1 and 4, the hexafluoroacetylacetonate complex 3 was molecular in the solid state. Furthermore, the triflate occupied an equatorial coordination site cis to the cyclopentadienyl ligand, while one diketone spanned an equatorial and axial site and the other spanned two equatorial sites. The aquo ligand in 11 was also coordinated in an equatorial site. By contrast, the pyridine ligand in 6 occupied the coordination site trans to the cyclopentadienyl ligand. It is not clear if the different binding preferences in 1 and 3 reflect the most Lewis acidic coordination sites or if it simply a measure of the size of aquo versus pyridine ligands.

Complexes 1-5 undergo stepwise hydrolysis to afford oxo clusters and, ultimately, titanium oxide (35,36). The alkyl-substituted complexes 1, 2, and 4 require a nitrogen base to promote hydrolysis, while the trifluoromethyl complexes 3 and 5 undergo spontaneous hydrolysis in the presence of water. This difference is proposed to arise from the electron-withdrawing nature of the hexafluoroacetylacetonate ligands, which make the titanium center a much stronger Lewis acid. Other differences between the alkyl and trifluoromethyl substituted complexes are observed. Complexes 3 and 5 both form stable aquo complexes upon exposure to ambient moisture in hexane, while it was not possible to prepare an aquo complex of 1, 2, or 4. Furthermore, 1 forms a stable pyridine adduct, which is an indication of a softer metal center than that found in 3 or 5. Finally, the hydrolyses of 1-5 provide a model for the hydrolysis of organometallic titanium(IV) complexes to titanium dioxide. It is clear that the ligands play an important role in determining the course of the hydrolyses.

While complexes 1-5 did not promote saturated alkane or fluorocarbon activation, the lessons learned from the synthetic and reactivity studies have led to the synthesis of the tris(triflate) complex 13, which is considerably more reactive due to the labile triflate ligand sphere. A promising example of the enhanced reactivity of 13 is its electrophilic substitution reactions with benzene and pyridine to form titanium-carbon bonds. These "titanations" are formal carbon-hydrogen bond activation processes and should allow access to the many useful organic reactions that titanium-carbon bonds are known to undergo (37,38).

We are continuing to study the synthesis, structure, and reactivity of highly electrophilic early transition metal complexes. Fluorine containing ligands and counterions are playing an increasingly important role in these studies because of the low reactivity associated with the strong carbon-fluorine bonds.

Acknowledgements. We thank the Donors of the Petroleum Research Fund, administered by the American Chemical Society, for support of this work and Mary Jane Heeg for help with the crystallography. We are grateful to the Wilfrid Heller Fund for a thesis fellowship to X.X.Z.

References

- (1) Mortreux, A.; Petit, F. *Industrial Applications of Homogeneous Catalysis*; D. Reidel: Dordrecht, Holland, 1988.
- (2) *Activation and Functionalization of Alkanes*; Hill, C.A., Ed.; Wiley Interscience: New York, 1989.

- (3) Hudlicky, M. *Organic Fluorine Chemistry*; Plenum Press: New York, 1971.
- (4) *Biochemistry Involving Carbon-Fluorine Bonds*; Filler, R.F., Ed.; ACS Symposium Series 28; American Chemical Society: Washington, D.C., 1976.
- (5) *Preparation, Properties, and Industrial Applications of Organofluorine Compounds*; Banks, R.E., Ed.; Ellis Horwood: Chichester, 1982.
- (6) Fisher, D.A.; Hales, C.H.; Filkin, D.L.; Ko, M.K.W.; Sze, N.D.; Connell, P.S.; Wuebbles, D.J.; Isaksen, I.S.A.; Stordal, F. *Nature* **1990**, *344*, 508.
- (7) Crabtree, R.H. *Chem. Rev.* **1985**, *85*, 245.
- (8) Crabtree, R.H.; Hamilton, D.G. *Adv. Organomet. Chem.* **1988**, *28*, 299.
- (9) Brookhart, M.; Green, M.L.H. *J. Organomet. Chem.* **1983**, *250*, 395.
- (10) Brookhart, M.; Green, M.L.H. *Prog. Inorg. Chem.* **1988**, *36*, 1.
- (11) For leading references, see: Thompson, M.E.; Baxter, S.M.; Bulls, A.R.; Burger, B.J.; Nolan, M.C.; Santarsiero, B.D.; Schaefer, W.P.; Bercaw, J.E. *J. Am. Chem. Soc.* **1987**, *109*, 203.
- (12) Richmond, T.G.; Osterberg, C.E.; Arif, A.M. *J. Am. Chem. Soc.* **1987**, *109*, 8091.
- (13) Watson, P.L.; Tulip, T.H.; Williams, I. *Organometallics* **1990**, *9*, 1999.
- (14) For an overview, see: *Zeolite Chemistry and Catalysis*; Rabo, J.A. Ed.; ACS Monograph 171; American Chemical Society: Washington, DC, 1976.
- (15) Olah, G.A.; Prakash, G.K.S.; Williams, R.E.; Field, L.D.; Wade, K. *Hypercarbon Chemistry*; Wiley-Interscience: New York, 1987; pp 218-235.
- (16) Olah, G.A.; Prakash, G.K.S.; Sommer, J. *Superacids*; Wiley-Interscience: New York, 1985; pp 243-249.
- (17) Olah, G.A.; Mo, Y.K. *Adv. Fluor. Chem.* **1973**, *7*, 69.
- (18) Chambers, R.D.; Parkin, A.; Matthews, R.S. *J. Chem. Soc., Perkin Trans. 1* **1976**, 2107.
- (19) Smart, B.E.; Reddy, G.S. *J. Am. Chem. Soc.* **1976**, *98*, 5593.
- (20) Winter, C.H.; Zhou, X.-X.; Heeg, M.J. *Inorg. Chem.* **1992**, *31*, 1808.
- (21) Gassman, P.G.; Deck, P.A.; Winter, C.H.; Dobbs, D.A.; Cao, D.H. *Organometallics* **1992**, *11*, 959.
- (22) Winter, C.H.; Zhou, X.-X.; Heeg, M.J. *Organometallics* **1991**, *10*, 3799.
- (23) Winter, C.H.; Pirzad, S.; Cao, D.H. *J. Chem. Soc., Chem. Commun.* **1991**, 1206.
- (24) Winter, C.H.; Dobbs, D.A.; Zhou, X.-X. *J. Organomet. Chem.* **1991**, *403*, 145.
- (25) Winter, C.H.; Zhou, X.-X.; Dobbs, D.A.; Heeg, M.J. *Organometallics* **1991**, *10*, 210.
- (26) Okuda, J.; Herdtweck, E. *Inorg. Chem.* **1991**, *30*, 1516.
- (27) Antiñolo, A.; Bristow, G.S.; Campbell, G.K.; Duff, A.W.; Hitchcock, P.B.; Kamarudin, R.A.; Lappert, M.F.; Norton, R.J.; Sarjudeen, N.; Winterborn, D.J.W.; Atwood, J.L.; Hunter, W.E.; Zhang, H. *Polyhedron* **1989**, *8*, 1601.
- (28) Lappert, M.F.; Singh, A.; Atwood, J.L.; Hunter, W.E. *J. Chem. Soc., Chem. Commun.* **1981**, 1190.
- (29) Beck, W.; Sünkel, K. *Chem. Rev.* **1988**, *88*, 1405.
- (30) All stable complexes described throughout this manuscript have been completely characterized by spectroscopic and analytical methods.

- (31) Winter, C.H.; Zhou, X.-X., unpublished results.
- (32) Winter, C.H.; Rivas, L.M., unpublished results.
- (33) Taylor, R. *Electrophilic Aromatic Substitutions*; Wiley: Chichester, 1990.
- (34) Aoyama, Y.; Yoshida, T.; Sakurai, K.; Ogoshi, H. *J. Chem. Soc., Chem. Commun.* **1983**, 478.
- (35) Babcock, L.M.; Klemperer, W.G. *Inorg. Chem.* **1989**, *28*, 2003.
- (36) Roth, A.; Floriani, C.; Chiesi-Villa, A.; Guastini, C. *J. Am. Chem. Soc.* **1986**, *108*, 6832.
- (37) Alelyunas, Y.W.; Jordan, R.F.; Echols, S.F.; Borkowsky, S.L.; Bradley, P.K. *Organometallics* **1991**, *10*, 1406.
- (38) Buchwald, S.L.; Nielsen, R.B. *Chem. Rev.* **1988**, *88*, 1047.

RECEIVED April 8, 1993

Chapter 24

New Synthetic Routes to Cyclopentadienyluranium(IV) Fluorides Redox and Atom-Abstraction Reactions

Marc Weydert and Richard A. Andersen¹

Department of Chemistry, University of California, and Chemical
Sciences Division, Lawrence Berkeley Laboratory,
Berkeley, CA 94720

A brief history of the preparation and physical properties of Cp_3UF and related metalloceneuranium fluorides is given. New synthetic routes that involve net redox or fluoride-atom abstraction reactions have been developed. These new developments offer new and improved ways to prepare more examples of this relatively rare type of organometallic compound.

Only four cyclopentadienyluranium(IV) fluorides have been described in the literature. Some synthesis details have been published though detailed procedures are not available; those details that are available are often in obscure places. This is unfortunate since Cp_3UF is a molecule with several unusual physical properties. Only one cyclopentadienyluranium(III) fluoride is known and it is mentioned in a scheme in a communication that lists its melting point and ^1H NMR spectrum. It is quite incorrect to say that cyclopentadienyluranium fluorides are well-known. This is, perhaps in part, due to the difficulty in synthesis as no generally applicable synthesis route has been developed. In this brief article we (a) describe the syntheses that have been used, (b) review the physical properties of Cp_3UF , and (c) describe the new synthetic methods that we have developed for cyclopentadienyluranium(IV) fluorides.

Synthesis

The unsubstituted cyclopentadienyl metallocene, Cp_3UF , has been prepared by the reaction of Cp_3UBr and NaF and isolated in 17% yield by vacuum sublimation at 170 °C (1). An apparently better synthesis is the melt reaction between Cp_2Mg and UF_4 giving Cp_3UF in 80% yield (1). The proton transfer reaction between Cp_4U and NH_4F in tetrahydrofuran also gives Cp_3UF in 41% yield (2). This latter

¹Corresponding author: Chemistry Department, University of California, Berkeley, CA 94720

method is not attractive since it is exceedingly difficult to prepare anhydrous NH_4F and the published synthesis of Cp_4U gives yields of 6% (3). The indenyl and methylcyclopentadienyl compounds, $(\text{C}_9\text{H}_7)_3\text{UF}$ (1) and $(\text{MeC}_5\text{H}_4)_3\text{UF}$ (4), respectively, have been mentioned though only in passing; no synthetic reaction nor details were given. The disubstituted metallocene derivative, $[(\text{Me}_3\text{Si})_2\text{C}_5\text{H}_3]_2\text{UF}_2(\text{thf})_n$ was mentioned as resulting from reaction of $\{[(\text{Me}_3\text{Si})_2\text{C}_5\text{H}_3]_2\text{U}(\text{BF}_4)(\text{F})\}_2$ and BF_3 in tetrahydrofuran (5).

The only uranium(III) compound mentioned is $[(\text{Me}_3\text{Si})_2\text{C}_5\text{H}_3]_2\text{UF}$, which is presumably a dimer with bridging fluorides since the other halides are dimers, though again no details are given other than melting point and the ^1H NMR absorption for the Me_3Si -groups (6). The insoluble, mixed-valence complex $[\text{Cp}_3\text{U}]_2\text{F}$ has been isolated, though its insolubility renders its purification and characterization difficult (7).

Physical Properties of Cp_3UF

The physical characterization of Cp_3UF was originally described without synthesis details by Fischer, Ammon and Kanellakopoulos (8). The compound is a monomer in the gas phase by mass spectroscopy, but it is suggested to be a dimer in benzene solution by osmometry. The other halides, *viz.*, Cp_3UX where $\text{X} = \text{Cl}, \text{Br}, \text{I}$, are monomeric in the gas and solution phase (1). In addition the ^1H NMR spectrum of the fluoride is unusual since a plot of the reciprocal of the chemical shift relative to absolute temperature (Curie law, $\chi = \text{CT}^{-1}$) is not linear; the other three halides follow the Curie law in all solvents studied (9). In toluene solution the inverse of the chemical shift of the cyclopentadienyl protons in Cp_3UF is essentially temperature independent below -25°C though at temperatures greater than 0°C it is essentially linear in absolute temperature. In tetrahydrofuran, the curves for all of the Cp_3UX compounds are parallel at temperatures above 0°C though below 0°C the slope for Cp_3UF sharply decreases then levels off. This "S" shaped curve is interpreted to be due to a temperature dependent equilibrium between solvated monomer and base-free dimer. Although the averaged chemical shift *i.e.*, a single resonance, (relative to the ^1H NMR time scale) is observed at all temperatures, the relative populations of each hypothetical species and its inherent chemical shift are changing, which gives rise to the non-linear behavior.

The dipole moment of Cp_3UF in benzene is 2.3D, whereas that of Cp_3UCl is 3.9D indicating that the U-F bond moment is greatly reduced upon dimer formation. Alternatively, the effective electronegativity of fluoride is reduced, relative to chloride, by localizing less negative charge on fluoride; *i.e.*, fluoride is acting as a π -donor in an intramolecular sense or as a σ -donor in an intermolecular sense.

The solution optical properties of Cp_3UF show subtle changes on going from toluene to tetrahydrofuran solution. The complex nature of the optical spectra renders them incomprehensible to all but the experts (10). It is noteworthy that, though the optical spectra of Cp_3UX ($\text{X} = \text{Cl}, \text{Br}, \text{I}$) in benzene are essentially superimposable on each other, they are not superimposable upon that of Cp_3UF . Further, the spectrum of Cp_3UF changes, in subtle ways, on lowering the temperature.

The variable temperature solid state magnetic susceptibility studies of Cp_3UF and Cp_3UX ($\text{X} = \text{Cl}, \text{Br}, \text{I}$) are similar, giving μ_{eff} (in Bohr magnetons) values of 2.38 (F), 2.66 (Cl), 2.74 (Br), and 2.75 (I) (11). The magnetic

susceptibility curves, however, behave differently at low temperature, the point at which the compounds become temperature independent depends upon the identity of the halide ligand.

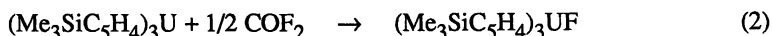
The difference between the properties of base-free Cp_3UF and the other metallocene halides has been rationalized by postulating that there is electron exchange between the two Cp_3U fragments in the fluoride-bridged dimer and this coupling is not possible in the other metallocenes as these are discrete monomers in solution and in the solid state. This postulate is weakened by the X-ray crystallographic study of Cp_3UF which shows it to be a "normal" monomer (12). The geometry about the uranium center is pseudo-tetrahedral with the averaged Cp (centroid) -U-Cp (centroid) angle of 117° and a U-F distance of $2.11(1)\text{\AA}$. The monomers are connected by long U-F...U intermolecular contacts of 3.9\AA . This contact brings the U-F bond into close proximity to the cyclopentadienyl ring hydrogen atoms of the adjacent molecule with a F...H-C(Cp) contact distance of 2.6\AA . The solid state structure of Cp_3UF casts doubt on the interpretation of the results of the "sporting techniques". The solid state structure does not rule out association in solution, though it does make this postulate tenuous. Nothing has appeared in the literature that addresses these apparent discrepancies in this most curious molecule, Cp_3UF .

New Synthesis Studies

The work that is discussed below illustrates two new types of reactions that are useful for the preparation of cyclopentadienyluranium fluorides, *viz.*, (1) redox reactions, in which the uranium center is oxidized from trivalent to tetravalent, and (2) fluoride-atom abstraction reactions, in which the uranium center does not change oxidation state in the net reaction. Our work usually is with substituted-cyclopentadienyl ligands such as MeC_5H_4 or $\text{Me}_3\text{SiC}_5\text{H}_4$ since the starting materials are more soluble in hydrocarbon solvents, making purification easier. In addition, the ^1H NMR spectrum consists of more than a single resonance, making impurities easier to detect.

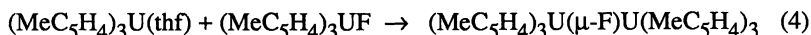
We developed the synthesis of the cyclopentadienyluranium fluorides by a serendipitous route; exploiting our good fortune led to good synthesis routes to these materials. Our initial intent was to explore the possibility of making a PF_3 coordination compound of $(\text{RC}_5\text{H}_4)_3\text{U}$, since PF_3 is a better σ -donor and comparable π -acceptor ligand than CO in d-transition metal chemistry. The trivalent metallocenes $(\text{RC}_5\text{H}_4)_3\text{U}(\text{L})$ molecules can be prepared. Competition studies in toluene solution and solid state X-ray crystallographic studies show that the trivalent uranium centers always prefer L to be a phosphine rather than an amine or an alkylisocyanide rather than an alkylcyanide (13). These semi-quantitative studies lead us to prepare the carbon monoxide coordination compound $(\text{Me}_3\text{SiC}_5\text{H}_4)_3\text{U}(\text{CO})$ (14). The compound is not isolable though the CO stretching frequencies (CO, ^{13}CO , C^{18}O) in solution and in the solid state leave no doubt that the monocarbonyl exists in these two phases. This series of experiments lead us to expose $(\text{MeC}_5\text{H}_4)_3\text{U}(\text{thf})$ to PF_3 in the hope that a solid phosphine complex analogous to that of $(\text{MeC}_5\text{H}_4)_3\text{U}(\text{PMe}_3)$ would result (15). Instead we isolated $(\text{MeC}_5\text{H}_4)_3\text{UF}$, presumably P_2F_4 is the other product (13b). From this beginning we developed the new synthetic routes that are described below.

1. Redox-Reactions: In the trimethylsilylcyclopentadienyl system, the base-free uranium(III) precursor $(\text{Me}_3\text{SiC}_5\text{H}_4)_3\text{U}$ is available (16). In contrast to the methylcyclopentadienyl system, tetrahydrofuran coordinates only weakly to $(\text{Me}_3\text{SiC}_5\text{H}_4)_3\text{U}$ and is easily removed under reduced pressure. A variety of substrates react smoothly with $(\text{Me}_3\text{SiC}_5\text{H}_4)_3\text{U}$ to form $(\text{Me}_3\text{SiC}_5\text{H}_4)_3\text{UF}$ in high yield as outlined in equations 1-3.



The byproduct in the silver fluoride reaction is metallic silver. Trityl fluoride is reduced to bitryl and carbonyl fluoride to carbon monoxide.

An interesting observation involves the reaction of $(\text{MeC}_5\text{H}_4)_3\text{UF}$ with $(\text{MeC}_5\text{H}_4)_3\text{U}(\text{thf})$. Upon mixing, an insoluble material is rapidly precipitated from the reaction mixture in toluene (equation 4). The precipitate was identified as having the proper stoichiometry for a mixed-valent bridging fluoride compound, similar to



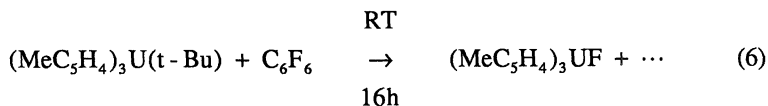
the reported $[(\text{C}_5\text{H}_5)_3\text{U}]_2\text{F}$ (7). Like the unsubstituted analogue, the MeC_5H_4 derivative is insoluble in all common solvents and a detailed characterization is therefore not possible. In an attempt to take advantage of the generally more favorable solubility properties of trimethylsilylcyclopentadienyl compounds, the interaction of $(\text{Me}_3\text{SiC}_5\text{H}_4)_3\text{UF}$ with $(\text{Me}_3\text{SiC}_5\text{H}_4)_3\text{U}$ was studied in hydrocarbons. However, no interaction between $(\text{Me}_3\text{SiC}_5\text{H}_4)_3\text{UF}$ and $(\text{Me}_3\text{SiC}_5\text{H}_4)_3\text{U}$ could be detected by ^1H NMR spectroscopy at room temperature in benzene- d_6 solution. Presumably, the increased bulk of the trimethylsilylcyclopentadienyl ligands does not permit the two metal centers to approach each other to form a fluoride bridge. In keeping with this hypothesis, upon mixing equimolar amounts of $(\text{Me}_3\text{SiC}_5\text{H}_4)_3\text{UCl}$ and $(\text{Me}_3\text{SiC}_5\text{H}_4)_3\text{U}$, only a time-averaged resonance was observed by ^1H NMR spectroscopy in benzene- d_6 solution at room temperature. The longer U-Cl bond (relative to the U-F bond) does not require such a close approach of the two metal centers, thereby reducing the steric hindrance to intermolecular association. However, upon attempted crystallization, $(\text{Me}_3\text{SiC}_5\text{H}_4)_3\text{UCl}$ crystallizes preferentially. This behavior indicates that in the chloride case a dynamic equilibrium is established, rather than the formation of a new static species in solution.

2. Atom-Abstraction Reactions: In addition to $(\text{MeC}_5\text{H}_4)_3\text{U}(\text{thf})$, we also found that $(\text{MeC}_5\text{H}_4)_3\text{U}(\text{t-Bu})$ reacts with trifluorophosphine (equation 5). This net reaction is not a redox-reaction, at least not in a formal sense.



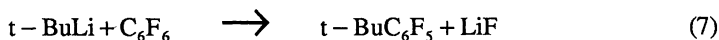
We attempted to expand the scope of this reaction by investigating substrates from which fluorine abstraction would be much more difficult. First, we

focused our attention on hexafluorobenzene, a fluorocarbon with a very strong carbon-fluorine bond (154 kcal/mol). Hexafluorobenzene also possesses aromatic π -electron density, which can allow it to coordinate to a metal center. Precoordination of the substrate to the metal center was shown to be an essential feature in the Cp^*_2Yb -system (18). Indeed, $(\text{MeC}_5\text{H}_4)_3\text{U}(\text{t-Bu})$ reacts with hexafluorobenzene in benzene or toluene solution to form $(\text{MeC}_5\text{H}_4)_3\text{UF}$ (equation 6).

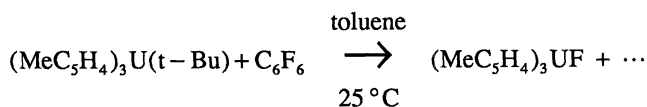


The reaction kinetics are dependent on the concentration of hexafluorobenzene; the more hexafluorobenzene is added to the reaction mixture, the faster the reaction proceeds.

By NMR-spectroscopy, GC and GC-MS techniques, the organic products of this reaction were found to be isobutane, isobutene, pentafluorobenzene and t-butylpentafluorobenzene. Note that by GC, the hexafluorobenzene used in these reactions was shown to be free of pentafluorobenzene. The identity of these products was confirmed by comparison to authentic compounds. A sample of t-butylpentafluorobenzene was synthesized independently from hexafluorobenzene and t-butyllithium (equation 7).



In addition, small amounts of 2,3,4,5,6-pentafluoro-4'-methylbiphenyl were isolated from the reaction mixture, when the reaction between hexafluorobenzene and $(\text{MeC}_5\text{H}_4)_3\text{U}(\text{t-Bu})$ was carried out in toluene. This compound was identified by comparison to reported literature data (19). Small quantities of bibenzyl were detected by GC. Traces of hexamethylethane, the coupling product of two t-butyl radicals, are found in all samples as well. Other products present in trace amounts were not characterized. The relative amounts of these organic products are given in Scheme 1.

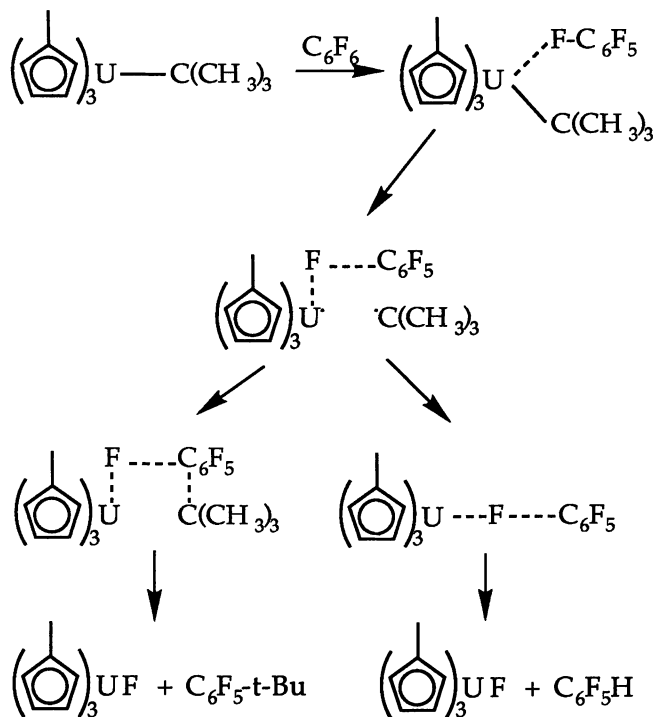


t-BuC ₆ F ₅	C ₆ F ₅ H	Isobutane	Isobutene
1	2	2	1

Scheme 1

This product distribution is temperature dependent. If the temperature is raised, the amount of coupled product t-butylpentafluorobenzene decreases with respect to the other reaction products, and the ratio of isobutane and isobutene approaches 1:1. The fact that the rate of reaction depends on the concentration of hexafluorobenzene is suggestive of a bimolecular reaction mechanism, rather than a

free-radical mechanism initiated by uranium-carbon bond homolysis. Thus, coordination of hexafluorobenzene followed by ligand-induced uranium-carbon bond homolysis is expected to initiate the reaction, similar to the reaction of other substrates with $(\text{MeC}_5\text{H}_4)_3\text{U}(\text{t-Bu})$ (20). In order to explain the formation of *t*-butylpentafluorobenzene one can assume a caged radical pair as shown in Scheme 2. If the *t*-butyl radical escapes from this solvent cage pentafluorobenzene

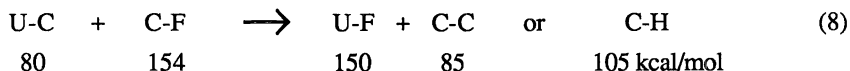


Scheme 2

and isobutane/isobutene are expected to be the products. But if the *t*-butylradical remains in the cage, radical coupling is expected to yield *t*-butylpentafluorobenzene. From this model the product distribution is expected to be temperature dependent, since at higher temperatures more radical escape from the solvent cage should take place. Thus the amount of *t*-butylpentafluorobenzene relative to pentafluorobenzene should decrease at higher reaction temperatures. This is indeed observed experimentally.

It is reasonable to postulate that the main driving force for the reaction of $(\text{MeC}_5\text{H}_4)_3\text{U}(\text{t-Bu})$ with hexafluorobenzene is thermodynamic. A weak uranium-carbon bond and a carbon-fluorine bond have to be broken. This is offset by the formation of a strong uranium-fluorine bond and either a carbon-carbon or a carbon-hydrogen bond. As illustrated in equation 8, the uranium-fluorine bond energy can be estimated to be on the order of 150 kcal/mol based on known thermochemical data for uranium fluorides (21). The carbon-fluorine bond dissociation energy for hexafluorobenzene is reported to be 154 kcal/mol (17). The

uranium-carbon bond energy can be estimated at 80 kcal/mol based on measurements in thorium organometallic compounds (22). Finally the carbon-carbon and carbon-hydrogen bond strengths are known to be on the order of 85 and 105 kcal/mol, respectively (23). Based on these data, the reaction should be enthalpically favored. Especially considering that the uranium-tertiary alkyl bond is probably quite a bit weaker than the 80 kcal/mol estimate based on measurements for primary alkyl compounds.



Conclusions

This brief manuscript summarizes the older literature about cyclopentadienyl-uranium fluorides and our new synthetic approaches to them. One of the motivations for these studies, other than the desire to learn how to prepare them in good yields, was to learn more about the postulated electron-exchange processes that are suggested to explain the magnetic behavior in the solid and solution phases, which in turn was motivated by our demonstration of such a phenomenon in the pentavalent uranium compound $[(\text{MeC}_5\text{H}_4)_3\text{U}]_2[\mu\text{-}1,4\text{-N}_2\text{C}_6\text{H}_4]$ (24). Alas, the variable temperature ^1H NMR spectra of $(\text{MeC}_5\text{H}_4)_3\text{UF}$ follow Curie Law behavior from $+90^\circ\text{C}$ to -90°C in toluene and in tetrahydrofuran- d_8 . This disturbing result suggests that either the experimental results on Cp_3UF are in error, as might be inferred from the X-ray crystal structure, or the small change in substituent on the cyclopentadienyl ring modifies the behavior of the resulting metallocene. Further experiments are needed to decide between these two alternatives.

Experimental Section

General. Unless otherwise noted, materials were obtained from commercial suppliers and were used without further purification. Toluene and hexane were distilled under nitrogen from sodium or sodium/benzophenone immediately prior to use. Deuterated solvents were heated at reflux over sodium and subsequently distilled from sodium. Silver fluoride was obtained from Pennwalt and washed with anhydrous HF. Trityl fluoride was obtained from Columbia and COF_2 was obtained from Matheson; both reagents were used without further purification. $(\text{Me}_3\text{SiC}_5\text{H}_4)_3\text{U}$ was prepared as reported previously (16a). Full experimental details on the reactions of $(\text{MeC}_5\text{H}_4)_3\text{U}(\text{t-Bu})$ will be reported elsewhere (20). All compounds were handled using standard Schlenk techniques under a nitrogen or argon atmosphere or in an inert atmosphere dry box under argon. Melting points were determined in sealed capillaries under argon and are uncorrected. Infrared spectra were recorded as Nujol mulls between CsI plates on a Perkin-Elmer 580 instrument. ^1H -NMR spectra were measured at 89.56 MHz on a JEOL-FX90Q instrument equipped with Tecmag Libra software and are reported in δ values relative to tetramethylsilane with positive values to high frequency. Mass spectra were obtained with an Atlas MS-12 spectrometer. Elemental analyses were performed by the Microanalytical Laboratory operated by the College of Chemistry, University of California, Berkeley.

(Me₃SiC₅H₄)₃UF: a) A solution of (Me₃SiC₅H₄)₃U (1.75 g; 2.69 mmol) in 50 mL of toluene was added by cannulae to AgF (0.34 g; 2.7 mmol). The reaction mixture was stirred for 48 h at room temperature. The solvent was removed under reduced pressure and the resulting solid was extracted with 150 mL of hexane. After filtration, the volume of the hexane extract was reduced to ca. 60 mL. Cooling to -80 °C yielded green crystals of (Me₃SiC₅H₄)₃UF (1.12 g; 62.2%), m.p. 73-75 °C. ¹H-NMR (C₆D₆; 30 °C): δ = 6.21 (s, 2H); -4.62 (s, 9H); -14.80 (s, 2H) ppm. EIMS: M⁺ = 668 amu. Anal. Calcd for C₂₄H₃₉FSi₃U: C 43.1, H 5.89. Found: C 42.7, H 5.83. IR (Nujol, CsI): 1310(w), 1260(w), 1245(s), 1175(m), 1045(m), 900(m), 835(s), 785(s), 750(m), 690(w), 635(s), 625(w), 490(s), 420(s) cm⁻¹. By comparison to the IR-spectrum of (Me₃SiC₅H₄)₃UCl the stretch at 490 cm⁻¹ can be assigned to the U-F stretching mode.

b) To a solution of (Me₃SiC₅H₄)₃U (1.38 g; 2.12 mmol) in 50 mL of hexane was added COF₂ (70 mg; 1.1 mmol) by vacuum transfer. The reaction mixture was stirred for 24 h at room temperature. The solvent was removed under reduced pressure and the resulting solid was extracted with 100 mL of hexane. After filtration, the volume of the hexane extract was reduced to ca. 50 mL. Cooling to -80 °C yielded green crystals of (Me₃SiC₅H₄)₃UF (0.46 g; 32%). The material obtained had physical and spectroscopic properties identical to the material obtained under a).

c) A solution of (Me₃SiC₅H₄)₃U (1.01 g; 1.55 mmol) in 50 mL of toluene was added by cannulae to Ph₃CF (0.41 g; 1.6 mmol). The reaction mixture was stirred for 48 h at room temperature. The solvent was removed under reduced pressure and the resulting solid was extracted with 100 mL of hexane. After filtration, the volume of the hexane extract was reduced to ca. 50 mL. Cooling to -80 °C yielded green crystals of (Me₃SiC₅H₄)₃UF (0.46 g; 45%). The material obtained had physical and spectroscopic properties identical to the material obtained under a).

Acknowledgment. We thank Prof. R.G. Bergman for helpful discussion. This work was supported by the Director, Office of Energy Research, Office of Basic Energy Sciences, Chemical Sciences Division of the U.S. Department of Energy under Contract No. DE-AC03-76SF00098.

Literature Cited.

1. Kanellakopulos, B. in "Gmelin Handbuch der Anorganische Chemie" Uranium Supplement, Vol. E2.
2. Dornberger, E.; Klenze, R.; Kanellakopulos, B. *Inorg. Nucl. Chem. Letters* **1978**, *14*, 319.
3. Fischer, E.O.; Hristidu, Y. Z. *Naturforsch.,B* **1962**, *17B*, 275.
4. Fischer, R.D. in "Fundamental and Technological Aspects of Organo-f-Element Chemistry," Marks, T.J. and Fragala, I. (eds.) **1985**, Reidel (Dordrecht), p. 306.
5. Hitchcock, P.B.; Lappert, M.F.; Taylor, R.G. *J. Chem. Soc. Chem. Comm.* **1984**, 1084.
6. Blake, P.C.; Lappert, M.F.; Taylor, R.G.; Atwood, J.L.; Hunter, W.E.; Zhang, H. *J. Chem. Soc. Chem. Comm.* **1986**, 1394.
7. Kanellakopulos, B.; Dornberger, E.; von Ammon, R.; Fischer, R.D. *Angew. Chem. Int. Ed. English* **1970**, *9*, 957.

8. Fischer, R.D.; von Ammon, R.; Kanellakopulos, B.K. *J. Organomet. Chem.* **1970**, *25*, 123.
9. For a review of paramagnetic NMR applied to the f-block metallocenes, see (a) Fischer, R.D. in "*Organometallics of the f-Elements*" Marks, T.J. and Fischer, R.D. (eds.) Reidel (Dordrecht) **1979**. (b) ref. 4, above, (c) von Ammon, R.; Fischer, R.D. *Angew. Chem. Int. Ed. English* **1972**, *11*, 675, and (d) Jahn, W.; Yünlü, K.; Oroschin, W.; Amberger, H.D. and Fischer, R.D. *Inorg. Chim. Acta* **1984**, *95*, 85.
10. For detailed reviews see (a) Edelstein, N.M. in "*Organometallics of the f-Elements*", Marks T.J. and Fischer, R.D. (eds.) Reidel (Dordrecht) **1979**, p. 37. (b) Edelstein, N.M. in "*Fundamental and Technological Aspects of Organo-f-Element Chemistry*" Marks T.J. and Fragala, I. Reidel (Dordrecht) **1985**, p. 229, and (c) Kanellakopulos, B. in "*Gmelin Handbuch der Anorganischen Chemie*" Uranium Supplement Vol. A6 **1983**.
11. Aderhold, C.; Baumgärtner, F.; Dornberger, E.; Kanellakopulos, B. *Z. Naturforsch.,A* **1978**, *33A*, 1268.
12. Ryan, R.R.; Penneman, R.A.; Kanellakopulos, B. *J. Am. Chem. Soc.* **1975**, *97*, 4258.
13. (a) Brennan, J.G.; Stults, S.D.; Andersen, R.A.; Zalkin, A. *Inorg. Chim. Acta* **1987**, *139*, 201. (b) Brennan, J.G.; Stults, S.D.; Andersen, R.A.; Zalkin, A. *Organometallics* **1988**, *7*, 1329.
14. Brennan, J.G.; Andersen, R.A.; Robbins, J.L. *J. Am. Chem. Soc.* **1986**, *108*, 335.
15. Brennan, J.G.; Zalkin, A. *Acta Crystallogr., Sect. C* **1985**, *C41*, 1038.
16. (a) Brennan, J.G.; Andersen, R.A.; Zalkin, A. *Inorg. Chem.* **1986**, *25*, 1756-1760. (b) Zalkin, A.; Brennan, J.G.; Andersen, R.A. *Acta Crystallogr., Sect C* **1988**, *C44*, 2104.
17. Smart, B.E. in "*The Chemistry of Functional Groups*", Supplement D, S.Patai and Z. Rapoport (eds.), **1983**, John Wiley, New York, Chapter 14.
18. Burns, C.J.; Andersen, R.A. *J. Chem. Soc. Chem. Commun.* **1989**, 136.
19. (a) Brune, H.A.; Hess, R.; Schmidtberg G. *Z. Naturforsch.,B* **1984**, *39B*, 1772. (b) Bolton, R.; Sandall, J.P.B. *J. Fluorine Chem.* **1978**, *12*, 463. (c) Birchall, J.M.; Hazard, R.; Haszeldine, R.N.; Wakalski, W.W. *J. Chem. Soc. (C)* **1967**, 47.
20. Weydert, M.; Brennan, J.G.; Andersen, R.A.; Bergman, R.G. manuscript in preparation.
21. Lau, K.H.; Hildenbrand, D.L. *J. Chem. Phys.* **1982**, *33*, 2646
22. (a) Bruno, J.W.; Marks, T.J.; Morss, L.R. *J. Am. Chem. Soc.* **1983**, *105*, 6824. (b) Sonnenberger, D.C.; Morss, L.R.; Marks, T.J. *Organometallics* **1985**, *4*, 352. (c) Bruno, J.W.; Stecher, H.A.; Morss, L.R.; Sonnenberger, D.C.; Marks, T.J. *J. Am. Chem. Soc.* **1986**, *108*, 7275.
23. McMillen, D.F.; Golden, D.M. *Ann. Rev. Phys. Chem.* **1982**, *33*, 493.
24. Rosen, R.K.; Andersen, R.A.; Edelstein, N.M.; *J. Am. Chem. Soc.* **1990**, *112*, 4588.

RECEIVED March 16, 1993

Chapter 25

Activation of Carbon–Fluorine Bonds by Oxidative Addition to Low-Valent Transition Metals

Carolyn E. Osterberg¹ and Thomas G. Richmond²

¹Department of Chemistry, Concordia College, Moorhead, MN 56560

²Department of Chemistry, University of Utah, Salt Lake City, UT 84112

Several zero valent transition metals [W(0), Mo(0), and Ni(0)] can insert into an aromatic carbon-fluorine bond of suitably designed Schiff base ligands to afford stable divalent oxidative addition products with new metal-carbon and metal-fluorine linkages. New compounds are characterized by multinuclear NMR and IR spectroscopic methods. These reactions proceed readily under mild conditions and show that transition metals can promote cleavage of the strongest single bond to carbon. Qualitatively, the rate of these reactions increase with increasing fluorination of the aromatic ring consistent with a nucleophilic mechanism for C-F activation. In addition the structure of the chelating ligand is crucial in promoting reactivity in these systems. In some instances, carbon monoxide scavenging blocks the open coordination site at the metal necessary for C-F activation. The crystal structure of a model metal-ligand complex prior to oxidative addition is reported. A summary of related examples of carbon-fluorine activation by organometallic complexes is provided and helps place our research in a broader context.

Early work in organometallic chemistry benefited greatly from contemporaneous developments in organofluorine chemistry which provided a new class of ligands which often yielded stable organometallic species (1). In particular, the low reactivity of the strong C-F bond stabilizes perfluoroalkyl complexes to β -elimination pathways (which are often facile in hydrocarbon analogues) and made the synthesis of a wide variety of thermally stable and chemically intriguing molecules. This trend continues to the present (2).

Although relatively uncommon, activation of C-F bonds has been noted in a number of reactions of metal complexes with fluorinated substrates usually under rather vigorous conditions and accompanying low chemical yields. These examples may provide insight into the nature of the high temperature defluorination technologies involving metals such as iron used in the synthesis of fluorinated arenes from saturated perfluorocarbons (3). Replacement of fluorine by hydrogen is sometimes observed in catalytic hydrogenations although usually under forcing conditions compared to the lower halogens (4). Our research group has sought to uncover the fundamental organometallic chemistry of fluorocarbon ligands as models for catalytic reactions and to develop new methods of C-F bond formation.

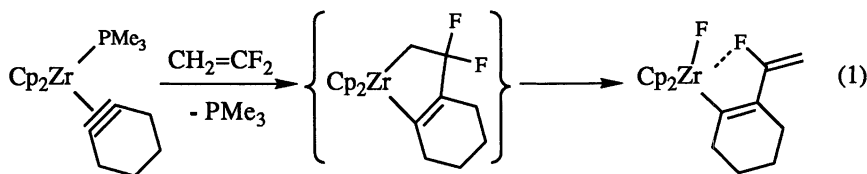
0097-6156/94/0555-0392\$08.00/0

© 1994 American Chemical Society

C-F Bond Activation by Electron Deficient Reagents

A diverse body of chemistry has been developed based on facile fluoride abstraction (5) or halide exchange (6) from perfluoroalkyl ligands by electrophilic reagents to afford perhaloalkylidene ligands (7). These transformations have been the subject of a recent review (8) and will not be discussed in detail since a main group electrophile is usually employed to remove the fluoride.

Thermolysis of $\text{Cp}_2\text{Ti}(\text{C}_6\text{F}_5)_2$ at 150 °C for 24 h affords an 8% yield of $\text{Cp}_2\text{Ti}(\text{C}_6\text{F}_5)\text{F}$ in which a C-F bond is presumably broken to afford the Ti-F bond perhaps through a benzyne intermediate (9). Not surprisingly, other early transition metal systems which have a high affinity for fluoride as a ligand have also been implicated in C-F bond activation. Thus Cp^*_2ScH reacts with tetrafluoroethylene to afford Cp^*_2ScF either through an initial insertion of the tetrafluoroethylene into the scandium-hydride bond followed by β -fluoro elimination or by a σ -bond metathesis pathway (10). Another apparent example of β -fluoro elimination at a zirconium metal center has also been noted (Buchwald, S. L., Massachusetts Institute of Technology, personal communication, 1992).

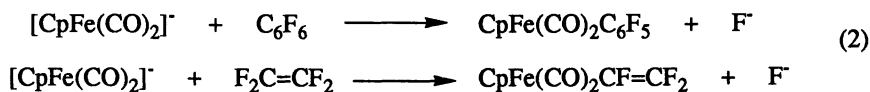


Attempts to prepare $\text{Cp}_2\text{Ti}(\text{CF}_3)_2$ invariably afford titanocene difluoride perhaps by an α -elimination pathway (11). Electron transfer is proposed to trigger C-F activation in tetrakis(trifluoromethyl)cyclopentadienone upon reaction with bis(cyclopentadienyl)-titanacyclobutanes (12).

Organometallic lanthanide and actinide complexes also extract fluoride from organofluorine compounds. Bis(pentamethylcyclopentadienyl)ytterbium reacts with hexafluorobenzene to afford the mixed valence dimer $[\text{Cp}^*_2\text{Yb}]_2(\mu\text{-F})$ and $\text{Cp}^*_2\text{YbC}_6\text{F}_5$ (13). The mixed valence dimer was also isolated from similar, but slower reactions with fluorinated ethylenes, PhCF_3 and PhF . Bis(pentamethylcyclopentadienyl) complexes of Yb, Sm and Eu have been shown to abstract two fluoride ions from perfluorinated olefins to afford dienes (14). Tungsten lamp photolysis accelerates this defluorination reaction. Examples of C-F activation in the chemistry of $(\text{C}_6\text{F}_5)_2\text{Yb}$ also have been noted (15). Fluorocarbons provide a novel mild fluorine source for the preparation of $(\text{MeC}_5\text{H}_4)_3\text{UF}$ from $(\text{MeC}_5\text{H}_4)_3\text{UCMe}_3$ and PhCF_3 (16). These reactions occur under mild conditions and most appear to be irreversible due to the strong metal-fluoride bond formed. Although detailed mechanistic studies have not been reported, initial interaction of these hard, coordinatively unsaturated metals centers with a fluorine lone pair of the fluorocarbon seems likely followed by atom or electron transfer.

C-F Activation by Electron Rich Reagents

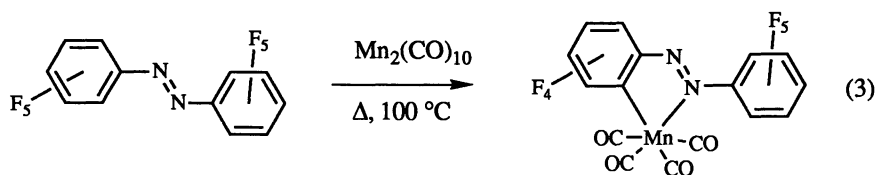
Electron rich d^n ($n = 6, 8, 10$) complexes have also been demonstrated to activate C-F bonds by nucleophilic or oxidative addition pathways. Most common is nucleophilic displacement of fluoride from a perfluoroaromatic or perfluoroolefinic substrate as typified by the chemistry of $[\text{CpFe}(\text{CO})_2]^-$ and related highly nucleophilic anions as in equation 2 (17).



Despite the strong C-F bond strength, fluoride is a good leaving group in these substitution reactions. Reactions such as these usually require highly fluorinated substrates for reasonable yields. No new metal-fluorine bond is formed.

Of particular interest to our research are reactions involving oxidative addition of a C-F bond by a transition metal complex which involve formation of both metal-fluorine and metal-carbon bonds. This transformation is the intellectual cousin of the important C-H oxidative addition process in hydrocarbon chemistry.

The pioneering *ortho*-metallation work carried out by Bruce and co-workers (18) showed that metal-carbon bond formation could be achieved from fluorinated substrates such as perfluoroazobenzene at low valent metal centers, albeit under forcing conditions and with low yields (equation 3).

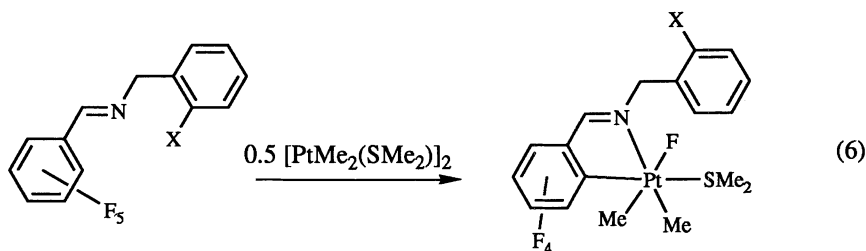
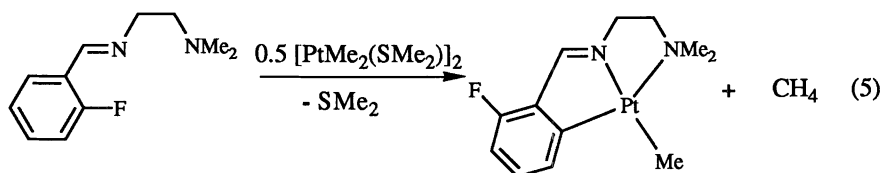
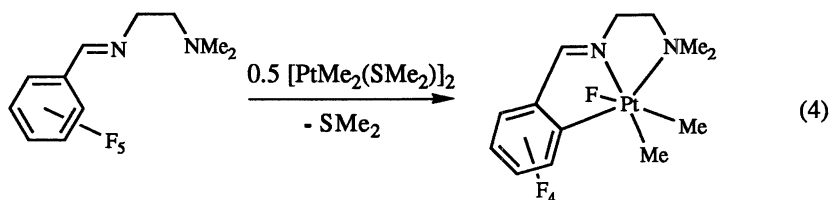


Similar reactions occur for $\text{Mn}(\text{CO})_5\text{H}$ and $\text{CpRu}(\text{PPh}_3)_2\text{Me}$ (19). The fate of the cleaved fluorine atom was not determined. In partially fluorinated systems, C-H and C-F bond activation were found to be competitive (20).

Pyrolysis of perfluoroalkyl iron(II) carbonyl complexes sometimes results in fluorocarbon products that involve shifts of C-F bonds although the role of the metal in these transformations is not clear. For example, heating $\text{CF}_3\text{Fe}(\text{CO})_4\text{I}$ to 160 °C affords tetrafluoroethylene and perfluoropropene perhaps by difluorocarbene formation by α -elimination (21). Quantitative formation of hexafluorocyclobutene is obtained in the decomposition of the octafluorocyclopentane complex $\text{C}_4\text{F}_8\text{Fe}(\text{CO})_4$ (21). β -elimination is proposed to account for the formation of hexafluoropropene by thermolysis of $\text{CF}_3\text{CF}_2\text{CF}_2\text{Fe}(\text{CO})_4\text{I}$ (22). Vicinal defluorination has been observed in the reaction of octafluorocyclooctatetraene with dicobalt octacarbonyl forming the (μ -hexafluorocyclooctatrieneynedicobalt hexacarbonyl (23).

In 1987, we reported the first high yield oxidative addition of a C-F bond to a transition metal center by treating the 1:1 Schiff base ligand derived from 1,2-diaminobenzene and pentafluorobenzaldehyde with $\text{W}(\text{CO})_3(\text{PrCN})_3$ (24). This transformation will be discussed in detail below. Later we demonstrated that ligands derived from *unsym*-N,N-dimethylethylenediamine and pentafluoro-, 2,6-difluoro- and even 2-fluoro- benzaldehydes undergo similar transformations, although heating to 60-100 °C is required for the di- and mono-fluoro systems (25). In the latter case, C-F activation takes place even in the presence of the weaker C-H bond.

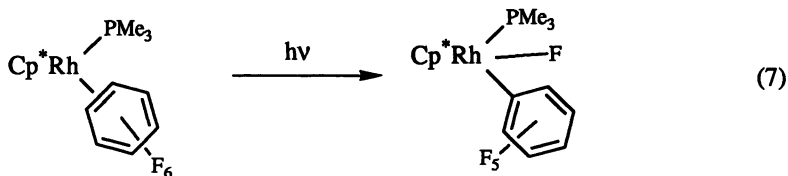
Puddephatt and co-workers have employed these ligand systems at a dimethylplatinum(II) center (equation 4) (26). Interestingly, facile C-F activation is observed for the pentafluorophenyl system, but the product of C-H activation (trapped by loss of methane) is noted for the monofluoro ligand (equation 5). Crespo and co-workers (27) have demonstrated that with proper ligand design (28), C-F activation takes place even in the presence of a weaker C-X (X = H, Cl, Br) bonds (equation 6). These ligand based systems provided the first examples of high yield C-F oxidative addition and continue to afford excellent opportunities to study these reactions.



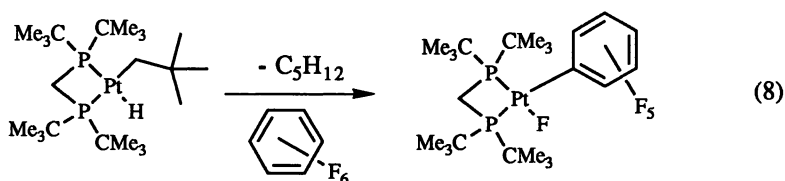
However, intermolecular C-F activation, as noted for some of the electron deficient reagents above, would be most important for catalytic or synthetic applications.

Several electron rich systems hold promise in this area. An early report by Fahey and Mahan noted a 7% yield of thermally unstable *trans*-Ni(PEt₃)₂(C₆F₅)F from C₆F₆ and Ni(PEt₃)₂(COD) over a period of days at 35 °C (29). Although obtained rapidly in 65 % isolated yield, the product of benzoylfluoride oxidative addition, *trans*-Ni(PEt₃)₂(COPh)F was also thermally unstable. An unusual case of C-F activation that may involve nickel was noted by Roundhill and co-workers in the novel synthesis of [PPh₃(C₆F₄H-4)]Br obtained by hydrolysis following reaction of NiBr₂ and C₆F₅Br in molten PPh₃ at 200 °C (30).

Somewhat better defined chemistry is observed for second and third row transition metals. Milstein and coworkers (31) treated C₆F₆ with CH₃Ir(PEt₃)₃ at 60 °C to afford Ir(PEt₃)₂(PEt₂F)C₆F₅ with the expulsion of CH₄ and C₂H₄. In this unique transformation, a C-F bond is broken and new Ir-C and P-F bonds are formed but the metal does not undergo a net change in oxidation state. A multistep mechanism involving electron transfer from a cyclometallated Ir(III) intermediate to hexafluorobenzene, P-C bond cleavage, transfer of fluoride from [C₆F₆]⁻ to iridium and finally to phosphorous was proposed. Only C-H activation is observed for fluorobenzene or 1,3,5-trifluorobenzene under similar conditions. Photochemical C-F activation is observed (equation 7) for Cp^{*}Rh(PMe₃)(η²-C₆F₆) but no C-F activation is detected under thermal conditions (32).



Interestingly, the fluoro complex is rather unstable and scavenges chloride from solvent to yield the crystallographically characterized chloro complex. Most recently, Hoffmann and Unfried (33) have reported the quantitative oxidative addition of C_6F_6 to a 14-electron $\text{Pt}(0)$ fragment generated by reductive elimination of neopentane in neat C_6F_6 (equation 8).



Although not detected, an $\eta^2\text{-C}_6\text{F}_6$ intermediate is suspected.

These examples show that both electron deficient and electron rich metal centers with appropriate ligand complements can serve to activate C-F bonds in well defined reactions. In the case of the early transition and rare earth metals, bimolecular fluoride abstraction seems to be the dominant and irreversible reaction pathway while oxidative addition with formation of new metal-carbon and metal-fluorine bonds is possible for electron rich metals capable of undergoing two electron oxidation. Clearly much mechanistic work remains to be accomplished to understand these important transformations.

Herein we report more details on our preliminary report (24) of C-F activation at tungsten(0) including its extension to molybdenum and nickel systems as well as qualitative observations concerning the mechanism of these transformations.

Results

Condensation in ethanol afford the fluorinated 1:1 Schiff base ligands **1-3** and **8** in high yield as yellow crystalline solids. The imine proton resonance and ^{19}F NMR resonances are collected in Table I.

Insertion of tungsten(0) into the ortho C-F bond of ligands **1-3** is achieved readily at room temperature in THF solution to afford the seven coordinate tungsten(II) products **4-6** in moderate to good yields as air and water stable red-orange crystalline solids (equation 9). The hydrogen bonding ability of the coordinated primary amine is demonstrated by the isolation of THF solvates which are stable to vacuum. Upon coordination to tungsten, the ligand imine resonance shifts downfield by 0.6 - 1 ppm and the typical three band pattern in the carbonyl region of the IR spectrum shifts to higher energy relative to the $\text{W}(\text{CO})_3(\text{EtCN})_3$ starting material (**34**) (Table II). Complexes **4-6** exhibit broad fluorine ($\nu_{1/2} \approx 25$ hz) resonances near -200 ppm in their ^{19}F NMR spectra assigned to the new tungsten-fluoride bond. This resonance shifts further upfield upon addition of water, alcohols or phenols capable of hydrogen bonding to the fluoride (**35**).

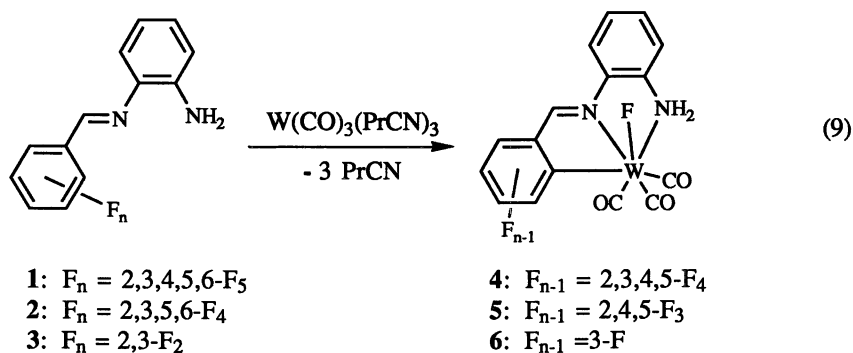


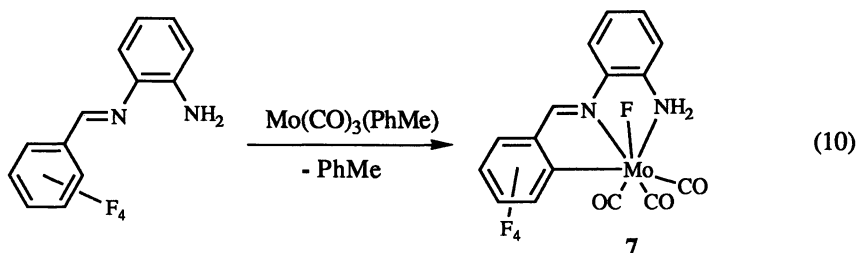
Table I. Selected NMR Data for Ligands and Metal Complexes

Compound	Imine	Aromatic ^{19}F Resonances
1	8.75	-142.85(dd, 2); -151.16(t, 1); -162.32(q, 2)
2	8.73	-139.50(m, 2); -143.64(m, 2)
3	8.87	-139.07(t, 1); -146.98(t, 1)
4	9.72	-113.24(ddd, 1); -139.99(t, 1); 153.56(t, 1), -164.03(t, 1)
5	9.70	-89.27(d, 1); -144.56(m, 2)
6	9.47	-87.38(m, 1)
7	9.42	-114.10(dd, 1); -138.82(t, 1); -153.64(t, 1); -162.97(t, 1)
8	8.56	-141.01(t, 2); -152.00(m, 1); -163.51(q, 2)
9	9.76	-115.84(dd, 1); -141.64(m, 1); -155.00(m, 1); -165.81(t, 1)
10	9.46	-138.89(m, 2); -152.65(dd, 1); -161.31(m, 2)
11 ^a	—	-138.91(dd, 2), -154.65(t, 1); -162.25(dd, 2)
11 ^b	9.29	-136.40(d, 1), -138.44(d, 1); -152.80(t, 1); -161.51(br, 2)
12	8.48	-132.55(dd, 1); -140.52(t, 1); -148.51(t, 1); -161.88(t, 1)

^aRecorded at 0 °C. ^bRecorded at -83 °C.

In addition, the fluorine adjacent to the newly formed tungsten-carbon bond shifts significantly to low field relative to the free ligand. The molecular structure of **4** was verified by X-ray crystallography as previously reported (24).

The molybdenum analogue of **4** may be conveniently prepared using $Mo(CO)_3(THF)_3$ generated *in situ* from the toluene complex (36), as starting material. An unknown deep maroon impurity can be removed by crystallization from THF/hexanes but results in the lower isolated yield than for **4**.



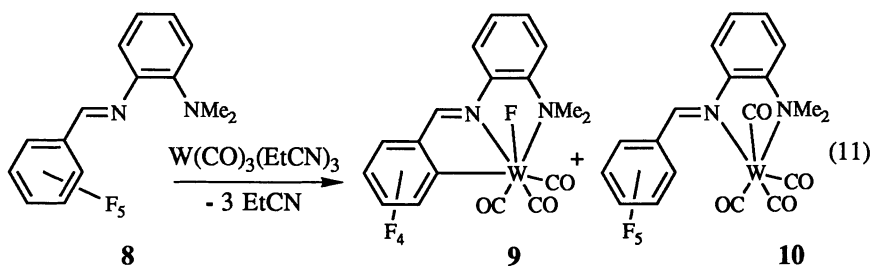
Spectroscopic and physical parameters of **7** are quite similar to **4** but the molybdenum complex is slightly air-sensitive.

Table II: Selected Data for Metal Carbonyl C-F Activation Products

Compound	Yield(%)	δ M-F (ppm) ^a	ν_{CO} (cm ⁻¹) ^b
4	69	-227.4	2020(m), 1937(s), 1906(s)
5	35	-231.5	2017(m), 1933(s), 1900(s)
6	61	-233.1	2012(m), 1927(s), 1892(s)
7	40	-206.1	2026(s), 1952(s), 1917(s)
9	67	-208.7	2020(m), 1937(s), 1907(s)

^aRecorded in (CD₃)₂CO. ^bRecorded in THF.

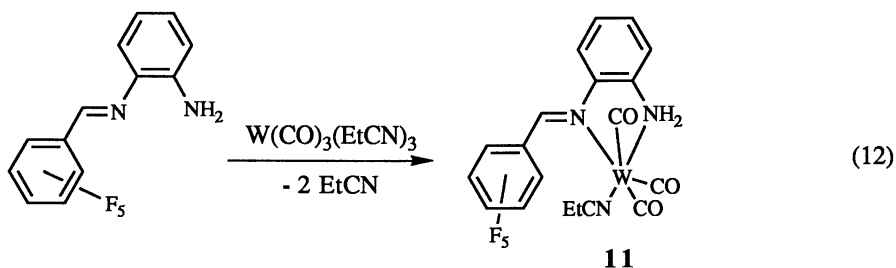
The solubility of **4-7** is somewhat limited in solvents of low coordinating ability as a consequence of their hydrogen bonding properties which leads to the formation of head-to-tail dimers in the solid state (37). Accordingly we have also explored the chemistry of the *N,N*-dimethyl ligand **8**. Under the usual synthetic conditions a 67 % yield of oxidative addition product **9** was crystallized and spectroscopic data are in accord with the proposed structure (equation 11).



Interestingly one of the diastereotopic methyl resonances exists as a doublet in the ¹³C{¹H} NMR spectrum of **9** with ³J_{CF} = 7 Hz. The observation of three distinct CO resonances with coupling to fluoride (δ 234.44 (²J_{CF} = 41 Hz); δ 225.23 (²J_{CF} = 13 Hz); δ 220.65 (²J_{CF} = 8 Hz) indicating that the seven coordinate structure is static and

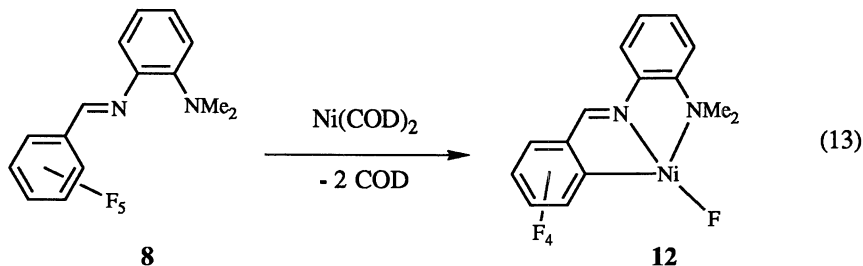
fluoride does not dissociate on the NMR time scale. The tetracarbonyl complex **10** was isolated from the supernatant in 16 % yield. The solution IR spectrum in the carbonyl region shows the expected 4-band pattern for this geometry. The imine resonance shifts downfield upon coordination but the ^{19}F NMR spectra shows an intact pentafluorophenyl group.

Additional insight into the nature of the tungsten(0)-ligand complex prior to oxidative addition is obtained by the generation of the purple mononitrile complex **11** by carrying out the ligand addition in dichloromethane and immediately isolating the precipitate that forms (equation 12).



The low field shift of the imine proton and strong metal carbonyl bands at 1907 and 1792 cm^{-1} are consistent with the proposed structure. Dissolution of the solid **11** in THF results in quantitative spectroscopic conversion to **4**. Dynamic behavior is observed in the ^{19}F NMR spectra of **11** with the most noticeable change being the inequivalence of the two *ortho*-fluorines in the slow exchange limit spectrum recorded at $-83\text{ }^\circ\text{C}$. Coalescence was observed at $-30\text{ }^\circ\text{C}$ and the expected three resonance pattern was obtained at $0\text{ }^\circ\text{C}$.

Since later transition metals are often used in catalytic transformation of C-X bonds (38), we also investigated the reactivity of ligand **8** with $\text{Ni}(0)$.



Four highly coupled aromatic fluorine resonances were observed in the ^{19}F NMR spectra characteristic of the metallacycle structure. Although the Ni-F resonance could not be located in the ^{19}F NMR spectra, its presence was inferred from the $^3\text{J}_{\text{CF}}$ coupling of 6 Hz observed to the carbons of the methyl groups of the ligand. In addition a parent ion was detected in the mass spectrum of **11**.

Discussion

Activation of aromatic carbon-fluorine bonds may be achieved at room temperature under mild condition by the use of appropriately designed chelating Schiff base ligands at low valent tungsten or molybdenum carbonyls. This is the first report of C-F bond activation at molybdenum. It is remarkable that the exceedingly strong C-F bond (154 kcal/mole for C_6F_6 (39)) can be cleaved under such mild conditions. Qualitatively, the pentafluorophenyl system reacts more readily than less heavily fluorinated ligands. For this class of ligands with a 1,2-diaminobenzene backbone, we were unable to detect C-F activation in the ligand derived from 2,4-difluorobenzaldehyde although the 2,3-isomer **3** does react. Kinetic studies show that C-Cl oxidative addition in similar systems is greatly accelerated by electron withdrawing groups on the aromatic ring (40, 41). This is consistent with a nucleophilic mechanism for C-F bond activation akin to nucleophilic aromatic substitution in organic systems (41). Both kinetic and thermodynamic factors appear to favor C-F, in preference to C-H activation in the chemistry of **3**. The metal carbonyl fluoride products are stable while we have demonstrated in related systems that the putative tungsten hydride product of C-H activation is thermodynamically unstable and could not be detected even at $-80\text{ }^\circ\text{C}$ (41). In addition, the carbon of a C-F bond should be more electrophilic than that of a C-H bond favoring attack at the C-F bond by the metal nucleophile.

A single crystal X-ray diffraction study of **10** was carried out since this provides a structural model of the metal-ligand complex before C-F bond activation. An ORTEP diagram with selected bond distances and angles is given in Figure 1. The bond distances and angles are unexceptional, but the favorable geometry for attack of an *ortho*-C-F bond is apparent and probably crucial for the facile reactivity observed. Dynamic ^{19}F NMR studies of **11** provide further insight into the nature of the metal-ligand interaction prior to oxidative addition. The observation of inequivalent *ortho*-fluorines at low temperature suggest that rotation around the F_5C_6 -imine carbon bond is restricted by the crowded nature of the complex. At the coalescence temperature of $-30\text{ }^\circ\text{C}$, $\Delta G^\ddagger = 10.4(5)\text{ kcal/mol}$. Steric interactions between the pentafluorophenyl group and ligands bound to tungsten are probably responsible for this behavior. Thus, after dissociation of the nitrile ligand, complex **11** is in an excellent geometry to insert into the C-F bond. The chelating ligand is crucial in enabling use to observe this reactivity; we have been unable to promote bimolecular C-F activation of C_6F_6 with $W(CO)_3(RCN)_3$ (42). The restricted conformation of the imine ligand once coordinated to the metal center seems most important in promoting C-F activation.

We have extended this chemistry to the later transition metals in the preparation of the "homoleptic" Ni(0) complex of ligand **8**. Based on its diamagnetic behavior, we propose a square planar geometry for **12**. Thus our ligand complement also promotes C-F activation with the metal undergoing a d^{10} to d^8 transformation. The coordinatively unsaturated nature of **12** may allow for further reaction chemistry.

Future Prospects

A wide variety of transition metals have now been shown to be capable of reacting with C-F bonds with highly fluorinated aromatic compounds most susceptible to attack (43). The stability of early transition metal-fluoride bonds suggests that catalytic reactions may be difficult to attain. Thus more work with low valent, later transition metal systems should be pursued. The microscopic reverse of oxidative addition—reductive elimination—may provide a new means of making C-F bonds but this has not yet been demonstrated. Saturated perfluorocarbons provide the next challenge for C-F bond activation by metal reagents (44). Understanding the organometallic chemistry of fluorocarbons may also lend insight into new strategies for destruction of chlorinated organic wastes and development of new synthetic methods for replacement CFC's.

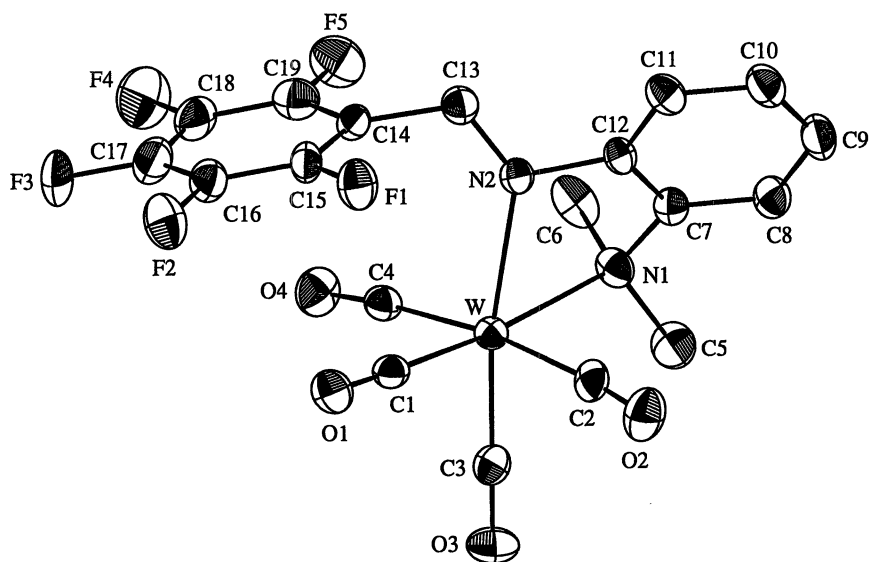


Figure 1. ORTEP representation of **10**. Selected bond distances (\AA): W-N1, 2.351(3); W-N2, 2.241(4); W-C1, 1.954(5); W-C2, 2.027(5); W-C3, 1.953(5); W-C4, 2.012(5); N2-C13, 1.263(6). Selected bond angles (deg): N1-W-N2, 71.3(1); W-N2-C13, 132.6(3); N2-C13-C14, 120.1(4); N1-W-C1, 172.1(2); N2-W-C3, 168.7(2); C2-W-C4, 172.4(2). Reproduced with permission from ref. 40. Copyright 1990 Elsevier Science Publishers BV.

Experimental Section

All manipulations were carried out under a nitrogen atmosphere using standard Schlenk or glove box techniques. Solvents were distilled from appropriate drying agents under nitrogen. FT-IR spectra were recorded in 0.1 mm CaF₂ solution cells and a Varian XL-300 spectrometer was used to record ¹H, ¹³C{¹H} and ¹⁹F (internal CCl₃F reference) NMR spectra. Elemental analysis were carried out by Desert Analytics, Tucson, AZ. Literature preparations were used for the following starting materials: W(CO)₃(PrCN)₃ (34), Mo(CO)₃(C₇H₈) (45), and Ni(COD)₂ (46). Schiff base ligands were isolated in greater than 80% yields as yellow crystalline solids by filtration of the precipitate formed upon condensation of the diamine with the appropriate fluoro-benzaldehyde in ethanol. Selected ¹H and ¹⁹F NMR data are given in Tables I and II.

4. A 100 mL flask was charged with **1** (0.572 g, 2.00 mmol) and W(CO)₃(PrCN)₃ (0.878 g, 2.03 mmol) and 30 mL THF. After stirring for 10 min, the volume of the burgundy solution was reduced under vacuum and 8 mL hexanes were added. Cooling this solution to -10 °C afforded **4** (0.90 g, 1.4 mmol) as a THF solvate (MP, 159 °C, dec). Anal. Calcd for C₂₀H₁₅N₂F₅O₄W: C, 38.36; H, 2.41; N, 4.47; F, 15.17. Found: C, 38.03; H, 2.27; N, 4.63; F, 15.36.

5. This compound was prepared in a similar manner to **4** from ligand **2** but the reaction mixture was twice evaporated to dryness and redissolved in THF to remove released PrCN prior to crystallization (MP = 141-142 °C, dec). Anal. Calcd for C₁₆H₈N₂F₄O₃W·0.2 THF: C, 36.39; H, 1.74; N, 5.05. Found: C, 36.19; H, 1.94; N, 5.04.

6. This compound was prepared as for **4** using ligand **3** but allowed to stir overnight prior to crystallization (MP = 138, dec). Anal. Calcd for C₁₆H₈N₂F₂O₃W·0.5 THF: C, 40.32; H, 2.63; N, 5.22. Found: C, 40.57; H, 2.98; N, 5.22.

7. In 25 mL of THF, Mo(CO)₃(PhMe) (1.07 g, 3.94 mmol) and **1** (1.10 g, 3.85 mmol) were combined. After stirring for 2 h, THF was removed under vacuum and the residue was extracted into 20 mL THF, filtered and evacuated to dryness. This solid was washed with CH₂Cl₂ to remove Mo(CO)₆ and then recrystallized from THF/hexanes to afford orange highly crystalline **7** as a THF solvate (0.71 g, 1.5 mmol). Anal. Calcd for C₂₀H₁₅N₂F₅O₄Mo: C, 44.30; H, 2.79; N, 5.18. Found: C, 44.36; H, 2.75; N, 5.42.

9. This compound was prepared in a similar manner to **5** in 67% isolated yield from ligand **8** (MP = 168, dec). Anal. Calcd for C₁₈H₁₁N₂F₅O₃W: C, 37.14; H, 1.90; N, 4.80. Found: C, 37.28; H, 1.86; N, 4.77.

10. Hexanes were added to the supernatant from the preparation of **9** and cooling to -10 °C produced orange-red crystals in 16 % isolated yield (MP 155-156 °C, dec). IR (THF): 2010(s), 1887(s), 1879(sh), 1844(s) cm⁻¹. Anal. Calcd for C₁₉H₁₁N₂F₅O₃W: C, 37.40; H, 1.82; N, 4.59. Found: C, 37.52; H, 1.69; N, 4.58.

12. Addition of 35 mL of THF to Ni(COD)₂ (2.6 g, 9.5 mmol) and **8** produced a red solution. After stirring overnight, the THF and COD were removed under vacuum. Stirring with an additional 35 mL of THF gave a purple powder (3.0 g, 8.0 mmol) which was isolated by filtration in 86 % yield. A parent peak was observed at 372 amu in the mass spectrum. Anal. Calcd for C₁₅H₁₁N₂F₅Ni: C, 48.31; H, 2.98; N, 7.47. Found: C, 48.17; H, 2.92; N, 7.51.

Single crystals of **10** were obtained from THF/hexanes in the monoclinic space group C2/c with $a = 22.785(3)$, $b = 13.280(2)$, $c = 11.634(2)$ Å, $\beta = 116.41(1)^\circ$ and $Z = 8$. Refinement based on 2521 data with $I > 3\sigma I$ collected on a Syntex P1 ($\lambda_{\text{Mo K}\alpha} = 0.71073$ Å, $\mu = 60.23$ cm⁻¹) and 280 variables gave $R = 0.0240$ and $R_w = 0.0275$ with GOF = 2.23.

Acknowledgments. We thank Dr. Atta M. Arif for solving the crystal structure reported in this work and the Presidential Young Investigator Program of the National Science Foundation for financial support. T. G. R. is an Alfred P. Sloan Research Fellow (1991-1993).

Literature Cited

1. Treichel, P. M.; Stone, F. G. A. *Adv. Organomet. Chem.* **1964**, *1*, 143.
2. Hughes, R. P. *Adv. Organomet. Chem.* **1990**, *31*, 183.
3. Chambers, R. D.; Lindley, A. *J. Chem. Soc., Perkin I*, **1981**, 1064.
4. Hudlicky, M. *J. Fluorine Chem.* **1989**, *44*, 345.
5. Reger, D. L.; Dukes, M. D. *J. Organomet. Chem.* **1978**, *153*, 67. Koola, J. D.; Roddick, D. M. *Organometallics* **1991**, *10*, 591.
6. Richmond, T. G.; Shriver, D. F. *Organometallics* **1983**, *2*, 1062. *Ibid.* **1984**, *3*, 305. Richmond, T. G.; Crespi, A. M.; Shriver, D. F. *Ibid.* **1984**, *3*, 314.
7. Crespi, A. M.; Shriver, D. F. *Organometallics* **1985**, *4*, 1830.
8. Brothers, P. J.; Roper, W. R. *Chem. Rev.* **1988**, *88*, 1293.
9. Chaudhari, M. A.; P. M. Treichel, P. M.; Stone, F. G. A. *J. Organomet. Chem.* **1964**, *2*, 206.
10. Burger, B. J. *Ph. D. Thesis, California Institute of Technology* **1987**.
11. Morrison, J. A. *Abstracts of the 203rd ACS National Meeting*, FLOU 007, **1992**.
12. Burk, M. J.; Staley, D. L.; Tumas, W. *J. Chem. Soc., Chem. Commun.* **1990**, 809.
13. Andersen, R. A.; Burns, C. J. *J. Chem. Soc., Chem. Commun.*, **1989**, 136.
14. Watson, P. L.; Tulip, T. H.; Williams, I. *Organometallics* **1990**, *7*, 1999.
15. Deacon, G. B.; MacKinnon, P. I.; Toung, T. D. *Aust. J. Chem.* **1983**, *36*, 43. Deacon, G. B.; Kopllick, A. J.; Raverty, W. D.; Vince, D. G.; *J. Organomet. Chem.* **1979**, *182*, 121.
16. Andersen, R. A. *Abstracts of the 203rd ACS National Meeting*, FLOU 058, **1992**.
17. King, R. B.; Bisnettee, M. B. *J. Organomet. Chem.* **1964**, *2*, 38.
18. Bruce, M. I.; Godall, B. L.; Sheppard, G. L.; Stone, F. G. A. *J. Chem. Soc., Dalton Trans.* **1975**, 591. Bruce, M. I. *Angew. Chem. Intl. Ed. Engl.* **1977**, *16*, 73.
19. Bruce, M. I.; Gardner, R. C. F.; Goodall, B. L.; Stone, F. G. A. *J. Chem. Soc., Chem. Commun.* **1974**, 186.
20. Bruce, M. I.; Gardner, R. C. F.; Stone, F. G. A. *J. Chem. Soc., Dalton Trans.* **1976**, 81.
21. King, R. B.; Stafford, S. L.; Theichel, P. M.; Stone, F. G. A. *J. Am. Chem. Soc.* **1961**, *83*, 3604.
22. Plowman, R. A.; Stone, F. G. A. *Inorg. Chem.* **1962**, *1*, 518. Krespan, C. G. *J. Fluorine Chem.* **1988**, *40*, 129.
23. Doig, S. J.; Hughes, R. P.; Davis, S. M.; Gadol, A. M.; Holland, K. D. *Organometallics* **1984**, *3*, 1921.
24. Richmond, T. G.; Osterberg, C. E.; Arif, A. M. *J. Am. Chem. Soc.* **1987**, *109*, 8091.
25. Lucht, B. L.; Poss, M. J.; King, M. A.; Richmond, T. G. *J. Chem. Soc., Chem. Commun.* **1991**, 400.
26. Anderson, C. M.; Puddephatt, R. J.; Ferguson, G.; Lough, A. J. *J. Chem. Soc., Chem. Commun.* **1989**, 1297. Anderson, C. M.; Crespo, M.; Ferguson, G.; Lough, A. J.; Puddephatt, R. J. *Organometallics* **1992**, *11*, 1177.

27. Crespo, M.; Martinez, M.; Sales, J. *J. Chem. Soc., Chem. Commun.* **1992**, 822.
28. Poss, M. J.; Arif, A. M.; Richmond, T. G. *Organometallics* **1988**, *7*, 1669.
29. Fahey, D. R.; Mahan, J. E. *J. Am. Chem. Soc.* **1977**, *99*, 2501.
30. Park, S.; Roundhill, D. M. *Inorg. Chem.* **1989**, *28*, 2906.
31. Blum, O.; Frolow, F.; Milstein, D. *J. Chem. Soc., Chem. Commun.* **1991**, 258.
32. Jones, W. D.; Partridge, M. G.; Perutz, R. N. *J. Chem. Soc., Chem. Commun.* **1991**, 264.
33. Hoffman, P.; Unfried, G. *Chem. Ber.* **1992**, *125*, 659.
34. Kubas, G. J. *Inorg. Chem.* **1983**, *22*, 692.
35. Osterberg, C. E.; King, M. A.; Arif, A. M.; Richmond, T. G. *Angew. Chem. Int. Ed. Engl.* **1990**, *29*, 888.
36. Cotton, F. A.; Poli, R. *J. Am. Chem. Soc.* **1988**, *110*, 830.
37. Osterberg, C. E.; Arif, A. M.; Richmond, T. G. *J. Am. Chem. Soc.* **1988**, *110*, 6903.
38. Stille, J. K. *Acc. Chem. Res.* **1977**, *10*, 434.
39. B. E. Smart, *Fluorocarbons*, in: S. Patai and Z. Rappoport (Eds.), *The Chemistry of the Functional Groups, Supplement D.*, Wiley, New York, **1983**, pp. 604-655.
40. Richmond, T. G. *Coord. Chem. Rev.* **1990**, *105*, 221.
41. Poss, M. J. *Ph. D. Thesis, University of Utah*, **1991**.
42. Osterberg, C. E. *Ph. D. Thesis, University of Utah*, **1990**.
43. For a recent photochemically initiated intermolecular C-F bond activation of C₆F₆ at (η⁵-C₅Me₅)Re(CO)₃ see: Klahn, A. H.; Moore, M. H.; Perutz, R. N. *J. Chem. Soc., Chem. Commun.* **1992**, 1699.
44. Selective reductive defluorination of perfluorodecalin to afford perfluoronaphthalene proceeds with good yield upon treatment with sodium benzophenone radical anion: Marsella, J. A.; Gilincinski, A. G.; Coughlin, A. M.; Pez, G. P. *J. Org. Chem.* **1992**, *57*, 2856.
45. Strohmeier, W. *Chem. Ber.* **1961**, *94*, 3337.
46. Krysan, D. J.; Mackenzie, P. B. *J. Org. Chem.* **1990**, *55*, 4229.

RECEIVED March 16, 1993

Chapter 26

Recent Developments in the Chemistry of Fluorinated Isopropoxides and Tertiary Butoxides

A. P. Purdy and C. F. George

Chemistry Division (Code 6120) and Laboratory for the Structure of Matter (Code 6030), Naval Research Laboratory, Washington, DC 20375

Studies on $\text{OCH}(\text{CF}_3)_2$, $\text{OCMe}(\text{CF}_3)_2$, $\text{OCMe}_2(\text{CF}_3)$, and $\text{OC}(\text{CF}_3)_3$ derivatives of the alkali metals, alkaline earth metals, transition metals, and the lanthanide elements are reviewed, with emphasis on work reported since 1988. Alkali and alkaline earth fluoroalkoxides are generally made from reaction between the alcohol and the metal, its hydride, or organometallics. Most syntheses of transition metal derivatives involve reaction between metal halides and alkali or alkaline earth salts, or the alcoholysis of metal alkyls, alkoxides and amides. Coordination between organic fluorine and electropositive metals (ie. Na, Ba, Tl, Pr) is often observed in the crystal structures of these fluoroalkoxides and may be related to their use as chemical vapor deposition precursors for metal fluorides.

Fluorinated metal alkoxides are of interest for a number of reasons. Complexes with bulky fluorinated alkoxy ligands usually have substantially greater volatility and solubility than their unfluorinated counterparts, primarily as a result of low polarizability of the C-F bond (1,2). In addition, the high electronegativity of R_F reduces the basicity of the alkoxy oxygen, which renders extended alkoxy bridged polymers less favorable than those with unfluorinated alkoxy groups (1). These properties are of interest in the design of new precursors for CVD (chemical vapor deposition) and sol-gel types of ceramic synthesis. Of note here is the ability of fluorinated metal complexes to serve as precursors for metal fluorides (3). The high electronegativity and oxidation resistance of fluorinated alkoxy groups can help to stabilize the higher oxidation states of some metals and also finds application in the design of new olefin metathesis catalysts.

Although many types of fluoro-alkoxy ligands are known, this chapter is primarily concerned with the alkoxy derivatives of 1,1,1,3,3,3-hexafluoroisopropanol ($\text{HOCH}(\text{CF}_3)_2$, H[HFIP]), 1,1,1-trifluoro-*tert*-butanol ($\text{HOCMe}_2\text{CF}_3$, H[TFTB]), 1,1,1,3,3,3-hexafluoro-*tert*-butanol ($\text{HOCMe}(\text{CF}_3)_2$, H[HFTB]), and perfluoro-*tert*-butanol ($\text{HOC}(\text{CF}_3)_3$, H[PFTB]). Emphasis is placed on compounds reported after 1988, as an excellent review by Willis details work prior to that time (1). Discussion will focus on the synthesis of these

This chapter not subject to U.S. copyright
Published 1994 American Chemical Society

compounds, their physical properties, and where available, crystal structures. Mention will also be made of CVD experiments using fluorinated alkoxides.

Alkali and Alkaline Earth Derivatives

Reactions between R_FOH and the alkali metals, or their hydrides in Et_2O (4), or with RLi in hexane (5) are the most effective means of preparing the alkali metal [HFIP], [HFTB], and [PFTB] complexes. These colorless, volatile solids are easily purified by vacuum sublimation or distillation. Heavy alkaline earth (Ca, Sr, Ba) complexes are prepared in a similar manner using THF as the solvent (6), and the coordinated THF is removed by heating to 100-130 °C under vacuum. Physical data on these compounds are listed in Table I.

Table I. Alkali and Alkaline Earth Fluoroalkoxides

	Mp (dec)	Subl (pressure)	bNMR $^{19}F(1H)$	ref
Li[HFIP]	194.5-196.5	50 (0.05 mm Hg)		4
Na[HFIP]	114-116(170)	70 (0.05 mm)	-79.25 (4.59)	4
K[HFIP]	--- (150)	30-100 (10^{-5} mm)	-77.47 (4.29) ^c	
Na[PFTB]	143	232 (1 atm) ^a	-77.5	4
Li[PFTB]	142	218 (1 atm) ^a		4
K[PFTB]	> 300(220)	140 (0.2 mm)		4
K[HFTB]	200 (w/dec)	105 (10^{-5} mm)	-80.34 (1.35)	
Ca[PFTB] ₂	--- (260)	140 (10^{-5} mm)	-75.6	6
Sr[PFTB] ₂	--- (320)	230 (10^{-5} mm)	-76.4	6
Ba[PFTB] ₂	--- (320)	280 (10^{-5} mm)	-75.9	6
Ba[HFIP] ₂	--- (260)	230 (10^{-5} mm)	-76.2, -76.1, -74.9 (5.0)	6
Ba[HFTB] ₂	---	---	-76.6 (1.35)	7

^aBoiling point. ^b δ relative to $CFCl_3$; C_4D_8O solvent unless stated otherwise.

^c C_6D_6 solvent.

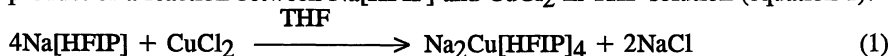
The crystal structure shows Na[HFIP] to be tetrameric, with the [HFIP] groups located at four tetrahedrally arranged corners of a $(Na-O)_4$ cube. Each sodium ion is coordinated to organic fluorine in addition to alkoxy oxygen, the Na-F interactions ranging from 2.365(2) to 2.805(3) Å v.s. 2.31 Å in sodium fluoride (8). As we shall see, this is a feature often observed whenever organofluorine ligands come in contact with electropositive metal ions. It may not be a coincidence that such fluorinated metal complexes usually deposit metal fluorides when used as CVD precursors, although alkali metal fluorides are thermodynamically stable and might be expected to form in any case (9,10). Several fluorinated organosodium complexes, including the alkoxides Na[HFIP] and Na[PFTB], were recently studied as CVD precursors for NaF. The best films were obtained using Na[HFIP] under vacuum with the substrate temperature between 250 and 300 °C (11).

Group 11 Derivatives.

Copper and silver fluoroalkoxides have been synthesized by primarily two methods. One method, ionic metathesis in ethereal solvents between alkali or alkaline earth salts and a copper or silver halide, usually results in a double metal alkoxide product. A second method, alcoholysis of organometallics or unfluorinated alkoxides avoids the presence of other metals but can result in mixed

ligand products. Composition and structure of the product(s) formed seem to be greatly influenced by the steric bulk of the fluorinated ligands.

Copper (II). The volatile double alkoxide $\text{Na}_2\text{Cu}[\text{HFIP}]_4$ is the sole alkoxide product of a reaction between $\text{Na}[\text{HFIP}]$ and CuCl_2 in THF solution (equation 1).

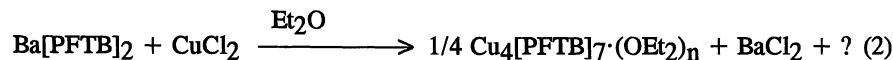


A related barium-copper complex, $\text{BaCu}[\text{HFIP}]_4$, and its THF adduct, $\text{BaCu}[\text{HFIP}]_4 \cdot (\text{THF})_4$, are synthesized in a similar manner from $\text{Ba}[\text{HFIP}]_2$ and CuCl_2 . Both complexes decompose near 200 °C, in marked contrast to the unfluorinated analogue, $\text{Na}_2\text{Cu}(\text{OCHMe}_2)_4$, which decomposes slowly at room temperature (6).

Crystal structures (Figures 1 and 2) show copper to be 4-coordinate in both complexes with a tetrahedrally distorted square planar geometry; the dihedral angle between the O1-Cu1-O1A and O2-Cu1-O2A planes in $\text{BaCu}[\text{HFIP}]_4 \cdot (\text{THF})_4$ and the O1-Cu-O2 and O1A-Cu-O2A planes in $\text{Na}_2\text{Cu}[\text{HFIP}]_4$ are 25.4° and 22.4° respectively. In $\text{Na}_2\text{Cu}[\text{HFIP}]_4$ the $\text{Cu}[\text{HFIP}]_4^{2-}$ ions are linked by both Na-O and Na-F bridges (Na-F 2.481(7)-2.791(7) Å) in a polymeric lattice, but ESR spectroscopy suggests a monomeric structure in THF solution (6). The barium-copper complex $\text{BaCu}[\text{HFIP}]_4 \cdot (\text{THF})_4$ (Figure 2) is monomeric in the solid state as a combination of two alkoxy oxygens, two fluorines, and four THF molecules are sufficient to satisfy the barium coordination sphere and prevent intermolecular association. The positional parameters of $\text{BaCu}[\text{HFIP}]_4 \cdot (\text{THF})_4$ are listed in Table II, and bond lengths and angles are listed in Table III.

Reactions between $\text{Ba}[\text{HFTB}]_2$ and CuCl_2 in ethereal solvents (3:2 mole ratio) initially produce a green-brown solid of empirical formula $\text{Ba}_2\text{Cu}_3[\text{HFTB}]_9\text{Cl}$. Vacuum sublimation above 90 °C affords $\text{Ba}\{\text{Cu}[\text{HFTB}]_3\}_2$, a monomeric, structurally unique alkoxide composed of two Y-shaped, planar $\text{Cu}[\text{HFTB}]_3^-$ ions coordinated to Ba through four of its alkoxy oxygens and eight fluorines (Figure 3) with Ba-F distances ranging from 2.94 to 3.14 Å. A combination of the completely encapsulated 12-coordinate Ba^{2+} ion and the low polarizability of fluorinated ligands make $\text{Ba}\{\text{Cu}[\text{HFTB}]_3\}_2$ one of the most volatile barium compounds known (sublimation 70-90 °C). Furthermore, the ability of sterically demanding ligands to stabilize low coordination numbers, in this case 3-coordinate Cu(II), is clearly demonstrated. The terminal Cu-OCMe(CF₂)₃ distance of 1.781 Å is one of the shortest observed in any Cu(II) complex. Strong nitrogen bases decompose $\text{Ba}\{\text{Cu}[\text{HFTB}]_3\}_2$, for instance $\text{Me}_2\text{N}(\text{CH}_2)_2\text{NMe}_2$ (TMEDA) reacts to afford $\text{Ba}[\text{HFTB}]_2$ and $\text{Cu}[\text{HFTB}]_2 \cdot (\text{TMEDA})$ (7).

With the bulkier [PFTB] ligand, no Ba-Cu(II) double alkoxides are isolated, as excess $\text{Ba}[\text{PFTB}]_2$ does not react. Instead, the reaction of $\text{Ba}[\text{PFTB}]_2$ with CuCl_2 in Et_2O affords a series of highly volatile etherates, from which an orange crystalline compound, tentatively identified as $\text{Cu}_4[\text{PFTB}]_7$ was obtained by vacuum distillation (equation 2).



$\text{Cu}_4[\text{PFTB}]_7$ orange solid MP = 68-71 °C Sublimation (vac) 0 °C
 $\text{Cu}_4[\text{PFTB}]_7 \cdot \text{OEt}_2$ lt. green solid
 $\text{Cu}_4[\text{PFTB}]_7 \cdot (\text{OEt}_2)_n$ n = 2-4 green liquid, n > 4 off-white solid

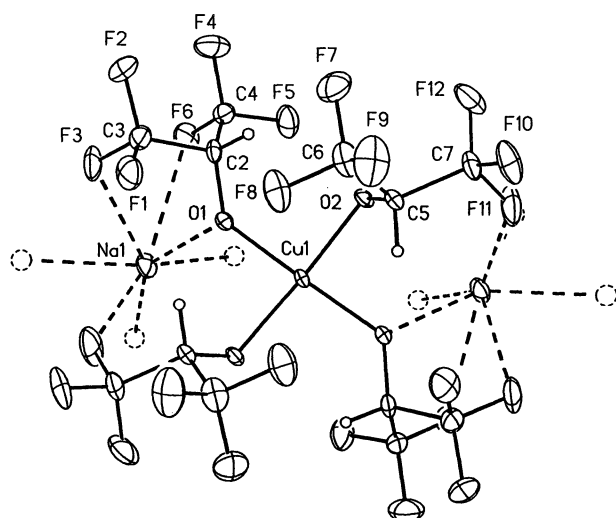


Figure 1. Structure of $\text{Na}_2\text{Cu}[\text{HFIP}]_4$, adapted from ref. 6.

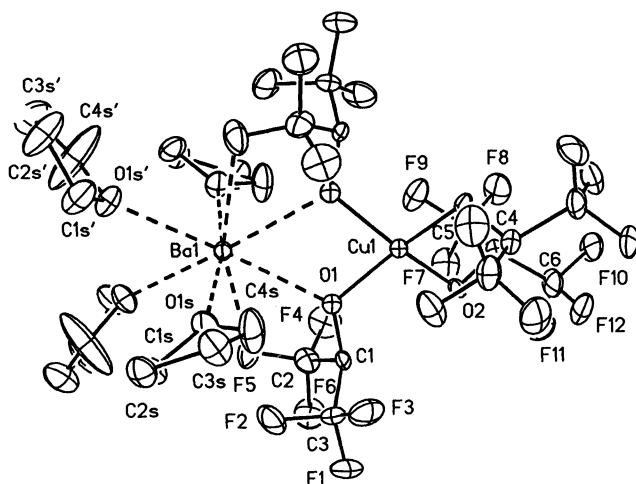


Figure 2. Structure of $\text{BaCu}[\text{HFIP}]_4 \cdot (\text{THF})_4$.

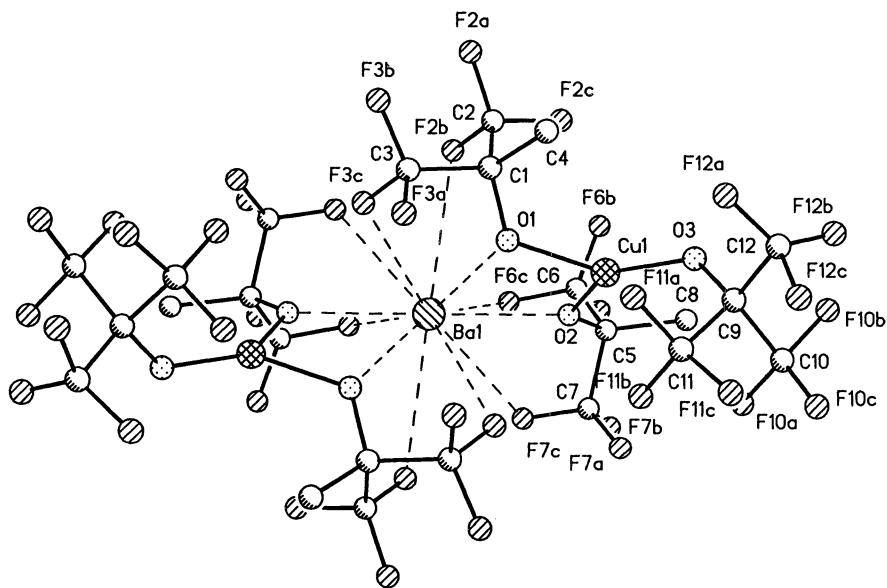


Figure 3. Structure of Ba{Cu[HFTB]₃}₂, adapted from ref 7.

Table II. Atomic Coordinates ($\times 10^4$) and Equivalent Isotropic Displacement Coefficients ($\text{\AA}^2 \times 10^3$) for $\text{BaCu}[\text{HFIP}]_4 \cdot (\text{THF})_4$

	x	y	z	U(eq)
Ba(1)	0	1617(1)	7500	37(1)
Cu(1)	0	-911(2)	7500	38(1)
O(1)	-664(6)	66(6)	6972(4)	41(2)
O(2)	-389(6)	-1785(5)	6777(5)	44(3)
C(1)	-1361(9)	-88(9)	6424(7)	45(5)
C(2)	-1192(13)	460(14)	5782(9)	73(7)
C(3)	-2241(1)	72(12)	6642(11)	69(7)
C(4)	237(10)	-2396(9)	6649(8)	52(6)
C(5)	847(15)	-2010(13)	6162(12)	81(9)
C(6)	-195(13)	-3283(12)	6344(11)	76(8)
F(1)	-2933(6)	-109(8)	6140(7)	115(5)
F(2)	-2327(7)	954(7)	6821(6)	104(5)
F(3)	-2327(6)	-391(8)	7215(6)	102(5)
F(4)	-507(8)	177(8)	5531(6)	110(6)
F(5)	-1081(8)	1331(7)	5955(5)	105(5)
F(6)	-1893(8)	435(8)	5249(5)	119(5)
F(7)	410(8)	-1748(7)	5536(6)	104(5)
F(8)	1481(7)	-2568(7)	6041(6)	106(5)
F(9)	1236(7)	-1257(7)	6466(6)	97(5)
F(10)	401(7)	-3927(6)	6281(7)	111(5)
F(11)	-695(7)	-3157(7)	5701(6)	97(5)
F(12)	-739(7)	-3607(6)	6770(6)	89(5)
O(1S)	-1349(7)	1778(8)	8280(6)	71(4)
C(1S)	-1964(11)	2479(13)	8299(10)	86(8)
C(2S)	-2179(11)	2491(12)	9046(9)	75(8)
C(3S)	-1945(12)	1546(13)	9319(10)	90(8)
C(4S)	-1569(15)	1119(13)	8756(12)	119(12)
O(1S')	447(8)	3130(7)	8345(6)	73(5)
C(1S')	242(14)	3404(15)	9024(11)	108(10)
C(2S')	1010(19)	3854(17)	9391(11)	142(13)
C(3S')	1497(14)	4118(18)	8882(14)	131(13)
C(4S')	1155(23)	3648(21)	8263(14)	263(24)

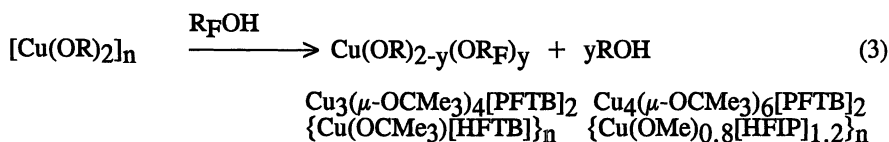
Crystal Data: $\text{MoK}\alpha$, C2/c , $a=15.213(4)\text{\AA}$, $b=14.742(3)\text{\AA}$, $c=19.031(5)\text{\AA}$, $\beta=99.57(2)^\circ$, $Z=4$, $R=7.40\%$. Compound was crystallized by cooling an NMR tube with THF-dg solution to -20°C in freezer.

Table III. Bond Lengths(Å) and Selected Bond Angles(°) for BaCu[HFIP]₄(THF)₄

Ba(1)··Cu(1)	3.726(3)	Ba(1)-O(1)	2.631(8)	Ba(1)-F(5)	3.150(10)
Ba(1)-O(1S)	2.736(12)	Ba(1)-O(1S')	2.768(10)	Ba(1)-O(1A)	2.631(8)
Ba(1)-F(5A)	3.150(10)	Ba(1)-O(1SA)	2.736(12)	Ba(1)-O(1SB)	2.768(10)
Cu(1)-O(1)	1.941(8)	Cu(1)-O(2)	1.906(8)	Cu(1)-O(1A)	1.941(8)
Cu(1)-O(2A)	1.906(8)	O(1)-C(1)	1.38(1)	O(2)-C(4)	1.36(2)
C(1)-C(2)	1.52(2)	C(1)-C(3)	1.49(2)	C(2)-F(4)	1.29(2)
C(2)-F(5)	1.33(2)	C(2)-F(6)	1.35(2)	C(3)-F(1)	1.33(2)
C(3)-F(2)	1.36(2)	C(3)-F(3)	1.31(2)	C(4)-C(5)	1.53(3)
C(4)-C(6)	1.53(2)	C(5)-F(7)	1.32(2)	C(5)-F(8)	1.32(3)
C(5)-F(9)	1.34(2)	C(6)-F(10)	1.33(2)	C(6)-F(11)	1.34(2)
C(6)-F(12)	1.34(2)	O(1S)-C(1S)	1.40(2)	O(1S)-C(4S)	1.41(3)
C(1S)-C(2S)	1.51(3)	C(2S)-C(3S)	1.51(3)	C(3S)-C(4S)	1.44(3)
O(1S')-C(1S')	1.44(3)	O(1S')-C(4S')	1.35(4)	C(1S')-C(2S')	1.42(3)
C(2S')-C(3S')	1.37(4)	C(3S')-C(4S')	1.39(4)		
O(1)-Ba(1)-F(5)	54.5(2)	O(1)-Ba(1)-F(5A)	110.4(3)		
O(1)-Ba(1)-O(1A)	59.3(3)	F(5)-Ba(1)-F(5A)	164.6(4)		
Ba(1)-O(1)-Cu(1)	108.3(3)	O(1)-Cu(1)-O(2)	93.2(3)		
O(1)-Cu(1)-O(1A)	84.2(5)	O(2)-Cu(1)-O(2A)	94.9(5)		
O(2)-Cu(1)-O(1A)	161.4(4)	O(1)-Cu(1)-O(2A)	161.4(4)		
O(1A)-Cu(1)-O(2A)	93.2(3)	Cu(1)-O(1)-C(1)	122.6(7)		
Ba(1)-O(1)-C(1)	129.2(7)	Cu(1)-O(2)-C(4)	115.7(8)		

The green etherates are relatively stable and require repeated vacuum distillation to remove all the ether (7). Performance of this reaction in THF affords a light blue-green sublimable solid whose elemental analysis approximates Cu₄[PFTB]₇(THF)₆. Stable ligation of Cu(II) by small monodentate ether ligands is relatively unusual and probably results from the strong electron withdrawing power of the C(CF₃)₃ group.

Several mixed ligand Cu(II) fluoroalkoxides have been prepared by alcohol exchange reactions (equation 3) (12, 13). Alcohol exchange reactions



are often incomplete as a result of both strongly bound bridging and more easily replaced terminal alkoxy groups being present in the starting alkoxides. (14,15) Steric effects of the substituting fluorinated groups may also limit the degree of ligand exchange, particularly with the [PFTB] group. The [PFTB] ligands in Cu₃(μ-OCMe₃)₄[PFTB]₂ and Cu₄(μ-OCMe₃)₆[PFTB]₂ are in terminal positions, attached to 3-coordinate Cu(II), which is consistent with the ligand's low basicity and large steric size. The geometries around the 3-coordinate copper atoms in Cu₄(μ-OCMe₃)₆[PFTB]₂ are nearly identical to those observed in Ba{Cu[HFTB]₃}₂. Magnetic measurements are reported for both complexes (12).

Mixed ligand copper(II) methoxide fluoroalkoxides such as {Cu(OMe)_{0.8}[HFIP]_{1.2}}_n redistribute to [Cu(OMe)₂]_n and Cu[HFIP]₂L_x when treated with a strong amine base such as TMEDA or pyridine. Several adducts of pyridine (Py), Bipyridine (BIPY), N,N,N',N'-tetraethylethylenediamine (TEED),

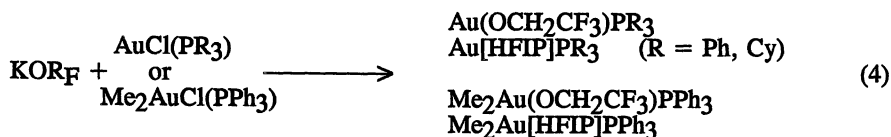
and TMEDA with $\text{Cu}[\text{HFIP}]_2$ and $\text{Cu}[\text{HFTB}]_2$ were prepared in this manner. Both TMEDA adducts, $\text{Cu}[\text{HFIP}]_2 \cdot (\text{TMEDA})$ and $\text{Cu}[\text{HFTB}]_2 \cdot (\text{TMEDA})$, have distorted square planar structures and $\text{Cu}[\text{HFIP}]_2 \cdot (\text{TMEDA})$ was found to serve as a CVD precursor for copper metal. (13)

A copper oxalate complex, $\{\text{Cu}[\text{PFTB}](\text{TMEDA})\}_2\text{C}_2\text{O}_4$ is obtained in very low yield from a reaction between $\text{Cu}(\text{OH})_2$, $\text{H}[\text{PFTB}]$, and TMEDA in a THF/benzene mixture (16). Apparently the copper hydroxide absorbed CO_2 from the air which was reduced to oxalate. Both $\text{Cu}(\text{II})$ centers are 5-coordinate in a distorted square pyramidal configuration, with the highly disordered $[\text{PFTB}]$ groups *trans* to each other (Figure 4).

Copper(I). Although unfluorinated $\text{Cu}(\text{I})$ alkoxides are readily prepared from NaOR and CuCl , $\text{Na}[\text{PFTB}]$ and CuCl hardly react at all when combined in ether or THF. Copper perfluoro-*tert*-butoxide is synthesized instead by alcoholysis of mesitylcopper in hexane at 60–70 °C (7). Reaction between $(\text{CuOCMe}_3)_4$ and various fluorinated alcohols including $\text{H}[\text{HFIP}]$, $\text{H}[\text{TFTB}]$, and $\text{H}[\text{PFTB}]$ affords complexes of the form $\text{Cu}(\text{OCMe}_3)_x(\text{OR}_F)_{1-x}$ with $x \approx 0.5$. The volatility and thermogravimetric analyses of these mixed ligand complexes was studied (17). A mixed ligand alkyl alkoxide $\text{Cu}(\text{CH}_2\text{SiMe}_3)_x[\text{PFTB}]_{1-x}$ ($x \approx 0.35$) is obtained by stirring $\text{Cu}(\text{CH}_2\text{SiMe}_3)_2$ (18) and $\text{H}[\text{PFTB}]$ in pentane at room temperature for 16 hours in the dark. The pentane is removed at 0 °C and the product purified by sublimation (19). This volatile alkyl alkoxide decomposes thermally or photochemically to leave a deposit of copper metal and might serve as a precursor for the latter. Both the $\text{Cu}(\text{OCMe}_3)_x(\text{OR}_F)_{1-x}$ and $\text{Cu}(\text{CH}_2\text{SiMe}_3)_x[\text{PFTB}]_{1-x}$ mixed ligand complexes show only one set of ^1H and ^{19}F NMR peaks for each type of ligand, which either indicates a symmetrical structure (17) or rapid exchange in solution.

Silver and Gold. Very few silver and gold fluoroalkoxides are known (20). An attempt to prepare an $\text{Ag}(\text{II})$ -Ba double alkoxide from a reaction between AgF_2 and $\text{Ba}[\text{PFTB}]_2$ in THF results instead in an $\text{Ag}(\text{I})$ -Ba complex $\text{BaAg}[\text{PFTB}]_3 \cdot (\text{THF})_4$, whose crystal structure is illustrated in Figure 5. Atomic coordinates are listed in Table IV, and selected bond lengths and angles are listed in Table V. Two bridging $[\text{PFTB}]$ groups link Ba1 and Ag1 with a Ba1–O1 and Ag1–O1 distances of 2.676(7) and 2.299(7) Å respectively, and the Ba1–O2 distance to the terminal $[\text{PFTB}]$ ligand is a rather short 2.45(1) Å. The terminal $[\text{PFTB}]$ ligand is highly disordered, possibly from free rotation, while the bridging ligands appear to be restrained in their motion by weak Ba–F contacts at 3.26(1) Å. Coordinated THF is readily lost by evaporation to afford a white unsolvated powder. This photosensitive compound is also readily prepared, in nearly quantitative yield, by stirring a mixture of AgF and 1.5 eq. of $\text{Ba}[\text{PFTB}]_2$ in THF in the dark for 3d at 25 °C, followed by filtration and solvent removal.

Synthesis of air and thermally stable $\text{Au}(\text{I})$ and $\text{Au}(\text{III})$ alkoxy complexes AuOR_FL and $\text{Me}_2\text{AuOR}_FL$ ($L = \text{PR}_3$) is readily accomplished by metathesis between KOR_F and the corresponding halide in THF (equation 4) (21,22). The $\text{Au}(\text{I})$ complexes are found to be highly nucleophilic, abstracting protons smoothly from malonitrile, methylcyanoacetate and even acetone to form the corresponding C-bonded $\text{Au}(\text{I})$ enolate and HOR_F . The volatility of these complexes is not mentioned. (Table VI)



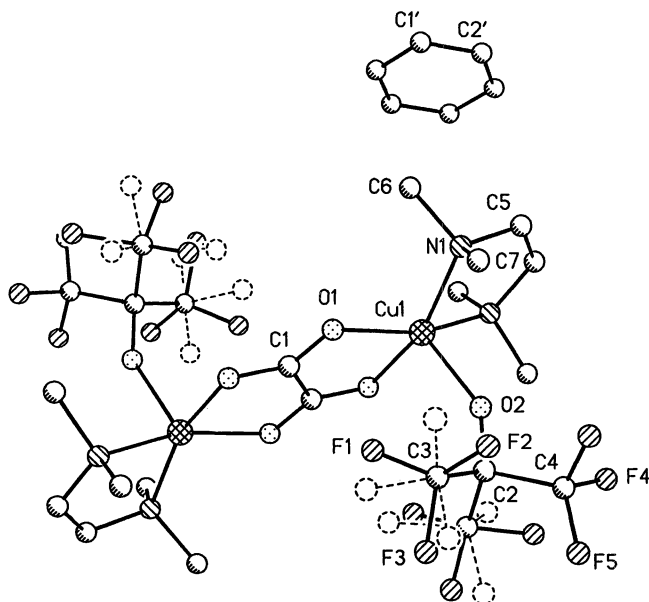


Figure 4. Structure of $\{\text{Cu}[\text{PFTB}](\text{TMEDA})\}_2\text{C}_2\text{O}_4$ benzene solvate, adapted from ref 16.

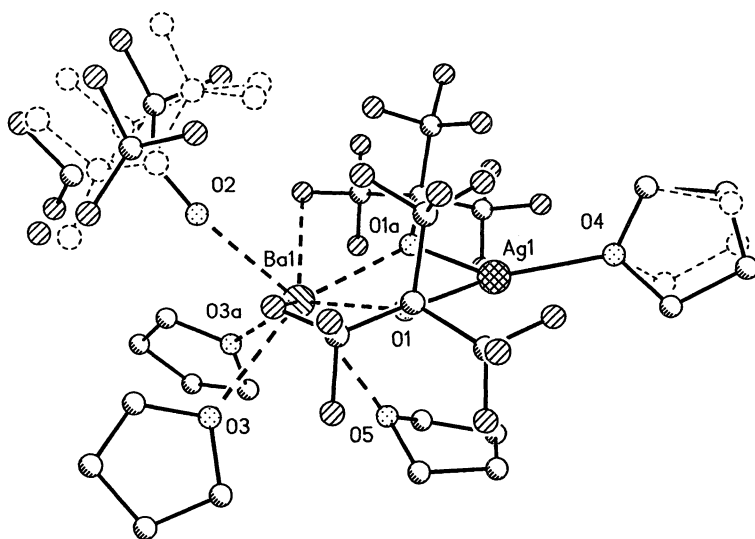


Figure 5. Structure of $\text{BaAg}[\text{PFTB}]_3 \cdot (\text{THF})_4$.

Table IV. Atomic Coordinates ($\times 10^4$) and Equivalent Isotropic Displacement Coefficients ($\text{\AA}^2 \times 10^{-3}$) for $\text{BaAg}[\text{PFTB}]_3 \cdot (\text{THF})_4$

	x	y	z	U(eq)
Ba(1)	9726(1)	2500	2832(1)	41(1)
Ag(1)	7411(2)	2500	400(1)	67(1)
O(1)	8223(7)	3526(5)	1522(5)	54(3)
C(1)	7618(10)	4243(7)	1551(9)	49(4)
C(2)	7448(16)	4690(9)	553(11)	83(5)
C(3)	6207(15)	4111(10)	1771(11)	86(5)
C(4)	8474(16)	4774(9)	2364(13)	98(5)
F(1)	6952(10)	5442(5)	542(7)	118(4)
F(2)	8543(11)	4752(7)	239(8)	159(4)
F(3)	6571(12)	4306(6)	-173(7)	143(4)
F(4)	5455(8)	3606(7)	1168(8)	141(4)
F(5)	6323(10)	3781(8)	2659(9)	165(4)
F(6)	5454(9)	4786(6)	1781(8)	135(4)
F(7)	9596(11)	5003(7)	2116(9)	151(4)
F(8)	7889(11)	5463(6)	2561(9)	179(4)
F(9)	8844(11)	4379(6)	3205(7)	137(4)
O(2)	9197(12)	2500	4512(9)	65(4)
C(5)	8695(17)	2500	5310(11)	69(5)
C(6)	8201(33)	3338(18)	5561(29)	308(6)
C(7)	9732(38)	2500	6285(27)	232(6)
F(10)	9357(16)	3829(14)	5792(19)	92(5)
F(11)	7219(19)	3636(17)	4819(15)	115(5)
F(12)	7414(32)	3301(20)	6257(22)	208(6)
F(13)	10759(17)	2922(15)	6428(15)	159(5)
F(14)	9328(47)	2500	7138(27)	259(6)
C(6')	8880(31)	1695(16)	5881(21)	162(6)
F(10')	7937(29)	1193(12)	5159(17)	200(6)
F(11')	8601(20)	1689(11)	6808(11)	141(5)
F(12')	10020(17)	1332(16)	5949(16)	171(5)
C(7')	7163(26)	2500	5073(21)	127(6)
F(13')	6570(15)	2222(14)	4266(12)	185(5)
F(14')	6382(18)	2500	5707(16)	142(5)
O(3)	11886(9)	3536(6)	3494(8)	101(4)
C(8)	12204(22)	3737(16)	4507(14)	238(6)
C(9)	13325(17)	4180(11)	4785(15)	138(5)
C(10)	13711(19)	4408(16)	3852(16)	214(6)
C(11)	12849(16)	3910(12)	3033(15)	160(5)
O(4)	5901(14)	2500	-1029(9)	90(4)
C(12)	6055(27)	2864(28)	-1936(14)	172(6)
C(13)	4707(29)	2884(20)	-2682(18)	139(6)
C(14)	3906(27)	2316(19)	-2197(17)	120(6)
C(15)	4505(25)	2500	-1096(17)	187(6)
O(5)	10899(14)	2500	1115(10)	81(4)
C(16)	11103(15)	3189(9)	525(10)	88(5)
C(17)	10442(16)	2959(9)	-515(10)	108(5)

Crystal Data: $\text{MoK}\alpha$, $P2_1/m$, $a = 10.074(9)\text{\AA}$, $b = 16.321(7)\text{\AA}$, $c = 13.580(4)\text{\AA}$, $\beta = 101.77(5)^\circ$, $Z = 2$, $R = 6.19\%$

Table V. Selected Bond Lengths and Angles for BaAg[PFTB]₃·(THF)₄

Ba(1)··Ag(1)	3.633(4)	Ba(1)-O(3)	2.758(10)	Ba(1)-O(1A)	2.676(7)
Ba(1)-O(3A)	2.758(10)	Ba(1)-O(1)	2.676(7)	Ba(1)-O(2)	2.448(12)
Ba(1)-O(5)	2.820(15)	Ba(1)··F(9A)	3.261(10)	Ba(1)··F(9)	3.261(10)
Ag(1)-O(4)	2.209(12)	Ag(1)-O(1)	2.299(7)	Ag(1)-O(1A)	2.299(7)
O(1)-C(1)	1.324(13)	O(2)-C(5)	1.286(21)		

Average C-CF₃ 1.52, C-F 1.31; in THF C-O 1.40, C-C 1.46

O(1)-Ba(1)-O(2)	114.7(3)	O(1)-Ba(1)-O(3)	97.8(3)
O(2)-Ba(1)-O(3)	90.2(3)	O(1)-Ba(1)-O(5)	74.1(3)
O(2)-Ba(1)-O(5)	168.1(4)	O(3)-Ba(1)-O(1A)	154.5(3)
O(3)-Ba(1)-O(5)	80.4(3)	O(1)-Ba(1)-O(1A)	77.5(3)
O(5)-Ba(1)-O(1A)	74.1(3)	O(2)-Ba(1)-O(1A)	114.7(3)
O(1)-Ba(1)-O(3A)	154.5(3)	O(3)-Ba(1)-O(3A)	75.7(4)
O(2)-Ba(1)-O(3A)	90.2(3)	O(5)-Ba(1)-O(3A)	80.4(3)
O(1)-Ag(1)-O(4)	132.1(2)	O(1A)-Ba(1)-O(3A)	97.8(3)
O(1)-Ag(1)-O(1A)	93.5(4)	Ba(1)-O(1)-Ag(1)	93.5(3)
Ag(1)-O(1)-C(1)	124.1(6)	Ba(1)-O(1)-C(1)	137.3(6)
Ba(1)-O(2)-C(5)	169.7(10)		

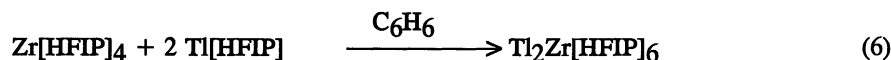
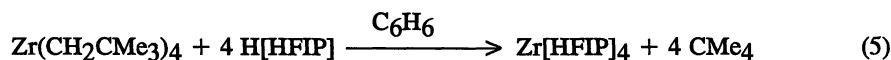
Table VI. Physical Data on Group 11 Fluoroalkoxides

Compound	Mp (dec)	Subl. ^a	¹⁹ F NMR ^b	ref.
Na ₂ Cu[HFIP] ₄	140-146 (200)	90	-60.5 ^c	6
BaCu[HFIP] ₄	(225)	220		6
BaCu[HFIP] ₄ ·(THF) ₄		(-THF)	-65.8 ^c	
Ba{Cu[HFIP] ₂ ·(TMEDA)}	124-126 (>250)	70-90	-51,-56.8,-60.2	7
Cu[HFIP] ₂ ·(TMEDA)	105-108	75		13
Cu[HFIP] ₂ ·(TMEDA)	137-140 (150)	60-80	-45.6	7,13
Cu[HFIP] ₂ ·(TEED)	97 -100	75		13
Cu[HFIP] ₂ ·(BIPY)	(150)	75		13
Cu[HFIP] ₂ ·(BIPY)	(150)	140		13
Cu[HFIP] ₂ ·(Py) ₂	63-66 (-Py 70)			13
Cu[HFIP] ₂ ·(Py) ₂	(-Py 70)			13
Cu ₄ [PFTB] ₇	68-71	<0	-1.6,-51.7	7
Cu ₄ [PFTB] ₇ ·OEt ₂		<0		7
Cu ₄ [PFTB] ₇ ·(OEt ₂) _n (n=2-4)	<20	<0		7
Cu ₄ [PFTB] ₇ ·(THF) ₆		60		
Cu ₄ (μ-OCMe ₃) ₆ [PFTB] ₂		90-110	-62.7	12
Cu ₃ (μ-OCMe ₃) ₄ [PFTB] ₂		90-110	-59.9	12
{Cu(OCMe ₃)[HFIP] _n }		110		12
(Cu[PFTB] _n) _n	67-151 (150)	40-50	-75.3	7
Cu(CH ₂ SiMe ₃) _{0.35} [PFTB] _{0.65}	55-85 (110 ^d)	40-70	-74.9 ^e	
Cu(OCMe ₃) _{0.47} [PFTB] _{0.53}	(125)	80		17
Cu(OCMe ₃) _{0.46} [HFIP] _{0.54}	(140)	90		17
Cu(OCMe ₃) _{0.4} [TFTB] _{0.6}		100		17
BaAg[PFTB] ₃	(140)	100-110		
BaAg[PFTB] ₃ ·(THF) ₄	(-THF)		-75.7 ^c	

^aSublimation under dynamic vacuum. ^bC₆D₆ solvent unless stated otherwise. ^cC₄D₈O solvent. ^dDeposits Cu metal at 270 °C under 1 Atm He. ^e0.11(SiMe₃), -0.62(CH₂) in ¹H spectrum.

Zirconium Derivatives

A sodium-zirconium alkoxide Na₂Zr[HFIP]₆·(C₆H₆)_n (n = 0-2) is obtained from a reaction between ZrCl₄ and Na[HFIP] (8). The crystal structure shows the n=1 and n=2 complexes to contain 6-coordinate zirconium and both Na-O and Na-F coordination, with additional π-bonding between the Na⁺ ion and coordinated benzene. These zirconium complexes are soluble in C₆F₆ but not C₆H₆. An analogous thallium complex Tl₂Zr[HFIP]₆, is synthesized from Tl[HFIP] (23) and Zr[HFIP]₄ (equations 5 & 6) (24).



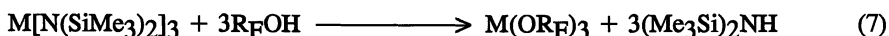
Although the crystal structure shows 6 strong Tl-F interactions, the ¹⁹F and ²⁰⁵Tl NMR spectra reveal each Tl to be equally coupled in C₆F₆ solution to all 36 fluorine atoms, the result of a fluxional process. The magnitude of the Tl-F

coupling (383 Hz) supports the notion that there is actually a coordinate bond between the fluorines and thallium and not just an electrostatic interaction.

It was found that $\text{Na}_2\text{Zr}[\text{HFIP}]_6$ deposits films of Na_3ZrF_7 in a CVD reactor at 275 °C (8). This is in contrast to the previous report that thermolysis of $\text{Zr}[\text{HFIP}]_4$ affords ZrO_2 quantitatively (25), the difference possibly due to the Na-F interaction in $\text{Na}_2\text{Zr}[\text{HFIP}]_6$.

Lanthanide Derivatives

A recent report (26) details the synthesis of various $[\text{HFIP}]$, $[\text{TFTB}]$, and $[\text{HFTB}]$ complexes of Sc, Y, La, and Pr by alcoholysis of the trimethylsilylamides in C_6H_6 (equation 7). The products sometimes contain



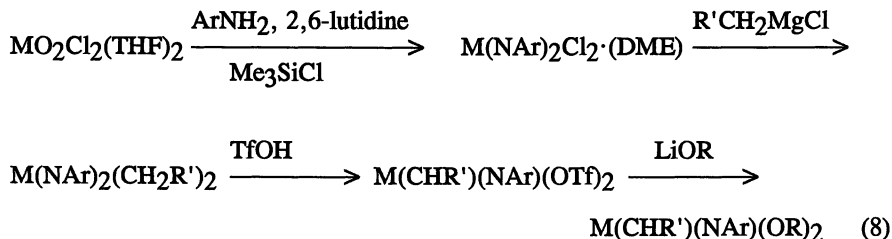
coordinated NH_3 from the action of excess alcohol on the $(\text{Me}_3\text{Si})_2\text{NH}$. *Bis* ammonia adducts are shown to be dimers with *trans*- NH_3 and *cis*-alkoxy ligands by NMR and x-ray crystallography, which contrasts with a previous report that suggested a monomeric composition (27). Monomeric THF adducts, *fac*- $\text{Ln}(\text{OR}_\text{F})_3 \cdot (\text{THF})_3$, are obtained when THF is used as the reaction solvent. A crystal structure of one homoleptic complex, $\text{Pr}[\text{TFTB}]_3$, shows a trinuclear structure with both Pr-O and Pr-F coordination; Pr-F bonds range from 2.76 to 3.00 Å. The $[\text{HFTB}]$ complexes are volatile under vacuum at temperatures ranging from 75 to 130 °C, but the volatility of the $[\text{TFTB}]$ complexes is not mentioned.

Group 6 and 7 Derivatives

A stable chromyl(VI) alkoxide, $\text{CrO}_2[\text{HFIP}]_2$ is prepared from $\text{Li}[\text{HFIP}]$ and CrO_2Cl_2 in refluxing CCl_4 (28). The thermal stability of this alkoxide is attributed to the oxidation resistance of $[\text{HFIP}]$ vs. unfluorinated alkoxy groups which are readily susceptible to hydride abstraction by Cr(VI).

Fluorinated alkoxides with $\text{Mo} \equiv \text{Mo}$ and $\text{W} \equiv \text{W}$ triple bonds can be prepared by the alcoholysis of $(\text{Me}_2\text{N})_3\text{Mo} \equiv \text{Mo}(\text{NMe}_2)_3$ and the analogous tungsten compound respectively. When $\text{H}[\text{PFTB}]$ reacts with $\text{Mo}_2(\text{NMe}_2)_6$ in a 8:1 mole ratio $\text{Mo}_2(\text{NMe}_2)_2[\text{PFTB}]_4$ and $[\text{NH}_2\text{Me}_2][\text{PFTB}]$ are obtained in good yield. However, an excess of the alcohol does not afford the homoleptic complex $\text{Mo}_2[\text{PFTB}]_6$; a difficult to separate mixture of products is formed instead (29).

Numerous alkoxy complexes of Mo(VI), W(VI), and Re(VII) (both fluorinated and unfluorinated) have been prepared by the Schrock group and others as part of their studies of olefin metathesis catalysts (1). Alkylidene complexes of the form $\text{M}(\text{CHR}')(\text{NAr})(\text{OR})_2$ (M = Mo, W) can be prepared by several different multistep syntheses; equation 8 shows one example (30,31). Catalytic activity is very sensitive to the nature of the alkoxy ligand OR; the more electron withdrawing alkoxides are the more active catalysts. Thus, $\text{W}(\text{CHCMe}_3)(\text{NAr})[\text{HFTB}]_2$ reacts rapidly with internal olefins while the $\text{OR} = \text{OCMe}_3$ derivative reacts only slowly. However, the latter is useful for controlled ring opening metathesis polymerization (ROMP) of strained cyclic olefins like norbornene. Molybdenum complexes are less active than their tungsten analogues. Complexes with different imido ligands ($=\text{NCMe}_3$ or $=\text{NC}_6\text{H}_3\text{Me}_2$) in place of $=\text{NAr}$ have also been studied (32, 33). Rhenium(VII) complexes of the form $\text{Re}(\text{NAr})_2(\text{CHCMe}_3)\text{OR}$ (OR = $[\text{HFIP}]$, $[\text{HFTB}]$, and OAr), are much less reactive, failing even to metathesize norbornene (34).



Metathesis of internal acetylenes via W(VI), Mo(VI), and Re(VII) alkylidyne complexes has also been reported (35-39). The two key requirements for a successful Mo(VI) or W(VI) acetylene metathesis catalyst are a crowded alkoxide coordination sphere to prevent further reaction of the metallacyclobutadiene intermediate with more of the acetylene (which forms polyacetylenes), and electronegative alkoxy groups to afford an electrophilic metal center. Thus a good metathesis catalyst is Mo(CCMe₃)[HFTB]₃; the [HFIP] analogue does not have sufficient steric hindrance to prevent a competing polymerization reaction (36). Rhenium(VII) alkylidyne complexes are found to participate in two different reaction pathways with internal acetylenes (39). With R = OCMe₃, Ar, [HFIP], or [TFTB] the resulting rhenacyclobutadiene ring is of a type that is stable to loss of acetylenes, but the [HFTB] derivative forms a second, more reactive isomer that acts as a metathesis catalyst.

General Conclusions

Hexafluoroisopropoxides and fluorinated *tert*-butoxides of the alkali and alkaline earth metals are readily synthesized by reactions between HOR_F and the metal in Et₂O or THF. These alkali and alkaline earth derivatives are useful in the synthesis of transition metal fluoroalkoxides by reaction with either a metal halide or a metal complex with good leaving groups. Complex ions such as Cu(OR_F)₄²⁻ often form in such reactions when the transition metal is coordinatively unsaturated, resulting in double metal alkoxides. A good ligand for the metal in the complex ion can cause double alkoxides MM'(OR_F)_n to rearrange to M(OR_F)_x and M'(OR_F)_{n-x}L. When ionic metathesis fails, or fails to produce the desired homoleptic single metal alkoxide, reactions between HOR_F and metal alkyls or trimethylsilylamides can be excellent routes to transition metal (or lanthanide) alkoxides M(OR_F)_n. Alcohol exchange reactions between HOR_F and other metal alkoxides typically produce mixed products M(OR)_{n-x}(OR_F)_x, but strongly coordinating ligands can induce a rearrangement to M(OR)_n and M(OR_F)_nL.

The presence of [HFIP], [TFTB], [HFTB], and [PFTB] groups can confer a number of desirable properties on metal alkoxides, that provide some advantage over their unfluorinated analogues. These include improved thermal and oxidative stability, enhanced catalytic activity, and higher volatility. The latter can sometimes be enhanced to a spectacular extent. This is not only due to the greater steric size and reduced bridging tendencies of OR_F, and the reduction of Van der Waals forces common to most heavily fluorinated compounds, but also to coordination between electropositive metals and organic fluorine. Organofluorine coordination has been observed to Na, Ba, Pr and Tl, but not to Cu. This

coordination can allow nominally unidentate alkoxy ligands to saturate the coordination sphere of the metal resulting in a volatile monomer, for example $\text{Ba}\{\text{Cu}[\text{HFTB}]\}_2$, and may contribute to deposition of metal fluorides from compounds such as $\{\text{Na}[\text{HFIP}]\}_4$ and $\text{Na}_2\text{Zr}[\text{HFIP}]_6$ during CVD experiments.

Acknowledgments

We thank K. G. Caulton (Indiana University) for providing unpublished data and the ONR for financial support.

Literature Cited

1. Willis, C. J. *Coord. Chem. Rev.* **1988**, *88*, 133-202.
2. Tatlow, J. C. In *Organofluorine Chemicals and their Industrial Applications*; Banks, R. E., Ed.; Ellis Horwood Publishers: London, 1979; pp 22-26.
3. Joosten, P. H.; Heller, P.; Nabben, H. J. P.; van Hal, H. A. M.; Popma, T. J. A.; Haisma, J. *Appl. Optics* **1985**, *24*, 2674-2678.
4. Dear, R. E. A.; Fox, W. B.; Fredericks, R. J.; Gilbert, E. E.; Huggins, D. K. *Inorg. Chem.* **1970**, *9*, 2590-2591.
5. Mahmood, T.; Shreeve, J. M. *Inorg. Chem.* **1986**, *25*, 3830-3837.
6. Purdy, A. P.; George, C. F.; Callahan, J. H. *Inorg. Chem.* **1991**, *30*, 2812-2819.
7. Purdy, A. P.; George, C. F. *Inorg. Chem.* **1991**, *30*, 1969-1970.
8. Caulton, K. G. *Unpublished Results*.
9. Zhao, J.; Dahmen, K.; Marcy, H. O.; Tonge, L. M.; Marks, T. J.; Wessels, B. W.; Kannewurf, C. R. *Appl. Phys. Lett.* **1988**, *53*, 1750-1752.
10. Purdy, A. P.; Berry, A. D.; Holm, R. T.; Fatemi, M.; Gaskill, D. K. *Inorg. Chem.* **1989**, *28*, 2799-2803.
11. Lingg, L. J.; Berry, A. D.; Purdy, A. P.; Ewing, K. J. *Thin Solid Films* **1992**, *209*, 9-16.
12. Purdy, A. P.; George, C. F.; Brewer, G. A. *Inorg. Chem.* **1992**, *31*, 2633-2638.
13. Jeffries, P. M.; Wilson, S. R.; Girolami, G. S. *Inorg. Chem.* **1992**, *31*, 4503-4509.
14. Caulton, K. G.; Hubert-Pfalzgraf, L. G. *Chem. Rev.* **1990**, *90*, 969.
15. Bradley, D. C.; Mehrotra, R. C.; Gaur, D. P. *Metal Alkoxides*; Academic Press: London, 1978.
16. George, C. F.; Purdy, A. P. *Acta. Cryst.* **1992**, 155-157.
17. Gross, M. E. *J. Electrochem. Soc.* **1991**, *138*, 2422-2426.
18. Jarvis, J. A.; Pearce, R.; Lappert, M. F. *J. Chem. Soc. Dalton Trans.* **1977**, 999-1003.
19. Purdy, A. P. *Patent application, Navy case #73102 and 73188*;
20. Mitchell, C. M.; Stone, F. G. A. *J. Chem. Soc. Dalton. Trans.* **1972**, 102-107.
21. Sone, T.; Iwata, M.; Kasuga, N.; Komiya, S. *Chem. Lett.* **1991**, 1949-1952.
22. Komiya, S.; Iwata, M.; Sone, T.; Fukuoka, A. *J. Chem. Soc. Chem. Commun.* **1992**, 1109-1110.
23. Skelcey, J. S.; Rumminger, J. E.; Groves, K. O. *US Patent 3,494,946* **1968**; CA 72:110787.
24. Samuels, J. A.; Zwanzinger, J. W.; Lobkovsky, E. B.; Caulton, K. G. *Inorg. Chem.* **1992**, *31*, 4046-4047.

25. Mazdiyasi, K. S.; Schaper, B. J.; Brown, L.M. *Inorg. Chem.* **1971**, *10*, 889-892.
26. Bradley, D. C.; Chudzynska, H.; Hammond, M. E.; Hursthouse, M. B.; Motevalli, M.; Ruowen, W. *Polyhedron* **1992**, *11*, 375-379.
27. Mazdiyasi, K. S.; Schaper, B. J. *J. Less-Common Met.* **1973**, *30*, 105-112.
28. Chadha, S. L. *Inorg. Chim. Acta.* **1989**, *156*, 173.
29. Abbott, R. G.; Cotton, F. A.; Falvello, L. R. *Polyhedron* **1990**, *9*, 1821-1827.
30. Schrock, R. R.; Murdzek, J. S.; Bazan, G. C.; Robbins, J.; DiMare, M.; O'Regan, M. *J. Am. Chem. Soc.* **1990**, *112*, 3875-3886.
31. Schrock, R. R.; DePue, R. T.; Feldman, J.; Yap, K. B.; Yang, D. C.; Davis, W. M.; Park, L.; DiMare, M.; Schofield, M.; Walborsky, A. E.; Evitt, E.; Kruger, C.; Betz, P. *Organometallics* **1990**, *9*, 2262-2275.
32. Schottel, G.; Kress, J.; Osborn, J. A. *J. Chem. Soc. Chem. Commun.* **1989**, 1062-1063.
33. Johnson, L. K.; Virgil, S. C.; Grubbs, R. H. *J. Am. Chem. Soc.* **1990**, *112*, 5384-5385.
34. Horton, A. D.; Schrock, R. R. *Polyhedron* **1988**, *7*, 1841-1853.
35. McCullough, L. G.; Schrock, R. R. *J. Am. Chem. Soc.* **1984**, *106*, 4067-4068.
36. McCullough, L. C.; Schrock, R. R.; Dewan, J. C.; Murdzek, J. C. *J. Am. Chem. Soc.* **1985**, *107*, 5987-5998.
37. Strutz, H.; Dewan, J. C.; Schrock, R. R. *J. Am. Chem. Soc.* **1985**, *107*, 5999-6005.
38. Freudenberger, J. H.; Schrock, R. R. *Organometallics* **1986**, *5*, 1411-1417.
39. Weinstock, I. A.; Schrock, R. R.; Davis, W. M. *J. Am. Chem. Soc.* **1991**, *113*, 135-144.

RECEIVED April 13, 1993

Chapter 27

(Fluoroalkyl)phosphine Coordination Chemistry

Dean M. Roddick and Richard C. Schnabel

Department of Chemistry, Box 3838, University of Wyoming,
Laramie, WY 82071

A general review of (fluoroalkyl)phosphine coordination chemistry and recent results concerning the synthesis and reactivity patterns of dimeric rhodium and iridium complexes incorporating the chelate $(C_2F_5)_2PCH_2CH_2P(C_2F_5)_2$ ("dfepe") are presented. $[(dfepe)M(\mu-Cl)]_2$ ($M = Rh$ (**1**), Ir (**2**)) and $[(dfepe)M(\mu-O_2CCF_3)]_2$ ($M = Rh$ (**3**), Ir (**4**)) are obtained in high yield from $[(cod)M(\mu-Cl)]_2$ and $[(cod)M(\mu-O_2CCF_3)]_2$, respectively. While **1**, **2** and **3** are inert toward oxidative addition reactions, **4** reacts readily with H_2 to form $(dfepe)_2Ir_2(H)(\mu-H)_2(\mu-O_2CCF_3)$ (**5**). Thermolysis of **4** in neat cyclopentane at $150\text{ }^\circ\text{C}$ affords a mixture of **5** and the alkane dehydrogenation product $CpIr(dfep)$ (**6**). Hydrogenolysis of $(dfep)Ir(\eta^3-C_3H_5)$ (**9**) affords the dimeric tetrahydride $(dfep)_2Ir_2(H)(\mu-H)_3$ (**10**), which in the presence of (*t*-butyl)ethylene also reacts with cyclopentane at $120\text{ }^\circ\text{C}$ to give **6**.

One of the principal goals in coordination chemistry and homogeneous catalysis is to control metal reactivity through systematic variation of ligand properties. To date, most research has focused on structure/reactivity relationships involving sigma and pi-donor ligands such as phosphines (*1,2*), alkoxides (*3-6*), thiolates (*7*), amides (*8-11*), phosphides (*12-14*), and alkyls (*15,16*). In contrast, the possibilities inherent in similar π -acceptor ligand modification remain largely unexplored. This imbalance in approach is particularly significant in light of the important role π -acceptor ligands play in the chemistry of low valent metal complexes.

The development of stable low coordinate metal systems incorporating bulky donor ligands has steadily expanded over the years and has no counterpart in acceptor ligand coordination chemistry. A graphical illustration of the steric range of typical acceptor and donor phosphine ligands is depicted in Figure 1. In comparison to the wide range of steric and electronic properties available to common donor phosphines (*1*), strong acceptor phosphine ligands are essentially limited to the sterically undemanding fluorophosphine, PF_3 . This marked differ-

ence between donor and acceptor phosphine size ranges is reflected more generally by the uniformly small size of the common π -acceptor ligands CO, NO⁺, and CNR. While isonitriles can in principle incorporate a range of R group functionalities, direct steric influence on the coordination sphere is minimized by the linear nature of the M-C-N-R moiety. In addition, isonitriles have a tendency to undergo coupling (17), insertion (18,19), and nucleophilic addition (19) side reactions that severely restrict their potential use as stable ancillary ligands. Because of these considerations, most efforts in acceptor ligand design have focused on modifying the basic PF₃ framework (20).

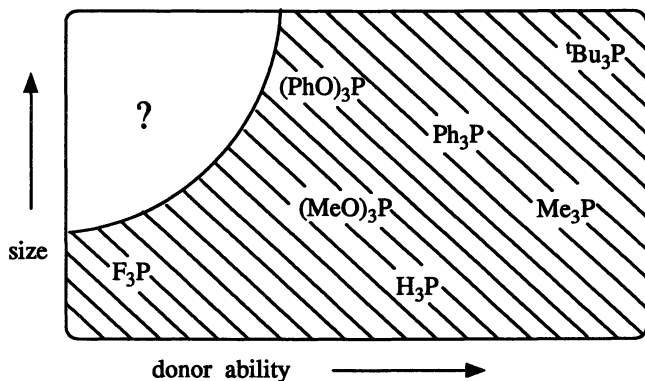
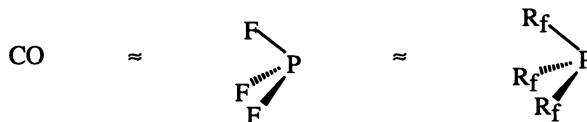


Figure 1. Qualitative range of steric and electronic properties for some common phosphine ligands

A sterically and electronically tunable CO analogue would have a profound impact on low valent coordination chemistry. Recognizing this challenge, numerous workers have attempted to prepare new types of acceptor ligands and establish systems which complement or parallel known metal carbonyl chemistry. Nixon (20), King (21,22), and others (23) have noted in particular the lack of polydentate acceptor ligands and have investigated the coordination chemistry of RN(PF₂)₂ and related fluorophosphine chelates (24) in a variety of metal systems. Although these ligands in several cases do substitute completely for CO in a manner similar to PF₃, they suffer from a number of limitations due to P-F and P-N cleavage side reactions and a preference for binuclear-bridging coordination modes. Examples of other substituted fluorophosphines that have been reported include R_xPF_{3-x} (R = CF₃ (25,26), OCH₃ (25,27), (CF₃)₂CHO (28,29), (CF₃)₂C(CN)O (30), Me₂N (31), Ph (32)) as well as the chelates F₂PCH₂CH₂PF₂, F₂PCF₂CF₂PF₂, and F₂PC₆H₁₀PF₂ (33,34). It is significant that the coordination chemistry of these ligands remains largely undeveloped.

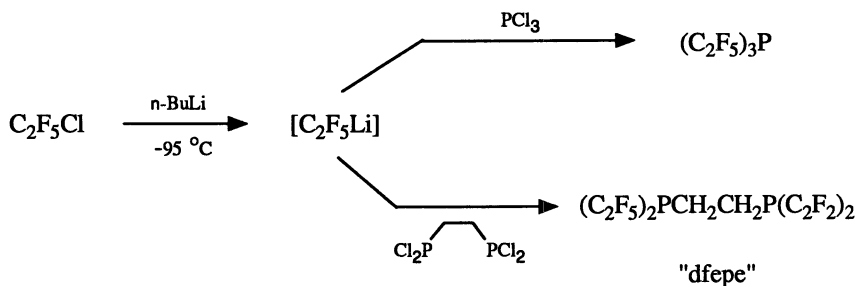
A promising class of ligands that has thus far received little attention is the fluorocarbon-substituted phosphines, $(R_f)_xPR_{3-x}$ (35). Substitution of inductively similar fluorocarbon groups for fluorine in PF_3 retains to a large degree the acceptor ability of the phosphorus center while at the same time providing the opportunity for steric manipulation of coordination properties. The greatest

Acceptor Ability:



advantage (fluoroalkyl)phosphines have over fluorophosphines is that P-C and C-F bonds are considerably more inert than P-F bonds, and thus are much better suited for applications in coordination chemistry where highly reactive metal centers are involved. Although the prototypical fluorinated trialkylphosphine $(CF_3)_3P$ has been the subject of a number of theoretical (36-39) and spectroscopic studies (40-43), the only transition metal complexes that have been reported are $((CF_3)_3P)_xNi(CO)_{4-x}$ ($X = 1 - 3$) (44), $((CF_3)_3P)Ni(NO)(CO)$ (45), $((CF_3P)_3P)_x-Fe(CO)_{5-x}$ ($X = 1 - 3$) (46), and $((CF_3)_3P)((CF_3)_2P(O))PtCl$ (47). Several reports of secondary and primary $(CF_3)_nPX_{3-n}$ ($n = 1, 2; X = H, \text{halide}$) coordination chemistry have also appeared (48-50). A number of years ago, Burg reported the synthesis of the trifluoromethyl-substituted phosphine chelates $(CF_3)_2P(B)P(CF_3)_2$ ($B = O, S, NR$) (51-53) and $(CF_3)_2PCX_2CX_2P(CF_3)_2$ ($X = H, F$) (25,54). These ligands were demonstrated to be π -acceptors comparable to CO in strength, with binding affinities superior to that of $(CF_3)_3P$. However, practical difficulties in the synthesis of the common precursor $(CF_3)_2PP(CF_3)_2$ have forestalled the development of trifluoromethylated phosphine coordination chemistry (55).

We have recently developed an efficient synthetic route to the perfluoroethyl-substituted diphosphine $(C_2F_5)_2PCH_2CH_2P(C_2F_5)_2$ (abbreviated "dfepe") (Scheme 1) (56). Using the readily available dichlorophosphine chelate $Cl_2PCH_2CH_2PCl_2$, 60 gram quantities of dfepe are conveniently prepared in



Scheme 1.

greater than 85% yield; $(\text{C}_2\text{F}_5)_3\text{P}$ has been prepared analogously from PCl_3 in 40% yield (unpublished results). An alternative synthetic procedure utilizing Schlenk techniques has recently been reported (57). Because of the greater thermal stability of the higher perfluoroalkyllithium homologues (58), this direct alkylation methodology may be easily extended to the synthesis of a broad array of (fluoroalkyl)phosphine ligands.

Physical and Coordination Properties of (Fluoroalkyl)phosphines.

Perfluoroalkyl substituents induce profound changes in the chemical properties of the phosphorus center. In comparison to conventional donor phosphines, the proton affinity of the central P atom is greatly reduced. Angelici has reported enthalpies of protonation (ΔH_p) for a range of monodentate and bidentate phosphines with 0.1 M $\text{CF}_3\text{SO}_3\text{H}$ in 1,2-dichloroethane as a measure of phosphine basicity (59). A good linear correlation between the $\text{p}K_a$ of the conjugate phosphonium ion $\text{R}_3\text{PH}^+\text{CF}_3\text{SO}_3^-$ and ΔH_p was found with $\text{p}K_a$'s varying in a predictable fashion based on the electron-donor ability of the phosphine substituent between (*p*- $\text{CF}_3\text{C}_6\text{H}_4$) $_3\text{P}$ (-1.32) and $(t\text{Bu})_3\text{P}$ (+11.4). For all phosphines examined, the protonation by $\text{CF}_3\text{SO}_3\text{H}$ was found to be rapid and quantitative. In contrast, *no reaction* is observed between excess $\text{CF}_3\text{SO}_3\text{H}$ and *dfepe* or $(\text{C}_2\text{F}_5)_3\text{P}$ in CH_2Cl_2 as judged by ^1H and ^{31}P NMR; extrapolation of a thermoneutral ΔH_p yields an estimated $\text{p}K_a$ value of -9.0 as an upper limit for these phosphines. The low basicity of the (perfluoroaryl)phosphine $(\text{C}_6\text{F}_5)_3\text{P}$, which is not protonated in neat H_2SO_4 , has previously been noted (60). The drastically-reduced basicity of the phosphorus lone pair in fluoroalkylphosphines is in accord with $(\text{CF}_3)_x\text{P}(\text{CH}_3)_{3-x}$ PES data, which show a 0.7 - 1.2 eV increase in lone pair ionization energy upon stepwise replacement of CH_3 by CF_3 (40).

The low donor ability of (fluoroalkyl)phosphines suggested by PES data and protonation experiments is similarly indicated by comparative infrared studies of isostructural *cis*- $(\text{R}_3\text{P})_2\text{Mo}(\text{CO})_4$ complexes. On the basis of IR data for group VI $(\text{L})\text{M}(\text{CO})_5$ and *cis*- $(\text{R}_3\text{P})_2\text{M}(\text{CO})_4$ (Table I) systems, the π -acceptor ligand ordering $(\text{CF}_3)_3\text{P} > \text{F}_3\text{P} > \text{CO} > \text{Cl}_3\text{P} > \text{Me}(\text{CF}_3)_2\text{P} > \text{Me}_2(\text{CF}_3)\text{P} \gg \text{Me}_3\text{P}$ has been proposed (42). A recent ligand effect study of *dfepe* by Brookhart places this ligand between PCl_2Ph and PCl_3 in acceptor ability (68). Two features relevant to the coordination chemistry of fluorinated phosphine ligands are evident from the data in Table I. First, although the electronegativity of CF_3 is considered to be less than that of fluorine (69), there is little variation in electronic properties between $(\text{CF}_3)_x\text{PF}_{3-x}$ ligands. This equivalence has been ascribed to a compensating interaction of the fluorine $\text{p}\pi$ lone pairs with the phosphorus acceptor orbitals (61). Second, a comparison between $(\text{CF}_3)_2\text{PCH}_2\text{CH}_2\text{P}(\text{CF}_3)_2$ and $(\text{C}_2\text{F}_5)_2\text{PCH}_2\text{CH}_2\text{P}(\text{C}_2\text{F}_5)_2$ shows that substitution of CF_3 by C_2F_5 does not affect the acceptor ability of the phosphorus center. Thus, for the full steric range of fluorine-modified phosphines $(\text{R}_f)_x\text{PF}_{3-x}$ ($\text{R}_f = \text{CF}_3, \text{C}_2\text{F}_5, \text{C}_n\text{F}_m$), the electronic properties should remain essentially constant.

An additional measure of the electronic properties of *dfepe* is provided by comparative infrared and electrochemical studies of piano-stool complexes $(\eta^5\text{-C}_n\text{-R}_n)\text{M}(\text{L})_3$, summarized in Table II. In general, substitution of *dfepe* for *dppe* or

Table I. Infrared and Cone Angle Data for *cis*-(R₃P)₂Mo(CO)₄ Complexes

phosphine	$\nu(\text{CO})(A_1^2)$, cm ⁻¹	ref	cone angle, deg ^a
2P(CF ₃)F ₂	2094	61	115
2P(CF ₃) ₂ F	2093	61	126
2PF ₃	2091	61	104
2P(CF ₃) ₃	2086	62	137
(CF ₃) ₂ PCF ₂ CF ₂ P(CF ₃) ₂	2082	55	120
F ₂ PCH ₂ CH ₂ PF ₂	2074	34	98
EtN(PF ₂) ₂	2066	63	94
2MeP(CF ₃) ₂	2066	62	131
(C ₂ F ₅) ₂ PCH ₂ CH ₂ P(C ₂ F ₅) ₂	2064	56	129 ^b
(CF ₃) ₂ PCH ₂ CH ₂ P(CF ₃) ₂	2063	55	120
2Me ₂ P(CF ₃)	2044	62	124
(C ₆ F ₅) ₂ PCH ₂ CH ₂ P(C ₆ F ₅) ₂	2041	64	151
(MeO) ₂ PCH ₂ CH ₂ P(OMe) ₂	2033	65	100
Ph ₂ PCH ₂ CH ₂ PPh ₂	2020	66	125
Et ₂ PCH ₂ CH ₂ PEt ₂	2012	66	115

^aValues taken from ref 1, except where noted. ^bValue taken from ref 67.

two Ph₃P ligands results in roughly a one volt anodic shift in oxidation potential and an increase of $\nu(\text{CO})$ for monocarbonyls of about 100 cm⁻¹. For (R₃P)₂M(CO)₄ (M = Cr, Mo) compounds, substitution of R₂PCH₂CH₂PR₂ (R = alkyl) by the perfluoroaryl chelate (C₆F₅)₂PCH₂CH₂P(C₆F₅)₂ induces a 0.7 V anodic shift in potential (64). It is not surprising in view of these large redox shifts that (perfluoroalkyl)phosphine complexes generally exhibit increased air stability and enhanced electrophilic chemical properties (*vide infra*).

Apart from their unique electronic and steric properties, fluorinated ligand complexes also exhibit unusually high volatilities due to reduced intermolecular Van der Waals attractive forces. Despite the significant increase in molecular weight relative to alkylphosphines, mixed perfluoroalkylphosphine carbonyl systems are typically liquids or readily sublimable low-melting solids (46,62,79). This trend is paralleled by the lower boiling points of the free phosphines (CF₃)₃P (17 °C) and (CF₃CF₂)₃P (70 °C) relative to their alkyl counterparts Me₃P (38 °C) and Et₃P (128 °C). The volatility imparted to metal complexes by fluorinated phosphine ligands is particularly intriguing and should prove advantageous in the design of CVD precursors for transition metal deposition (80).

An additional interesting physical property associated with perfluorinated phosphine transition metal complexes is fluorocarbon solubility. In contrast to the generally poor solubility of complexes with hydrocarbon ligand substituents in fluorocarbon media, (dfep)Cr(CO)₄ (68) and ((CF₃)₃P)_xFe(CO)_{5-x} (46) are moderately soluble in perfluoroalkane solvents. While *cis*-(dfep)₂RuH₂ (81) is only sparingly soluble in most polar and nonpolar solvents, it is substantially more

soluble in perfluorohexane (0.03M) than hexane (< 0.002M). The ability of fluoroalkylphosphine ligands to promote fluorocarbon solubility offers a distinct advantage for the study of weak ligand interactions in non-coordinating media (68).

Table II. Comparison of Infrared and Electrochemical Data for $(\eta^6\text{-arene})\text{Mo}(\text{L})_3$, $\text{CpMn}(\text{L})_3$, and $\text{CpRu}(\text{L})_3^+$ Complexes

complex	$\nu(\text{CO}), \text{cm}^{-1}$	$E_{1/2}(\text{ox}), \text{V (vs. SCE)}$	ref
$(\text{C}_6\text{H}_5\text{Me})\text{Mo}(\text{dfepe})(\text{CO})$	1922	+1.06	67
$(\text{C}_6\text{H}_5\text{Me})\text{Mo}(\text{dfepe})(\text{py})$		+0.37	67
$(\text{C}_6\text{H}_5\text{PPh}_2)\text{Mo}(\text{dppe})(\text{CO})$	1817	+0.15	70
$(\text{C}_6\text{H}_5\text{Me})\text{Mo}(\text{py})_3$		-1.09	71
$\text{CpMn}(\text{dfepe})(\text{CO})$	1933	+1.09	72
$\text{CpMn}(\text{Me}_2\text{NPF}_2)_2(\text{CO})$	1920		73
$\text{CpMn}(\text{PhO})_3\text{P}(\text{CO})_2$	1961, 1893	+0.98	74
$\text{CpMn}(\text{Ph}_3\text{P})(\text{CO})_2$	1931, 1863	+0.65	74
$\text{CpMn}(\text{Ph}_3\text{P})_2(\text{CO})$	1824	-0.21	74
$\text{CpRu}(\text{dfepe})(\text{CO})^+$	2075		75
$\text{CpRu}(\text{MeCN})_2(\text{CO})^+$	2000		76
$\text{CpRu}(\text{Ph}_3\text{P})_2(\text{CO})^+$	1980		77
$\text{CpRu}(\text{Me}_3\text{P})_2(\text{CO})^+$	1961		78

To date, much of our fluoroalkylphosphine work has focused on the coordination chemistry of the dfepe chelate. Substitution of sterically demanding dfepe for small monodentate carbonyl ligands should maintain the electron-poor nature of the metal center and provide unprecedented access to stable low coordinate electrophilic metal systems with unusual structural and electronic properties. As a useful qualitative guideline, $(\text{dfepe})\text{ML}_n$ complexes are conceptually viewed as chelating electronic mimics to $(\text{CO})_2\text{ML}_n$ complexes with steric properties equal to or exceeding that of $(\text{dppe})\text{ML}_n$ donor phosphine analogues.

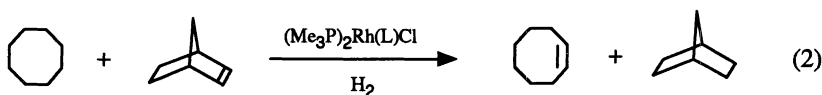
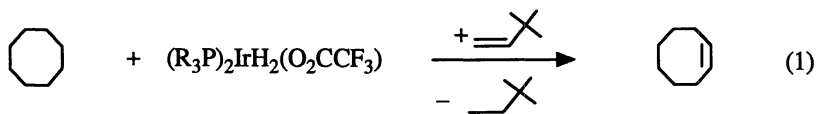
Group IX Reactivity Studies.

The coordination chemistry of the cobalt triad has received considerable attention in the areas of organometallic reaction mechanisms and homogeneous catalysis (82-84). Of particular interest have been processes such as hydrogenation, carbonylation, and hydroformylation, where the oxidative addition of substrate C-X or H-X bonds to coordinatively-unsaturated M(I) centers plays a critical role. Systems which have received the most attention thus far have been electron-rich

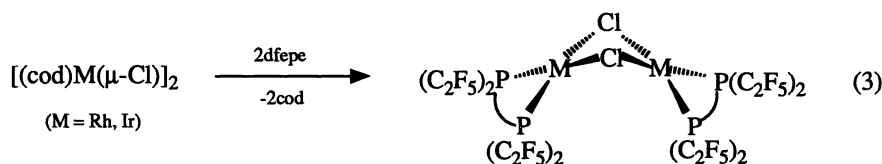


alkylphosphine or mixed phosphine-carbonyl complexes such as $(R_3P)_2M(solvent)_2^+$, $(R_3P)_3MX$, or $(R_3P)_2M(CO)X$ ($X = H$ or halide). In contrast, comparatively little is known regarding the chemistry of the related electron-poor carbonyls, $(CO)_nMX$ ($n = 2-4$). In comparison to well-studied $(CO)_4CoH$, which has marginal stability, the heavier metal homologues $(CO)_4MH$ ($M = Rh, Ir$) rapidly aggregate to form binary carbonyl clusters $M_4(CO)_{12}$ in the absence of high CO pressures (85,86). Although simple carbonyl halides such as $[(CO)_2Rh(\mu-Cl)]_2$ and $(CO)_3IrCl$ are known, much of the chemistry reported for these compounds concerns their use as synthetic precursors to carbonyl clusters and ligand addition products (87).

Our interest in the development of (fluoroalkyl)phosphine analogues to Group IX carbonyl systems stems from our work on the dehydrogenation of cycloalkanes by $(dfep)_2RuH_2$ (81). Since the extreme conditions (200 °C, days) required for dehydrogenation by this complex are attributable to its substitutionally-inert octahedral d^6 18 e^- configuration, preparative routes to coordinatively-unsaturated 16 e^- square-planar rhodium and iridium complexes have been examined. Alkane dehydrogenation is well preceded for Group IX systems (88-94). For hydrogen transfer systems reported by Crabtree (90) and Goldman (93) (equations 1 and 2), 14 e^- reactive intermediates have been proposed. Accordingly, initial efforts have been directed toward the synthesis of rhodium and iridium $dfep$ derivatives which could readily access similar 14 e^- species.

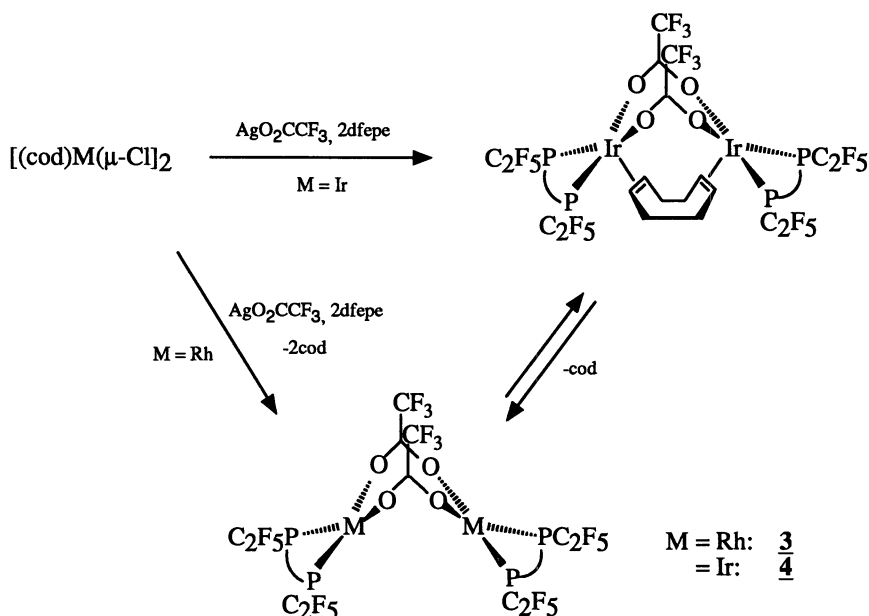


$[(\text{cod})\text{M}(\mu\text{-Cl})_2]$ ($\text{M} = \text{Rh}, \text{Ir}$) compounds provide a convenient entry to dfepe systems (95). Direct substitution of cyclooctadiene by dfepe occurs under mild conditions to afford the μ -chloro dimers $[(\text{dfepe})\text{M}(\mu\text{-Cl})_2]$ ($\text{M} = \text{Rh}, \mathbf{1}$; $\text{Ir}, \mathbf{2}$) in high yield as air-stable crystalline solids (equation 3). X-ray diffraction studies reveal that $\mathbf{1}$ and $\mathbf{2}$ have isostructural hinged $\text{M}_2(\mu\text{-Cl})_2$ core geometries. Unlike donor phosphine derivatives, the chloride bridges are quite robust and do not cleave in the presence of excess dfepe to form $(\text{dfepe})_2\text{MCl}$. In keeping with the expected electron-poor nature of these compounds, no oxidative additions of substrates such as CH_3I , O_2 , or H_2 to the $\text{Ir}(\text{I})$ center of $\mathbf{2}$ have been observed. Although the thermal stability of $\text{Ir}(\text{I})$ phosphine complexes is often limited by



facile orthometallation reactions involving the phosphine substituent alkyl groups (96,97), $\mathbf{2}$ may be heated to $150\text{ }^\circ\text{C}$ in cyclohexane for extended periods without decomposition. This enhanced stability may be due to both a general reluctance toward oxidative addition as well as the inertness of the phosphine substituent's C-F bonds.

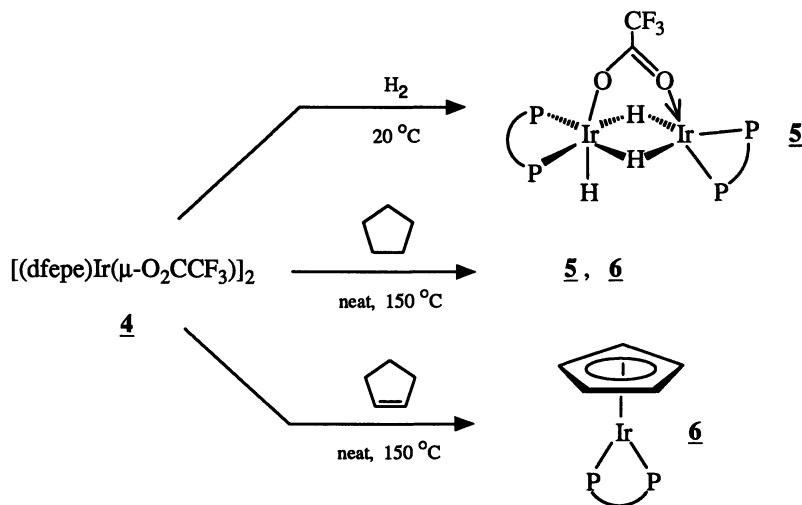
Synthesis and Reactivity of $[(\text{dfepe})\text{M}(\mu\text{-O}_2\text{CCF}_3)_2]$ Complexes. The inertness of both $\mathbf{1}$ and $\mathbf{2}$ to C-X or H-H bond addition does not necessarily imply that $(\text{dfepe})\text{M}(\text{I})$ centers are incapable of hydrocarbon activation. Rather, access to a more reactive 14-electron intermediate via chloride bridge dissociation may be a limiting factor. To test this notion, the replacement of chloride by a potentially more labile CF_3CO_2^- bridging ligand was examined. Treatment of $[(\text{cod})\text{Ir}(\mu\text{-Cl})_2]$ with AgO_2CCF_3 in CH_2Cl_2 followed by the addition of dfepe yielded an isolable deep red cyclooctadiene adduct $[(\text{dfepe})\text{Ir}(\mu\text{-O}_2\text{CCF}_3)_2](\mu\text{-cod})$, which when heated in benzene under dilute conditions quantitatively formed the desired cod-free acetate dimer, $[(\text{dfepe})\text{Ir}(\mu\text{-O}_2\text{CCF}_3)_2]$ ($\mathbf{4}$) (Scheme 2). The rhodium analogue $\mathbf{3}$ was obtained directly without evidence of a stable cyclooctadiene intermediate adduct. The dimeric bent geometries of $\mathbf{3}$ and $\mathbf{4}$, as drawn in Scheme 2, have been confirmed by IR data and an x-ray diffraction study of $\mathbf{4}$. The triphenylphosphine rhodium analogue of $\mathbf{3}$, $(\text{Ph}_3\text{P})_2\text{Rh}(\text{O}_2\text{CCF}_3)$ has been reported (98). Though initially formulated as a monomer, the close similarity in $\nu(\text{O}_2\text{CCF}_3)$ IR data for both $\mathbf{3}$, $\mathbf{4}$, and $(\text{Ph}_3\text{P})_2\text{Rh}(\text{O}_2\text{CCF}_3)$ indicate that the latter complex is most likely dimeric as well. Crabtree has reported $(\text{R}_3\text{P})_2\text{Ir}(\text{H})_2(\eta^2\text{-O}_2\text{CCF}_3)$ ($\text{R} = p\text{-FC}_6\text{H}_4, \text{Cy}$); however, attempts to isolate dehydrogenated $(\text{R}_3\text{P})_2\text{Ir}(\text{O}_2\text{CCF}_3)$ compounds were unsuccessful (88). It is possible that the cis phosphine orientation required for dimer formation is sterically unfavorable for these monodentate phosphine systems.



Scheme 2.

The reactivity properties of **4** differ markedly from the chloro-bridged dimer **2** (**99**). As noted above, cyclooctadiene weakly binds in a bridging mode to the iridium centers of **4**. The reversible binding of ethylene to **4** has similarly been observed by variable temperature NMR. In contrast, there is no evidence for cod or ethylene binding to **2**. While **2** and the rhodium acetate dimer **3** are similarly unreactive with H_2 , exposure of a benzene solution of **4** to 1 atm H_2 at ambient temperature results in the loss of one equivalent of $\text{CF}_3\text{CO}_2\text{H}$ and the formation of the unsymmetrical trihydride dimer $(\text{dfepe})_2\text{Ir}_2(\text{H})(\mu\text{-H})_2(\mu\text{-O}_2\text{CCF}_3)$ (**5**) in high yield (Scheme 3). The assignment of **5** is supported by NMR data and the recent preparation of the analogous structurally-characterized bridging triflate dimer $(\text{dfepe})_2\text{Ir}_2(\text{H})(\mu\text{-H})_2(\mu\text{-O}_3\text{SCF}_3)$, in our laboratory (*100*). The olefin hydrogenation activity of **5** has been briefly examined. No spectral changes are noted for **5**; however, in the presence of excess ethylene at 20 °C the addition of H_2 (*ca.* 800 torr) initiates ethane formation at a rate of approximately 50 turnovers/hour. **5** was the sole iridium species observed during the course of the hydrogenation.

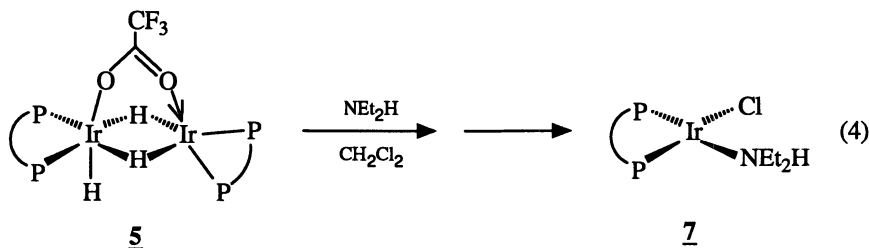
In light of the hydrogenation reactions described above, it is not surprising that **4** also participates in dehydrogenation reactions. Thermolysis of **4** in neat cyclopentene at 150 °C for one day quantitatively affords $\text{CpIr}(\text{dfepe})$ (**6**). Under the same temperature conditions, **4** in neat cyclopentane yields a mixture of the trihydride dimer **5** and $\text{CpIr}(\text{dfepe})$ (Scheme 3). The relative yield of **5** diminishes under dilute conditions, indicating that this product is formed via a secondary reaction of **4** with released H_2 . No discernible reaction between the rhodium analog **3** and cyclopentane occurs at this temperature. **5** is itself inactive toward

**Scheme 3.**

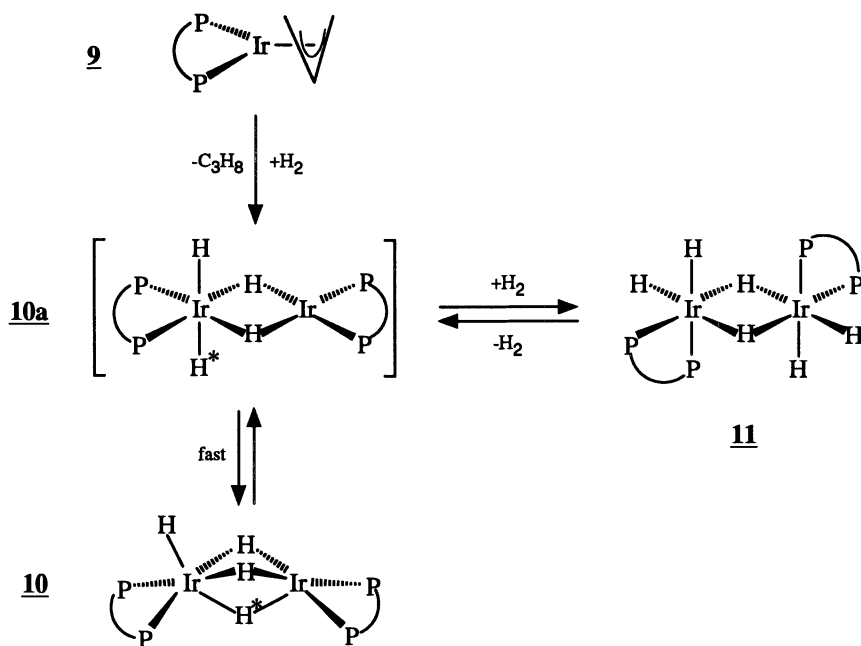
dehydrogenation and appears to be a thermodynamic sink for this system in the absence of a hydrogen acceptor. The qualitative similarity in dehydrogenation rates between cyclopentene and cyclopentane media for **4** differs from the selectivity $k(C_5H_8) \gg k(C_5H_{10})$ found for *cis*-(dfepe)₂RuH₂ (**81**), suggesting that the rate limiting step for **4** may involve the dissociation of one or both acetate bridges to access reactive 14 e⁻ metal centers, rather than a direct C-H addition to the dimer.

Synthesis of Binuclear Iridium Polyhydrides. It is clear from the preceding observations concerning chloro and acetato-bridged dimers that iridium reactivity patterns are highly sensitive to the nature of the bridging ligand group. Since the trihydride dimer **5** is effectively the CF₃CO₂H protonation product of the Ir(I) dihydride dimer, [(dfepe)Ir(μ-H)]₂, synthetic routes to this parent system have been examined. The direct deprotonation of **5** or the triflate analogue has thus far proven unsuccessful. In one instance, treatment of the triflate complex with diethylamine in CH₂Cl₂ quantitatively afforded the previously-characterized amine chloride (dfepe)Ir(NEt₂H)Cl (**7**) (**95**). This product is presumably derived from the reaction of initially-formed [(dfepe)Ir(μ-H)]₂ with the chlorinated solvent.

A well-precedented route to cobalt and rhodium phosphine hydride complexes of the general form [(R₃P)_nM(H)_m]_x is via the hydrogenolysis of the corresponding allyl compounds, (R₃P)_nM(η³-allyl) (n = 2 or 3). Depending on the nature of the ancillary phosphine, dimeric complexes (R₃P)₄Rh₂(H)₂ (**101-103**) and (R₃P)₄M₂(H)₄ (M = Co (**104**), Rh (**102,103**)) as well as higher oligomeric products [(R₃P)₂Rh(H)]_n (n = 3, 4) (**101,105**) have been characterized. To date, the development of iridium phosphine hydride chemistry has been primarily limited to higher valent Ir(III) and Ir(V) monomeric (R₃P)₃IrH₃ (**106**) and (R₃P)₂IrH₅ (**107-109**) systems; moreover, the hydrogenolysis chemistry of iridium allyls remains essentially unexplored. The allyl complexes (dfepe)M(η³-C₃H₅) (M = Rh



(**8**); Ir (**9**) are readily obtained as sublimable crystalline solids by treatment of the appropriate chloro-dimer with allylmagnesium bromide (unpublished results). Whereas the hydrogenolysis of **8** under 2 atm H_2 in hexane proceeds quite slowly over the course of several days to give an uncharacterized thermally unstable insoluble dark green solid, the corresponding reaction with **9** rapidly affords an air-stable red binuclear tetrahydride, $(dfepe)_2Ir_2(H)_4$ (**10**) in high yield (Scheme 4).

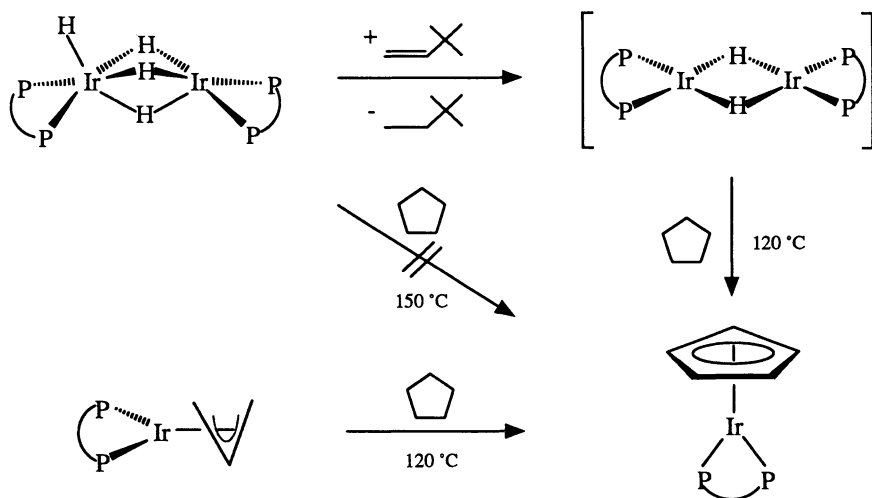


Scheme 4.

Variable temperature 1H and ^{31}P NMR data for **10** are fully consistent with a triply-bridged ground state structure $(dfepe)_2Ir_2(H)(\mu-H)_3$ that undergoes rapid exchange of the terminal hydride ligand and a unique trans bridging hydride; analogous dynamic behavior has been reported by Fryzuk for $(R_3P)_4Rh_2(H)_4$ systems (**102**).

The accessibility of a coordinatively-unsaturated intermediate **10a** suggested by NMR data for **10** is supported by its reactivity with hydrogen. In polar solvents, deep red solutions of **10** exhibit no spectroscopic changes under 2 atm H₂. However, exposure of a hexane slurry of **10** to 2 atm hydrogen at 20 °C for 24 hours results in the quantitative precipitation of a new pale yellow crystalline solid. Redissolving this insoluble product in acetone or other coordinating solvents leads to rapid loss of H₂ and regeneration of **10**. Based on hydrogen uptake and preliminary diffraction data, this unstable product is tentatively formulated as the binuclear Ir(III)-Ir(III) hexahydride, [(dfep)₂Ir(H)₂]₂(μ-H)₂ (**11**). To our knowledge only a single well-characterized donor phosphine dimeric hexahydride similar to **11** has been reported (*110*).

The activation of C-H bonds by iridium polyhydrides has been reported in the presence of olefinic hydrogen acceptors. For the pentahydride (iPr₃P)₂IrH₅, phosphine-metallation (*111*) as well as catalytic hydrocarbon and vinylic H-D exchange (*107*) has been observed. In all cases, an unsaturated Ir(III) or Ir(I) species generated by olefin hydrogenation has been proposed as the reactive intermediate. The direct hydrogenation of the tetrahydride **10** to give **11** suggested that direct C-H activation in the absence of a hydrogen acceptor might be possible. Indeed, slow H-D exchange between **10** and deuterobenzene is observed over the course of several days at 120 °C. However, no H-D exchange with deuterocyclohexane or dehydrogenation of cyclopentane is found at temperatures up to 150 °C. In the presence of (*t*-butyl)ethylene, formation of CpIr(dfep) (**6**) in neat

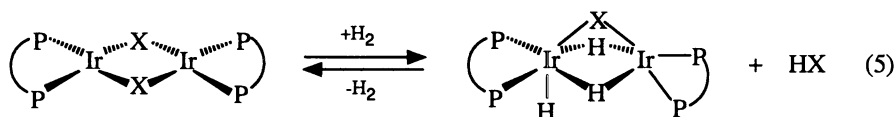


Scheme 5.

cyclopentane is quantitative after one day at 120 °C (Scheme 5). A likely active intermediate involved in this process is the dihydride, [(dfep)₂Ir(μ-H)₂]. Interestingly, **6** may also be prepared by the direct thermolysis of (dfep)Ir(η³-allyl) in cyclopentane at 120 °C. This latter reaction provides an interesting model for the reverse process of arene hydrogenation reactions reported for (R₃P)₂Co(η³-allyl) systems (*112*).

Summary.

The oxidative addition of substrate bonds to electron-rich low-valent metal centers of the platinum group metals has guided much of our thinking in the area of organometallic reaction mechanisms. Although the relative reactivities of elementary addition processes such as hydrogen or C-H addition to Vaska's complex and related M(I) systems correlate well with metal electron density, it is clear that for more complicated transformations additional driving forces may become important. The relative reactivities of the (fluoroalkyl)phosphine dimers [(dfepe)Ir(μ -X)]₂ (X = Cl, O₂CCF₃) toward H₂ illustrate this point (equation 5).



The overall equilibrium depicted in equation 5 involves both the heterolysis of H₂ to release HX and the formation of stable 3-center 2-electron hydride bridges. For X = Cl, release of the strong acid HCl would be disfavored relative to the release of CF₃CO₂H from the hydrogenolysis of **4**. This does not appear to be the critical factor, however, since the addition of Et₃N to [(dfepe)Ir(μ -Cl)]₂ under 1 atm H₂ does not drive hydride product formation. Pending further studies on bridging ligand effects, it is not obvious why the Ir₂(μ -Cl)₂ core of **2** is inert relative to the Ir₂(μ -O₂CCF₃)₂ and Ir₂(μ -H)₂ cores of **4** and **10**.

The perturbation of conventional donor phosphine coordination chemistry induced by the perfluorination of alkyl substituents is readily manifested in a range of metal systems. For the iridium compounds described in this chapter, the thermal and air stability of electron-poor Ir(I) complexes is quite exceptional. Nevertheless, both H-H and C-H activation reactivity patterns commonly associated with electron-rich Ir(I) systems are accessible. Rhodium dfepe analogues examined thus far do not exhibit similar reactivity patterns, suggesting that generation of (dfepe)Rh(III) intermediates is unfavorable. We are currently extending our studies to potentially more labile and reactive [(dfepe)Ir(μ -X)]₂ complexes in order to explore C-H activation reactions of electrophilic iridium centers in more detail.

Acknowledgments. This work has been supported by the National Science Foundation (Grant No. CHE-8912697) and the donors of the Petroleum Research Fund, administered by the American Chemical Society. Johnson Matthey is gratefully acknowledged for a generous loan of iridium and rhodium trichlorides.

Literature Cited

1. Tolman, C. A. *Chem. Rev.* **1977**, *77*, 313.
2. *Homogeneous Catalysis with Metal Phosphine Complexes*; Pignolet, L. H., Ed.; Plenum Press: New York, N.Y., 1983.

3. Shaverein, C. J.; Dewar, J. C.; Schrock, R. R. *J. Am. Chem. Soc.* **1986**, *108*, 2771.
4. Lubben, T. V.; Wolczanski, P. T.; Van Duyne, G. D. *Organometallics* **1984**, *3*, 977.
5. Kerschner, J. L.; Fanwick, P. E.; Rothwell, I. P. *J. Am. Chem. Soc.* **1987**, *109*, 5840.
6. Weese, K. J.; Bartlett, R. A.; Decker, D.; Olmstead, M. M.; Power, P. P. *Inorg. Chem.* **1987**, *26*, 2409.
7. Yoshida, T.; Adachi, T.; Kaminaka, M.; Ueda, T.; Higuchi, T. *J. Am. Chem. Soc.* **1988**, *110*, 4872.
8. Lappert, M. F.; Power, P. P.; Sanger, A. R.; Srivastava, R. C. *Metal and Metalloid Amides*; Ellis Horwood Ltd.: Chichester, 1980.
9. Hillhouse, G. L.; Bulls, A. R.; Santarsiero, B. D.; Bercaw, J. E. *Organometallics* **1988**, *7*, 1309.
10. Andersen, R.A. *Inorg. Chem.* **1979**, *18*, 2928.
11. Nugent, W. A. *Inorg. Chem.* **1983**, *22*, 965.
12. Baker, R. T.; Whitney, J. F.; Wreford, S. S. *Organometallics* **1983**, *2*, 1049.
13. Jones, R. A.; Wright, T. L.; Atwood, J. L.; Hunter, W. E. *Organometallics* **1983**, *2*, 470.
14. Roddick, D. M.; Santarsiero, B. D.; Bercaw, J. E. *J. Am. Chem. Soc.* **1985**, *107*, 4670.
15. Schrock, R. R.; Parshall, G. W. *Chem. Rev.* **1976**, *76*, 243.
16. Davidson, P. J.; Lappert, M. F.; Pierce, R. *Chem. Rev.* **1976**, *76*, 219.
17. Giandomenico, C. M.; Lam, C. T.; Lippard, S. J. *J. Am. Chem. Soc.* **1984**, *104*, 1263.
18. Wolczanski, P. T.; Bercaw, J. E. *J. Am. Chem. Soc.* **1979**, *101*, 6450.
19. Singleton, E.; Oosthuizen, H. E. *Adv. Organomet. Chem.* **1983**, *22*, pp 209-310.
20. Johnson, T. R.; Nixon, J. F. *J. Chem. Soc. A* **1969**, 2518.
21. King, R. B. *Acc. Chem. Res.* **1980**, *13*, 243.
22. King, R. B.; Shimura, M.; Brown, G. M. *Inorg. Chem.* **1984**, *23*, 1398.
23. Mague, J. T.; Johnson, M. P.; Lloyd, C. L. *J. Am. Chem. Soc.* **1989**, *111*, 5012.
24. Brown, G. M.; Finholt, J. E.; King, R. B.; Lee, T. W. *J. Am. Chem. Soc.* **1981**, *103*, 5249.
25. Burg, A. B.; Street, G. B. *Inorg. Chem.* **1966**, *5*, 1532.
26. Udovich, C. A.; Clark, R. J.; Haas, H. *Inorg. Chem.* **1969**, *8*, 1066.
27. Mathieu, R.; Poilblanc, R. *Inorg. Chem.* **1972**, *11*, 1858.
28. Lustig, M. *Inorg. Chem.* **1968**, *10*, 2054.
29. Bauer, D. P.; Ruff, J. K. *Inorg. Chem.* **1983**, *22*, 1686.
30. Van Leeuwen, P. W. N. M.; Roobeek, C. F. *J. Organomet. Chem.* **1983**, *258*, 343.
31. Montemayor, R. G.; Sawyer, D. T.; Fleming, S. S.; Bennett, D. W.; Thomas, M. G.; Parry, R. W. *J. Am. Chem. Soc.* **1978**, *100*, 2231.
32. Douglas, W. M.; Ruff, J. K. *J. Chem. Soc. A* **1971**, 3558.
33. Cook, R. L.; Morse, J. G. *Inorg. Chem.* **1984**, *23*, 2332.
34. Gallup, D. L.; Morse, J. G. *J. Organomet. Chem.* **1978**, *159*, 477.

35. Burg, A. B. *Acc. Chem. Res.* **1969**, *2*, 353.
36. Magnusson, E. *Aust. J. Chem.* **1985**, *38*, 23.
37. Whangbo, M. -H.; Stewart, K. R. *Inorg. Chem.* **1982**, *21*, 1720.
38. Marsden, C. J.; Bartell, L. S. *Inorg. Chem.* **1976**, *15*, 2713.
39. Oberhammer, H. *J. Mol. Struct.* **1975**, *28*, 349.
40. Gleiter, R.; Goodmann, W. D.; Schäfer, W.; Grobe, J.; Apel, J. *Chem. Ber.* **1983**, *116*, 3745.
41. Lee, T. H.; Jolly, W. L.; Bakke, A. A.; Weiss, R.; Verkade, J. G. *J. Am. Chem. Soc.* **1980**, *102*, 2631.
42. Apel, V. J.; Grobe, J. Z. *Anorg. Allg. Chem.* **1979**, *453*, pp. 28 and 53.
43. Burg, A. B. *Inorg. Nucl. Chem. Lett.* **1977**, *13*, 199.
44. Kang, D. -K.; Burg, A. B. *Inorg. Chem.* **1972**, *11*, 902.
45. Burg, A. B.; Sabherwal, I. H. *Inorg. Chem.* **1970**, *9*, 974.
46. Burg, A. B. *Inorg. Chem.* **1986**, *25*, 4751.
47. Khokhryakov, K. A.; Maslennikov, I. G.; Grigorev, E. I.; Kukushkin, Y. N. *J. Gen. Chem. U.S.S.R.* **1985**, *55*, 2331.
48. Grobe, J.; Le Van, D.; Meyring, W. Z. *Anorg. Allg. Chem.* **1990**, *586*, 149.
49. Clegg, W.; Morton, S. *Inorg. Chem.* **1979**, *18*, 1189.
50. Dobbie, R. C.; Hopkinson, M. J.; Whittaker, D. *J. Chem. Soc., Dalton Trans.* **1972**, 1030.
51. Sinclair, R. A.; Burg, A. B. *Inorg. Chem.* **1968**, *7*, 2160.
52. Burg, A. B.; Sinclair, R. A. *J. Am. Chem. Soc.* **1966**, *88*, 5354.
53. Einspar, H.; Donohue, J. *Inorg. Chem.* **1974**, *13*, 1839.
54. Grant, L. R., Ph. D. Dissertation, University of Southern California, 1961, pg 29.
55. A more broadly applicable synthesis of trifluoromethylated phosphine chelates has been reported: Phillips, I. G.; Ball, R. G.; Cavell, R. G. *Inorg. Chem.* **1988**, *27*, 4038.
56. Ernst, M. F.; Roddick, D. M. *Inorg. Chem.* **1989**, *28*, 1624.
57. Brookhart, M.; Chandler, W. A.; Pfister, A. C.; Santini, C. C.; White, P. S. *Organometallics* **1992**, *11*, 1263.
58. Gassman, P. G.; O'Reilly, N. J. *Tetrahedron* **1985**, *26*, 5243.
59. Sowa, J. R.; Angelici, R. J. *Inorg. Chem.* **1991**, *30*, 3534.
60. Kemmit, R. D. W.; Nichols, D. I.; Peacock, R. D. *J. Chem. Soc. A* **1968**, 1898.
61. Barlow, C. G.; Nixon, J. F.; Webster, M. *J. Chem. Soc. A* **1968**, 2216.
62. Apel, V. J.; Bacher, R.; Grobe, J.; Le Van, D. Z. *Anorg. Allg. Chem.* **1979**, *453*, 39.
63. Johnson, T. R.; Nixon, J. F. *J. Chem. Soc. A* **1969**, 2518.
64. Cook, R. L.; Morse, J. G. *Inorg. Chem.* **1984**, *23*, 2332.
65. King, R. B.; Rhee, W. M. *Inorg. Chem.* **1978**, *17*, 2961.
66. Chatt, J.; Watson, H. R. *J. Chem. Soc.* **1961**, 4980.
67. Ernst, M. F.; Roddick, D. M. *Organometallics* **1990**, *9*, 1586.
68. Brookhart, M.; Chandler, W.; Kessler, R. J.; Liu, Y.; Pienta, N. J.; Santini, C. C.; Hall, C.; Perutz, R. N.; Timney, J. A. *J. Am. Chem. Soc.* **1992**, *114*, 3802.

69. Huheey, J. E. *Inorganic Chemistry*; 3rd Ed., Harper & Row: New York, N.Y., 1983, pp 144-160.
70. Morris, R. H.; Earl, K. A.; Luck, R. L.; Lazarowych, N. J.; Sella, A. *Inorg. Chem.* **1987**, *26*, 2674.
71. Silverthorn, W. E. *Inorg. Chem.* **1979**, *18*, 1835.
72. Merwin, R. K.; Roddick, D. M., unpublished results.
73. King, R. B.; Zipperer, W. C.; Ishaq, M. *Inorg. Chem.* **1972**, *11*, 1361.
74. Connelly, N. G.; Kitchen, M. D. *J. Chem. Soc., Dalton Trans.* **1977**, 931.
75. Keady, M. S.; Koola, J. D.; Ontko, A. C.; Merwin, R. K.; Roddick, D. M. *Organometallics* **1992**, *11*, 3417.
76. Crocker, M.; Green, M.; Morton, C. E.; Nagle, K. R.; Orpen, A. G. *J. Chem. Soc., Dalton Trans.* **1985**, 2145.
77. Blackmore, T.; Bruce, M. I.; Stone, F. G. A. *J. Chem. Soc. A* **1971**, 2376.
78. Bruce, M. I.; Wong, F. S.; Skelton, B. W.; White, A. H. *J. Chem. Soc., Dalton Trans.* **1981**, 1398.
79. Barlow, C. G.; Nixon, J. F.; Webster, M. *J. Chem. Soc. A* **1968**, 2216.
80. Jensen, F.; Kern, W. In *Thin Film Processes II*; J. L. Vossen, W. Kern Eds.; Academic Press Inc.: San Diego, CA, 1991, Part III.
81. Koola, J. D.; Roddick, D. M. *J. Am. Chem. Soc.* **1991**, *113*, 1450.
82. Collman, J. P.; Hegedus, L. S.; Norton, J. R.; Finke, R. G. *Principles and Applications of Organotransition metal Chemistry*; University Science Books: Mill Valley, CA, 2nd Ed., 1987.
83. Jardine, F. H. In *Chemistry of the Platinum Group Metals*; Hartley, F. R., Ed.; Elsevier: New York, NY, 1991; Chapter 13.
84. Dickson, R. S. *Homogeneous Catalysis with Compounds of Rhodium and Iridium*; D. Reidel Publ. Co.: Dordrecht, Holland, 1985.
85. Vidal, J. L.; Walker, W. E. *Inorg. Chem.* **1981**, *20*, 249.
86. Whyman, R. *J. Chem. Soc., Dalton Trans.* **1972**, 1375.
87. Dickson, R. S. *Organometallic Chemistry of Rhodium and Iridium*; Academic Press: New York, NY, 1983, pp 10-107.
88. Burk, M. J.; Crabtree, R. H. *J. Am. Chem. Soc.* **1987**, *109*, 8025.
89. Crabtree, R. H.; Parnell, C. P.; Uriarte, R. J. *Organometallics* **1987**, *6*, 696.
90. Burk, M. J.; Crabtree, R. H.; Parnell, C. P.; Uriarte, R. J. *Organometallics* **1984**, *3*, 816.
91. Sakakura, T.; Sodeyama, T.; Tokunaga, Y.; Tanaka, M. *Chem. Lett.* **1988**, 263.
92. Fujii, T.; Saito, Y. *J. Chem. Soc., Chem. Commun.* **1990**, 757.
93. Maguire, J. A.; Petrillo, A.; Goldman, A. S. *J. Am. Chem. Soc.* **1991**, *114*, 9492.
94. Maguire, J. A.; Boese, W. T.; Goldman, M. E.; Goldman, A. S. *Coord. Chem. Rev.* **1990**, *97*, 179.
95. Schnabel, R. C.; Roddick, D. M., *Inorg. Chem.* **1993**, *32*, in press.
96. Dahlenburg, L.; Yardimcioglu, A. *J. Organomet. Chem.* **1986**, *299*, 149.
97. Bennett, M. A.; Milner, D. L. *J. Am. Chem. Soc.* **1969**, *91*, 6983.
98. Commereuc, D.; Douek, I.; Wilkinson, G. *J. Chem. Soc. A* **1970**, 1771.
99. Schnabel, R. C.; Roddick, D. M., manuscript in preparation.
100. Schnabel, R. C.; Roddick, D. M., *Organometallics* **1993**, *12*, in press.

101. Sivak, A. J.; Meuterties, E. L. *J. Am. Chem. Soc.* **1979**, *101*, 4878.
102. Fryzuk, M. D.; Piers, W. E. *Can. J. Chem.* **1989**, *67*, 883.
103. Fryzuk, M. D.; Piers, W. E.; Rettig, S. J.; Einstein, F. W. B.; Jones, T.; Albright, T. A. *J. Am. Chem. Soc.* **1989**, *111*, 5709.
104. Fryzuk, M. D.; Ng, J. B.; Rettig, S. J.; Huffman, J. C.; Jonas, K. *Inorg. Chem.* **1991**, *30*, 2437.
105. Fryzuk, M. D. *Organometallics* **1982**, *1*, 408.
106. Ahmad, N.; Robinson, S. D.; Uttley, M. F. *J. Chem. Soc., Dalton Trans.* **1972**, 843.
107. Faller, J. W.; Smart, C. J. *Organometallics* **1989**, *8*, 602.
108. Cameron, C. J.; Felkin, H.; Fillebeen-Khan, T.; Forrow, N. J.; Guittet, E. *J. Chem. Soc., Chem. Commun.* **1986**, 801.
109. Mann, B. E.; Masters, C.; Shaw, B. L. *J. Inorg. Nucl. Chem.* **1971**, *33*, 2195.
110. Robertson, G. B.; Tucker, P. A. *Aust. J. Chem.* **1984**, *37*, 257.
111. Clerici, M. G.; Giocchino, S. D.; Maspero, F.; Perrotti, E.; Zanobi, A. *J. Organomet. Chem.* **1975**, *84*, 379.
112. Bleeke, J. R.; Muetterties, E. L. *J. Am. Chem. Soc.* **1981**, *103*, 556.

RECEIVED June 10, 1993

Author Index

- Andersen, Richard A., 383
Aubke, F., 350
Bäck, Birgit, 90
Barren, Elizabeth, 286
Bartlett, Neil, 26
Brand, Holger, 286
Brodbelt, Jennifer S., 216
Brosius, A., 104
Burton, Donald J., 297
Chopra, Suman K., 167
Christe, K. O., 66
Cicha, Walter V., 181
Clark, Wayne D., 216
Cockman, R. W., 326
Covey, Jane, 181
Curnow, Owen J., 252
Curtis, E. C., 66
Dixon, D. A., 66
Ebsworth, E. A. V., 326
Edelmann, Frank T., 309
Farnham, William B., 209
Fernandez, Richard E., 237
FitzPatrick, J. R., 40
Foropoulos, J., Jr., 40
Gard, Gary L., 128
George, C. F., 405
Haas, A., 104
Hagiwara, Rika, 26
Holloway, J. H., 326
Hughes, Russell P., 252
Hurlburt, Paul K., 338
Kinkead, S. A., 40
Kissane, R. J., 40
Konieczny, Linda, 286
Lagow, Richard J., 216
Lentz, Dieter, 265
Lin, Tzuhn-Yuan, 216
Lin, Wen-Huey, 216
Liou, Chien Chung, 216
Mairs, Erin N., 252
Maleknia, Simin D., 216
Mallouk, Thomas E., 26
Martin, J. C., 167
Mercier, H. P. A., 66
Mews, R., 148
Minkwitz, Rolf, 90
Moon, Chester D., 167
Murdoch, H., 326
Osterberg, Carolyn E., 392
Purdy, A. P., 405
Purson, J. D., 40
Rack, Jeffrey J., 338
Rheingold, Arnold L., 252
Richmond, Thomas G., 392
Robertson, N., 326
Roddick, Dean M., 421
Roesky, Herbert W., 216
Rose, Peter R., 252
Sanders, J. C. P., 66
Schermerhorn, E. James, 286
Schnabel, Richard C., 421
Schrobilgen, G. J., 66
Seggen, Dawn M. Van, 338
Seppelt, Konrad, 56
Shen, Ciping, 26
Shufon, Kevin, 286
Strauss, Steven H., 1,338
Thrasher, Joseph S., 1,237
Toscano, Paul J., 286
Wang, John H., 181
Watson, P. G., 326
Weydert, Marc, 383
Wilson, W. W., 66
Winkler, Stephen van, 286
Winter, Charles H., 366
Winter, Rolf, 128
Zane, Stephen G., 209
Zheng, Xiaoming, 252
Zhou, Xiao-Xing, 366

Affiliation Index

- BP Chemicals Ltd., 326
 Colorado State University, 1,338
 Concordia College, 392
 Crisla Technologies Research and Development, 181
 Dartmouth College, 252
 DuPont, 66,209,237
 Durham University, 326
 Edinburgh University, 326
 Freie Universität Berlin, 56,265,326
 Los Alamos National Laboratory, 40
 McMaster University, 66
 Naval Research Laboratory, 405
 Portland State University, 128
 Rocketdyne, 66
 Ruhr-Universität Bochum, 104
 State University of New York at Albany, 286
 Universität Bremen, 148,326
 Universität Dortmund, 90
 Universität Göttingen, 309
 The University—Leicester, 326
 The University of Alabama, 1,237
 The University of British Columbia, 350
 University of California—Berkeley, 26,383
 University of Delaware, 252
 University of Iowa, 297
 The University of Texas at Austin, 216
 University of Utah, 392
 University of Wyoming, 421
 Vanderbilt University, 167
 Wayne State University, 366

Subject Index

A

- AB_x (*x* = 5 or 6), geometries, 56
 Acetylenes, addition of SF₅ halides, 136
 Activation of carbon–fluorine bonds
 conditions, 400
 electron-deficient reagents, 393
 electron-rich reagents, 393–396
 experimental procedure, 402
 future prospects, 400
 NMR data, 396,397*t*
 ORTEP diagram, 400,401*f*
 product data, 396–397,398*t*
 reactivity, 399–400
 Addition reaction, alkali metal polyhydrogen
 fluorides as halogen exchange media,
 240–242
 Ag²⁺, stabilization by very weakly basic
 fluoro anions, 355–357
 Alkali and alkaline earth fluoroalkoxides,
 chemistry, 406*t*
 Alkali metal fluorides, functions
 and limitations, 237
 Alkali metal polyhydrogen fluorides as
 halogen exchange media
 addition reaction, 240–242
 concept, 237–238
 previous studies, 238–239
 regeneration reaction, 241–248
 substitution reaction, 240–242
 thermodynamics, 237–239
 Alkane(s), functionalization strategies, 366
 Alkane activation, 366–367
 Alkenyl cadmium reagents, synthesis,
 298–300
 Al(OCH₂CF₃)₃, polymerization of
 fluorinated aldehyde, 214
 Anion(s), polyfluorinated, *See*
 Polyfluorinated anions
 Anion basicity scale, dimethyltin(IV)
 cation, 352–354
 Antimony(V) fluoride, carbonylation and
 solvolysis for synthesis of weakly
 basic fluoro anions, 352
 (ArF)⁺ species, binding, 26
 ArF⁺ salts, prospects, 37–38

Affiliation Index

- BP Chemicals Ltd., 326
 Colorado State University, 1,338
 Concordia College, 392
 Crisla Technologies Research and Development, 181
 Dartmouth College, 252
 DuPont, 66,209,237
 Durham University, 326
 Edinburgh University, 326
 Freie Universität Berlin, 56,265,326
 Los Alamos National Laboratory, 40
 McMaster University, 66
 Naval Research Laboratory, 405
 Portland State University, 128
 Rocketdyne, 66
 Ruhr-Universität Bochum, 104
 State University of New York at Albany, 286
 Universität Bremen, 148,326
 Universität Dortmund, 90
 Universität Göttingen, 309
 The University—Leicester, 326
 The University of Alabama, 1,237
 The University of British Columbia, 350
 University of California—Berkeley, 26,383
 University of Delaware, 252
 University of Iowa, 297
 The University of Texas at Austin, 216
 University of Utah, 392
 University of Wyoming, 421
 Vanderbilt University, 167
 Wayne State University, 366

Subject Index

A

- AB_x (*x* = 5 or 6), geometries, 56
 Acetylenes, addition of SF₅ halides, 136
 Activation of carbon–fluorine bonds
 conditions, 400
 electron-deficient reagents, 393
 electron-rich reagents, 393–396
 experimental procedure, 402
 future prospects, 400
 NMR data, 396,397*t*
 ORTEP diagram, 400,401*f*
 product data, 396–397,398*t*
 reactivity, 399–400
 Addition reaction, alkali metal polyhydrogen
 fluorides as halogen exchange media,
 240–242
 Ag²⁺, stabilization by very weakly basic
 fluoro anions, 355–357
 Alkali and alkaline earth fluoroalkoxides,
 chemistry, 406*t*
 Alkali metal fluorides, functions
 and limitations, 237
 Alkali metal polyhydrogen fluorides as
 halogen exchange media
 addition reaction, 240–242
 concept, 237–238
 previous studies, 238–239
 regeneration reaction, 241–248
 substitution reaction, 240–242
 thermodynamics, 237–239
 Alkane(s), functionalization strategies, 366
 Alkane activation, 366–367
 Alkenyl cadmium reagents, synthesis,
 298–300
 Al(OCH₂CF₃)₃, polymerization of
 fluorinated aldehyde, 214
 Anion(s), polyfluorinated, *See*
 Polyfluorinated anions
 Anion basicity scale, dimethyltin(IV)
 cation, 352–354
 Antimony(V) fluoride, carbonylation and
 solvolytic synthesis of weakly
 basic fluoro anions, 352
 (ArF)⁺ species, binding, 26
 ArF⁺ salts, prospects, 37–38

- AsF₅, high F⁻ affinity, 31
- Au²⁺, stabilization by very weakly basic fluoro anions, 355–357
- B**
- Bifunctional SN systems, addition of fluoride ions, 157–163
- Binuclear iridium polyhydrides, synthesis, 430–432
- Bis(dimethylglyoximate)cobalt(III) complexes, studies, 286
- Bis(fluorosulfonyl) peroxide, oxidation for synthesis of weakly basic fluoro anion compounds, 351
- Bonds, novel types to noble gases, 3–4
- Bonds in organic molecules, selective functionalization, 366
- B(OTeF₅)₄⁻, role in coordinative unsaturation in cations, 341–344, 346
- Br²⁺, stabilization by very weakly basic fluoro anions, 354–355
- 4-(*tert*-Butyl)- $\alpha,\alpha,\alpha',\alpha'$ -tetrakis(trifluoromethyl)-2,6-pyridinedimethanolato-(2-)-*N*¹,*O*^a,*O* ^{α} -substituted silicate, synthesis, 170–175
- C**
- C–F bond(s)
- activation, 7,392–402
 - function, 392
- ¹³C-NMR spectroscopy, characterization of fluoroalkyl cobaloximes, 290–291
- (C₂F₅)₂PCH₂CH₂P(C₂F₅)₂, synthesis, 423–424
- C₇F₁₅CHO, polymerization with CF₃CH₂OTiL₃, 213–214
- Cadmium reagents, perfluorovinyl, *See* Perfluorovinyl cadmium reagents
- Carbenes, fluorine-containing, chemistry, 105–108
- Carbon–carbon bonds, addition of SF₅ halides, 135–136
- Carbonyl(s), fluorine-containing, chemistry, 114
- Carbonyl derivatives, noble metal, stabilization by very weakly basic fluoro anions, 357–362
- Cation(s), unusual, stabilization by very weakly basic fluoro anions, 350–362
- Cationic complexes, coordinative unsaturation, 338–346
- CF₃CH₂OCF₂CHFOCF₂CF(CF₃)OCF₂CF₂CHO end capping with PCl₃ and Cl₂, 213
- polymerization
- Al(OCH₂CF₃)₃, 214
 - TAS Me₃SiF₂, 213
- synthesis, 213
- CF₃CH₂OTiL₃, polymerization of fluorinated aldehydes, 213–214
- CF₃SO₂ group, superacid development, 8
- Chemical vapor deposition of inorganic materials, precursors, development, 1
- Chemistry
- dinuclear trifluoromethyl isocyanide complexes and cluster compounds, 270,272f,273,275–278f
 - fluorinated isopropoxides and tertiary butoxides
 - alkali and alkaline earth derivatives, 406f
 - experimental description, 405–406
 - group 6 and 7 derivatives, 417–418
 - group 11 derivatives, 406–416
 - lanthanide derivatives, 417
 - zirconium derivatives, 416–417
 - group 6 fluoroalkoxides, 417–418
 - group 7 fluoroalkoxides, 417–418
 - group 11 fluoroalkoxides, 406–416
 - lanthanide fluoroalkoxides, 417
 - mononuclear trifluoromethyl isocyanide complexes, 269–270
 - pentafluorophenyl isocyanide, 281
 - perfluoro macrocycles, 216–235
 - trifluorovinyl isocyanide, 281,282f
 - zirconium fluoroalkoxides, 416–417
- Chlorofluorocarbon alternatives, development, 1
- Cobaloximes, studies, 286
- Collisionally activated dissociation, MS characterization of perfluoro macrocycles, 229–230
- Computational chemistry, relationship to experimental chemistry, 4–5
- Coordinated trifluoromethyl isocyanide ligand, reactions, 273,279–280,282
- Coordination chemistry, (fluoroalkyl)phosphines, 421–432

- Coordination number 7 fluorides
geometries, 56–61
transition metal compounds, 61
- Coordination number 8 fluorides,
geometries, 61, 62*f*
- Coordination numbers greater than six among
fluorides and oxofluorides, description, 2
- Coordination properties,
(fluoroalkyl)phosphines, 424–426
- Coordinative unsaturation
description, 338–339
generation by polyfluorinated anions in
cations, 340–346
- Copper fluoroalkoxides, chemistry, 406–412
- Copper reagents, perfluorovinyl, *See*
Perfluorovinyl copper reagents
- CsF, role as fluoride ion donor, 150, 152–157
- Cyclopentadienyluranium fluorides
experimental procedure, 389–390
physical properties, 384–385
synthesis, 383, 385–389
- D**
- [(dfepe)M(ν -O₂CCF₃)₂]₂ complexes
reactivity and synthesis, 428–430
- Difluoroethyne, description, 5
- Difluoromethyl isocyanide, synthesis, 279
- Difluoromethylidene, description, 5
- Dimethyltin(IV) cation, scale of anion
basicity, 352–354
- Dinuclear trifluoromethyl isocyanide
complexes and cluster compounds,
reactions and synthesis, 270–282
- Dioxygen difluoride, physical properties, 41*t*
- Diphosphene derivatives, kinetic
stabilization, 309–310
- Disulfanes, reactions with monofluoro-
xonium hexafluorometalates, 93, 94*f*
- E**
- Electron-deficient reagents, activation of
carbon–fluorine bonds, 393
- Electron-rich reagents, activation of
carbon–fluorine bonds, 393–396
- Entropy, estimation for fluorine–Lewis
fluoroacid mixtures, 31–32, 33*r*, 34*f*
- Experimental chemistry, relationship to
computational chemistry, 4–5
- F**
- 10-F-2 trifluoride anion, calculated
charges, 168
- ¹⁹F-NMR spectroscopy, characterization of
fluoroalkyl cobaloximes, 291
- F₂C(SF₃)₂, gas-phase structure, 150, 151*f*
- F₂SCF=CF₂, reactions, 140–144
- Fifth main group elements, reactions with
monofluoroxenonium hexafluorometalates,
97–98, 101*f*
- Five-coordinated Ir(I), reactions with
XeF₂, 328–331
- Fluoride(s)
coordination numbers greater than six,
description, 2
nonmetal, *See* Nonmetal
fluoride–platinum metal complexes
See also Heptacoordinated main group
fluorides and oxofluorides
See also Main group fluorides with
coordination numbers greater than six
- Fluoride affinity, definition, 27
- Fluoride ion(s), addition to bifunctional SN
systems, 157–163
- Fluoride ion donors, examples, 148
- Fluorinated aldehyde(s)
polymerization, 211–214
previous studies, 211
synthesis, 209
- Fluorinated aldehyde polymers,
synthesis, 211–214
- Fluorinated alkyl cobaloximes
representation, 286
structural studies, 291–294
synthesis, 286, 288–289
- Fluorinated allotropes of carbon,
description, 3
- Fluorinated isocyanides, description, 6
- Fluorinated isopropoxides, 405–418
- Fluorinated metal alkoxides, reasons for
interest, 405
- α -Fluorinated organocobaloxime
complexes, synthesis, 286, 288–289
- Fluorinated sulfonium cations, synthesis,
90–91

- Fluorinated sulfur anions and cations, intermediates in sulfur chemistry, 148
- Fluorinated sulfuramide anions intermediates, 156–157 reactions, 155–156
- Fluorinated tertiary butoxides, 405–418
- Fluorine, constants as aliphatic and aromatic substituents, 104,106*t*
- Fluorine and parahalogen substituent effect on chemistry of functional groups
- carbenes, 105–107,108*f*
 - carbonyls, 114
 - isocyanates, 120,123–126
 - ketenes, 120
 - nitrenes, 105–107,109–113
 - selenocarbonyls, 114–117
 - sulfines, 120,123–126
 - sulfinylamines, 120,123–126
 - tellurocarbonyls, 114–116,118–119
 - thiocarbonyls, 114
 - thioketenes, 120–122
- Fluorine chemistry, inorganic, *See* Inorganic fluorine chemistry
- Fluorine-containing carbenes, 105–108
- Fluorine-containing carbonyls, 114
- Fluorine-containing isocyanates, 120,123–126
- Fluorine-containing ketenes, 120
- Fluorine-containing ligands, 5
- Fluorine-containing main group element ligands, description, 6–7
- Fluorine-containing nitrenes, 105–107,109–113
- Fluorine-containing selenocarbonyls, 114–117
- Fluorine-containing substituent groups, description, 7–8
- Fluorine-containing sulfines, 120,123–126
- Fluorine-containing sulfinylamines, 120,123–126
- Fluorine-containing tellurocarbonyls, 114–116,118–119
- Fluorine-containing thiocarbonyls, 114
- Fluorine-containing thioketenes, 120–122
- Fluorine–Lewis fluoroacid mixtures, thermodynamics of oxidizing capabilities, 26–38
- Fluoro anions, very weakly basic, stabilization of unusual cations, 350–362
- Fluoroalkyl cobaloximes, characterization by NMR spectroscopy, 290–291
- (Fluoroalkyl)phosphines
- acceptor ability, 423
 - coordination properties, 424–426
 - group 9 reactivity studies, 426–432
 - physical properties, 424
 - synthesis, 423–424
- Fluorodienes, transition metal chemistry, 252–263
- Fluoromethyl isocyanides, synthesis, 279
- Fluoromethylidyne, description, 5
- Fluoro-olefins, transition metal chemistry, 252–263
- Fluoro-onium salts, synthesis, 26
- Fluorophosphines, 6,422
- Fluorosilanes, importance, 181
- Fluorosulfuranide anions chemistry, 155
- donor–acceptor properties, 148–149
 - ¹⁹F-NMR spectroscopy, 153*t*
 - gas-phase structure, 150,151*f*
 - interactions, 149–150
 - intermediates, 152–153,155
 - reagents, 150,152–153
 - X-ray structure, 150–154
- Four-coordinated Ir(I), reactions with XeF₂, 327–328,329*t*
- Functionalization, pentafluoro-*l*6-sulfanyl olefins and acetylenes, 128–144
- G
- Gas-phase reactions, perfluoro macrocycles, 221,225–229
- Gold fluoroalkoxides, chemistry, 412,416*t*
- Group 6 and 7 fluoroalkoxides, chemistry, 417–418
- Group 9 reactivity studies, (fluoroalkyl)phosphines, 426–432
- Group 11 fluoroalkoxides, chemistry, 406–416
- Group 15–17 onium cations, syntheses, 7–8
- H
- ¹H-NMR spectroscopy, characterization of fluoroalkyl cobaloximes, 290

- $\text{H}_2\text{SF}_6^+\text{SbF}_6^-$, 95–96
- Halogen exchange media, use of alkali metal polyhydrogen fluorides, 237–248
- Heptacoordinated main group fluorides and oxofluorides
 experimental description, 67
 SF_5E_2 species, 67–69
 XF_6E species, 67
 XF_6 species, 69–78,80
 XOF_6 species, 78–87
- Hexafluorobutadiene, transition metal chemistry, 255–261,263
- HF, reaction with SiH_4 , 181–207
- High coordination number fluoride species with one nonbonding electron pair, geometries, 61,63–65
- Highly soluble cationic organotitanium Lewis acids
 experimental description, 367
 hydrolysis, 372–378
 reaction chemistry, 371
 reactive complexes, 377–379
 solid-state structures, 368–371,373
 solubility in nonpolar solvents, 371*t*
 synthesis, 367–369
- Homogeneous catalysis, goals, 421
- HSO_3F , reductive carbonylation for synthesis of weakly basic fluoro anions, 352
- Hydrolysis, highly soluble cationic organotitanium Lewis acids, 372–378
- Hypervalent, description, 167
- Hypervalent bonding, orbital diagram, 167–168
- I
- I^{2+} , stabilization by very weakly basic fluoro anions, 354–355
- IF_7 , ab initio calculations, 69–71
 axial–equatorial ligand exchange, 75
 force constants, 73,74*t*
 mean square amplitudes of vibration, 73,74*t*
 Raman spectrum, 71,72*f*
 structure and bonding, 69,75–78
 vibrational assignments, 71,73
- Inorganic fluorine chemistry
 C–F bond activation, 7
 computational–experimental chemistry relationship, 4–5
- Inorganic fluorine chemistry—*Continued*
 coordination numbers greater than 6
 among fluorides and oxofluorides, 2
 difluoroethyne, 1
 difluoromethylidene, 5–6
 fluorinated allotropes of carbon, 3
 fluorinated isocyanides, 6
 fluorine-containing main group element ligands, 5
 fluorine-containing substituent groups, 7–8
 fluoromethylidyne, 5–6
 fluorophosphines, 6
 importance to industry, 1
 naked fluoride transfer to least coordinating anion, 2–3
 novel bond types to noble gases, 3–4
 pentafluorocyclopentadienyl, 5
- Inorganic main group fluorides and oxofluorides, reasons for interest, 66–67
- Intermediates, fluorinated sulfur anions, 148–163
- IOF_6^-
 ab initio calculations, 85,86*t*
 equatorial puckering, 79,81,82*f*
 ^{19}F -NMR spectrum, 81,82*f*
 normal coordinate analyses, 85,87*t*
 structure and bonding, 85–87
 vibrational spectra, 81,83–84
- Ir(I), reactions with XeF_2 , 327–331
- Ir(III), reactions with XeF_2 , 332
- Iridium polyhydrides, binuclear, synthesis, 430–432
- Isocyanates, fluorine-containing, chemistry, 120,123–126
- Isocyanides
 complex formation, 265
 fluorinated, description, 6
- Isopropoxides, fluorinated, chemistry, 405–418
- K
- Ketenes, fluorine-containing, 120
- Kinetic stabilization
 description, 309
 2,4,6-tris(trifluoromethyl)phenyl substituent, 310–322
- $\text{Kr}(\text{OTeF}_5)_2$, evidence, 4

Krypton difluoride
 applications, 40–41
 photochemical and thermal dissociation
 synthesis, 42–54
 physical properties, 41*t*
 synthetic methods, 41–42

L

Lanthanide fluoroalkoxides, chemistry, 417
 Lattice enthalpy, size effect for
 fluorine–Lewis fluoroacid mixtures,
 30–31,33*f*
 Least coordinating anion, formation from
 naked fluoride, 2–3
 Lewis acid–elemental fluorine mixtures,
 oxidizing power, 26–27
 Lewis fluoroacid–fluorine mixtures,
 thermodynamics of oxidizing
 capabilities, 26–38
 Lewis' octet rule, purpose, 16
 Liquid antimony(V) fluoride, solvolysis
 for synthesis of weakly basic fluoro
 anion compounds, 351
 Low-valent transition metals, activation
 of C–F bonds by oxidative addition,
 392–402

M

Main group fluorides and oxofluorides,
 heptacoordinated, *See* Heptacoordinated
 main group fluorides and oxofluorides
 Main group fluorides with coordination
 numbers greater than 6
 coordination number 7, 56–61
 coordination number 8, 61,62*f*
 high coordination number species with
 one nonbonding electron pair,
 61,63–65
 Mass spectrometric characterization by
 collisionally activated dissociation,
 perfluoro macrocycles, 229–230
 $(\text{Me}_2\text{N})_3\text{S}^+\text{Me}_3\text{SiF}_2^-$, role as fluoride
 ion donor, 150–163
 Metal derivatives, 2,4,6-tris(trifluoro-
 methyl)phenyl substituent, 319–322

Monofluoroxenonium hexafluorometalates
 reactions
 disulfanes, 93,94*f*
 fifth main group elements, 97–98,101*f*
 seventh main group elements, 99–100,101*f*
 SH derivatives, 93,95
 sixth main group elements, 98–99
 sulfanes, 91–93,94*f*
 sulfuranes, 96–97
 synthesis, 91
 Mononuclear trifluoromethyl isocyanide
 complexes
 chemistry, 269–270
 synthesis, 266–269

N

$\text{N}_2\text{F}^+\text{AsF}_6^-$, reactions with fifth main group
 elements, 97–98,101*f*
 Naked fluoride, transfer to least
 coordinating anion, 2–3
 $\text{N}(\text{CH}_3)_4^+\text{IOF}_6^-$
 ab initio calculations, 85,86*t*
 equatorial puckering, 79,81,82*f*
 ^{19}F -NMR spectrum, 81,82*f*
 normal coordinate analyses, 85,87*t*
 properties, 78–79,80*f*
 structure and bonding, 85–87
 synthesis, 78
 vibrational spectra, 81,83–84
 Ni^{2+} , stabilization by very weakly basic
 fluoro anions, 355–356
 Nitrenes, fluorine-containing, chemistry,
 105–107,109–113
 Noble gases, novel bond types, 3–4
 Noble metal carbonyl derivatives,
 stabilization by very weakly basic
 fluoro anions, 357–362
 Noncoordinating anions
 coordination to metal ions, 338
 examples, 338
 Nonmetal fluoride–platinum metal complexes
 experimental description, 327
 previous studies, 326
 XeF_2 reactions, 327
 YF_4 reactions, 332–336
 Nonmetal fluoride–transition metal
 complexes, 326

O

- O_2^+ , stabilization by very weakly basic fluoro anions, 354–355
- $O_2^+AF^-$ salts, physical properties, 32,35f,36
- $O_2^+AsF_6^-$
comparison to $XeF^+AsF_6^-$, 36–37
synthesis, 27
- O_2-F_2-A reaction, pathway, 37
- Olefins, addition of SF_5 halides, 136–137
- Onium cations, synthesis using monofluoro-xenonium hexafluorometalates, 90–101
- Organic chemistry, 2,4,6-tris(trifluoromethyl)phenyl substituent, 313–320
- Organocobaloxime complexes, α -fluorinated, 286,288–289
- Organometallic chemistry, fluorinated isocyanides, 265–282
- Organometallic compounds with perfluorinated ligands, studies, 252
- Organotitanium Lewis acids, highly soluble cationic, *See* Highly soluble cationic organotitanium Lewis acids
- $OTeF_5$ group anions, role in coordinative unsaturation in cations, 340–346
- Oxidative addition to low-valent transition metals, activation of C–F bonds, 392–402
- Oxidizing capabilities of fluorine–Lewis fluoroacid mixtures, thermodynamics, 26–38
- Oxofluorides
coordination numbers greater than six, description, 2
See also Heptacoordinated
main group fluorides and oxofluorides

P

- Palladium-catalyzed coupling reactions, perfluorovinyl zinc reagents, 304–307
- Parahalogen substituents, role in chemistry of functional groups, 104–126
- Pd^{2+} , stabilization by very weakly basic fluoro anions, 355–356
- Pentafluoro-16-sulfanylolefins and acetylenes
addition of SF_5 halides to acetylenes, 136
addition of SF_5 halides to multiple C–C bonds, 135–136
- Pentafluoro-16-sulfanylolefins and acetylenes—*Continued*
addition of SF_5 halides to olefins, 136–137
examples, 128,130–134f
reactions, 139–144
structures of gases and solids, 144
synthesis
 SF_5 alkenes, 136–139
 SF_5 halides, 135
- Pentafluoro-oxotellurate anions, role in coordinative unsaturation in cations, 340–346f
- Pentafluorocyclopentadienyl
description, 5
transition metal chemistry, 258,262–263
- Pentafluorophenyl isocyanide, 281
- (Pentafluorothio)alkenes, synthesis, 136–139
- Pentafluorothio halides
addition to acetylenes, 136
addition to multiple C–C bonds, 135–136
synthesis, 135
- (Pentafluorothio)olefins, reactions, 139–140
- Perfluoroalkenyl lithium and Grignard reagents, thermal stability, 297
- Perfluoroalkynes, stereospecific addition of perfluorovinyl copper reagents, 303–304
- Perfluoro-*cis,syn,cis*- and -*cis,anti,cis*-dicyclohexyl-18-crown-6 ether
single-crystal X-ray structure, 221–223f
synthesis, 219
unit cell packing, 221,223f
- Perfluoroaryl copper reagents, 307–308
- Perfluoro crown ether(s)
applications, 216–219
binding, 230
characterization, 216,219–222
crystal structures, 231–234f
- Perfluoro macrocycles
cation binding, 230–231
gas-phase reactions, 221,225–229
MS characterization by collisionally activated dissociation, 229–230
synthesis, 216–219,230–231,235
- Perfluoro-12-crown-4 ether, characterization, 219,220f
- Perfluoro-15-crown-5 ether, characterization, 219,220f
- Perfluoro-18-crown-6 ether
ORTEP drawing, 219,220f
packing diagram, 219,222f

- Perfluorocryptands, 221,224*f*
- Perfluorovinyl cadmium reagents
 reactivity, 299
 stability, 300
 stereospecific addition to
 perfluoroalkynes, 303–304
 synthesis, 298–300
- Perfluorovinyl copper reagents
 reactivity and stability, 303
 synthesis, 302*t*
- Perfluorovinyl zinc reagents
 palladium-catalyzed coupling reactions,
 304–307
 reactivity and stability, 302
 synthesis, 300–301
- Phosphine ligands, steric and electronic
 property range, 421–422
- Photochemical synthesis of krypton difluoride
 advantages, 54
 apparatus, 42–46*f*
 experimental procedure, 42–43
 ideal Kr : F mole ratio, 50,52
 lamp power vs. yield, 52*t*
 mechanism, 50
 quantum yield, 48–49
 synthetic procedure, 46*f*,47
 UV–visible spectrum, 46*f*,47–48
 UV wavelength effect, 48–49
 yield vs. mole fraction of krypton, 50,51*f*
- Physical properties
 cyclopentadienyluranium fluorides, 385
 dioxygen difluoride, 41*t*
 (fluoroalkyl)phosphines, 424
 krypton difluoride, 41*t*
- Platinum complexes, reactions with YF_4 ,
 332–336
- Polyfluorinated anions
 $B(OTeF_3)_4^-$, 341–346
 examples, 338
 ideal properties, 339–340
 $M(OTeF_3)_4$, 340–341,343*f*
 $M(OTeF_3)_6^m$, 344–345,346*f*
 role in coordinative unsaturation in
 cations, 338–339
- Precursor for chemical vapor deposition of
 inorganic materials, importance of
 development, 1
- Protonic acids, acidolysis for synthesis
 of weakly basic fluoro anion
 compounds, 351
- R
- Reaction(s)
 coordinated trifluoromethyl isocyanide
 ligand, 273,279–280,282
 $F_5SCF=CF_2$, 140–144
 pentafluorothio olefins, 139–140
- Reaction chemistry, highly soluble cationic
 organotitanium Lewis acids, 371
- Reactivity
 $[(dfepe)M(v-O_2CCF_3)]_2$ complexes, 429–430
 perfluoroaryl copper reagents, 307–308
 perfluorovinyl cadmium reagents, 299
 perfluorovinyl copper reagents, 303
 perfluorovinyl zinc reagents, 302
- Reactor walls, UF_6-SiH_4 system reactions,
 193,194*f*,195,196*f*
- Reagents, fluorinated sulfur anions, 148–163
- Regeneration reaction, alkali metal
 polyhydrogen fluorides as halogen
 exchange media, 241–248
- S
- SbF_5 , high F^- affinity, 31
- Scale of anion basicity, dimethyltin(IV)
 cation, 352–354
- SeF_4 , reactions with platinum metal
 complexes, 334
- Selenocarbonyls, fluorine-containing,
 chemistry, 114–117
- Seventh main group elements, reactions
 with monofluoroxenonium
 hexafluorometalates, 99–100,101*f*
- SH derivatives, reactions with
 monofluoroxenonium
 hexafluorometalates, 93,95
- SiH_4-HF system, vapor-phase
 Fourier transform IR studies, 198–202
- SiH_4-UF_6 and $-HF$ reactions
 apparatus, 183–184
 catalysis, 206
 experimental procedure, 182–185
 reaction, 206
 reaction(s) on reactor walls, 193–196
 reaction procedure, 182–183
 reactivity, 206–207
 SiH_4-HF vapor-phase Fourier transform IR
 studies, 198–202

- SiH₄-UF₆ and -HF reactions—*Continued*
 solid products, 201,203–205
 UF₆-SiH₄-HF vapor-phase Fourier
 transform IR studies, 197–198
 UF₆-SiH₄ vapor-phase Fourier transform
 IR studies, 185–193
- Silane, 181–182
- Silver fluoroalkoxides, chemistry,
 406–407,412–415
- Six-coordinated Ir(III), reactions with
 XeF₂, 332
- Sixth main group elements, reactions with
 monofluoroxenonium
 hexafluorometalates, 98–99
- Size, lattice energy effect for fluorine–Lewis
 fluoroacid mixtures, 30–31,33f
- SN systems, bifunctional, addition of
 fluoride ions, 157–163
- Solid products of SiH₄-UF₆ and -HF
 reactions, vapor-phase Fourier transform
 IR studies, 201,203–205
- Solid-state structures, highly soluble
 cationic organotitanium Lewis acids,
 368–371,373
- Solubility in nonpolar solvents, highly
 soluble cationic organotitanium Lewis
 acids, 367
- Stability
 perfluorovinyl cadmium reagents, 300
 perfluorovinyl copper reagents, 303
 perfluorovinyl zinc reagents, 302
- Stabilization of unusual cations by very
 weakly basic fluoro anions
 Ag₂⁺, 355–357
 anions, 350
 Au₂⁺, 355–357
 Br₂⁺, 354–355
 definition of unusual, 350
 I₂⁺, 354–355
 Ni²⁺, 355–356
 noble metal carbonyl derivatives, 357–362
 O₂⁺, 354–355
 Pd²⁺, 355–356
 scale of anion basicity, 352–354
 synthesis, 351–352
- Structural studies, fluorinated alkyl
 cobaloximes, 291–294
- Substitution reaction, alkali metal
 polyhydrogen fluorides as halogen
 exchange media, 240–242
- Sulfanes, reactions with monofluoro-
 xenonium hexafluorometalates, 91–93,94f
- Sulfines, fluorine-containing, chemistry,
 120,123–126
- Sulfinylamines, fluorine-containing,
 chemistry, 120,123–126
- Sulfur hexafluoride, chemical stability, 128
- Sulfur tetrafluoride, donor–acceptor
 properties, 148–149
- Sulfuranes, reactions with monofluoro-
 xenonium hexafluorometalates, 96–97
- Synthesis
 binuclear iridium polyhydrides, 430–432
 cyclopentadienyluranium fluorides,
 383,385–389
 [(dfepe)M(v-O₂CCF₃)]₂ complexes, 428–429
 difluoromethyl isocyanide, 279
 dinuclear trifluoromethyl isocyanide
 complexes and cluster compounds,
 270–271,273–274,276,278
 fluorinated alkyl cobaloximes, 286,288–289
 α-fluorinated organocobaloxime complexes
 fluorine-containing ligand introduction
 via highly fluorinated olefins, 288–289
 fluoroalkyl ligand introduction via
 fluorinated aliphatic alkyl halides,
 286,288
 pyridine ligand substitution, 289
 fluoromethyl isocyanides, 279
 highly soluble cationic organotitanium
 Lewis acids, 367–369
 iridium polyhydrides, binuclear, 430–432
 mononuclear trifluoromethyl isocyanide
 complexes, 266–269
 pentafluorophenyl isocyanide, 281
 perfluoroaryl copper reagents, 307–308
 perfluoro macrocycles, 216–235
 perfluorovinyl cadmium reagents, 298–300
 perfluorovinyl copper reagents, 302t
 perfluorovinyl zinc reagents, 300–301
 trifluorovinyl isocyanide, 279,281
 weakly basic fluoro anion compounds
 acidolysis in protonic acids, 351
 carbonylation and solvolysis in
 antimony(V) fluoride, 352
 element oxidation by
 bis(fluorosulfuryl)peroxide, 351
 reductive carbonylation in HSO₃F, 352
 solvolysis in liquid antimony(V)
 fluoride, 351

T

TeF₄, reactions with platinum metal complexes, 336

TeF₇⁻, structure, 78,80f

Tellurocarbonyls, fluorine-containing, chemistry, 114–116,118–119

TeOF₆²⁻, structure, 87

Tertiary butoxides, fluorinated, chemistry, 405–418

Tetrafluoroethylene complexes with metallocyclopropane structures, chemistry, 253–256

Thermal dissociation of krypton difluoride advantages, 54
 apparatus, 43,47
 experimental procedure, 42–43
 factors affecting yields, 52–54
 synthetic procedure, 47
 UV–visible spectrum, 46f,47–48
 yield vs. mole fraction of krypton, 50,51f

Thermodynamics
 alkali metal polyhydrogen fluorides as halogen exchange media, 237–239
 oxidizing capabilities of fluorine–Lewis fluoroacid mixtures
 comparison of O₂⁺AsF₆⁻ and XeF⁺AsF₆⁻, 36–37
 entropy estimation, 31–32,33t,34f
 experimental reagents, 28
 high F⁻ affinity of AsF₅ and SbF₅, 31
 pathway for Xe–F₂–A and O₂–F₂–A reactions, 37
 physical properties of O₂⁺AF⁻ salts, 32,35–36
 prospects for ArF⁺ salts, 37–38
 reaction(s), 29–30
 reaction procedures, 28–29
 reactors, 27–28
 size vs. lattice enthalpy, 30–31,33f
 X-ray powder diffraction procedure, 28

Thiocarbonyls, fluorine-containing, chemistry, 114

Thioketenes, fluorine-containing, chemistry, 120–122

Transition metal chemistry of fluoro-olefins and fluorodienes
 hexafluorobutadiene, 255–261,263
 pentafluorocyclopentadienyl ligand, 258,262–263

Transition metal chemistry of fluoro-olefins and fluorodienes—*Continued*
 tetrafluoroethylene complexes with metallocyclopropane structures, 253–256

Transition metal compounds, geometries for complexes with fluorides with coordination number 7, 61

Transition states, fluorinated sulfur anions, 148–163

Trifluoromethyl constants, aliphatic and aromatic substituents, 104,106r

Trifluoromethyl isocyanide, studies of transition metal chemistry, 265–266

Trifluoromethyl isocyanide complexes mononuclear, *See* Mononuclear trifluoromethyl isocyanide complexes dinuclear, *See* Dinuclear trifluoromethyl isocyanide complexes and cluster compounds (Trifluoromethyl)sulfonyl, constants as aliphatic and aromatic substituents, 104,106r

Trifluorovinyl isocyanide chemistry, 281,282f
 synthesis, 279,281

Tris(dimethylamino)sulfonium trimethyldifluorosilicate, polymerization of fluorinated aldehyde, 213

2,4,6-Tris(trifluoromethyl)phenyl substituent metal derivatives, 319–322
 organic chemistry, 313–320
 previous studies, 310
 synthesis of starting materials, 310–313

Twenty-first century, developments in inorganic fluorine chemistry, 8

U

UF₆–SiH₄–HF system, vapor-phase Fourier transform IR studies, 197–198

UF₆–SiH₄ system, vapor-phase Fourier transform studies, 185–193

Unusual, definition, 350

Unusual cations, stabilization by very weakly basic fluoro anions, 350–362

V

Vacant coordination site, terminology, 339

- Vapor-phase Fourier transform IR studies
 reactions on reactor walls, 193–196
 SiH_4 –HF system, 198–202
 solid products, 201,203–205
 UF_6 – SiH_4 system, 185–193
 UF_6 – SiH_4 –HF system, 197–198
 Very weakly basic fluoro anions, stabilization
 of unusual cations, 350–362
- W
- Weakly coordinating anions, ideal
 properties, 339–340
- X
- Xe– F_2 –A reaction, pathway, 37
 $\text{Xe}(\text{CF}_3)_2$, evidence, 4
 $\text{XeF}^+\text{AsF}_6^-$
 comparison to $\text{O}_2^+\text{AsF}_6^-$, 36–37
 reactions
 disulfanes, 93,94f
 fifth main group elements, 97–98,101f
 seventh main group elements, 99–100,101f
 SH derivatives, 93,95
 sixth main group elements, 98–99
 sulfanes, 91–93,94f
 sulfuranes, 96–97
 $\text{XeF}^+\text{SbF}_6^-$ reactions
 disulfanes, 93,94f
 fifth main group elements, 97–98,101f
 seventh main group elements, 99–100,101f
 SH derivatives, 93,95
 sixth main group elements, 98–99
 sulfanes, 91–93,94f
 sulfuranes, 96–97
 XeF_2 reactions
 4-coordinated Ir(I), 327–328,329t
 5-coordinated Ir(I), 328–331
 6-coordinated Ir(III), 332
 XeF_5^- anion, structure, 67–69
 XF_3E_2 species, structure, 67–69
 XF_6E species, structures, 67
 XF_6 species
 ab initio calculations, 69–71
 axial–equatorial ligand exchange, 75
 force constants, 73,74t
 mean square amplitudes of vibration,
 73,74t
 Raman spectrum, 71,72f
 structure and bonding, 75–78
 structure studies, 69
 vibrational assignment, 71,73
 XOF_6 species
 ab initio calculations, 85,86t
 equatorial puckering, 79,81,82f
 ^{19}F -NMR spectrum, 81,82f
 normal coordinate analyses, 85,87t
 properties, 78–79,80f
 structure and bonding, 85–87
 synthesis, 78
 TeOF_6^{2-} , 87
 vibrational spectra, 81,83–84
- Y
- YF_4 , reactions with $[\text{M}(\text{CO})\text{X}(\text{PEt}_3)_2]$,
 332–336
- Z
- Zinc reagents, perfluorovinyl, *See*
 Perfluorovinyl zinc reagents
 Zirconium fluoroalkoxides, chemistry,
 416–417

Production: Susan F. Antigone

Indexing: Deborah H. Steiner & Colleen P. Stamm

Acquisition: Rhonda Bitterli

Cover design: Cesar Caminero

Printed and bound by Maple Press, York, PA